PHOSPHORUS ALONG THE SOIL-FRESHWATER-OCEAN CONTINUUM

EDITED BY: Barbara J. Cade-Menun, Solange Duhamel, Rosalind J. Dodd, Christian Lønborg, Chris T. Parsons and William D. Taylor

PUBLISHED IN: Frontiers in Marine Science, Frontiers in Microbiology, Frontiers in Earth Science and Frontiers in Environmental Science

frontiers Research Topics

frontiers

ISSN 1664-8714
ISBN 978-2-88945-829-5
DOI 10.3389/978-2-88945-829-5

About Frontiers

Frontiers is more than just an open-access publisher of scholarly articles: it is a pioneering approach to the world of academia, radically improving the way scholarly research is managed. The grand vision of Frontiers is a world where all people have an equal opportunity to seek, share and generate knowledge. Frontiers provides immediate and permanent online open access to all its publications, but this alone is not enough to realize our grand goals.

Frontiers Journal Series

The Frontiers Journal Series is a multi-tier and interdisciplinary set of open-access, online journals, promising a paradigm shift from the current review, selection and dissemination processes in academic publishing. All Frontiers journals are driven by researchers for researchers; therefore, they constitute a service to the scholarly community. At the same time, the Frontiers Journal Series operates on a revolutionary invention, the tiered publishing system, initially addressing specific communities of scholars, and gradually climbing up to broader public understanding, thus serving the interests of the lay society, too.

Dedication to Quality

Each Frontiers article is a landmark of the highest quality, thanks to genuinely collaborative interactions between authors and review editors, who include some of the world's best academicians. Research must be certified by peers before entering a stream of knowledge that may eventually reach the public - and shape society; therefore, Frontiers only applies the most rigorous and unbiased reviews.
Frontiers revolutionizes research publishing by freely delivering the most outstanding research, evaluated with no bias from both the academic and social point of view. By applying the most advanced information technologies, Frontiers is catapulting scholarly publishing into a new generation.

What are Frontiers Research Topics?

Frontiers Research Topics are very popular trademarks of the Frontiers Journals Series: they are collections of at least ten articles, all centered on a particular subject. With their unique mix of varied contributions from Original Research to Review Articles, Frontiers Research Topics unify the most influential researchers, the latest key findings and historical advances in a hot research area! Find out more on how to host your own Frontiers Research Topic or contribute to one as an author by contacting the Frontiers Editorial Office: researchtopics@frontiersin.org

PHOSPHORUS ALONG THE SOIL-FRESHWATER-OCEAN CONTINUUM

Topic Editors:
Barbara J. Cade-Menun, Agriculture & Agri-Food Canada, Canada
Solange Duhamel, Columbia University, United States
Rosalind J. Dodd, Lincoln University, New Zealand
Christian Lønborg, Australian Institute of Marine Science, Australia
Chris T. Parsons, University of Waterloo, Canada
William D. Taylor, University of Waterloo, Canada

Phosphorus (P) is an essential element for all organisms. However, there is a P paradox, whereby P concentrations considered deficient in some environments such as in agricultural soils are considered excessive in water, where they trigger eutrophication. Ensuring adequate P for crop production while minimizing water quality degradation requires consideration of the P continuum from soils to freshwater and oceans. It also requires an international, interdisciplinary approach to monitoring and scientific research. This eBook brings together P studies in soil science, lakes, rivers, estuaries and oceans, with 74 authors from 12 countries in Asia, Europe and North America. The papers assembled here provide important new information to address knowledge gaps, cover P forms and cycling in soil and water, and identify key priorities for future research. Thus, the papers assembled here provide current and interdisciplinary information about P forms and their cycling along the soil-freshwater-ocean continuum, which is essential for environmentally sustainable P use.

Citation: Cade-Menun, B. J., Duhamel, S., Dodd, R. J., Lønborg, C., Parsons, C. T., Taylor, W. D., eds. (2019). Phosphorus Along the Soil-Freshwater-Ocean Continuum. Frontiers Media. doi: 10.3389/978-2-88945-829-5

Table of Contents

SECTION 3
PHOSPHORUS FORMS AND CYCLING IN OCEANS

frontiers in Marine Science

EDITORIAL
published: 25 February 2019
doi: 10.3389/fmars.2019.00028

Editorial: Phosphorus Along the Soil-Freshwater-Ocean Continuum

Barbara J. Cade-Menun[1], Solange Duhamel[2], Rosalind J. Dodd[3], Christian Lønborg[4], Chris T. Parsons[5] and William D. Taylor[6]*

[1] Agriculture and Agri-Food Canada, Swift Current Research and Development Centre, Swift Current, SK, Canada, [2] Lamont Doherty Earth Observatory, Division of Biology and Paleo Environment, Columbia University, Palisades, NY, United States, [3] Faculty of Agriculture and Life Sciences, Lincoln University, Lincoln, New Zealand, [4] Australian Institute of Marine Science, Townsville, QLD, Australia, [5] Department of Earth and Environmental Sciences and the Water Institute, University of Waterloo, Waterloo, ON, Canada, [6] Department of Biology, University of Waterloo, Waterloo, ON, Canada

Keywords: phosphorus, land-water continuum, lakes, estuaries, oceans, soil

Editorial on the Research Topic

Phosphorus Along the Soil-Freshwater-Ocean Continuum

Phosphorus (P) is an essential element for all organisms. However, there is a P paradox, whereby P concentrations considered deficient in some environments such as in agricultural soils are considered excessive in freshwater, where they trigger eutrophication (e.g., Sims and Sharpley, 2005 and references therein; Elser and Bennet, 2011; Lougheed, 2011). Geographical imbalances also occur, with excesses in Western Europe and North America and deficiencies in regions with highly weathered soils, such as sub-Saharan Africa. There is a strong link between soil P stores and P mobilization and transfer to receiving waters, termed the P transfer continuum (Haygarth et al., 2005). Ensuring adequate P for crop production while minimizing water quality degradation requires consideration of this continuum and an international, interdisciplinary approach. This research topic brings together P studies in soil science, lakes, rivers, estuaries, and oceans, with 74 authors from 12 countries in Asia, Europe, and North America, and identifies key priorities for future research.

In all ecosystems, P exists in many chemical forms. Inorganic P compounds include phosphate, pyrophosphate, and polyphosphate, with organisms directly using phosphate ($H_2PO_4^-$ or HPO_4^{2-} at the pH range of most natural ecosystems). Organic P compounds contain a link to carbon (C), and include orthophosphate monoesters [e.g., glucose 6-phosphate and *myo*-inositol hexakisphosphate (*myo*-IHP or phytate)]; orthophosphate diesters (e.g., nucleic acids, phospholipids); phosphonates (e.g., aminoethyl phosphonate), and biological polyphosphates (e.g., ATP). In all environments, P cycles geochemically and biologically. Geochemical processes include adsorption/desorption of organic and inorganic P compounds with mineral particles, and precipitation with cations in solution. In biological cycling, phosphate is taken up by organisms and converted to organic P forms such as nucleic acids or is stored in cells as phytate or polyphosphate. This P can be released by secretion or after cell death, and converted back to phosphate by mineralization, primarily an enzymatic process involving P-specific enzymes (phosphatases). For more information on P cycling, a number of review papers are available (e.g., Condron et al., 2005; Pierzynski et al., 2005; Paytan and McLaughlin, 2007; Baldwin, 2013; Karl, 2014; Orihel et al., 2017).

There are similarities and differences in P cycling in terrestrial and aquatic ecosystems. Terrestrial organisms obtain phosphate from the pool that is dissolved in the soil solution, in the space between the solid components of soil (minerals and organic matter). Here, P availability is limited by moisture. Easily-obtained (labile) phosphate is taken up from the soil solution, then replenished by desorption, dissolution, or mineralization.

OPEN ACCESS

Edited and reviewed by:
Eric 'Pieter Achterberg, GEOMAR Helmholtz Center for Ocean Research Kiel, Germany

****Correspondence:***
Barbara J. Cade-Menun
barbara.cade-menun@canada.ca

Specialty section:
This article was submitted to Marine Biogeochemistry, a section of the journal Frontiers in Marine Science

Received: *20 December 2018*
Accepted: *21 January 2019*
Published: *25 February 2019*

Citation:
Cade-Menun BJ, Duhamel S, Dodd RJ, Lønborg C, Parsons CT and Taylor WD (2019) Editorial: Phosphorus Along the Soil-Freshwater-Ocean Continuum. Front. Mar. Sci. 6:28. doi: 10.3389/fmars.2019.00028

Because terrestrial plants are fixed in place, strategies have evolved to improve their P acquisition. This includes changes in rooting structure or associations with rhizosphere microbes and symbionts, which can enhance access to phosphate, or production of phosphatases or organic acids to desorb P compounds from mineral surfaces (Richardson et al., 2011). Aquatic environments include sediments, benthic biofilms, and the water column. In sediments, organic and inorganic P compounds will be associated with mineral particles, algal and bacterial biomass (particularly at the sediment-water interface) and organic matter, or occur in aqueous form in pore water. Phosphate and other P forms can exchange with the water column through adsorption/desorption and precipitation/dissolution, and through uptake and remineralization by organisms in the sediment and in the water column. Within the water column, organic and inorganic P compounds can be dissolved, associated with colloids, or associated with larger particulates including plankton (e.g., Paytan and McLaughlin, 2007; Orihel et al., 2017; Taylor and Lean, 2018).

Although it can be the most limiting nutrient, or second to nitrogen (N) in many environments, P cycling in terrestrial and aquatic ecosystems in still poorly understood relative to C or N, because P concentrations are orders of magnitude lower than those of C and N, and due to methodological limitations. Unlike C and N, P has no significant natural gaseous forms, and only one stable isotope (^{31}P), which can hamper tracing P sources in the environment, but it does have two radioisotopes (^{32}P and ^{33}P) that occur naturally or can be added as tracers. Total P is determined by digestion of solids, or by inductively coupled argon plasma optical emission spectroscopy (ICP-OES) of liquids, and phosphate concentrations in liquids or extracted samples are analyzed by colorimetric techniques such as the molybdate blue method (Murphy and Riley, 1962). However, characterization of specific P compounds requires advanced techniques such as ^{31}P-nuclear magnetic resonance (P-NMR) spectroscopy or P-X-ray Absorption Near Edge Structure (P-XANES) spectroscopy that are not readily available to all researchers. Information about biological P cycling is also limited, particularly the roles of specific organisms. The links between the P cycle and those of other elements, including C and N, are also poorly understood.

The papers assembled here provide important new information to address knowledge gaps, and cover all aspects of the soil-freshwater-ocean continuum. Liu et al. examined P cycling in agricultural lands in Canada. Bol et al. and Reid et al. addressed P transfer from agricultural land to water, with Reid et al. assessing the components of P loss and assessment tools, and Bol et al. discussing the need for more integrated research efforts into the processes and mechanisms controlling P loss. In aquatic environments, P cycling in lakes was investigated by Thompson and Cotner; Anderson; and Depew et al; in estuaries by Watson et al.; in rivers by Felgentreu et al. and Gomes et al. and in oceans by Björkman et al.; Diaz et al. and Djaoudi et al. Across disciplines, several themes emerged. With respect to methods, colorimetric techniques were frequently used. However, Felgentreu et al. assessed filtration and colorimetric methods in river samples to improve routine monitoring programs, while Djaoudi et al. used techniques to improve the sensitivity of the Murphy and Riley (1962) colorimetric technique to determine nanomolar concentrations of dissolved inorganic P in the Mediterranean Sea. Liu et al. and Watson et al. both used P-NMR to characterize organic P forms, in soils and estuary sediments respectively, and Liu et al. used P-XANES to characterize soil inorganic P species. Oxygen isotope ratios of phosphate were used by Depew et al. to identify sources of P to Lake Erie and pathways of cycling.

Biological P cycling and P bioavailability in different ecosystems was a common theme. Liu et al. identified microbial communities in various agricultural soils, showing that soil disturbance controlled P forms and cycling in these ecosystems. Gomes et al. demonstrated that Amazon and Changjiang river plume phytoplankton communities were shaped by river N:P ratios. Björkman et al. assessed spatial variability in the dynamics of inorganic and organic P compounds in the North Pacific Tropical Gyre with radio tracer techniques, while Diaz et al. estimated the lability of model P compounds by diatom cultures and used proteomics to examine phosphatase diversity. Anderson measured alkaline phosphomonoesterase activities in freshwater microbial communities, while Thompson and Cotner investigated the bioavailability of dissolved organic P in lakes in Minnesota and South Dakota; both studies linked P and C biogeochemical cycles.

Thus, the articles in this research topic provide current and interdisciplinary information about P forms and their cycling along the soil-freshwater-ocean continuum, which is essential for environmentally sustainable P use.

AUTHOR CONTRIBUTIONS

All authors listed have made a substantial, direct and intellectual contribution to the work, and approved it for publication.

REFERENCES

Baldwin, D. S. (2013). Organic phosphorus in the aquatic environment. *Environ. Chem.* 10, 439–454. doi: 10.1071/EN13151

Condron, L. M., Turner, B. L., and Cade-Menun, B. J. (2005). "Chemistry and dynamics of soil organic phosphorus," in *Phosphorus, Agriculture and the Environment*, eds J. T. Sims and A. N. Sharpley (Madison, WI: American Society of Agronomy), 87–121.

Elser, J., and Bennet, E. (2011). A broken biogeochemical cycle. *Nature* 478, 29–31. doi: 10.1038/478029a

Haygarth, P. M., Condron, L. M., Heathwaite, A. L., Turner, B. L., and Harris, G. P. (2005). The phosphorus transfer continuum: linking source to impact with an interdisciplinary and multi-scaled approach. *Sci. Tot. Environ.* 344, 5–14. doi: 10.1016/j.scitotenv.2005.02.001

Karl, D. M. (2014). Microbially mediated transformation of phosphorus in the sea: new views of an old cycle. *Ann. Rev. Mar. Sci.* 6, 279–335. doi: 10.1146/annurev-marine-010213-135046

Lougheed, T. (2011). Phosphorus paradox: scarcity and overabundance of a key nutrient. *Environ. Health. Perspect.* 119, A209–A213. doi: 10.1289/ehp.119-a208

Murphy, J., and Riley, J. P. (1962). A modified single solution method for the determination of phosphate in natural water. *Anal. Chim. Acta* 27, 31–36. doi: 10.1016/S0003-2670(00)88444-5

Orihel, D. M., Baulch, H. M., Casson, N. J., North, R. L., Parsons, C. T., Seckar, D. C. M., et al. (2017). Internal phosphorus loading in Canadian freshwater lakes: a critical review and data analysis. *Can. J. Fish. Aquat. Sci.* 74, 2005–2029. doi: 10.1139/cjfas-2016-0500

Paytan, A., and McLaughlin, K. (2007). The oceanic phosphorus cycle. *Chem. Rev.* 107, 563–576. doi: 10.1021/cr0503613

Pierzynski, G. M., McDowell, R. W., and Sims, J. T. (2005). "Chemistry and dynamics of soil organic phosphorus," in *Phosphorus, Agriculture and the Environment*, eds J. T. Sims and A. N. Sharpley (Madison, WI: American Society of Agronomy), 53–86.

Richardson, A. E., Lynch, J. P., Ryan, P. R., Delhaize, E., Smith, F. A., Smith, S. E., et al. (2011). Plant and microbial strategies to improve the phosphorus efficiency of agriculture. *Plant Soil* 349, 121–156. doi: 10.1007/s11104-011-0950-4.

Sims, J. T., and Sharpley, A. N. (eds.) (2005). *Phosphorus: Agriculture and the Environment*. Madison, WI: American Society of Agronomy, 1121.

Taylor, W. D., and Lean, D. R. S. (2018). Observations on the dynamics and fate of dissolved organic phosphorus in lake water and a new model of epilimnetic P cycling. *Aquat. Sci.* 80:13. doi: 10.1007/s00027-018-0564-5

Conflict of Interest Statement: The authors declare that the research was conducted in the absence of any commercial or financial relationships that could be construed as a potential conflict of interest.

frontiers in Microbiology

ORIGINAL RESEARCH
published: 20 July 2018
doi: 10.3389/fmicb.2018.01643

Long-Term Land Use Affects Phosphorus Speciation and the Composition of Phosphorus Cycling Genes in Agricultural Soils

*Jin Liu[1,2], Barbara J. Cade-Menun[3], Jianjun Yang[4], Yongfeng Hu[5], Corey W. Liu[6], Julien Tremblay[7], Kerry LaForge[3], Michael Schellenberg[3], Chantal Hamel[3] and Luke D. Bainard[3]**

[1] College of Agronomy and Biotechnology, China Agricultural University, Beijing, China, [2] Visiting Scientist, Agriculture and Agri-Food Canada, Swift Current Research and Development Centre, Swift Current, SK, Canada, [3] Swift Current Research and Development Centre, Agriculture and Agri-Food Canada, Swift Current, SK, Canada, [4] Institute of Environment and Sustainable Development in Agriculture, Chinese Academy of Agricultural Sciences, Beijing, China, [5] Canadian Light Source, University of Saskatchewan, Saskatoon, SK, Canada, [6] Stanford Magnetic Resonance Laboratory, Stanford University School of Medicine and ChEM-H-Stanford University, Stanford, CA, United States, [7] Energy, Mining and Environment, National Research Council of Canada, Montreal, QC, Canada

OPEN ACCESS

Edited by:
Rosalind Jane Dodd, Bangor University, United Kingdom

Reviewed by:
John W. Moreau, University of Melbourne, Australia
Mustafa Yucel, Middle East Technical University, Turkey

***Correspondence:**
Luke D. Bainard
luke.bainard@agr.gc.ca

Specialty section:
This article was submitted to Microbiological Chemistry and Geomicrobiology, a section of the journal Frontiers in Microbiology

Received: *31 March 2018*
Accepted: *02 July 2018*
Published: *20 July 2018*

Citation:
Liu J, Cade-Menun BJ, Yang J, Hu Y, Liu CW, Tremblay J, LaForge K, Schellenberg M, Hamel C and Bainard LD (2018) Long-Term Land Use Affects Phosphorus Speciation and the Composition of Phosphorus Cycling Genes in Agricultural Soils. Front. Microbiol. 9:1643. doi: 10.3389/fmicb.2018.01643

Agriculturally-driven land transformation is increasing globally. Improving phosphorus (P) use efficiency to sustain optimum productivity in diverse ecosystems, based on knowledge of soil P dynamics, is also globally important in light of potential shortages of rock phosphate to manufacture P fertilizer. We investigated P chemical speciation and P cycling with solution ^{31}P nuclear magnetic resonance, P K-edge X-ray absorption near-edge structure spectroscopy, phosphatase activity assays, and shotgun metagenomics in soil samples from long-term agricultural fields containing four different land-use types (native and tame grasslands, annual croplands, and roadside ditches). Across these land use types, native and tame grasslands showed high accumulation of organic P, principally orthophosphate monoesters, and high acid phosphomonoesterase activity but the lowest abundance of P cycling genes. The proportion of inositol hexaphosphates (IHP), especially the *neo*-IHP stereoisomer that likely originates from microbes rather than plants, was significantly increased in native grasslands than croplands. Annual croplands had the largest variances of soil P composition, and the highest potential capacity for P cycling processes based on the abundance of genes coding for P cycling processes. In contrast, roadside soils had the highest soil Olsen-P concentrations, lowest organic P, and highest tricalcium phosphate concentrations, which were likely facilitated by the neutral pH and high exchangeable Ca of these soils. Redundancy analysis demonstrated that IHP by NMR, potential phosphatase activity, Olsen-P, and pH were important P chemistry predictors of the P cycling bacterial community and functional gene composition. Combining chemical and metagenomics results provides important insights into soil P processes and dynamics in different land-use ecosystems.

Keywords: land use, soil, phosphorus, solution NMR, XANES, shotgun metagenomics

INTRODUCTION

Driven by the increasing demand for agricultural production, land-use change has been widespread globally over the last several decades (Guillaume et al., 2015). In most parts of the world, the original vegetation has been cleared for the expansion of croplands and pastures, both of which are typical land uses crucial for food production (Houghton, 1994). Agricultural areas mostly devoted to either arable croplands or grazed pastures comprise about one third of the land surface globally (FAO/UNEP, 2015). The global effects of land-use change also contribute to global changes in nutrient cycling and dynamics (Houghton, 1994). This is especially significant for phosphorus (P), which often limits the productivity and sustainability of agriculture, requiring fertilization. Rock phosphate sources used to produce fertilizers are globally limited, and there are concerns about their long-term availability (Elser and Bennett, 2011; Sharpley et al., 2013). Additionally, P loss from agriculture can have a negative effect on the aquatic environment. This is expected to continue even if P fertilization is reduced due to the large amount of residual P accumulated in agricultural soils through time in many regions (Garcia-Montiel et al., 2000; Sharpley et al., 2013; Stutter et al., 2015). Efficient P use is therefore a priority when replacing natural ecosystems with managed ecosystems (Stutter et al., 2015).

Conversion of land-use is expected to change soil P dynamics. Changes in P inputs and outputs through management practices that alter soil physical, chemical and biological properties affect the chemical nature of different P species in soils and ultimately their bioavailability (Condron et al., 2005; Maranguit et al., 2017). A full understanding of the effects of land-use and management systems on soil P composition remains obscure, partially due to methodological limitations such as a reliance on the widely used but operationally defined sequential fractionation approach (Guggenberger et al., 1996; Negassa and Leinweber, 2009; Crews and Brookes, 2014; Maranguit et al., 2017). A more useful method, capable of identifying P species, particularly organic P (P_o) compounds, in soils at the molecular level, is solution ^{31}P nuclear magnetic resonance (P-NMR) spectroscopy. With P-NMR, more detailed insights into P_o species behind the P pools have been revealed in recent years (Condron et al., 2005; McDowell and Stewart, 2006; Stutter et al., 2015). Nevertheless, many published studies have limited peak identification to clearly separated, distinct peaks only (e.g., orthophosphate and pyrophosphate) and have grouped the remaining peaks together into broad compound classes such as orthophosphate monoesters and diesters; this provides limited information about P cycling and availability (Cade-Menun, 2017). Additionally, even within a single broad category such as orthophosphate monoesters or orthophosphate diesters, P_o forms differ in their bioavailability and reactivity. As such, a full understanding of P cycling in soils requires identifying as many specific P_o species as possible (Cade-Menun, 2015; Cade-Menun, 2017). Additionally, P K-edge X-ray absorption near-edge structure (P-XANES) spectroscopy provides a new and powerful approach to directly identify inorganic P (P_i) compounds (Prietzel et al., 2013; Liu et al., 2015). Therefore, the combined application of P K-edge XANES and P-NMR spectroscopy allows for a comprehensive identification of soil P species across ecosystems with different land uses, to an extent not accomplished with previous studies.

Land use change will introduce significant changes in vegetation, which can alter soil biology and nutrient cycling. Vegetation changes will change rooting depth, nutrient and water uptake, soil chemistry and symbioses, such as N fixation or mycorrhizae (Bainard et al., 2017; Cade-Menun et al., 2017a). Plants and microorganisms are essential drivers of soil P turnover and dynamics. They enhance the solubilization of P by the release of low molecular weight acids and phosphatases that mineralize P_o (Richardson et al., 2011). Under conditions of phosphate deficiency, bacteria can induce the phosphate (Pho) regulon to excrete phosphatases to obtain bioavailable orthophosphate (Santos-Beneit, 2015). Land use has been shown to influence specific functional genes (e.g., phytase and phosphatase genes), and the composition of microbial communities associated with P cycling in soils (Jangid et al., 2008; Neal et al., 2017). Few studies to date have generated a thorough insight into the response of soil microbial communities and their P cycling capacity, coupled with soil P chemistry (e.g., soil physico-chemical parameters and P speciation) to land use.

The general objective of this study was to investigate the effects of land use change on P cycling, using advanced chemical techniques and metagenomics sequencing. We chose four agricultural areas in southwestern Saskatchewan, with adjacent sites of four typical agricultural land uses in the region: annual cropland, native grassland, tame grassland and roadsides. The close proximity of these locations and their historical continuity of land use (each $>$ 50 years) kept all otherwise interrelated variables relatively constant (climate, topography, parent material, etc.) except land use. Samples from the four locations were patterned as replicated sites for each land use, providing a unique and valuable research platform to clarify soil P cycling induced by land use change. Combining state-of-the-art spectroscopic approaches (solution P-NMR and P K-edge XANES spectroscopy) with metagenomics, the specific objectives of this study were: (1) to characterize the composition of P_i and P_o in the soils under various land uses; (2) to investigate the abundance and composition of P functional genes and the microbial community within various ecosystems; and (3) to link these chemical and metagenomics results together for a better understanding of P cycling processes under different land uses.

MATERIALS AND METHODS

Field Sites and Sample Collection

The four experimental sites [Auvergne Wise Creek (AWC), Val Marie (VM), Masefield (MF1, MF2)], located in southwestern Saskatchewan, have the same soil type (well-drained Orthic Brown Chernozems; Saskatchewan Environment, and Resource Management [SERM], 1997) and a known history of more than 50 years in each studied land use type (Cade-Menun et al., 2017a). The native grasslands were a mixed grass prairie community, and tame grasslands were crested wheatgrass [*Agropyron cristatum* (L.) Gaetern.] stands that had been established for over 50 years.

The native and tame grasslands used for this study were in pastures grazed for beef production. Croplands were in dryland (unirrigated) annual wheat-based production. The fourth land use type in this study was roadside ditches, which serve as buffers between roads and fields. More details of the experimental sites and the broader land use study are available in Cade-Menun et al. (2017a). For the current study, soil samples were collected in July 2013 from the 0 to 30 cm depth from four land use types at four locations (n = 16). At each location, six soil cores (1.9 cm diameter) were collected inside four 1 m^2 quadrats that were situated along a 10 m transect for a total of 24 total soil cores per location. This differs from Cade-Menun et al. (2017a) with respect to date, sampling depth and number of study sites. Soil samples were stored in a cooler with ice packs while in the field. At the lab, field-moist soil cores from each location were pooled together and sieved (<2 mm) to form one composite sample per location and to remove rocks, larger roots, and coarse plant material. A portion of each composite soil sample was air-dried and stored at room temperature for chemical analysis, including XANES. An additional sub-sample was immediately stored at −20°C for molecular analysis, and the remainder was refrigerated (4°C) for enzyme assays and extraction for P-NMR.

Chemical Analysis

Soil pH was measured in $CaCl_2$ (1:2 w/v; Hendershot et al., 2008). Soils were analyzed for total C, total N, and organic C (after acidification) by dry combustion (Vario Micro Cube, Elementar). Total P was determined by digestion (Parkinson and Allen, 1975), total P_o was determined by the ignition method (Saunders and Williams, 1955), and Olsen-P was determined with sodium bicarbonate extraction (Sims, 2009), all followed by colorimetric analysis (Murphy and Riley, 1962). Mehlich-3 extraction (Sims, 2009) was used to determine P, Al, Ca, and Fe through analysis of extracts by inductively coupled plasma optical emission spectroscopy (ICP-OES; Thermo Scientific ICAP 6300 Duo). Exchangeable Ca was extracted in ammonium acetate and measured by ICP-OES (Hendershot et al., 2008). The activities of acid and alkaline phosphomonoesterase were assayed with *p*-nitrophenyl phosphate as substrates with the buffer pH-values adjusted to 6.5 and 11, respectively, phosphodiesterase activity was assayed with *bis-p*-nitrophenyl phosphate as substrate with the buffer pH 8.0 (Tabatabai, 1994).

Solution P-NMR Spectroscopy

Refrigerated soils were extracted with NaOH-EDTA in a 1:10 soil: extract ratio for P-NMR as previously described (Liu et al., 2015). Solution P-NMR spectra were collected as described in Cade-Menun et al. (2017b), using a Varian INOVA 600 MHz (202.5 MHz for P) spectrometer with a 10 mm broadband probe at the Stanford Magnetic Resonance Laboratory. The NMR parameters were: 90° pulse (30 μs), 0.675 s acquisition time, 4.32 s pulse delay, 20°C, 2,160–11,520 scans (3–16 h); no proton decoupling. The delay time used was based on the P:(Fe + Mn) concentrations in extracts (McDowell et al., 2006; Cade-Menun and Liu, 2014). To facilitate peak identification, spiking experiments with phytate, α- and β-glycerophosphate and adenosine monophosphate were conducted (Cade-Menun, 2015; Liu et al., 2015; Cade-Menun et al., 2017b). Compounds were identified by their chemical shifts after the orthophosphate peak in each spectrum was standardized to 6.0 ppm during processing. Peak areas were calculated by integration on spectra processed with 7 and 2 Hz line-broadening, using NUTS software (2000 edition; Acorn NMR, Livermore, CA, United States) and manual calculation. Percentages of orthophosphate monoesters and diesters were corrected for degradation of diesters to monoesters during NMR analysis (Liu et al., 2015; Cade-Menun et al., 2017b).

Phosphorus K-Edge XANES Spectroscopy

Phosphorus K-edge XANES spectra were collected at the Soft X-ray Micro-characterization Beamline (SXRMB) equipped with a InSb(111) double-crystal monochromator at the Canadian Light Source (CLS), Saskatoon, SK, Canada. Detailed information on instrument setting, sample preparation and data collection was described previously (Liu et al., 2014, 2015). In brief, soil samples were thinly spread over a P-free and double-sided carbon tape for the XANES measurements. The soil spectra were collected in partial fluorescence yield (PFY) mode using a four-element fluorescence detector. At least three XANES spectra were collected and averaged for each soil sample to obtain acceptable signal-to-noise level. Radiation damage during XANES experiment was excluded by a good reproducibility of the repeated measurements on the same spot and repeated scans over different spots for each sample. All XANES spectra were analyzed by Athena (Ravel and Newville, 2005). The absolute energy scale was calibrated to 2,149 eV (E_0) as the maximum energy of the first peak in the first derivative spectrum of $AlPO_4$ (Beauchemin et al., 2003). Spectra were background corrected by a linear regression fit through the pre-edge region and normalized total K-edge intensity to one unit edge jump by defining the continuum regions (>50 eV above absorption edge) as the post-edge region. Principal component analysis (PCA) was performed on the set of 16 soil XANES spectra using the program SixPack (Webb, 2005). According to PCA results (Supplementary Table S1), the minimum indicator (IND) suggested that four components were optimal for linear combination fitting (LCF) analysis of these soil samples. Consistently, the variations of the fifth component almost represented random variations due to noise rather than real spectral variations (Supplementary Figure S1). As there were up to four components contributing to 92.5% of spectra variations for all of the investigated samples (Supplementary Table S1 and Supplementary Figure S1), LCF of soil spectra were performed over the spectral energy region from 2,139 to 2,164 eV using all possible binary, ternary, and quaternary combinations of our reference spectra which were collected at the same beamline and reported in our previous studies (Liu et al., 2013, 2015). The E_0 was fixed during LCF analysis and weights of all P standards used were forced to sum 1. Phosphorus forms with proportions <10% were excluded from the fit set and replaced with other possible P species (Weyers et al., 2016). The goodness-of-fit was judged by the Chi-squared values and R values, and P standards yielding

the best fit were considered as the most possible P species in the investigated soil samples (Supplementary Figure S2 and Supplementary Table S2).

Metagenomic Analysis

Total nucleic acids were extracted from 1 g (2 × 0.5 g) frozen soil from each sample using the PowerSoil DNA Isolation Kit (Mo Bio Laboratories, Carlsbad, CA, United States) following the manufacturer's recommended protocol. The DNA samples were quantified using the Qubit dsDNA BR Assay Kit (ThermoFisher Scientific) and 2,100 Bioanalyzer instrument. Metagenomic libraries were prepared and sequenced on an Illumina HiSeq2500 system on a rapid mode 2 × 150 bp configuration. A total of 20 samples were submitted for metagenome sequencing of which the resulting data (273 Giga-bases) were processed through our metagenomics bioinformatics pipeline (Tremblay et al., 2017). Read count summaries and mapping statistics are provided (Supplementary Table S3). Sequencing adapters were removed from each read and bases at the end of reads having a quality score <30 were cut off (Trimmomatic v0.32; Bolger et al., 2014) and scanned for sequencing adapters contaminants reads using DUK[1] to generate quality controlled (QC) reads. The QC-passed reads from each sample were co-assembled using Megahit v1.1.2 (Li et al., 2015) on a 3 Tera-Bytes of RAM compute node with iterative kmer sizes of 31, 41, 51, 61, 71, 81, and 91 bases (see Supplementary Table S4 for assembly statistics). Gene prediction was performed by calling genes on each assembled contig using Prodigal v2.6.2 (Hyatt et al., 2010). Genes were annotated following the JGI's guidelines (Huntemann et al., 2015) including the assignment of KEGG orthologs (KO; Kanehisa and Goto, 2000). The QC-passed reads were mapped (BWA mem v0.7.15[2]) against contigs to assess quality of metagenome assembly and to obtain contig abundance profiles. Alignment files in bam format were sorted by read coordinates using samtools v1.2 (Li et al., 2009), and only properly aligned read pairs were kept for downstream steps. Each bam file (containing properly aligned paired-reads only) was analyzed for coverage of called genes and contigs using bedtools (v2.17.0; Quinlan and Hall, 2010) using a custom bed file representing gene coordinates on each contig. Only paired reads both overlapping their contig or gene were considered for gene counts. Coverage profiles of each sample were merged to generate an abundance matrix (rows = contig, columns = samples) for which a corresponding CPM (Counts Per Million–normalized using the TMM method; edgeR v3.10.2; Robinson et al., 2010). Taxonomic summaries were performed using a combination of in-house Perl and R scripts and Qiime v.1.9.1 (Caporaso et al., 2010).

Statistical Analyses

One-way ANOVAs were conducted for all the data of each land use (n = 4) separately, using SPSS 13.0 (SPSS, Inc), followed by a least significant difference (LSD) test with $\alpha = 0.05$. The P-NMR data were clr transformed prior to statistical analysis (Abdi et al., 2015; Liu et al., 2015); other data were transformed as needed for normality. Redundancy analysis (RDA) was used to identify the important P chemistry-related drivers of the P-cycling soil bacterial community and functional gene composition. A set of nonredundant predictors of the bacterial community and functional gene composition were selected using the *ordistep* and *envfit* functions (*vegan* package, R 3.4.3). Only the significant variables were included in the final models, excluding collinear variables with a variance inflation factor >10.

[1]http://duk.sourceforge.net/

[2]http://bio-bwa.sourceforge.net

RESULTS

Soil Properties

Among the investigated land uses, there were no significant differences in soil pH, total P, total C, organic C, total N, Mehlich-extractable P, Al, Fe, and Ca (**Table 1**). The percentage of P_o was significantly higher for both native and tame grasslands (both 75.4%) than for annual croplands (52.6%) and roadside soils (54.4%, **Table 1**). The highest Olsen-P concentration was observed in roadside soils (12.5 mg kg^{-1}), which was significantly higher than native grasslands (3.8 mg kg^{-1}) and annual croplands (5.6 mg kg^{-1}, **Table 1**). The highest exchangeable Ca occurred in roadside soils and the lowest in tame grasslands (**Table 1**).

Solution P-NMR Spectroscopy and Soil Phosphatase Activities

Examples of P-NMR spectra for these samples are shown in **Figure 1** and Supplementary Figure S3; chemical shifts of identified peaks are shown in Supplementary Table S5, and proportions of P forms and compound classes determined by P-NMR are shown in **Table 2** and Supplementary Table S6. Extraction with NaOH-EDTA recovered 34.9–50.5% of total P without significant differences among the land use types (**Table 2**). Inorganic P in the NaOH-EDTA extracts was significantly greater in roadside samples (46.3%) than native and tame grasslands (31.5 and 30.9%; **Table 2**), and was mainly orthophosphate (27.8–43.1%) with traces of polyphosphate (2.2–2.4%) and pyrophosphate (0.7–1.3%, Supplementary Table S6). The percentage of phosphonates was low (1.3–1.8%) with no differences among land use types. There were no significant differences among land use types for orthophosphate diesters with (CDiest, 19.5–24.0%) and without (Di, 2.5–4.1%) correction for degradation products (Deg, **Table 2**). In these samples, diester degradation was primarily from RNA to mononucleotides (Nucl, Supplementary Table S6), because the percentages of α- and β-glycerophosphates (degradation products of phospholipids) were low, and peaks were identified in the OthDi1 category where undegraded phospholipids would be observed (Supplementary Table S6). There were significant differences among the land use types for orthophosphate monoesters, with (Mono) and without (Cmono) correction for degradation (**Table 2**), with native and tame grasslands greater than roadside and annual cropland samples.

By NMR, P_o represented 53.7–69.2% of the NaOH-EDTA extracted P in the tested soils (**Table 2**). The greatest P_o proportions were in native and tame grasslands (**Table 2**) and the

TABLE 1 | Selected physiochemical properties of the soils under different land uses (means ± standard errors, $n = 4$)[a].

Land uses	pH	Total P	Organic P	Total C	Org C	Total N	Olsen-P	Mehlich P	Mehlich Al	Mehlich Fe	Mehlich Ca	NH_4OAc extracted Ca
		mg kg^{-1}	%	%	%	%	mg kg^{-1}					
Roadside soils	7.1 ± 0.1 a	479.3 ± 46.4 a	54.4 ± 2.6 b	2.2 ± 0.2 a	1.6 ± 0.2 a	0.15 ± 0.03 a	12.5 ± 3.9 a	22.8 ± 6.4 a	373.8 ± 106.5 a	140.6 ± 37.1 a	5223.3 ± 188.9 a	3698.4 ± 100.7 a
Native grasslands	6.6 ± 0.2 a	381.3 ± 24.3 a	75.4 ± 3.2 a	2.1 ± 0.3 a	1.7 ± 0.2 a	0.18 ± 0.03 a	3.8 ± 0.4 b	15.0 ± 2.9 a	532.0 ± 63.0 a	97.1 ± 7.0 a	3250.4 ± 1130.1 a	2446.1 ± 496.5 ab
Tame grasslands	6.3 ± 0.3 a	401.2 ± 42.7 a	75.4 ± 8.0 a	1.9 ± 0.2 a	1.7 ± 0.2 a	0.18 ± 0.03 a	6.9 ± 1.8 ab	19.0 ± 4.2 a	630.0 ± 138.5 a	127.6 ± 24.4 a	2662.5 ± 772.2 a	1759.4 ± 290.8 b
Annual croplands	7.1 ± 0.3 a	381.1 ± 32.9 a	52.6 ± 8.3 b	2.0 ± 0.3 a	1.2 ± 0.4 a	0.14 ± 0.07 a	5.6 ± 2.6 b	12.1 ± 5.3 a	372.2 ± 163.3 a	81.0 ± 18.8 a	6037.0 ± 2403.1 a	3006.9 ± 732.6 ab

[a]*Values in each column followed by the same lowercase letters are not significantly different according to LSD ($P < 0.05$).*

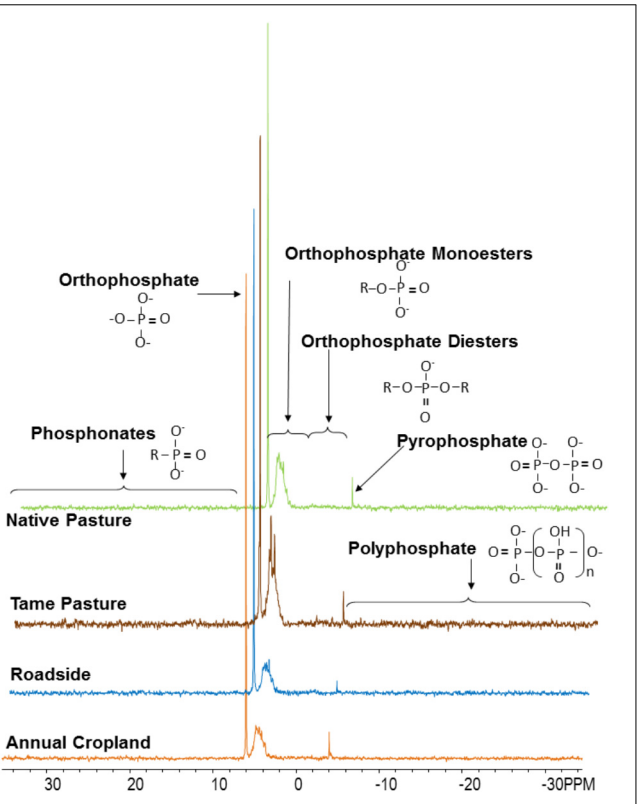

FIGURE 1 | Spectra (P-NMR) for each land use type from the Masefield 1 location. Spectra were processed with 7 Hz line-broadening, and are plotted to full height and scaled to the height of the orthophosphate peak.

least was in roadside soils, consistent with general soil chemical results (**Table 1**). The significant differences among the land use types for P_o predominantly occurred through differences in inositol hexakisphosphates (IHP, **Table 2**) and an unidentified P compound resolved at 4.9 ppm (Supplementary Tables S5, S6). Among the four stereoisomers of IHP, the 4 equatorial/2 axial configuration of *neo*-IHP in native grasslands (1.1%) was significantly higher than that in annual croplands (0.6%). The unidentified peak at 4.9 ppm, which was significantly higher for tame and native grasslands, may be the 4 axial/2 equatorial configuration of *neo*-IHP (Turner et al., 2012), but this could not be confirmed with spiking. There were no significant differences among other land use types for the other IHP stereoisomers (Supplementary Table S6), or for the other P_o compound classes and identified species, although some of them showed higher proportions in grasslands than other land uses (**Table 2** and Supplementary Table S6).

Phosphatases play a key role in catalyzing the hydrolysis of P_o to release orthophosphate for plant uptake. The activity of acid phosphomonoesterase, produced by plants and microbes (Tabatabai, 1994), was significantly lower in soils from annual cropland than other land use types (Supplementary Figure S4). There were no significant differences among land use types for alkaline phosphatase, which is produced by microbes only, and the activity of this enzyme was lower

TABLE 2 | Phosphorus form classes or ratios of form classes[a] determined by ^{31}P nuclear magnetic resonance spectroscopy for the studied soil samples under different land uses (means ± standard errors, $n = 4$)[b].

Land uses	Recovery	P_i	P_o	TotPoly	IHP	Myo:other	Mono	Di	M:D	Cmono	CDiest	Deg	CM:D
Roadside	34.9 ± 3.6 a	46.3 ± 5.7 a	53.7 ± 5.7 b	3.2 ± 0.7 a	13.8 ± 1.0 b	0.4 ± 0 ab	48.6 ± 4.5 b	3.7 ± 1.8 a	20.9 ± 6.5 a	32.8 ± 3.3 c	19.5 ± 2.5 a	15.8 ± 1.7 a	1.7 ± 0.1 a
Native grasslands	43.1 ± 2.4 a	31.5 ± 2.6 b	68.5 ± 2.6 a	3.7 ± 0.4 a	18.4 ± 1.2 ab	0.3 ± 0.1 ab	63.1 ± 2.4 a	3.9 ± 0.9 a	19.3 ± 4.9 a	43.0 ± 1.2 ab	24.0 ± 1.8 a	20.1 ± 1.4 a	1.8 ± 0.1 a
Tame grasslands	50.5 ± 6.6 a	30.9 ± 2.7 b	69.2 ± 2.7 a	3.1 ± 0.2 a	24.9 ± 3.8 a	0.2 ± 0 b	64.9 ± 2.8 a	2.5 ± 0.6 a	31.6 ± 7.8 a	46.7 ± 3.8 a	20.7 ± 1.9 a	18.2 ± 2.4 a	2.4 ± 0.4 a
Annual crop	47.6 ± 6.7 a	41.4 ± 2.3 ab	58.6 ± 2.3 ab	3.0 ± 0.6 a	16.8 ± 2.3 b	0.4 ± 0.1 a	53.2 ± 1.7 b	4.1 ± 0.7 a	13.7 ± 1.6 a	35.9 ± 1.9 bc	21.4 ± 0.8 a	17.3 ± 0.7 a	1.7 ± 0.1 a

[a,b]Values in each column followed by the same lowercase letters are not significantly different according to LSD ($P < 0.05$). P_i, inorganic P; P_o, organic P; TotPoly, total polyphosphate, IHP, inositol hexakisphosphate; Myo:other, the ratio of myo-IHP to other IHP species; Mono, orthophosphate monoester; Di, orthophosphate diesters; M:D, the ratio of orthophosphate monoester to orthophosphate diesters; Deg, degradation; C denotes a correction for degradation products.

than that of acid phosphatase for all but annual cropland soils. Phosphodiesterase activities were lowest for land use types compared to phosphomonoesterase activities, and were significantly lower in annual cropland soils than roadside soils.

Phosphorus K-Edge XANES Spectroscopy

Supplementary Figure S5 shows the K-edge XANES spectra of P standards in this study, where similar shapes with both the white line peak (ii) and oxygen oscillation peak (v) are observed. In addition, these P standards exhibited fingerprinting features that allow for identification and quantification of different P species in soil samples. For example, all Ca-associated P (Ca-P) standards exhibit a post-edge shoulder (iii) that is sharper for compounds containing many Ca atoms [HAP and $Ca_3(PO_4)_2$] than for monocalcium phosphates [$Ca(H_2PO_4)_2$ and $CaHPO_4$], and another signal (iv). Iron phosphate ($FePO_4$) displayed a pre-edge feature (i). Aluminum phosphate ($AlPO_4$), without the pre-edge feature (i) seen for $FePO_4$, shows a post-edge feature (iv) similar to Ca-P. These features agree well with previous reports (Beauchemin et al., 2003; Lombi et al., 2006; Prietzel et al., 2013). Spectra of native and grassland soils (**Figures 2C,B**), rather similar across locations, resembled the spectra of IHP (Supplementary Figure S5). As the K-edge XANES spectra of P_o compounds are mostly featureless and hard to differentiate, the contribution of IHP is interpreted as the presence of all possible organically bound P rather than specifically to IHP in the samples. Roadside soils showed spectra with a broad post-edge feature and slight shoulders (iii and iv, **Figure 2D**), demonstrating the presence of Ca-P in these soils. In contrast, spectra of cropland soils showed more variation than those of other land uses (**Figure 2A**).

The LCF for each soil sample, shown in Supplementary Figure S2 and Supplementary Table S2, indicated that IHP was present in all soil samples, in greater proportions for the native (92%) and tame (82%) grasslands than that for the roadside soils (50%, **Table 3**). The roadside soils from all four locations also contained some Ca-P in the form of tricalcium phosphate (TCP, 42–54%), which was absent from the native grassland samples, the tame grassland samples, and two cropland samples (Supplementary Table S2). Additionally, small amounts of P (<17%, Supplementary Table S2) in the forms of dibasic calcium phosphate (DCP), monobasic calcium phosphate (MCP), hydroxyapatite (HAP), or $FePO_4$ were also fitted in some samples. This indicated that these P species may be present in the soils, but there were no significant differences of these P species among land uses types (**Table 3**).

Metagenomic Analysis

Land use had a strong effect on the taxonomic composition of the soil microbial community. Although the archaeal community did not differ, the bacterial and fungal communities significantly differed among the land use types (Supplementary Table S7). Tame and native grassland soils harbored similar bacterial and fungal communities, whereas annual cropland and roadsides clustered separately in the principle coordinate analysis

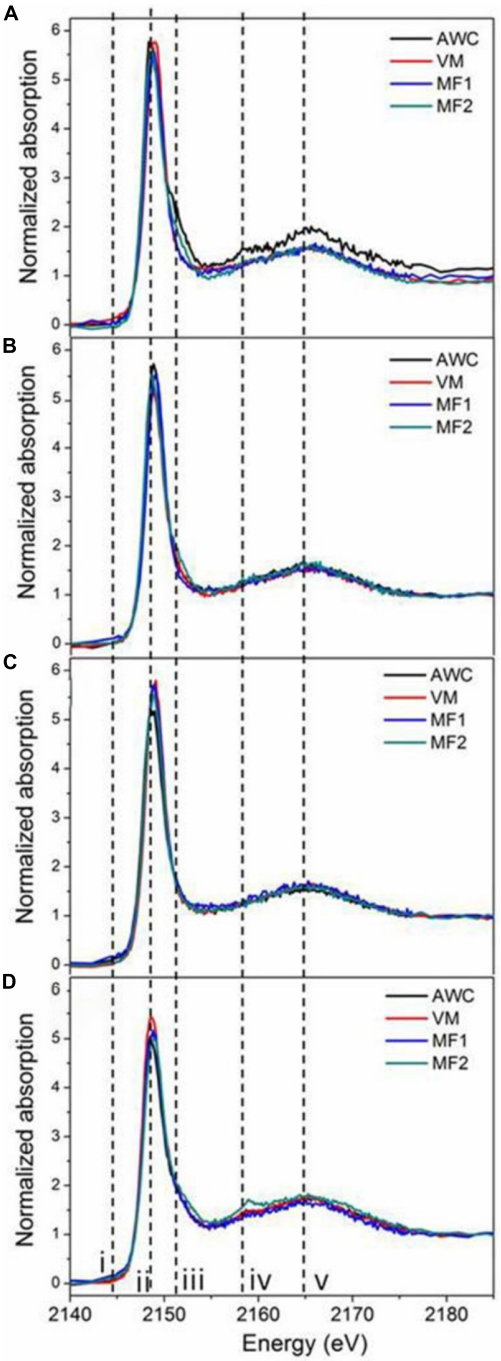

FIGURE 2 | P K-edge XANES spectra of soils under different land uses. Figure panels are for soils from annual croplands **(A)**, tame grasslands **(B)**, native grasslands **(C)**, roadsides **(D)**. Samples from each land use type were collected at four locations: Val Marie (VM), Auvergne Wise Creek (AWC), Masefield1 (MF1), and Masefield2 (MF2).

(PCoA, Supplementary Figure S6), indicating they had distinct communities.

The microbial genes coding for various P cycling processes were broadly grouped into six functional categories based on Bergkemper et al. (2016), and these included phosphoesterase, phytase, phosphonate degradation, inorganic phosphate solubilizing, P transporter, and regulation of phosphate starvation genes (**Table 4**). Taxonomic classification of the P cycling genes revealed that the majority of the reads (76.1%) were assigned or classified as bacteria, 0.9% archaea, 0.8% eukaryota, and the remaining 22.1% of the reads were unclassified (**Figure 3**). Actinobacteria and Alphaproteobacteria were the most abundant bacterial classes but did not significantly differ among the land use types. Significant differences were observed for the Betaproteobacteria, Deinococci, Deltaproteobacteria, Gammaproteobacteria, Gemmatimonadetes, and Eukaryota, all of which were the most abundant in annual cropland soils and least abundant in native grassland soils (**Figure 3**). Overall, annual cropland soils had the highest number of reads assigned to P cycling coding genes; native grassland soils had the lowest.

The permanova results showed a significant difference in the composition of the P cycling bacterial communities and composition of the P cycling functional genes among the four land use types (Supplementary Table S7). The PCoA (Supplementary Figure S7A) revealed a similar clustering of the P cycling bacterial communities compared to the total bacterial community (which included taxa that were not linked to P cycling functional genes) among the land use types, with roadside communities being the most distinct and dissimilar to native and tame grassland communities. However, PCoA of the P cycling gene composition revealed that native grassland and annual cropland soils had the most dissimilar P cycling gene compositions, with roadside and tame grassland soils being intermediary (Supplementary Figure S7B).

The abundance of most P cycling genes significantly differed among the land use types (**Table 4**). Genes coding for phosphoesterase enzymes were the most abundant in annual cropland and roadside soils, and least abundant in native grassland soils. Alkaline phosphatase (*phoD*, *phoA*, *phoX*) and glycerophosphoryl diester phosphodiesterase (*upgQ*) were the most abundant phosphoesterase enzyme coding genes for all land use types, possibly indicating that these enzymes have a higher capacity for P mineralization in the soils from this region compared to acid phosphatase and phytase enzymes. Roadside soils had the highest abundance of genes coding for phosphonate degradation enzymes, and this was particularly evident of genes coding for enzymes involved in the carbon-phosphorus (C-P) lyase core complex (*phnG*, *phnH*, *phnI*, *phnJ*, *phnM*). Genes coding for inorganic phosphate solubilizing enzymes (*ppa*, *ppx*, *ppk*, *gcd*) were the most abundant group of P cycling genes for all land use types. Annual cropland and roadside soils appeared to have the highest inorganic phosphate solubilizing capacity based on the abundance of these genes, and native grassland soils the lowest capacity. Annual cropland soils also had the highest abundance of genes coding for P transporter subunits (phosphate-specific transporter, phosphonate transporter, and glycerol-3-phosphate transporter) and genes regulating phosphate starvation (*phoB*, *phoR*, *phoU*). Native grassland and tame grassland soils exhibited a lower phosphate uptake and regulation capacity based on the lower abundance of these genes.

TABLE 3 | Phosphorus K-edge XANES fitting results showing the relative percent of each phosphate species[a] in the studied soils under different land uses (means ± standard errors, $n = 4$)[b].

Land uses	IHP	TCP	DCP	MCP	HAP	$FePO_4$
				%		
Roadside	50 ± 3 b	47 ± 3 a	0 a	0 a	3 ± 3 a	0 a
Native grasslands	92 ± 5 a	0 b	6 ± 3 a	0 a	0 a	2 ± 2 a
Tame grasslands	82 ± 4 a	3 ± 3 b	2 ± 2 a	2 ± 2 a	7 ± 4 a	3 ± 3 a
Annual Crop	67 ± 17 ab	24 ± 19 ab	2 ± 2 a	0 a	4 ± 4 a	3 ± 3 a

[a]*IHP, inositol hexakisphosphate; TCP, tricalcium phosphate; DCP, dibasic calcium phosphate; MCP, monobasic calcium phosphate; HAP, hydroxyapatite.* [b]*Values in each column followed by the same lowercase letters are not significantly different according to LSD ($P < 0.05$).*

Supplementary Figure S8 shows the taxonomic composition (at the class level) of each P cycling gene. There are similarities in the taxonomic composition of genes that are functionally related. For example, most genes coding for the C-P lyase multienzyme complex are primarily from Alphaproteobacteria and from Actinobacteria and Betaproteobacteria to a lesser extent. The genes coding for the phosphate-specific transport subunit (*pstA*, *pstB*, *pstC*, *pstS*), phosphonate transporter subunit (*phnC*, *phnD*, *phnE*), and glycerol-3-phosphate transporter subunit (*ugpA*, *ugpB*, *ugpC*, *ugpE*) each had similar taxonomic compositions among the genes that make up their respective subunits. In contrast, other genes coding for similar functions such as alkaline phosphatase (*phoA*, *phoX*, *phoD*) and acid phosphatase (*phoN*, *aphA*, K01078) had higher variability in their respective taxonomic compositions.

Redundancy Analysis

Redundancy analysis (RDA) was used to identify the most important P chemistry predictors of the P cycling bacterial community composition (**Figure 4A**) and P cycling gene composition (**Figure 4B**). Similar P chemistry predictors were identified for both the bacterial community and gene compositions with a few exceptions. Overall, NMR (*myo*-IHP and IHP), enzyme activity (acid and alkaline phosphatase), Olsen P, and pH were significantly correlated with the composition of both the bacterial and functional gene compositions. In contrast, P-XANES species exhibited a limited relationship as only TCP was identified as a significant predictor of the P cycling bacterial community composition. The P chemistry predictors were able to explain a high proportion of the P cycling bacterial community and functional gene composition as the adjusted r^2-values for each RDA was 0.34 and 0.75, respectively.

DISCUSSION

The results by the ignition method, NMR, and XANES consistently indicated that native and tame grasslands had higher total P_o proportions among the investigated land use types. In grazed grasslands, the majority of the P (∼85%) taken up in the form of orthophosphate by plants is returned to the soil in the form of P_o through dung, providing a significant P_o stock (Nash et al., 2014). Specifically, differences among land use types were significant for monoesters, principally total IHP and the *neo*-IHP stereoisomer. Higher proportions of monoester P in grasslands than cultivated soils have been reported previously (Condron et al., 1990; Stutter et al., 2015), although these studies did not correct for diester degradation or identify specific P forms. Using an improved method of P-NMR spectra interpretation to identify specific P forms, we found a significantly higher abundance of *neo*-IHP in native grasslands and an unidentified monoester species resolved at 4.9 ppm, which might also be *neo*-IHP (Turner et al., 2012), in tame grasslands compared to croplands. The abundance of *chiro*-IHP was extremely high in the tame pasture soil from one location, but the overall abundance of either of the two configurations of *chiro*-IHP was not significantly different among land use types. The specific origins and function of *chiro*-IHP and *neo*-IHP in soils are unknown, but they are thought to be synthesized by soil microbes (Turner et al., 2002, 2014; Giles et al., 2011). The higher abundance of these stereoisomers and lower ratio of *myo*-IHP:other IHP forms (**Table 2**) in grassland soils indicates that microbes are likely responsible for the higher accumulation of IHP compared to annual cropland and roadside soils.

The higher abundance of *neo*-IHP in grassland soils may be linked to reduced P turnover or cycling in these land use types. For example, Young et al. (2013) reported significantly higher *neo*-IHP concentrations under conditions (i.e., poor drainage) that constrain microbial P cycling. In the present study, native and tame grassland soils had the lowest abundance of genes coding for most P cycling processes (except phosphonate degradation) compared to other land use types, which may be an indicator of reduced P cycling capacity. The accumulation of *neo*-IHP in the grassland soils of this study is consistent with the results of Young et al. (2013), supporting their speculation that this IHP stereoisomer accumulates when microbial P cycling is reduced.

The native grassland soils of this study had a greater abundance of the 4-phytase gene (*appA*) than cropland soils, although there were no significant differences among land use types for the more abundant 3-phytase genes (K01083). Differing from other P_o mineralization processes, phytases may not be controlled by the PhoBR two component regulatory system, but likely respond to the presence or absence of phytate in the soil (Lidbury et al., 2016). However, the ability of these genes to degrade other stereoisomers besides phytate (*myo*-IHP) is unknown, and previous research suggests *neo*-, *chiro*-, and

TABLE 4 | Abundance of microbial genes associated with phosphorus cycling in soil.

Functional group		Gene	KEGG orthology	Native	Tame	Roadside	Annual
Phosphoesterase genes	Acid phosphatase		K01078	161.39	190.80	155.67	178.88
	Acid phosphatase	phoN	K09474***	32.51 b	35.70 b	48.10 a	52.06 a
	Acid phosphatase	aphaA	K03788	0.32	0.44	0.35	0.27
	Alkaline phosphatase	phoA	K01077*	36.35 b	41.98 ab	48.40 a	40.33 b
	Alkaline phosphatase	phoX	K01077	0.05	0.00	0.12	0.08
	Alkaline phosphatase	phoD	K01113	411.74	430.55	467.28	505.17
	GP phosphodiesterase	ugpQ	K01126*	323.30 b	354.98 ab	360.65 ab	401.54 a
	Phosphotriesterase		K07048	100.08	105.33	99.03	119.70
Phytase genes	3-Phytase		K01083	77.96	78.82	97.27	116.39
	4-Phytase	appA	K01093*	1.94 a	1.54 ab	2.13 a	1.09 b
Phosphonate degradation genes	C-P lyase multienzyme complex	phnF	K02043**	6.30b	6.25b	7.81a	4.89c
	C-P lyase multienzyme complex	phnG	K06166	4.18	4.19	4.77	3.07
	C-P lyase multienzyme complex	phnH	K06165*	5.14 a	5.39 a	5.62 a	4.03 b
	C-P lyase multienzyme complex	phnI	K06164*	9.61 b	9.03 b	13.18 a	9.49 b
	C-P lyase multienzyme complex	phnJ	K06163*	8.14 b	7.86 b	11.38 a	7.89 b
	C-P lyase multienzyme complex	phnK	K05781*	7.02 ab	6.43 b	8.82 a	6.32 b
	C-P lyase multienzyme complex	phnL	K05780**	7.17 b	6.39 b	9.08 a	6.16 b
	C-P lyase multienzyme complex	phnM	K06162*	18.77 b	19.94 ab	23.27 a	15.82 b
	C-P lyase multienzyme complex	phnN	K05774**	6.89 b	7.46 ab	8.95 a	4.92 c
	C-P lyase multienzyme complex	phnO	K09994*	26.77 ab	29.78 a	22.06 b	30.37 a
	C-P lyase multienzyme complex	phnP	K06167	60.08	63.01	67.10	73.69
	AEP-Pyruvate transaminase	phnW	K03430***	22.15 b	22.73 b	31.96 a	32.54 a
	Phosphonatase	phnX	K05306	3.76	4.18	4.31	4.75
	Phosphonoacetate hydrolase	phnA	K06193**	2.09 b	2.11 b	3.83 a	1.49 b
Inorganic phosphate solubilizing genes	Inorganic pyrophosphatase	ppa	K01507**	127.67 c	142.46 bc	144.40 ab	159.73 a
	Exopolyphosphatase	ppx	K01524*	377.44 b	399.73 ab	395.58 b	443.40 a
	Polyphosphate kinase	ppk	K00937*	733.09 b	814.99 ab	809.87 ab	856.84 a
	PQQGDH	gcd	K00117**	762.19 b	811.18 b	1206.06 a	1142.91 a
Phosphorus transporter genes	Phosphate inorganic transporter	pit	K03306	266.88	303.67	268.24	280.36
	Low-affinity inorganic phosphate transporter	pitA	K16322*	0.28 ab	0.12 b	0.48 a	0.14 b
	Phosphate-specific transport system subunit	pstA	K02038*	211.81 b	224.38 b	232.04 ab	257.92 a
	Phosphate-specific transport system subunit	pstB	K02036*	199.29 b	218.36 b	221.83 b	252.92 a
	Phosphate-specific transport system subunit	pstC	K02037*	236.61 b	255.90 ab	254.61 ab	286.45 a
	Phosphate-specific transport system subunit	pstS	K02040**	298.59 b	325.53 b	332.87 b	375.87 a
	Phosphonate transporter subunit	phnC	K02041*	46.32 b	48.50 b	54.06 ab	62.21 a
	Phosphonate transporter subunit	phnD	K02044*	87.21 b	93.51 b	105.91 ab	128.44 a
	Phosphonate transporter subunit	phnE	K02042*	46.41 b	46.12 b	63.65 a	64.02 a
	Glycerol-3-phosphate transporter subunit	ugpA	K05814*	38.74 c	42.49 bc	51.72 a	49.14 ab
	Glycerol-3-phosphate transporter subunit	ugpB	K05813**	74.76 b	78.02 b	93.49 a	95.93 a
	Glycerol-3-phosphate transporter subunit	ugpC	K05816***	36.76 b	37.08 b	44.76 a	42.56 a
	Glycerol-3-phosphate transporter subunit	ugpE	K05815**	38.10 b	40.95 b	48.95 a	49.53 a
Regulation of phosphate starvation inducible genes	Phosphate regulon response regulator	phoB	K07657**	215.10 b	229.43 b	237.40 b	278.42 a
	Phosphate regulon sensor histidine kinase	phoR	K07636**	718.51 b	799.38 b	768.48 b	943.60 a
	PhoR/PhoB inhibitor protein	phoU	K02039*	188.29 b	204.46 b	208.66 ab	237.55 a

*Mean values (n = 4) represent counts per million of mapped reads for each land use type. Values within a row that have different letters indicate a significant difference between land use types (P < 0.05).*P < 0.05, **P < 0.01, ***P < 0.001.*

scyllo-IHP are more resistant to phytase hydrolysis than the *myo*-IHP stereoisomer (Turner et al., 2012). It has been suggested that microbes synthesize these stereoisomers as a potential strategy to preserve phosphorus from competing organisms under limiting P conditions (Turner, 2007). Contrary to the anecdotal evidence that P_o mineralization in pastures might be high (Nash et al., 2014), our results demonstrated that the abundance of most P cycling genes was lowest in native

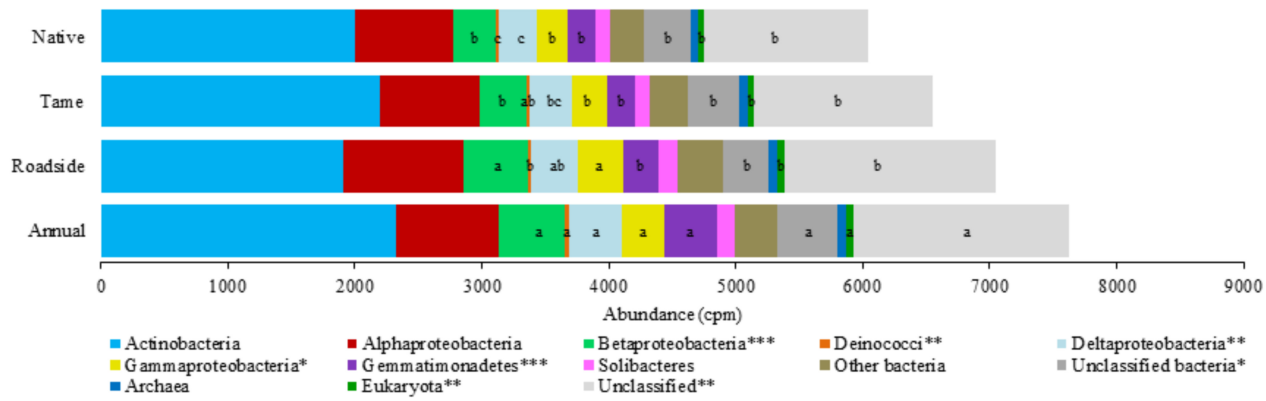

FIGURE 3 | Taxonomic classification and relative abundance (copies per million reads) of the phosphorus cycling genes among the four land use types. Mean values (copies per million reads) within a taxonomic classification that have a different letter indicate a significant difference between land use types ($P < 0.05$). An asterisk (*) indicates a significant land use type effect at $P < 0.05$ (**$P < 0.01$ and ***$P < 0.001$).

grasslands, except for the 4-phytase gene. This suggests that P_o turnover in grasslands from this region may not be as active as other more intensive land use types, allowing P_o to accumulate or become immobilized in soils via microbial processes. This is particularly relevant in grassland soils with low P_i availability (Bünemann et al., 2012). Given the lower degree of disturbance in grasslands as a long-term stable ecosystem (Cade-Menun et al., 2017a), the transformation of P_o in grasslands is likely more tightly regulated than arable systems and driven by intrinsic soil-plant-microbial cycling demands for P. It is clear that P_o serves as a substantial reserve of P for plant nutrition in grasslands. As such, further investigations linking the supply of orthophosphate from these P_o species with plant needs warrants further studies (Nash et al., 2014).

In annual croplands, P_o returns to soils are interrupted at crop harvest, which may account for the limited P_o accumulation in this study. However, enhanced mineralization of P_o by microbe-mediated activities due to low soil Olsen-P cannot be excluded, since annual croplands had the highest total abundance of genes coding for phosphoesterase and phytase enzymes. This contradicts the lower acid phosphatase and phosphodiesterase activity we observed in annual cropland soil despite the higher abundance of genes coding for these enzymes (*phoN*, *ugpQ*) compared to the other land use types. One explanation for this observation may be linked to the pH conditions of the enzyme assays as this can affect the relationships between gene abundance and enzyme activity (Fraser et al., 2017).

The high abundance of P cycling genes suggests a greater capacity for P transformation in cropland soils of this study. This may be a strategy utilized by the soil microbial community to adapt to the high temporal variability in P forms and availability (Hedley et al., 1982; Bainard et al., 2016) associated with the intensive practices of annual crop production (e.g., fertilization, tillage, harvest, weed management and fallow). There was considerable variability in crop management practices among the annual cropland sampling sites, including fertilizer and P-containing herbicide inputs (Cade-Menun et al., 2017a), which may have contributed to the high site variance in P_i species and the insignificant differences among the four land use types. Additionally, the relatively higher TCP in the annual croplands than grasslands may arise from tillage, because the surface of annual croplands could be replenished by the deeper soil containing high levels of carbonates after repeated tillage. The higher abundance of P_i solubilizing genes in annual cropland soils could indicate a higher capacity for the microbial community to access these P_i forms compared to the grasslands. Interestingly, glyphosate was commonly used in three of the four annual cropping sites, but these soils had the lowest abundance of genes coding for the polypeptides that make up the core complex or reaction of the C-P lyase pathway, which is one of the primary pathways for the catabolism of phosphonates (Hove-Jensen et al., 2014). However, all polypeptides involved in the C-P lyase pathway (*phnCDEFGHIJKLMNOP*) are required for the utilization of glyphosate as a phosphate source (Chen et al., 1990; Hove-Jensen et al., 2014), including those that are more abundant in annual cropland soil (phosphonate transporters *phnCDE*, aminoalkylphosphonate N-acetyltransferase *phnO*, and phosphoribosyl cyclic phosphodiesterase *phnP*). Glyphosate has a distinctive peak in P-NMR spectra (Cade-Menun, 2015), which was not detected in the cropland soils, and the concentrations of phosphonates in general were not significantly greater in cropland soils than other land use types in this study. Further investigation is warranted to understand the factors controlling the degradation of agricultural compounds such as glyphosate in the soils of this region.

Annual crop production practices appear to have an impact on the PhoBR two component regulatory system based on the higher abundance of P-starvation-inducible genes compared to the other land use types. This is consistent with the low Olsen *P*-values for the cropland soils. This system regulates several important P cycling processes controlled by genes coding for phosphoesterase, phosphonate degradation, inorganic phosphate solubilizing, and P transporter enzymes (Furtwängler et al., 2010; Lidbury et al., 2016). Bergkemper et al. (2016) suggested that a high abundance of P-starvation-inducible genes can enable microbial communities to utilize alternative P forms

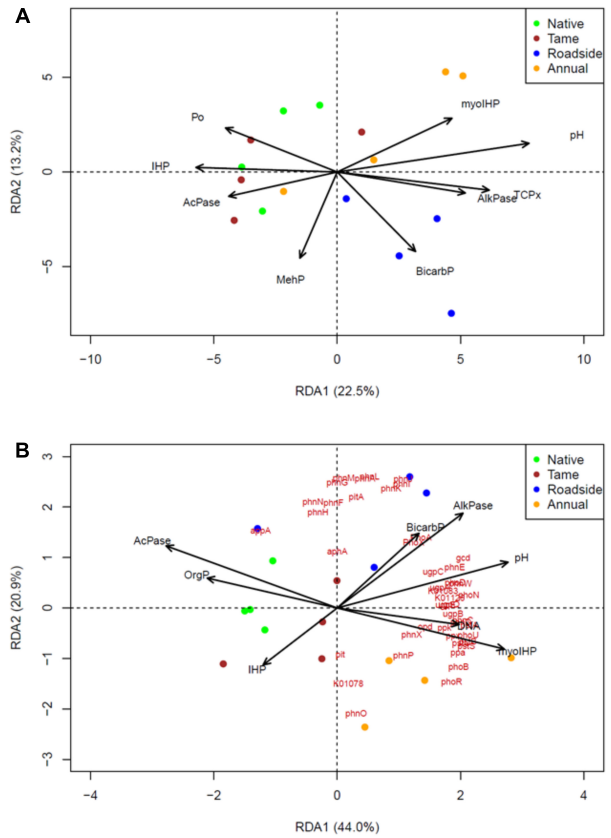

FIGURE 4 | Identification of the P chemistry related drivers of **(A)** the P-cycling soil bacterial community, and **(B)** soil P-cycling functional gene composition among the four land use types based on the metagenomic data sets and redundancy analysis (RDA). A step-wise selection of important predictors of gene and community composition was used in conjunction with the RDA. The biplot arrows represent the P-chemistry related variables and red text in **(B)** represent the P-cycling functional genes or KEGG orthology numbers. Green, brown, blue and yellow colors, respectively, represent native grasslands, tame grasslands, roadsides, and annual croplands.

under P limiting conditions. This may be more important in annual cropland soils compared to perennial grasslands, because grassland ecosystems likely experience fewer disturbances and fluxes in P availability.

Roadside soils differ from the other land use types because they are disturbed environments that have high variability in terms of soil chemical and physical properties and soil moisture gradients due to runoff from adjacent roads and croplands and nutrient removal via haying and mowing (Dai et al., 2013; Cade-Menun et al., 2017a). Roadside soils distinguished from other land use types in this study based on having the highest Olsen P and TCP concentrations and low P_o. In a separate study, Cade-Menun et al. (2017a) showed that roadside soils collected from the same sampling locations as the current study at the 0–7.5 cm depth had the greatest percentage of clay, the highest soil pH and higher total C relative to the other land use types. There were generally no differences among land use types at lower depths; thus, sampling at 0–30 cm may have obscured some differences for the current study. Roadsides in Saskatchewan are subjected to snowmelt runoff, in which dissolved reactive P accounted for 97–100% of the dissolved total P loss from croplands and pastures (Cade-Menun et al., 2013), which would account for the high Olsen P concentrations in these roadside soils. These roadside soils would also experience deposition of clays during wind erosion (Cade-Menun et al., 2017a). This, with the neutral pH (7.1) and high NH_4OAC-extracted Ca are expected to facilitate the formation of TCP in these roadside soils (Sato et al., 2005). From the microbial perspective, the relatively high abundance of P cycling functional genes along with high phosphatase activity and low abundance of P_o indicate that microbe-mediated P dynamics in roadsides are active but highly variable.

To the best of our knowledge, this is the first study to combine state-of-the art spectroscopic methods for P chemistry with shotgun metagenomics to provide an in depth evaluation of the dominant mechanisms involved in P cycling in soils with different land uses. Grasslands had high abundances of monoesters, principally IHP stereoisomers, and high acid phosphomonoesterase activities but lower abundance of genes coding for P cycling processes. In particular, the significantly higher proportion of *neo*-IHP in the native grasslands than in croplands confirms the important role of microbes in P_o transformation in grassland soils. In contrast, croplands showed the largest variance of P speciation among the land use types, illustrating the crucial role of specific field management practices within croplands. Furthermore, the conversion of native grassland to annual crop production appears to increase the abundance of P-cycling genes, which may be required in soils that are under intensive management practices. Future studies are warranted to design tailored agronomic practices that directly facilitate functional genes and microbial communities for certain P cycling processes (e.g., P_o mineralization) to optimize P-use efficiency. Roadside soils had the highest Olsen-P due to inputs from erosion and runoff, and had high proportions of TCP, reflecting clay inputs, neutral pH and high exchangeable Ca concentrations. The RDA results demonstrated that IHP by NMR, enzyme activity, Olsen-P, and pH were important P chemistry predictors of the P cycling bacterial community composition and functional gene composition.

AUTHOR CONTRIBUTIONS

LB, BC-M, MS, KL, and CH designed and conducted the study. The NMR analysis was performed by CL and interpreted by BC-M. JL and JY conducted the synchrotron experiments. JL, JY, and YH analyzed the data. LB and JT performed the soil microbial and bioinformatic analyses. JL, LB, and BC-M wrote the manuscript with inputs from all authors. All authors read and approved the manuscript.

ACKNOWLEDGMENTS

This project was funded by the Agriculture & Agri-Food Canada A-Base project 1154 (Impact of Land Use on Soil Functional

Diversity and Nutrient Cycling in Prairie Ecosystems). We gratefully thank staff and students at the SCRDC for assistance with sample collection and analysis. The NMR analysis was conducted at the Stanford Magnetic Resonance Laboratory at Stanford University, and the metagenomic analysis was done at the Biotechnology Research Institute of the National Research Council of Canada. Synchrotron measurement was carried out at the SXRMB beamline of the Canadian Light Source, which is financially supported by the Natural Sciences and Engineering Research Council of Canada, the National Research Council of Canada, the Canadian Institutes of Health Research, the Province of Saskatchewan, Western Economic Diversification Canada, and the University of Saskatchewan. We also wish to acknowledge Compute Canada for access to the University of Waterloo High Performance Computing (HPC) infrastructure (Graham system).

SUPPLEMENTARY MATERIAL

The Supplementary Material for this article can be found online at: https://www.frontiersin.org/articles/10.3389/fmicb.2018.01643/full#supplementary-material

REFERENCES

Abdi, D., Cade-Menun, B. J., Ziadi, N., and Parent, L.-É. (2015). Compositional statistical analysis of soil ^{31}P-NMR forms. *Geoderma* 257–258, 40–47. doi: 10.1016/j.geoderma.2015.03.019

Bainard, L. D., Chagnon, P. L., Cade-Menun, B. J., Lamb, E. G., LaForge, K., Schellenberg, M., et al. (2017). Plant communities and soil properties mediate agricultural land use impacts on arbuscular mycorrhizal fungi in the mixed prairie ecoregion of the North American great plains. *Agric. Ecosyst. Environ.* 249, 187–195. doi: 10.1016/j.agee.2017.08.010

Bainard, L. D., Hamel, C., and Gan, Y. (2016). Edaphic properties override the influence of crops on the composition of the soil bacterial community in a semiarid agroecosystem. *Appl. Soil Ecol.* 105, 160–168. doi: 10.1016/j.apsoil.2016.03.013

Beauchemin, S., Hesterberg, D., Chou, J., Beauchemin, M., Simard, R. R., and Sayers, D. E. (2003). Speciation of phosphorus in phosphorus-enriched agricultural soils using X-ray absorption near-edge structure spectroscopy and chemical fractionation. *J. Environ. Qual.* 32, 1809–1819. doi: 10.2134/jeq2003.1809

Bergkemper, F., Schöler, A., Engel, M., Lang, F., Krüger, J., Schloter, M., et al. (2016). Phosphorus depletion in forest soils shapes bacterial communities towards phosphorus recycling systems. *Environ. Microbiol.* 18, 1988–2000. doi: 10.1111/1462-2920.13188

Bolger, A. M., Lohse, M., and Usadel, B. (2014). Trimmomatic: a flexible trimmer for Illumina sequence data. *Bioinformatics* 30, 2114–2120. doi: 10.1093/bioinformatics/btu170

Bünemann, E. K., Oberson, A., Liebisch, F., Keller, F., Annaheim, K. E., Huguenin-Elie, O., et al. (2012). Rapid microbial phosphorus immobilization dominates gross phosphorus fluxes in a grassland soil with low inorganic phosphorus availability. *Soil Biol. Biochem.* 51, 84–95. doi: 10.1016/j.soilbio.2012.04.012

Cade-Menun, B., Bainard, L., LaForge, K., Schellenberg, M., Houston, B., and Hamel, C. (2017a). Long-term agricultural land use affects chemical and physical properties of soils from Southwest Saskatchewan. *Can. J. Soil Sci.* 97, 650–666. doi: 10.1139/CJSS-2016-0153

Cade-Menun, B. J., Doody, D. G., Liu, C. W., and Watson, C. J. (2017b). Long-term changes in grassland soil phosphorus with fertilizer application and withdrawal. *J. Environ. Qual.* 46, 537–545. doi: 10.2134/jeq2016.09.0373

Cade-Menun, B. J. (2015). Improved peak identification in P-31-NMR spectra of environmental samples with a standardized method and peak library. *Geoderma* 257, 102–114. doi: 10.1016/j.geoderma.2014.12.016

Cade-Menun, B. J. (2017). Characterizing phosphorus forms in cropland soils with solution ^{31}P-NMR: past studies and future research needs. *Chem. Biol. Technol. Agric.* 4:19. doi: 10.1186/s40538-017-0098-4

Cade-Menun, B. J., Bell, G., Baker-Ismail, S., Fouli, Y., Hodder, K., McMartin, D. W., et al. (2013). Nutrient loss from Saskatchewan cropland and pasture in spring snowmelt runoff. *Can. J. Soil Sci.* 93, 445–458. doi: 10.1139/CJSS2012-042

Cade-Menun, B. J., and Liu, C. W. (2014). Solution ^{31}P-NMR spectroscopy of soils from 2005 to 2013: a review of sample preparation and experimental parameters. *Soil Sci. Soc. Am. J.* 78, 19–37. doi: 10.2136/sssaj2013.05.0187dgs

Caporaso, J. G., Kuczynski, J., Stombaugh, J., Bittinger, K., Bushman, F. D., Costello, E. K., et al. (2010). QIIME allows analysis of high-throughput community sequencing data. *Nat. Methods* 7, 335–336. doi: 10.1038/nmeth.f.303

Chen, C. M., Ye, Q. Z., Zhu, Z. M., Wanner, B. L., and Walsh, C. T. (1990). Molecular biology of carbon-phosphorus bond cleavage. Cloning and sequencing of the phn (psiD) genes involved in alkylphosphonate uptake and C-P lyase activity in *Escherichia coli B. J. Biol. Chem.* 265, 4461–4471.

Condron, L. M., Frossard, E., Tiessen, H., Newmans, R. H., and Stewart, J. W. B. (1990). Chemical nature of organic phosphorus in cultivated and uncultivated soils under different environmental conditions. *J. Soil Sci.* 41, 41–50. doi: 10.1111/j.1365-2389.1990.tb00043.x

Condron, L. M., Turner, B. L., and Cade-Menun, B. J. (2005). "Chemistry and Dynamics of Soil Organic Phosphorus," in *Phosphorus: Agriculture and the Environment*, eds J. T. Sims and A. N. Sharpley (Madison, WI: American Society of Agronomy), 87–121.

Crews, T. E., and Brookes, P. C. (2014). Changes in soil phosphorus forms through time in perennial versus annual agroecosystems. *Agric. Ecosyst. Environ.* 184, 168–181. doi: 10.1016/j.agee.2013.11.022

Dai, M., Bainard, L. D., Hamel, C., Gan, Y., and Lynch, D. (2013). Impact of land use on arbuscular mycorrhizal fungal communities in rural Canada. *Appl. Environ. Microbiol.* 79, 6719–6729. doi: 10.1128/aem.01333-13

Elser, J., and Bennett, E. (2011). A broken biogeochemical cycle. *Nature* 478, 29–31. doi: 10.1038/478029a

FAO/UNEP. (2015). *FAO Statistical Pocketbook*. Rome: FAO.

Fraser, T. D., Lynch, D. H., Gaiero, J., Khosla, K., and Dunfield, K. E. (2017). Quantification of bacterial non-specific acid (phoC) and alkaline (phoD) phosphatase genes in bulk and rhizosphere soil from organically managed soybean fields. *Appl. Soil Ecol.* 111, 48–56. doi: 10.1016/j.apsoil.2016.11.013

Furtwängler, K., Tarasov, V., Wende, A., Schwarz, C., and Oesterhelt, D. (2010). Regulation of phosphate uptake via Pst transporters in *Halobacterium salinarum* R1. *Mol. Microbiol.* 76, 378–392. doi: 10.1111/j.1365-2958.2010.07101.x

Garcia-Montiel, D. C., Neill, C., Melillo, J., Thomas, S., Steudler, P. A., and Cerri, C. C. (2000). Soil phosphorus transformations following forest clearing for pasture in the Brazilian Amazon. *Soil Sci. Soc. Am. J.* 64, 1792–1804. doi: 10.2136/sssaj2000.6451792x

Giles, C., Cade-Menun, B., and Hill, J. (2011). The inositol phosphates in soils and manures: abundance, cycling, and measurement. *Can. J. Soil Sci.* 91, 397–416. doi: 10.4141/cjss09090

Guggenberger, G., Christensen, B. T., Rubaek, G., and Zech, W. (1996). Land-use and fertilization effects on P forms in two European soils: resin extraction and P-31-NMR analysis. *Eur. J. Soil Sci.* 47, 605–614. doi: 10.1111/j.1365-2389.1996.tb01859.x

Guillaume, T., Damris, M., and Kuzyakov, Y. (2015). Losses of soil carbon by converting tropical forest to plantations: erosion and decomposition estimated by δ13C. *Glob. Change Biol.* 21, 3548–3560. doi: 10.1111/gcb.12907

Hedley, M. J., Stewart, J. W. B., and Chauhan, B. S. (1982). Changes in inorganic and organic soil phosphorus fractions induced by cultivation practices and by laboratory incubations. *Soil Sci. Soc. Am. J.* 46, 970–976. doi: 10.2136/sssaj1982.03615995004600050017x

Hendershot, W. H., Lalande, H., and Duquette, M. (2008). "Soil sampling and methods of analysis," in *Soil Sampling and Methods of Analysis*, eds M. R. Carter and E. G. Gregorich (Boca Raton, FL: CRC Press), 173–178.

Houghton, R. A. (1994). The worldwide extent of land-use change. *Bioscience* 44, 305–313. doi: 10.2307/1312380

Hove-Jensen, B., Zechel, D. L., and Jochimsen, B. (2014). Utilization of glyphosate as phosphate source: biochemistry and genetics of bacterial carbon-phosphorus lyase. *Microbiol. Mol. Biol. Rev.* 78, 176–197. doi: 10.1128/mmbr.00040-13

Huntemann, M., Ivanova, N. N., Mavromatis, K., Tripp, H. J., Paez-Espino, D., Palaniappan, K., et al. (2015). The standard operating procedure of the DOE-JGI microbial genome annotation pipeline (MGAP v.4). *Stand. Genomic Sci.* 10:86. doi: 10.1186/s40793-015-0077-y

Hyatt, D., Chen, G., LoCascio, P. F., Land, M. L., Larimer, F. W., and Hauser, L. J. (2010). Prodigal: prokaryotic gene recognition and translation initiation site identification. *BMC Bioinformatics* 11:119. doi: 10.1186/1471-2105-11-119

Jangid, K., Williams, M. A., Franzluebbers, A. J., Sanderlin, J. S., Reeves, J. H., Jenkins, M. B., et al. (2008). Relative impacts of land-use, management intensity and fertilization upon soil microbial community structure in agricultural systems. *Soil Biol. Biochem.* 40, 2843–2853. doi: 10.1016/j.soilbio.2008.07.030

Kanehisa, M., and Goto, S. (2000). KEGG: kyoto encyclopedia of genes and genomes. *Nucleic Acids Res.* 28, 27–30. doi: 10.1093/nar/28.1.27

Li, D., Liu, C., Luo, R., Sadakane, K., and Lam, T. (2015). MEGAHIT: an ultra-fast single-node solution for large and complex metagenomics assembly via succinct de Bruijn graph. *Bioinformatics* 31, 1674–1676. doi: 10.1093/bioinformatics/btv033

Li, H., Handsaker, B., Wysoker, A., Fennell, T., Ruan, J., Homer, N., et al. (2009). The sequence alignment/map format and SAMtools. *Bioinformatics* 25, 2078–2079. doi: 10.1093/bioinformatics/btp352

Lidbury, I. D., Murphy, A. R., Scanlan, D. J., Bending, G. D., Jones, A. M., Moore, J. D., et al. (2016). Comparative genomic, proteomic and exoproteomic analyses of three *Pseudomonas* strains reveals novel insights into the phosphorus scavenging capabilities of soil bacteria. *Environ. Microbiol.* 18, 3535–3549. doi: 10.1111/1462-2920.13390

Liu, J., Hu, Y., Yang, J., Abdi, D., and Cade-Menun, B. J. (2015). Investigation of soil legacy phosphorus transformation in long-term agricultural fields using sequential fractionation, P K-edge XANES and solution P NMR spectroscopy. *Environ. Sci. Technol.* 49, 168–176. doi: 10.1021/es504420n

Liu, J., Yang, J., Cade-Menun, B. J., Liang, X., Hu, Y., Liu, C. W., et al. (2013). Complementary phosphorus speciation in agricultural soils by sequential fractionation, solution P-31 nuclear magnetic resonance, and phosphorus K-edge X-ray absorption near-edge structure spectroscopy. *J. Environ. Qual.* 42, 1763–1770. doi: 10.2134/jeq2013.04.0127

Liu, J., Yang, J., Liang, X., Zhao, Y., Cade-Menun, B. J., and Hu, Y. (2014). Molecular speciation of phosphorus present in readily dispersible colloids from agricultural soils. *Soil Sci. Soc. Am. J.* 78, 47–53. doi: 10.2136/sssaj2013.05.0159

Lombi, E., Scheckel, K. G., Armstrong, R. D., Forrester, S., Cutler, J. N., and Paterson, D. (2006). Speciation and distribution of phosphorus in a fertilized soil: a synchrotron-based investigation. *Soil Sci. Soc. Am. J.* 70, 2038–2048. doi: 10.2136/sssaj2006.0051

Maranguit, D., Guillaume, T., and Kuzyakov, Y. (2017). Land-use change affects phosphorus fractions in highly weathered tropical soils. *Catena* 149, 385–393. doi: 10.1016/j.catena.2016.10.010

McDowell, R. W., and Stewart, I. (2006). The phosphorus composition of contrasting soils in pastoral, native and forest management in Otago, New Zealand: sequential extraction and ^{31}P NMR. *Geoderma* 130, 176–189. doi: 10.1016/j.geoderma.2005.01.020

McDowell, R. W., Stewart, I., and Cade-Menun, B. J. (2006). An examination of spin–lattice relaxation times for analysis of soil and manure extracts by liquid state phosphorus-31 nuclear magnetic resonance spectroscopy. *J. Environ. Qual.* 35, 293–302. doi: 10.2134/jeq2005.0285

Murphy, J., and Riley, J. P. (1962). A modified single solution method for the determination of phosphate in natural waters. *Anal. Chim. Acta* 27, 31–36. doi: 10.1016/S0003-2670(00)88444-5

Nash, D. M., Haygarth, P. M., Turner, B. L., Condron, L. M., McDowell, R. W., Richardson, A. E., et al. (2014). Using organic phosphorus to sustain pasture productivity: a perspective. *Geoderma* 221, 11–19. doi: 10.1016/j.geoderma.2013.12.004

Neal, A. L., Rossmann, M., Brearley, C., Akkari, E., Guyomar, C., Clark, I. M., et al. (2017). Land-use influences phosphatase gene microdiversity in soils. *Environ. Microbiol.* 19, 2740–2753. doi: 10.1111/1462-2920.13778

Negassa, W., and Leinweber, P. (2009). How does the Hedley sequential phosphorus fractionation reflect impacts of land use and management on soil phosphorus: a review. *J. Plant Nutr. Soil Sci.* 172, 305–325. doi: 10.1002/jpln.200800223

Parkinson, J. A., and Allen, S. E. (1975). A wet oxidation procedure suitable for the determination of nitrogen and mineral nutrients in biological material. *Commun. Soil Sci. Plant Anal.* 6, 1–11. doi: 10.1080/00103627509366539

Prietzel, J., Duemig, A., Wu, Y., Zhou, J., and Klysubun, W. (2013). Synchrotron-based P K-edge XANES spectroscopy reveals rapid changes of phosphorus speciation in the topsoil of two glacier foreland chronosequences. *Geochim. Cosmochim. Acta* 108, 154–171. doi: 10.1016/j.gca.2013.01.029

Quinlan, A. R., and Hall, I. M. (2010). BEDTools: a flexible suite of utilities for comparing genomic features. *Bioinformatics* 26, 841–842. doi: 10.1093/bioinformatics/btq033

Ravel, B., and Newville, M. (2005). ATHENA, ARTEMIS, HEPHAESTUS: data analysis for X-ray absorption spectroscopy using IFEFFIT. *J. Synchrotron Radiat.* 12, 537–541. doi: 10.1107/s0909049505012719

Richardson, A. E., Lynch, J. P., Ryan, P. R., Delhaize, E., Smith, F. A., Smith, S. E., et al. (2011). Plant and microbial strategies to improve the phosphorus efficiency of agriculture. *Plant Soil* 349, 121–156. doi: 10.1007/s11104-011-0950-4

Robinson, M. D., McCarthy, D. J., and Smyth, G. K. (2010). edgeR: a Bioconductor package for differential expression analysis of digital gene expression data. *Bioinformatics* 26, 139–140. doi: 10.1093/bioinformatics/btp616

Santos-Beneit, F. (2015). The Pho regulon: a huge regulatory network in bacteria. *Front. Microbiol.* 6:402. doi: 10.3389/fmicb.2015.00402

Saskatchewan Environment, and Resource Management [SERM]. (1997). *Saskatchewan's State of the Environment Report 1997 - The Prairie Ecozone, Our Agricultural Heartland*. Regina, SK: Saskatchewan Enviornment and Resource Management.

Sato, S., Solomon, D., Hyland, C., Ketterings, Q. M., and Lehmann, J. (2005). Phosphorus speciation in manure and manure-amended soils using XANES spectroscopy. *Environ. Sci. Technol.* 39, 7485–7491. doi: 10.1021/es050313o

Saunders, W. M. H., and Williams, E. G. (1955). Observations on the determinations of total organic phosphorus in soils. *J. Soil Sci.* 6, 254–267. doi: 10.1111/j.1365-2389.1955.tb00849.x

Sharpley, A., Jarvie, H. P., Buda, A., May, L., Spears, B., and Kleinman, P. (2013). Phosphorus legacy: overcoming the effects of past management practices to mitigate future water quality impairment. *J. Environ. Qual.* 42, 1308–1326. doi: 10.2134/jeq2013.03.0098

Sims, J. T. (2009). "Soil test phosphorus: Principles and methods," in *Methods of Phosphorus Analysis for Soil, Sediments, Residuals, and Waters*, ed. G. M. Pierzynski (Raleigh, NC: North Carolina State University), 9–19.

Stutter, M. I., Shand, C. A., George, T. S., Blackwell, M. S. A., Dixon, L., Bol, R., et al. (2015). Land use and soil factors affecting accumulation of phosphorus species in temperate soils. *Geoderma* 257, 29–39. doi: 10.1016/j.geoderma.2015.03.020

Tabatabai, M. A. (1994). "Soil enzymes," in *Methods of Soil Analysis. Part 2: Microbiological and Biochemical Properties*, eds S. H. Mickelson and J. M. Bifham (Madison, WI: Soil Science Society of America, Inc.), 775–833.

Tremblay, J., Yergeau, E., Fortin, N., Cobanli, S., Elias, M., King, T. L., et al. (2017). Chemical dispersants enhance the activity of oil- and gas condensate-degrading marine bacteria. *ISME J.* 11, 2793. doi: 10.1038/ismej.2017.129

Turner, B. L. (2007). "Inositol phosphates in soil: amounts, forms and significance of the phosphorlyated inositol stereoisomers," in *Inositol phosphates: linking agriculture and the environment*, eds B. L. Turner, A. E. Richardson, and E. J. Mullaney (Wallingford: CAB International), 186–207. doi: 10.1079/9781845931520.0186

Turner, B. L., Cheesman, A. W., Godage, H. Y., Riley, A. M., and Potter, B. V. L. (2012). Determination of neo- and D-chiro-inositol hexakisphosphate in soils by solution ^{31}P NMR spectroscopy. *Environ. Sci. Technol.* 46:11479. doi: 10.1021/es204446z

Turner, B. L., Papházy, M. J., Haygarth, P. M., and McKelvie, I. D. (2002). Inositol phosphates in the environment. *Philos. Trans. R. Soc. Lond. B Biol. Sci.* 357, 449–469. doi: 10.1098/rstb.2001.0837

Turner, B. L., Wells, A., and Condron, L. M. (2014). Soil organic phosphorus transformations along a coastal dune chronosequence under New Zealand temperate rain forest. *Biogeochemistry* 121, 595–611. doi: 10.1007/s10533-014-0025-8

Webb, S. M. (2005). SIXpack: a graphical user interface for XAS analysis using IFEFFIT. *Phys. Scr.* 115, 1011–1014. doi: 10.1238/Physica.Topical.115a01011

Weyers, E., Strawn, D. G., Peak, D., Moore, A. D., Baker, L. L., and Cade-Menun, B. (2016). Phosphorus speciation in calcareous soils following annual dairy manure amendments. *Soil Sci. Soc. Am. J.* 80, 1531–1542. doi: 10.2136/sssaj2016.09.0280

Young, E. O., Ross, D. S., Cade-Menun, B. J., and Liu, C. W. (2013). Phosphorus speciation in riparian soils: a phosphorus-31 nuclear magnetic resonance spectroscopy and enzyme hydrolysis study. *Soil Sci. Soc. Am. J.* 77, 1636–1647. doi: 10.2136/sssaj2012.0313

Conflict of Interest Statement: The authors declare that the research was conducted in the absence of any commercial or financial relationships that could be construed as a potential conflict of interest.

frontiers in Earth Science

REVIEW
published: 05 September 2018
doi: 10.3389/feart.2018.00135

Components of Phosphorus Loss From Agricultural Landscapes, and How to Incorporate Them Into Risk Assessment Tools

Keith Reid[1], Kimberly Schneider[1] and Brian McConkey[2]*

[1] Science and Technology Branch, Agriculture and Agri-Food Canada, Guelph, ON, Canada, [2] Science and Technology Branch, Agriculture and Agri-Food Canada, Swift Current, SK, Canada

Phosphorus (P) loss to surface freshwater is a key driver of environmental degradation, including blooms of both harmful (e.g., microcystis) and nuisance (e.g., cladophora) algae, along with the development of hypoxic zones that could significantly impact fish habitat. Mitigating P losses from agricultural land will require a detailed understanding of the forms (particulate versus dissolved, and chemical speciation), sources (soil erosion, desorption of soil P, dissolved P from fertilizer or manure application, or release from frozen vegetation) and transport pathways (surface runoff, or subsurface runoff through tile drains). This paper describes each of these components in detail, and discusses how this can guide the adoption of appropriate beneficial management practices to effectively reduce P losses. Further, it describes how this component structure has been incorporated into the Canadian national Indicator of Risk of Water Contamination by Phosphorus (IROWC-P) as an example of a risk assessment tool.

Keywords: phosphorus, nutrient loss, risk assessment tools, component P index, P source, P transport

OPEN ACCESS

Edited by:
Chris Thomas Parsons, University of Waterloo, Canada

Reviewed by:
Yi Zhang, University of Maryland, College Park, United States
Ryuichiro Shinohara, National Institute for Environmental Studies, Japan

****Correspondence:***
Keith Reid
keith.reid@canada.ca

Specialty section:
This article was submitted to Marine Biogeochemistry, a section of the journal Frontiers in Earth Science

Received: *26 January 2018*
Accepted: *20 August 2018*
Published: *05 September 2018*

Citation:
Reid K, Schneider K and McConkey B (2018) Components of Phosphorus Loss From Agricultural Landscapes, and How to Incorporate Them Into Risk Assessment Tools. Front. Earth Sci. 6:135. doi: 10.3389/feart.2018.00135

INTRODUCTION

Phosphorus (P) loss to surface freshwater is a key driver of environmental degradation (Sharpley et al., 2003; Jarvie et al., 2013; Scavia et al., 2014), including blooms of both harmful (e.g., microcystis) (Conroy et al., 2014; Steffen et al., 2014; Simic et al., 2017) and nuisance (e.g., cladophora) algae (Auer et al., 2010; Depew et al., 2011; Howell and Dove, 2017), along with contributing to the development of hypoxic zones that impact fish habitat (Bouffard et al., 2013; Scavia et al., 2014). While agricultural runoff is not the only source of P loading to surface water, it is significant in many areas and is implicated as the dominant source to some of the most heavily impacted waters (Sharpley et al., 2003; Michaud et al., 2004; Joosse and Baker, 2011; Bunting et al., 2016).

Given the importance of agricultural runoff in P loading to surface water, there is great interest in finding ways to mitigate these losses (Haygarth et al., 2005; OLEPTF, 2010; Reutter et al., 2011; Osmond et al., 2012a; Kerr et al., 2016). The success of these mitigation activities depends on how well our understanding of the source and transport processes for P represent what is actually happening in an individual field, farm or catchment (Gburek et al., 2002; Osmond et al., 2012b; Sharpley et al., 2012; Radcliffe et al., 2015). Unfortunately, this linkage is often less than perfect for a number of reasons. For example, models may be adapted from other jurisdictions that are dominated by different processes; our understanding of the underlying processes for the transport

of P may be flawed, or based on outdated research; or the models chosen may be biased by tightly held cultural, political or economic preferences (Kleinman et al., 2015b).

This paper will attempt to outline our current understanding of the dominant sources and transport pathways for phosphorus loss from agricultural land under varying inherent conditions and management practices, and how the relative importance of each may be assessed. The Indicator of Risk of Water Contamination by Phosphorus (IROWC-P) will be discussed as an example of one type of assessment tool, including describing the areas for future improvement.

THE SOURCE × TRANSPORT PARADIGM FOR UNDERSTANDING P LOSS

The earliest P indexes considered sources of P independently from the risk of transport (Lemunyon and Gilbert, 1993) and did not always assign risk correctly if there was, for example, a large source of P with no transport risk. Gburek et al. (2000) pointed out this flaw, and suggested an alternative model which determined the potential P source for loss, and multiplied it by a transport modifier to assess the risk of P loss to surface water. This forms the basis for our understanding of P losses, where water movement is needed before any P transport can occur. The unfortunate corollary is that some models assume that any water leaving the landscape will carry the same concentration of P, which ignores the differences in the ways that P is released into water traveling by different pathways, the opportunities for mitigation of P traveling through different pathways, and the ways that different forms of P will be transported.

This weakness is addressed by using a component model to understand and predict P losses, where the combinations of P sources and transport pathways are assessed individually, and then summed to determine the total risk of P loss from the field or region being assessed. The focus in this paper is on P transport by water, although atmospheric deposition of P can also occur, and may be a significant fraction of P inputs to some smaller water bodies adjacent to sources of P (Anderson and Downing, 2006), and this could be included in as a component in a P loss model. The factors that make up each of the components are discussed in the following sections.

PARTICULATE VERSUS DISSOLVED P

Phosphorus exported from terrestrial systems is a combination of dissolved P, and P that is bound to soil as particulate P. Dissolved P is predominantly phosphate ions [also identified as dissolved reactive P (DRP) due to its reactivity with molybdate to form a blue colored complex (Joosse and Baker, 2011)], but it can also contain P sorbed to colloidal particles, organic P compounds (Heathwaite et al., 2005), and non-reactive mineral forms including polyphosphates and phosphonates (Turner and Newman, 2005; Weihrauch and Opp, 2018). The phosphate ion is extremely reactive, and therefore tends to form insoluble or slightly soluble compounds if a suitable counter ion is available (Sharpley, 1995). Most P in the soil is in the particulate form, as precipitates of iron, aluminum or calcium phosphates, bound to soil minerals (clay, calcite, aluminum hydroxides, etc.), or occluded within soil granules (Wang et al., 2010). This has led to the misconception that controlling soil erosion will effectively control P export from agricultural land (Baker et al., 2014), but recent developments have shown that a significant portion of P losses can be in the dissolved form (Baker et al., 2007; Joosse and Baker, 2011).

This is relevant to water quality because of the relative availability of each P form to freshwater algae. Dissolved P, especially PO_4^{3-}, is immediately available to algae, and is absorbed within a time frame of minutes to hours (Barlow-Busch et al., 2006), so many lake water analyses ignore the dissolved fraction completely since the majority is in the algal biomass (Lin and Guo, 2016). The particulate fraction is, generally, more slowly available, as the recalcitrant compounds gradually dissolve. This proportion will vary with the soil chemistry, and with the amount of P in the soil. Estimates of the proportion of total particulate P that is bioavailable vary widely, with Sharpley et al. (1991) reporting a range from 0 to 95%, and Young et al. (1985) reporting a range from 0 to 70% for sediments in the Great Lakes basin. The most frequently used estimates, however, are in the range of 10% (Fang et al., 2002) to 30% (Sharpley and Smith, 1993), which is within the range reported for five lower Great Lakes tributaries by DePinto et al. (1981). A full discussion of the complexity of various P forms in soils and sediments is beyond the scope of this paper, but the topic has been well summarized by Condron and Newman (2011) and Weihrauch and Opp (2018).

The biological response of lakes and streams to P inputs will depend on the total amount of bioavailable P. This can be calculated as the total of dissolved P and the bioavailable portion of particulate P.

P SOURCES

One of the limitations of P risk assessments is focusing on a limited number of potential sources, which may lead to ignoring sources that are relevant to the conditions in a given area. This is a particular danger if P indexes are adopted from other regions with different dominant P sources. While it may be appropriate to focus on particular sources, this should only be done after an objective assessment of the relative importance of each source within the area of interest, rather than adopting the assumptions made in different geographies.

Particulate P From Eroded Soil

In many environments, the particulate P fraction represents the majority of total P leaving a field, although it may not represent the largest amount of bioavailable P. Nonetheless, it is important to consider in any assessment of P loss.

The factors affecting particulate P loss include the quantity of eroded soil, and the P concentration within that sediment. It is difficult to measure soil loss directly, but there are a number of tools available to estimate soil erosion from soil, landscape,

climate, and management factors. These are generally based on the Universal Soil Loss Equation (USLE), which is a mixed model that combines both source and transport factors to predict soil delivery to the bottom of a 22.7 m slope (Foster et al., 2003; Kinnell, 2008). This helps to explain why soil erosion is often included as a transport factor rather than a source factor. Variations on USLE, like RUSLE (Renard et al., 1995) or WEPP (Flanagan et al., 2007), use similar equations to estimate the quantity of soil detached but also account for additional landscape factors to improve estimates of P delivery to the edge of field.

Two different methods have been used for estimation of the particulate P concentration within the soil. Some studies have shown a correlation between the soil test P (STP) of the soil and total P concentration (van der Perk et al., 2007; Withers et al., 2009). The second method is to assume that particulate P concentration is a constant fraction of the soil, which is supported by data showing a weak relationship between STP and PP (Uusitalo et al., 2003; Reid, 2011; Glæsner et al., 2013; Borda et al., 2014). It is likely that this proportion varies with mineralogy as well as organic matter content and composition, so there may be significant differences between regions that are independent of STP.

Complicating the estimation of PP losses are the issues of P stratification and P enrichment. P stratification is the accumulation of elevated levels of P at the soil surface, either by the deposition of plant residues on the soil surface or by the surface application of fertilizer or manure (Smith et al., 2017). P stratification is an important consideration because the runoff water interacts with a very shallow layer of soil at the surface (Sharpley, 1985). P enrichment refers to the selective erosion of sediments with a higher P concentration than the bulk soil during small erosion events (Sharpley, 1980).

Some risk assessment tools are attempting to estimate the bioavailable fraction of PP, rather than the total, to better predict the biological consequences of the P loss. This can be estimated as a constant proportion of the PP (see previous section), or related to the STP (Sharpley et al., 1992; Sharpley and Smith, 1993). Ellison and Brett (2006) showed the proportion of bioavailable particulate P (BAPP) ranging from 12 to 29% in runoff from rural areas in Washington State, United States. DePinto et al. (1981) found that the BAPP of suspended sediments in tributaries of Lakes Erie and Ontario were relatively consistent within tributary samples, but varied between tributaries with a range of 6.1–35.8% of total sediment P.

Dissolved P Desorbed From Soil

When rain or snow-melt interacts with the soil surface, a small part of the P contained in that soil will dissolve and be transported with runoff water, either across the soil surface in surface runoff or diverted vertically through macropores to tile drains. The exact proportion of soil P that desorbs will vary with P content of the soil, and the soil mineralogy. A number of studies have shown that DP losses are related to the agronomic soil tests that are appropriate for that region, which provides a readily available tool for estimating the risk of DP losses (Vadas et al., 2005; Little et al., 2007; Wang et al., 2012, 2015). Some of these studies have shown greater accuracy when the STP is expressed as a degree of P saturation (DPS), calculated as the STP divided by the P sorption capacity of the soil. The importance of this increased accuracy for routine evaluations is unclear, however, since it would require soil analyses that are not included as part of most STP evaluations, and the increase in accuracy is modest relative to the range of STP values found under field conditions (Vadas et al., 2005; Wang et al., 2010, 2015).

The proportion of desorbed P has generally been assessed using artificial rainfall on small field plots or repacked soil boxes (National Phosphorus Research Project [NPRP], 2001; Wang et al., 2010). This consistent approach has been very good for assessing the relative difference between different soils and STP values, although there is evidence that it may be underestimating the concentration of P in runoff water from small rain events (Shigaki et al., 2007; Srinivasan et al., 2007; Dougherty et al., 2008; Dunkerley, 2017). It is speculated that the intensive rainfall in the rainfall simulators limits the opportunity for rainwater to interact with the soil surface due to the rapid runoff, and that the estimated proportions should be increased for light rain.

Dissolved P Desorbed From Applied Fertilizer

Fertilizer applied to the soil surface represents a highly soluble source of phosphorus, which can readily be mobilized in runoff water. Vadas et al. (2008) summarized the state of knowledge regarding interactions of fertilizer with soil and precipitation, noting that fertilizer granules dissolve over time with successive rainfall events. The resulting solution is more concentrated than what would result from the interaction of runoff water with soil, so the soil represents a net sink for the P desorbed from fertilizer. Using the assumption that the P in water which infiltrates into the soil will be retained there, the P losses from fertilizer can be estimated by using a distribution factor to account for the partitioning between runoff and infiltration (Vadas et al., 2008).

It is important to note that losses from applied P are only relevant from fertilizer that remains on the surface. Subsurface banding or incorporation by tillage should, theoretically, eliminate losses from applied P fertilizer, although the reality is that a small amount of the applied P remains on the surface. The degree of incorporation, and the lag time between application and incorporation, if known, should be considered in P loss risk assessments.

Dissolved P Released From Applied Manure

Similar to fertilizer, manure is a highly available source of P for runoff, but has two key differences. The first is that manure contains a range of organic and mineral forms of P (Johannesson et al., 2017), so not all is immediately soluble although some compounds will degrade to release soluble P over time (Sharpley and Moyer, 2000; Vadas et al., 2011). The rate of release of these compounds can also vary with soil conditions, e.g., redox potential (Turner and Newman, 2005). The second is the physical form of the manure, as there may be immediate infiltration of liquid manure (Vadas, 2006), or reduced effectiveness of

incorporation due to the larger volume applied and the clumpy nature of solid manure (Vadas et al., 2007). The net result is that the immediate release from applied manure may be less than from an equivalent amount of fertilizer P, but the concentration of P in runoff water will not decline as quickly.

Dissolved P release from applied manure can be estimated from the total P application rate multiplied by the water extractable P proportion in the manure, which varies among livestock species (Kleinman et al., 2002, 2005, 2006), minus the amount of liquid manure that has infiltrated (Vadas et al., 2007). This dissolved P is then subject to a similar partitioning between runoff and infiltration as fertilizer, but with a different partitioning coefficient to reflect the slower rate but longer duration of P release from manure (Vadas et al., 2008, 2009).

Dissolved P Released From Frozen Plant Residue

In areas where annual runoff is dominated by snowmelt, P that is released from frozen plant residue can represent a significant part of annual P losses to surface water (Elliott, 2013). It has been well established that the rate of P release from plant tissue is accelerated by freezing and thawing (Miller et al., 1994; Bechmann et al., 2005; Liu J. et al., 2013; Kirchmann and Wessling, 2017), although this has not translated into increased P losses to surface water under all conditions (Lozier et al., 2017). The most likely explanation for this seeming discrepancy is the difference in water infiltration under different climatic conditions. Where freezing conditions are followed by warm weather and rainfall, the P leached out of the plant residues will have to opportunity to interact with the soil and be adsorbed. In contrast, if there is little or no rainfall between freezing conditions and the onset of winter with snow accumulation, most of the P would remain in the residue in soluble form until it is carried off the field during snowmelt (Roberson et al., 2007).

This can be modeled by assuming the labile portion of the P in crop residue (roughly 50% for most residues) is converted to soluble forms according to an exponential decay function (Damon et al., 2014). This soluble P is then washed out of the residue by rainwater or by "steeping" in the water from snowmelt (Elliott, 2013), and partitions between infiltration and runoff in the same manner as dissolved P from fertilizer (Vadas et al., 2009). Modeling the P in alfalfa residue against actual weather conditions in southwestern Ontario (Harrow) and southern Saskatchewan (Swift Current) showed that most of the P was leached out of the Ontario residue by January with relatively little carried off the field, while significant amounts remained over winter in the prairie environment (Saskatchewan) and was exported in runoff during snowmelt (**Figure 1**).

P TRANSPORT PATHWAYS

As already noted, P movement in runoff cannot occur unless there is also water movement (Chardon and Schoumans, 2002). Most models of P loss account for surface runoff, but in regions with extensive tile drainage it is important to consider this pathway, as well (Reid et al., 2012; Jarvie et al., 2017). In some environments, subsurface lateral movement of P can contribute to P losses, but this requires preferential flow pathways in both vertical and horizontal directions, that discharge to surface water (Allen et al., 2012; McGrath et al., 2013; Kleinman et al., 2015a).

It should be noted that, although it is common to refer to the vertical movement of P as "leaching," that this is a different process from the leaching of compounds like nitrate. Both dissolved and particulate forms of P are significantly retarded by contact with the soil matrix, so the vertical movement of P to tile drains is through preferential flow pathways rather than through the soil matrix (Radcliffe et al., 2015). Leaching to deep aquifers is not assessed as part of P loss, both because dissolved P does not pose a direct human health risk, and because the conditions to support the biological response to P loading (i.e., algae growth) are not present in groundwater.

Transport of P through the air to surface water is ignored in most models, because, unlike N, there are no gaseous losses of P from the soil surface and it is considered to be a relatively minor contributor to P loading. There can, however, be significant generation of dust by soil disturbance that can then be deposited on surface water, which can contribute a significant part of P loading to water bodies that are relatively small (Anderson and Downing, 2006).

Surface Runoff

Surface runoff will be generated whenever water inputs from precipitation or snowmelt exceed the capacity of the soil to absorb that water. This exceedance may occur because the rate of precipitation exceeds the infiltration capacity of the soil (Infiltration excess runoff, or Hortonian flow), or because the soil is already saturated and cannot absorb any more water (saturation excess runoff). The amount of runoff, and therefore the risk of P loss in that runoff, is driven by the total amount of precipitation, the intensity of that precipitation, and the proportion of that precipitation that becomes runoff. Runoff from any landscape will be a combination of both processes, although the dominant process will depend on climate, topography, and soils.

Infiltration excess is the basis of runoff predictions using the SCS Curve Number approach (Garen and Moore, 2005; Singh et al., 2010). The underlying assumption is that areas with similar infiltration capacity (hydrologic response units, or HRUs), as determined by soil type, crop types, soil management and antecedent moisture, will all generate runoff at the same time when an intense rain event occurs. The corollary of this assumption is that the runoff generated will all run downslope to surface water, so the entire HRU is a source for P transport. Infiltration excess runoff will dominate in areas where soil permeability is low and precipitation is concentrated into intense storm events. Because of the influence of crop type and soil management (particularly tillage system), this form of runoff generation will change in response to management (Garen and Moore, 2005).

Saturation excess flow, in contrast, occurs in parts of the landscape where the water table is close to the surface of the soil. This may be due to topographic position (i.e., low elevation),

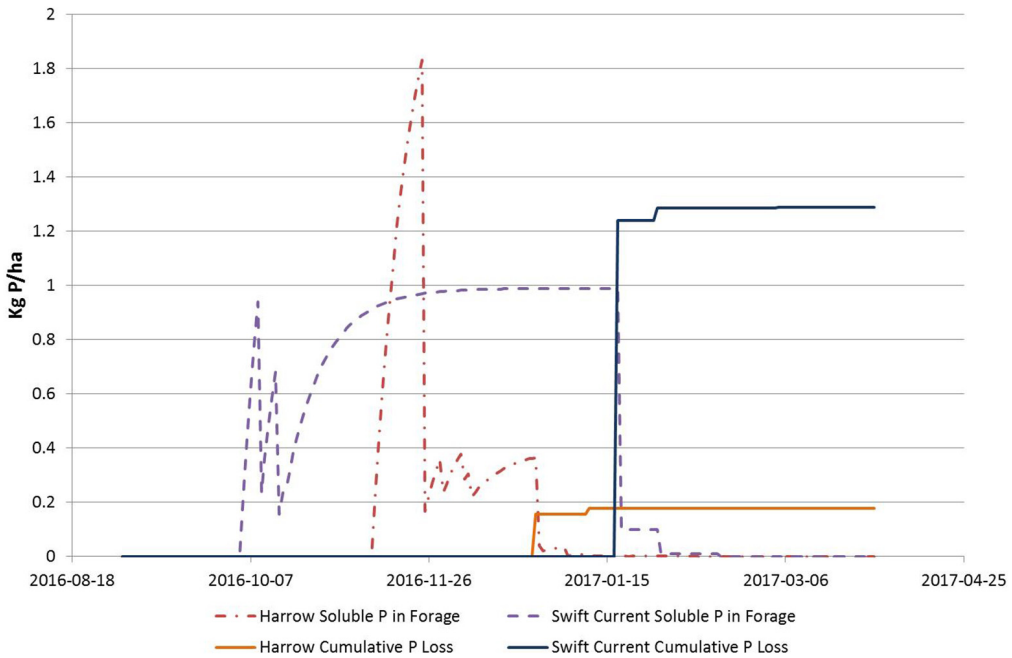

FIGURE 1 | Predicted plant residue P available for loss from forages in different climate zones.

or to impermeable layers in (cemented horizons or shallow bedrock) or at the surface (compacted soils) of the soil. It is the basis for variable source areas for runoff (Gburek et al., 2006; Schneiderman et al., 2007; Dahlke et al., 2009). Runoff will generally occur from only a small part of the landscape, but can have a disproportionate effect because they are concentrated close to surface water. The proportion of precipitation that becomes runoff is related to the proportion of the landscape with saturated conditions; this parameter will not be affected by changes in crop type or soil management.

Both of these methods can be calibrated to provide good estimations of total runoff volume from a landscape, but the parts of that landscape that are assumed to be generating runoff can be quite different for each (Lyon et al., 2006). Models based on infiltration excess will predict most of the runoff coming from upland areas within a watershed, while saturation excess models will predict that most runoff comes from the lower reaches. Understanding the relative importance of each process within an area will be critical to the choice of P source mitigation efforts, if the goal is to reduce P losses to surface water.

Runoff from snowmelt is a special case, since large parts of the landscape may be either saturated or frozen. If this occurs, the differences between infiltration and saturation excess disappear. One of the major challenges, from both a modeling and a management perspective, is that there are also conditions where the snow melts gradually over a permeable soil so almost all of it infiltrates (Zhang, 2005; Dutta et al., 2017). This process has not been extensively researched, and the process of infiltration into unfrozen soils is not included in the Cold Regions Hydrologic Model (Pomeroy et al., 2007), although it does include a factor for infiltration into unsaturated frozen soils.

The impact of the interactions between regional climate variation and the seasonality of runoff generation on potential source areas for P loss can be illustrated by some examples. In the northern Great Plains, dry conditions dictate that there is virtually no runoff except during spring snowmelt (Liu K. et al., 2013; Liu et al., 2014; Mahmood et al., 2017), but there is also little opportunity for infiltration of P into frozen soils. Surface applied P during the fall or winter, or P from frozen plant residues, would represent a high risk of P loss. In contrast, runoff generation in much of south-eastern United States is dominated by infiltration excess from summer storms so losses from spring applied nutrients are more problematic than from fall applications (Osmond et al., 2012b; Woodbury et al., 2014). The Eastern Corn Belt is a transition zone, where runoff in the spring freshet mimics infiltration excess, while during the growing season there are seldom storms intense enough to exceed soil infiltration capacity so runoff is dominated by saturation excess (Gburek et al., 2006; Easton et al., 2008).

Tile Runoff

Tile drainage is widely used in many humid temperate agricultural areas to manage excess soil moisture and improve crop growth, with some of the most intensive areas of tile drainage in the southern parts of the Great Lakes basin (Tan and Zhang, 2011; Reid et al., 2012; King et al., 2015), the Mississippi River basin (Blann et al., 2009), and northern Europe (Uusitalo et al., 2007; Ulén et al., 2011). Tile drains have a marked effect on hydrology by reducing the volume of surface runoff, lowering the water table within the soil, and changing the timing and duration of peak runoff flows (Sloan et al., 2016), although the total runoff from an individual field may not increase very much

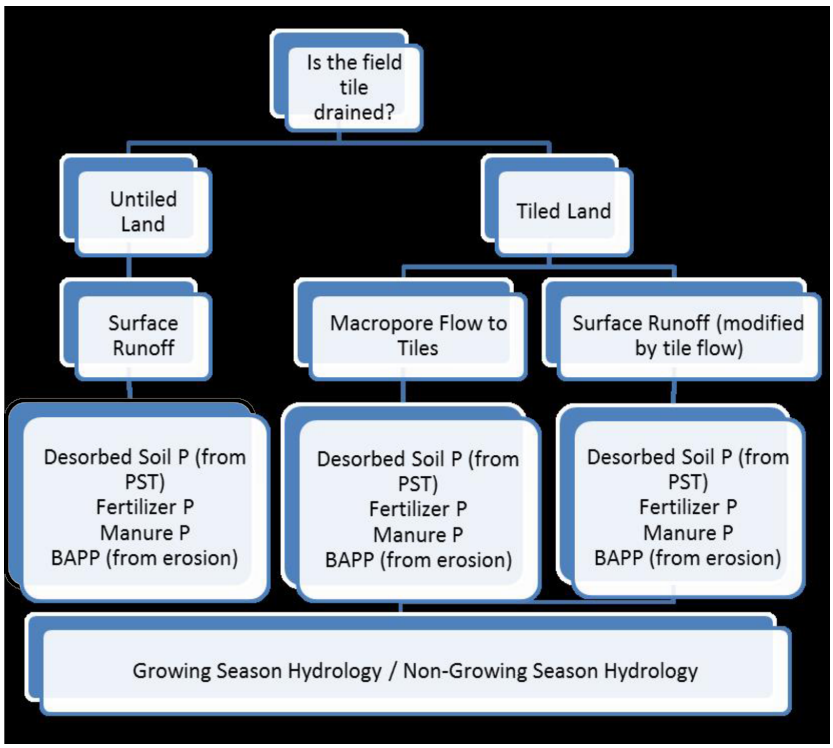

FIGURE 2 | Flow chart to determine transport coefficients for various P sources in tiled or non-tiled agricultural fields.

(King et al., 2014) if at all (Singh et al., 2006; Turunen et al., 2013). At the same time, the increased connectivity of the upper parts of the landscape and the greater conductivity of straightened streams and surface drains installed to receive tile water can increase the total water export from the landscape (Blann et al., 2009).

Although tile drains may have limited impact on total water movement off the landscape, they typically carry a significant part of the total annual runoff. King et al. (2014) measured tile contribution to stream flow on a silt loam to clay loam watershed in Ohio that ranged from 0 to 100% of total runoff in any month, with a mean annual value of 41%. This is similar to the 42% of total streamflow from tiles found by Macrae et al. (2007) on a watershed with coarse to medium texture soils in southern Ontario. Van Esbroeck et al. (2016) found a higher proportion of tile runoff at edge of field on three coarse to medium textured sites, ranging from 78 to 90% of total runoff. Tan and Zhang (2011) found that 96% of the total runoff, averaged over 5 years, was through tile drains on a clay soil in Essex County, ON, Canada.

Phosphorus export through tile drains in all of the above studies was less than the proportion of total flow, indicating that either movement of P from the surface to the tile drains was being partially impeded, or that the tile flow was a mix of surface runoff diverted to the tiles through macropores and water that had percolated through the soil matrix. Given the propensity of most soils in the tile drained regions to adsorb P (Richards et al., 1995; Wang et al., 2014), the latter mechanism seems much more likely, and has been proposed by a number of authors as an explanation for the P concentrations found in tile flow (Stamm et al., 1998; Chikhaoui et al., 2008; Van Bochove et al., 2010; Reid et al., 2012; Beven and Germann, 2013; Radcliffe et al., 2015; Jarvis et al., 2016). Further evidence that P transport to tile drains is occurring through macropores is that the proportion of particulate P in the tiles is similar to that in the surface runoff, when averaged over a year (Ball Coelho et al., 2010; Radcliffe et al., 2015; Pease et al., 2017), although there can be significant variability between individual flow events, and the application of fertilizer or manure can temporarily increase the proportion of dissolved P (Macrae et al., 2007). Within this framework, the main determinant of P movement to tile drains will be the partitioning of water reaching the tile drains between macropore flow, with a relatively high P concentration, and matrix flow which carries very little P. This partitioning is not well represented in most models of P transport (Radcliffe et al., 2015), but there has been some progress in empirical determination of macropore flow showing a strong influence of soil texture (Allaire et al., 2009; Eastman et al., 2010; Karahan and Erşahin, 2017). The textural influence may be directly affecting the propensity of the soil to form shrinkage cracks, or indirectly affect the population of anecic earthworms, both of which can contribute to macroporosity (van Bochove et al., 2007; Fox et al., 2008; Koestel et al., 2011; Jarvis et al., 2016). The general trend, where there have been direct comparisons, is for greater macropore flow in fine than coarse textured soils (Eastman et al., 2010).

Since the installation of tile drains reduces the volume of surface runoff, proper accounting for the contribution of tile drains to P transport requires estimation of the reduced surface runoff, as well as the macropore portion of tile flow as shown in **Figure 2**. Since the macropores with direct connection to the tiles are concentrated in a narrow strip over the tile drains, the spacing between the tile runs will influence the amount of P that could move to the tile. An additional complication is the extent of many subsurface drainage systems. Within an individual field, the catchment areas for surface runoff and subsurface runoff may correspond fairly closely, but modern tile drainage systems may encompass many fields and extend for a kilometer or more into the landscape. This represents a large increase in the connectivity of the landscape to surface water, and since there is essentially no mitigation of P in the tile flow and the drain outlets are generally directly into surface water, it can bypass the riparian buffers that can reduce the P entrained in surface runoff.

Sub Surface Lateral Flow

Preferential flow is generally considered to be vertical, but there are situations where there are horizontal preferential pathways, often where there is an impervious layer beneath the surface that impedes vertical flow and creates a perched water table. Water reaching these lateral flow paths, either through vertical macropores or by matrix flow through a soil that is saturated with P, can be carried horizontally to side-hill seeps (where the impervious layer reaches the soil surface along a slope) or into drainage ditches that intersect the impervious layer. This is the dominant pathway for P loss in the Delmarva Peninsula (Kleinman et al., 2007, 2015a).

MITIGATION FROM EDGE-OF-FIELD TO EDGE-OF-WATER

The sources of P from agricultural land, and the transport factors that are calculated are operating within the same geography, so the end result is an estimate of P delivery to the edge of the field. If this coincides with the shore of a water body it is a reasonable estimate of risk, but more often the field is at some distance from surface water, and runoff must travel over other fields or buffer areas where mitigation of the P losses could occur. The actual risk to surface water quality, therefore, will depend on the distance from the edge of field to the stream, and on the nature of the soils and vegetation in this area.

Mitigation of P runoff can occur in several ways. Particulate P can be trapped or filtered by growing vegetation, particularly if there is a dense sward of grasses (Butler et al., 2006). Surface runoff can infiltrate into the soil in a buffer zone, which will reduce both dissolved and particulate P (Leguédois et al., 2008; Dosskey et al., 2010). There can even be some mitigation of P in runoff over a field, as the P concentration in the runoff water reaches equilibrium with the soil surface. All of these mechanisms will be most effective if there is sheet flow, to maximize the area of interaction. Concentrated flow will have enough energy to travel through the buffer without any appreciable reduction in P (Dosskey et al., 2002).

This mitigation is generally accounted for in models as a delivery ratio. This may be a single coefficient for buffers of a given width, or there may be more complex models that account for landscape types and vegetation (Li et al., 2011). Neither of these approaches has been well calibrated, and this remains an area requiring further work.

THE COMPONENT MODEL STRUCTURE

The principle of the component model structure is that each source has a unique transport modifier, and the product of each source × transport calculation is summed to determine the total risk of P loss. If taken to this extreme, the component model would become complex to the point of being impractical. Fortunately, it is possible to lump together many of the sources to simplify the calculations. The transport of dissolved P is going to be similar, for example, whether it came from applied fertilizer or released from frozen vegetation.

Even with the rationalization of transport coefficients, there are many possible combinations of source and transport which could make the model unwieldy. Anyone developing a P Index using this approach should apply judgment as to which components are most important for the conditions within their jurisdiction, and which can be safely excluded. This will mean that indexes will vary between jurisdictions, but if both are using the component structure the results should still be comparable. This structure also encourages an objective assessment of which components should be included or excluded, and a framework for explaining why there are differences across jurisdictional boundaries.

Key considerations in the development of a component P index are consistency of units, and ensuring that the weighting of each of the individual components is correct. Ignoring either of these details can result in a model that is highly skewed because one of the components is generating results on a different scale than the others, and so is off by an order of magnitude or more. One advantage of the component structure is that, while the models are not complex enough to generate P loadings from individual storm events, the results should correlate with water quality measurements over the annual time scale and so can be validated as to whether they meet the goal of being "directionally and magnitudinally correct" (Sharpley et al., 2012).

We will discuss the IROWC-P model as an example of the component structure in the Section "IROWC-P as an Example of P Loss Risk Assessment."

SETTING CATEGORIES FOR RISK OF P LOSS

The numbers generated by any index do not, without context, provide any useful information, so it is important to assign the results into categories. This will allow users to quickly determine if they are at a high or low risk. For risk indicators that cover a broad area, it will also facilitate visual representation of the data on a map. There are a number of ways to define risk categories,

but two of the most common are to relate the categories to environmental outcomes (or reduction targets), or to use the frequency distribution of the index results to base the categories on percentiles.

The idea of classifying risk categories by environmental outcomes is attractive, but it overestimates the model's ability to quantify the losses from the landscape. There is also a danger that the choice of thresholds, even if the model were accurate, would be set so that the highest level of risk would not exceed environmental outcomes, even though the majority of the catchment is already below that level. In this case, the categories could provide an unrealistically harsh perception of the performance of farmers in a region.

Another approach is to use the frequency distribution to separate the risk categories, either as even quartiles or quintiles, or using a skewed distribution of the percentiles. This latter approach can use the cumulative risk at each level to inform the setting of the categories, since a few very large scores at the top of the range can have a much greater impact than a large number of low scores. This focuses attention on the relatively few operations that contribute disproportionately to environmental impact, and allows for continuous improvement as the frequency distribution moves downward. It depends, however, on knowing the distribution of index scores. Since this is not possible before the use of the index is widespread, the distribution can be estimated by using Monte Carlo simulations as a proxy.

IROWC-P AS AN EXAMPLE OF P LOSS RISK ASSESSMENT

Developing models to assess the risk of P loss from terrestrial systems is a balancing act between representing all of the source and transport processes as accurately as possible, the availability of input data at an appropriate level of detail to run a process-based model, and the complexity of the model, at a scale that is useful to the end user (Sharpley et al., 2002). One of the key challenges is that individual source and transport factors have been quantified through research, but there are few studies that account for the relative weighting of these factors in describing P losses at the field or landscape scale under varying soil types, topography, vegetation, P inputs and weather. Osmond et al. (2012b) found that P Indices developed using professional judgment about local conditions were more accurate at predicting runoff water quality than process based models. This may stem, in part, from imperfect representation of P loss processes in the model, or from over-parameterization where the errors associated with input variables propagate through the model to skew the final results (Vadas et al., 2013).

IROWC-P is one of the agri-environmental indicators developed by Agriculture and Agri-Food Canada (AAFC) to provide information on the status and trends of environmental performance by Canadian agricultural producers (Reid et al., 2016). Although this indicator operates at a regional rather than field scale – the basic spatial unit is a Soil Landscape of Canada (SLC) polygon, or 1:1,000,000 scale – the calculations used to estimate risk of P loss are parallel to those used in a field scale P Index. Each SLC polygon is treated as a virtual field, with input parameters to the model estimated from publicly available data. The version used in the last report was a multiplicative approach to P risk assessment, with a single transport coefficient, but it is currently being updated to a component model. The discussion in this paper will focus on the updated version, and on the algorithms used for determining risk of P loss but not the estimation procedures for the input parameters.

IROWC-P first determines the risk of P loss at the edge of field, and then applies a delivery ratio to estimate the proportion of this loss that reaches surface water. The source and transport factors for each of the components are summarized in **Table 1**.

BioAvailable Particulate P

The developers of this indicator chose to express the results in terms of bioavailable P rather than total P to provide better information on the potential impact of P loss in different forms on water quality. The sediment loss to the edge of field is derived from the water erosion component of the AAFC Soil Erosion indicator (Lobb et al., 2016), and the bioavailable portion of this sediment is predicted from the STP levels according to the method of Sharpley and Smith (1993). A P enrichment factor is also included to account for the increased P concentrations in eroded sediment relative to the bulk soil in the field, particularly under small runoff events (Sharpley, 1980). The product of this equation is multiplied by a scaling factor to align the units of the outputs with the rest of the components in IROWC-P (Reid et al., 2016).

Soil erosion models combine sediment source and transport to predict delivery of sediment to the bottom of a slope or, in this case, to the edge of a field. A separate transport modifier is not required, except where tile drains are present. The tile drains reduce the amount of surface runoff, diverting that water into the tile drains, but also carrying the portion of the sediment that is carried with the portion of tile flow that has reached the tile through macropores rather than soil matrix flow. The partitioning of water between surface runoff and tile flow is predicted using the hydrology module of the DNDC model (Kröbel et al., 2010; Dutta et al., 2016; Guest et al., 2017), and the fraction of tile flow from macropores is derived from the probability of burrow flow (through anecic worm burrows) (Dadfar et al., 2010a) and crack flow (Dadfar et al., 2010b). In general, the macropore flow is highest for the fine and medium textured soils, and lowest for the coarse textured soils. Since there is compelling evidence that macropore flow represents diverted surface runoff, and that the ratio of dissolved to particulate P in macropore flow tracks that in surface runoff (Radcliffe et al., 2009; Reid et al., 2012), this partitioning of water into surface runoff, macropore tile flow and matrix tile flow will be used for all of the components.

Dissolved P Desorbed From Soil

This component represents the release of dissolved P from the soil surface as it interacts with runoff water. Water Extractable P (WEP), derived from the STP values, is used as an indicator of the amount of P that could be desorbed from the soil surface. This is multiplied by an extraction coefficient to convert the

TABLE 1 | Source and transport components in IROWC-P.

Component	Source	Transport
BioAvailable Particulate P (BAPP) (annual)	T/ha eroded sediment from WatERI indicator * STP (Mehlich-3 equivalent) * enrichment ratio	Transport to edge of field is implicit in the WatERI calculations. Where tile drains are present, surface runoff is reduced and BAPP is partitioned to tile flow in proportion to macropore flow
Dissolved P desorbed from soil (annual)	Soil WEP (derived from STP) * extraction coefficient * stratification factor	Runoff volume (mm * 10,000), predicted for soil types from DNDC hydrology module Where tile drains are present, surface runoff is reduced and DP is partitioned to macropore flow fraction of tile flow
Dissolved P from applied fertilizer (growing season)	Applied P rate (GS) * application method factor	(GS runoff/GS precipitation) * P distribution factor for fertilizer (PDFfert) Where tile drains are present, this quantity is multiplied by the (surface runoff with tiles/total surface runoff) to determine the surface runoff contribution, and by (macropore flow volume/total surface runoff) to determine the tile contribution
Dissolved P from applied fertilizer (non-growing season)	Applied P rate (NGS) * application method factor	Same as for growing season, except runoff/precipitation ratio and PDF are both calculated for non-growing season conditions
Dissolved P from applied manure (growing season)	Applied P rate (GS) * application method factor * P availability	(GS runoff/GS precipitation) * P distribution factor for manure (PDFman) Where tile drains are present, this quantity is multiplied by the (surface runoff with tiles/total surface runoff) to determine the surface runoff contribution, and by (macropore flow volume/total surface runoff) to determine the tile contribution
Dissolved P from applied manure (non-growing season)	Applied P rate (NGS) * application method factor * P availability	Same as for growing season, except runoff/precipitation ratio and PDF are both calculated for non-growing season conditions
Dissolved P from over-winter plant residue (non-growing season)	Plant biomass * P content * labile P fraction * release of labile P into soluble P (function of time after freezing)	Rainfall > 3 mm (movement of soluble P from residue); partitioning of desorbed P between infiltration and runoff using the PDFfert

potentially desorbed P into actual dissolved P (Wang et al., 2010), and modified by a stratification factor based on tillage system to account for the build-up of P in the shallow surface layer that runoff water interacts with (Sharpley, 1985).

The transport factor for this component is the total volume of runoff, as predicted by the DNDC hydrology module (Dutta et al., 2016; Guest et al., 2017). This is assessed on an annual basis, since the pool of P available for desorption is very large relative to the actual losses and so does not vary over the year. Adjustments for tile drains are the same as for BAPP.

Dissolved P From Applied Fertilizer

Because the risk of P loss from applied nutrients is highest immediately after application and declines quickly as they interact with the soil (Vadas et al., 2008), both fertilizer and manure applications are assessed separately for the growing- and non-growing-seasons. Under Canadian climatic conditions, the partitioning of water between infiltration and runoff is markedly different between these two periods (Liu K. et al., 2013; Mahmood et al., 2017). The source factor for this component is the rate of fertilizer P applied, modified by an application factor to account for the proportion of fertilizer remaining on the soil surface. Incorporation has been shown to effectively shield the applied P from immediate losses (Sharpley, 1985), but there will always be a small amount remaining at the surface so the application factor estimates these proportions for different application systems.

The concentration of P in runoff water from applied fertilizer will be high relative to the P desorbed from soil, so the transport factor needs to account for the soil as a sink for this dissolved P. IROWC-P follows the method of Vadas et al. (2008), using a P distribution factor (PDF) multiplied by the ratio of runoff:precipitation to partition the applied P between adsorption by the soil and loss in runoff. The proportion of precipitation that runs off is much greater in the non-growing season under Canadian climatic conditions, so differentiating between P applications in the growing- versus non-growing-season is important for predicting risk of P loss. As noted above, the impact of tile drainage is predicted using the same algorithms as for BAPP.

Dissolved P From Applied Manure

The prediction of P losses from applied manure parallels that of applied fertilizer, with three exceptions. The source factor is based on the water extractable P in the manure, so only a portion of the total P applied is considered to be available for loss. The application factors are also modified to reflect the difficulty in achieving complete incorporation of the large volumes normally associated with manure application. On the transport side, the PDF is specific to manure (Vadas et al., 2004), reflecting the difference in the timing of P release from manure compared to fertilizer.

Dissolved P From Over-Wintering Vegetation

This component only applies to the non-growing season, from the time of killing frost until the spring freshet prior to the next growing season. The source factor for this component is the labile, or easily degraded, portion of the P contained in the above-ground portion of plant residues at the time of killing frost in the fall. This is calculated as the plant biomass times the P concentration times the labile fraction, which is assumed to be 0.50 after Damon et al. (2014). An exponential decay function is used to estimate the conversion of labile P to soluble P within the plant biomass from freezing until the P is leached

out by rainfall. These calculations can be applied to crop residue remaining in the field post-harvest (in which case the harvest date is used as a proxy for plant maturity and the beginning of plant senescence) or for forage regrowth. The current version of the indicator is not assessing the P contributions from cover crops because of insufficient data regarding the area of cover crops, the biomass production and the P concentration, although it would be desirable to include this in future versions.

The transport of P from the frozen plant residues is in two steps, with the first being the leaching of the P out of the plant residue. It is assumed that rainfall must be >3 mm to initiate this process, or that the residue is in contact with meltwater from the accumulated snowpack, and that the dissolution of the soluble P in the residue follows a similar pattern to that of fertilizer P as described in Vadas et al. (2008), but with the duration of rainfall used by Vadas et al. (2008) replaced by the accumulated rainfall. The dissolved P that was then entrained in the runoff water was distributed between soil adsorption and runoff using the PDF for fertilizer (Vadas et al., 2009). Melt water runoff that occurs on frozen soils will carry much of the over-winter accumulation of soluble P from the field, because of limited infiltration.

Aggregate Risk of P Loss

Since the components are designed so that all of the outputs are at the same scale, the total risk of P loss at the edge of field is calculated by summing the values for each of the components.

Delivery Ratio From Edge of Field to Surface Water

To assess the potential impact of agricultural P losses on surface water quality, it is necessary to estimate how much of the P leaving the edge of a field actually reaches surface water. The underlying assumption in assessing connectivity to surface water is that there is mitigation of P losses with greater transport distance to surface water. Processes that could contribute to this mitigation include:

- infiltration of runoff water or trapping of water in ponds (Li et al., 2011), so less water (with its associated P load) reaches surface water, or
- trapping of sediment (Leguédois et al., 2008) or adsorption of dissolved P to the underlying soil (Sharpley et al., 1981), so the concentration of P in runoff water is reduced, or
- both operating simultaneously.

These processes are not well quantified, and have seldom been included in P transport models beyond rudimentary estimates. Gburek et al. (2006), for example, estimated the proportion of the landscape that was contributing surface runoff from the proportion of precipitation that contributed to increased streamflow during storm events. Other models have simply assumed a delivery ratio based on the measured P loading at a watershed scale, relative to modeled or measured P losses within fields in the watershed, but without any understanding in the processes involved in P delivery from the field to the stream.

The AAFC Soil Erosion indicator (Lobb et al., 2016) includes calculations for sediment reaching surface water based on the stream density (defined as the kilometers of shoreline per square kilometer of watershed), and the landform type and slope within the watershed. This has been modified to assume the greatest mitigation of BAPP losses in overland runoff, less mitigation of dissolved P in surface runoff, and no mitigation of either BAPP or dissolved P in tile flow.

Additional Considerations

Phosphorus losses in sub-surface lateral flow are not included as part of the IROWC-P model. The conditions favorable for this type of P transport from Canadian agricultural land are considered to be rare enough that ignoring it will not introduce a significant source of error in the estimates of P loss.

One of the desired outcomes from this indicator is an assessment of the impact of changes in management on the risk of P loss from agricultural landscapes, but extreme weather events can completely eclipse the effect of management changes in any given year. This could be addressed by using average weather conditions in model runs, so that regional variations in climate are accounted for but annual weather is de-emphasized. The drawback to this approach is that responses to weather conditions non-linear and losses from areas with more variable weather may be underestimated. Calculations for IROWC-P are conducted using weather data from each year within the 30-year window that makes up the climate norm, and then the results averaged.

GAPS AND NEXT STEPS

While the authors consider this revision of IROWC-P to be a significant advance in accurately representing the geographic distribution and temporal trends in the relative risk of P losses from Canadian agricultural land, there are still some areas in need of improvement. The individual components have been derived from a large body of scientific research, but not all of them have been validated for Canadian conditions. The aggregate values for edge of field losses are also in need of validation to ensure that the relative contribution from each of the components has been captured correctly. This model does not, nor was it intended to, provide a quantitative estimate of P loss from agricultural land during individual runoff events, so validation needs to be based on whether the relative P losses from contrasting fields matches the relative predicted risk of P loss, over an annual period or longer.

As previously mentioned, the delivery ratios from edge of field to surface water are an area of significant uncertainty. The scope of this issue means that it will require a large research effort to adequately address. The mandate to conduct this research, however, or the funding availability, often falls between the areas of responsibility of organizations with a primary focus on land management, and those focused on water quality impacts.

A perennial challenge for any regional or national scale indicator is the availability of input data to run the models. We do not know what each individual land manager is doing on their properties, so average or typical values are inferred from public data sources. In the case of IROWC-P,

these values are based on interpretation of data from the Census of Agriculture, supplemented by data from surveys (Reid et al., 2016), but it is recognized that the information about nutrient management practices is extremely limited. In the United States, the Conservation Effects Assessment Program (CEAP, 2011) has addressed this issue through detailed interviews with a stratified sample of farmers within a region, but this requires a large resource commitment, and while it provides a more complete picture of individual farmer activities there is limited opportunity to assess how well this represents the population as a whole. We can expect future improvements in some of the input data using remote sensing, which can detect topography and soil moisture, and enumerate areas of different crops or amount of soil cover, but this will be of little use for capturing data about management. Better methods of data collection will improve the accuracy of the model predictions, but they will need to meet the multiple requirements of protecting individual privacy, ensuring accuracy of the collected data, and being economical to collect and store.

The focus to this point has been on understanding the spatial variation in risk of P loss to surface water, and how it is changing over time. The indicator has been designed in such a way, however, that data for individual crops or farming systems can be extracted, although it will have to be at a coarser spatial scale to be meaningful. This creates the opportunity to work with commodity organizations to generate intensity based indicators of risk of P loss per unit of production. An additional benefit to this type of assessment might be the ability for individual farmers to compare the performance of their own farms to regional averages.

SUMMARY AND CONCLUSION

Phosphorus loss from a landscape is not a single process, but rather is the aggregate of a number of different source × transport interactions. Which of these components will dominate in a particular area, or on a particular farm, is a function of climate, soils, topography, and both long- and short-term management. The choice of options to mitigate these losses will, necessarily, be equally complex. It also renders useless the application of static coefficients to predict the effectiveness of mitigation practices, since the effectiveness of each practice will depend on the conditions where it is applied.

Progress is being made in developing risk indicators that address this complexity in a meaningful way, although much work remains to be done. IROWC-P has been presented as one example of how this could be approached, but other examples include models developed in North Carolina (N.C. PLAT Committee, 2005) and Wisconsin (Vadas et al., 2013). It is likely that selecting the best features from each of these component models for the individual conditions within a given jurisdiction will result in the most accurate representation of P loss risk.

AUTHOR CONTRIBUTIONS

The majority of the writing in this paper was contributed by KR, with significant additions from KS and BM.

FUNDING

Research and development activities described in this paper were funded as part of the Agriculture and Agri-Food Canada internal Research, Development and Transfer project funds.

ACKNOWLEDGMENTS

The authors would like to acknowledge the contributions of all of the scientists and professionals who contributed to the development of the Sustainability Metrics for Canadian Agriculture, as well as the programs which preceded it (Agri-Environmental Indicators for Canadian Agriculture, and the National Agri-Environmental Standards Initiative).

REFERENCES

Allaire, S. E., Roulier, S., and Cessna, A. J. (2009). Quantifying preferential flow in soils: a review of different techniques. *J. Hydrol.* 378, 179–204. doi: 10.1016/j.jhydrol.2009.08.013

Allen, B. L., Mallarino, A. P., Lore, J. F., Baker, J. L., and Haq, M. U. (2012). Phosphorus lateral movement through subsoil to subsurface tile drains. *Soil Sci. Soc. Am. J.* 76, 710–717. doi: 10.2136/sssaj2011.0150

Anderson, K. A., and Downing, J. A. (2006). Dry and wet atmospheric deposition of nitrogen, phosphorus and silicon in an agricultural region. *Water Air Soil Pollut.* 176, 351–374. doi: 10.1007/s11270-006-9172-4

Auer, M. T., Tomlinson, L. M., Higgins, S. N., Malkin, S. Y., Howell, E. T., and Bootsma, H. A. (2010). Great lakes *Cladophora* in the 21st century: same algae—different ecosystem. *J. Great Lakes Res.* 36, 248–255. doi: 10.1016/j.jglr.2010.03.001

Baker, D., Richards, R., and Crumrine, J. (2007). *Increasing Dissolved Phosphorus Loading to Lake Erie from Agricultural Watersheds: a Conservation Tillage Trade-Off.* Tampa, FL: Soil and Water Conservation Society.

Baker, D. B., Confesor, R., Ewing, D. E., Johnson, L. T., Kramer, J. W., and Merryfield, B. J. (2014). Phosphorus loading to lake erie from the Maumee, Sandusky and Cuyahoga rivers: the importance of bioavailability. *J. Great Lakes Res.* 40, 502–517. doi: 10.1016/j.jglr.2014.05.001

Ball Coelho, B., Bruin, A. J., Staton, S., and Hayman, D. (2010). Sediment and nutrient contributions from subsurface drains and point sources to an agricultural watershed. *Air Soil Water Res.* 3, 1–21. doi: 10.4137/ASWR.S4471

Barlow-Busch, L., Baulch, H. M., and Taylor, W. D. (2006). Phosphate uptake by seston and epilithon in the Grand River, southern Ontario. *Aquat. Sci.* 68, 181–192. doi: 10.1007/s00027-006-0806-9

Bechmann, M. E., Kleinman, P. J. A., Sharpley, A. N., and Saporito, L. S. (2005). Freeze–thaw effects on phosphorus loss in runoff from manured and catch-cropped soils. *J. Environ. Qual.* 34, 2301–2309. doi: 10.2134/jeq2004.0415

Beven, K., and Germann, P. (2013). Macropores and water flow in soils revisited. *Water Resour. Res.* 49, 3071–3092. doi: 10.1002/wrcr.20156

Blann, K. L., Anderson, J. L., Sands, G. R., and Vondracek, B. (2009). Effects of agricultural drainage on aquatic ecosystems: a review. *Crit. Rev. Environ. Sci. Technol.* 39, 909–1001. doi: 10.1080/10643380801977966

Borda, T., Celi, L., Bünemann, E. K., Oberson, A., Frossard, E., and Barberis, E. (2014). Fertilization strategies affect phosphorus forms and release from soils and suspended solids. *J. Environ. Qual.* 43, 1024–1031. doi: 10.2134/jeq2013.11.0436

Bouffard, D., Ackerman, J. D., and Boegman, L. (2013). Factors affecting the development and dynamics of hypoxia in a large shallow stratified lake: hourly to seasonal patterns. *Water Resour. Res.* 49, 2380–2394. doi: 10.1002/wrcr.20241

Bunting, L., Leavitt, P. R., Simpson, G. L., Wissel, B., Laird, K. R., Cumming, B. F., et al. (2016). Increased variability and sudden ecosystem state change in Lake Winnipeg, Canada, caused by 20th century agriculture. *Limnol. Oceanogr.* 61, 2090–2107. doi: 10.1002/lno.10355

Butler, D. M., Franklin, D. H., Ranells, N. N., Poore, M. H., and Green, J. T. (2006). Ground cover impacts on sediment and phosphorus export from manured riparian pasture. *J. Environ. Qual.* 35, 2178–2185. doi: 10.2134/jeq2005.0351

CEAP. (2011). *Assessment of the Effects of Conservation Practices on Cultivated Cropland in the Great Lakes Region*. Washington, DC: USDA.

Chardon, W. J., and Schoumans, O. F. (2002). *Phosphorus Losses from Agricultural Soils: Processes at the Field Scale*. Wageningen: Alterra.

Chikhaoui, M., Madramootoo, C. A., Eastman, M., and Michaud, A. (2008). "Estimating preferential flow to agricultural tile drains," in *Proceedings of the 2008 ASABE Annual International Meeting*, Providence.

Committee, N. C. P. L. A. T. (2005). *North Carolina Phosphorus Loss Assessment: I. Model Description and II. Scientific Basis and Supporting Literature, Department of Soil Science*. Raleigh, NC: North Carolina State University.

Condron, L. M., and Newman, S. (2011). Revisiting the fundamentals of phosphorus fractionation of sediments and soils. *J. Soils Sediments* 11, 830–840. doi: 10.1007/s11368-011-0363-2

Conroy, J. D., Kane, D. D., Briland, R. D., and Culver, D. A. (2014). Systemic, early-season *Microcystis* blooms in western Lake Erie and two of its major agricultural tributaries (Maumee and Sandusky rivers). *J. Great Lakes Res.* 40, 518–523. doi: 10.1016/j.jglr.2014.04.015

Dadfar, H., Allaire, S. E., Bochove, E. V., Denault, J.-T., Thériault, G., and Charles, A. (2010a). Likelihood of burrow flow in Canadian agricultural lands. *J. Hydrol.* 386, 142–159. doi: 10.1016/j.jhydrol.2010.03.016

Dadfar, H., Allaire, S. E., De Jong, R., van Bochove, E., Denault, J.-T., Theriault, G., et al. (2010b). Development of a method for estimating the likelihood of crack flow in Canadian agricultural soils at the landscape scale. *Can. J. Soil Sci.* 90, 129–149. doi: 10.4141/CJSS09066

Dahlke, H. E., Easton, Z. M., Fuka, D. R., Lyon, S. W., and Steenhuis, T. S. (2009). Modelling variable source area dynamics in a CEAP watershed. *Ecohydrology* 2, 337–349. doi: 10.1002/eco.58

Damon, P. M., Bowden, B., Rose, T., and Rengel, Z. (2014). Crop residue contributions to phosphorus pools in agricultural soils: a review. *Soil Biol. Biochem.* 74, 127–137. doi: 10.1016/j.soilbio.2014.03.003

Depew, D. C., Houben, A. J., Guildford, S. J., and Hecky, R. E. (2011). Distribution of nuisance *Cladophora* in the lower Great lakes: patterns with land use, near shore water quality and dreissenid abundance. *J. Great Lakes Res.* 37, 656–671. doi: 10.1016/j.jglr.2011.08.011

DePinto, J. V., Young, T. C., and Martin, S. C. (1981). Algal-available phosphorus in suspended sediments from lower great lakes tributaries. *J. Great Lakes Res.* 7, 311–325. doi: 10.1016/S0380-1330(81)72059-8

Dosskey, M. G., Helmers, M. J., Eisenhauer, D. E., Franti, T. G., and Hoagland, K. D. (2002). Assessment of concentrated flow through riparian buffers. *J. Soil Water Conserv.* 57, 336–343.

Dosskey, M. G., Vidon, P., Gurwick, N. P., Allan, C. J., Duval, T. P., and Lowrance, R. (2010). The role of riparian vegetation in protecting and improving chemical water quality in streams1. *JAWRA J. Am. Water Res. Assoc.* 46, 261–277. doi: 10.1111/j.1752-1688.2010.00419.x

Dougherty, W. J., Nash, D. M., Cox, J. W., Chittleborough, D. J., and Fleming, N. K. (2008). Small-scale, high-intensity rainfall simulation under-estimates natural runoff P concentrations from pastures on hill-slopes. *Soil Res.* 46, 694–702. doi: 10.1071/SR07232

Dunkerley, D. (2017). An approach to analysing plot scale infiltration and runoff responses to rainfall of fluctuating intensity. *Hydrol. Process.* 31, 191–206. doi: 10.1002/hyp.10990

Dutta, B., Grant, B. B., Congreves, K. A., Smith, W. N., Wagner-Riddle, C., VanderZaag, A. C., et al. (2017). Characterising effects of management practices, snow cover, and soil texture on soil temperature: model development in DNDC. *Biosyst. Eng.* 168, 54–72. doi: 10.1016/j.biosystemseng.2017.02.001

Dutta, B., Smith, W. N., Grant, B. B., Pattey, E., Desjardins, R. L., and Li, C. (2016). Model development in DNDC for the prediction of evapotranspiration and water use in temperate field cropping systems. *Environ. Model. Softw.* 80, 9–25. doi: 10.1016/j.envsoft.2016.02.014

Eastman, M., Gollamudi, A., Stämpfli, N., Madramootoo, C. A., and Sarangi, A. (2010). Comparative evaluation of phosphorus losses from subsurface and naturally drained agricultural fields in the Pike River watershed of Quebec. Canada. *Agric. Water Manag.* 97, 596–604. doi: 10.1016/j.agwat.2009.11.010

Easton, Z. M., Fuka, D. R., Walter, M. T., Cowan, D. M., Schneiderman, E. M., and Steenhuis, T. S. (2008). Re-conceptualizing the soil and water assessment tool (SWAT) model to predict runoff from variable source areas. *J. Hydrol.* 348, 279–291. doi: 10.1016/j.jhydrol.2007.10.008

Elliott, J. (2013). Evaluating the potential contribution of vegetation as a nutrient source in snowmelt runoff. *Can. J. Soil Sci.* 93, 435–443. doi: 10.4141/cjss2012-050

Ellison, M. E., and Brett, M. T. (2006). Particulate phosphorus bioavailability as a function of stream flow and land cover. *Water Res.* 40, 1258–1268. doi: 10.1016/j.watres.2006.01.016

Fang, F., Brezonik, P. L., Mulla, D. J., and Hatch, L. K. (2002). Estimating runoff phosphorus losses from calcareous soils in the Minnesota River Basin. *J. Environ. Qual.* 31, 1918–1929. doi: 10.2134/jeq2002.1918

Flanagan, D. C., Gilley, J. E., and Franti, T. G. (2007). Water Erosion Prediction Project (WEPP): development history, model capabilities, and future enhancements. *Trans. ASABE* 50, 1603–1612. doi: 10.13031/2013.23968

Foster, G. R., Toy, T. E., and Renard, K. G. (2003). "Comparison of the USLE, RUSLE1.06c, and RUSLE2 for application to highly disturbed lands," in *Proceedings of the 1st Interagency Conference on Research in Watersheds*, Washington, DC.

Fox, C. A., Jarvis, I., Behan-Pelletier, V., Dalpe, Y., Clapperton, J., Prevost, D., et al. (2008). "Progress towards developing a soil biodiversity indicator for Canada," in *Agricultural Impacts on Soil Erosion and Soil Biodiversity: Developing Indicators for Policy Analysis*, ed. R. Francaviglia (Paris: OECD).

Garen, D. C., and Moore, D. S. (2005). Curve number hydrology in water quality modeling: uses, abuses and future directions. *JAWRA J. Am. Water Resour. Assoc.* 41, 377–388. doi: 10.1111/j.1752-1688.2005.tb03742.x

Gburek, W. J., Drungil, C. C., Srinivasan, M. S., Needelman, B. A., and Woodward, D. E. (2002). Variable-source-area controls on phosphorus transport: bridging the gap between research and design. *J. Soil Water Conserv.* 57, 534–543.

Gburek, W. J., Sharpley, A. N., and Beegle, D. B. (2006). *Incorporation of Variable Source Area Hydrology in the Phosphorus Index: a Paradigm for Improving Relevancy of Watershed Research*. Washington,DC: USDA.

Gburek, W. J., Sharpley, A. N., Heathwaite, L., and Folmar, G. J. (2000). Phosphorus management at the watershed scale: a modification of the phosphorus index. *J. Environ. Qual.* 29, 130–144. doi: 10.2134/jeq2000.00472425002900010017x

Glæsner, N., Kjaergaard, C., Rubæk, G. H., and Magid, J. (2013). Relation between soil P test values and mobilization of dissolved and particulate P from the plough layer of typical Danish soils from a long-term field experiment with applied P fertilizers. *Soil Use Manag.* 29, 297–305. doi: 10.1111/sum.12060

Guest, G., Kröbel, R., Grant, B., Smith, W., Sansoulet, J., Pattey, E., et al. (2017). Model comparison of soil processes in eastern Canada using DayCent, DNDC and STICS. *Nutr. Cycling Agroecosyst.* 109, 211–232. doi: 10.1007/s10705-017-9880-8

Haygarth, P. M., Condron, L. M., Heathwaite, A. L., Turner, B. L., and Harris, G. P. (2005). The phosphorus transfer continuum: linking source to impact with an interdisciplinary and multi-scaled approach. *Sci. Total Environ.* 344, 5–14. doi: 10.1016/j.scitotenv.2005.02.001

Heathwaite, L., Haygarth, P., Matthews, R., Preedy, N., and Butler, P. (2005). Evaluating colloidal phosphorus delivery to surface waters from diffuse agricultural sources. *J. Environ. Qual.* 34, 287–298.

Howell, E. T., and Dove, A. (2017). Chronic nutrient loading from Lake Erie affecting water quality and nuisance algae on the St. Catharines shores of Lake Ontario. *J. Great Lakes Res.* 43, 899–915. doi: 10.1016/j.jglr.2017.06.006

Jarvie, H. P., Johnson, L. T., Sharpley, A. N., Smith, D. R., Baker, D. B., Bruulsema, T. W., et al. (2017). Increased soluble phosphorus loads to lake Erie: unintended consequences of conservation practices? *J. Environ. Qual.* 46, 123–132. doi: 10.2134/jeq2016.07.0248

Jarvie, H. P., Sharpley, A. N., Withers, P. J. A., Scott, J. T., Haggard, B. E., and Neal, C. (2013). Phosphorus mitigation to control river eutrophication: murky waters, inconvenient truths, and "Postnormal" science. *J. Environ. Qual.* 42, 295–304. doi: 10.2134/jeq2012.0085

Jarvis, N., Koestel, J., and Larsbo, M. (2016). Understanding preferential flow in the vadose zone: recent advances and future prospects. *Vadose Zone J.* 15, 1–11. doi: 10.2136/vzj2016.09.0075

Johannesson, G. H., Lauzon, J., Crolla, A., Gilroyed, B., Vanderzaag, A., and Gordon, R. (2017). Impact of manure storage conditions and time on decomposition of and losses from liquid dairy manure stored in a temperate climate. *Can. J. Soil Sci.* 98, 148–160. doi: 10.1139/CJSS-2017-0083

Joosse, P. J., and Baker, D. B. (2011). Context for re-evaluating agricultural source phosphorus loadings to the great Lakes. *Can. J. Soil Sci.* 91, 317–327. doi: 10.4141/cjss10005

Karahan, G., and Erşahin, S. (2017). Relating macropore flow to soil parametric and morphological variables. *Soil Sci. Soc. Am. J.* 81, 1014–1024. doi: 10.2136/sssaj2016.10.0327

Kerr, J. M., DePinto, J. V., McGrath, D., Sowa, S. P., and Swinton, S. M. (2016). Sustainable management of great Lakes watersheds dominated by agricultural land use. *J. Great Lakes Res.* 42, 1252–1259. doi: 10.1016/j.jglr.2016.10.001

King, K. W., Fausey, N. R., and Williams, M. R. (2014). Effect of subsurface drainage on streamflow in an agricultural headwater watershed. *J. Hydrol.* 519(Part A), 438–445. doi: 10.1016/j.jhydrol.2014.07.035

King, K. W., Williams, M. R., Macrae, M. L., Fausey, N. R., Frankenberger, J., Smith, D. R., et al. (2015). Phosphorus transport in agricultural subsurface drainage: a review. *J. Environ. Qual.* 44, 467–485. doi: 10.2134/jeq2014.04.0163

Kinnell, P. I. A. (2008). Discussion: misrepresentation of the USLE in 'Is sediment delivery a fallacy?'. *Earth Surf. Process. Landf.* 33, 1627–1629. doi: 10.1002/esp.1629

Kirchmann, H., and Wessling, J. (2017). Kinetics of inorganic and organic P release from red clover (*Trifolium pratense* L.) and ryegrass *(Lolium multiflorum L.*) upon frost or drying. *Acta Agric. Scand. B Soil Plant Sci.* 67, 693–696. doi: 10.1080/09064710.2017.1339823

Kleinman, P. J. A., Allen, A. L., Needelman, B. A., Sharpley, A. N., Vadas, P. A., Saporito, L. S., et al. (2007). Dynamics of phosphorus transfers from heavily manured coastal plain soils to drainage ditches. *J. Soil Water Conserv.* 62, 225–235.

Kleinman, P. J. A., Church, C., Saporito, L. S., McGrath, J. M., Reiter, M. S., Allen, A. L., et al. (2015a). Phosphorus leaching from agricultural soils of the Delmarva Peninsula. USA. *J. Environ. Qual.* 44, 524–534. doi: 10.2134/jeq2014.07.0301

Kleinman, P. J. A., Smith, D. R., Bolster, C. H., and Easton, Z. M. (2015b). Phosphorus fate, management, and modeling in artificially drained systems. *J. Environ. Qual.* 44, 460–466. doi: 10.2134/jeq2015.02.0090

Kleinman, P. J. A., Sharpley, A. N., Wolf, A. M., Beegle, D. B., Elliott, H. A., Weld, J. L., et al. (2006). Developing an environmental manure test for the phosphorus index. *Commun. Soil Sci. Plant Anal.* 37, 2137–2155. doi: 10.1080/00103620600817242

Kleinman, P. J. A., Sharpley, A. N., Wolf, A. M., Beegle, D. B., and Moore, P. A. (2002). Measuring water-extractable phosphorus in manure as an indicator of phosphorus in runoff. *Soil Sci. Soc. Am. J.* 66, 2009–2015. doi: 10.2136/sssaj2002.2009

Kleinman, P. J. A., Wolf, A. M., Sharpley, A. N., Beegle, D. B., and Saporito, L. S. (2005). Survey of water-extractable phosphorus in livestock manures. *Soil Sci. Soc. Am. J.* 69, 701–708. doi: 10.2136/sssaj2004.0099

Koestel, J. K., Moeys, J., and Jarvis, N. J. (2011). Meta-analysis of the effects of soil properties, site factors and experimental conditions on preferential solute transport. *Hydrol. Earth Syst. Sci. Discuss.* 8, 10007–10052. doi: 10.5194/hessd-8-10007-2011

Kröbel, R., Sun, Q., Ingwersen, J., Chen, X., Zhang, F., Müller, T., et al. (2010). Modelling water dynamics with DNDC and DAISY in a soil of the North China Plain: a comparative study. *Environ. Model. Softw.* 25, 583–601. doi: 10.1016/j.envsoft.2009.09.003

Leguédois, S., Ellis, T. W., Hairsine, P. B., and Tongway, D. J. (2008). Sediment trapping by a tree belt: processes and consequences for sediment delivery. *Hydrol. Process.* 22, 3523–3534. doi: 10.1002/hyp.6957

Lemunyon, J. L., and Gilbert, R. G. (1993). The concept and need for a phosphorus assessment tool. *J. Prod. Agric.* 6, 483–486. doi: 10.2134/jpa1993.0483

Li, S., Elliott, J. A., Tiessen, K. H. D., Yarotski, J., Lobb, D. A., and Flaten, D. N. (2011). The effects of multiple beneficial management practices on hydrology and nutrient losses in a small watershed in the canadian prairies. *J. Environ. Qual.* 40, 1627–1642. doi: 10.2134/jeq2011.0054

Lin, P., and Guo, L. (2016). Dynamic changes in the abundance and chemical speciation of dissolved and particulate phosphorus across the river-lake interface in southwest Lake Michigan. *Limnol. Oceanogr.* 61, 771–789. doi: 10.1002/lno.10254

Little, J. L., Nolan, S. C., Casson, J. P., and Olson, B. M. (2007). Relationships between soil and runoff phosphorus in small alberta watersheds. *J. Environ. Qual.* 36, 1289–1300. doi: 10.2134/jeq2006.0502

Liu, J., Khalaf, R., Ulén, B., and Bergkvist, G. (2013). Potential phosphorus release from catch crop shoots and roots after freezing-thawing. *Plant Soil* 371, 543–557. doi: 10.1007/s11104-013-1716-y

Liu, K., Elliott, J. A., Lobb, D. A., Flaten, D. N., and Yarotski, J. (2013). Critical factors affecting field-scale losses of nitrogen and phosphorus in spring snowmelt runoff in the Canadian prairies. *J. Environ. Qual.* 42, 484–496. doi: 10.2134/jeq2012.0385

Liu, K., Elliott, J. A., Lobb, D. A., Flaten, D. N., and Yarotski, J. (2014). Nutrient and sediment losses in snowmelt runoff from perennial forage and annual cropland in the Canadian prairies. *J. Environ. Qual.* 43, 1644–1655. doi: 10.2134/jeq2014.01.0040

Lobb, D. A., Li, S. T., and McConkey, B. G. (2016). "Soil Erosion," in *Environmental Sustainability of Canadian Agriculture: Agri-Environmental Indicator Report Series*, ed. W. Eilers (Ottawa: Agriculture and Agri-Food Canada), 79–100.

Lozier, T. M., Macrae, M. L., Brunke, R., and Van Eerd, L. L. (2017). Release of phosphorus from crop residue and cover crops over the non-growing season in a cool temperate region. *Agric. Water Manag.* 189, 39–51. doi: 10.1016/j.agwat.2017.04.015

Lyon, S. W., McHale, M. R., Walter, M. T., and Steenhuis, T. S. (2006). The impact of runoff generation mechanisms on the location of critical source areas. *J. Am. Water Resour. Assoc.* 42, 793–804. doi: 10.1111/j.1752-1688.2006.tb04493.x

Macrae, M. L., English, M. C., Schiff, S. L., and Stone, M. (2007). Intra-annual variability in the contribution of tile drains to basin discharge and phosphorus export in a first-order agricultural catchment. *Agric. Water Manag.* 92, 171–182. doi: 10.1016/j.agwat.2007.05.015

Mahmood, T. H., Pomeroy, J. W., Wheater, H. S., and Baulch, H. M. (2017). Hydrological responses to climatic variability in a cold agricultural region. *Hydrol. Process.* 31, 854–870. doi: 10.1002/hyp.11064

McGrath, J. M., Penn, C. J., and Coale, F. J. (2013). A modelling approach to the design of in situ agricultural drainage filters. *Soil Use Manag.* 29, 155–161. doi: 10.1111/j.1475-2743.2011.00381.x

Michaud, A. R., Lauzier, R., and Laverdiere, M. R. (2004). "Temporal and spatial variability in non-point source phosphorus in relation to agricultural production and terrestrial indicators: the Beaver Brook case study, Pike River basin, Quebec," in *Lake Champlain: Partnership and Research in the New Millenium*, ed. T. Mihuc (Dordrecht: Kluwer Academic/Plenum Pub), 97–121.

Miller, M. H., Beauchamp, E. G., and Lauzon, J. D. (1994). Leaching of nitrogen and phosphorus from the biomass of three cover crop species. *J. Environ. Qual.* 23, 267–272. doi: 10.2134/jeq1994.00472425002300020007x

National Phosphorus Research Project [NPRP] (2001). *Rain Simulator Protocols*. Heinsberg: SERA-17.

OLEPTF (2010). *Ohio Lake Erie Phosphorus Task Force Final Report*. Columbus, OH: Ohio Environmental Protection Agency.

Osmond, D., Meals, D., Hoag, D., Arabi, M., Luloff, A., Jennings, G., et al. (2012a). Improving conservation practices programming to protect water quality in agricultural watersheds: lessons learned from the National Institute of Food and Agriculture-Conservation Effects Assessment Project. *J. Soil Water Conserv.* 67, 122A–127A. doi: 10.2489/jswc.67.5.122A

Osmond, D., Sharpley, A., Bolster, C., Cabrera, M., Feagley, S., Lee, B., et al. (2012b). Comparing phosphorus indices from twelve southern U.S. states against monitored phosphorus loads from six prior southern studies. *J. Environ. Qual.* 41, 1741–1749. doi: 10.2134/jeq2012.0013

Pease, L. A., King, K. W., Williams, M. R., LaBarge, G. A., Duncan, E. W., and Fausey, N. R. (2017). Phosphorus export from artificially drained fields across the eastern corn belt. *J. Great Lakes Res.* 44, 43–53. doi: 10.1016/j.jglr.2017.11.009

Pomeroy, J. W., Gray, D. M., Brown, T., Hedstrom, N. R., Quinton, W. L., Granger, R. J., et al. (2007). The cold regions hydrological model: a platform for basing process representation and model structure on physical evidence. *Hydrol. Process.* 21, 2650–2667. doi: 10.1002/hyp.6787

Radcliffe, D. E., Freer, J., and Schoumans, O. (2009). Diffuse phosphorus models in the United States and Europe: their usages, scales, and uncertainties. *J. Environ. Qual.* 38, 1956–1967. doi: 10.2134/jeq2008.0060

Radcliffe, D. E., Reid, D. K., Blombäck, K., Bolster, C. H., Collick, A. S., Easton, Z. M., et al. (2015). Applicability of models to predict phosphorus losses in drained fields: a review. *J. Environ. Qual.* 44, 614–628. doi: 10.2134/jeq2014.05.0220

Reid, D. K. (2011). A modified Ontario P index as a tool for on-farm phosphorus management. *Can. J. Soil Sci.* 91, 455–466. doi: 10.4141/CJSS09088

Reid, D. K., Ball, B., and Zhang, T. Q. (2012). Accounting for the risks of phosphorus losses through tile drains in a P index. *J. Environ. Qual.* 41, 1720–1729. doi: 10.2134/jeq2012.0238

Reid, D. K., Western, W., Rounce, T., Bogdan, D., Churchill, J., van Bochove, E., et al. (2016). "Risk of water contamination by phosphorus (IROWC-P)," in *Environmental Sustainability of Canadian Agriculture: Agri-Environmental Indicator Report Series*, ed. W. Eilers (Ottawa: Agriculture and Agri Food Canada), 131–142.

Renard, K. G., Foster, G. R., Weesies, G. A., and Porter, J. P. (1995). RUSLE: revised universal soil loss equation. *J. Soil Water Conserv.* 46, 30–33.

Reutter, J. M., Ciborowski, J., DePinto, J., Bade, D., Baker, D., and Bridgeman, T. B. (eds). (2011). "Lake Erie nutrient loading and harmful algal blooms," in *Research Findings and Management Implications* (Columbus, OH: Final Report of the Lake Erie Millennium Network Synthesis Team).

Richards, J. E., Bates, T. E., and Sheppard, S. C. (1995). Changes in the forms and distribution of soil phosphorus due to long-term corn production. *Can. J. Soil Sci.* 75, 311–318. doi: 10.4141/cjss95-045

Roberson, T., Bundy, L. G., and Andraski, T. W. (2007) Freezing and drying effects on potential plant contributions to phosphorus in runoff. *J. Environ. Qual.* 36, 532–539. doi: 10.2134/jeq2006.0169

Scavia, D., David Allan, J., Arend, K. K., Bartell, S., Beletsky, D., Bosch, N. S., et al. (2014). Assessing and addressing the re-eutrophication of Lake Erie: central basin hypoxia. *J. Great Lakes Res.* 40, 226–246. doi: 10.1016/j.jglr.2014.02.004

Schneiderman, E. M., Steenhuis, T. S., Thongs, D. J., Easton, Z. M., Zion, M. S., Neal, A. L., et al. (2007). Incorporating variable source area hydrology into a curve-number-based watershed model. *Hydrol. Process.* 21, 3420–3430. doi: 10.1002/hyp.6556

Sharpley, A., Beegle, D., Bolster, C., Good, L., Joern, B., Ketterings, Q., et al. (2012). Phosphorus indices: why we need to take stock of how we are doing. *J. Environ. Qual.* 41, 1711–1719. doi: 10.2134/jeq2012.0040

Sharpley, A., Daniel, T., Sims, T., Lemunyon, J. L., Stevens, R., and Parry, R. (2003). *Agricultural Phosphorus and Eutrophication*. Washington, DC: United States Department of Agriculture.

Sharpley, A., and Moyer, B. (2000). Phosphorus forms in manure and compost and their release during simulated rainfall. *J. Environ. Qual.* 29, 1462–1469. doi: 10.2134/jeq2000.00472425002900050012x

Sharpley, A. N. (1980). The enrichment of soil phosphorus in runoff sediments. *J. Environ. Qual.* 9, 521–526. doi: 10.2134/jeq1980.00472425000900030039x

Sharpley, A. N. (1985). Depth of surface soil-runoff interaction as affected by rainfall, soil slope, and management1. *Soil Sci. Soc. Am. J.* 49, 1010–1015. doi: 10.2136/sssaj1985.03615995004900040044x

Sharpley, A. N. (1995). Soil phosphorus dynamics: agronomic and environmental impacts. *Ecol. Eng.* 5, 261–279. doi: 10.1016/0925-8574(95)00027-5

Sharpley, A. N., Kleinman, P. J. A., McDowell, R. W., Gitau, M., and Bryant, R. B. (2002). Modeling phosphorus transport in agricultural watersheds: processes and possibilities. *J. Soil Water Conserv.* 57, 425–439.

Sharpley, A. N., Menzel, R. G., Smith, S. J., Rhoades, E. D., and Olness, A. E. (1981). The sorption of soluble phosphorus by soil material during transport in runoff from cropped and grassed watersheds1. *J. Environ. Qual.* 10, 211–215. doi: 10.2134/jeq1981.00472425001000020018x

Sharpley, A. N., and Smith, S. J. (1993). Prediction of bioavailable phosphorus loss in agricultural runoff. *J. Environ. Qual.* 22, 32–37. doi: 10.2134/jeq1993.00472425002200010004x

Sharpley, A. N., Smith, S. J., Jones, O. R., Berg, W. A., and Coleman, G. A. (1992). The transport of bioavailable phosphorus in agricultural runoff. *J. Environ. Qual.* 21, 30–35. doi: 10.2134/jeq1992.00472425002100010003x

Sharpley, A. N., Troeger, W. W., and Smith, S. J. (1991). The measurement of bioavailable phosphorus in agricultural runoff. *J. Environ. Qual.* 20, 235–238. doi: 10.2134/jeq1991.00472425002000010037x

Shigaki, F., Sharpley, A., and Prochnow, L. I. (2007). Rainfall intensity and phosphorus source effects on phosphorus transport in surface runoff from soil trays. *Sci. Total Environ.* 373, 334–343. doi: 10.1016/j.scitotenv.2006.10.048

Simic, S. B., Đorđevic, N. B., and Milosevic, D. (2017). The relationship between the dominance of Cyanobacteria species and environmental variables in different seasons and after extreme precipitation. *Fundam. Appl. Limnol.* 190, 1–11. doi: 10.1127/fal/2017/0975

Singh, P. K., Gaur, M. L., Mishra, S. K., and Rawat, S. S. (2010). An updated hydrological review on recent advancements in soil conservation service-curve number technique. *J. Water Clim. Change* 1, 118–134. doi: 10.2166/wcc.2010.022

Singh, R., Helmers, M. J., and Qi, Z. (2006). Calibration and validation of DRAINMOD to design subsurface drainage systems for Iowa's tile landscapes. *Agric. Water Manag.* 85, 221–232. doi: 10.1016/j.agwat.2006.05.013

Sloan, B. P., Basu, N. B., and Mantilla, R. (2016). Hydrologic impacts of subsurface drainage at the field scale: climate, landscape and anthropogenic controls. *Agric. Water Manag.* 165, 1–10. doi: 10.1016/j.agwat.2015.10.008

Smith, D. R., Huang, C., and Haney, R. L. (2017). Phosphorus fertilization, soil stratification, and potential water quality impacts. *J. Soil Water Conserv.* 72, 417–424. doi: 10.2489/jswc.72.5.417

Srinivasan, M. S., Kleinman, P. J. A., Sharpley, A. N., Buob, T., and Gburek, W. J. (2007). Hydrology of small field plots used to study phosphorus runoff under simulated rainfall. *J. Environ. Qual.* 36, 1833–1842. doi: 10.2134/jeq2007.0017

Stamm, C., Flühler, H., Gächter, R., Leuenberger, J., and Wunderli, H. (1998). Preferential transport of phosphorus in drained grassland soils. *J. Environ. Qual.* 27, 515–522. doi: 10.2134/jeq1998.00472425002700030006x

Steffen, M. M., Belisle, B. S., Watson, S. B., Boyer, G. L., and Wilhelm, S. W. (2014). Status, causes and controls of cyanobacterial blooms in Lake Erie. *J. Great Lakes Res.* 40, 215–225. doi: 10.1016/j.jglr.2013.12.012

Tan, C. S., and Zhang, T. Q. (2011). Surface runoff and sub - surface drainage phosphorus losses under regular free drainage and controlled drainage with sub - irrigation systems in southern Ontario. *Can. J. Soil Sci.* 91, 349–359. doi: 10.4141/cjss09086

Turner, B. L., and Newman, S. (2005). Phosphorus cycling in wetland soils. *J. Environ. Qual.* 34, 1921–1929. doi: 10.2134/jeq2005.0060

Turunen, M., Warsta, L., Paasonen-Kivekäs, M., Nurminen, J., Myllys, M., Alakukku, L., et al. (2013). Modeling water balance and effects of different subsurface drainage methods on water outflow components in a clayey agricultural field in boreal conditions. *Agric. Water Manag.* 121, 135–148. doi: 10.1016/j.agwat.2013.01.012

Ulén, B., Djodjic, F., Etana, A., Johansson, G., and Lindström, J. (2011). The need for an improved risk index for phosphorus losses to water from tile-drained agricultural land. *J. Hydrol.* 400, 234–243. doi: 10.1016/j.jhydrol.2011.01.038

Uusitalo, R., Turtola, E., and Lemola, R. (2007). Phosphorus losses from a subdrained clayey soil as affected by cultivation. *Agric. Food Sci.* 16, 352–365. doi: 10.2137/145960607784125393

Uusitalo, R., Turtola, E., Puustinen, M., Paasonen-Kivekäs, M., and Uusi-Kamppa, J. (2003). Contribution of particulate phosphorus to runoff phosphorus bioavailability. *J. Environ. Qual.* 32, 2007–2016. doi: 10.2134/jeq2003.2007

Vadas, P. A. (2006). Distribution of phosphorus in manure slurry and its infiltration after application to soils. *J. Environ. Qual.* 35:6. doi: 10.2134/jeq2005.0214

Vadas, P. A., Aarons, S. R., Butler, D. M., and Dougherty, W. J. (2011). A new model for dung decomposition and phosphorus transformations and loss in runoff. *Soil Res.* 49, 367–375. doi: 10.1071/SR10195

Vadas, P. A., Bolster, C. H., and Good, L. W. (2013). Critical evaluation of models used to study agricultural phosphorus and water quality. *Soil Use Manag.* 29, 36–44. doi: 10.1111/j.1475-2743.2012.00431.x

Vadas, P. A., Gburek, W. J., Sharpley, A. N., Kleinman, P. J. A., Moore, P. A., Cabrera, M. L., et al. (2007). A model for phosphorus transformation and runoff loss for surface-applied manures. *J. Environ. Qual.* 36, 324–332. doi: 10.2134/jeq2006.0213

Vadas, P. A., Good, L. W., Moore, P. A. J., and Widman, N. (2009). Estimating phosphorus loss in runoff from manure and fertilizer for a phosphorus loss quantification tool. *J. Environ. Qual.* 38, 1645–1653. doi: 10.2134/jeq2008.0337

Vadas, P. A., Kleinman, P. J. A., and Sharpley, A. (2004). A simple method to predict dissolved phosphorus in runoff from surface - applied manures. *J. Environ. Qual.* 33, 749–756. doi: 10.2134/jeq2004.7490

Vadas, P. A., Kleinman, P. J. A., Sharpley, A. N., and Turner, B. L. (2005). Relating soil phosphorus to dissolved phosphorus in runoff. *J. Environ. Qual.* 34, 572–580. doi: 10.2134/jeq2005.0572

Vadas, P. A., Owens, L. B., and Sharpley, A. N. (2008). An empirical model for dissolved phosphorus in runoff from surface-applied fertilizers. *Agric. Ecosyst. Environ.* 127, 59–65. doi: 10.1016/j.agee.2008.03.001

van Bochove, E., Thériault, G., Dechmi, F., Leclerc, M.-L., and Goussard, N. (2007). Indicator of risk of water contamination by phosphorus: temporal trends for the province of Quebec from 1981 to 2001. *Can. J. Soil Sci.* 87, 121–128. doi: 10.4141/s06-067

Van Bochove, E., Theriault, G., Denault, J. T., Dechmi, F., Rousseau, A. N., and Allaire, S. E. (2010). "Phosphorus," in *Environmental Sustainability of Canadian Agriculture: Agri-Environmental Indicator Report Series*, ed. W. Eilers (Ottawa: Agriculture and Agri-Food Canada).

van der Perk, M., Owens, P. N., Deeks, L. K., Rawlins, B. G., Haygarth, P. M., and Beven, K. J. (2007). Controls on catchment-scale patterns of phosphorus in soil, streambed sediment, and stream water. *J. Environ. Qual.* 36, 694–708. doi: 10.2134/jeq2006.0175

Van Esbroeck, C. J., Macrae, M. L., Brunke, R. I., and McKague, K. (2016). Annual and seasonal phosphorus export in surface runoff and tile drainage from agricultural fields with cold temperate climates. *J. Great Lakes Res.* 42, 1271–1280. doi: 10.1016/j.jglr.2015.12.014

Wang, Y., Tang, J., Zhang, H., Schroder, J. L., and He, Y. (2014). Phosphorus availability and sorption as affected by long-term fertilization. *Agron. J.* 106, 1583–1592. doi: 10.2134/agronj14.0059

Wang, Y. T., Zhang, T. Q., Hu, Q. C., Tan, C. S., Halloran, I. P. O., Drury, C. F., et al. (2010). Estimating dissolved reactive phosphorus concentration in surface runoff water from major Ontario soils. *J. Environ. Qual.* 39, 1771–1781. doi: 10.2134/jeq2009.0504

Wang, Y. T., Zhang, T. Q., O'Halloran, I. P., Hu, Q. C., Tan, C. S., Speranzini, D., et al. (2015). Agronomic and environmental soil phosphorus tests for predicting potential phosphorus loss from Ontario soils. *Geoderma* 241–242, 51–58. doi: 10.1016/j.geoderma.2014.11.001

Wang, Y. T., Zhang, T. Q., O'Halloran, I. P., Tan, C. S., Hu, Q. C., and Reid, D. K. (2012). Soil tests as risk indicators for leaching of dissolved phosphorus from agricultural soils in Ontario. *Soil Sci. Soc. Am. J.* 76, 220–229. doi: 10.2136/sssaj2011.0175

Weihrauch, C., and Opp, C. (2018). Ecologically relevant phosphorus pools in soils and their dynamics: the story so far. *Geoderma* 325, 183–194. doi: 10.1016/j.geoderma.2018.02.047

Withers, P. J. A., Hartikainen, H., Barberis, E., Flynn, N. J., and Warren, G. P. (2009). The effect of soil phosphorus on particulate phosphorus in land runoff. *Eur. J. Soil Sci.* 60, 994–1004. doi: 10.1111/j.1365-2389.2009.01161.x

Woodbury, J. D., Shoemaker, C. A., Easton, Z. M., and Cowan, D. M. (2014). Application of SWAT with and without variable source area hydrology to a large watershed. *JAWRA J. Am. Water Resour. Assoc.* 50, 42–56. doi: 10.1111/jawr.12116

Young, T. C., DePinto, J. V., Martin, S. C., and Bonner, J. S. (1985). Algal-available particulate phosphorus in the great lakes Basin. *J. Great Lakes Res.* 11, 434–446. doi: 10.1016/S0380-1330(85)71788-1

Zhang, T. (2005). Influence of the seasonal snow cover on the ground thermal regime: an overview. *Rev. Geophys.* 43:RG4002. doi: 10.1029/2004RG000157

Conflict of Interest Statement: The authors declare that the research was conducted in the absence of any commercial or financial relationships that could be construed as a potential conflict of interest.

frontiers in Marine Science

REVIEW
published: 23 August 2018
doi: 10.3389/fmars.2018.00276

Challenges of Reducing Phosphorus Based Water Eutrophication in the Agricultural Landscapes of Northwest Europe

Roland Bol[1], Gerard Gruau[2], Per-Erik Mellander[3], Rémi Dupas[4], Marianne Bechmann[5], Eva Skarbøvik[5], Magdalena Bieroza[6], Faruk Djodjic[6], Miriam Glendell[7], Philip Jordan[8], Bas Van der Grift[9], Michael Rode[10], Erik Smolders[11], Mieke Verbeeck[11], Sen Gu[2], Erwin Klumpp[1], Ina Pohle[7], Maelle Fresne[3] and Chantal Gascuel-Odoux[4]*

[1] Agrosphere (IBG-3), Institute of Bio- and Geosciences, Forschungszentrum Jülich, Jülich, Germany, [2] CNRS, Géosciences Rennes - UMR 6118, FranceOSUR, University of Rennes, Rennes, France, [3] Agricultural Catchments Program, Department of Environment, Soils and Landuse, TEAGASC, Johnstown Castle, Ireland, [4] INRA, Agrocampus-Ouest, UMR1069 SAS, Rennes, France, [5] Norwegian Institute of Bioeconomy Research, Ås, Norway, [6] Department of Soil and Environment, Swedish University of Agricultural Sciences, Uppsala, Sweden, [7] Environmental and Biochemical Sciences Group, James Hutton Institute, Aberdeen, Scotland, [8] Environmental Sciences Research Institute, Ulster University, Londonderry, Ireland, [9] Subsurface and Groundwater Quality, Deltares, Delft, Netherlands, [10] Department of Aquatic Ecosystem Analysis, Helmholtz Centre for Environmental Research-UFZ, Magdeburg, Germany, [11] Division of Soil and Water Management, KU Leuven, Leuven, Belgium*

OPEN ACCESS

Edited by:
Rosalind Jane Dodd, Lincoln University, New Zealand

Reviewed by:
Sönke Hohn, Leibniz Centre for Tropical Marine Research (LG), Germany
Verena Pfahler, Rothamsted Research (BBSRC), United Kingdom

***Correspondence:**
Roland Bol
r.bol@fz-juelich.de

Specialty section:
This article was submitted to Marine Biogeochemistry, a section of the journal Frontiers in Marine Science

Received: *26 March 2018*
Accepted: *20 July 2018*
Published: *23 August 2018*

Citation:
Bol R, Gruau G, Mellander P-E, Dupas R, Bechmann M, Skarbøvik E, Bieroza M, Djodjic F, Glendell M, Jordan P, Van der Grift B, Rode M, Smolders E, Verbeeck M, Gu S, Klumpp E, Pohle I, Fresne M and Gascuel-Odoux C (2018) Challenges of Reducing Phosphorus Based Water Eutrophication in the Agricultural Landscapes of Northwest Europe. Front. Mar. Sci. 5:276. doi: 10.3389/fmars.2018.00276

In this paper, we outline several recent insights for the priorities and challenges for future research for reducing phosphorus (P) based water eutrophication in the agricultural landscapes of Northwest Europe. We highlight that new research efforts best be focused on headwater catchments as they are a key influence on the initial chemistry of the larger river catchments, and here many management interventions are most effectively made. We emphasize the lack of understanding on how climate change will impact on P losses from agricultural landscapes. Particularly, the capability to disentangle current and future trends in P fluxes, due to climate change itself, from climate driven changes in agricultural management practices and P inputs. Knowing that, future climatic change trajectories for Western Europe will accelerate the release of the most bioavailable soil P. We stress the ambiguities created by the large varieties of sources and storage/transfer processes involved in P emissions in landscapes and the need to develop specific data treatment methods or tracers able to circumvent them, thereby helping catchment managers to identify the ultimate P sources that most contribute to diffuse P emissions. We point out that soil and aqueous P exist not only in various chemical forms, but also in range of less considered physical forms e.g., dissolved, nanoparticulate, colloidal and other particulates, all affected differently by climate as well as other environmental factors, and require bespoke mitigation measures. We support increased high resolution monitoring of headwater catchments, to not only help verify the effectiveness of catchments mitigation strategies, but also add data to further develop new water quality models (e.g., those include Fe-P interactions) which can deal with climate and land use change effects within an uncertainty framework. We finally conclude that there is a crucial need for more integrative research efforts to deal with our incomplete understanding

of the mechanisms and processes associated with the identification of critical source areas, P mobilization, delivery and biogeochemical processing, as otherwise even high-intensity and high-resolution research efforts will only reveal an incomplete picture of the full global impact of the terrestrial derived P on downstream aquatic and marine ecosystems.

Keywords: phosphorus, cycling, soil, eutrophication, climate change, colloidal and particulate, water quality

INTRODUCTION

The increasing world-wide issue of the eutrophication of our lakes, reservoirs, rivers and coastal waters has highlighted an urgent need for interdisciplinary action across research fields (e.g., Moss, 2012; Withers et al., 2014; Elmgren et al., 2015; Pinay et al., 2017; Charlton et al., 2018). It is now well documented that anthropogenically derived phosphorus (P) and nitrogen (N) pollution are currently the main drivers of eutrophication, with the excessive inputs of these two nutrients into freshwater and estuarine water bodies being considered as one of the most urgent environmental issues that human societies face (Rockström et al., 2009; Steffen et al., 2015; George et al., 2017). Agricultural activities and urbanization can both deliver excess P and N to aquatic ecosystems, which may cause eutrophication of water courses and which in turn may alter the native ecological communities, degrade ecosystem services and directly or indirectly impact water supply, recreational uses, and human health (e.g., cyanobacteria blooms). Already, in the late 1960s a fundamental change started to occur in most developed countries regarding the type of P input (see **Table S1** for P terminology and additionally Haygarth and Sharpley, 2000), namely a very marked decrease of point-source P due to an increased waste water treatment (Persson, 2001; Billen et al., 2007; Grizzetti et al., 2012; Scavia et al., 2014; Minaudo et al., 2015). This decrease has had rapid and marked effects on the P loading and trophic status of downstream water bodies (e.g., a 75% reduction in 25 years of the P flux in the Seine River and Lake Geneva; disappearance of cyanobacteria blooms in some lakes, such as Lake Erie in the USA, Lake du Bourget in France, and Lake Mjosa in Norway; Nesheim et al., 2010**;** Jacquet et al., 2014; Scavia et al., 2014; Romero et al., 2016). However, this reduction in point sources has been counterbalanced by the stagnation or even the increase of diffuse P emissions from agricultural soils (Scavia et al., 2014; Dupas et al., 2015d; Stoddard et al., 2016). This has happened even despite the fact that overall fertilizer usage in NW Europe since the 1980's has decreased significantly (Schoumans et al., 2015). For example in Sweden, lower P fertilizer use is now accompanied by more or less balanced P inputs and outputs in agriculture (Bergström et al., 2015). Both dissolved/colloidal P, i.e., the most bio-available forms of P for algae (Dupas et al., 2015a; Mellander et al., 2016; Gu et al., 2017), as well as particulate P (Bechmann and Deelstra, 2013) are involved in this increase of P emissions from agricultural soils. For Norway increased delivery of particulate P to surface waters can partly be assigned to higher soil erosion due to climate change effects (i.e., increased runoff) (Deelstra et al., 2011). Whereas, for Sweden a modeling study (Arheimer and Donnelly, 2013) suggested that the total mean load to the Baltic Sea will increase for P, but may decrease for N by 2100 due to climate-induced changes. Enhanced particulate P can be formed in the surface waters due to the discharge of iron (Fe) and calcium (Ca)-bearing groundwater and subsequent precipitation of P-rich minerals (Baken et al., 2013; Van der Grift et al., 2014, 2018). Depending on the receiving water body, most of this particulate P could in the long run become available to algae (e.g., Yang et al., 2016; Yao et al., 2017).

Maintaining high levels or even increasing diffuse P losses from agricultural landscapes hampers any expected improvements in water quality, thereby challenging our society's ability to combat eutrophication. The issue here concerns not only lakes, rivers and estuaries, but also the multitude of small water bodies of natural and artificial origin, some which may serve as reservoirs for drinking water production.

For 30 years or more, much knowledge has been gained on the basic physico-chemical processes by which P is mobilized in soils and transported to rivers, as well as on the chemical forms of the mobilized and transported P. For example, the role of wetting-drying cycles as catalysts for the production and transfer of dissolved and colloidal phosphorus is now well known (e.g., Turner et al., 2003; Butterly et al., 2011; Blackwell et al., 2013; Chen et al., 2016; Gu et al., 2018). In particular, the important role of colloids to serve as carrier of P in soils and waters has been highlighted (e.g., Henderson et al., 2012; Gottselig et al., 2014; Liu et al., 2014; Baken et al., 2016; Jiang et al., 2017; Gu et al., 2018; Missong et al., 2018). Also well-constrained is the capacity of P to bind with manganese (Mn) and iron oxides and the influence the redox state of soils and waters has on P mobility in the environment (Scalenghe et al., 2012; Van der Grift et al., 2014; Jiang et al., 2015a,b; Smolders et al., 2017). Along with these understandings, novel high resolution P water quality monitoring, such as sensor technology, can be used to understand the processes of dissolved and particle-bound substances in waters. For example by using turbidity as a proxy for particulate P we can now reliably achieve high-frequency observations of P losses from agricultural landscapes over multi-annual periods (Jordan et al., 2007; Skarbøvik and Roseth, 2014; Rode et al., 2016; Shore et al., 2017). This information, combined with ever advancing analytical techniques (Kruse et al., 2015) as well as improvements in landscape visualization tool kits, is helping to facilitate efforts to better quantify P dynamics in time and space, from plot to catchment and landscape.

Transforming this knowledge into appropriate cost effective mitigation strategies remains a major challenge (Schoumans

et al., 2014, 2015; Dodds and Sharpley, 2015; Kleinman et al., 2015; Sharpley et al., 2015; Withers et al., 2015a,b; Rowe et al., 2016). The degree of integration and knowledge is such today that some of the most recent studies can go as far as integrating the costs of management in the reduction of diffuse phosphorus emissions, in connection with national or local legislation or land property issues (e.g., McDowell et al., 2016; Vinten et al., 2017; Zhang et al., 2017).

The EU Water Framework Directive (WFD) has since its emergence in the beginning of this millennium set the scene for water management in Europe. Its implementation has resulted in massive efforts to classify all water bodies according to their ecological status, within this context monitoring of European waters has, at least tentatively, become more harmonized through the Common Implementation Strategy (CIS) guidelines. Achieving Good Ecological Status of waterbodies across Europe under the Water Framework Directive will require an improved understanding of the link between P concentrations, loads and sources in the soil and recipient freshwater ecosystems within the context of multiple stressors (Whitehead and Crossman, 2012; Crossman et al., 2013). However, in this paper, we will not focus on all the aspects of the WFD or other EU legislation, but only few aspects that are linked to the main foci of our review. These include the types of monitoring that can give new insight into catchment processes, including investigative monitoring and source apportionment.

Furthermore, we are taking into account the considerable amount of papers already published on the topic of P transfer and P management in agricultural landscapes, including several recent review papers (e.g., Kleinman et al., 2011; Chowdhury et al., 2014; Schoumans et al., 2014; Sharpley et al., 2015; Kadlec, 2016; McDowell et al., 2016). As well as related contemporary topical reviews on aspects like scenario analysis and mitigation (Roberts et al., 2012; Schoumans et al., 2014; Dodd and Sharpley, 2016; Ahmad et al., 2017; Liu et al., 2017; Wu et al., 2017), policy and implementation (Christen and Dalgaard, 2013; McDowell et al., 2016), novel modeling approaches and management insights Shepherd et al., 2011; Radcliffe et al., 2015; Xie et al., 2015; Ouyang et al., 2017, water quality modeling (Rode et al., 2010; Wellen et al., 2015; Hashemi et al., 2016), erosion (Panagos et al., 2017) and other more general appraisal of future needs and directions (Fernandez-Mena et al., 2016; Garnache et al., 2016). Hence our intention in this article is not to produce an exhaustive review which also covers the state of knowledge in these related research fields. Rather, our paper is aimed at highlighting certain important knowledge gaps and research challenges on P cycling and transfer processes in agricultural landscapes in Northwest Europe in relation to the continued issue of eutrophication of inland and coastal surface waters. Thereby, implicitly also identifying research needs for these 4 key challenges. These main challenges for us concern: (i) a better understanding of the processes and variables controlling P mobilization and P transfer in headwater catchments, (ii) a better consideration of how the basic mechanisms involved in P mobilization in soils at the small scale aggregate themselves at larger scales, and how this aggregation ultimately control P diffuse emissions in agricultural landscapes, (iii) the resolution of ambiguities in the interpretation of river P dynamics for identification of sources in catchments, and (iv) a better understanding and prediction of the effects of climate change on P fluxes and P physical-chemical forms.

HEADWATER CATCHMENTS: THE RIGHT PLACE TO BE TO MANAGE AND MONITOR DIFFUSE PHOSPHORUS EMISSIONS

Combating eutrophication relies on effective reduction in P losses from land to water through appropriate management of P sources and pathways in the landscape. The key scientific and management questions are: where is the excess P coming from? How are these P sources mobilized and delivered to surface waters? What is their impact on water bodies? For still unknown reasons, some headwater catchments (surface area <50 km^2) in agricultural landscapes appear more resilient (have more buffering capacity) than others with regards to P loading, resulting in huge differences in average annual P concentrations and annual P fluxes, as exemplified by the case of Brittany, one of the most intensively farmed regions of France (Legeay et al., 2015; Abbott et al., 2017). This increased variability of P concentration and P fluxes with decreasing catchment size is as a result of headwater catchments having lower intense cultivation rates. In fact the majority of these Brittany headwater catchments shown in **Figure 1** are intensively cultivated (>80% of arable land) throughout (Legeay et al., 2015; Abbott et al., 2017). They were also found to be insensitive to the general decreased particulate P emissions that has been recorded in Brittany since the beginning of the 1990's, as this decrease left the amplitude of particulate P flux variability in headwater catchments unchanged (see **Figure 1**).

The increased variability of P emissions when moving upstream in headwater catchments is found both for dissolved and particulate P fluxes (**Figure 1**). Land use, and especially the share of arable land within a catchment, is known to have a strong positive relationship on nutrient losses (Evans et al., 2014). Indeed, plotting median TP (total P) losses against the share of arable land in Swedish catchments included in the monitoring program River outlets and Trend Watercourses results in strong ($R^2 = 0.79$, $p < 0.005$) and positive relationship (**Figure 2**). However, long term data from another Swedish water quality program, monitoring program arable catchments, also highlighted an inherent great variability in nutrient delivery among small catchments (<50 km^2) with high portion of the arable land (**Figure 2**). For these small catchments with high share of arable land, the relationship was not statistically significant at all ($R^2 = 0.02$, $p = 0.41$). Consequently, measured P concentrations from some small catchments were remarkably low in spite of intensive agricultural production, whereas other catchments were found to be less resilient and much more vulnerable to P losses.

The high spatial variability observed among headwater catchments appears persistent over time suggesting that occasional synoptic sampling of headwater catchments can provide valuable information for catchment characterization and

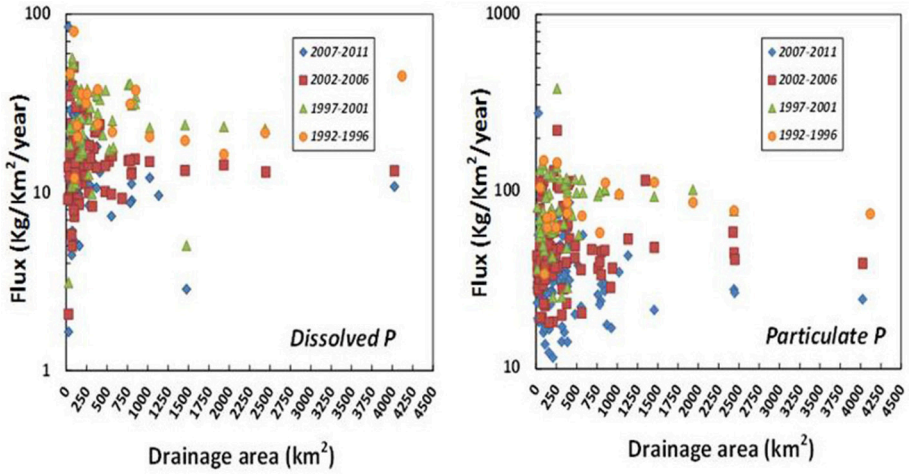

FIGURE 1 | The relationship between dissolved an particulate P fluxes and drainage areas as observed in Brittany rivers, Western France. Fluxes have been calculated as average values for periods of four consecutive years, in order to minimize flux uncertainities. The two plots data from 117 monitoring station. Drainage areas ranges from 11 to 4,000 km^2. For both dissolved and particulate P fluxes, an increase variability is observed when moving from large rivers toward headwater catchments, the maximum of variability occurring for headwater catchments of drainage area <50 km^2 (Legeay et al., 2015).

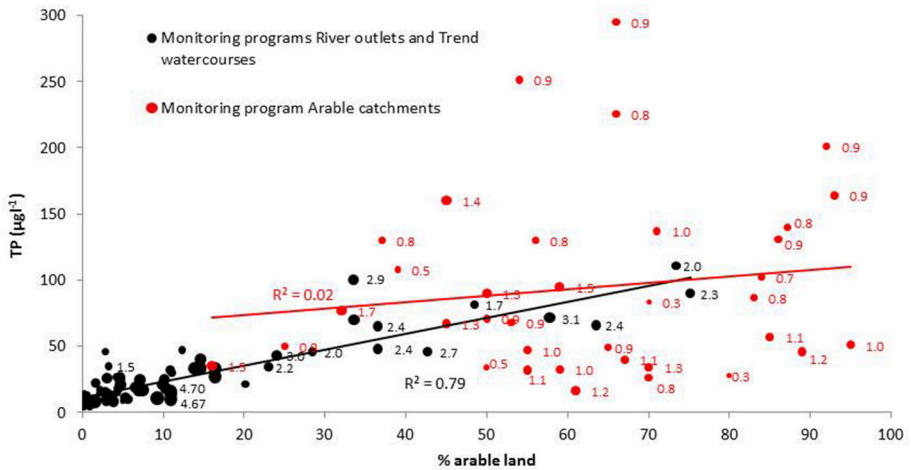

FIGURE 2 | The relationship between the portion of a arable land and median total phosphorus (TP) concentration for the period 2000–2016 included in two Swedish water equality monitoring program: (a) 77 catchments (area 8–50,110 km^2). River outlets and trend watercourses (black filled circles) and (b) 36 smaller (area 1.8–54 km^2) catchments dominated by agriculture (red filled circles). The size of the filled circles is proportional to the catchment area, and the label value stands for the $\log_{10}$ area of the catchment (km^2).
Original source data:
Monitoring programs River outlets and Trend Watercourses: http://miljodata.slu.se/
Monitoring programs Arable catchments:;http://jordbruksvatten.slu.se/.

management with regards to P emissions. This finding also raises the question of the spatial threshold at which the landscape splits into poorly and highly contributing headwater catchments with regards to P emissions, which has been recently referred as to the "landscape grain size" concept (Abbott et al., 2017). There are many potential parameters that could modify the capacity of headwater catchments to release P to river networks, and thus create variations in P emission properties at a specific spatial threshold, or given landscape grain size (see also Dodds and Oakes, 2008; Haygarth et al., 2012). Included are the extent of preferential flow paths in soils and aquifers, which determine residence times in different catchment components, as well as the connectivity between land and water which may strongly vary among headwater catchments (Dahlke et al., 2012; Dupas et al., 2015d, 2016; Mellander et al., 2015). Differences in P applied to or present in soils, the biogeochemical cycling in soils, linked with variations in groundwater dynamics, themselves influenced topography, could be also involved (e.g., Gu et al.,

2017). Differences in past land-use history and soil properties will likewise will play a role (Stutter et al., 2015; Gu et al., 2017).

Irrespective of the processes and factors that control the ability of headwater catchments to act as sinks or sources for P, the understanding where P is coming from is important both to target and reduce these sources and also to establish who is responsible for their management according to the polluter pays principle (as defined in the WFD). There is however less clarity in WFD who will pay for the monitoring to obtain this information, in fact, the direct monitoring of point sources is often left to the owner of the waste water treatment plants (Skarbøvik et al., 2014).

Knowing the spatial structure and the typical grain size of source and sink headwater catchments with regards to diffuse P emissions in the landscape could improve site selection for targeted management efforts. Should the difference in resilience properties be of high spatial and temporal stability as found by Legeay et al. (2015) and Abbott et al. (2017), then the intervention in those headwater catchments showing the lowest resilience or highest source properties would potentially yield the largest catchment-level improvements at the lowest cost.

Knowing the landscape typical threshold or grain size could be also helpful for rationalizing water quality monitoring networks. Owing to the temporal stationarity of the spatial distribution of poorly and highly contributing headwater catchments, occasional synoptic sampling of headwater catchments would provide valuable information for identifying high and low contributing headwater catchments in agricultural landscapes. The redistribution of agricultural activity based on the difference in P emission properties of headwater catchments could be a cost effective management strategy for decreasing P loads of larger rivers. This could be implemented even in the absence of a clear understanding of the underlying mechanisms and factors that cause differences in headwater catchment properties. The implementation over the long-term of high frequency monitoring devices at the outlet of larger river basins where the river channel integrates multiple headwater catchments would make it possible to assess the effectiveness of the mitigation strategies thus deployed in the most contributive headwater catchment areas.

DIFFICULTIES IN DISENTANGLING POINT-SOURCE, DIFFUSE PHOSPHORUS EMISSIONS AND PRE-AGRICULTURAL PHOSPHORUS CONCENTRATION BASELINES

Load apportionment models are often used to distinguish between diffuse (mainly from agriculture) and point P sources (sewage treatments, industry sources, fish farming etc.) (Bowes et al., 2008). In many European countries, monitoring networks (statutory monitoring) were established well before 2000 to monitor pollution from point sources and to assess long-term water quality status (Bieroza et al., 2014; Kyllmar et al., 2014), but recently more new emphasis has been put on such networks as part of the obligations and the verification of compliance with EU legislative directives (e.g., WFD). Furthermore, both the location of the sampling points and the monitoring interval are not always suitable to capture the spatial and temporal dynamics of diffuse sources (Jordan and Cassidy, 2011; Bieroza et al., 2014). Thus, targeting diffuse P is difficult, since the sources operate sparsely in both space and time, except for specific locations in the catchment, so-called Critical Source Areas (CSA), and during specific times e.g., rainfall and snowmelt events (Djodjic and Villa, 2015).

Haygarth and Jarvis (1999) stated that having good quantitative knowledge of the baseline P concentrations is necessary when assessing spatiotemporal trends in water quality in agricultural areas. This is also a requirement in the WFD, which states that the environmental goals should deviate only slightly from the background or reference conditions. However, the baseline P concentrations can be expected to vary widely among regions. For example, Phillips and Pitt (2015) demonstrated the differences between European countries of nutrient boundaries used for the WFD. This may be due to natural variations in soil types and topography, but may also be a result of limitations in catchment understanding.

At any rate, such baseline levels should be based on scientific methods, and not on political concerns. Estimations of baseline P is especially difficult in the lower lying areas where the land has been used for agricultural production for centuries, and where such baseline P concentrations must either be modeled or estimated based on limited data. Additionally, those P sources originating from forests and highlands areas ("background runoff"), which are generally poorly quantified themselves, do also contribute to overall baseline P concentrations in the waters of agricultural and urban catchments. Furthermore, the baseline P values may also change, due to large-scale changes such as climate change or the reductions in acid rain. The latter has led to brownification (increased darkening of the water color, due to the increase of dissolved organic carbon content) of Scandinavian waters, which again may have impacted on P losses (Fölster et al., 2014).

CHALLENGES TO MONITOR AND MODEL PHOSPHORUS TRANSFER AT THE LANDSCAPE SCALE

Monitoring and modeling of P transport pathways in the landscape remains a challenge. This is particularly true for the transfer of particulate P, which is a highly dynamic process, and targeting particulate P sources depends on the exact timing of mitigation measures in relation to plant growth, soil management and soil moisture. Modeling approaches based on detailed measurements of topography (e.g., Lidar) are normally used to target both sources and pathways (e.g., erosion gullies) of sediment-bound P (Thomas et al., 2016). On tile drained soils, significant amounts of particulate P can also be transferred through macropores, which are difficult to monitor and manage (Bechmann et al., 2017a). In addition, elucidating the sources and pathways of dissolved P is also a challenge since it involves understanding of sub-surface pathways (e.g., shallow

groundwater) and their connectivity with water bodies as well as its interactions with soil chemistry governing P sorption and release. Shallow sub-surface pathways and hyporheic flow have been found to be important for dissolved P delivery to streams (Bieroza and Heathwaite, 2015; Mellander et al., 2015). Recent advances in high-temporal resolution sampling with *in situ* analyzers and sensors have yielded information to help delineate potential pathways through hysteresis pattern analysis (Bieroza and Heathwaite, 2015; Dupas et al., 2015b). Furthermore, establishing robust correlations between routinely measured parameters (e.g., turbidity) or smart environmental tracers and P fractions can further help to gain improved understanding of processes and assist to reduce the monitoring cost (Bieroza and Heathwaite, 2016; Minaudo et al., 2017; Stutter et al., 2017).

Statutory monitoring data are used to assess chemical and ecological status of water bodies and to evaluate the impacts of diffuse pollution on stream nutrient concentrations. Despite intensive efforts to reduce these negative impacts, many rural catchments still show increasing long-term P concentration trends (Bechmann et al., 2017b), possibly due to the influence of weather events on local landscape P dynamics, highlighting the continued need for a deeper understanding of these weather-related processes (Bieroza et al., 2014). Seemingly similar catchments (e.g., percentage arable land in a catchment) are known to show opposing nutrient trends, which in turn may indicate a differing resilience to environmental change (Legeay et al., 2015). The observed disconnection between management practices and water quality in many catchments necessitates further efforts to better target P sources and pathways in space and time. The persistence of P pollution also requires more catchment-tailored approaches to mitigate diffuse pollution. Use of high-resolution mapping of CSAs, including soil chemistry, topography and soil type, can help to identify locations in the landscape that will benefit most from the implementation of mitigation measures (Thomas et al., 2016; Djodjic et al., 2017). Using statutory and high-frequency P monitoring in parallel could further help in identifying the most critical time periods and pathways of diffuse pollution (Dupas et al., 2015c). Additionally, new upscaling modeling approaches are needed to link single location patterns to landscape-wide process understanding.

AMBIGUITIES IN THE INTERPRETATION OF RIVER P DYNAMICS FOR IDENTIFICATION OF SOURCES IN CATCHMENTS

In order to limit P transfer and reduce eutrophication, it is important to identify the sources and the mobilization/delivery mechanisms of P into rivers. One commonly used method for source identification is statistical analysis of water quality time series. In particular, load apportionment models (LAMs) based on concentration - discharge (C-Q) relationships (Bowes et al., 2008, 2014, 2015; Greene et al., 2011; Lamba et al., 2015; Crockford et al., 2017; Glendell et al., 2018) or the identification of periods of the year when one source is believed to dominate over other sources, a method is used to disentangle point sources from diffuse sources (Legeay et al., 2015). Equations in LAMs all rely on the assumption that point source emissions are constant in time (leading to negative C-Q relationships due to dilution when discharge increases) while diffuse source emissions increase with discharge (leading to positive C-Q relationships due to mobilization and delivery of P during storm events). Furthermore, analysis of C-Q hysteresis loops during storm events has been used to distinguish proximal (remobilization of stream bed sediments, bank erosion, erosion of riparian area) and distal sources (hillslope erosion, subsurface transfer) (Stutter et al., 2008; Outram et al., 2014, 2016; Bieroza and Heathwaite, 2015; Bowes et al., 2015; Dupas et al., 2015a,b; Perks et al., 2015; Sherriff et al., 2016). Clockwise loops are often interpreted as originating from proximal sources whereas anticlockwise loops are interpreted as originating from distal sources. However the interpretation of P dynamics observed in rivers, and both LAMs and analysis of C-Q hysteresis loops are subject to "ambiguity" problems. Here, the term ambiguity describes situations when several processes (or sources) can lead to the same observed P dynamics in rivers. This can lead to difficulties in inferring the dominant controlling process (or source) from statistical analysis of water quality time series. Jarvie et al. (2012) have shown that remobilization of streambed sediment during winter high flow is often (wrongly) attributed to diffuse source, whereas these sediments may have been enriched by point sources during the summer low flow period, and thus the primary source is predominantly a point source. This ambiguity may lead to overestimation of diffuse sources in LAMs.

The reductive dissolution of Fe oxyhydroxides in sediments of lowland rivers (Smolders et al., 2017) or riparian wetlands in upland systems (Dupas et al., 2017) can lead to soluble reactive phosphorus (SRP) release during summer low flows, increasing summer SRP concentrations in rivers in the same manner as does an undiluted point source. This ambiguity may lead to overestimation of point sources in LAMs. Likewise, ambiguities in river P dynamics have been highlighted in the identification of proximal versus distal sources within hillslopes. Bieroza and Heathwaite (2015) have shown that in the case of two successive storm events, the first event could transport a distal P source to the near-stream zone, which can be remobilized during a second event (exhibiting a clockwise hysteresis loop). Therefore, if only the second event was monitored, there is an ambiguity in the location (proximal/distal) of the primary source, because the primary mobilization of a proximal source can lead to the same observed P dynamics pattern as the secondary mobilization of a distal source (both would exhibit clockwise hysteresis loops). Furthermore, *in-situ* monitoring of uncultivated soils in the near stream zone have highlighted that these zones represented a significant contribution to annual SRP exports in a temperate agricultural catchment (Gu et al., 2017). However, it is not clear to which extend these zones are primary sources (due to legacy P inputs before their conversion into uncultivated buffers) or secondary sources (as they accumulate and re mobilize P rich eroded soils from cultivated upslope areas). At the scale of the hyporheic zone, Van der Grift et al. (2014, 2018) have shown that

SRP via Fe(II) oxidatie at the groundwater-surface water interface can be followed by remobilization of newly formed particulate P. Thus, there can be an ambiguity in the location (proximal/distal) of the source of the particulate P, which can be attributed to a proximal source (the river bank) whereas it may stem from remobilization of a more distal primary source. Another example of ambiguity is the P release pulses observed in summer from river sediments whose ultimate source can be a mixture of several point and diffuse sources, located further upstream (Cooper et al., 2015a; Dupas et al., 2017; Smolders et al., 2017).

Given the important implications of these ambiguities in the identification of P sources and pathways in rural landscapes, several improved methods can be proposed. Firstly, it is possible to use tracers (e.g., stable isotopes and plant-specific biomarkers) and/or complementary water quality parameters in addition to P (Jarvie et al., 2012; Cooper et al., 2015b; Alewell et al., 2016; Glendell et al., 2018) to trace the primary sediment source. For example, Ahlgren et al., 2012 found Barium (Ba) being a promising tracer element, being present in significantly higher amounts in waters affected by agricultural runoff. Whereas Paruch and co-authors developed microbial source-tracking techniques based on advanced DNA methods to distinguish between different sources of microbial contamination (Paruch et al., 2015; Paruch and Paruch, 2017). Furthermore, recent work do suggest that the composition of P carrier colloids could also be a 'tracer/fingerprint' the source of P (Missong et al., 2018). Secondly, more observational data is needed, combining monitoring at the catchment outlet with *in situ* observation within functional zones such as riparian wetland or groundwater (Mellander et al., 2016; Gu et al., 2017) to disentangle primary mobilization from secondary delivery/remobilization. Thirdly, interpretation of long term change in water quality dynamics ("trajectory") in catchments where management changes, such as removal of point sources, decrease in soil P status or installation of buffer zones, have been recorded over several decades (Bieroza et al., 2014) may help to resolve ambiguities in river P dynamics. Therefore, meta-analysis of large catchment datasets may help to identify typical situations where one mechanism (e.g., summer sediment P release versus point source P input) dominates over others. In doing so, "typical" situations can be identified without ambiguity and the P dynamics pattern can be transferred to other, less studied areas as a guide to infer what are the key mechanisms controlling P loads. Finally, consideration of time lags and legacy effects is crucial when communicating results of source identification studies to catchment managers, so that they do not only target secondary proximal sources (short term vision) but also primary more distal sources (long term vision).

DIFFICULTIES IN PREDICTIONS OF DISSOLVED/COLLOIDAL/PARTICULATE CATCHMENT PHOSPHORUS "HOT SPOTS" AND "HOT/CRITICAL" MOMENTS

The difficulty in attributing spatio-temporal variations in P fluxes and P concentrations in streams and rivers draining agricultural landscapes to specific sources or specific mobilization/transfer processes is well known (e.g., Haygarth et al., 2005; Edwards and Withers, 2007; Granger et al., 2010; Trevisan et al., 2012; Hahn et al., 2013; Sharpley et al., 2015). This difficulty mainly arises from the fact that the transfer of P in agricultural landscapes is not often caused by a single process or a single source, rather being the consequence of a series of processes, mobilizing P from several permanent or temporary sources. A good illustration of this difficulty and of the ambiguities it may create in terms of process and source identification was provided by the dissolved/colloidal P release pulses observed in riparian wetland zones. Riparian zones in agricultural catchments are active in transforming poorly mobile particulate P into highly mobile dissolved and colloidal P, which is directly or indirectly bioavailable (Stutter et al., 2009; Dupas et al., 2015a; Gu et al., 2017). Indeed, these P release pulses come from the solubilisation of particulate P eroded from the upland cultivated fields which are temporarily accumulated in wetland zones. This implies that the primary sources of the released P are the upland cultivated fields from which P originates. Quite clearly, such entanglement of processes and existence of temporary sources may lead to ambiguities in the clear identification of the zones and processes contributing most to the risk of P mobilization and P transfer at the catchment scale. Therefore, moving toward full understanding the overall sequence of transfer and retainment of P process chain and how P release capacities vary in space and time is challenging, but it is a knowledge prerequisite to better control and reduce P loss in agricultural landscapes.

In order to better evaluate and quantify how the above mentioned processes control P emissions in catchments, we need to understand how their spatio-temporal occurrence and intensity is controlled by landscape properties, and how the zones where these processes take place are connected with each other and to the river network. Though relevant for particulate P, the issue is particularly relevant for dissolved and colloidal P, which both appear much more significant contributors to P losses from agricultural lands than previously assumed (Kleinman et al., 2011, 2015; Dupas et al., 2015c; Jiang et al., 2015a; Mellander et al., 2015, 2016; Gu et al., 2017), and are also potentially bioavailable P forms. From the perspective of locating dissolved and colloidal P sources in the landscape, the way landscape structures, in interaction with climatic variables, control ground- and surface water dynamics is of fundamental importance. Groundwater level changes in the overall landscape, in response to precipitation and evapotranspiration, influence the location, timing and duration of soil water saturation and wetting-drying episodes that in turn cause reduction of soil Fe-oxyhydroxides. Ground- and surface water dynamics are thus anticipated to be the important determinants of hot spots and hot moment release of dissolved/colloidal P in catchments. An example of such complex control of landscape structure on P release dynamics in catchments has been provided in a recent study conducted on riparian wetlands in a small French catchment (Gu et al., 2017). Large differences have been observed with regards to P release dynamics in the riparian zone, depending on the topography and the control it exerts on the location and timing of biogeochemical processes such as soil Fe-oxyhydroxide reduction or P leaching following soil rewetting. This study

has led to the development of a coherent, spatially integrated concept of "landscape biogeochemistry" (see **Figure 3**) in which the topography, as a first-order control on spatial variation of hydrological conditions (Sørensen et al., 2006), appears to control spatial and temporal distribution of P release processes, the inputs of P from cultivated soils situated upslope (control of topography on soil erosion) and the organic and inorganic nature of released P through indirect control of topography on the rate of soil organic matter mineralization.

The chemistry of P in the soil-water continuum is often controlled through interactions with iron (Fe). Iron is a redox sensitive element and is commonly present in the soil-groundwater-surface water system. Mechanisms such as reduction of soil Fe-oxyhydroxides or rewetting of dried soils are known to trigger the release of P in soils, notably that of dissolved and colloidal P fractions (Turner and Haygarth, 2001; Stutter et al., 2009; Blackwell et al., 2010, 2013; Obour et al., 2011; Scalenghe et al., 2012; Gu et al., 2017; Missong et al., 2018). Redox gradients also result in the precipitation or dissolution of Fe-rich particles, which have a major impact on the fate and bioavailability of P (Jiang et al., 2017). Particulate or colloidal P is formed at the groundwater-surface water interface in groundwater-fed lowland catchments (Van der Grift et al., 2014, 2018; Baken et al., 2015). The formation of Fe hydroxyphosphate precipitates, with molar P/Fe ratio of 0.5 is the main immobilization process of dissolved P during Fe(II) oxidation (Voegelin et al., 2013; Van der Grift et al., 2016) and therefore a major control on the P retention in natural waters that drain anaerobic aquifers. As a consequence, Fe-bound P can be the dominant P fraction in suspended particulate matter under such conditions (Van der Grift, 2017). The Fe(II) oxidation may also lead to formation of Fe(III) bearing colloids. Furthermore, redox mediated P release from river sediments in lowland rivers has been identified as dissolved reactive P (DRP) release mechanism during summer anoxia (Smolders et al., 2017). Reductive dissolution of ferric Fe oxides was found to be associated with mobilization of P to the water column from sediments with a molar P/Fe ratio >0.4. In contrast, no sediment DRP release was found for a lower P/Fe ratio irrespective of temperature and dissolved oxygen treatments. Hence, the P/Fe molar ratio in sediments is an indicator for P mobilization. Clearly, Fe redox dynamics should be taken into account when describing and predicting P transfer from both soils and sediments to surface water.

Particulate P, the dominant P form in many agricultural areas in Northwest European countries like Norway (Bechmann et al., 2008), may be transferred within the headwater catchments adsorbed onto soil particles, but it may also be released from the soil particles when it reaches the recipient waterbody. In addition, some algae can also use particulate P directly. When soil particles do contain high levels of P (high soil P status), these particles may release high amounts of P when diluted in water. Therefore, the importance of particulate (including colloidal) associated phosphorus for algal growth, both on a short and long-term time-scale requires further investigation.

Locating and apportionment of the sources and fluxes of the dissolved vs. collodial P conveyed by rivers in landscapes remains a longstanding and fundamental challenge for catchment scientists (see McClain et al., 2003; Bol et al., 2016; Gottselig et al., 2017b; Missong et al., 2018), with major implications for land management and nutrient pollution mitigation strategies. Colloidal P is characterized as dissolved P in most routine water quality monitoring programs (Gottselig et al., 2017a), however, it is believed to have reduced bioavailability compared to the truly dissolved P (Baken et al., 2014). Furthermore, colloids which consist of organic matter, Fe/Al oxyhydroxides and clay minerals (Jiang et al., 2015a; Missong et al., 2017) are important P carriers in and to surface waters (Gottselig et al., 2014, 2017a,b) and thus should be more explicitly accounted for in P budgets. These interactions between P and colloids need to be understood to better assess and predict P mobility, availability and eutrophication in surface waters, such as homo- and hetero-aggregation behavior of colloidal particles as a controlling factor for P retention. While the mobilization and retention of P cannot be fully understood without understanding its interaction with Fe it is currently omitted from current water quality models and one of their important limitations.

UNCERTAIN IMPACTS OF WEATHER AND CLIMATE CHANGE ON P STATUS

Human influence on the global climate and a range of future climate projections are now well established (Jenkins et al., 2010; IPCC, 2014). However, less information is currently available in the literature on how climate change will impact on current and future P losses from agricultural landscapes (Ockenden et al., 2017). Similarly, how to disentangle current and future trends in P fluxes due to climate change itself from those related to climate driven changes in agricultural management practices and P inputs (Dupas et al., 2016; Bussi et al., 2017). Furthermore, the responses to climate change could vary widely across geographical scales due to localized differences in the sensitivity of catchment P losses to climatic drivers (Mellander et al., 2018), thus highlighting the need to establish climate vulnerability maps for better assessments of the sensitivity of P water quality trends (such as eutrophication potential) to climatic factors. For example, in Western Europe the weather patterns are influenced by both anthropogenic warming and by decadal trends in the North Atlantic Oscillation (NAO) (Hurrell, 1995). Thus long term changes in weather are not spatially uniform and the effects on water quality are expected to vary for different physical and chemical settings, making an area more or less susceptible to P loss (Mellander et al., 2018). We therefore need to better understand both the heterogeneity in large scale weather changes and the influence on small scale processes of P release, retention and transfer pathways within the landscape, as each pathway has a different impact on water quality at the catchment scale. This knowledge is needed both in order to assess current water quality trends (concentrations and loads) and to model future scenarios for specific regions.

As said, while the impacts of projected climate on river hydrological regimes are widely studied, fewer projections of the likely impact on future P pollution in running waters exist

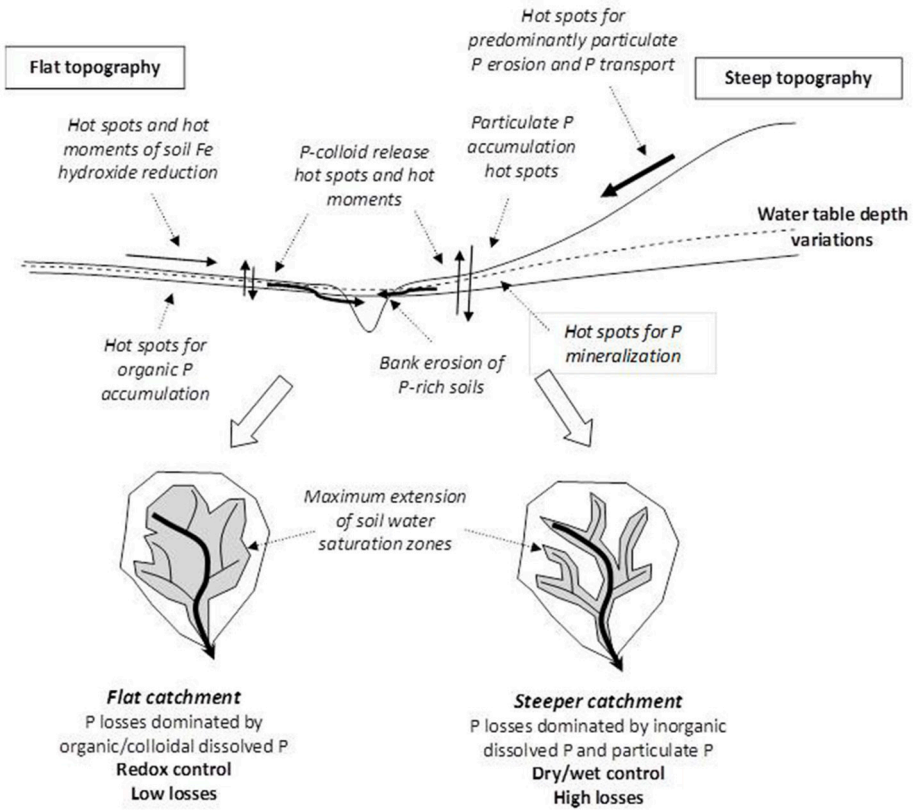

FIGURE 3 | Sketch illustrating the concept of landscape biogeochemistry applied to dissolved, colloidal and particulate P emissions in catchments (adapted from Gu et al., 2017).

FIGURE 4 | Overland flow on an arable field with well drained soils (country Wexford, Ireland), following heavy rainfall in November 2014 [photo: Michael Fleming].

(Whitehead et al., 2009; Dunn et al., 2015; Mehdi et al., 2015; Hesse and Krysanova, 2016; Ockenden et al., 2016, 2017). This may be related to the continuing complexity of human activities and its impact on water quality across a range of different spatial scales, including the small headwater catchment scale, while climate scientists traditionally focus their work mostly only at the larger scales (Michalak, 2016). In addition, while it is possible to model the link between precipitation and discharge with reasonable certainty, the relationship between climate change and water quality is subject to uncertainties in our understanding of the potential effects of climate change on the physical and biogeochemical processes along the nutrient source-mobilization-delivery-impact continuum. Furthermore, it is difficult to disentangle direct climate change impacts from the indirect consequences of adaptive land use mediated by climate change (Bussi et al., 2016, 2017). Thus, water quality modeling with respect to climate change impacts is subject to more weaknesses and uncertainties compared to rainfall-runoff modeling (Hesse and Krysanova, 2016). Understanding the impact of climate change on water quality will require an understanding of the link between P concentrations, loads and recipient freshwater ecosystems within the context of multiple stressors (Whitehead and Crossman, 2012; Crossman et al., 2013), including point source and diffuse pollution sources and water abstraction.

Across NW Europe, national scale climate projections vary from relatively straightforward patterns of drier summers and wetter winters in the Atlantic climate across the British Isles (Jenkins et al., 2010), to more complicated regional patterns and higher uncertainty related to both the direction and magnitude of change in precipitation in the more continental climatic regime of Germany (e.g., Van der Linden and Mitchell, 2009; Gädeke et al., 2017). Meanwhile, in Scandinavian countries (Norway and Sweden), climate projections have indicated greater warming in the northern latitudes than in southern latitudes, particularly during winter. The precipitation in Sweden is expected to increase throughout the country but more moderately in summer (Lind and Kjellström, 2008), while in Norway precipitation is expected to increase across the country with the highest increase expected during spring in Mid-Norway (Hanssen-Bauer et al., 2009). Air temperatures affect soil P mineralization, therefore increased temperatures in summer will likely lead to a buildup of labile P pool in the soil (Turner and Haygarth, 2001), ready for transfer to waterbodies by the autumn/winter rains. Thus, areas where both summer temperatures and winter rainfall are projected to increase are likely to become more prone to P mobilization and thus vulnerable to P loss to water (Jordan et al., 2012) (**Figure 4**). Soil rewetting after a dry summer will mobilize P of mostly microbial origin, largely controlled by the soil P status (Dupas et al., 2015a), while prolonged wet periods due to more rain or more frequent rain may further enhance P release due to reductive dissolution of Fe (hydr)oxides (Van der Grift et al., 2016; Gu et al., 2017). In both cases, the mobilized P consists mainly of dissolved (both organic and inorganic) P forms, i.e., of P forms which are potentially highly bioavailable to algae.

Drying-rewetting and freezing-thawing episodes of soils are two of the most common forms of abiotic soil perturbation, resulting in solubilisation and release of P (Blackwell et al., 2009). In response to climate change it is likely that the frequency of such episodes and/or the duration of the dry and frozen periods will change differently in different areas. Furthermore, soil freezing-thawing events can increase the rates of P losses due to freezing of plant material (e.g., Bechmann et al., 2005). In Northern European countries, such as Sweden, projected warmer temperatures will likely shorten the period of persistent snowpack and cause more soil freezing-thawing episodes (Mellander et al., 2007) with increased erosion and loss of particulate P. In German lower mountain ranges snowmelt events are often an important source of sediment and P loss (Ollesch et al., 2005, 2006). Increasing temperatures may therefore shorten periods with snow cover, but could in contrast to Northern Europe also lower surface runoff due to smaller number of snowmelt events (Anis and Rode, 2015). These may mobilize both the dissolved and particulate P. In Norway, the trend in the number of freeze-thaw events depends on altitude, with an increasing number observed in the mountains (Hanssen-Bauer et al., 2009) and a decrease observed in the lower lying agricultural areas along the coast (Bechmann and Eggestad, 2016).

Catchments at high risk of P transfer are particularly responsive to changes in climate. For example, in a hydrologically flashy agricultural catchment in Ireland the total reactive phosphorus (TRP) loss was threefold that of a more hydrologically buffered catchment, despite similar soil P status (Mellander et al., 2015). The inter-annual variability in P loss in the flashy catchment was larger than the difference between the two catchments, highlighting the catchment dependence of P transfer risk and sensitivity to more rain, or more frequent rain, to catchment different hydrological flow paths. In another example from Norway, soil erosion was found to be the main process of P transfer in agricultural catchments with arable land and a flashy hydrology. In these catchments the soil P status appeared to have an influence on the catchment P loss (Bechmann et al., 2008). Thus changing rainfall patterns and rainfall intensity under climate change may affect rainfall erosivity and therefore particulate P mobilization and transfer to watercourses (Panagos et al., 2017; Poggio et al., 2018).

An understanding of the magnitude of different hydrological flow paths, their response to climate change and their potential effects on nutrient and soil loss processes will be necessary for choosing the right mitigation measures under future climate scenarios. While the amount of P lost from catchments increases with runoff, several mitigation measures, such as sedimentation ponds, have been implemented to reduce P loading from agricultural catchments, with an effective annual retention of 8–35% of TP (average 18%) (Blankenberg et al., 2013). However, a recent study found that current mitigation efforts will not be sufficient to combat the effects of climate change on P losses, particularly in areas where increased winter runoff will lead to an overriding increase in P loads (Ockenden et al., 2017).

The importance of concentrations vs. loads and seasonality of climate change impacts (i.e., summer vs. winter) will vary with the type of receptor waterbodies (e.g., headwater catchments vs. downstream river reaches and lakes) and will have different

impacts on freshwater ecology. For example, increased winter river flows may lead to increased total annual P loads (Ockenden et al., 2017), leading to negative impacts on standing waters such as lakes and reservoirs during the ecologically active period of spring and summer (Stamm et al., 2014). Conversely, increased P concentration during reduced summer flows (Bussi et al., 2017), could lead to negative impacts on river ecosystems (Stamm et al., 2014). These likely differential seasonal and water-body effects will be important to consider when modeling the impact of climate change scenarios on aquatic ecology. Thus improvement of our mechanistic understanding at multiple scales along with development of novel methods for accommodating rigorous error analysis are the imperative challenges for the future of integrated water quality modeling (Rode et al., 2010). Meanwhile, modeling the complex interactions between climate change impacts, social and economic adaptation and land use change is not a trivial task and whilst it is critical for future adaptation policies, to our knowledge, only limited examples of such integrated analysis are available to date (Dunn et al., 2012; Mehdi et al., 2015; Sample et al., 2016).

CONCLUSION FOR FUTURE RESEARCH

Independent of the variety of issues highlighted in the present paper which do highlight the fact that the reduction of phosphorus (P) based water eutrophication in the agricultural landscapes of Northwest Europe is neither simple nor straightforward. We like to conclude that there is a crucial need for more integrative research efforts to deal with our incomplete understanding of the mechanisms and processes associated with the identification of critical source areas, P mobilization, delivery and biogeochemical processing, as otherwise even high-intensity and high-resolution research efforts will likely only reveal an incomplete picture of the full global impact of the role of terrestrial derived P on downstream aquatic and marine ecosystems.

AUTHOR CONTRIBUTIONS

All authors listed have made a substantial, direct and intellectual contribution to the work, and approved it for publication.

ACKNOWLEDGMENTS

The INSU-CNRS Earth Sciences and Astronomy Observatory of Rennes (OSUR), the Loire-Brittany Water Agency (AELB), and the French Catchment Network Observatory (SOERE Réseau des Bassins Versants) are thanked for their financial support to the international workshop meeting which was held in Rennes (France) between 24th and 26th October 2017 and whose outputs and discussions have served as a basis for constructing this paper.

SUPPLEMENTARY MATERIAL

The Supplementary Material for this article can be found online at: https://www.frontiersin.org/articles/10.3389/fmars.2018.00276/full#supplementary-material

REFERENCES

Abbott, B. W., Gruau, G., Zarnetske, J. P., Moatar, F., Barbe, L., Thomas, Z., et al. (2017). Unexpected spatial stability of water chemistry in headwater stream networks. *Ecol. Lett.* 21, 296–308. doi: 10.1111/ele.12897

Ahlgren, J., Djodjic, F., and Wallin, M. (2012). Barium as a potential indicator of phosphorus in agricultural runoff. *J. Environ. Qual.* 41, 208–216. doi: 10.2134/jeq2011.0220

Ahmad, Z. U., Sanin, M., Lian, Q., Zappi, M., and Gang, D. D. (2017). Nonpoint source pollution. *Water Environ. Res.* 89, 1580–1602. doi: 10.2175/106143017X15023776270593

Alewell, C., Birkholz, A., Meusburger, K., Schindler Wildhaber, Y., and Mabit, L. (2016). Quantitative sediment source attribution with compound-specific isotope analysis in a C3 plant-dominated catchment (central Switzerland). *Biogeoscience* 13, 1587–1596. doi: 10.5194/bg-13-1587-2016

Anis, M. R., and Rode, M. (2015). Effect of climate change on runoff components using high resolution rainfall-runoff modelling. *Hydrol. Process.* 29, 2478–2490. doi: 10.1002/hyp.10381

Arheimer, B. C.,Donnelly, and Strömqvist, J. (2013). Large-scale effects of climate change on water resources in Sweden and Europe. *J. Water Man. Res.* 69, 201–207.

Baken, S., Moens, C., Van der Grift, B., and Smolders, E. (2016). Phosphate binding by natural irion-rich colloids in streams. *Water Res.* 98, 326–333. doi: 10.1016/j.watres.2016.04.032

Baken, S., Nawara, S., Van Moorleghem, C., and Smolders, E. (2014). Iron colloids reduce the bioavailability of phosphorus to the green alga *Raphidocelis subcapitata*. *Water Res.* 59, 198–206. doi: 10.1016/j.watres.2014.04.010

Baken, S., Salaets, P., Desmet, N., Seuntjens, P., Vanlierde, E., and Smolders, E. (2015). Oxidation of iron causes removal of phosphorus and arsenic from streamwater in groundwater-fed lowland catchments. *Environ. Sci. Technol.* 49, 2886–2894. doi: 10.1021/es505834y

Baken, S., Sjöstedt, C., Gustafsson, J. P., Seuntjens, P., Desmet, N., De Schutter, J., et al. (2013). Characterisation of hydrous ferric oxides derived from iron-rich groundwaters and their contribution to the suspended sediment of streams. *Appl. Geochem.* 39, 59–68. doi: 10.1016/j.apgeochem.2013.09.013

Bechmann, M., and Deelstra, J. (2013). *Agriculture and Environment-Long Term Monitoring in Norway*. Trondheim: Akademika.

Bechmann, M., Deelstra, J., Stålnacke, P., Eggestad, H. O., Øygarden, L., and Pengerud, A. (2008). Monitoring catchment scale agricultural pollution in Norway – policy instruments, implementation of mitigation methods and trends in nutrient and sediment losses. *Environ. Sci. Policy* 11, 102–114. doi: 10.1016/j.envsci.2007.10.005

Bechmann, M., and Eggestad, H. O. (2016). *Temperaturendringer, Plantevekst og Avrenning*. NIBIO popular articles 2, 1–4 (In Norwegian).

Bechmann, M., Starkloff, T., Kværnø, S., and Eklo, O. M. (2017a). *Plot Study. Soil and Nutrient Losses through Surface and Subsurface Pathways with Different Soil Tillage*. NIBIO report 3, 1–48 (In Norwegian).

Bechmann, M., Stenrød, M., Greipsland, I., Hauken, M., Deelstra, J., Eggestad, H. O., et al. (2017b). *Erosion and Loss of Nutrients and Pesticides from Agricultural Dominated Catchments*. NIBIO report 3, 1–104 (In Norwegian).

Bechmann, M. E., Kleinman, P. J., Sharpley, A. N., and Saporito, L. S. (2005). Freeze-thaw effects on phosphorus loss in runoff from manured and catch-cropped soils. *J. Environ. Qual.* 34. 2301–2309. doi: 10.2134/jeq2004.0415

Bergström, L. Kirchmann, H., Djodjic, F., Kyllmar, K., Ulén, B., Liu, J., et al. (2015). Turnover and losses of phosphorus in Swedish agricultural soils: long-term changes, leaching trends, and mitigation measures. *J. Environ. Qual.* 44, 512–523. doi: 10.2134/jeq2014.04.0165

Bieroza, M. Z., and Heathwaite, A. L. (2015). Seasonal variation in phosphorus concentration–discharge hysteresis inferred from high-frequency *in situ* monitoring. *J. Hydrol.* 524, 333–347. doi: 10.1016/j.jhydrol.2015.02.036

Bieroza, M. Z., and Heathwaite, A. L. (2016). Unravelling organic matter and nutrient biogeochemistry in groundwater-fed rivers und er baseflow conditions: uncertainty in *in situ* high-frequency analysis. *Sci. Total Environ.* 572, 1520–1533. doi: 10.1016/j.scitotenv.2016.02.046

Bieroza, M. Z., Heathwaite, A. L., Mullinger, N. J., and Keenan, P. O. (2014). Understanding nutrient biogeochemistry in agricultural catchments: the challenge of appropriate monitoring frequencies. *Environ. Sci. Proc. Imp.* 16, 1676–1691. doi: 10.1039/C4EM00100A

Billen, G., Garnier, J., Némery, J., Sebilo, M., Ferratore, A., Barles, S., et al. (2007). A long-term view of nutrient transfers through the Seine river continuum. *Sci. Total Environ.* 375, 80–97. doi: 10.1016/j.scitotenv.2006.12.005

Blackwell, M. S. A., Brookes, P. C., de la Fuente-Martinez, N., Gordon, H., Murray, P. J., Snars, K. E., et al. (2010). Phosphorus solubilization and potential transfer to surface waters from the soil microbial biomass following drying-rewetting and freezing-thawing. *Adv. Agron.* 106, 1–35. doi: 10.1016/S0065-2113(10)06001-3

Blackwell, M. S. A., Brookes, P. C., de la Fuente-Martinez, N., Murray, P. J., Snars, K. E., Williams, J. K., et al. (2009). Effects of soil drying and rate of re-wetting on concentrations and forms of phosphorus in leachate. *Biol. Fert. Soils* 45, 635–643. doi: 10.1007/s00374-009-0375-x

Blackwell, M. S. A., Carswell, A. M., and Bol, R. (2013). Variations in concentrations of N and P forms in leachates from dried soils rewetted at different rates. *Biol. Fertil. Soils* 49, 79–87. doi: 10.1007/s00374-012-0700-7

Blankenberg, A. G. B., Deelstra, J., Øgaard, A. F., and Pedersen, R. (2013). "Phosphorus and sediment retention in a constructed wetland," in *Agriculture and Environment- Long Term Monitoring in Norway*. Trondheim: Akademika.

Bol, R., Julich, D., Brödlin, D., Siemens, J., Dippold, M. A., Spielvogel, S., et al. (2016). Dissolved and colloidal phosphorus fluxes in forest ecosystems - an almost blind spot in ecosystem research. *J. Plant Nutr. Soil Sci.* 179, 425–438. doi: 10.1002/jpln.201600079

Bowes, M. J., Jarvie, H. P., Halliday, S. J., Skeffington, R. A., Wade, A. J., Loewenthal, M., et al. (2015). Characterising phosphorus and nitrate inputs to a rural river using high-frequency concentration-flow relationships. *Sci. Total Environ.* 511, 608–620. doi: 10.1016/j.scitotenv.2014.12.086

Bowes, M. J., Jarvie, H. P., Naden, P. S., Old, G. H., Scarlett, P. M., Roberts, C., et al. (2014). Identifying priorities for nutrient mitigation using river concentration-flow relationships: the Thames basin, UK. *J. Hydrol.* 517, 1–12. doi: 10.1016/j.jhydrol.2014.03.063

Bowes, M. J., Smith, J. T., Jarvie, H. P., and Neal, C. (2008). Modelling of phosphorus inputs to rivers from diffuse and point sources. *Sci. Total Environ.* 395, 125–138. doi: 10.1016/j.scitotenv.2008.01.054

Bussi, G., Janes, V., Whitehead, P. G., Dadson, S. J., and Holman, I. P. (2017). Dynamic response of land use and river nutrient concentration to long-term climatic changes. *Sci. Total Environ.* 590–591, 818–831. doi: 10.1016/j.scitotenv.2017.03.069

Bussi, G., Whitehead, P. G., Bowes, M. J., Read, D. S., Prudhomme, C., and Dadson, S. J. (2016). Impacts of climate change, land-use change and phosphorus reduction on phytoplankton in the river Thames (UK). *Sci. Total Environ.* 572, 1507–1519. doi: 10.1016/j.scitotenv.2016.02.109

Butterly, C. R., McNeill, A. M., Baldock, J. A., and Marschner, P. (2011). Rapid changes in carbon and phosphorus after rewetting of dry soil. *Biol. Fertil. Soils* 47, 41–50. doi: 10.1007/s00374-010-0500-x

Charlton, M. B., Bowes, M. J., Hutchins, M. G., Orr, H. G., Soley, R., and Davison, P. (2018). Mapping eutrophication risk from climate change: future phosphorus concentrations in English rivers. *Sci. Total Environ.* 613, 1510–1526. doi: 10.1016/j.scitotenv.2017.07.218

Chen, H., Lai, L., Zhao, X., Li, G., and Lin, Q. (2016). Soil microbial biomass carbon and phosphorus as affected by frequent drying-rewetting. *Soil Res.* 54, 321–327. doi: 10.1071/SR14299

Chowdhury, R. B., Moore, G. A., and Weatherley, A. J. (2014). A review of recent substance flow analyses of phosphorus to identify priority management areas at different geographical scales. *Res. Conserv. Recycl.* 83, 213– 228. doi: 10.1016/j.resconrec.2013.10.014

Christen, B., and Dalgaard, T. (2013). Buffers for biomass production in temperate European agriculture: a review and synthesis on function, ecosystem services and implementation. *Biomass Bioenergy* 55, 53–67. doi: 10.1016/j.biombioe.2012.09.053

Cooper, R. J., Pedentchouk, N., Hiscock, K. M., Disdle, P., Krueger, T., and Rawlins, B. G. (2015b). Apportioning sources of organic matter in streambed sediments: an integrated molecular and compound-specific stable isotope approach. *Sci. Total Environ.* 520, 187–197. doi: 10.1016/j.scitotenv.2015.03.058

Cooper, R. J., Rawlins, B. G., Krueger, T., Lézé, B., Hiscock, K. M., and Pedentchouk, N. (2015a). Contrasting controls on the phosphorus concentration of suspended particulate matter under baseflow and storm event conditions in agricultural headwater streams. *Sci. Total Environ.* 533, 49–59. doi: 10.1016/j.scitotenv.2015.06.113

Crockford, L., O'Riordain, S., Taylor, D., Melland, A. R., Shortle, G., and Jordan, P. (2017). The application of high temporal resolution data in river catchment modelling and management strategies. *Environ. Monit. Assess.* 189:461. doi: 10.1007/s10661-017-6174-1

Crossman, J., Whitehead, P. G., Futter, M. N., Jin, L., Shahgedanova, M., Castellazzi, M., et al. (2013). The interactive responses of water quality and hydrology to changes in multiple stressors, and implications for the long-term effective management of phosphorus. *Sci. Total Environ.* 454–455, 230–244. doi: 10.1016/j.scitotenv.2013.02.033

Dahlke, H. E., Easton, Z. M., Lyon, S. W., Walter, M. T., Destouni, G., and Steenhuis, T. S. (2012). Dissecting the variable source area concept – subsurface flow pathways and water mixing processes in a hillslope. *J. Hydrol.* 420–421, 125–141. doi: 10.1016/j.jhydrol.2011.11.052

Deelstra, J., Øygarden, L., Blankenberg, A. G. B., and Eggestad, H. O. (2011). Climate change and runoff from agricultural catchments in Norway. *Int. J. Clim. Change Strateg. Manag.* 3, 345–360. doi: 10.1108/17568691111175641

Djodjic, F., Elmquist, H., and Collentine, D. (2017). Targeting critical source areas for phosphorus losses: evaluation with soil testing, farmers' assessment and modelling. *Ambio* 47, 45–56. doi: 10.1007/s13280-017-0935-5

Djodjic, F., and Villa, A. (2015). Distributed, high-resolution modelling of critical source areas for erosion and phosphorus losses. *Ambio* 44, S241–S251. doi: 10.1007/s13280-014-0618-4

Dodd, R. J., and Sharpley, A. N. (2016). Conservation practice effectiveness and adoption: unintended consequences and implications for sustainable phosphorus management. *Nutr. Cycle Agroecosyst.* 104, 373–392. doi: 10.1007/s10705-015-9748-8

Dodds, R. J., and Sharpley, A. N. (2015). Recognizing the role of soil organic phosphorus in soil fertility and water quality. *Res. Conserv. Recycl.* 105, 282–293. doi: 10.1016/j.resconrec.2015.10.001

Dodds, W. K., and Oakes, R. M. (2008). Headwater influences on downstream water quality. *Environ. Manag.* 41, 367–377. doi: 10.1007/s00267-007-9033-y

Dunn, S. M., Brown, I., Sample, J., and Post, H. (2012). Relationships between climate, water resources, land use and diffuse pollution and the significance of uncertainty in climate change. *J. Hydrol.* 434–435, 19–35. doi: 10.1016/j.jhydrol.2012.02.039

Dunn, S. M., Towers, W., Dawson, J. J. C., Sample, J., and McDonald, J. (2015). A pragmatic methodology for horizon scanning of water quality linked to future climate and land use scenarios. *Land Use Policy* 44, 131–144. doi: 10.1016/j.landusepol.2014.12.007

Dupas, R., Delmas, M., Dorioz, J. M., Granier, J., Moatar, F., and Gascuel-Odoux, C. (2015d). Assessing the impact of agricultural pressures on N and P loads and eutrophication risks. *Ecol. Indic.* 48, 396–407. doi: 10.1016/j.ecolind.2014.08.007

Dupas, R., Gascuel-Odoux, C., Gillet, N., Grimaldi, C., and Gruau, G. (2015c). Distinct export dynamics for dissolved and particulate phosphorus reveal independent transport mechanisms in an arable headwater catchment. *Hydrol. Proces.* 29, 3162–3178. doi: 10.1002/hyp.10432

Dupas, R., Gruau, G., Gu, S., Guillaume, H., Jaffrézic, A., and Gascuel-Odoux, C. (2015a). Groundwater control of biogeochemical processes causing phosphorus release from riparian wetlands. *Water Res.* 84, 307–314. doi: 10.1016/j.watres.2015.07.048

Dupas, R., Jomaa, S., Musolff, A., Borchardt, D., and Rode, M. (2016). Disentangling the influence of hydroclimatic patterns and agricultural management on river nitrate dynamics from sub-hourly to decadal time scales. *Sci. Total Environ.* 571, 791–800. doi: 10.1016/j.scitotenv.2016.07.053

Dupas, R., Musolff, A., Jawitz, J. W., Suresh, P., Rao, C., Jäger, C. G., et al. (2017). Carbon and nutrient export regimes from headwater

catchments to downstream reaches. *Biogeosciences* 14, 4391–4407. doi: 10.5194/bg-14-4391-2017

Dupas, R., Tavenard, R., Fovet, O., Gilliet, N., Grimaldi, C., and Gascuel-Odoux, C. (2015b). Identifying seasonal patterns of phosphorus storm dynamics with dynamic time warping. *Water Resour. Res.* 51, 8868–8882. doi: 10.1002/2015WR017338

Edwards, A. C., and Withers, P. J. A. (2007). Linking phosphorus sources to impacts in different types of water body. *Soil Use Manag.* 23, 133–143. doi: 10.1111/j.1475-2743.2007.00110.x

Elmgren, R., Blenckner, T., and Andersson, A. (2015). Baltic sea management: successes and failures. *Ambio* 44, S335–S344. doi: 10.1007/s13280-015-0653-9

Evans, D. M., Schoenholtz, S. H., Wigington P. J. Jr., Griffith, S. M., and Floyd, W. C. (2014). Spatial and temporal patterns of dissolved nitrogen and phosphorus in surface waters of a multi-land use basin. *Environ. Monit. Assess.* 186, 873–887 doi: 10.1007/s10661-013-3428-4

Fernandez-Mena, H., Nesme, T., and Pellerin, S. (2016). Towards an agro-industrial ecology: a review of nutrient flow modelling and assessment tools in agro-food systems at the local scale. *Sci. Total Environ.* 543, 467–479. doi: 10.1016/j.scitotenv.2015.11.032

Fölster, J., Johnson, R. K., Futter, M. N., and Wilander, A. (2014). The swedish monitoring of surface waters: 50 years of adaptive monitoring. *Ambio* 43, 3–18. doi: 10.1007/s13280-014-0558-z

Gädeke, A., Pohle, I., Koch, H., and Grünewald, U. (2017). Trend analysis for integrated regional climate change impact assessments in the Lusatian river catchments (North-eastern Germany). *Reg. Environ. Change* 17, 1751–1762. doi: 10.1007/s10113-017-1138-0

Garnache, C., Swinton, S. M., Herriges, J. A., Lupi, F., and Stevenson, R. J. (2016). Solving the phosphorus pollution puzzle: synthesis and directions for future research. *Am. J. Agric. Econ.* 98, 1334–1359. doi: 10.1093/ajae/aaw027

George, T. S., Giles, C. D., Menezes-Blackburn, D., Condron, L. M., Gama-Rodrigues, A. C., Jaisi, D., et al. (2017). Organic phosphorus in the terrestrial environment: a perspective on the state of the art and future priorities. *Plant Soil* 427, 191–208. doi: 10.1007/s11104-017-3391-x

Glendell, M., Jones, R., Dungait, J. A. J., Meusburger, K., Schwendel, A. C., Barclay, R., et al. (2018). Tracing of particulate organic C sources across the terrestrial-aquatic continuum, a case study at the catchment scale (Carminowe Creek, southwest England). *Sci. Total Environ.* 616–617, 1077–1088. doi: 10.1016/j.scitotenv.2017.10.211

Gottselig, N., Amelung, W., Bol, R., Nischwitz, V., Siemens, J., Kirchner, J., et al. (2017b). Natural nanoparticles and colloids in European forest stream waters and their role for phosphorus transport. *Glob. Biogeochem. Cycl.* 31, 1592–1607.

Gottselig, N., Bol, R., Nischwitz, V., Vereecken, H., Amelung, W., and Klumpp, E. (2014). Distribution of phosphorus-containing fine colloids and nanoparticles in stream water of a forest catchment. *Vad. Zone J.* 13, 1–11. doi: 10.2136/vzj2014.01.0005

Gottselig, N., Nischwitz, V., Meyn, T., Amelung, W., Bol, R., Halle, C., et al. (2017a). Phosphorus binding to nanoparticles and colloids in forest stream waters. *Vad. Zone J.* 16, 1–12. doi: 10.2136/vzj2016.07.0064

Granger, S. J., Hawkins, J. M. B., Bol, R., Anthony, S., White, S. M., Owens, P., et al. (2010). Towards a holistic classification of diffuse agricultural water pollution from intensively managed grasslands on heavy soils. *Adv. Agron.* 105, 83–115. doi: 10.1016/S0065-2113(10)05003-0

Greene, S., Taylor, D., McElarney, Y. R., Foy, R. H., and Jordan, P. (2011). An evaluation of catchment-scale phosphorus mitigation using load apportionment modelling. *Sci. Total Environ.* 409, 2211–2221. doi: 10.1016/j.scitotenv.2011.02.016

Grizzetti, B., Bouraoui, F., and Aloe, A. (2012). Changes of nitrogen and phosphorus loads to European seas. *Glob. Change Biol.* 18, 769–782. doi: 10.1111/j.1365-2486.2011.02576.x

Gu, S., Gruau, G., Dupas, R., Rumpel, C., Crème, A., Fovet, O., et al. (2017). Release of dissolved phosphorus from riparian wetlands: evidence for complex interactions among hydroclimate variablilty, topography and soil properties. *Sci. Total Environ.* 598, 421–431. doi: 10.1016/j.scitotenv.2017.04.028

Gu, S., Gruau, G., Malique, F., Dupas, R., Petitjean, P., Gascuel-Odoux, C., et al. (2018). Drying/rewetting cycles stimulate release of colloid-bound phosphorus in riparian soils. *Geoderma* 321, 32–41. doi: 10.1016/j.geoderma.2018.01.015

Hahn, C., Prasuhn, V., Stamm, C., Lazzarotto, P., Evangelou, M. W. H., and Schulin, R. (2013). Prediction of dissolved reactive phosphorus losses from small agricultural catchments: calibration and validation of a parsimonious model. *Hydrol. Earth Syst. Sci.* 17, 3679–3693. doi: 10.5194/hess-17-3679-2013

Hanssen-Bauer, I., Drange, H., Førland, E. J., Roald, L. A., Børsheim, K. Y., Hisdal, H., et al. (2009). *Klima I Norge 2100. Bakgrunnsmateriale til NOU Klimatilplassing*, Norsk klimasenter, Oslo.

Hashemi, F., Olesen, J. E., Dalgaard, T., and Børgesen, C. D. (2016). Review of scenario analyses to reduce agricultural nitrogen and phosphorus loading to the aquatic environment. *Sci. Total Environ.* 573, 608–626. doi: 10.1016/j.scitotenv.2016.08.141

Haygarth, P. M., Condron, L. M., Heathwaite, A. L., Turner, B. L., and Harris, G. P. (2005). The phosphorus transfer continuum: linking source to impact with an interdisciplinary and multi-scaled approach. *Sci. Total Environ.* 344, 5–14. doi: 10.1016/j.scitotenv.2005.02.001

Haygarth, P. M., and Jarvis, S. C. (1999). Transfer of phosphorus from agricultural soil. *Adv. Agron.* 66, 195–249. doi: 10.1016/S0065-2113(08)60428-9

Haygarth, P. M., Page, T. J. C., Beven, K. J., Freer, J., Joynes, A., Butler, P., et al. (2012). Lancaster Environment Centre, Scaling up the phosphorus signal from soil hillslopes to headwater catchments. *Freshw. Biol.* 57, S7–25. doi: 10.1111/j.1365-2427.2012.02748.x

Haygarth, P. M., and Sharpley, A. N. (2000). Terminology for phosphorus transfer. *JEQ* 29, 10–15. doi: 10.2134/jeq2000.00472425002900010002x

Henderson, R., Kabengi, N., Mantripragada, N., Cabrera, M., Hassan, S., and Thompson, A. (2012). Anoxia-induced release of colloid- and nanoparticle-bound phosphorus in grassland soils. *Environ. Sci. Technol.* 46, 11727–11734. doi: 10.1021/es302395r

Hesse, C., and Krysanova, V. (2016). Modeling climate and management change impacts on water quality and in-stream processes in the Elbe River Basin. *Water* 8:40. doi: 10.3390/w8020040

Hurrell, J. W. (1995). Decadal trends in the North Atlantic oscillation: regional temperatures and precipitation. *Science* 269, 676–679. doi: 10.1126/science.269.5224.676

IPCC (2014). *Climate Change 2014: Synthesis Report. Contribution of Working Groups, I., II and III to the Fifth Assessment Report of the Intergovernmental Panel on Climate Change*, eds Core Writing Team, R. K. Pachauri and L. A. Meyer (Geneva: IPCC).

Jacquet, S., Kerimoglu, O., Rimet, F., and Paolini, G. (2014). Cyanobacterial bloom termination: the disappearance of Planktothrix rubescens from Lake Bourget (France) after restoration. *Freshw. Biol.* 59, 2472–2487. doi: 10.1111/fwb.12444

Jarvie, H. P., Sharpley, A. N., Scott, J. T., Haggard, B. E., Bowes, M. J., and Massey, L. B. (2012). Within-river phosphorus retention: accounting for a missing piece in the watershed phosphorus puzzle. *Environ. Sci. Technol.* 46, 13284–13292. doi: 10.1021/es303562y

Jenkins, G. J., Murphy, J. M., Sexton, D. M. H., Lowe, J. A., Jones, P., and Kilsby, C. G. (2010). *UK Climate Projections: Briefing Report*. Version 2, December 2010. Available online at: http://ukclimateprojections.metoffice.gov.uk/22536

Jiang, X., Bol, R., Nischwitz, V., Siebers, N., Willbold, S., Vereecken, H., et al. (2015a). Phosphorus containing water dispersible nanoparticles in arable soil. *J. Environ. Qual.* 44, 1772–1778. doi: 10.2134/jeq2015.02.0085

Jiang, X.-Q., Bol, R., Willbold, S., Vereecken, H., and Klumpp, E. (2015b). Speciation and distribution of P associated with Fe and Al oxides in aggregate-sized fraction of an arable soil. *Biogeosciences* 12, 6443–6452. doi: 10.5194/bg-12-6443-2015

Jiang, X. -Q., Bol, R., Cade-Menun, B. J., Nischwitz, V., and Willbold, S., Bauke, S. L., et al. (2017). Colloid-bound and dissolved phosphorus species in topsoil water extracts along a grassland transect from Cambisol to Stagnosol. *Biogeosciences* 14, 1153–1164. doi: 10.5194/bg-14-1153-2017

Jordan, P., Arnscheidt, J., McGrogan, H., and McCormick, S. (2007). Characterising phosphorus transfers in rural catchments using a continuous bank-side analyser. *Hydrol. Earth Syst. Sci.* 11, 372–381. doi: 10.5194/hess-11-372-2007

Jordan, P., and Cassidy, R. (2011). Technical note: assessing a 24/7 solution for monitoring water quality loads in small river catchments. *Hydrol. Earth Syst. Sci.* 15, 3093–3100. doi: 10.5194/hess-15-3093-2011

Jordan, P., Melland, A. R., Mellander, P. E., Shortle, G., and Wall, D. (2012). The seasonality of phosphorus transfers from land to water: implications for trophic impacts and policy evaluation. *Sci. Total Environ.* 434, 101–109. doi: 10.1016/j.scitotenv.2011.12.070

Kadlec (2016). Large constructed wetlands for phosphorus control: a review. *Water* 8:243. doi: 10.3390/w8060243

Kleinman, P. J., Sharpley, A. N., Withers, P. J., Bergström, L., Johnson, L. T., and Doody, D. G. (2015). Implementing agricultural phosphorus science and management to combat eutrophication. *Ambio* 44, 297–310. doi: 10.1007/s13280-015-0631-2

Kleinman, P. J. A., Sharpley, A. N., McDowell, R. W., Flaten, D. N., Buda, A. R., Tao, L., et al. (2011). Managing agricultural phosphorus for water quality protection: principles for progress. *Plant Soil* 349, 169–182. doi: 10.1007/s11104-011-0832-9

Kruse, J., Abraham, M., Amelung, W., Baum, C., Bol, R., Kühn, O., et al. (2015). Innovative methods in soil phosphorus research: a review. *J. Plant Nutr. Soil Sci.* 178, 43–88. doi: 10.1002/jpln.201400327

Kyllmar, K., Bechmann, M., Deelstra, J., Iital, A., Blicher-Mathiesen, G., Jansons, V., et al. (2014). Long-term monitoring of nutrient losses from agricultural catchments in the Nordic–Baltic region – a discussion of methods, uncertainties and future needs. *Agric. Ecosyst. Environ.* 198, 4–12. doi: 10.1016/j.agee.2014.07.005

Lamba, J., Karthikeyan, K. G., and Thompson, A. M. (2015). Using radiometric fingerprinting and phosphorus to elucidate sediment transport dynamics in an agricultural watershed. *Hydrol. Proc.* 29, 2681–2693. doi: 10.1002/hyp.10396

Legeay, P. L., Gruau, G., and Moatar, F. (2015). *Une Analyse de la Variabilité Spatio-temporelle des Flux et Des Sources Du Phosphore Dans Les Cours D'eau Bretons., Agence de l'Eau.* Loire, Bretagne, 1–104 (in French).

Lind, P., and Kjellström, E. (2008). *Temperature and Precipitation Changes in Sweden, a Wide Range of Model-Based Projections for the 21st Century.* SMHI Reports Meteorology and Climatology.

Liu, J., Yang, J., Liang, X., Zhao, Y., Cade-Menun, B., and Hu, Y. (2014). Molecular speciation of phosphorus present in readily dispersible colloids from agricultural soils. *Soil Sci. Soc. Am. J.* 78, 47–53. doi: 10.2136/sssaj.2013.05.0159

Liu, Y., Engel, B. A., Flanagan, D. C., Gitaua, M. W., McMillan, S. K., and Chaubey, I. (2017). A review on effectiveness of best management practices in improving hydrology and water quality: needs and opportunities. *Sci. Total Environ.* 601–602, 580–593. doi: 10.1016/j.scitotenv.2017.05.212

McClain, M. E., Boyer, E. W., Dent, L., Gergel, S. E., Grimm, N. B., Groffman, P. M., et al. (2003). Biogeochemical hot spots and hot moments at the interface of terrestrial and aquatic ecosystems. *Ecosystems* 3, 301–312. doi: 10.1007/s10021-003-0161-9

McDowell, R. W., Dils, R. M., Collins, A. L., Flahive, K. A., Sharpley, A. N., and Quinn, J. (2016). A review of the policies and implementation of practices to decrease water quality impairment by phosphorus in New Zealand, the UK, and the US. *Nutr. Cycl. Agroecosyst.* 104, 289–305. doi: 10.1007/s10705-015-9727-0

Mehdi, B., Ludwig, R., and Lehner, B. (2015). Regional Studies Evaluating the impacts of climate change and crop land use change on streamflow, nitrates and phosphorus: a modelling study in Bavaria. *J. Hydrol.* 4, 60–90. doi: 10.1016/j.ejrh.2015.04.009

Mellander, P.-E., Jordan, P., Shore, M., Melland, A. R., and Shortle, G. (2015). Flow paths and phosphorus transfer pathways in two agricultural streams with contrasting flow controls. *Hydrol. Process.* 29, 3504–3518. doi: 10.1002/hyp.10415

Mellander, P.-E., Ottosson Löfvenius, M., and Laudon, H. (2007). Climate change impact on snow and soil temperature in boreal scots pine stands. *Clim. Change* 85, 179–193. doi: 10.1007/s10584-007-9254-3

Mellander, P. E., Jordan, P., Bechmann, M., Fovet, O., Shore, M. M., McDonald, N. T., et al. (2018). Integrated climate-chemical indicators of diffuse pollution from land to water. *Sci. Rep.* 8:944. doi: 10.1038/s41598-018-19143-1

Mellander, P. E., Jordan, P., Shore, M., McDonald, N. T., Wall, D. P., Shortle, G., et al. (2016). Identifying contrasting influences and surface water signals for specific groundwater phosphorus vulnerability. *Sci. Total Environ.* 541, 292–302. doi: 10.1016/j.scitotenv.2015.09.082

Michalak, A. (2016). Study role of climate change in extreme threats to water quality. *Nature* 535, 349–350. doi: 10.1038/535349a

Minaudo, C., Dupas, R., Gascuel-Odoux, C., Fovet, O., Mellander, P.-E., Jordan, P., et al. (2017). Nonlinear empirical modeling to estimate phosphorus exports using continuous records of turbidity and discharge. *Water Resour. Res.* 53, 7590–7606. doi: 10.1002/2017WR020590

Minaudo, C., Meybeck, M., Moatar, F., Gassama, N., and Curie, F. (2015). Eutrophication mitigation in rivers: 30 Years of trends in spatial and seasonal patterns of biogeochemistry of the Loire River (1980-2012). *Biogeoscience* 12, 2549–2563. doi: 10.5194/bg-12-2549-2015

Missong, A., Bol, R., Nischwitz, V., Siemens, J., Krüger, J., and , Lang, F., et al. (2017). Phosphorus in water dispersible colloids of forest soil profiles. *Plant Soil* 427, 71–86. doi: 10.1007/s11104-017-3430-7

Missong, A., Holzmann, S., Bol, R., Nischwitz, V., Puhlmann, H., v. Wilpert, K., et al. (2018). Leaching of natural colloids from forest topsoils and their relevance for phosphorus transfer. *Sci. Total Environ.* 634, 305–315. doi: 10.1016/j.scitotenv.2018.03.265

Moss, B. (2012). Cogs in the endless machine: lakes, climate change and nutrient cycles: a review. *Sci. Total Environ.* 434, 130–142. doi: 10.1016/j.scitotenv.2011.07.069

Nesheim, I., Stålnacke, P., Nagothu, U. S., Skarbøvik, E., Barkved, L. J., and Thaulow, H. (2010). "IWRM status in the Glomma River basin," in *Integrating Water Resources Management. Interdisciplinary Methodologies and Strategies,* eds G. D. PracticGooch, A. Rieu-Clarke, and P. Stålnacke (London: IWA-Publishing), 13–23.

Obour, A. K., Silveira, M., Vendraminin, J. M. B., Sollenberger, L. E., and O'Connor, G. A. (2011). Fluctuating water table effect on phosphorus release and availability from a Florida Spodsol. *Nutr. Cycl. Agroecosyst.* 91, 207–217. doi: 10.1007/s10705-011-9456-y

Ockenden, M. C., Deasy, C. E., Benskin, C. M. H., Beven, K. J., Burke, S., Collins, A. L., et al. (2016). Changing climate and nutrient transfers: evidence from high temporal resolution concentration-flow dynamics in headwater catchments. *Sci. Total Environ.* 548–549, 325–339. doi: 10.1016/j.scitotenv.2015.12.086

Ockenden, M. C., Hollaway, M. J., Beven, K. J., Collins, A. L., Evans, R., Falloon, P. D., et al. (2017). Major agricultural changes required to mitigate phosphorus losses under climate change. *Nat. Commun.* 8:161. doi: 10.1038/s41467-017-00232-0

Ollesch, G., Kistner, I., Meissner, R., and Lindenschmidt, K. E. (2006). Modelling of snowmelt erosion and sediment yield in a small low-mountain catchment in Germany. *Catena* 68, 161–176. doi: 10.1016/j.catena.2006.04.005

Ollesch, G., Sukhanovski, Y., Kistner, I., Rode, M., and Meissner, R. (2005). Characterisation and modelling of the spatial heterogeneity of snowmelt erosion. *Earth Surf. Process. Land.* 30, 197–211. doi: 10.1002/esp.1175

Outram, F. N., Cooper, R. J., Sünnenberg, G., Hiscock, K. M., and Lovett, A. A. (2016). Antecedent conditions, hydrological connectivity and anthropogenic inputs: factors affecting nitrate and phosphorus transfers to agricultural headwater streams. *Sci. Total Environ.* 545–546, 184–199. doi: 10.1016/j.scitotenv.2015.12.025

Outram, F. N., Lloyd, C. E. M., Jonczyk, J., Benskin, C. M. H., Grant, F., Perks, M. T., et al. (2014). High-frequency monitoring of nitrogen and phosphorus response in three rural catchments to the end of the 2011-2012 drought in England. *Hydrol. Earth Syst. Sci.* 18, 3429–3448. doi: 10.5194/hess-18-3429-2014

Ouyang, W., Gao, X., Wei, P., Gao, B., Lin, C. Y., and Hao, F. H. (2017). A review of diffuse pollution modelling and associated implications for watershed management in China. *J. Soils Sediments* 17, 1527–1536. doi: 10.1007/s11368-017-1688-2

Panagos, P., Ballabio, C., Meusburger, K., Spinoni, J., Alewell, C., and Borrelli, P. (2017). Towards estimates of future rainfall erosivity in Europe based on REDES and worldclim datasets. *J. Hydrol.* 548, 251–262 doi: 10.1016/j.jhydrol.2017.03.006

Paruch, A. M., Blankenberg, A. G. B., Bechmann, M., and Mæhlum, T. (2015). Application of host-specific genetic markers for microbial source tracking of faecal water contamination in an agricultural catchment. *Acta Agric. Scand.* 65, 164–172. doi: 10.1080/09064710.2014.941392

Paruch, L., and Paruch, A. M. (2017). The importance of melting curve analysis in discriminating faecal and environmental *Bacteroidales* bacteria. *Microbiology* 86, 536–538. doi: 10.1134/S0026261717040117

Perks, M. T., Owen, G. J., Benskin, C. M., Jonczyk, J., Deasy, C., Burke, S., et al. (2015). Dominant mechanisms for the delivery of fine sediment and phosphorus to fluvial networks draining grassland dominated headwater catchments. *Sci. Total Environ.* 523, 178–190. doi: 10.1016/j.scitotenv.2015.03.008

Persson, G. (2001). Phosphorus in tributaries to lake Mälaren, Sweden: analytical fractions, anthropogenic contribution and bioavailability. *Ambio* 30, 486–495. doi: 10.1579/0044-7447-30.8.486

Phillips, G., and Pitt, J. A. A. (2015). Comparison of European Freshwater Nutrient Boundaries Used for the Water Framework Directive: A Report to ECOSTATP. 1–176.

Pinay, G., Gascuel, C., Ménesguen, A., Souchon, Y., Le Moal, M., Levain, A., et al. (2017). *L'eutrophisation: Manifestations, Causes,Conséquences et Prédictibilité. Synthèse de l'Expertise Scientifique Collective CNRS - Ifremer - INRA -Irstea (France),* 1–148.

Poggio, L., Simonettia, E., and Gimona, A. (2018). Enhancing the worldclim data set for national and regional applications. *Sci. Total Environ*. 625, 1628–1643. doi: 10.1016/j.scitotenv.2017.12.258

Radcliffe, D. E., Reid, K. D., Blombäck, K., Bolster, C. H., Collick, A. S., Easton, Z. M., et al. (2015). Applicability of models to predict phosphorus losses in drained fields: a review. *J. Environ. Qual.* 44, 614–628. doi: 10.2134/jeq2014.05.0220

Roberts, W. M., Stutter, M. I., and Haygarth, P. M. (2012). Phosphorus retention and remobilization in vegetated buffer strips: a review. *J. Environ. Qual.* 41, 389–399. doi: 10.2134/jeq2010.0543

Rockström, J., Steffen, W., Noone, K., Persson, Å., Chapin, F. S., Lambin, E., et al. (2009). Planetary boundaries: exploring the safe operating space for humanity. *Ecol. Soc.* 14:32. doi: 10.5751/ES-03180-140232

Rode, M., Arhonditsis, G., Balin, D., Kebede, T., Krysanova, V., van Griensven, A., et al. (2010). New challenges in integrated water quality modelling. *Hydrol. Process.* 24, 3447–3461. doi: 10.1002/hyp.7766

Rode, M., Wade, A. J., Cohen, M. J., Hensley, R. T., Bowes, M. J., Kirchner, J. W., et al. (2016). Sensors in the stream: the high-frequency wave of the present. *Environ. Sci. Technol.* 50, 10297–10307. doi: 10.1021/acs.est.6b02155

Romero, E., Le Gendre, R., Garnier, J., Billen, G., Fisson, C., Silvestre, M., et al. (2016). Long-term water quality in the lower seine: lessons learned over 4 decades of monitoring. *Environ. Sci. Pol.* 58, 141–154. doi: 10.1016/j.envsci.2016.01.016

Rowe, H., Withers, P. J. A., Baas, P., Chan, N. I., Doody, D., Holiman, J., et al. (2016). Integrating legacy soil phosphorus into sustainable nutrient management strategies for future food, bioenergy and water security. *Nutr. Cycl. Agroecosyst.* 104, 393–412. doi: 10.1007/s10705-015-9726-1

Sample, J. E., Baber, I., and Badger, R. (2016). A spatially distributed risk screening tool to assess climate and land use change impacts on water-related ecosystem services. *Environ. Model. Softw.* 83, 12–26. doi: 10.1016/j.envsoft.2016.05.011

Scalenghe, R., Edwards, A. C., Barberis, E., and Ajmone-Marsan, F. (2012). Release of phosphorus under reducing and simulated open drainage conditions from overfertilised soils. *Chemosphere* 95, 289–294. doi: 10.1016/j.chemosphere.2013.09.016

Scavia, D., Allan, J. D., Arend, K. K., Bartell, S., Beletsky, D., Bosch, N. S., et al. (2014). Assessing and addressing the re-eutrophication of Lake Erie: central basin hypoxia. *J. Great Lakes Res.* 40, 226–246. doi: 10.1016/j.jglr.2014.02.004

Schoumans, O. F., Bouraoui, F., Kabbe, C., Oenema, O., and van Dijk, K. C. (2015). Phosphorus management in Europe in a changing world. *Ambio* 44, 180–192. doi: 10.1007/s13280-014-0613-9

Schoumans, O. F., Chardon, W. J., Bechmann, M. E., Gascuel-Odoux, C., Hofman, G., Kronvang, B., et al. (2014). Mitigation options to reduce phosphorus losses from the agricultural sector and improve surface water quality: a review. *Sci. Total Environ.* 468–469, 1255–1266. doi: 10.1016/j.scitotenv.2013.08.061

Sharpley, A. N., Bergström, L., Aronsson, H., Bechmann, M., Bolster, C. H., Börling, K., et al. (2015). Future agriculture with minimized phosphorus losses to waters: research needs and direction. *Ambio* 44, 163–179. doi: 10.1007/s13280-014-0612-x

Shepherd, A., Wu, L. H., Chadwick, D., and Bol, R. (2011). A review of quantitative tools for assessing the diffuse pollution response to farmer adaptions and mitigation methods under climate change. *Adv. Agron.* 112, 1–54. doi: 10.1016/B978-0-12-385538-1.00001-9

Sherriff, S. C., Rowan, J. S., Fenton, O., Jordan, P., Melland, A. R., Mellander, P. E., et al. (2016). Storm event suspended sediment-discharge hysteresis and controls in agricultural watersheds: implications for watershed scale sediment management. *Environ. Sci. Technol.* 50, 1769–1778. doi: 10.1021/acs.est.5b04573

Shore, M., Murphy, S., Mellander, P.-E., Short, G., Melland, A. R., Crockford, L., et al. (2017) Influence of storm flow and base flow phosphorus pressures on stream ecology in agricultural catchments. *Sci. Total Environ.* 590–591, 469–483. doi: 10.1016/j.scitotenv.2017.02.100

Skarbøvik, E., and Roseth, R. (2014). Use of sensor data for turbidity, pH and conductivity as an alternative to conventional water quality monitoring in four Norwegian case studies. *Acta Agric. Scand. Sect. B Soil Plant Sci.* 65, 63–73.doi: 10.1080/09064710.2014.966751

Skarbøvik, E., Stålnacke, P., Kaste, Ø., and Austnes, K. (2014). Trends in nutrients and metals in Norwegian rivers and point sources 1990–2009. *Hydrol. Res.* 45, 441–454. doi: 10.2166/nh.2013.233

Smolders, E., Baetens, E., Verbeeck, M., Nawara, S., Diels, J., Verdievel, M., et al. (2017). Internal loading and redox cycling of sediment iron explain reactive phosphorus concentrations in lowland rivers. *Environ. Sci. Technol.* 51, 2584–2592. doi: 10.1021/acs.est.6b04337

Sørensen, R., Zinko, U., and Seibert, J. (2006). On the calculation of the topographic wetness index: evaluation of different methods based on field observations. *Hydrol. Earth Syst. Sci.* 10, 101–112. doi: 10.5194/hess-10-101-2006

Stamm, C., Jarvie, H. P., and Scott, T. (2014). What's more important for managing phosphorus: loads, concentrations or both? *Environ. Sci. Technol.* 48, 23–24. doi: 10.1021/es405148c

Steffen, W., Richardson, K., Rockström, J., Cornell, S. E., Fetzer, I., Bennett, E. M., et al. (2015). Planetary boundaries: guiding human development on a changing planet. *Science* 347:1259855. doi: 10.1126/science.1259855

Stoddard, J. L., Van Sickle, J., Herlihy, A. T., Brahney, J., Paulsen, S., Peck, D. V., et al. (2016). Continental-Scale Increase in lake and stream phosphorus: are oligotrophic systems disappearing in the United States? *Environ. Sci. Technol.* 50, 3409–3415. doi: 10.1021/acs.est.5b05950

Stutter, M., Dawson, J. J. C., Glendell, M., Napier, F., Potts, J. M., Sample, J., et al. (2017). Evaluating the use of *in-situ* turbidity measurements to quantify fluvial sediment and phosphorus concentrations and fluxes in agricultural streams. *Sci. Total Environ.* 607–608, 391–402. doi: 10.1016/j.scitotenv.2017.07.013

Stutter, M. I., Langan, S. J., and Cooper, R. J. (2008). Spatial contributions of diffuse inputs and within-channel processes to the form of stream water phosphorus over storm events. *J. Hydrol.* 350, 203–214. doi: 10.1016/j.jhydrol.2007.10.045

Stutter, M. I., Langan, S. J., and Lumsdon, D. (2009). Vegetated buffer strips can lead to increased release of phosphorus to waters: a biogechemical assessment of the mechanisms. *Environ. Sci. Technol.* 43, 1858–1863. doi: 10.1021/es8030193

Stutter, M. I., Shand, C. A., George, T. S., Blackwell, M. S. A., Dixon, L., Bol, R., et al. (2015). Land use and soil factors affecting accumulation of phosphorus species in temperate soils. *Geoderma* 257–258, 29–39. doi: 10.1016/j.geoderma.2015.03.020

Thomas, I. A., Jordan, P., Mellander, P. E., Fenton, O., Shine, O., Creamer, R., et al. (2016). Improving the identification of hydrologically sensitive areas using LiDAR DEMs for the delineation and mitigation of critical source areas of diffuse pollution. *Sci. Total Environ.* 556, 276–290. doi: 10.1016/j.scitotenv.2016.02.183

Trevisan, D., Quétin, P., Barbet, D., and Dorioz, J. M. (2012). POPEYE: a river-load oriented model to evaluate the efficiency of environmental policy measures for reducing phosphorus losses. *J. Hydrol.* 450–451, 254–266. doi: 10.1016/j.jhydrol.2012.05.001

Turner, B. L., Dressen, J. P., Haygarth, P. M., and Mckelvie, I. D. (2003). Potential contribution of lysed bacterial celles to phosphorus solubilisation in two rewetted Australian pasture soils. *Soil Biol. Biochem.* 35, 187–189. doi: 10.1016/S0038-0717(02)00244-4

Turner, B. L., and Haygarth, P. M. (2001). Biogeochemistry: phosphorus solubilisation in rewetted soils. *Nature* 411:258. doi: 10.1038/35077146

Van der Grift, B. (2017). *Geochemical and Hydrodynamic Phosphorus Retention Mechanisms in Lowland Catchments*. Ph.D. thesis, Universiteit Utrecht.

Van der Grift, B., Behrends, T., Osté, L. A., Schot, P. P., Wassen, M. J., and Griffioen, J. (2016). Fe hydroxyphosphate precipitation and Fe(II) oxidation kinetics upon aeration of Fe(II) and phosphate-containing synthetic and natural solutions. *Geochim. Cosmochim. Acta* 186, 71–90. doi: 10.1016/j.gca.2016.04.035

Van der Grift, B., Osté, L., Schot, P. P., Kratz, A., Van Popta, E., Wassen, M., et al. (2018). Forms of phosphorus in suspended particulate matter in agriculture-dominated lowland catchments: iron as phosphorus carrier. *Sci. Total Environ.* 631–632, 115–129. doi: 10.1016/j.scitotenv.2018.02.266

Van der Grift, B., Rozemeijer, J. C., Griffioen, J., and van der Velde, Y. (2014). Iron oxidation kinetics and phosphate immobilization along the flow-path

from groundwater into surface water. *Hydrol. Earth Syst. Sci.* 18, 4687–4702. doi: 10.5194/hess-18-4687-2014

Van der Linden, P., and Mitchell, J. F. (2009). *ENSEMBLES Climate, Change, and Its Impacts: Summary of Research and Results from the, ENSEMBLES Project*. Exeter: Met Office Hadley Centre, 1–160.

Vinten, A., Sample, J., Ibiyemi, A., Abdul-Salama, Y., and Stutter, M. (2017). A tool for cost-effectiveness analysis of field scale sediment-bound phosphorus mitigation measures and application to analysis of spatial and temporal targeting in the Lunan Water catchment, Scotland. *Sci. Total Environ.* 586, 631–641. doi: 10.1016/j.scitotenv.2017.02.034

Voegelin, A., Senn, A. C., Kaegi, R., Hug, S. J., and Mangold, S. (2013). Dynamic Fe-precipitate formation induced by Fe(II) oxidation in aerated phosphate-containing water. *Geochim. Cosmochim. Acta* 117, 216–231. doi: 10.1016/j.gca.2013.04.022

Wellen, C., Kamran-Disfani, A. R., and Arhonditsis, G. B. (2015). Evaluation of the current state of distributed watershed nutrient water quality modeling. *Environ. Sci. Technol.* 49, 3278–3290. doi: 10.1021/es50 49557

Whitehead, P. G., and Crossman, J. (2012). Macronutrient cycles and climate change: key science areas and an international perspective. *Sci. Total Environ.* 434, 13–17. doi: 10.1016/j.scitotenv.2011.08.046

Whitehead, P. G., Wade, A. J., and Butterfield, D. (2009). Potential impacts of climate change on water quality and ecology in six UK rivers. *Hydrol. Res.* 40, 113–122. doi: 10.2166/nh.2009.078

Withers, P. J., van Dijk, K. C., Neset, T. S., Nesme, T., Oenema, O., Rubæk, G. H., et al. (2015b). Stewardship to tackle global phosphorus inefficiency: the case of Europe. *Ambio* 44, 193–206. doi: 10.1007/s13280-014-0614-8

Withers, P. J. A., Elser, J. J., Hilton, J., Ohtake, H., Schippere, W. J., and van Dijk, K. C. (2015a). Greening the global phosphorus cycle: how green chemistry can help achieve planetary P sustainability. *Green Chem.* 17, 2087–2099. doi: 10.1039/C4GC02445A

Withers, P. J. A., Neal, C., Jarvie, H. P., and Doody, D. G. (2014). Agriculture and eutrophication: where do we go from here? *Sustainability* 6, 5853–5875. doi: 10.3390/su6095853

Wu, Y., Liu, J., Shena, R., and Fub, B. (2017). Mitigation of nonpoint source pollution in rural areas: from control to synergies of multi ecosystem services. *Sci. Total Environ.* 607–608, 1376–1380. doi: 10.1016/j.scitotenv.2017.07.105

Xie, H., Chen, L., and Shen, Z. (2015). Assessment of agricultural best management practices using models: current issues and future perspectives. *Water* 7, 1088–1108. doi: 10.3390/w7031088

Yang, B., Liu, S. M., and Zhang, J. (2016). Phosphorus speciation and availability in sediments off the eastern coast of Hainan Island, South China Sea. *Cont. Shelf Res.* 118, 111–127. doi: 10.1016/j.csr.2016.03.003

Yao, Q. Z., Du, J. T., Chen, H. T., and Yu, Z. G. (2017). Particle-size distribution and phosphorus forms as a function of hydrological forcing in the Yellow River. *Environ. Sci. Poll. Res.* 23, 3385–3398. doi: 10.1007/s11356-015-5567-3

Zhang, Y., Collins, A. L., Johnes, P. J., and Jones, J. I. (2017). Projected impacts of increased uptake of source control mitigation measures on agricultural diffuse pollution emissions to water and air. *Land Use Policy* 62, 185–201. doi: 10.1016/j.landusepol.2016.12.017

Conflict of Interest Statement: The authors declare that the research was conducted in the absence of any commercial or financial relationships that could be construed as a potential conflict of interest.

frontiers in Marine Science

ORIGINAL RESEARCH
published: 05 February 2018
doi: 10.3389/fmars.2018.00020

Evidence for Coupling of the Carbon and Phosphorus Biogeochemical Cycles in Freshwater Microbial Communities

*O. Roger Anderson**

Department of Biology, Lamont-Doherty Earth Observatory, Columbia University, Palisades, NY, United States

Considerable attention has been given to the roles of the carbon and phosphate cycles in aquatic environments, but less attention has been given to an experimental analysis of the coupling of the C and P cycles in freshwater and marine ecosystems. Using laboratory microcosm experiments, prepared with natural pond-water microbial communities, evidence is presented for the coupling of dissolved organic C with microbial production of alkaline phosphatase driving the phosphorus cycle in freshwater microbial communities. The effects of glucose C-supplementation in microcosm microbial communities (including bacteria and heterotrophic nanoflagellates) on gains in microbial C-content and alkaline phosphatase activity (APA) were estimated in relation to control microcosms without C-supplementation. The C-supplementation increased total microbial APA (pmol min^{-1} μg^{-1} bacterial C) in the C-supplemented treatment (6.5 ± 0.6) compared to the non-supplemented cultures (5.1 ± 1.7). Microbial-bound APA in the C-supplemented treatment was particularly enhanced (4.4 ± 0.9) compared to control cultures (1.3 ± 0.8), but the amount of free (soluble) APA in the aquatic phase was less compared to the controls ($n = 5$, $p < 0.001$). Alkaline phosphatase activity was highly correlated ($r = 0.97$) with bacterial densities in the C-supplemented cultures, further supporting the hypothesis that C-supplementation can increase phosphorus remineralization through elevated production of microbial alkaline phosphatase. This laboratory-based, experimental study suggests that additional research on the coupling of the C and P cycles in freshwater and marine environments may yield productive insights into the finer details of the roles of these two biogeochemical cycles in aquatic microbial community dynamics.

Keywords: aquatic alkaline phosphatase, bacterial C biomass, biogeochemical cycles, heterotrophic nanoflagellate C biomass, microbial food webs, phosphorus biomineralization, planktonic microbial communities

OPEN ACCESS

Edited by:
Christian Lønborg, Australian Institute of Marine Science, Australia

Reviewed by:
L. Antonio Cuevas, EULA-Chile, Universidad de Concepcion, Chile
Renata Zaccone, Istituto per l'Ambiente Marino Costiero (CNR), Italy
Casey Michael Godwin, University of Michigan, United States

***Correspondence:**
O. Roger Anderson
ora@ldeo.columbia.edu

Specialty section:
This article was submitted to Marine Biogeochemistry, a section of the journal Frontiers in Marine Science

Received: *11 November 2017*
Accepted: *16 January 2018*
Published: *05 February 2018*

Citation:
Anderson OR (2018) Evidence for Coupling of the Carbon and Phosphorus Biogeochemical Cycles in Freshwater Microbial Communities. Front. Mar. Sci. 5:20. doi: 10.3389/fmars.2018.00020

INTRODUCTION

There is considerable evidence that eukaryotic microbial communities serve a significant role in fertility of aquatic and terrestrial environments (e.g., Bloem et al., 1989; Adl, 2003; Anderson, 2014b), particularly the contribution of heterotrophic protists such as nanoflagellates that prey on bacteria and promote remineralization of mineral and carbon compounds (e.g., Cole et al., 1977; Clarholm, 1989; Caron, 1994; Selph et al., 2003; Anderson, 2012). Some of this effect can

be attributed to nutrient release during phagotrophic feeding, especially in the microbial loop (e.g., Güde, 1985; Caron, 1994). Further contributions come from the death and lysis of bacteria (Renn, 1937) and by stimulation of bacterial hydrolytic enzymes mediating remineralization of inorganic nutrients such as phosphorus and nitrogen (Hadas et al., 1992; Ferrier-Pagès and Rassoulzadegan, 1994). In heterotrophic microbial communities, organic carbon compounds are a major source of nutrients for bacteria at the base of the food web (e.g., Ducklow, 2000; Anderson and McGuire, 2013). Heterotrophic nanoflagellates (HNAN) are often abundant major predators on bacteria, and are important links in the trophic hierarchy between bacteria and higher biota such as invertebrates (Caron et al., 1985; Anderson, 2012); therefore, the abundance and C-content of HNAN are analyzed in addition to bacteria. Moreover, because there is a focus in this study on C enrichment, and the C and P biogeochemical cycles in microbial communities, the alkaline phosphatase activity (APA) is normalized to bacterial C-biomass, expressed as APA units μg^{-1} bacterial C-content.

Although there is substantial published research on the role of organic C in microbial community dynamics, there is less research on the coupling of organic C with the phosphorus cycle, including production of microbial phosphatases, a potentially significant source of phosphate remineralization, especially in aquatic environments (Gibson et al., 1996; Dyhrman et al., 2007; Duhamel and Moutin, 2009; Ruttenberg and Dyhrman, 2012; Duhamel et al., 2014). Because of the potential threats from global warming, considerable research has been done on the coupling of nitrogen and carbon cycles, largely in relation to the effect of nitrogen on primary production, thus enhancing CO_2 sequestration (Esser et al., 2011; Zaehle, 2013). However, there is a relative lack of ecological experimental research on the potential role of organic C in driving the phosphorus cycle as mediated by microbial organo-phosphohydrolytic enzymes within the context of a community level analysis. A complex network of interactions link microbial communities to the biogeochemical changes of C and P (e.g., Anderson et al., 2018), including the role of increased atmospheric C as CO_2 that drives primary production, thus producing more soluble organic nutrients in aquatic ecosystems. Soluble nutrients potentially enhance heterotrophic microbial production, including release of enzymes such as alkaline phosphatases that convert organic phosphates into free phosphate available to support further growth of primary producers, and micro-heterotrophs. Understanding the dynamics and inter-relations of these processes can yield deeper insights into aquatic microplankton interactions.

This is a report of the effects of dissolved organic C (DOC) enrichment on alkaline phosphatase activity in freshwater heterotrophic microbial communities with a goal of estimating the role of DOC in phosphorus remineralization. The major research questions addressed are as follows: (1) What is the effect of emending freshwater microbial cultures with glucose-C on the relative gain in densities and C-content of bacteria and heterotrophic nanoflagellates? (2) To what extent does enrichment with glucose-C affect the alkaline phosphatase activity in these cultures? (3) Is there experimental evidence of coupling of the C cycle and phosphorus cycle in aquatic microbial communities?

MATERIALS AND METHODS

Laboratory Cultures

Laboratory cultures of microbial communities were established using a standard source of pond water distributed by Carolina Biological (Burlington, NC), a filtered and pasteurized water obtained from a local freshwater pond at Burlington, NC. To establish a sufficiently robust microbial community in laboratory cultures, the pond water was inoculated with a suspension of dark, rich sediment obtained from the margin of a freshwater pond on the Lamont-Doherty Earth Observatory Campus (41.004247, - 73.911677). A sample of the surface sediment (0.1 g) was added to 5 ml of the Carolina pond water in a 15-ml plastic conical centrifuge tube and thoroughly suspended using a vortex mixer. One milliliter of the suspension was added to 100 ml of Carolina pond water to be used for the experimental laboratory cultures. Fifty milliliter of this prepared pond water was distributed into each of two sterile 250 ml Falcon culture flasks (Thermo Fisher Scientific, Waltham, MA). One flask served as a control and the other flask served as a C-enrichment culture, emended with reagent grade glucose at a final concentration of 4 mg glucose-C ml^{-1} water. The cultures were maintained in the dark at 20°C (a reasonable growth temperature in a temperate pond) in a constant temperature incubator (Percival Scientific, Inc., Perry, IA) for 6 days before analysis; assuming the glucose remained labile. Experiments were replicated 5 times during 2 weeks. Because a different 0.1 g portion of sediment was used for each replication, the initial composition of the inoculating biota varied. At 6 days, the final biomass varied sufficiently to permit correlation of enzyme activity with densities.

Microbial Densities and C-Content

After 6-d incubation, 5 ml of thoroughly suspended culture were withdrawn from each of the control and treatment flasks and fixed by addition of pure glutaraldehyde (Ladd Research, Williston, VT), final concentration of 3% (v/v). Bacterial and heterotrophic flagellate densities and C-content were assessed at 1000x magnification by UV epifluorescent microscopy (Anderson et al., 2001). During microscopic enumeration of bacteria and HNAN, they were sized within 0.5 μm using an ocular reticule, deemed sufficiently accurate for the purposes of this research. While counting cocci, the diameter of representative individuals was measured and used in the formula for a sphere to estimate the volume. Likewise, the major and minor axes of bacilli were measured and used in the formula for a prolate spheroid to estimate the cell volume. The length and width of HNANs was assessed during counting and converted to volume using the formula for a prolate spheroid. The C-content of each group of microbes was estimated using a size-based regression equation relating C-content to cell volume (125.3 fg C μm^{-3}) as previously published by Pelegri et al. (1999). Densities of the microbes and their biomasses were expressed as number ml^{-1} and $\mu g\ ml^{-1}$, respectively, and reported as means ± SE based on data from the five replicate experiments. The

Pelegri et al. coefficient for conversion of volume to C-content was deemed to be adequate for both bacteria and HNAN, because the HNAN are relatively small in the range of 2–3 μm. Thus the differences in size ranges are not likely to cause a major bias in C-content estimates, at least within the precision needed for the limited comparisons made in this study.

Alkaline Phosphatase Activity Assays

Alkaline phosphatase activity in the control and treatment cultures was assayed using a Sigma APO100 colorimetric kit with paranitrophenylphosphate (pNPP) substrate as specified by the supplier (Sigma-Aldrich, St. Louis, MO). Blank cuvettes were prepared by adding 980 μL of buffer (1.0 M Diethanolamine and 0.50 mM Mg Cl_2, pH 9.8). Test cuvettes were prepared by adding 20 μL pNPP substrate solution and 960 μL of the buffer. The cuvettes were equilibrated to 37°C before adding 20 μL of the microcosm test sample to the test and blank cuvettes, respectively. The contents of the cuvettes were each immediately mixed by inversion and incubated for 30 min. The absorbance of the test sample vs. the blank was measured at a wavelength of 405 nm using a Beckman DU dual beam spectrophotometer (Beckman, Indianapolis, IN). Triplicate measurements were made for each assay and a mean value was calculated. Total enzyme activity in the control and treatment cultures was obtained using unaltered aliquots of samples from each condition. Free activity (non-bacterial bound) was assayed by passing samples of the cultures through 0.22 μm pore-sized filters (EMD Millipore Corp., Billerica, MA) before enzyme analysis. The enzyme assays were done immediately after sample aliquots were taken from the microcosms and also immediately after filtration through the micropore filters. Bacterial-bound activity was estimated by subtraction of the free activity from the total activity. Enzyme activity was expressed as $\mu mol\ min^{-1}\ ml^{-1}$ of culture, or converted to $pmol\ min^{-1}\ \mu g^{-1}$ of bacterial C in samples from each culture condition. The enzyme activities were converted from $\mu mol\ min^{-1}\ ml^{-1}$ to $pmol\ min^{-1}\ \mu g^{-1}$ C, by first converting the volume in ml to μg-C based on the estimated $C\ ml^{-1}$ for the density of bacteria in the sample. The alkaline phosphatase activity was converted from $\mu mol\ min^{-1}$ to $pmol\ min^{-1}$ by dividing it by 10^6, the number of pmols in a μmol. APA activity was normalized to only the bacterial C-content, because the HNAN C-content was relatively negligible; i.e., as much as two orders of magnitude less. Therefore, for purposes of approximation suitable for this analysis, the APA was normalized only to bacterial C-content. Bacteria can be good proxies for microbial contributions to some ecologically relevant measurements, such as correlation with total soil respiration in some ecosystems (e.g., Anderson, 2014a). Moreover, expressing APA units in terms of bacterial C-content is consistent with prior studies in our research program.

Statistical Analyses

Correlation analyses were obtained using StatPlus® (AnalystSoft, Inc., Alexandria, VA) for Microsoft Excel (Microsoft Corp., Redmond, WA), Student's *t*-test (GraphPad Software, La Jolla, CA) was used to assess the statistical significance of differences ($p \leq 0.05$) in mean data for the experimental and control samples, because it is an appropriate analysis to use for data from two groups. Additionally, the change in value (gain) for each of the two means was also reported.

RESULTS

Question 1: C Enhancement Effects on Microbial Densities and C-Content

What is the effect of emending freshwater microbial cultures with glucose-C on the relative gain in densities and C-content of bacteria and heterotrophic nanoflagellates? Mean densities and C-content of bacteria and heterotrophic nanoflagellates, including gains resulting from C enrichment (experimental treatment values minus control values), are presented in **Table 1**. As would be expected, the data for heterotrophic nanoflagellates (higher up the trophic hierarchy) were substantially lower than for the bacteria at the base of the food chain. The relative gains in density for the two groups of microbes expressed as percentage increase of the C-supplemented cultures relative to the controls are: bacteria (189%), and HNAN (192%). With respect to the relative gains in C-content, the corresponding proportional increases expressed as percentages are: bacteria (195%), and HNAN (188%).

Question 2: C Enhancement of Alkaline Phosphatase Activity

To what extent does enrichment with glucose-C affect the alkaline phosphatase activity in these cultures? Mean data for alkaline phosphatase activities (total, free, and bacterial-bound) for the C-enriched and control cultures are presented in **Table 3**. The amount of enzyme activity was larger in the C-enriched cultures compared to the control cultures. The gain for the total enzyme activity, normalized to bacterial C, was 1.4 $pmol\ min^{-1}\ \mu g^{-1}$ bacterial C. For free activity, there was a relatively greater amount in the control than the treatment culture with a difference of −1.7. The relative gain in bacterial-bound activity, obtained by algebraic subtraction of the mean free value (−1.7) from the total (1.4), was 3.1 (**Table 3**). The gain in bound APA is larger than the estimated total gain, because the free enzyme activity was lower in the control culture than the C-enriched culture. This indicates that C-enrichment tended to increase the bacterial-bound enzyme activity relative to that of the controls. It is important to note that these values are gains (difference values), hence it is possible for the estimate of the gain in bacterial-bound

TABLE 1 | Mean ± SE densities (no. ml^{-1}) of bacteria ($\times 10^9$), heterotrophic nanoflagellates (HNAN) ($\times 10^6$) in glucose-supplemented (+Gluc.) and non-supplemented (–Gluc.) cultures, and the gain expressed as the mean difference between the two conditions.

Microbiota	+Gluc.	–Gluc.	Gain
Bacteria	1.7 ± 0.3	0.9 ± 0.3	0.8[a]
HNAN	2.5 ± 1.8	1.3 ± 1.1	1.2[b]

Gains based on differences between means, and t-test for differences in means: [a]Bacteria ($t = 4.24$, $p = 0.003$, $df = 8$), [b]HNAN ($t = 1.26$, $p = 0.243$, $df = 8$).

TABLE 2 | Mean ± SE carbon content ($\mu g\,ml^{-1}$) of bacteria and heterotrophic nanoflagellates (HNAN) in glucose-supplemented (+Gluc.) and non-supplemented (–Gluc.) cultures, and the gain in C expressed as the mean difference between the two conditions.

Microbiota	+Gluc.	–Gluc.	Gain
Bacteria	227.5 ± 44.1	116.5 ± 32.9	111.0[a]
HNAN	3.0 ± 2.2	1.6 ± 1.3	1.4[b]

Gains based on differences between means, and t-test for differences in means: [a]Bacteria (t = 4.51, p =0.002), df = 8), [b]HNAN (t = 1.23, p = 0.255, df = 8).

TABLE 3 | Mean ± SE of total, free, and bacterial-bound alkaline phosphatase activity (pmol $min^{-1}\,\mu g^{-1}$ bacterial C) in glucose-supplemented (+Gluc.) and non-supplemented (–Gluc.) cultures, and the gain expressed as the mean difference between the two conditions.

Treatment	Total	Soluble free	Bacterial-bound
+Gluc.	6.5 ± 0.8	2.1 ± 0.2	4.4 ± 0.9
–Gluc.	5.1 ± 1.7	3.8 ± 0.9	1.3 ± 0.8
Gain	1.4[a]	−1.7[b]	3.1[c]

Gains based on differences between means, and t-test for differences in means: [a]Total (t = 1.67, p = 0.13, df = 8), [b]Soluble free (t = 4.12, p < 0.001, df = 8), [c]Bacterial-bound (t = 5.76, p < 0.001, df = 8).

activity to be greater than the gain in total activity. The linear correlation of the enzyme activity with bacterial densities was $r = 0.97$ ($p < 0.001$, $N = 5$). Thus, bacterial densities accounted for ∼94% of the variance in APA based on the square of the correlation coefficient.

Question 3: Coupling of the C and Phosphorus Cycles

Is there evidence of coupling of the C cycle and phosphorus cycle in aquatic microbial communities? Based on the foregoing data, evidence indicates that soluble organic C enrichment in the aquatic microbial communities not only increases the C-content of the microbiota, but secondarily also increases the alkaline phosphatase activity (particularly bacterial-bound APA), thus potentially driving phosphorus remineralization due to organo-phosphate hydrolysis. As reported above, in this experimental preparation, the total APA enzyme activity increased by a factor of 1.4 for every μg of glucose-C added, when compared to the control; and there was a substantial increase in bacterial-bound APA activity. Based on the statistical analyses in **Tables 1**–**3**, the increase in bacterial abundance and bacterial-bound APA in the C-enriched treatments are statistically significant ($p < 0.05$).

DISCUSSION

Summary of Conclusions

Glucose enrichment of the freshwater culture medium produced a gain of 111 μg bacterial C ml^{-1} of culture medium. This represents ∼3% of the amount of glucose-C added ml^{-1} (i.e., 4.0 mg ml^{-1}). A positive correlation between alkaline phosphatase activity and bacterial densities was found accounting for ∼94% of the variance in the enzyme activity, estimated from the square of the correlation coefficient. Based on this experiment, for every μg of C added above that in the control culture, the microcosm alkaline phosphatase activity (pmol $min^{-1}\,\mu g^{-1}$ bacterial C) increased by a factor of 1.4. Moreover, C-enrichment tends to increase the amount of bacterial-bound alkaline phosphatase, compared to that in control cultures lacking C-enrichment. In this study, the APA was normalized to estimated total bacterial C biomass, because the focus was on the C-budget and relevance of the APA to the C-cycle. However, this does not provide an estimate of the APA relative to the standing stock of metabolically active bacteria. Such estimates can be achieved by using fluorescent staining techniques that permit microscopic identification of the bacteria exhibiting surface APA activity. Some of these methods are discussed more fully in Section Relationships to prior research.

In this study, glucose was used as the sole C source. Glucose is commonly used in experimental microbe ecological research as representative of smaller, soluble organic nutrients (e.g., Hanson and Snyder, 1980; Shiah and Ducklow, 1994; Frost and Elser, 2002; Meon and Amon, 2004; Valliéres et al., 2008). Moreover, phytoplankton can be a significant source of glucose, in natural aquatic systems (e.g., Fogg, 1971; Moshiri et al., 1979). However, further research using a broader range of organic nutrients is needed to more fully document the effects of soluble C-enrichment on community structure and the production of APA, as well as the fate of soluble P produced as a result of organic phosphohydrolysis. Among other aspects, the molecular size and chemical composition of the organic matter, as well as its state (dissolved or particulate), needs to be examined in relation to the role of microbial communities in the aquatic P cycle.

Both the quality (kind) and quantity of soluble organic matter in natural aquatic ecosystems affect the composition and activity of microbial communities (e.g., Pérez and Sommaruga, 2006; Apple and del Giorgio, 2007). Although the use of a single C source in this study provided initial, experimental evidence of coupling of the C and P cycles, further studies with a broader composition of soluble organic matter may contribute greater predictability of the microbial community activity relative to the natural environment. Moreover microcosm, and other "bottle," experiments can introduce artifacts during laboratory incubation. Among other factors, the composition and activity of the prokaryote community may change during incubation, especially with longer durations such as days (e.g., Massana et al., 2001), especially if predator-prey relationships are not typical of the natural environment. In this study, heterotrophic nanoflagellate predators were present, and their densities and estimated C-biomass were included in addition to estimates for the bacteria (**Tables 1**, **2**).

Relationships to Prior Research

These data support the hypothesis of close coupling of the carbon and phosphorus biogeochemical cycles in freshwater aquatic microbial communities and provides a quantitative estimate of the likely gain in phosphorus remineralization that can occur due to soluble organic C enrichment. Organic C derived potentially from primary production, from decaying

biota, or from allochthonous sources, can enhance microbial alkaline phosphatase production and thus increase phosphorus remineralization by organo-phosphate hydrolysis. Based on the evidence in this research, it appears that C-enrichment produces less free enzyme and more bacterial-bound enzyme compared to control conditions without C-enrichment. This has also been reported in studies of organic C enrichment in natural environments (e.g., Chróst et al., 1989). It is not immediately clear why this is the case. However, further research is needed to better document changes in the cellular physiology of the microbes, particularly examining the localization of the APA on the bacterial surface, perhaps by using modern fluorescent labeling techniques (e.g., Giepmans et al., 2006). Moreover, additional insights may be obtained by transcriptome analyses to determine if there are changes temporally in the transcription of alkaline phosphatase mRNA and other proteins of biogeochemical significance (e.g., Mark et al., 2005). This avenue of research may be enhanced by examining the effects of different levels of aquatic C enrichment on microbial APA, and possible variations in its transcription.

Although prior research has documented the role of phagotrophic predation in the release of organo-phosphohydrolases, thus promoting phosphorus remineralization, the data presented here augments these prior findings by adding experimental evidence of C-based increase in APA production within the context of as somewhat broader community-based analysis, including major bacterial predators (e.g., HNAN). Free phosphate is typically assimilated much more rapidly by bacteria than heterotrophic eukaryotic microbes and bacteria may be one of the more important contributors to the phosphorous cycle in marine ecosystems (Duhamel and Moutin, 2009; Popendorf and Duhamel, 2015). Moreover, among lake microplankton, bacteria may account for as much as 94% of the APA (Chróst et al., 1984). Overall, the increased available phosphorus due to C enrichment as observed in the research reported here may enhance bacterial growth, thus providing a positive forcing function on growth of bacterial predators higher up the food web. In some marine environments, however, bacterial remineralization of soluble phosphates may exceed the immediate needs of the bacteria, thus making the excess P directly available to drive primary production of phytoplankton, and consequently increased biomass of their predators (White et al., 2012).

The research reported here expands our knowledge base of the dynamic role of organic C, beyond its role as a nutrient source, to include a link to increased alkaline phosphatase activity, thus driving phosphorus remineralization in freshwater heterotrophic microbial communities. This is one of the first experimental microcosm studies to provide a quantitative estimate of the C-supplementation effect on APA in microbial communities. It is consistent with prior published research in the natural environment showing that dissolved organic C has significant contributory effects on activity of bacterial alkaline phosphatase and primary productivity in freshwater and marine ecosystems (e.g., Stewart and Wetzel, 1982; Chróst et al., 1989; Boyer et al., 2006). Moreover, similar results of C-enrichment effects on APA were recently reported for laboratory microcosm studies using organic-rich arctic soil microbial communities (Anderson et al., 2018). Elucidation of the finer ecological implications will require additional research on how environmental variables interact with the organic C enhancement effect, including variations in temperature, oxygen concentration, organic and mineral nutrient concentrations (particularly organo-phosphate substrates and available free phosphate), and interactions of the heterotrophic microbiota with photosynthetic protists in the aquatic environment. Further comparative microcosm, and field-based studies, across a continuum of different terrestrial and aquatic ecosystems (e.g., coastal and oceanic), correlating organic C concentrations with microbial alkaline phosphatase activity, are needed to provide further evidence of the coupling of carbon and phosphate cycles in the natural environment as suggested by this laboratory experimental study.

AUTHOR CONTRIBUTIONS

The author confirms being the sole contributor of this work and approved it for publication.

ACKNOWLEDGMENTS

This is Lamont-Doherty Earth Observatory Contribution number 8179.

REFERENCES

Adl, S. M. (2003). *The Ecology of Soil Decomposition*. Wallingford: CAB International.

Anderson, O. R. (2012). The role of bacterial-based protist communities in aquatic and soil ecosystems and the carbon biogeochemical cycle, with emphasis on naked amoebae. *Acta Protozool.* 51, 209–221. doi: 10.4467/16890027AP.12.017.0763

Anderson, O. R. (2014a). Bacterial and heterotrophic nanoflagellate densities and C-biomass estimates along an Alaskan tundra transect with prediction of respiratory CO_2 efflux. *J. Eukaryot. Microbiol.* 61, 11–16. doi: 10.1111/jeu.12081

Anderson, O. R. (2014b). "The role of soil microbial communities in soil carbon processes and the biogeochemical carbon cycle" in *Soil Carbon: Types, Management Practices and Environmental Benefits*, ed A. Margit (New York, NY: Nova Publishers), 1–50.

Anderson, O. R., Gorrell, T., Bergen, A., Kruzansky, R., and Levandowsky, M. (2001). Naked amoebas and bacteria in an oil-impacted salt marsh community. *Microb. Ecol.* 42, 474–481. doi: 10.1007/s00248-001-0008-x

Anderson, O. R., Juhl, A. R., and Bock, N. (2018). Effects of organic carbon enrichment on respiration rates, phosphatase activities, and abundance of heterotrophic bacteria and protists in organic-rich Arctic and mineral-rich temperate soil samples. *Polar Biol.* 41, 11–24. doi: 10.1007/s00300-017-2166-4

Anderson, O. R., and McGuire, K. (2013). C-biomass of bacteria, fungi, and protozoan communities in arctic tundra soil, including some trophic relationships. *Acta Protozool.* 52, 217–227. doi: 10.4467/16890027AP.14.002.1439

Apple, J. K., and del Giorgio, P. A. (2007). Organic substrate quality as the link between bacterioplankton carbon demand and growth efficiency in a temperate salt-marsh estuary. *ISME J.* 1, 729–742. doi: 10.1038/ismej.2007.86

Bloem, J., Albert, C., Bär-Gillissen, M.-J. B., Berman, T., and Cappenberg, T. E. (1989). Nutrient cycling through phytoplankton bacteria and protozoa in selectively filtered Lake Vechten Netherlands water. *J. Plankton Res.* 11, 119–131.

Boyer, J. N., Dailey, S. K., Gibson, P. J., Rogers, M. T., and Mir-Gonzalez, D. (2006). The role of dissolved organic matter bioavailability in promoting phytoplankton blooms in Florida Bay. *Hydrobiologia* 569, 71–85. doi: 10.1007/s10750-006-0123-2

Caron, D. A. (1994). Inorganic nutrients, bacteria, and the microbial loop. *Microb. Ecol.* 28, 295–298.

Caron, D. A., Goldman, J. C., Andersen, O. K., and Dennett, M. R. (1985). Nutrient cycling in a microflagellate food chain II. Population dynamics and carbon cycling. *Mar. Ecol. Prog. Ser.* 24, 243–254.

Chróst, R. J., Münster, U., Rai, H., Albrecht, D., Witzel, P. K., and Overbeck, J. (1989). Photosynthetic production and exoenzymatic degradation of organic matter in the euphotic zone of a eutrophic lake. *J. Plankton Res.* 11, 223–242.

Chróst, R. J., Waldemar, S., and Halemejko, G. Z. (1984). Longterm studies on alkaline phosphatase activity (APA) in a lake with fish-aquaculture in relation to lake eutrophication and phosphorus cycle. *Arch. Hydrobiol. Suppl.* 70, 1–32.

Clarholm, M. (1989). Effects of plant-bacterial-amoebal interactions on plant uptake of nitrogen under field conditions. *Biol. Fertil. Soils* 8, 373–378.

Cole, C. V., Elliottt, E. T., Hunt, H. W., and Coleman, D. C. (1977). Trophic interactions in soils as they affect energy and nutrient dynamics. V. Phosphorus transformations. *Microbial. Ecol.* 4, 381–387.

Ducklow, H. (2000). "Bacterial production and biomass in the oceans." in *Microbial Ecology of the Oceans*, ed D. L. Kirchman (Wilmington, DE: Wiley-Liss, Inc.), 85–120.

Duhamel, S., Björkman, K. M., Doggett, J. K., and Karl, D. M. (2014). Microbial response to enhanced phosphorus cycling in the North Pacific Subtropical Gyre. *Mar. Ecol. Prog. Ser.* 504, 43–58. doi: 10.3354/meps10757

Duhamel, S., and Moutin, T. (2009). Carbon and phosphate incorporation rates of microbial assemblages in contrasting environments in the Southeast Pacific. *Mar. Ecol. Prog. Ser.* 375, 53–64. doi: 10.3354/meps07765

Dyhrman, S. T., Ammerman, J. W., and Van Mooy, B. A. S. (2007). Microbes and the marine phosphorus cycle. *Oceanography* 20, 110–116. doi: 10.5670/oceanog.2007.54

Esser, G., Kattge, J., and Sakalli, A. (2011). Feedback of carbon and nitrogen cycles enhances carbon sequestration in the terrestrial biosphere. *Glob. Change Biol.* 17, 819–842. doi: 10.1111/j.1365-2486.2010.02261.x

Ferrier-Pagès, C., and Rassoulzadegan, F. (1994). Seasonal impact of the microzooplankton on pico- and nanoplankton growth rates in the northwest Mediterranean Sea. *Mar. Ecol Prog. Ser.* 108, 283–294.

Fogg, G. E. (1971). Extracellular products of algae in freshwater. *Arch. Hydrobiol, Ergebn. Limnol.* 5, 1–25.

Frost, P. C., and Elser, J. J. (2002). Effects of light and nutrients on the net accumulation and elemental composition of epilithon in boreal lakes. *Freshw. Biol.* 47, 173–183. doi: 10.1046/j.1365-2427.2002.00796.x

Gibson, C. E., Foy, R. H., and Bailey-Watts, A. E. (1996). An analysis of the total phosphorus cycle in some temperate lakes: the response to enrichment. *Freshw. Biol.* 35, 525–532. doi: 10.1111/j.1365-2427.1996.tb01766.x

Giepmans, B. N., Adams, S. R., Ellisman, M. H., and Tsien, R. Y. (2006). The fluorescent toolbox for assessing protein location and function. *Science* 312, 217–224. doi: 10.1126/science.1124618

Güde, H. (1985). Influence of phagotrophic processes on the regeneration of nutrients in two-stage continuous culture systems. *Microbial. Ecol.* 11, 193–204.

Hadas, O., Pinkas, R., and Wynne, D. (1992). Nitrate reductase activity, ammonium regeneration, and orthophosphate uptake in protozoa isolated from Lake Kinneret, Israel. *Microbial. Ecol.* 23, 107–115.

Hanson, R. B., and Snyder, J. (1980). Glucose exchanges in a salt marsh estuary: biological activity and chemical measurements. *Limnol. Oceanogr.* 25, 633–642.

Mark, G. L., Dow, J. M., Kiely, P. D., Higgins, H., Haynes, J., Baysse, C., et al. (2005). Transcriptome profiling of bacterial responses to root exudates identifies genes involved in microbe-plant interactions. *Proc. Natl. Acad. Sci. U.S.A* 102, 17454–17459. doi: 10.1073/pnas.0506407102

Massana, R., Pedrós-Ali,ó, C., Casamayor, E. O., and Gasol, J. M. (2001). Changes in marine bacterioplankton phylogenetic composition during incubations designed to measure biogeochemically significant parameters. *Limnol. Oceanogr.* 46, 1181–1188. doi: 10.4319/lo.2001.46.5.1181

Meon, B., and Amon, R. M. W. (2004). Heterotrophic bacterial activity and fluxes of dissolved free amino acids and glucose in the Arctic rivers Ob, Yenisei and the adjacent Kara Sea. *Aquat. Microb. Ecol.* 37, 121–135. doi: 10.3354/ame037121

Moshiri, G. A., Crumpton, W. G., and Aumen, N. G. (1979). Dissolved glucose in a bayou estuary, possible sources and utilization by bacteria. *Hydrobiologia* 62, 71–74.

Pelegri, S. P., Dolan, J., and Rassoulzadegan, F. (1999). Use of high temperature catalytic oxidation (HTCO) to measure carbon content of microorganisms. *Aquat. Microb. Ecol.* 16, 273–280.

Pérez, M. T., and Sommaruga, R. (2006). Differential effect of algal- and soil-derived dissolved organic matter on alpine lake bacterial community composition and activity. *Limnol. Oceanogr.* 51, 2527–2537. doi: 10.4319/lo.2006.51.6.2527

Popendorf, K. J., and Duhamel, S. (2015). Variable phosphorus uptake rates and application across microbial groups in the oligotrophic Gulf of Mexico. *Environ. Microbiol.* 17, 3992–4006. doi: 10.1111/1462-2920.12932

Renn, C. E. (1937). Bacteria and the phosphorus cycle in the sea. *Biol. Bull.* 72, 190–195.

Ruttenberg, K. C., and Dyhrman, S. T. (2012). Dissolved organic phosphorus production during simulated phytoplankton blooms in a coastal upwelling system. *Front. Microbiol.* 3:274. doi: 10.3389/fmicb.2012.00274

Selph, K. E., Landry, M. R., and Laws, E. A. (2003). Heterotrophic nanoflagellate enhancement of bacterial growth through nutrient remineralization in chemostat culture. *Aquat. Microb. Ecol.* 32, 23–37. doi: 10.3354/ame032023

Shiah, F.-K., and Ducklow, H. W. (1994). Temperature and substrate regulation of bacterial abundance, production and specific growth rate in Chesapeake Bay, USA. *Mar. Ecol. Prog. Ser.* 103, 297–308.

Stewart, A. J., and Wetzel, R. G. (1982). Influence of dissolved humic materials on carbon assimilation and alkaline phosphatase activity in natural algal-bacterial assemblages. *Freshw. Biol.* 12, 369–380.

Vallières, C., Retamal, L., Ramlal, P., Osburn, C. L., and Vincent, W. F. (2008). Bacterial production and microbial food web structure in a large arctic river and the coastal Arctic Ocean. *J. Marine Syst.* 74, 756–773. doi: 10.1016/j.jmarsys.2007.12.002

White, A. E., Watkins-Brandt, K. S., Engle, M. A., Burkhardt, B., and Paytan, A. (2012). Characterization of the rate and temperature sensitivities of bacterial remineralization of dissolved organic phosphorus compounds by natural populations. *Front. Microbiol.* 3:276. doi: 10.3389/fmicb.2012.00276

Zaehle, S. (2013). Terrestrial nitrogen-carbon cycle interactions at the global scale. *Philos. T. Roy. Soc. B.* 368:20130125. doi: 10.1098/rstb.2013.0125

Conflict of Interest Statement: The author declares that the research was conducted in the absence of any commercial or financial relationships that could be construed as a potential conflict of interest.

frontiers in Marine Science

ORIGINAL RESEARCH
published: 19 June 2018
doi: 10.3389/fmars.2018.00215

Phosphorus Dynamics and Availability in the Nearshore of Eastern Lake Erie: Insights From Oxygen Isotope Ratios of Phosphate

David C. Depew[1]*, *Geoffrey Koehler*[2] *and Veronique Hiriart-Baer*[1]

[1] Watershed Hydrology and Ecology Research Division, Environment and Climate Change Canada, Burlington, ON, Canada,
[2] Watershed Hydrology and Ecology Research Division, Environment and Climate Change Canada, Saskatoon, SK, Canada

Blooms of filamentous benthic algae that plagued Lake Erie in the 1950s through 1970s were largely reduced through reductions of phosphorus (P) loading from point sources. Since the mid-1990s, these blooms have returned despite a period of relatively stable external P inputs. While increased loadings of dissolved P have been causally linked to cyanobacterial blooms in some parts of the lake, the impacts of ecosystem changes such as the effect of invasive species on nutrient cycling and availability have not been fully elucidated, leading to uncertainty as to the effectiveness of additional non-point P management actions. Here we use the oxygen isotope ratios ($\delta^{18}O_P$) of phosphate in concert with measures of water quality along the northern shore of the east basin of Lake Erie to identify sources and pathways of P cycling and infer potential importance in relation to annual blooms of *Cladophora* that foul the shorelines of eastern Lake Erie. $\delta^{18}O_P$ data indicate that potential external source signatures are rapidly overprinted by biological cycling of P by the plankton community and that much of the available phosphate in the nearshore waters is derived from hydrolysis of dissolved organic P compounds. Near the dreissenid-colonized lake bed, $\delta^{18}O_P$ was persistently and significantly enriched in ^{18}O relative to $\delta^{18}O_P$ measured in surface waters and was similar to $\delta^{18}O_P$ of phosphate excreted by dreissenid mussels in incubations. These results implicate dreissenid mussels as key agents in nearshore P cycling and highlight the importance of considering ecosystem changes in the development of nutrient management strategies designed to ameliorate symptoms of eutrophication.

Keywords: Lake Erie, phosphorus, *Cladophora*, oxygen isotopes, dreissenids

OPEN ACCESS

Edited by:
Christian Lønborg,
Australian Institute of Marine Science, Australia

Reviewed by:
Michael R. Twiss,
Clarkson University, United States
Federica Tamburini,
ETH Zürich, Switzerland

***Correspondence:**
David C. Depew
david.depew@canada.ca

Specialty section:
This article was submitted to Marine Biogeochemistry, a section of the journal Frontiers in Marine Science

Received: *28 February 2018*
Accepted: *30 May 2018*
Published: *19 June 2018*

Citation:
Depew DC, Koehler G and Hiriart-Baer V (2018) Phosphorus Dynamics and Availability in the Nearshore of Eastern Lake Erie: Insights From Oxygen Isotope Ratios of Phosphate. Front. Mar. Sci. 5:215. doi: 10.3389/fmars.2018.00215

INTRODUCTION

In the North American Laurentian Great Lakes, blooms of filamentous green algae (mostly *Cladophora* sp.) were one of the most visible signs of cultural eutrophication in the early 1950s through to the late 1970s, particularly in Lake Erie (Shear and Konasewich, 1975; Higgins et al., 2008). Phosphorus (P) abatement programs under the Great Lakes Water Quality Agreement (GLWQA) resulted in rapid and substantial reductions in external P inputs, that while primarily aimed at reducing extensive phytoplankton blooms, hypoxia, and fish kills, also appeared to reduce *Cladophora* blooms although confirmational data are limited (Painter and McCabe, 1987). Despite

these apparent improvements, reports of expansive blooms of *Cladophora* increased in frequency in eastern Lake Erie in the mid to late 1990s (Higgins et al., 2005) following P load reductions but also colonization of Lake Erie by exotic zebra (*Dreissena polymorpha*) and quagga (*D. rostriformis bugensis*) mussels (Griffiths et al., 1991; Roe and MacIsaac, 1997). It was postulated that the recurrence of these blooms during a period of stable or declining P loads (Dolan and Chapra, 2012) was in part related to structural and functional changes to the ecosystem mediated by large populations of filter feeding dreissenid mussels (Hecky et al., 2004) that increased water clarity (Howell et al., 1996), expanded areas of hard substrate for algal attachment (Haltuch et al., 2000), and enriched the benthic environment through the excretion of metabolic wastes and undigested algae (Arnott and Vanni, 1996; Conroy et al., 2005). At the same time, changing agricultural practices, precipitation patterns, and weather conditions have increased soluble P loadings to western Lake Erie, resulting in a recurrence of cyanobacterial blooms (Michalak et al., 2013). While there is general agreement reductions in P availability are the most practical means with which to reduce the extent and severity of *Cladophora* blooms (Auer et al., 2010), uncertainty remains as to the relative importance of direct P inputs, P circulating within the lake, and P potentially recycled in the benthic environment by dreissenid mussels (Bootsma et al., 2015). These uncertainties have confounded efforts to develop revised P loading targets for the east basin of Lake Erie to address *Cladophora* blooms (GLWQA, 2015).

Several recent studies have indicated that the relative abundance of oxygen stable isotopes in phosphate ($\delta^{18}O_P$) carries information regarding the sources and biological cycling of phosphate (PO_4, hereafter P_i) in aquatic environments (Colman et al., 2005; McLaughlin et al., 2006b, 2013; Elsbury et al., 2009; Joshi et al., 2015; Li et al., 2017). The strong bond between oxygen and phosphorus atoms in phosphate are resistant to oxygen exchange under most environmentally relevant conditions (Paytan and McLaughlin, 2012). While isotopic fractionation effects of abiotic processes such as sorption and desorption appear to be relatively minor (Jaisi et al., 2010, 2011), fractionation during biologically mediated enzymatic reactions can be large and at times, substrate and enzyme dependent (Blake, 2005; Liang and Blake, 2006, 2009). The uptake and internal cycling of P_i by intracellular pyrophosphatases (EC 3.6.1.1) results in complete exchange of all oxygen atoms from P_i with oxygen atoms from water, leading to a rapid temperature-dependent equilibrium between oxygen in P_i and intracellular water (Longinelli and Nuti, 1973; Blake, 2005), which is expected to be equal to that of ambient water ($\delta^{18}O_W$) (but see Li et al., 2016b). This isotopic equilibration has been observed in many environments to be an indicator of P_i turnover (McLaughlin et al., 2006b, 2013). Hydrolysis of organic phosphorus (OP) by various extra- and intracellular phosphatases and phosphohydrolases (for example, alkaline phosphatase; EC 3.1.3.1, 5' nucleotidase; EC 3.1.3.5, phosphodiesterase EC 3.1.4.1) impart a negative fractionation at the P-O bond site, shifting the $\delta^{18}O_P$ of the product (P_i) further away from equilibrium (Liang and Blake, 2006, 2009). Consequently, knowledge of these reactions and pathways may provide a means to identify sources of P or the importance of specific P cycling pathways governing P_i availability in aquatic ecosystems (Elsbury et al., 2009; McLaughlin et al., 2013; Joshi et al., 2015; Granger et al., 2017b; Li et al., 2017).

Initial application of this approach in central and western Lake Erie indicated the presence of two distinct sources of P_i; riverine inputs (∼+12‰) and a second, isotopically heavier source (∼+17‰) of unknown origin (Elsbury et al., 2009). Subsequent investigations have suggested that this P_i is derived primarily by redox mediated release from anoxic sediments in the central basin (Paytan et al., 2017). Given the apparent success at identifying different P_i sources in central and western Lake Erie and the residual uncertainty regarding the relevance of external vs. internal sources of P_i associated with *Cladophora* blooms, we sought to apply this approach to (1) examine the influence of the Grand River on nearshore phosphorus concentrations (2) investigate the utility of stable isotopes of oxygen in phosphate for differentiating P_i sources in the nearshore of the eastern basin and (3) to improve our understanding of P dynamics in a dynamic coastal environment. Our results presented here add to the expanding library of freshwater $\delta^{18}O_P$ data, particularly at the oligotrophic end of the spectrum. In addition, we provide data from a eutrophic river and to our knowledge, the first measurements of $\delta^{18}O_P$ generated by filter feeding bivalves. An improved understanding of the sources of P_i and the manner in which it is processed and recycled within the nearshore are of critical importance to establishing effective nutrient management strategies to ameliorate *Cladophora* blooms as required by the amended (GLWQA, 2012).

MATERIALS AND METHODS

Study Region

The eastern basin of Lake Erie is the deepest of the three basins (64 m maximum depth) and is considered oligotrophic based on long term monitoring of phosphorus concentrations (mean spring TP ∼0.32 μM; Dove and Chapra, 2015). The eastern basin receives ∼40% of its total P load from the Grand River (**Figure 1**) while the remainder comes via exchange with the central basin and other smaller tributaries around the north and south shores of the basin (Maccoux et al., 2016). With prevailing winds from the southwest direction, the north shore littoral region is subjected to a large fetch and this highly exposed shoreline is dominated by limestone bedrock with smaller regions of glacial till and sand (Rukavina and St. Jacques, 1971). Dreissenid mussels have colonized most of the hard substrate along this shore and remain a dominant feature of the benthos (Patterson et al., 2005; Chomicki et al., 2016).

Water Sample Collection and Nutrient Analysis

Water samples were collected on four to five occasions in 2013 and 2014 between the months of April and September at 12 sites along the northern shore of the east basin of Lake Erie (**Figure 1**). Vertical profiles of temperature, specific conductivity, pH, dissolved oxygen, the physical structure of

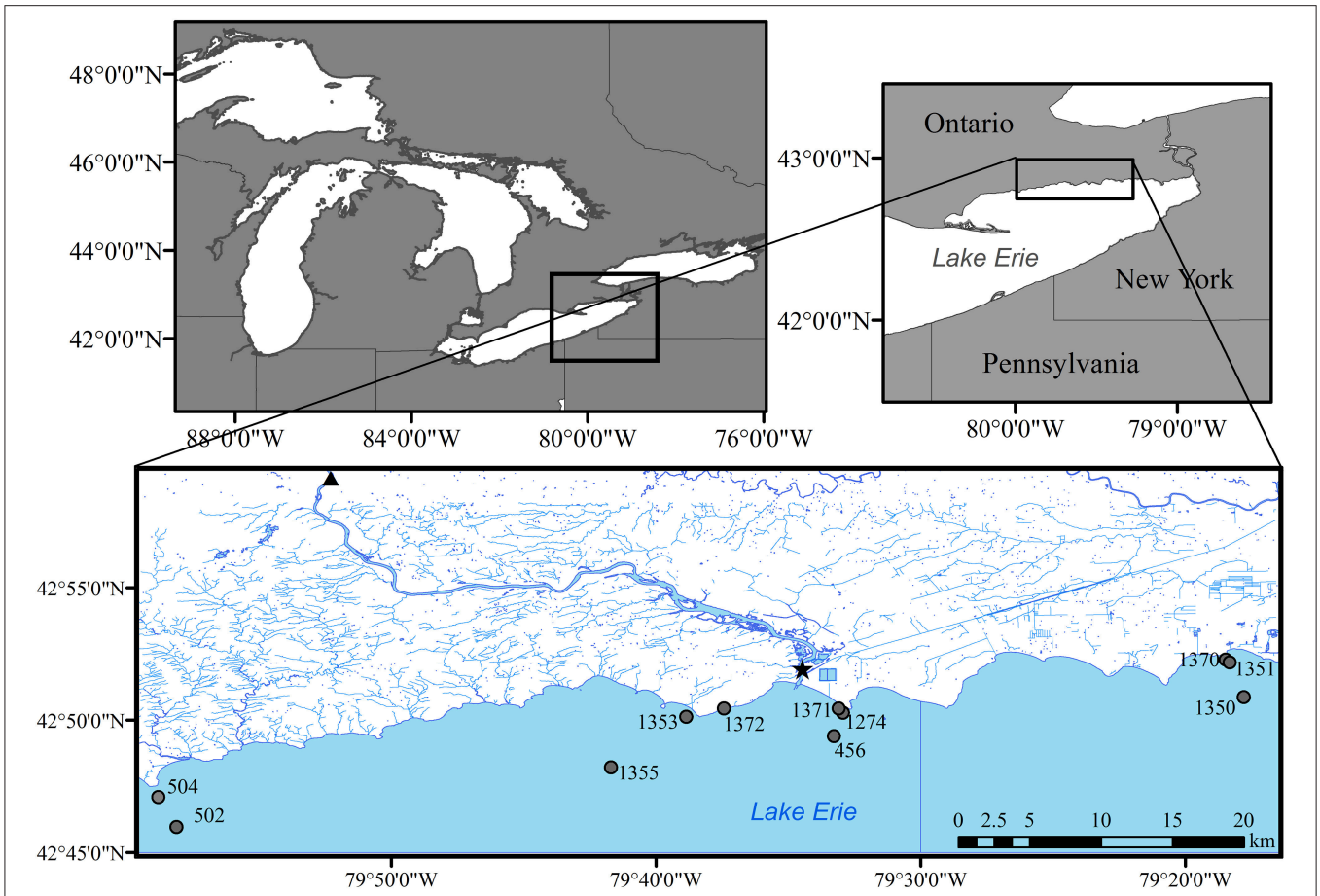

FIGURE 1 | Sampling sites in eastern Lake Erie during 2014, including lake stations (circles), river mouth (star), and long term nutrient loading station (triangle) for the Grand River at York, Ontario.

the water column were collected at each site with a YSI-6600 or EXO-2 water quality sonde prior to initiation of sampling. All water samples were collected using a submersible pump and stored in acid-cleaned 4 L HDPE jugs, placed on ice in coolers until processing for total phosphorus (TP), total dissolved phosphorus (TDP), soluble reactive phosphorus (SRP), ammonia (NH_3), nitrate/nitrite (NO_3/NO_2), total chlorophyll a (CHLA), particulate carbon (PC), and particulate nitrogen (PN). Water samples were processed for the above parameters following (Dove et al., 2009) and analyzed at the National Laboratory for Environmental Testing, Burlington ON. Particulate P (PP) was calculated as TP—TDP and dissolved organic P (DOP) was calculated as TDP-SRP.

For isotopic analyses of water and P_i, additional samples were collected with a target volume of ~200 L (to attain a minimum of 10 μM P_i) from selected depths using a submersible pump mounted on a tripod (**Table 1**): surface (S; 1.0 m depth) and ~0.1 m above the lake bottom (LB). To minimize boundary layer disturbance, the pump flow rates were set to ~50–60 mL min^{-1}, resulting in collection times of ~1 h. Pumped water was passed under low pressure first through a 1 μm polypropylene depth cartridge filter (Hytrex®) and then through a 0.2 μm pleated polypropylene filter (Flotrex®; FPN921BGS) to remove particles and colloidal material and collected in 10 20 L acid cleaned carboys. To each carboy, ~50 g of $MgCl_2$ (Fisher Scientific, ACS grade) was added and dissolved followed by an addition of 100 mL of 1M NaOH (Fisher Scientific, ACS grade) to achieve a loading of ~0.3% v:v to induce precipitation of brucite ($MgOH_2$) (Karl and Tien, 1992; Thomson-Bulldis and Karl, 1998). Fixed sample bottles were kept darkened and cool until further processing upon return to shore (see below).

Phosphate and Water Oxygen Isotope Analysis

To analyze $\delta^{18}OP$ in P_i, the brucite floc from each set of carboys was allowed to settle before siphoning supernatant water away. Samples were combined into a smaller number of carboys and this process was repeated until ~10 L of brucite floc remained. Sufficient 1M HNO_3 (ACS grade) was added to dissolve the brucite floc, but keep the pH of the sample between 5 and 7. 1M NaOH was then added to re-precipitate brucite and reduce the overall sample volume. At least three cycles were required to reduce sample volumes from

TABLE 1 | Oxygen isotopic compositions of water ($\delta^{18}O_W$), phosphate ($\delta^{18}O_P$), and calculated equilibrium phosphate oxygen isotopic compositions ($\delta^{18}O_{P-EQ}$) for different sites, dates, and depths in eastern Lake Erie and the lower Grand River.

PSN	Date	Type	Depth (m)	Temp (°C)	$\delta^{18}O_W$	$\delta^{18}O_P$	$\delta^{18}O_{P\text{-}Eq}$
River	10/04/14	S	0.5	5.0	−12.6	11.1 ± 0.6	12.7 (12.7–16.8)
River	16/04/14	S	0.5	5.0	−10.7	11.5 ± 0.5	14.7 (12.7–16.8)
River	23/04/14	S	0.5	9.0	−11.2	11.9 ± 0.7	13.4 (12.0–16.1)
River	02/05/14	S	0.5	9.5	−10.0	11.9	14.6 (11.9–16.0)
River	14/05/14	S	0.5	19.0	−9.8	11.0 ± 0.5	13.1 (10.2–14.3)
1370	23/05/14	LB	1.0	9.8	−7.3	7.5	17.3 (16.6–18.6)
1372	23/05/14	LB	1.0	10.0	−6.3	9.7	18.2 (16.6–18.5)
1371	26/05/14	LB	1.0	17.0	−8.0	6.9	15.3 (15.3–17.3)
River	26/05/14	S	0.5	19.5	−8.7	9.4 ± 1.6	14.2 (10.1–14.2)
1274	28/05/14	LB	3.7	9.1	−7.1	10.4	17.6 (16.8–18.7)
1355	29/05/14	LB	10.1	9.3	−7.1	11.9	17.6 (16.7–18.7)
1355	29/05/14	S	1.0	11.2	−6.8	9.6	17.8 (16.7–18.6)
1353	29/05/14	LB	3.8	9.7	−7.3	8.2	17.3 (16.7–18.6)
456	29/05/14	LB	11.9	10.5	−7.6	11.2	16.9 (16.5–18.5)
456	29/05/14	S	1.0	11.4	−6.9	8.9	17.4 (16.4–18.3)
1350	05/06/14	S	1.0	12.7	−6.9	6.4	17.2 (16.1–18.1)
1350	05/06/14	LB	13.5	8.2	−7.9	8.7	16.9 (16.9–18.9)
1351	05/06/14	LB	3.4	9.7	−6.4	6.0	18.2 (16.7–18.6)
P3	06/06/14	LB	4.0	9.2	−6.8	9.8	17.9 (16.7–18.7)
P10	06/06/14	S	1.0	12.7	−6.2	8.3	17.9 (16.1–18.1)
P10	06/06/14	LB	11.4	8.2	−6.6	10.2	18.3 (16.9–18.9)
1350	16/06/14	S	1	15.5	−6.4	11.8	17.2 (15.6–17.6)
1350	16/06/14	LB	13.4	10.3	−6.9	14.9	17.6 (16.6–18.5)
1351	16/06/14	LB	3.7	14.6	−7.1	4.7	16.6 (15.8–17.7)
1355	17/06/14	LB	12	11.3	−7.3	10.8	17.0 (16.4–18.3)
1355	17/06/14	S	1	16.1	−7.1	8.2	16.4 (15.5–17.3)
1353	17/06/14	LB	4.7	13.1	−7.2	9.9	16.8 (16.1–18.0)
456	17/06/14	LB	11.9	9.1	−6.8	12.1	17.9 (16.8–18.7)
456	17/06/14	S	1	16.1	−6.6	8.7	16.9 (15.5–17.5)
1274	17/06/14	LB	1.9	17.1	−6.9	7.4	16.4 (15.4–17.3)
P10	18/06/14	S	1	15.5	−6.6	7.5	17.0 (15.6–17.6)
P10	18/06/14	LB	11.6	7.3	−6.6	9.4	18.4 (17.1–19.1)
P3	18/06/14	LB	4.1	8.7	−6.6	8.1	18.2 (16.9–18.8)
River	18/06/14	S	1	23.5	−9.6	7.8	12.5 (9.4–13.6)
1370	24/06/14	LB	1	22.0	−6.7	7.1	15.7 (14.5–16.5)
1371	24/06/14	LB	1	21.0	−6.9	8.9	15.7 (14.7–16.6)
1372	24/06/14	LB	1	20.0	−7.2	7.1	15.6 (14.9–16.8)
1353	10/07/14	LB	4.7	19.7	−6.7	6.8	16.1 (14.9–16.8)
1355	10/07/14	S	1	20.2	−6.0	ND	16.7 (14.8–16.7)
1355	10/07/14	LB	11.6	19.0	−6.4	10.8	16.5 (15.0–16.9)
456	10/07/14	S	1	21.1	−6.8	5.3	15.8 (14.7–16.6)
456	10/07/14	LB	11.2	19.9	−7.0	9.2	15.8 (14.9–16.8)
1274	10/07/14	LB	3.9	20.7	−7.2	6.8	15.4 (14.7–16.7)
1350	11/07/14	S	1	21.5	−7.1	9.3	15.4 (14.6–16.5)
1350	11/07/14	LB	12.3	21.0	−6.9	11.3	15.7 (14.6–16.6)
1351	11/07/14	LB	3.2	21.7	−6.8	ND	15.7 (14.6–16.5)
1370	14/07/14	LB	1.1	23.6	−6.4	9.7	15.8 (14.2–16.2)
1371	14/07/14	LB	1.1	23.2	−6.8	9.5	15.4 (14.3–16.3)

(Continued)

TABLE 1 | Continued

PSN	Date	Type	Depth (m)	Temp (°C)	$\delta^{18}O_W$	$\delta^{18}O_P$	$\delta^{18}O_{P\text{-}Eq}$
1372	14/07/14	LB	1.1	23.0	−7.0	6.3	15.3 (14.3–16.3)
River	17/07/14	S	1	22.9	−9.8	6.9	12.4 (9.5–13.6)
1355	21/08/14	S	1	20.8	−6.8	4.7	15.9 (14.7–16.6)
1355	21/08/14	LB	10.8	18.4	−6.4	ND	16.6 (15.1–17.1)
1353	21/08/14	LB	4.2	21.3	−6.9	7.8	15.7 (14.6–16.6)
1274	21/08/14	LB	3.9	21.9	−6.3	7.2	16.2 (14.5–16.5)
456	21/08/14	S	1	22.1	−6.5	8.9	16.0 (14.5–16.5)
456	21/08/14	LB	11	19.8	−6.9	10.1	15.9 (14.9–16.8)
1350	22/08/14	S	1	21.7	−6.6	9.5	15.9 (14.6–16.5)
1350	22/08/14	LB	11.4	20.2	−6.5	11.2	16.3 (14.8–16.8)
1351	22/08/14	LB	2.8	21.6	−7.1	7.8	15.3 (14.6–16.6)
502	28/08/14	LB	4.1	21.3	−7.2	14.0	15.3 (14.6–16.6)
River	28/08/14	S	1	24.4	−10.2	5.7	11.8 (9.3–13.4)
504	28/08/14	S	1	21.5	−6.5	ND	16.1 (14.6–16.5)
504	28/08/14	LB	10.4	19.9	−6.9	7.0	15.9 (14.8–16.8)

Note $\delta^{18}O_{P-EQ}$ is calculated following Chang and Blake (2015) using the measured $\delta^{18}O_w$ at the time of sampling, while the range in brackets represents the uncertainty window calculated using the minimum and maximum $\delta^{18}O_w$.

200 L to ∼50 mL. At each stage, SRP and TDP concentrations in both the sample and supernatant were measured after reagent addition to ensure >99% recovery of SRP (i.e., SRP in supernatant was not detectable). Recovery of SRP was always >99% while recovery of TDP varied between 5 and 53%, depending on the sample and amount of 1M NaOH required.

Initially, we sought to precipitate silver phosphate (Ag_3PO_4) following the protocol of McLaughlin et al. (2004). However, we were unable to generate Ag_3PO_4 that was sufficiently clean of contaminant oxygen using this approach. Consequently samples collected in 2013 were deemed contaminated and are not presented herein. For samples collected in 2014, we adapted the approach of Colman et al. (2005) to remove organic matter prior to undergoing sequential precipitation and crystallization steps. Briefly, concentrated samples (∼50 mL) were run through Oasis HLB resin columns (1 mL min^{-1} flow rate) to remove organic matter. P_i in the now cleaned sample was first precipitated as ammonium phosphomolybdate (APM) and then magnesium ammonium phosphate (MAP) (Kolodny et al., 1983; Tamburini et al., 2010) to separate P_i from remaining impurities. Following dissolution of the MAP precipitate, cations were removed with BioRad AGx50 cation resin, and samples were evaporated to a total volume of ∼1.0 mL prior to precipitation of Ag_3PO_4. Ag_3PO_4 crystals were cleaned with H_2O_2 (15%; Tamburini et al., 2010), washed copiously with distilled water, dried at 60°C and stored in a dessicator prior to analysis. When possible, samples were processed in duplicate with ^{18}O enriched reagents (±59.7‰) to assess potential for hydrolysis of organic P compounds. For the limited number of samples with sufficient phosphate recovered that we could process with enriched reagents ($n = 9$), the difference between spiked and un-spiked samples was on average <1.5‰, thus we conclude that minimal hydrolysis occurred during processing and purification.

Between 0.25 and 0.35 mg of sample and nickelized carbon were added to silver capsules (pre-baked @ 500 C, 4 h) and shipped to the National Hydrology Research Centre in Saskatoon, SK. Samples were run in duplicate or triplicate if sufficient Ag_3PO_4 was recovered, but the majority of samples only had sufficient Ag_3PO_4 for a single analysis. Oxygen stable isotope analyses were accomplished by thermal conversion of Ag_3PO_4 to CO by reaction with glassy carbon at 1450°C in a Thermo Finnigan TC/EA device. Reaction gasses were separated by gas chromatography and the resultant CO introduced to a Thermo Finnigan Delta V Isotope Ratio Mass Spectrometer (IRMS). We used crimped silver capillaries (Longinelli and Nuti, 1973) containing amount equivalent aliquots of USGS UC03 ($\delta^{18}O = +29.8‰$) and IAEA VSMOW ($\delta^{18}O = 0.0‰$) to normalize raw $\delta^{18}O$ values from the mass spectrometer to the SMOW scale. An internal laboratory standard (0.3 μM; K_2HPO_4; Fisher, ACS Grade) was prepared in 10 L of filtered (<0.2 μm) Lake Erie water that had been previously stripped of P_i using brucite flocculation as above. Internal standards were run as samples and averaged +9.6 ± 0.3‰ (un-spiked reagents) and + 9.9 ± 0.1‰ (spiked reagents). Certified reference material B2207 (Isomass Scientific) measured 22.1 ± 0.5‰. Analytical precision averaged 0.6‰. All values are reported using standard delta notation relative to Vienna Standard Mean Ocean Water (VSMOW).

Samples for water $\delta^{18}O_W$ were collected whenever samples were taken for $\delta^{18}O_P$ by filtering ∼2 mL of lake water through a 0.45 μm cellulose acetate syringe filter into 2 mL glass vials. Vials were stored on ice and refrigerated until analysis by Off-Axis Integrated Output Spectroscopy (OA-ICOS) on a Los Gatos Research DLT-100 Liquid Water Isotope Analyser. We used two internal references waters, ROD3 and INV1 ($\delta^{18}O = -1.1$ and −28.3‰, respectively), to calibrate the raw values to the SMOW scale. The analytical precision of $\delta^{18}O_W$ values was determined by duplicate analyses of samples and internal references and is ± 0.2‰.

Dreissenid Mussel and Cladophora Sampling

Benthic surveys to collected dreissenid mussels and *Cladophora* were conducted at similar intervals in 2013 and 2014 at a larger number of stations in the study area as part of a targeted monitoring effort, however we only report data relevant to the stations identified in this study for 2014 as these surveys were conducted within 1 to 4 days of sampling for water chemistry and isotopes. Briefly, mussels and algae were harvested from three 0.15 m^2 quadrats at each station (with the exception of 1 m depth stations where a 0.125 m^2 quadrat was used). Mussels were removed by hand or by scraping while applying an airlift device to collect samples in a mesh bag. Samples were stored cool on ice until return to the laboratory in Burlington, ON and subsequently cleaned of debris and frozen prior to analysis. After lyophilization, mussels were counted, weighed, measured, and soft tissue removed to estimate densities of live individuals and biomass (as shell free dry mass, SFDM m^{-2}). For sites with algae collected concurrently, algal filaments were first cleaned in the field by washing with lake water. Upon return to the laboratory, algal filaments were cleaned under DI water and subsequently frozen. Algal biomass was determined after lyophilization and expressed as dry mass (g DM m^{-2}).

Dreissenid Incubations

Live dreissenid mussels were collected in July of 2013 and May of 2014 to aid in characterizing the $\delta^{18}O_P$ of P_i excreted by mussels ($\delta^{18}O_{P\_DM}$). Divers harvested intact mussels by hand into a fine mesh bag. Mussels were placed in ziplock bags with damp paper towel and stored on ice for transport to the laboratory in Burlington, ON. Upon arrival, mussels were gently separated from rocks, shell material and other debris, brushed clean with a toothbrush under running DI water. Between 75 and 150 individual mussels (10–30 mm valve length) were placed into acid washed 4 L polypropylene jars filled with filtered (<0.2 μm) Lake Erie water. Jars were aerated with air stones, and mussels were allowed to defecate and excrete for 12–36 h under a 16:8 L:D cycle at ± 2°C of lake temperature. SRP concentrations were monitored in the chambers until sufficient P had accumulated for analysis (∼10 μmol). Lakewater was gently decanted and siphoned from the jar, filtered through a 0.45 μm cellulose acetate filter, and processed as described above for $\delta^{18}O_P$.

Calculation of Isotopic Equilibrium Values for Phosphate

The theoretical isotopic equilibrium values for P_i ($\delta^{18}O_{P\_EQ}$) can be calculated using P_i water fractionation equations derived by Chang and Blake (2015) using Equation (1);

$$\delta^{18}O_{P\_EQ} = \left(\delta^{18}O_w \pm 1000\right) \times e^{\left[14.43\times\left(\frac{1000}{T(K)}-26.54\right]/1000} - 1000 \quad (1)$$

$\delta^{18}O_{P\_EQ}$ values were calculated for each sample using the measured $\delta^{18}O_w$ and temperature from the water column profiles. To assess uncertainty, we calculated $\delta^{18}O_{P\_EQ}$ using the minimum and maximum $\delta^{18}O_w$ for the entire study period for lake and river sites respectively.

Fraction of River Water and Expected Nutrient Concentrations

To estimate the relative influence of the river on nutrient conditions at the study sites, we used a linear mixing model to estimate the fractional contribution of river water (FRW) at lake sites using the measured values of δ^{18}Ow

$$FRW = \frac{\delta^{18}O_{ws} - \delta^{18}O_{wl}}{\delta^{18}O_{wr} - \delta^{18}O_{wl}} \quad (2)$$

where $\delta^{18}O_{ws}$ is the water $\delta^{18}O_w$ value at each site, $\delta^{18}O_{wr}$ is the water $\delta^{18}O_w$ value at the river mouth and $\delta^{18}O_{wl}$ is the highest water $\delta^{18}O_w$ value observed at the open lake sites. We elected to use the highest $\delta^{18}O_w$ value for each survey period as there was some spatial and temporal variation in $\delta^{18}O_w$, possibly due to larger scale circulation features. For each site (*i*), we calculated the expected concentration of PP, TDP, and SRP assuming conservative mixing between the open lake and river;

$$C_{P(i)} = C_{P(l)}\,(1 - FRW) \pm C_{P(r)}FRW \quad (3)$$

Where $C_{P(i)}$ is the expected concentration of P (PP, TDP, or SRP) at each site, $C_{P(l)}$ is the concentration of P for the open lake end member, and $C_{P(r)}$ is the concentration of P at the river mouth. We used the average concentrations for sites with FRW < 0.1 to derive the open lake end member values for each survey, and $C_{P(r)}$ is represented by the phosphorus concentration at the river mouth.

RESULTS

Influence of the Grand River and Patterns of Nutrient Variation in the Nearshore

$\delta^{18}O_w$ values ranged from −12.6 to −8.6‰ at the river mouth but were more constrained at the lake sites, ranging from −7.9 to −6.0‰ (**Table 1**). The calculated fraction of river water (FRW) was variable over all surveys but was highest in late May—early June, reaching up to 0.8 at shallow stations ∼2 km due east of the river mouth (**Figure 2**). While FRW was highest after the spring runoff period, values ranged from near 0 to ∼0.35 between June and August surveys, particularly at stations east of the river mouth (**Figure 2**). FRW tended to increase with increasing river discharge (**Figure 2**) although the correlation was weak ($r = 0.23$, $p < 0.1$).

Nutrient concentrations were often higher and more variable in proximity to the Grand River mixing area. Total phosphorus, total dissolved phosphorus and soluble reactive phosphorus (TP, TDP, and SRP) were negatively correlated with distance from the river mouth ($r = -0.42$, $r = -0.39$, $r = -0.34$, $p < 0.001$, $p < 0.001$, $p < 0.01$, respectively). Nitrate (NO_3) and dissolved organic carbon (DOC) concentrations were also strongly negatively related to distance from the Grand River mouth ($r = -0.48$, $r = -0.48$, $p < 0.001$, respectively). Ammonia (NH_3) was the only nutrient parameter measured that did not

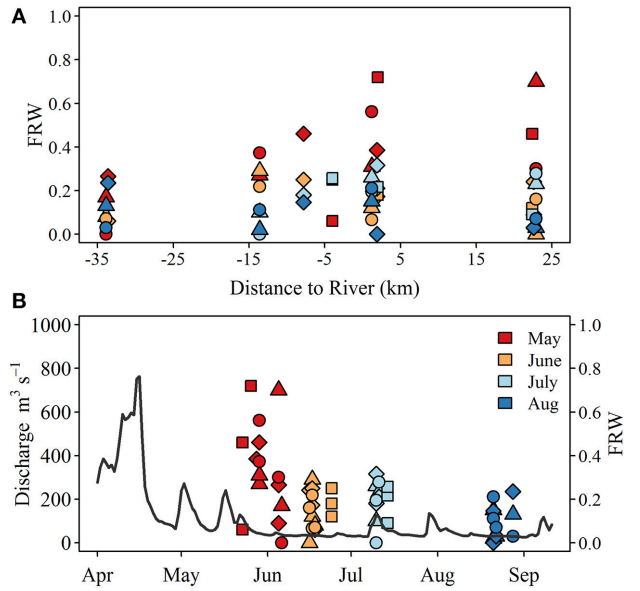

FIGURE 2 | (A) Spatial and **(B)** temporal pattern of the estimated fraction of river water (FRW) observed at lake sites. Symbols indicate sample type including surface (S; circle), lakebed 10 m (LB10; triangle), lakebed 3 m (LB3; diamond), and lakebed 1 m (LB1; squares). Gray line in **(B)** represents Grand River discharge measured at the monitoring station located at York (see **Figure 1**). Note the x-axis in **(A)** denotes the west (negative) and east (positive) distances of each sampling site from the mouth of the Grand River.

display any spatial gradient in relation to the Grand River ($r = -0.17, p > 0.2$).

Despite apparently elevated phosphorus concentrations at sites close to the river, deviation from expected concentrations based on a simple two member mixing model indicated strongly non-conservative behavior for both particulate and dissolved fractions in late May—early June. Notably, the deviations were strongest as FRW increased suggesting rapid consumption/settling or uptake processes were active (**Figure 3A**). From mid-June to August, the same general trend was apparent for particulate P, but was somewhat attenuated for TDP and SRP, largely because the concentration difference of TDP and SRP between river mouth station and open lake sites was small (**Figures 3B–D**). Some positive excursions for particulate P were evident at 1 m depth sites (**Figures 3B,C**) suggesting possible resuspension of sediment or sloughed periphyton. During mid-June, July and August surveys, TDP and SRP were generally lower than predicted for LB samples from shallow water (1 and 3 m depth) sites, with the exception of PSN 1371 and 1274 in July (**Figure 3C**). TDP and SRP in LB samples at 10 m sites were often (but not always) elevated relative to expected concentrations predicted from mixing alone (**Figure 3**).

Dreissenid Mussel and Cladophora Distribution

Plots of *Cladophora* and dreissenid mussel abundance and biomass (SFDM m^{-2}) are shown in **Figure 4**. *Cladophora* biomass ranged from 0 to 189 g DM m^{-2}, reaching maximum values at 1 m depth in June and July (**Figure 4**). *Cladophora* biomass at 3 m depth sites did not exceed 25 g DM m^{-2} and at 10 m sites did not exceed 2 g DM m^{-2} (**Figure 4**). Dreissenid abundance and biomass varied widely between surveys and locations (6–2131 m^{-2} and 0.2–65 g SFDM m^{-2} respectively). Dreissenid abundance and biomass was clearly higher at 10 m depth sites than 3 m sites. No strong spatial patterns in dreissenid abundance or biomass were observed, and although *Cladophora* biomass was high at the 1 m sites close to the Grand River, we do not have data for similar depths at greater distances to the west side of the river, which obscures the lack of spatial patterns observed in other years (D.Depew, unpubl.data).

Oxygen Isotopic Composition of River and Lake Samples

$\delta^{18}O_P$ and calculated $\delta^{18}O_{P\_EQ}$ values for all stations and dates are shown in **Table 1**; and their spatial/seasonal and depth distributions in **Figure 5** through **Figure 7**. $\delta^{18}O_{P\_EQ}$ values at the river mouth were isotopically lighter compared to lake sites (**Table 1**). The seasonal dynamics of $\delta^{18}O_P$ at the river mouth are displayed in **Figure 5**. During freshet period (April-late May), despite large variation in river discharge, $\delta^{18}O_P$ varied relatively little, ranging between $+11.1 \pm 0.6$ and $+11.9 \pm 0.7$‰ and overlapped the $\delta^{18}O_{P\_EQ}$ window at times (**Figure 5**). From mid-May to late August, $\delta^{18}O_P$ declined steadily ($\delta^{18}O_P$ in the river was significantly correlated with day of year; $r = -0.95$, $p < 0.001$) through the season reaching a low of +5.7‰ in late August (**Figure 5**).

The spatial and temporal variation of $\delta^{18}O_P$ at lake sites are shown in **Figure 6**. $\delta^{18}O_P$ at lake sites ranged from +4.7 to +14.9‰ and did not show strong relationships with FRW or with distance from the Grand River (**Figure 6**). Within-transect variation (i.e., variation across different depths) in $\delta^{18}O_P$ was often greater than differences from west to east (**Figure 6**). No obvious differences were observed for samples collected near the lake bed at 1 and 3 m sites and surface samples at 10 m sites, but samples collected near the lake bed at 10 m sites (LB10) were consistently isotopically heavier than companion surface samples (paired *t*-test, $t = 11.1$, $n = 12$, $p < 0.001$) and frequently overlapped the range of $\delta^{18}O_{P\_DM}$ (**Figure 7**). Notably, all but one lake sample are below the calculated theoretical equilibrium based on water temperature and $\delta^{18}O_W$ (**Figure 6**, **Table 1**).

The degree of isotopic offset of $\delta^{18}O_P$ from the calculated $\delta^{18}O_{P\_EQ}$ was strongly correlated to SRP concentration and negatively correlated to the seston N:P ratio, suggesting larger negative excursions for samples associated with low P availability (**Figure 8**). Such patterns are expected if the hydrolysis of DOP is an important mechanism of P_i regeneration. Indeed, we observed low $\delta^{18}O_P$ values and larger negative excursions from the $\delta^{18}O_{P\_EQ}$ values as the TDP pool became increasingly dominated by DOP (**Figure 8**). The only samples that appeared to not follow this pattern were those collected at the lakebed at 10 m depth sites.

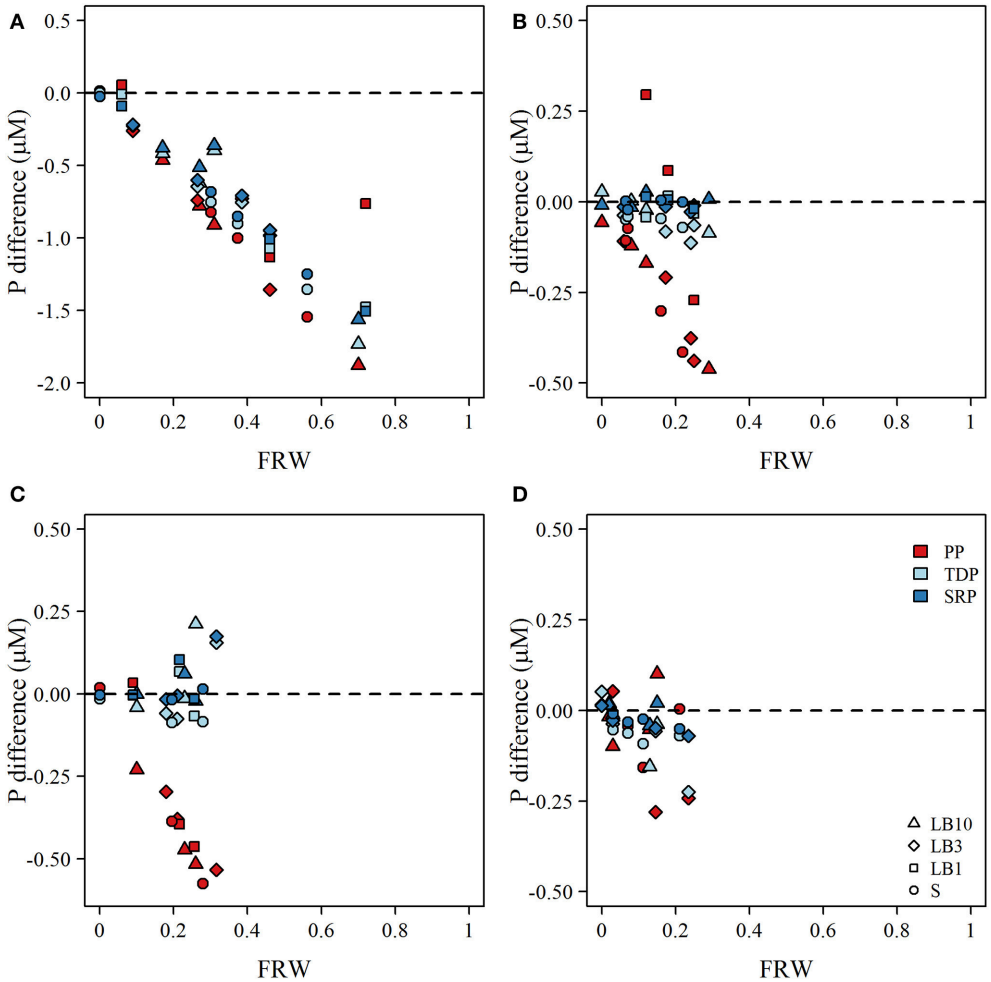

FIGURE 3 | Plot the calculated difference between observed and expected concentrations of particulate P (PP), total dissolved P (TDP), and soluble reactive P (SRP) as a function of the fraction of river water (FRW) at each site for **(A)** late-May to early-June, **(B)** June, **(C)** July, and **(D)** August. Symbols correspond to surface (S; circles), lakebed 10 m (LB10; triangle), lakebed 3 m (LB3; diamond), and lakebed 1 m (LB1; squares). Dashed line in each panel indicates the difference in concentration that would occur if mixing PP, TDP, and SRP of river and lake water were conservative assuming a two−member mixing model.Expected concentrations were calculated collowing Equation (3).

Oxygen Isotopic Composition of Phosphorus Excreted by Dreissenid Mussels

Oxygen isotopic compositions of phosphate collected during dreissenid excretion experiments ($\delta^{18}O_{P\_DM}$) ranged from +10.2 to +13.5‰ and averaged +11.9 ± 1.1‰ (**Table 2**). $\delta^{18}O_P$ at LB10 and LB3 sites were positively related to dreissenid abundance and shell free biomass (**Figure 9**).

DISCUSSION

Variation in water quality and nutrient conditions along the north shore of the eastern basin are shaped to a large degree by the discharge of nutrient rich water from the Grand River (Chomicki et al., 2016) as well as interaction with hydrodynamic features. Wind forcing (He et al., 2006) and large scale circulation features (Rao and Schwab, 2007) often trap river inputs alongshore, creating a band of enriched water that extends to approximately the 5 m depth contour (Chomicki et al., 2016). Estimates of FRW at our study sites are in general agreement with prior studies and existing knowledge and observations of nearshore circulation and river plume dynamics. For example, we observed FRW estimates approaching 80% at sites to the east of the river mouth, with larger values typically encountered at 1 and 3 m depth sites which are <1 km from the shoreline. It is unclear if the high FRW observed ∼20 km to the east represents input from the Grand River as there are a number of smaller tributaries that discharge along the shore between the Grand River and the eastern-most study sites. Previous estimates of river influence extent range from 8 to 10 km (Nicholls et al., 1983; Howell and Hobson, 2003) although these are generally based on seasonal data and use other semi-conservative tracers. Discharge from the Grand River in April and May of 2014 exceeded the

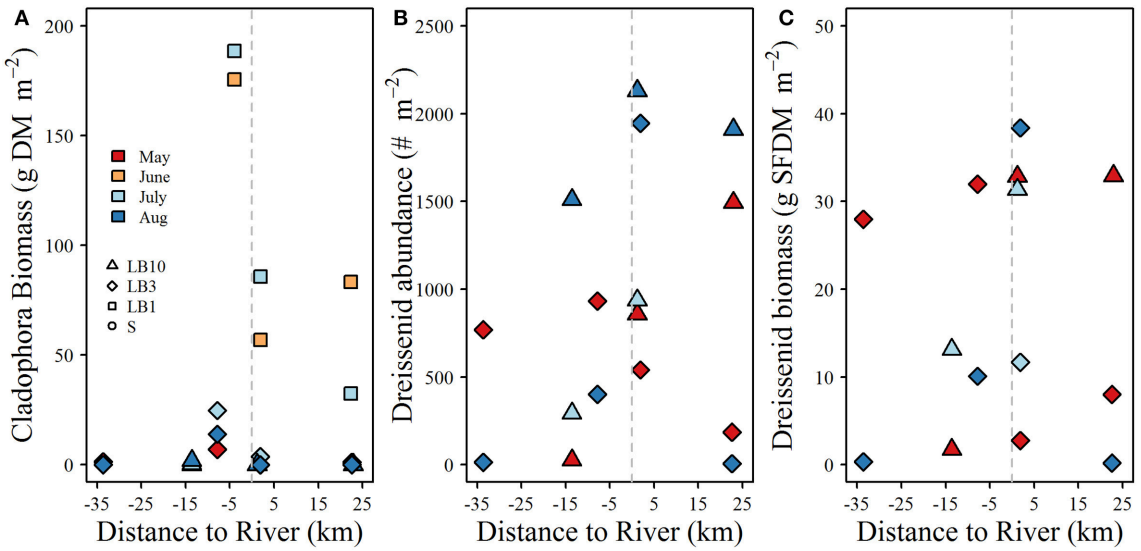

FIGURE 4 | (A) *Cladophora* biomass, **(B)** dreissenid mussel abundance, and **(C)** dreissenid biomass as a function of distance from the Grand River at study sites where isotope samples were collected. Note the x-axis in each panel denotes the west (negative) and east (positive) distances of each sampling site from the mouth of the Grand River. All benthic samples were collected within the same week as water quality and stable isotope samples.

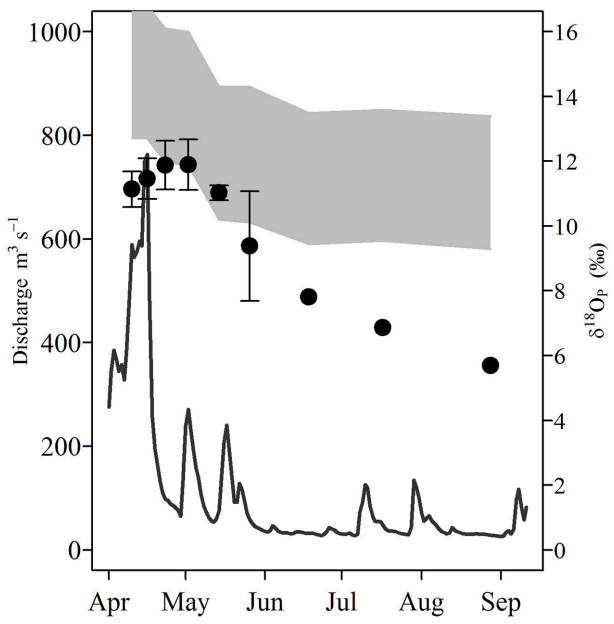

FIGURE 5 | Temporal variation of Grand River discharge (m^{-3} s^{-1}; solid line) and $\delta^{18}O_P$ measured at the river mouth during the study period (circles, error bars represent 1 SD of multiple measurements). Shaded gray area represents the equilibrium window ($\delta^{18}O_{P\_EQ}$) based on the minimum and maximum measured water $\delta^{18}O_W$ at the river site using the equation of Chang and Blake (2015).

long term (1913–2016) 75th percentile of ~300 m^3 s^{-1} by nearly a factor 2–3 (https://wateroffice.ec.gc.ca/report/historical_e.html?mode=Graph&type=h2oArc&stn=02GB001&dataType=Daily&parameterType=Flow&year=2014&y1Max=1&y1Upper=1&scale=normal), and given that river water temperatures at this time were approximately double those encountered in the lake (~19.5°C compared to 11–12°C), the river plume would have likely been thermally buoyant, spreading thinly over large distances before mixing completely. The FRW was less variable during low flow periods ranging from 0 to ~20%. FRW was generally higher at shallow stations (i.e., the 1 and 3 m depth sites), consistent with the alongshore entrapment of the plume.

Although nutrient concentrations were generally elevated closer to the river mouth and the river water clearly influenced our study sites, we observed strong non-conservative behavior of all forms of phosphorus across the river mouth—lake mixing area. During late May—early June, when concentrations of PP, TDP, and SRP were highest at the river mouth, the measured concentrations in the lake were considerably lower than would be expected based on simple dilution, even at sites in close proximity (<2 km) with FRW approaching 80% (**Figure 3**). In fact, losses of PP, TDP, and SRP appeared to be strongest at the sites closest to the river mouth, suggesting rapid sedimentation, consumption, and/or uptake (**Figure 3A**). Losses of particulate P could reflect the settling of large and coarser organic P particles owing to reductions in flow velocity and turbulence, or perhaps consumption of organic P by dreissenid mussels (Chomicki et al., 2016). Smaller particles such as non-apatite inorganic P (~4–7 μm diameter; Chomicki et al., 2016) would likely remain in suspension for a greater duration and be subjected to more widespread mixing and dispersion. Declines in SRP and to an extent TDP may reflect uptake by phytoplankton as chlorophyll a concentrations increased from ~0.5 μg L^{-1} at open lake sites (e.g., 502 and 1350) to a maximum of 15.3 μg L^{-1} at PSN 1371, 2 km east of the river mouth. Similar results have been observed

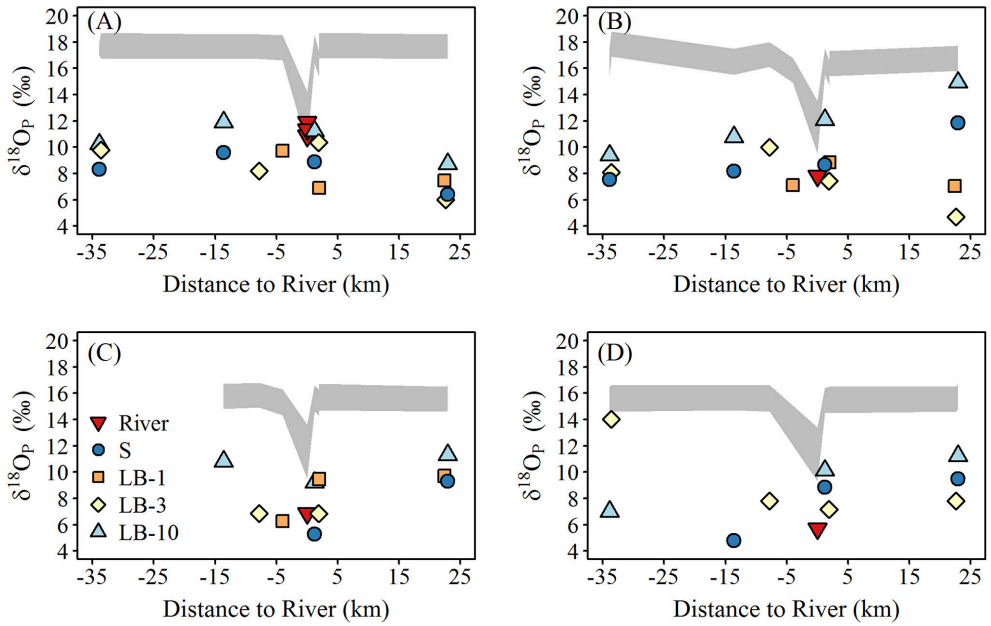

FIGURE 6 | Spatial variation of $\delta^{18}O_P$ (‰; symbols) and the calculated equilibrium window ($\delta^{18}O_{P\_EQ}$) at lake sites during **(A)** late May—early June, **(B)** mid-June, **(C)** mid-July, and **(D)** late August. The equilibrium window ($\delta^{18}O_{P\_EQ}$) was calculated using the minimum and maximum measured water $\delta^{18}O_W$ over the study period using the equation of Chang and Blake (2015).

across the Milwaukee River mixing zone in Lake Michigan, where biological processes have been implicated in removal of SRP in close proximity to the point of discharge (Lin and Guo, 2016).

Over the late June to August surveys, losses of particulate P remained consistently strong in close proximity to the river mouth although there were instances of resuspension elevating PP concentrations, particularly at 1 m depth sites (**Figure 3B**). The responses of TDP and SRP were generally consistent, although the magnitude of difference between observed and expected concentrations was small owing to the relatively small difference between TDP and SRP concentrations at the river mouth and lake sites. At times, TDP and SRP concentrations were larger than expected based on the mixing model calculations. Elevated concentrations of SRP were often observed for LB samples at 10 m sites (**Figures 3B–D**), but were also observed at 1 m and 3 m sites in July (**Figure 3C**). The proximate cause of these elevated concentrations could be due to leakage of nutrient rich groundwater (e.g., Robinson, 2015) or perhaps due to the decomposition of *Cladophora* that had accumulated at the adjacent shoreline as decomposing *Cladophora* is known to lose phosphorus slowly over a period of several weeks *in situ* (Paalme et al., 2002).

Oxygen Isotope Ratios of Phosphate Indicate Extensive Phosphorus Cycling

Compared to marine systems (Colman et al., 2005; McLaughlin et al., 2006a,b, 2013; Goldhammer et al., 2011; Jaisi et al., 2011; Joshi et al., 2015; Li et al., 2017) and soils (Zohar et al., 2010; Angert et al., 2012; Tamburini et al., 2012; Granger et al., 2017a), freshwater environments are poorly characterized with respect to $\delta^{18}O_P$ [but see (Elsbury et al., 2009; Granger et al., 2017b; Pistocchi et al., 2017)]. The $\delta^{18}O_P$ we measured in the Grand River during April and early May (+9.4 ± 1.7 to +11.9 ± 0.7‰) are similar to values reported for Lake Erie tributaries in the central and western basins over summer and fall (Elsbury et al., 2009), but lower than those reported for the River Taw, UK (Granger et al., 2017b). $\delta^{18}O_P$ at the river mouth site was near or overlapped $\delta^{18}O_{P\_EQ}$ in late April and early May, but declined steadily from +9.4 ± 1.7‰ to a minimum of +5.7‰ through August, with the departure from $\delta^{18}O_{P\_EQ}$ increasing to the end of August(**Figure 5**). Similarly, $\delta^{18}O_P$ at lake sites are considerably lower than those reported by (Elsbury et al., 2009) for the west and central basin of Lake Erie (∼+11 to +17‰), and all but one LB sample were below the calculated $\delta^{18}O_{P\_EQ}$ based on $\delta^{18}O_W$ and water temperature.

It is important to keep in mind that $\delta^{18}O_P$ measured at a given site at a given time represents a snapshot of a variety of processes occurring along a continuum of P cycling. For example, the P_i pool may be affected to varying degrees by the intensity of (1) P_i that has been equilibrated internally and released by microbes and/or phytoplankton (Blake et al., 1997; Paytan et al., 2002), (2) P_i excreted by zooplankton (Taylor and Lean, 1981), (3) remineralization of DOP excreted by phytoplankton (Bentzen et al., 1992) or liberated via zooplankton grazing and/or viral lysis (Taylor and Lean, 1981), and (4) mixing with an external P_i source with a distinct $\delta^{18}O_P$ (Paytan et al., 2017). The strong negative deviations from theoretical equilibrium values observed here are anticipated in systems where ambient levels of P are limiting and arise due to the large inheritance effects associated with isotopic fractionation during the incorporation

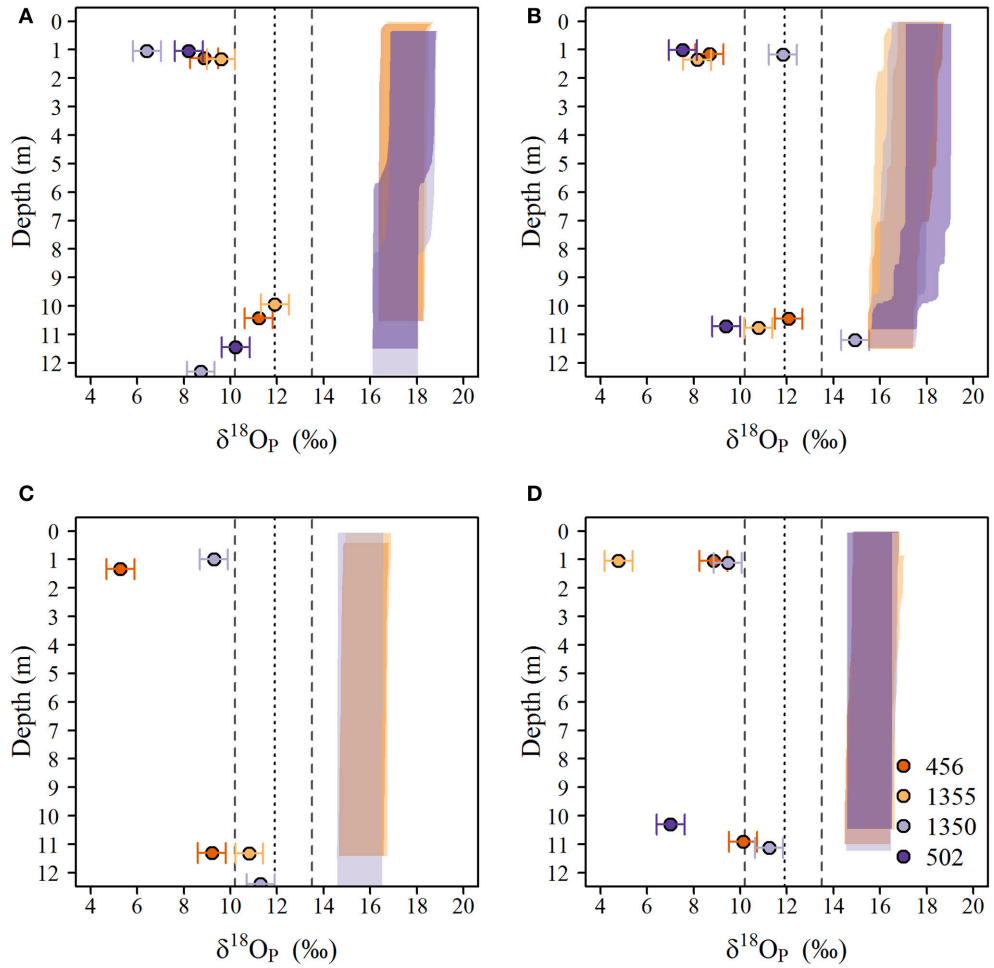

FIGURE 7 | Vertical distribution of $\delta^{18}O_P$(circles) and calculated equilibrium $\delta^{18}O_{P\_EQ}$) (shaded polygons) in the water column at the 10 m depth sites in eastern lake Erie during **(A)** late-May to early June, **(B)** June, **(C)** July, and **(D)** August of 2014. The equilibrium window was determined by interpolating $\delta^{18}O_W$ as function of depth and calculating the range of $\delta^{18}O_{P\_EQ}$ using the temperatures derived from vertical profiles and the equation Chang and Blake (2015) for the minimum and maximum $\delta^{18}O_W$ observed over the study period. The dotted (dashed) vertical line(s) represent the average (range) $\delta^{18}O_{P\_DM}$ measured in laboratory experiments.

of water oxygen into the P_i ion during enzymatic hydrolysis (Liang and Blake, 2006, 2009). Forms of DOP commonly found in aquatic ecosystems include phosphomonoesters, phosphodiesters, and phospholipids produced by organisms *in situ* (Baldwin, 2013) but may also include phosphomonesters, phosphodiesters and inositol phosphates exported from the surrounding catchment (Monbet et al., 2009). Monoesters are generally considered bioavailable due to the presence of enzymes such alkaline phosphatase (EC 3.1.3.1) (Bentzen et al., 1992), but phosphodiesterases and phytases may make diesters and inotisol phosphates potentially bioavailable (Cheng and Lim, 2006). Although we do not have detailed information on the nature and composition of DOP or enzyme activity in eastern Lake Erie (but see North et al., 2012), if we assume that organic P contained within organisms in the lake is at or near equilibrium (e.g., Paytan et al., 2002, based on known fractionation factors for various DOP compounds, the $\delta^{18}O_P$ of released P_i recycled from the DOP pool is expected to be $< \sim+14$‰, and even lower $< +11$‰ if substrates such as phytate is not a major component of the bioavailable DOP pool (**Table 3**). While these are generalizations, they illustrate the relative magnitude expected if regeneration of P_i from DOP is an important P recycling pathway. This is further supported by the significant relationships we observed between $\delta^{18}O_P$ and other proxies of P availability such as %DOP, SRP concentration and seston N:P ratios (**Figure 8**), and we infer that the recycling of DOP by the plankton community is a major determinant of the isotopic composition of the available P_i pool in eastern Lake Erie.

Oxygen Isotope Ratios Cannot Be Used to Track Riverine Input to Eastern Erie

Concentrations of SRP at the river mouth site were high (up to 6.9 μM) between April and early June. Despite large variation in river discharge volume, $\delta^{18}O_P$ was relatively invariant (**Figure 5**).

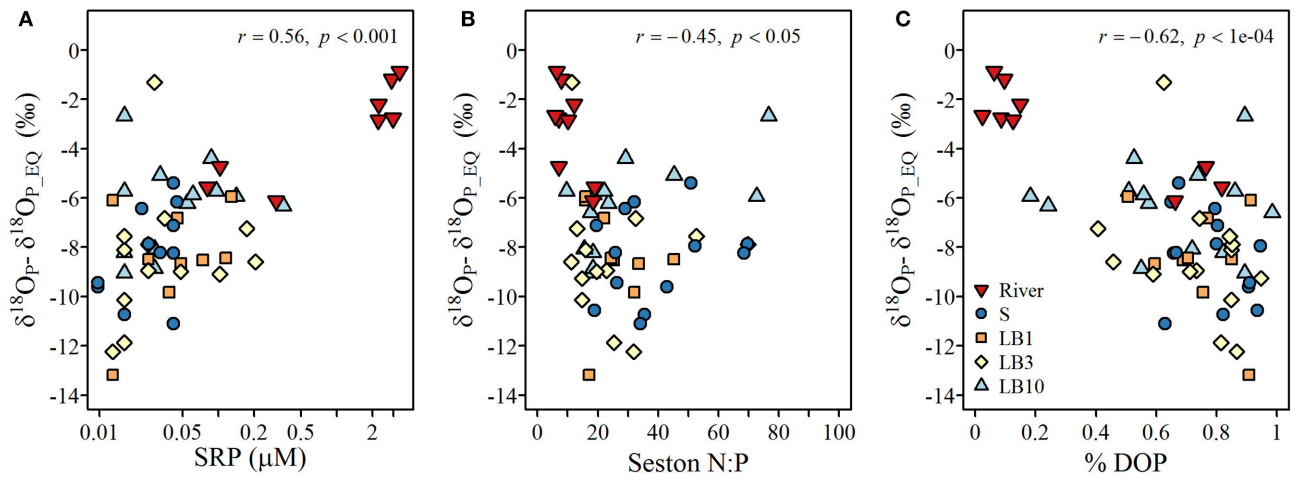

FIGURE 8 | Relationships between **(A)** the offset of measured $\delta^{18}O_P$ (‰; symbols) from theoretical $\delta^{18}O_{P\_EQ}$ and soluble reactive P concentrations, **(B)** offset of measured $\delta^{18}O_P$ (‰; symbols) from $\delta^{18}O_{P\_EQ}$ and seston N:P ratios, and **(C)** offset of measured $\delta^{18}O_P$ (‰; symbols) from $\delta^{18}O_{P\_EQ}$ and % DOP (calculated as (TDP-SRP)/TDP).

TABLE 2 | Oxygen isotopic composition of phosphate collected $\delta^{18}O_P$ in incubations with dreissenid mussels ($\delta^{18}O_{P\_DM}$) harvested from eastern Lake Erie in 2013 and 2014.

PSN	Date	Station depth (m)	$\delta^{18}O_{P\ DM}$(‰)
1350	May	10.1	+11.3
1345	May	6.2	+12.6
1352	May	6.1	+11.5
1342	May	5.9	+12.1
1349	July	18.2	+13.5
1342	July	5.9	+10.2
Average			+11.9 ± 1.08

*PSN denotes station ID as in **Figure 1**.*

This is somewhat surprising given that land use in the Grand River watershed is a mixture of intensive agricultural and urban use (Holeton, 2013). Although we do not have a detailed inventory of $\delta^{18}O_P$ of different sources within the Grand River watershed, based on existing data it seems likely that $\delta^{18}O_P$ might vary according to the relative inputs of P_i from different sources (e.g., Young et al., 2009). In addition,the short residence time of the river (∼3 d, Rosamond, 2013) and low temperatures (<10°C) should have acted to minimize any uptake and cycling of P_i in the river at this time. While it is possible that $\delta^{18}O_P$ within the watershed might not vary across different sources, or perhaps simply reflected thorough mixing of source inputs, we note that our SRP concentrations measured at the river mouth site were up to 2 to 6-fold higher compared to concentrations measured the same day at a nutrient monitoring station ∼40 km upstream (Supplemental Information Figure S1), indicating a significant input of P_i below the monitoring station. While further work will be required to identify the proximate source of this P_i, we note that this section of the river is characterized by extensive wetland complexes, some of which at times can have very high TDP concentrations (6–190 μM; (Gilbert and Ryan, 2007), and may explain lack of variation in $\delta^{18}O_P$ during this period.

Despite high concentrations of SRP, a relatively constant $\delta^{18}O_P$ and high discharge during the April to early June we did not observe any evidence of mixing between riverine $\delta^{18}O_P$ and lake $\delta^{18}O_P$ at any of our sites. During the cooler spring months, P uptake by phytoplankton is generally reduced relative to summer months (Lean et al., 1983), yet at sites closest to the river mouth (i.e., those with high FRW), $\delta^{18}O_P$ was no different than lake sites far removed from the river mixing zone. Only LB samples from 10 m depth sites had $\delta^{18}O_P$ that was reasonably close to riverine $\delta^{18}O_P$, but these samples had low FRW and are likely affected by recycling of P by dreissenid mussels (see below).

Between June and August, $\delta^{18}O_P$ at the river mouth site declined steadily, departing further from $\delta^{18}O_{P\_EQ}$ (**Figure 7**). Such observations are not uncommon in P–rich systems (Paytan and McLaughlin, 2012), however, $\delta^{18}O_P$ moved further away from $\delta^{18}O_{P\_EQ}$ as SRP concentrations declined from 6.9 μM in late May to a low of 0.08 μM in July, which is counter to expectation (McLaughlin et al., 2006b; Granger et al., 2017b). On one hand, this could indicate an input of an isotopically light source of P_i such as waste water treatment plant (WWTP) effluent (Young et al., 2009) or P_i liberated via the degradation of glyphosate (Li et al., 2016a). During summer base flow periods, WWTP inputs become a larger component of the total P mass load to the river (Holeton, 2013), however, $\delta^{18}O_P$ of treated WWTP effluent from plants within the Grand River watershed are reported to be higher than values we measured [+11.4 to +22.8‰ (Morrison, 2014)] and P uptake studies downstream of WWTP discharges indicate relatively short uptake lengths (<5500 m; Barlow-Busch et al., 2006). Similarly, while glyphosate is a common herbicide in southern Ontario, concentrations typically peak during rain events (Struger et al., 2015) and since we observed low $\delta^{18}O_P$ at near base flow conditions, this is unlikely to explain the values measured here. Rather, we

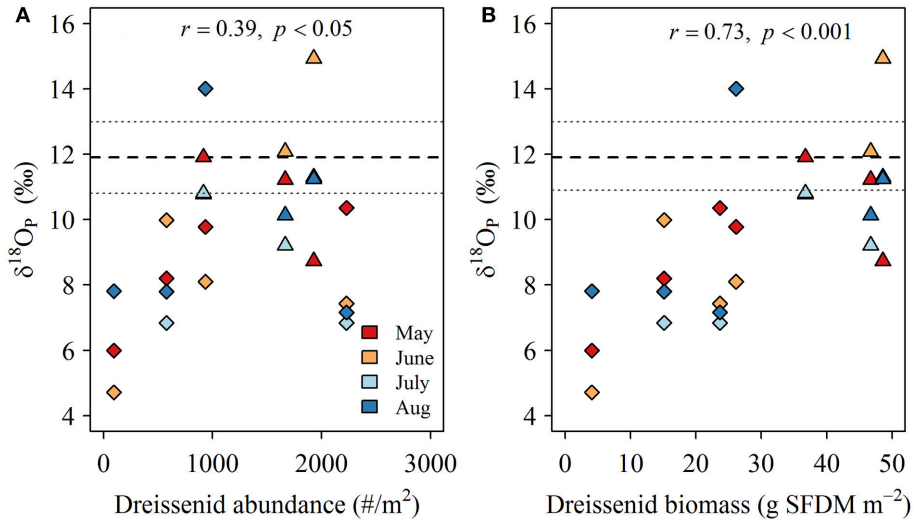

FIGURE 9 | (A) Relationship between the offset of $\delta^{18}O_p$ in LB samples from $\delta^{18}O_{P\_DM}$ (‰; symbols) and dreissenid abundance (# m^{-2}) and **(B)** shell free dreissenid biomass (g SFDM m^{-2}). Long (short) dashed lines represents the mean (range) of experimentally determined $\delta^{18}O_{p\_DM}$.

speculate that P_i is extensively processed within the lower river by the attendant phytoplankton community. Previous studies of the lower Grand have indicated that an appreciable portion of dissolved P is converted into phytoplankton biomass prior to entering Lake Erie (Kuntz, 2008). Despite the overall eutrophic conditions, the increasing disequilibrium from $\delta^{18}O_{P\_EQ}$ at the river mouth during the summer in combination with high chlorophyll a concentrations (25–48 $\mu g\ L^{-1}$) is not inconsistent with a highly productive river estuary where even the use of DOP can be important (Larson et al., 2016; Yuan et al., 2017). Further study of phosphorus sources to the lower river and speciation would be required to confirm such pathways, particularly in order to trace back to specific input sources of P. Nonetheless, even though riverine $\delta^{18}O_P$ appears to be altered prior to discharge into the lake, when our $\delta^{18}O_P$ data are considered together with evidence of strongly non-conservative mixing behavior of SRP, we infer that most of the P_i discharged by the river is quickly assimilated into phytoplankton and rapidly overprinted via DOP recycling.

Isotopic Enrichment at the Lake Bottom Indicates Benthic P Recycling

Samples collected near the lake bed at 10 m depth sites were persistently isotopically heavier than paired surface samples at all sites on all dates, and most samples overlapped the $\delta^{18}O_P$ measured in our excretion experiments ($\delta^{18}O_{P\_DM}$) (**Figure 7**). In some cases, differences between lakebed and surface SRP concentrations were large (up to 10-fold) indicating enrichment of the near bottom waters while in others, the differences were smaller. Overall, SRP was significantly higher in LB samples compared to surface samples (paired *t*-test, $t = 2.24$, $p < 0.05$) and chlorophyll *a* concentrations were lower (paired *t*-test, $t = 2.89$, $p < 0.05$) consistent with known impacts of dreissenid grazing of phytoplankton and excretion of soluble P (Ackerman et al., 2001; Conroy et al., 2005; Ozersky et al., 2009). Differences in TDP displayed similar patterns but were not significant (paired *t*-test, $t = 1.69$, $p < 0.1$) and differences in NH_4, NO_3 and PC, PN or PP were not different (data not shown).

The experimentally determined $\delta^{18}O_{P\_DM}$ was constrained relative to $\delta^{18}O_P$ collected at lake sites, regardless of where or when dreissenid mussels were collected for incubations. Dreissenid mussels excrete P_i directly (Arnott and Vanni, 1996), DOP (Mosley and Bootsma, 2015), and deposit a larger quantity of nutrients (including P) as partially digested pseudofaeces and feces on the surrounding sediments/lakebed (Nalepa et al., 1991). The smaller range of $\delta^{18}O_{P\_DM}$ compared to $\delta^{18}O_{P\_}$ from LB samples might be due to differences in the quantities of P_i derived from direct excretion vs mineralization of pseudofecal and fecal material, as our incubation time required to generate sufficient P_i for recovery (~10 μM; 12–36 h) were of sufficient duration to permit accumulation of feces and psuedofaeces, and although we did not measure microbial activity, decomposition of fecal and pseudofecal material generally occurs over a longer time frame than employed here (Roditi et al., 1997). In contrast, our LB samples could contain P_i excreted directly by dreissenids, or derived from the re-mineralization of pseudofaeces and/or feces. P_i excreted directly by dreissenids is likely liberated through the action of acid phosphatases (EC 3.1.3.2) in the acidic gut (Sauey et al., 2016), and based on examples in **Table 3**, released P_i could range between +7.0 and +14‰. Many of our $\delta^{18}O_{P\_DM}$ fall within this range, as do $\delta^{18}O_P$ from LB samples at 10 m sites. The generally consistent overlap between $\delta^{18}O_{P\_DM}$ from incubations and $\delta^{18}O_P$ from LB sites is further supported by positive relationships observed between the degree of offset of $\delta^{18}O_P$ from our experimentally determined $\delta^{18}O_{P\_DM}$ and dreissenid abundance and shell free biomass (**Figure 9**) and support the role of dreissenid mussels as active recyclers of P in the benthic environment.

TABLE 3 | Examples of mass balance calculations* for the oxygen isotopic composition of phosphate ($\delta^{18}O_P$; ‰) released by enzymatic hydrolysis for different enzymes and substrates using literature values for isotopic fractionation (ε).

$\delta^{18}O_P$	ε	Substrate	Enzyme	References
7.9–10.5	−8.1	AMP	AcidPase[1] EC 3.1.3.2	Von Sperber et al., 2014
7.0–9.5	−11.8	GPO_4	AcidPase[1] EC 3.1.3.2	Von Sperber et al., 2014
11.7–14.3	+7.2	Phytic acid	AcidPase[1] EC 3.1.3.2	Von Sperber et al., 2015
7.7–10.3	−8.9	AMP	AcidPase[2] EC 3.1.3.2	Von Sperber et al., 2014
7.2–9.7	−11	GPO_4	AcidPase[2] EC 3.1.3.2	Von Sperber et al., 2014
9.7–12.3	−0.9	Phytic acid	AcidPase[2] EC 3.1.3.2	Von Sperber et al., 2015
11.9–14.4	+7.7	Phytic acid	Phytase EC 3.1.3.26	Von Sperber et al., 2015
6.9–9.4	−12.3	AMP	Phytase EC 3.1.3.26	Von Sperber et al., 2015
6.9–9.5	−12.0	GPO_4	Phytase EC 3.1.3.26	Von Sperber et al., 2015
4.2–6.7	−23	Glu-1-P	AlkPase[3] EC 3.1.3.1	Liang and Blake, 2006
1.7–4.2	−33	GPO_4	AlkPase[3] EC 3.1.3.1	Liang and Blake, 2006
2.4–5.0	−30	AMP	AlkPase[3] EC 3.1.3.1	Liang and Blake, 2006
5.2–7.7	−19	Glu-1-P	AlkPase[4] EC 3.1.3.1	Liang and Blake, 2006
3.2–5.7	−27	GPO_4	AlkPase[4] EC 3.1.3.1	Liang and Blake, 2006
7.4–10.0	−10	AMP	5'Nase EC 3.6.1.1	Liang and Blake, 2006
1.9–3.6	+20/−30	RNA	PDase + AlkPase (EC 3.1.4.1/EC.3.1.3.1)	Liang and Blake, 2009
6.9–8.6	+20/−10	RNA	PDase + 5'Nase (EC 3.1.4.1/EC.3.6.1.1)	Liang and Blake, 2009
−8.2 to −6.5	−20/−30	DNA	PDase + AlkPase (EC 3.1.4.1/EC.3.1.3.1)	Liang and Blake, 2009
−3.2 to −1.5	−20/−10	DNA	PDase + 5'Nase (EC 3.1.4.1/EC.3.6.1.1)	Liang and Blake, 2009

**For these calculations, it is assumed that organic P (dissolved or particulate) retains an equilibrium signature (isotope equilibrium value associated with pyrophosphatase P cycling at measured temperatures and $\delta^{18}O_w$). The lower and upper values represent the range of possible $\delta^{18}O_P$ of released phosphate assuming the $\delta^{18}O_P$ of organic P ranges between +15.5 and +18.9, which represent equilibrium values for an average $\delta^{18}O_w$ of −6.8‰ for eastern Lake Erie, and water temperatures of 23° and 4°C respectively. Mass balance equations for each enzyme and substrate are found in listed references. AcidPase[1], Potato AcidPase; AcidPase[2], Wheat germ AcidPase; AlkPase[3], calf AlkPase; AlkPase[4], E. coli AlkPase; AMP, adenosine 5'-monophosphate; GPO4, glycerophosphate; Glu-1-P, glucose-1-phosphate.*

Alternative explanations for isotopic enrichment of $\delta^{18}O_P$ near the lake bed could include possible desorption of P_i from clays or iron minerals, or injection of isotopically heavier P_i from the hypolimnion. Chomicki et al. (2016) suggested that ∼50% of the particulate P leaving the Grand River is non-apatite inorganic P (NAIP), of which iron oxides are a dominant component (Mayer and Manning, 1989). While much of this material likely settles out within a short distance of the river mouth, it is nonetheless subject to resuspension and subsequent dispersal by wind and waves (Chomicki et al., 2016). The structurally complex and rough surfaces created by abundant dreissenid mussels may retain settled material in interstitial spaces and enhanced O_2 demand from fecal material and respiratory activity of mussels (Turner, 2010) could promote release of P_i from redox sensitive P bearing sediments. While we did not directly measure the $\delta^{18}O_P$ of redox sensitive NAIP, we consider this to be an unlikely explanation for the persistently heavy $\delta^{18}O_P$ near the lake bed. Jaisi et al. (2010) have shown that P_i adsorbed to mineral surfaces are constantly exchanged with P_i in the surrounding water such that fractionation associated with adsorption/desorption is negligible over a matter of hours. Since NAIP particles near the Grand River are small (4–7 μm; Chomicki et al., 2016) and likely to stay in suspension for several days (DePinto et al., 1981), we would expect P_i retained on NAIP particles that eventually settles within mussel beds to be equilibrated with $\delta^{18}O_P$ in the water column. If P_i is released via redox mediated dissolution, we infer that such P_i would retain $\delta^{18}O_P$ closer to that of lake water, and would be unlikely to explain the higher $\delta^{18}O_P$ values observed near the lake bed.

Entrainment of cooler water from the hypolimnion could theoretically account for near bed enrichment via (1) remineralization of sinking P by bacteria or (2) release of P_i from anoxic sediments. In the open ocean, $\delta^{18}O_P$ shifts toward the theoretical equilibrium with increasing depth as sinking organic matter is re-mineralized and microbes become carbon limited (Colman et al., 2005). Demand for P_i by phytoplankton and activity of hydrolytic enzymes should also be reduced in the cooler and darker hypolimnion compared to the illuminated surface layers (Pick, 1987). Cooler temperatures would favor an isotopically heavier $\delta^{18}O_{P\_EQ}$. Upwelling has been identified as a potentially significant transport mechanism for hypolimnetic SRP in some years (Valipour et al., 2016) which could affect our measures of $\delta^{18}O_P$. Wind speed and direction data from buoy #C45142, prior to and during our sampling trips did not indicate the presence of conditions favorable for upwelling (Supplemental Figure S2), nor did we observe any deviations in water temperature profiles during surveys associated with hypolimnetic intrusions (data not shown), thus we infer that upwelling cannot explain the heavier $\delta^{18}O_P$ observed near the lake bed. Similarly, Paytan et al. (2017) have linked release of isotopically heavier $\delta^{18}O_P$ in the central basinto sediment release during hypoxic events. However, hypolimnetic oxygen

concentrations in the much less productive eastern basin rarely fall below 0.3 mM during the stratified period (Carrick, 2004). Consequently, high rates of sediment P release from internal loading is unlikely to explain the $\delta^{18}O_P$ measured at our 10 m sites.

The lack of a similar degree of isotopic enrichment in the LB samples at 1 and 3 m sites is not easily explained. On one hand, the relationship between $\delta^{18}O_P$ and dreissenid biomass might suggest that dreissenid biomass at these shallow depths was insufficient to generate a strong isotope signal. Rapid uptake of released P_i by *Cladophora* might also attenuate an isotopic signal, however, *Cladophora* biomass in 2014 was relatively low, in large part because water clarity in 2014 was poor owing to high inputs of suspended solids from the Grand River (Valipour et al., 2016). It is also possible that the length of time required (~1 h) to collect sufficient sample volume (~200 L) whilst minimizing the disturbance near the lake bed may have compromised our samples to varying degrees if vertical mixing was sufficient to mix surface waters (containing lighter $\delta^{18}O_P$) with bottom waters (containing heavier $\delta^{18}O_P$). We evaluated this possibility by calculating the characteristic time scale for diffusive mixing of the water column following Boegman et al. (2008)

$$T_D^{mix} = \frac{N^2}{3}\left(\frac{H}{1.4u_*}\right)^3 \quad (4)$$

where N is the buoyant frequency (calculated as $\sqrt{-g/\rho_0\left(\frac{\partial\rho}{\partial z}\right)}$, H is the water column depth (m), and u_* is the surface shear velocity (calculated as $\sqrt{\frac{\tau_w}{\rho_0}}$; where τ_w can be estimated from $C_D\rho_A U_{10}^2 e^{-\beta z}$; with $C_{D=}$ 1.3 × 10^{-3}, ρ_0 = 1,000 kg m^{-3}, ρ_A = 1.2 kg m^{-3}, and U_{10} is the average daily wind speed (m s^{-1}) adjusted to a height of 10 m above surface recorded at buoy #C45142). Note since τ_w was evaluated at surface, the exponential term is neglected (Boegman et al., 2008). For many samples, it is clear that the time to completely mix the water column was shorter than our sample collection time (**Figure 10**)—thus we cannot exclude the possibility that our samples may have been compromised by mixing of lower $\delta^{18}O_P$ from surface waters. Furthermore, the degree of $\delta^{18}O_P$ offset from $\delta^{18}O_{P\_DM}$ appeared to be reduced as T_D^{mix} increased for samples collected in May and June when density gradients were greatest (**Figure 10**). Although the low sample size likely precludes statistical significance, these calculations are consistent with our hypothesis.

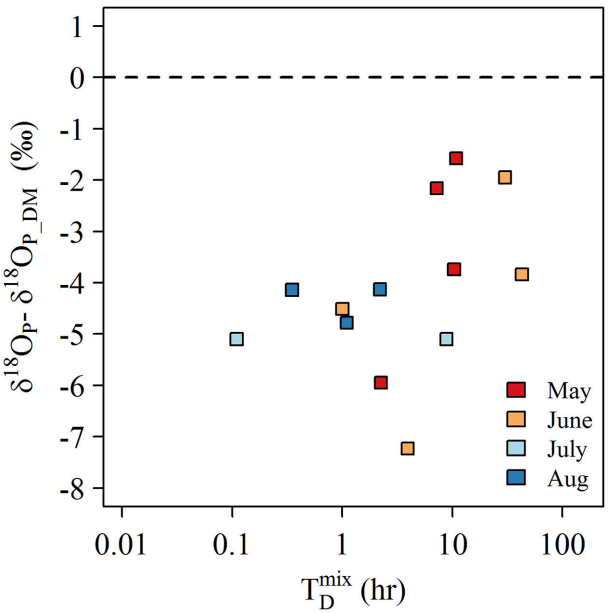

FIGURE 10 | Plot of the offset of $\delta^{18}O_P$ in LB samples from the average experimentally determined $\delta^{18}O_{P\_DM}$ (11.9 ± 1.1‰) against the estimated time to completely mix the water column (T_D^{mix}) for samples collected 0.1 m above bottom at stationsof 3 m depth.

CONCLUSIONS

One of our original objectives was to assess the utility of $\delta^{18}O_P$ to delineate the impact of riverine P_i in the nearshore and determine any potential association with *Cladophora* blooms. This proved to be challenging as the $\delta^{18}O_P$ of riverine P_i appeared to be rapidly altered by in-river and in-lake processes. Based on the nature and magnitude of deviations from $\delta^{18}O_{P\_EQ}$, $\delta^{18}O_P$, we infer that internal recycling of DOP by the plankton community is a dominant pathway determining the overall $\delta^{18}O_P$ of the available P_i pool in eastern Lake Erie. In addition, our data provide compelling evidence for the release of P_i at the lake bed, facilitated by dreissenid mussels. Management actions aimed at reducing the extent and severity of *Cladophora* blooms in Lake Erie will likely require consideration of linking the magnitude of external P inputs to the in-lake growth response in a more complex framework than prior to the advent of dreissenid populations. The ability of dreissenid mussels to function as a P trap in the nearshore as proposed by Hecky et al. (2004) poses distinct challenges. Dreissenid mussels in eastern Lake Erie are highly reliant on phytoplankton (Campbell et al., 2009), and the open waters represents a large reservoir of P that would have been previously unavailable to *Cladophora*. At the same time, local inputs of P_i from tributaries may be rapidly incorporated into phytoplankton, which while formerly unavailable to *Cladophora*, must now pass through the littoral zone which is dominated by expansive mussel populations and such P may ultimately be trapped and made available in the nearshore through the feeding activity of mussels. While it is clear that reductions in P inputs are the appropriate management tool, further work will be required to better quantify if reductions in *Cladophora* growth are achievable and whether these changes will require more stringent P controls than already proposed for Lake Erie.

AUTHOR CONTRIBUTIONS

DD and VH-B designed the study. DD carried out the study. GK conducted isotope analysis. DD wrote manuscript.

FUNDING

This study was funded by Environment Canada through the Great Lakes Nutrient Initiative.

ACKNOWLEDGMENTS

The authors thank the Technical Operations Services at Environment and Climate Change Canada for field and laboratory support. Greg Boulton, Karina Tsang, Danielle Bruyns, and Jacqui Milne provided tireless assistance in the field. Alice Dove provided nutrient data collected at York, ON, and data on dreissenid abundance and biomass Sandra Cooke (Grand River Conservation Authority) provided valuable input on the Grand River ecology. Comments and advice regarding purification protocols from Federica Tamburini, Adina Paytan, and Deb Jaisi are appreciated and were essential for improving sample processing.

SUPPLEMENTARY MATERIAL

The Supplementary Material for this article can be found online at: https://www.frontiersin.org/articles/10.3389/fmars.2018.00215/full#supplementary-material

REFERENCES

Ackerman, J. D., Loewen, M. R., and Hamblin, P. F. (2001). Benthic-Pelagic coupling over a zebra mussel reef in western Lake Erie. *Limnol. Oceanogr.* 46, 892–904. doi: 10.4319/lo.2001.46.4.0892

Angert, A., Weiner, T., Mazeh, S., and Sternberg, M. (2012). Soil phosphate stable oxygen isotopes across rainfall and bedrock gradients. *Environ. Sci. Technol.* 46, 2156–2162. doi: 10.1021/es203551s

Arnott, D. L., and Vanni, M. J. (1996). Nitrogen and phosphorus recycling by the zebra mussel (*Dreissena polymorpha*) in the western basin of Lake Erie. *Can. J. Fish. Aquat. Sci.* 53, 646–659. doi: 10.1139/f95-214

Auer, M. T., Tomlinson, L. M., Higgins, S. N., Malkin, S. Y., Howell, E. T., and Bootsma, H. A. (2010). Great lakes *Cladophora* in the 21st century: same algae—different ecosystem. *J. Gt. Lakes Res.* 36, 248–255. doi: 10.1016/j.jglr.2010.03.001

Baldwin, D. S. (2013). Organic phosphorus in the aquatic environment. *Environ. Chem.* 10, 439–454. doi: 10.1071/EN13151

Barlow-Busch, L., Baulch, H. M., and Taylor, W. D. (2006). Phosphate uptake by seston and epilithon in the Grand River, southern Ontario. *Aquat. Sci.* 68, 181–192. doi: 10.1007/s00027-006-0806-9

Bentzen, E., Taylor, W. D., and Millard, E. S. (1992). The importance of dissolved organic phosphorus to phosphorus uptake by limnetic plankton. *Limnol. Oceanogr.* 37, 217–231. doi: 10.4319/lo.1992.37.2.0217

Blake, R. E. (2005). Biogeochemical cycling of phosphorus: insights from oxygen isotope effects of phosphoenzymes. *Am. J. Sci.* 305, 596–620. doi: 10.2475/ajs.305.6-8.596

Blake, R. E., O'neil, J. R., and Garcia, G. A. (1997). Oxygen isotope systematics of biologically mediated reactions of phosphate: I. Microbial degradation of organophosphorus compounds. *Geochim. Cosmochim. Acta* 61, 4411–4422. doi: 10.1016/S0016-7037(97)00272-X

Boegman, L., Loewen, M. R., Hamblin, P. F., and Culver, D. A. (2008). Vertical mixing and weak stratification over zebra mussel colonies in western Lake Erie. *Limnol. Oceanogr.* 53, 1093–1110. doi: 10.4319/lo.2008.53.3.1093

Bootsma, H. A., Rowe, M. D., Brooks, C. N., and Vanderploeg, H. A. (2015). Commentary: the need for model development related to *Cladophora* and nutrient management in Lake Michigan. *J. Gt. Lakes Res.* 41, 7–15. doi: 10.1016/j.jglr.2015.03.023

Campbell, L. M., Thacker, R., Barton, D., Muir, D. C. G., Greenwood, D., and Hecky, R. E. (2009). Re-engineering the eastern Lake Erie littoral food web: the trophic function of non-indigenous Ponto-Caspian species. *J. Gt. Lakes Res.* 35, 224–231. doi: 10.1016/j.jglr.2009.02.002

Carrick, H. J. (2004). Algal distribution patterns in Lake Erie: implications for oxygen balances in the Eastern Basin. *J. Gt. Lakes Res.* 30, 133–147. doi: 10.1016/S0380-1330(04)70336-6

Chang, S. J., and Blake, R. E. (2015). Precise calibration of equilibrium oxygen isotope fractionations between dissolved phosphate and water from 3 to 37°C. *Geochim. Cosmochim. Acta* 150, 314–329. doi: 10.1016/j.gca.2014.10.030

Cheng, C., and Lim, B. L. (2006). Beta-propeller phytases in the aquatic environment. *Arch. Microbiol.* 185, 1–13. doi: 10.1007/s00203-005-0080-6

Chomicki, K. M., Howell, E. T., Defield, E., Dumas, A., and Taylor, W. D. (2016). Factors influencing the phosphorus distribution near the mouth of the Grand River, Ontario, Lake Erie. *J. Gt. Lakes Res.* 42, 549–564. doi: 10.1016/j.jglr.2016.03.014

Colman, A. S., Blake, R. E., Karl, D. M., Fogel, M. L., and Turekian, K. K. (2005). Marine phosphate oxygen isotopes and organic matter remineralization in the oceans. *Proc. Natl. Acad. Sci. U.S.A.* 102, 13023–13028. doi: 10.1073/pnas.0506455102

Conroy, J. D., Edwards, W. J., Pontius, R. A., Kane, D. D., Zhang, H., Shea, J. F., et al. (2005). Soluble nitrogen and phosphorus excretion of exotic freshwater mussels (Dreissena spp.): potential impacts for nutrient remineralisation in western Lake Erie. *Freshw. Biol.* 50, 1146–1162. doi: 10.1111/j.1365-2427.2005.01392.x

DePinto, J. V., Young, T. C., and Martin, S. C. (1981). Algal-available phosphorus in suspended sediments from lower great lakes tributaries. *J. Gt. Lakes Res.* 7, 311–325. doi: 10.1016/S0380-1330(81)72059-8

Dolan, D. M., and Chapra, S. C. (2012). Great Lakes total phosphorus revisited: 1. Loading analysis and update (1994–2008). *J. Gt. Lakes Res.* 38, 730–740. doi: 10.1016/j.jglr.2012.10.001

Dove, A., and Chapra, S. C. (2015). Long-term trends of nutrients and trophic response variables for the great lakes: great lakes nutrient trends. *Limnol. Oceanogr.* 60, 696–721. doi: 10.1002/lno.10055

Dove, A., L'Italien, S., and Gilroy, D. (2009). *Great Lakes Surveillance Program Field Methods Manual*. Burlington, ON: Environment Canada.

Elsbury, K. E., Paytan, A., Ostrom, N. E., Kendall, C., Young, M. B., McLaughlin, K., et al. (2009). Using oxygen isotopes of phosphate to trace phosphorus sources and cycling in Lake Erie. *Environ. Sci. Technol.* 43, 3108–3114. doi: 10.1021/es8034126

Gilbert, J. M., and Ryan, P. A. (2007). *Southern Grand River Wetland Report*. Port Dover, ON: Lake Erie Management Unit, Ontario Ministry of Natural Resources.

GLWQA (2012). *The 2012 Great Lakes Water Quality Agreement - Annex 4*. Available online at: https:tinyurl.com/gt92hrh

GLWQA (2015). *Recommended Phosphorus Loading Targets for Lake Erie - Annex 4 Objectives and Targets Task Team Final Report to the Nutrients Annex Subcommittee*.

Goldhammer, T., Brunner, B., Bernasconi, S. M., Ferdelman, T. G., and Zabel, M. (2011). Phosphate oxygen isotopes: insights into sedimentary phosphorus cycling from the Benguela upwelling system. *Geochim. Cosmochim. Acta* 75, 3741–3756. doi: 10.1016/j.gca.2011.04.006

Granger, S. J., Harris, P., Peukert, S., Guo, R., Tamburini, F., Blackwell, M. S., et al. (2017a). Phosphate stable oxygen isotope variability within a temperate agricultural soil. *Geoderma* 285, 64–75. doi: 10.1016/j.geoderma.2016.09.020

Granger, S. J., Heaton, T. H. E., Pfahler, V., Blackwell, M. S. A., Yuan, H., and Collins, A. L. (2017b). The oxygen isotopic composition of phosphate in river water and its potential sources in the Upper River Taw catchment, UK. *Sci. Tot. Environ.* 574, 680–690. doi: 10.1016/j.scitotenv.2016.09.007

Griffiths, R. W., Schloesser, D. W., Leach, J. H., and Kovalak, W. P. (1991). Distribution and dispersal of the zebra mussel (*Dreissena polymorpha*)

in the Great Lakes Region. *Can. J. Fish. Aquat. Sci.* 48, 1381–1388. doi: 10.1139/f91-165

Haltuch, M. A., Berkman, P. A., and Garton, D. W. (2000). Geographic information system (GIS) analysis of ecosystem invasion: exotic mussels in Lake Erie. *Limnol. Oceanogr.* 45, 1778–1787. doi: 10.4319/lo.2000.45.8.1778

He, C., Rao, Y. R., Skafel, M. G., and Howell, T. (2006). Numerical modelling of the Grand River plume in Lake Erie during unstratified period. *Water Qual. Res. J. Can.* 41, 16–23. doi: 10.2166/wqrj.2006.002

Hecky, R. E., Smith, R. E., Barton, D. R., Guildford, S. J., Taylor, W. D., Charlton, M. N., et al. (2004). The nearshore phosphorus shunt: a consequence of ecosystem engineering by dreissenids in the Laurentian Great Lakes. *Can. J. Fish. Aquat. Sci.* 61, 1285–1293. doi: 10.1139/f04-065

Higgins, S. N., Howell, E. T., Hecky, R. E., Guildford, S. J., and Smith, R. E. (2005). The wall of green: the status of *Cladophora* glomerata on the Northern shores of Lake Erie's Eastern Basin, 1995–2002. *J. Gt. Lakes Res.* 31, 547–563. doi: 10.1016/S0380-1330(05)70283-5

Higgins, S. N., Malkin, S. Y., Todd Howell, E., Guildford, S. J., Campbell, L., Hiriart-Baer, V., et al. (2008). An ecological review of *Cladophora glomerata* (CHLOROPHYTA) in the Laurentian Great Lakes [1]. *J. Phycol.* 44, 839–854. doi: 10.1111/j.1529-8817.2008.00538.x

Holeton, C. (2013). *Sources of Nutrients and Sediments in the Grand River Watershed*. Cambridge, ON: Grand River Conservation Authority.

Howell, E. T., and Hobson, G. (2003). *Water Quality on the Lake Erie Shores of Wainfleet Township in 2002*. Toronto, ON: Environmental Monitoring and Reporting Branch, Ontario Ministry of Environment.

Howell, E. T., Marvin, C. H., Bilyea, R. W., Kauss, P. B., and Somers, K. (1996). Changes in environmental conditions during Dreissena colonization of a monitoring station in Eastern Lake Erie. *J. Gt. Lakes Res.* 22, 744–756. doi: 10.1016/S0380-1330(96)70993-0

Jaisi, D. P., Blake, R. E., and Kukkadapu, R. K. (2010). Fractionation of oxygen isotopes in phosphate during its interactions with iron oxides. *Geochim. Cosmochim. Acta* 74, 1309–1319. doi: 10.1016/j.gca.2009.11.010

Jaisi, D. P., Kukkadapu, R. K., Stout, L. M., Varga, T., and Blake, R. E. (2011). Biotic and abiotic pathways of phosphorus cycling in minerals and sediments: insights from oxygen isotope ratios in phosphate. *Environ. Sci. Technol.* 45, 6254–6261. doi: 10.1021/es200456e

Joshi, S. R., Kukkadapu, R. K., Burdige, D. J., Bowden, M. E., Sparks, D. L., and Jaisi, D. P. (2015). Organic matter remineralization predominates phosphorus cycling in the mid-bay sediments in the Chesapeake Bay. *Environ. Sci. Technol.* 49, 5887–5896. doi: 10.1021/es5059617

Karl, D. M., and Tien, G. (1992). MAGIC: a sensitive and precise method for measuring dissolved phosphorus in aquatic environments. *Limnol. Oceanogr.* 37, 105–116. doi: 10.4319/lo.1992.37.1.0105

Kolodny, Y., Luz, B., and Navon, O. (1983). Oxygen isotope variations in phosphate of biogenic apatites, I. Fish bone apatite—rechecking the rules of the game. *Earth Planet. Sci. Lett.* 64, 398–404. doi: 10.1016/0012-821X(83)90100-0

Kuntz, T. (2008). *System and Plankton Metabolism in the Lower Grand River*, Waterloo, ON: Ontario.

Larson, J. H., Frost, P. C., Vallazza, J. M., Nelson, J. C., and Richardson, W. B. (2016). Do rivermouths alter nutrient and seston delivery to the nearshore? *Freshw. Biol.* 61, 1935–1949. doi: 10.1111/fwb.12827

Lean, D. R. S., Abbott, A. P., Charlton, M. N., and Rao, S. S. (1983). Seasonal phosphate demand for Lake Erie Plankton. *J. Gt. Lakes Res.* 9, 83–91. doi: 10.1016/S0380-1330(83)71875-7

Li, H., Joshi, S. R., and Jaisi, D. P. (2016a). Degradation and isotope source tracking of glyphosate and aminomethylphosphonic acid. *J. Agric. Food Chem.* 64, 529–538. doi: 10.1021/acs.jafc.5b04838

Li, H., Yu, C., Wang, F., Chang, S. J., Yao, J., and Blake, R. E. (2016b). Probing the metabolic water contribution to intracellular water using oxygen isotope ratios of PO_4. *Proc. Natl. Acad. Sci.U.S.A.* 113, 5862–5867. doi: 10.1073/pnas.1521038113

Li, J., Bai, Y., Bear, K., Joshi, S., and Jaisi, D. (2017). Phosphorus availability and turnover in the Chesapeake Bay: insights from nutrient stoichiometry and phosphate oxygen isotope ratios. *J. Geophys. Res. Biogeosci.* 122, 811–824. doi: 10.1002/2016JG003589

Liang, Y., and Blake, R. E. (2006). Oxygen isotope signature of Pi regeneration from organic compounds by phosphomonoesterases and photooxidation. *Geochim. Cosmochim. Acta* 70, 3957–3969. doi: 10.1016/j.gca.2006.04.036

Liang, Y., and Blake, R. E. (2009). Compound- and enzyme-specific phosphodiester hydrolysis mechanisms revealed by $\delta^{18}O$ of dissolved inorganic phosphate: implications for marine P cycling. *Geochim. Cosmochim. Acta* 73, 3782–3794. doi: 10.1016/j.gca.2009.01.038

Lin, P., and Guo, L. (2016). Dynamic changes in the abundance and chemical speciation of dissolved and particulate phosphorus across the river-lake interface in southwest Lake Michigan. *Limnol. Oceanogr.* 61, 771–789. doi: 10.1002/lno.10254

Longinelli, A., and Nuti, S. (1973). Revised phosphate-water isotopic temperature scale. *Earth Planet. Sci. Lett.* 19, 373–376. doi: 10.1016/0012-821X(73)90088-5

Maccoux, M. J., Dove, A., Backus, S. M., and Dolan, D. M. (2016). Total and soluble reactive phosphorus loadings to Lake Erie. *J. Gt. Lakes Res.* 42, 1151–1165. doi: 10.1016/j.jglr.2016.08.005

Mayer, T., and Manning, P. G. (1989). Variability of phosphorus forms in suspended solids at the Lake Erie-Grand River Confluence. *J. Gt. Lakes Res.* 15, 687–699. doi: 10.1016/S0380-1330(89)71521-5

McLaughlin, K., Cade-Menun, B. J., and Paytan, A. (2006a). The oxygen isotopic composition of phosphate in Elkhorn Slough, California: a tracer for phosphate sources. *Estuar. Coast. Shelf Sci.* 70, 499–506. doi: 10.1016/j.ecss.2006.06.030

McLaughlin, K., Kendall, C., Silva, S. R., Young, M., and Paytan, A. (2006b). Phosphate oxygen isotope ratios as a tracer for sources and cycling of phosphate in North San Francisco Bay, California. *J. Geophys. Res.* 111. doi: 10.1029/2005JG000079

McLaughlin, K., Silva, S., Kendall, C., Stuart-Williams, H., and Paytan, A. (2004). A precise method for the analysis of $\delta^{18}O$ of dissolved inorganic phosphate in seawater: method for oxygen isotopic analysis of DIP. *Limnol. Oceanogr. Methods* 2, 202–212. doi: 10.4319/lom.2004.2.202

McLaughlin, K., Sohm, J. A., Cutter, G. A., Lomas, M. W., and Paytan, A. (2013). Phosphorus cycling in the Sargasso Sea: investigation using the oxygen isotopic composition of phosphate, enzyme-labeled fluorescence, and turnover times: sargasso sea phosphorus cycling. *Glob. Biogeochem. Cycles* 27, 375–387. doi: 10.1002/gbc.20037

Michalak, A. M., Anderson, E. J., Beletsky, D., Boland, S., Bosch, N. S., Bridgeman, T. B., et al. (2013). Record-setting algal bloom in Lake Erie caused by agricultural and meteorological trends consistent with expected future conditions. *Proc. Natl. Acad. Sci. U.S.A.* 110, 6448–6452. doi: 10.1073/pnas.1216006110

Monbet, P., McKelvie, I. D., and Worsfold, P. J. (2009). Dissolved organic phosphorus speciation in the waters of the Tamar estuary (SW England). *Geochim. Cosmochim. Acta* 73, 1027–1038. doi: 10.1016/j.gca.2008.11.024

Morrison, A. (2014). *Assessing the Use of 18O-PO4 Analysis for Tracing Source Inputs and the Cycling of Phosphorus.* Application to the Grand River.

Mosley, C., and Bootsma, H. (2015). Phosphorus recycling by profunda quagga mussels (Dreissena rostriformis bugensis) in Lake Michigan. *J. Gt. Lakes Res.* 41, 38–48. doi: 10.1016/j.jglr.2015.07.007

Nalepa, T. F., Gardner, W. S., and Malczyk, J. M. (1991). Phosphorus cycling by mussels (Unionidae: Bivalvia) in Lake St. *Clair. Hydrobiologia* 219, 239–250. doi: 10.1007/BF00024758

Nicholls, K. H., Taylor, R., and Hamdy, Y. S. (1983). The influence of the Grand River on phytoplankton near the northeastern shore of Lake Erie during 1979. *Arch. Hydrobiol.* 98, 146–172.

North, R. L., Smith, R. E. H., Hecky, R. E., Depew, D. C., León, L. F., Charlton, M. N., et al. (2012). Distribution of seston and nutrient concentrations in the eastern basin of Lake Erie pre- and post-dreissenid mussel invasion. *J. Gt. Lakes Res.* 38, 463–476. doi: 10.1016/j.jglr.2012.06.012

Ozersky, T., Malkin, S. Y., Barton, D. R., and Hecky, R. E. (2009). Dreissenid phosphorus excretion can sustain C. glomerata growth along a portion of Lake Ontario shoreline. *J. Gt. Lakes Res.* 35, 321–328. doi: 10.1016/j.jglr.2009.05.001

Paalme, T., Kukk, H., Kotta, J., and Orav, H. (2002). "'*In vitro*' and '*in situ*' decomposition of nuisance macroalgae *Cladophora glomerata* and *Pilayella littoralis*," in *Nutrients and Eutrophication in Estuaries and Coastal Waters Developments in Hydrobiology*, eds E. Orive, M. Elliott, and V. N. de Jonge (Dordrecht: Springer), 469–476.

Painter, D. S., and McCabe, K. J. (1987). *The Influence of the Grand River on Eastern Lake Erie Cladophora*. Burlington, ON: National Water Research Institute.

Patterson, M. W. R., Ciborowski, J. J. H., and Barton, D. R. (2005). The distribution and abundance of Dreissena species (Dreissenidae) in Lake

Erie, 2002. *J. Gt. Lakes Res.* 31, 223–237. doi: 10.1016/S0380-1330(05)70316-6

Paytan, A., Kolodny, Y., Neori, A., and Luz, B. (2002). Rapid biologically mediated oxygen isotope exchange between water and phosphate: oxygen isotopes in phosphate. *Glob. Biogeochem. Cycles* 16, 13.1–13.8. doi: 10.1029/2001GB001430

Paytan, A., and McLaughlin, K. (2012). "Tracing the sources and biogeochemical cycling of phosphorus in aquatic systems using isotopes of oxygen in phosphate," in *Handbook of Environmental Isotope Geochemistry*, ed M. Baskaran (Berlin; Heidelberg: Springer Berlin Heidelberg), 419–436.

Paytan, A., Roberts, K., Watson, S., Peek, S., Chuang, P. C., Defforey, D., et al. (2017). Internal loading of phosphate in Lake Erie Central Basin. *Sci. Tot. Environ.* 579, 1356–1365. doi: 10.1016/j.scitotenv.2016.11.133

Pick, F. R. (1987). Interpretations of alkaline phosphatase activity in Lake Ontario. *Can. J. Fish. Aquat. Sci.* 44, 2087–2094. doi: 10.1139/f87-258

Pistocchi, C., Tamburini, F., Gruau, G., Ferhi, A., Trevisan, D., and Dorioz, J. M. (2017). Tracing the sources and cycling of phosphorus in river sediments using oxygen isotopes: methodological adaptations and first results from a case study in France. *Water Res.* 111, 346–356. doi: 10.1016/j.watres.2016.12.038

Rao, Y. R., and Schwab, D. J. (2007). Transport and mixing between the coastal and offshore waters in the great lakes: a review. *J. Gt. Lakes Res.* 33, 202–218. doi: 10.3394/0380-1330(2007)33[202:TAMBTC]2.0.CO;2

Robinson, C. (2015). Review on groundwater as a source of nutrients to the great lakes and their tributaries. *J. Great Lakes Res.* 41, 941–950.doi: 10.1016/.j.jglr.205.08.001

Roditi, H. A., Strayer, D. L., and Findlay, S. E. G. (1997). Characteristics of zebra mussel (*Dreissena polymorpha*) biodeposits in a tidal freshwater estuary. *Arch. Hydrobiol.* 140, 207–219. doi: 10.1127/archiv-hydrobiol/140/1997/207

Roe, S. L., and MacIsaac, H. J. (1997). Deepwater population structure and reproductive state of quagga mussels (*Dreissena bugensis*) in Lake Erie. *Can. J. Fish. Aquat. Sci.* 54, 2428–2433. doi: 10.1139/f97-151

Rosamond, M. (2013). *Nitrous Oxide and Nitrate in the Grand River, Ontario: Sources, Production Pathways and Predictability*. Waterloo, ON.

Rukavina, N. A., and St. Jacques, D. A. (1971). "Lake Erie nearshore sediments Fort Erie to Mohawk Pt, Ontario," in *Proc. 14th Conf Great Lakes Res.* (International Association for Great Lakes Research), 387–393.

Sauey, B. W., Amberg, J. J., Cooper, S. T., Grunwald, S. K., Haro, R. J., and Gaikowski, M. P. (2016). Digestive physiology comparisons of aquatic invertebrates in the Upper Mississippi River Basin. *J. Freshw. Ecol.* 31, 303–314. doi: 10.1080/02705060.2015.1132485

Shear, H., and Konasewich, D. (1975). *Cladophora in the Great Lakes*. Windsor, ON: International Joint Commission.

Struger, J., van Stempvoort, D. R., and Brown, S. J. (2015). Sources of aminomethylphosphonic acid (AMPA) in urban and rural catchments in Ontario, Canada: glyphosate or phosphonates in wastewater? *Environ. Pollut.* 204, 289–297. doi: 10.1016/j.envpol.2015.03.038

Tamburini, F., Bernasconi, S. M., Angert, A., Weiner, T., and Frossard, E. (2010). A method for the analysis of the $\delta^{18}O$ of inorganic phosphate extracted from soils with HCl. *Eur. J. Soil Sci.* 61, 1025–1032. doi: 10.1111/j.1365-2389.2010.01290.x

Tamburini, F., Pfahler, V., Bünemann, E. K., Guelland, K., Bernasconi, S. M., and Frossard, E. (2012). Oxygen isotopes unravel the role of microorganisms in phosphate cycling in soils. *Environ. Sci. Technol.* 46, 5956–5962. doi: 10.1021/es300311h

Taylor, W. D., and Lean, D. R. S. (1981). Radiotracer experiments on phosphorus uptake and release by limnetic microzooplankton. *Can. J. Fish. Aquat. Sci.* 38, 1316–1321. doi: 10.1139/f81-177

Thomson-Bulldis, A., and Karl, D. (1998). Application of a novel method for phosphorus determinations in the oligotrophic North Pacific Ocean. *Limnol. Oceanogr.* 43, 1565–1577. doi: 10.4319/lo.1998.43.7.1565

Turner, C. B. (2010). Influence of zebra (*Dreissena polymorpha*) and quagga (*Dreissena rostriformis*) mussel invasions on benthic nutrient and oxygen dynamics. *Can. J. Fish. Aquat. Sci.* 67, 1899–1908. doi: 10.1139/F10-107

Valipour, R., León, L. F., Depew, D., Dove, A., and Rao, Y. R. (2016). High-resolution modeling for development of nearshore ecosystem objectives in eastern Lake Erie. *J. Gt. Lakes Res.* 42, 1241–1251. doi: 10.1016/j.jglr.2016.08.011

Von Sperber, C., Kries, H., Tamburini F., Bernasconi, S.M., and Frossard, E. (2014). The effect of phosphomonoesterases on the oxygen isotope composition of phosphate. *Geochim. Cosmochim. Acta* 125, 519–527. doi: 10.1016/j.gca.2013.10.010

Von Sperber, C., Tamburini, F., Brunner, B., Bernasconi, S.M., Frossard, E. (2015). The oxygen isotope composition of phosphate released from phytic acid by the activity of wheat and Aspergillus niger phytase. *BioGeosciences,* 12, 4175–4184. doi: 10.5194/bg-12-4175-2015

Young, M. B., McLaughlin, K., Kendall, C., Stringfellow, W., Rollog, M., Elsbury, K., et al. (2009). Characterizing the oxygen isotopic composition of phosphate sources to aquatic ecosystems. *Environ. Sci. Technol.* 43, 5190–5196. doi: 10.1021/es900337q

Yuan, Y., Bi, Y., and Hu, Z. (2017). Phytoplankton communities determine the spatio-temporal heterogeneity of alkaline phosphatase activity: evidence from a tributary of the Three Gorges Reservoir. *Sci. Rep.* 7:16404. doi: 10.1038/s41598-017-16740-4

Zohar, I., Shaviv, A., Young, M., Kendall, C., Silva, S., and Paytan, A. (2010). Phosphorus dynamics in soils irrigated with reclaimed waste water or fresh water — A study using oxygen isotopic composition of phosphate. *Geoderma* 159, 109–121. doi: 10.1016/j.geoderma.2010.07.002

Conflict of Interest Statement: The authors declare that the research was conducted in the absence of any commercial or financial relationships that could be construed as a potential conflict of interest.

frontiers in Marine Science

ORIGINAL RESEARCH
published: 19 June 2018
doi: 10.3389/fmars.2018.00212

Colorimetric Chemical Differentiation and Detection of Phosphorus in Eutrophic and High Particulate Waters: Advantages of a New Monitoring Approach

Lisa Felgentreu[1], Günther Nausch[1], Franziska Bitschofsky[2], Monika Nausch[2] and Detlef Schulz-Bull[1]*

[1] Department of Marine Chemistry, Leibniz-Institute of Baltic Sea Research, Warnemünde, Germany, [2] Department of Marine Biology, Leibniz-Institute of Baltic Sea Research, Warnemünde, Germany

OPEN ACCESS

Edited by:
Barbara Cade-Menun, Agriculture and Agri-Food Canada (AAFC), Canada

Reviewed by:
Raghab Ray, University of Tokyo, Japan
Sheree J. Watson, University of Hawaii at Manoa, United States

***Correspondence:**
Lisa Felgentreu
lisa.felgentreu@io-warnemuende.de

Specialty section:
This article was submitted to Coastal Ocean Processes, a section of the journal Frontiers in Marine Science

Received: *29 January 2018*
Accepted: *29 May 2018*
Published: *19 June 2018*

Citation:
Felgentreu L, Nausch G, Bitschofsky F, Nausch M and Schulz-Bull D (2018) Colorimetric Chemical Differentiation and Detection of Phosphorus in Eutrophic and High Particulate Waters: Advantages of a New Monitoring Approach. Front. Mar. Sci. 5:212. doi: 10.3389/fmars.2018.00212

Phosphorus (P) is a key factor forcing eutrophication in limnic and marine systems, and all monitoring programs for water quality accordingly include P determinations. However, traditional monitoring does not allow an analysis of the different components involved in the P cycle taking place in the water column. Nonetheless, the implementation of measures addressing eutrophication requires a full understanding of the processes involved in the transformation and transport of P, in all its chemical forms. In this study, the P categories present in a river and its estuary in northern Germany, which discharge into the Baltic Sea, were characterized. Using the molybdenum blue method we found that the classification of P into the traditional fractions (DIP, DOP, POP) applied in the ocean cannot be applied to turbid waters such as rivers because interferences between the fractions seems to occur. Therefore a new nomenclature has been introduced. In addition to total phosphorus (TP) and dissolved molybdate-reactive phosphorus (DRP; previously referred to as inorganic phosphorus), dissolved non-molybdate-reactive phosphorus (DNP), particulate molybdatereactive phosphorus (PRP), and particulate non-molybdate-reactive phosphorus (PNP) were distinguished. The high spatial and temporal variations in the proportions of these forms with respect to the TP concentration well-demonstrate the complexity of the P cycle and the involved P fractions and emphasize the need for expanded monitoring approach. The potential of eutrophication could be underestimated if not all P categories were considered. With the new operational nomenclature the common and standardized molybdenum blue reaction could be used to implement the analysis of various P components into regular monitoring programs.

Keywords: phosphorus categories, differentiation, detection, monitoring program, contribution to eutrophication, Baltic Sea

INTRODUCTION

To address eutrophication in European waters and adopt measures aimed at restoring their good ecological status, the European Water Framework Directive and the European Marine Strategy Framework Directive were established. However, phosphorus (P) is a critical element forcing eutrophication in aquatic systems throughout the world, especially in surface waters (OECD, 1982; Hecky and Kilham, 1988). Moreover, eutrophication is reinforced by the presence of internal P cycles, for example, the P released from the sediment under anoxic conditions.

Both the cycling of P and the intense P transformations in the environment have been characterized and include biotic (uptake and release by organisms) and abiotic (adsorption onto and desorption from particles, precipitation and dissolution, advection and diffusion) processes in which both dissolved and particulate P forms are generated. In the literature, these functionally distinct forms of organic and inorganic P that make up the P cycle have been variably named (Jarvie et al., 2002; Withers and Jarvie, 2008; Worsfold et al., 2016). Traditional terms for the same P component include orthophosphate (ortho-P), dissolved inorganic P (DIP), or simply phosphate (PO_4^{3-}), but also soluble reactive P (SRP/srP), dissolved reactive P (DRP), filterable reactive P (FRP), and molybdate-reactive P (MRP) are used. While at times confusing, the use of operational (e.g., FRP, used in analytical determinations) and functional (e.g., DIP, as applied to analyses of an ecosystem or microbial forms) terminologies can also be possible. The functional differentiation of organic and inorganic P requires a big effort which takes much time. It is hardly realizable to measure organic P in its entirety rather its single compounds like DNA and RNA or ATP which have a minor part in the DOP (Unger et al., 2013). Furthermore, when using the molybdenum blue method, labile P components other than DIP, e.g., labile organic P or colloidal bound P, may also be bound to the molybdenum blue complex (Rigler, 1968; Stainton, 1980; Haygarth and Sharpley, 2000; Jarvie et al., 2002).

Our studies within the PhosWaM project (phosphorus from the source to the sea) have focused on the Warnow catchment area (**Figure 1**), specifically: (1) P fractions in the Warnow river and its estuary, as a transition zone between an agrarian catchment area and the Baltic Sea, and (2) P fluxes, especially with respect to the transport and exchange of P with coastal waters. Rivers play a key role in transporting and processing P from source to sea (Withers and Jarvie, 2008), especially when diffuse sources are the main factor for eutrophication after the elimination of point sources. During the second half of the twentieth century, environmental inputs of P have increased worldwide (Gustafsson et al., 2012). Despite numerous efforts to reduce nutrient inputs (Backer et al., 2010) into the coastal waters of the southern Baltic Sea, inputs of P have led to a shift in the trophic status and the degree of eutrophication remains high (Nausch et al., 2011). Effective measures are therefore needed to control P inputs reaching rivers and estuaries characterized by high organic loads. Although a large number of monitoring programs targeting the nutrient status of these waters are in place, they typically measure only two forms of P, total P (TP) and DIP (Baldwin, 1998; Jarvie et al., 2002; Jescovitch et al., 2017; Stammler et al., 2017). However, because all P fractions can contribute to eutrophication and all of them can be successfully targeted for reduction, the proportions of each one must be considered. For example, among the various forms of P, dissolved organic P is counted to be the most relevant P source for the growth of algae and bacteria during the productive season (Nausch and Nausch, 2006) and is therefore a major contributor to eutrophication.

Reducing the P that contributes to eutrophication requires a revised approach to P monitoring and is one of the primary aims of the PhosWaM project. In this study we demonstrate the importance of measuring the various components of P and their implementation into regular monitoring measures. Therefore, we introduce a nomenclature for the different operational P forms, one that is tailored to those in the turbid riverine and estuarine waters of the investigated area (lowland agricultural dominated catchment) and applicable to similar areas. Additionally, the nomenclature is more accurate according to the widely common and standardized molybdenum blue colorimetric method.

MATERIALS AND METHODS

Phosphorus (P) categories were analyzed in surface water samples taken monthly since August 2016 along the river Warnow and its estuary to the Baltic Sea (**Figure 1**). The Warnow river, in which the sampling station "Bützow" is located, has a low current velocity. The Warnow estuary, where the station "Hundsburg" is located, is a typical partially mixed estuary. The sampling station "Baltic Sea" is located at the mouth of the river in the coastal zone of the Baltic Sea.

Our newly established nomenclature differentiates P categories based on their dissolved and particulate forms. The detection of dissolved P is standardized using the molybdenum blue colorimetric method (Murphy and Riley, 1962), which should quantify the amount of DIP, also referred to as ortho-P or SRP. However, when used in a water sample, the molybdenum blue can also bind labile P components as described above (Rigler, 1968; Stainton, 1980; Haygarth and Sharpley, 2000; Jarvie et al., 2002). Using the molybdenum blue method in unfiltered and filtered estuarine and river water samples resulted in remarkable different P values, indicating the presence of a labile particulate P forms, the particulate molybdate-reactive P fraction (PRP). It thus became evident that the traditionally measured and named fractions were not suitable for use in the lowland catchment area investigated in this study. Hence,

Abbreviations: DHP, dissolved hydrolysable phosphorus; DIP, dissolved inorganic phosphorus; DNP, dissolved non-molybdate-reactive phosphorus; DP, (total) dissolved phosphorus; DRP, dissolved reactive phosphorus, dissolved molybdate-reactive phosphorus (new); DUP, dissolved unreactive phosphorus; FOP, filterable organic phosphorus; FRP, filterable reactive phosphorus; MRP, molybdate reactive phosphorus; ortho-P, orthophosphate; P, phosphorus; PNP, particulate non-molybdate-reactive phosphorus; PO_4^{3-}, phosphate; PP, particulate phosphorus; PRP, particulate molybdate-reactive phosphorus; SRP/srP, soluble reactive phosphorus; SUP, soluble unreactive phosphorus; TDP, total dissolved phosphorus; TFP, total filterable phosphorus; TP, total phosphorus; TPP, total particulate phosphorus; TRP, total molybdate-reactive phosphorus.

we developed a detection scheme (**Figure 2**) and renamed the traditional terms of P categories (**Table 1**).

Analysis of Molybdate-Reactive Phosphorus Categories

For these components the water sample should be analyzed as soon as possible after sampling (Jarvie et al., 2002). Dissolved P and particulate P are separated by filtration (maximum 250 ml) over precombusted (4 h at 450°C) filters (GF/F-filter, retention range 0.7 µm) using a vacuum pressure constantly adjusted to 850 hPa. The P concentrations are measured in duplicates using the molybdenum blue colorimetric method (Murphy and Riley, 1962) in which a blue phosphomolybdate complex is formed. The reaction requires a reductant, typically acidified ascorbic acid solution, and a mixed reagent consisting of ammonium heptamolybdate tetrahydrate-solution, potassium antimony tartrate-solution, and 50% sulfuric acid. The procedure generally follows that of Koroleff (1983) but with the following modifications. After the addition of 1 ml of the mixed reagent to a 50 ml water sample, the absorbance at a wavelength of 885 nm is immediately measured to obtain a turbidity blank. This is followed by the addition of 0.5 ml of the reductant to the sample-reagent mixture. Over a period of 20–60 min (depending on the ambient temperature) the P in the sample reacts with the molybdate to form a bluish complex. The absorbance of this sample is then measured again at 885 nm and the P concentration calculated according to Koroleff (1983).

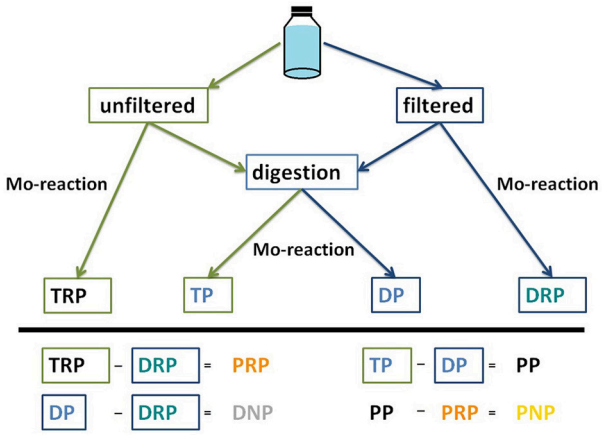

FIGURE 2 | Scheme used in the detection of the various phosphorus (P) fractions. Mo-reaction, reaction of phosphate with molybdate whereby a blue phosphomolybdate complex is generated; TP, total P; DP, total dissolved P; PP, total particulate P; TRP, total molybdate-reactive P; DRP, dissolved molybdate-reactive P; PRP, particulate molybdate-reactive P; DNP, dissolved non-molybdate-reactive P; PNP, particulate non-molybdate-reactive P.

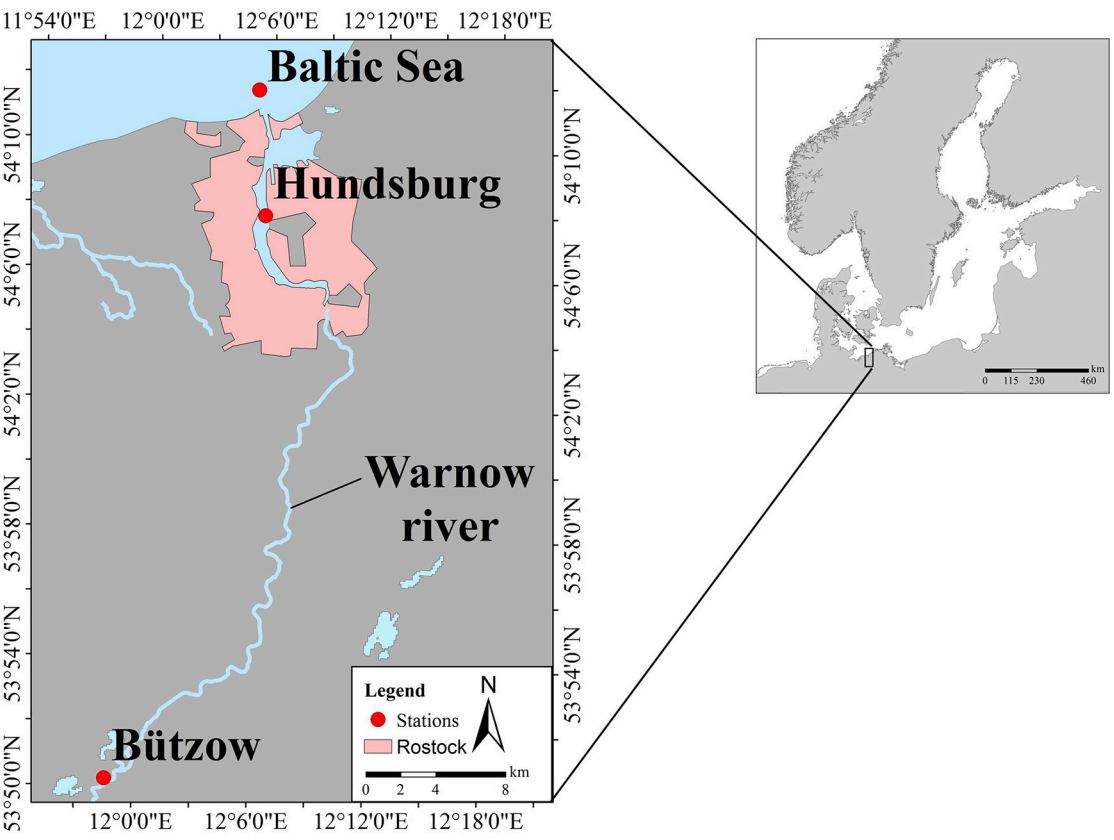

FIGURE 1 | Study area showing the three stations in a lowland catchment area in northern Germany: Bützow (Warnow river), Hundsburg (Warnow estuary, city of Rostock), and Baltic Sea (coastal zone of Baltic Sea).

The concentration of the dissolved molybdate-reactive P (DRP) in the filtrate is determined together with the concentration of total molybdate-reactive P (TRP) in the unfiltered water sample. The difference between the TRP and DRP values is the amount of particulate molybdate-reactive P (PRP).

The calibration curve, which is renewed with every new regent and reductant solution, for this method is linear up to 10 μM, and in the present study the detection limit was reached at an absorbance of 0.007 (equal to ca. 0.07 μM), measured in a 5 cm cuvette. The measured standard (potassium-dihydrogen phosphate) has a concentration of 5 μM which fitted in a 10%–variance. At least one blank and one standard was applied at every measurement.

Analysis of Total Phosphorus Categories

The determination of TP and total dissolved P (DP) requires a digestion of the sample so that all of the P in the sample is converted to DRP. The previously frozen (−20°C), stored water samples (exact 40 ml) were thawed and then transferred to Teflon PFA®-bottles. The digestion is achieved by the addition of an oxidant (4 ml), usually potassium peroxydisulfate (Koroleff, 1983). The oxidation was done in an alkaline medium.

The digestion was carried out in a lab-microwave. In this study, the CEM MARS Xpress and the following protocol were used: After a short initialization phase of a few seconds, the oxidant-containing samples were subjected to a 70 min heating phase during which they were heated to 180°C. This temperature was held for 50 min, after which the samples were cooled down over 30 min in the microwave to 70–80°C. The amount of DRP in the completely cooled samples was then measured using the molybdenum blue colorimetric method, in a mixture containing 0.8 ml of reductant and reagent. The samples were analyzed as duplicates.

The TP concentration was determined in the unfiltered water sample, and the DP concentration in the filtrate. The total particulate P (PP) concentration was calculated as the difference between TP and DP.

Every new solution of the oxidant is calibrated with standards concentrated between 0 and 20 μM. In each digestion two to three blanks and two 2 μM-standard (glucose-6-phosphate) were included. The detection limit was reached at an absorbance of 0.008 (equal to ca. 0.08 μM), measured in a 5 cm cuvette. The variance of the 2 μM-standard was within the 5% of the reference value. The measurement of the standard was linear up to a concentration of 15 μM.

TABLE 1 | Comparison of the traditional and new nomenclatures used to describe the different phosphorus (P) categories.

Traditional nomenclature	New nomenclature
Dissolved inorganic P (DIP)	Dissolved molybdate-reactive P (DRP)
Particulate inorganic P (PIP)	Particulate molybdate-reactive P (PRP)
Dissolved organic P (DOP)	Dissolved non-molybdate-reactive P (DNP)
Particulate organic P (POP)	Particulate non-molybdate-reactive P (PNP)

Analysis of Non-molybdate-reactive Phosphorus Categories

The two non-molybdate-reactive P categories were determined by calculation. Dissolved non-molybdate-reactive P (DNP) was defined as the difference between DP and DRP. Thus, the particulate non-molybdate-reactive P (PNP) was calculated out as the difference between PP and PRP (**Figure 2**).

RESULTS

In our area of investigation (**Figure 1**) the concentration of the different P categories vary seasonally and spatially. In general the TP concentrations decreased from the Warnow river to the Baltic Sea (**Table 2**) and thus so did the various P fractions, except PRP,

TABLE 2 | The variability of the concentration ranges of the phosphorus (P) fractions at the different stations of the study vs. that reported in the literature for different study areas.

Station	TP[a] (μM)	DRP[a]		DNP		PRP		PNP		Study area
		(μM)	(%)	(μM)	(%)	(μM)	(%)	(μM)	(%)	
Bützow	1.04–6.52	0.05–2.68	2.4–65.7	0–2.51	0–51.4	0.33–0.58	7.5–53.4	0–2.44	0–55.8	Warnow River
Hundsburg	0.30–4.07	0.01–2.81	0.3–100	0–1.73	0–100	0–0.64	0–100	0–2.31	0–78.6	Warnow estuary
Baltic Sea	0.19–1.14	0–0.80	0–100	0–0.42	0–56.5	0–0.89	0–100	0–0.44	0–56.7	Baltic Sea
Nausch et al., 2017	1.54–2.82	0.06–1.22	–	0–0.46	–	0.16–1.94	–	0.22–1.01	–	Warnow River
Nausch et al., 2011[b]	2.6	0.7	–	–	–	–	–	–	–	Warnow estuary
Nausch et al., 2011[b]	1.1	0.7	–	–	–	–	–	–	–	Baltic Sea
Stammler et al., 2017[c]	1.29–9.04	0.10–3.23	–	–	–	–	–	–	–	River system in Ontario
Han et al., 2018	5.49–807.23	1.94–2.26	–	0.32–1.94	–	–	–	–	–	Zhutuo River[d]

[a] *P categories measured in traditional monitoring.*
[b] *mean values in winter 2007.*
[c] *different stations at the Great Lakes (USA) with mixed type of land use in adjacent areas.*
[d] *Three Gorges Reservoir (China).*

which increased toward the Baltic Sea. The contribution to TP of the measured P forms varied over a wide range. Thus, at the river station (Bützow, **Figure 1**) DRP concentrations ranged between 2.4 and 65.7%, DNP concentrations between 0 and 100%, PRP concentrations between 7.5 and 53.4%, and PNP concentrations between 0 and 55.8%. Similarly high variations were measured at the estuarine station (Hundsburg, **Figure 1**), where the DRP concentrations were between 0.3 and 100%, the DNP and PRP concentrations between 0 and 100%, and the PNP concentrations up to 78.6%. At the "Baltic Sea" station (**Figure 1**), DRP and PRP, as molybdate-reactive P fractions, accounted for 0–100%, and DNP and PNP, as non-molybdate-reactive P fractions, for 0–56.5 and 0–56.7%, respectively. According to this we calculated the difference of the mean values of TP and DRP, as the traditional measured P components (**Table 3**) to show the importance of measuring the different P categories. In "Bützow," the river station, the TP and DRP values differed with 1.97 μM. At the station in the estuary the difference was with 1.62 μM lower and at the "Baltic Sea" station was a TP-DRP-difference of 0.44 μM. In addition, the DNP concentrations as mean values also decreased from 0.38 μM in the river (Bützow) to 0.26 μM at the "Baltic Sea."

Seasonal variations were exemplified by the data from February 2017 and June 2017 (**Figure 3**). Additional abiotic parameters (water temperature, rainfall, wind, and discharge) and biotic parameters (chlorophyll a and seston) were given in **Table 4**. In February 2017 it was stormy during the sampling at the stations "Hundsburg" and "Baltic Sea" and also in June 2017 at the river station in "Bützow." Moreover, the salinity situation was different in the 2 months (**Figure 4**). In February, the water column was locally nearly totally mixed at the different stations. In June, however, the water column was a bit stratified with freshwater (1 to 8 g kg^{-1}) at the surface and saltwater (8 to 10/11 g kg^{-1}) below the surface layer to the bottom layer. Furthermore, the chlorophyll a concentration was higher in February 2017 than in June 2017 at the stations "Bützow" (25.10 μg l^{-1} in February and 8.76 μg l^{-1} in June) and "Baltic Sea" (4.05 μg l^{-1} in February and 2.63 μg l^{-1} in June). In contrast, the Secchi depth at "Hundsburg" and "Baltic Sea" were in February deeper than in June. At all stations TP concentration is higher in June than in February. In February the particulate fractions dominated both at the "Baltic Sea" (∼60% PRP from a TP of 0.89 μM) and the river (∼20% PRP and 50% PNP from a TP of 2.01 μM) stations. By contrast, at the estuary station the dissolved fractions dominated (∼50% DRP and 30% DNP from a TP of 1.07 μM). In June, the conditions were reversed. At the "Baltic Sea" station (TP = 0.95 μM), DRP accounted for ∼40% and DNP for ∼30%, and at the river station (TP = 3.03 μM) DRP for 60% and DNP for ∼20%. At the estuary (TP = 1.96 μM), PNP dominated, with ∼60%.

TABLE 3 | Differences of TP and DRP/DIP as traditional monitoring parameter in comparison with differences of DP and DRP (DNP/DOP) at the three stations of the study area as mean values from September 2016 to 2017.

Station	TP (μM)	DRP/DIP (μM)	TP minus DRP (μM)	DP (μM)	DP minus DRP/ DNP/DOP (μM)
Bützow	3.04	1.07	1.97	1.30	0.38
Hundsburg	1.73	0.12	1.62	0.70	0.37
Baltic Sea	0.75	0.31	0.44	0.50	0.26

DISCUSSION

Detection of Different Phosphorus Categories and Their Impact

The nomenclature presented herein is an operational one and was developed to address the large variety of terms used to describe the same P form, and the resulting confusion (**Table 5**). The terms we introduced for the different P categories are consistent for us and our further work in the project. Moreover, it allows a more accurate description of the P fractions usually detected in monitoring programs (**Table 2**), especially in eutrophic waters with high amount of particles like our study area (**Table 3**). It does not replace the functional terms of organic and inorganic P forms, which are chemically-defined on the bonding of P with carbon. Instead, the proposed nomenclature has its antagonist in the traditional nomenclature (**Table 1**). Nevertheless, the functional terms of P categories could not be differentiated

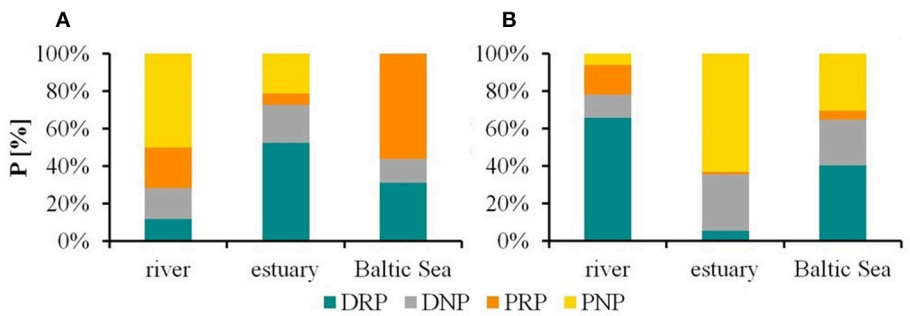

FIGURE 3 | Proportions (%) of the phosphorus (P) categories as a function of total P at the three study sites (Warnow River "Bützow," its estuary "Hundsburg," and the southern Baltic Sea "Baltic Sea") during two different seasons: **(A)** February 2017, **(B)** = June 2017. DRP, dissolved molybdate-reactive P; DNP, dissolved non-molybdate-reactive P; PRP, particulate molybdate-reactive P; PNP, particulate non-molybdate-reactive P.

TABLE 4 | Abiotic and biotic parameter during sampling in February 2017 (Feb 17) and June 2017 (Jun 17) at the three stations of the study area; T_{water}, water temperature in °C; RF, rainfall as daily mean value in the area around the city of Rostock in mm; Q, discharge as daily mean value in $m^3\ s^{-1}$; FM, mean wind velocity measured at the DWD-weather station in Rostock-Warnemünde in $m\ s^{-1}$; FX, maximum wind velocity measured at the DWD-weather station in Rostock-Warnemünde in $m\ s^{-1}$; O_2, oxygen saturation in %; Chl a, chlorophyll a concentration in $\mu g\ l^{-1}$; Seston, content of seston in $mg\ l^{-1}$.

Station	Month	T_{water} (°C)	RF (mm)	Q ($m^3\ s^{-1}$)	FM ($m\ s^{-1}$)	FX ($m\ s^{-1}$)	O_2 (%)	Chl a ($\mu g\ l^{-1}$)	Seston ($mg\ l^{-1}$)	Secchi depth (m)
Bützow	Feb 17	2.8	0	9.61	2.3	7	85.8	25.10	6.06	–
	Jun 17	18.4	4.7	4.94	4.4	15	69.9	8.76	4.68	–
Hundsburg	Feb 17	4.5	3.4	18.45*	8.8	16	92.9	13.10	2.14	4.5
	Jun 17	22.6	0	7.12*	2.2	4.8	78.1	16.02	2.68	1.5
Baltic Sea	Feb 17	3.7	3.4	–	8.8	16	100.6	4.05	1.19	5
	Jun 17	17.5	0	–	2.2	4.8	80.4	2.63	1.36	4.5

**Measured where the river change into the estuary.*

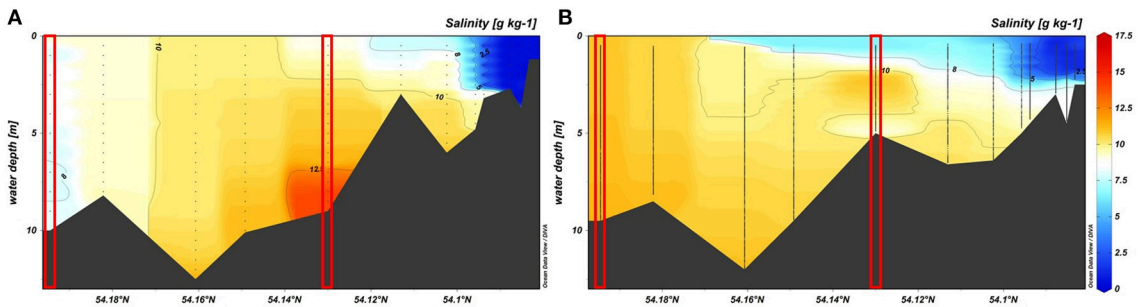

FIGURE 4 | Salinity profiles in the Warnow estuary in **(A)** February 2017 and **(B)** June 2017; red lined boxes mark the stations "Baltic Sea" and "Hundsburg".

accurately by the common and standardized molybdenum blue colorimetric method.

While the molybdenum blue colorimetric method for the analytical detection of P categories has been used for many years, discrepancies have often been reported (e.g., Murphy and Riley, 1962; Rigler, 1968; Baldwin, 1998). For example, the terms SRP and ortho-P have been variably used to refer often to the same P fraction (**Table 5**; Jarvie et al., 2002) although they do not describe the same fraction (Rigler, 1968; Stainton, 1980). Their synonymous use may reflect the fact that labile forms of organic P might be hydrolyzed in the acidic milieu of the molybdenum blue reaction (Rigler, 1968; Baldwin, 1998; Jarvie et al., 2002). Additionally, the P associated with colloids could be released during the reaction between molybdate and phosphates (Stainton, 1980; Baldwin, 1998). Therefore, a consistent operational nomenclature is necessary to prevent misinterpretation of results from molybdenum blue method. For example, DNP is indeed DOP but it will be underestimated because an amount of it is measured with the DRP which is dominated by DIP. In literature most studies and environmental reports refer to functional terms of P forms (e.g., organic, inorganic), which are also detected by molybdenum blue method (e.g., Nausch and Nausch, 2006).

In the traditional monitoring praxis as well as in most environmental studies (**Table 2**) only TP and DRP (after introduced nomenclature) are measured. On this basis the ecological status of an aquatic system is evaluated and potential aquatic management measures are developed. The DRP is presumed to be the P category available for phytoplankton and therefore the main source for eutrophication. **Table 3** shows, that with ∼40 to 50% of TP the DRP amount in the aquatic environment is not specified. This results in an underestimation of eutrophication potential, since at least DNP is known to be bioavailable (Nausch and Nausch, 2006). An advantage of the additional measurement of TRP is the calculation of PRP, which, as demonstrated by our results, plays an important role in the P cycle of the study area, especially during regeneration periods. Furthermore, because PRP is bound in labile form to particulate material, it is potentially bioavailable.

A problem of the method occurs with the unfiltered water samples which often had a high turbidity as we worked in waters with a high level of eutrophication (Nausch et al., 2011). The presence of particles that remain after the digestion can result in an underestimation of TP (Jarvie et al., 2002). In this study, this was avoided by exemplarily diluting the samples to a median sample:Milli-Q water ratio of 4:3 and 1:2.

Furthermore, because of the pressure exerted by the vacuum pump during the filtration (Rigler, 1968), the cells might collapse such that P of particulate origin contaminates the dissolved P fractions. This would lead to an underestimation of the particulate P fractions. To avoid this problem, we prevented crowding of the cells as described above.

Apparently, the traditional nomenclature is adaptable in less eutrophic waters or rather in waters with less turbidity like

TABLE 5 | Overview of the various nomenclatures and the terms used to detect the various phosphorus (P) categories.

Handling	Traditional nomenclature	Additional nomenclature used in the literature	New nomenclature
Phosphomolybdate reaction in the filtered sample	Dissolved inorganic P (DIP)	SRP^{2-6}, ortho-$P^{2,3,4,6}$, PO_4^{3-1}, dissolved reactive P (DRP)[4,6], FRP[4,6], MRP (filtered samples)[4,6]	Dissolved molybdate-reactive P (DRP)
Difference between TRP and DRP	Particulate inorganic P (PIP)	–	Particulate molybdate-reactive P (PRP)
Phosphomolybdate reaction in the unfiltered sample	–	MRP[4]	Total molybdate-reactive P (TRP)
Difference between DP and DRP	Dissolved organic P (DOP)	Dissolved hydrolyzable P (DHP)[4,5], dissolved unreactive P (DUP)[4], soluble unreactive P (SUP)[4], filterable organic P (FOP)[6]	Dissolved non-molybdate-reactive P (DNP)
Difference between PP and PRP	Particulate organic P (POP)	–	Particulate non-molybdate-reactive P (PNP)
Digestion of the unfiltered sample	Total P (TP)	–	Total P (TP)
Digestion of the filtered sample	Dissolved P (DP)	Total dissolved P (TDP)[4–6], total filterable P (TFP)[4,6]	Total dissolved P (DP)
Difference between TP and DP	Particulate P (PP)	Total particulate P (TPP)[6]	Total particulate P (PP)

[1]Murphy and Riley (1962); [2]Rigler (1968); [3]Baldwin (1998); [4]Jarvie et al. (2002); [5]Withers and Jarvie (2008); [6]Worsfold et al. (2016).

the station "Baltic Sea" (**Table 3**). Here, the difference between TP and DRP/DIP are less and the amount of particulate P is negligible. Thus, the proposed P categories could be used in waters with less turbidity but are advisable in waters with a high level of eutrophication and particles.

Differentiation of the Phosphorus Categories

The P fractions (TP and DRP) of the traditional monitoring (Nausch et al., 2011; Stammler et al., 2017; Han et al., 2018) and that of the extended programs (Nausch et al., 2017, own data) are highly variable, regardless of the chosen study area (**Table 2**). This was evidenced by the similar ranges of our own data from the estuary and the Baltic Sea and the mean TP and DRP values reported by Nausch et al. (2011). Especially in summer, the export of dissolved P forms out of the Warnow river may support primary production in the estuary and the southern Baltic Sea. Therefore, the proportion of PNP increased. The general trend of a decrease in TP towards the Baltic Sea suggested either the dilution of inflowing Baltic Sea water (**Figure 4**) or smaller inflows in the municipal area of Rostock together with the sedimentation of particulate P forms. In a seasonal comparison, the TP concentrations were higher in June 2017 than in February 2017. The reason therefore is a higher biomass in June than in February. In February the phytoplankton is dominant whereas in June the community consists of phytoplankton and zooplankton. Additionally, the Secchi depth is lower in June than in February which points to higher biomass in June.

In contrast to TP the PRP fraction was larger in February than in June at all three stations. This may have been a consequence of the high turbidity caused by a storm event that occurred during sampling in February, especially at the station "Baltic Sea." Higher turbidity and PRP concentrations could be positively correlated because dissolved P adsorb on particular material like on resuspended sediment (Stainton, 1980). Except for the river station, the amount of PNP in February was less than in June, most likely due to particulate material that was autochthonously built and not exported. Moreover, the chlorophyll a concentration was in "Bützow" in February higher than in June so that the high PNP data could be explained by a possible phytoplankton bloom.

The values of the TP and DRP concentrations reported by Stammler et al. (2017) in their study of the river system associated with the Great Lakes (USA) and by Han et al. (2018), who analyzed P concentrations in the Three Gorges Reservoir (China), were higher than those determined at the Warnow stations representing the Baltic Sea and the Warnow estuary but also analyzed by Nausch et al. (2011). They were also higher than those measured in a portion of the Warnow catchment area (Nausch et al., 2017). This large variety in TP and DRP may reflect regional differences between the different study areas. Additionally, according to Stammler et al. (2017), the deviation in the range of P values is allegeable by the different sampling rhythms. The data used in that study were collected between 1979 and 2011, with monthly sampling during the growing season (April to November). Our data were obtained from monthly samples collected between September 2016 and September 2017. On the other hand, Han et al. (2018) used data from four samplings timed according to the water cycle of the examined reservoir. In that study, sampling was performed in October 2014 (impounding period), January 2015 (high water level period), July 2015 (low water level period), and April 2016 (sluicing period).

Our results demonstrate that the various P forms occurring in aquatic systems depend on the season and the hydrology. Further research is needed to specify the single P components and their function within the P cycle. They also showed that the transformation processes taking place between the single P fractions are not reflected in the traditional monitoring, which detect only TP and DRP concentrations.

CONCLUSION

In traditional monitoring programs, only TP and DRP concentrations are measured. This does not reflect the diversity and complexity of P cycle in aquatic environment and

underestimates the eutrophication potential. The determination of all P categories is important both for comparison to data reported in the literature and to own data within a single multi-year study. However, because P forms are not stable, spatially and even within the same season, all P categories must be measured if effective nutrient reduction is to be successfully implemented. Additionally, an understanding of the function of the individual P components, such as their bioavailability, is important to determine to identify their contribution to eutrophication.

Furthermore, it is necessary to communicate research results to stake holders and implement the measurement of all P categories into monitoring strategies. Therefore, a simple and standardized method and concise nomenclature is helpful. The molybdenum blue reaction is a common and standardized method to determine P. The operative nomenclature, we presented in this study, based on reactivity of P with molybdenum blue. This should simplify research communication and prevent misinterpretation due to the functional terms of organic and inorganic P given to operational differentiated P components.

AUTHOR CONTRIBUTIONS

All authors were involved in contributing the conception and design of the study and performed the experiments; FB and LF analyzed the data; LF wrote the first and following drafts of the manuscript; DS-B supported LF during the writing process with ideas for the manuscript design. All authors are involved in manuscript revision, read, and approved the submitted version.

ACKNOWLEDGMENTS

We thank Christoph Kamper and Carmen Esser for their technical assistance in the lab. Additionally, we thank Sandra Jahn who aided during the development of the filtration scheme. This study is part of the PhosWaM project (Phosphorus from source to sea—Integrated phosphorus and water resources management for sustainable water protection), funded by the Federal Ministry of Education and Research, Germany (FKZ 033W042A). It also was performed within the scope of the Leibniz ScienceCampus Phosphorus Research Rostock.

REFERENCES

Backer, H., Leppänen, J. M., Brusendorff, A. C., Forsius, K., Stankiewicz, M., Mehtonen, J., et al. (2010). HELCOM Baltic Sea Action Plan – A regional programme of measures for the marine environment based on the Ecosystem Approach. *Mar. Pollut. Bull.* 60, 642–649. doi: 10.1016/j.marpolbul.2009.11.016

Baldwin, D. S. (1998). Reactive "organic" phosphorus revisited. *Water Res.* 32, 2265–2270. doi: 10.1016/S0043-1354(97)00474-0

Gustafsson, B. G., Schenk, F., Blenckner, T., Eilola, K., Meier, H. E. M., Müller-Karulis, B., et al. (2012). Reconstructing the development of Baltic Sea Eutrophication 1850-2006. *Ambio* 41, 534–548. doi: 10.1007/s13280-012-0318-x

Han, C., Zheng, B., Qin, Y., Ma, Y., Yang, C., Liu, Z., et al. (2018). Impact of upstream river inputs and reservoir operation on phosphorus fractions in water-particulate phases in the Three Gorges Reservoir. *Sci. Tot. Environ.* 610, 1546–1556. doi: 10.1016/j.scitotenv.2017.06.109

Haygarth, P. M., and Sharpley, A. N. (2000). Terminology for phosphorus transfer. *J. Environ. Qual.* 29, 10–15. doi: 10.2134/jeq2000.00472425002900010002x

Hecky, R. E., and Kilham, P. (1988). Nutrient limitation of phytoplankton in freshwater and marine environments: a review of recent evidence on the effects of enrichment. *Limnol. Oceanogr.* 33(4Pt 2), 796–822. doi: 10.4319/lo.1988.33.4part2.0796

Jarvie, H. P., Withers, P. J. A., and Neal, C. (2002). Review of robust measurement of phosphorus in river water: sampling, storage, fractionation and sensitivity. *Hydrol. Earth Syst. Sci.* 6, 113–131. doi: 10.5194/hess-6-113-2002

Jescovitch, L. N., Boyd, C. E., and Whitis, G. N. (2017). Effects of mechanical aeration in the waste-treatment cells of split-pond aquaculture systems on water quality. *Aquaculture* 480, 32–41. doi: 10.1016/j.aquaculture.2017.08.001

Koroleff, F. (1983). "Determination of phosphorus," in *Methods of Seawater Analysis, 2nd Edn.*, eds K. Grasshoff, M. Ehrhardt, and K. Kremling (Weinheim: Verlag Chemie), 125–138, 168–169.

Murphy, J., and Riley, J. P. (1962). A modified single solution method for the determination of phosphate in natural waters. *Anal. Chim. Acta* 27(Suppl. C), 31–36. doi: 10.1016/S0003-2670(00)88444-5

Nausch, G., Bachor, A., Petenati, T., Voß, J., and Von Weber, M. (2011). Nährstoffe in den deutschen Küstengewässern der Ostsee und angrenzenden Gebieten. *Meeresumwelt Aktuell Nord Ostsee* 1, 1–16.

Nausch, M., and Nausch, G. (2006). Bioavailability of dissolved organic phosphorus in the Baltic Sea. *Mar. Ecol. Prog. Ser.* 321, 9–17. doi: 10.3354/meps321009

Nausch, M., Woelk, J., Kahle, P., Nausch, G., Leipe, T., and Lennartz, B. (2017). Phosphorus fractions in discharges from artificially drained lowland catchments (Warnow River, Baltic Sea). *Agric. Water Manage.* 187, 77–87. doi: 10.1016/j.agwat.2017.03.006

OECD (1982). *Eutrophication of Waters: Monitoring, Assessment and Control.* Paris: Organisation for Economic Co-Operation and Development (Publié en français sous le titre "Eutrophication des Eaux. Méthodes de Surveillance, d'Evaluation et de Lutte").

Rigler, F. (1968). Further observations inconsistent with the hypothesis that the molybdenum blue method measures orthophosphate in lake water. *Limnol. Oceanogr.* 13, 7–13. doi: 10.4319/lo.1968.13.1.0007

Stainton, M. P. (1980). Errors in the molybdenum blue methods for determining ortho-phosphate in freshwater. *Can. J. Fish. Aquat. Sci.* 37, 472–478. doi: 10.1139/f80-061

Stammler, K. L., Taylor, W. D., and Mohamed, M. N. (2017). Long-term decline in stream total phosphorus concentrations: a pervasive pattern in all watershed types in Ontario. *J. Great Lakes Res.* 43, 930–937. doi: 10.1016/j.jglr.2017.07.005

Unger, J., Endres, S., Wannicke, N., Engel, A., Voss, M., Nausch, G., et al. (2013). Response of Nodularia spumigena to pCO(2) - Part 3: turnover of phosphorus compounds. *Biogeosciences* 10, 1483–1499. doi: 10.5194/bg-10-1483-2013

Withers, P. J., and Jarvie, H. P. (2008). Delivery and cycling of phosphorus in rivers: a review. *Sci. Tot. Environ.* 400, 379–395. doi: 10.1016/j.scitotenv.2008.08.002

Worsfold, P., McKelvie, I., and Monbet, P. (2016). Determination of phosphorus in natural waters: a historical review. *Anal. Chim. Acta* 918, 8–20. doi: 10.1016/j.aca.2016.02.047

Conflict of Interest Statement: The authors declare that the research was conducted in the absence of any commercial or financial relationships that could be construed as a potential conflict of interest.

frontiers in Marine Science

ORIGINAL RESEARCH
published: 25 September 2018
doi: 10.3389/fmars.2018.00343

The Influence of Riverine Nutrients in Niche Partitioning of Phytoplankton Communities–A Contrast Between the Amazon River Plume and the Changjiang (Yangtze) River Diluted Water of the East China Sea

Helga do Rosario Gomes[1], Qian Xu[2], Joji Ishizaka[2], Edward J. Carpenter[3], Patricia L. Yager[4] and Joaquim I. Goes[1]*

[1] Lamont Doherty Earth Observatory at Columbia, Palisades, NY, United States, [2] Institute for Space-Earth Environmental Research, Nagoya University, Nagoya, Japan, [3] Estuary & Ocean Science Center, San Francisco State University, Tiburon, CA, United States, [4] School of Biology, Georgia Institute of Technology, Atlanta, GA, United States

OPEN ACCESS

Edited by:
Christian Lønborg, Australian Institute of Marine Science (AIMS), Australia

Reviewed by:
María Fróján, Instituto de Investigaciones Marinas, Vigo, Consejo Superior de Investigaciones Científicas (CSIC), Spain
Bingzhang Chen, Tokyo University of Marine Science and Technology, Japan
Maria Aranguren-Gassis, University of Vigo, Spain

***Correspondence:**
Helga do Rosario Gomes
helga@ldeo.columbia.edu

Specialty section:
This article was submitted to Marine Biogeochemistry, a section of the journal Frontiers in Marine Science

Received: *05 April 2018*
Accepted: *06 September 2018*
Published: *25 September 2018*

Citation:
Gomes HdR, Xu Q, Ishizaka J, Carpenter EJ, Yager PL and Goes JI (2018) The Influence of Riverine Nutrients in Niche Partitioning of Phytoplankton Communities–A Contrast Between the Amazon River Plume and the Changjiang (Yangtze) River Diluted Water of the East China Sea. Front. Mar. Sci. 5:343. doi: 10.3389/fmars.2018.00343

Riverine nutrients act in concert with local hydrographic conditions to create distinct ecological niches for phytoplankton communities across river-ocean continuums. Here we compare two of the world's largest river-ocean systems, the Amazon River Plume (ARP) which outflows into the Western Tropical North Atlantic and the Changjiang Diluted Water (CDW) which empties into the East China Sea to show how distinctly different N:P supply ratios of their source waters, shape phytoplankton communities along the river-ocean continuum. Sampling in the relatively unpolluted surface waters of the ARP during peak river discharge revealed that phytoplankton communities along the river-ocean continuum were strongly limited by Dissolved Inorganic Nitrogen (DIN, nitrate plus nitrite) which was low or beyond detectable, while Dissolved Inorganic Phosphorous (DIP, phosphate) and Silica were not limiting. The resulting low N:P supply ratio allowed diazotrophs to co-exist with non-diazotrophs. Diatom-Diazotroph Associations (DDAs) such as *Hemiaulus hauckii-Richelia* proliferated, while in the oligotrophic oceanic waters, *Trichodesmium* spp. thrived. In contrast, in the CDW, anthropogenic nitrogen inputs from human pressures in the Changjiang River system has led to a system where the changing supply rate of the single nutrient (DIP) is responsible for the interannual variability seen in the phytoplankton community structure of the CDW. During years of low discharge, DIP limitation can be ameliorated by on-shelf upwelling of DIP rich Kuroshio Intermediate Waters leading to domination of diatoms and dinoflagellates. Conversely, during years of heavy discharge, the westward flowing CDW plume was severely DIP limited, probably because water column stratification dampened upwelling of subsurface waters. The consequent DIP limitation led to the proliferation of small phytoplankton such as Chlorophytes and Cyanobacteria. The absence of diazotrophs in the CDW, leads us to hypothesize that river-ocean continuums, whose source waters

are heavily impacted by anthropogenic activities and with high nitrate concentrations often substantially in excess of Redfield ratios, may not support diatoms offshore on account of DIP limitation nor diazotrophy because of excess DIN.

Keywords: Amazon River Plume, Changjiang River Diluted Water, East China Sea, resource competition, nutrient stoichiometry, phytoplankton communities, diazotrophy

INTRODUCTION

Rivers are the primary conduit transporting weathered, leached, and human-derived material from land to the oceans (Sharples et al., 2017). In addition to carbon, rivers export nitrogen, phosphorus and silica which are the key potentially limiting nutrients required for phytoplankton growth. Thus riverine nutrients can not only augment primary productivity but also contribute to regulating the long-term biological productivity of the ocean and hence ocean carbon storage (Jickells et al., 2017). Several studies show that anthropogenic disturbance of river nutrient loads and export to coastal and ocean marine systems has increased, creating a global problem affecting water quality, and biodiversity (Bouwman et al., 2005). Increasing inputs of nitrogen and phosphorous from human activity, predominantly from land-based activities, now have the potential to modify oceanic, and even global, biogeochemical systems. The total river input of nitrogen and phosphorous to the coastal seas has approximately doubled over the last few hundred years (Seitzinger et al., 2010; Beusen et al., 2016; Jickells et al., 2017). Nitrogen inputs are a consequence of urbanization, sanitation, development of sewerage systems, and lagging wastewater treatment, as well as increasing food production and associated inputs of N fertilizer, animal manure, atmospheric N deposition, and biological N fixation in agricultural systems. P has increased through the use of rock phosphate as fertilizer, detergent additives, animal feed supplements etc. (Seitzinger et al., 2010). Sharples et al. (2017) calculated that globally 75 and 80% Dissolved Inorganic Nitrogen (DIN) and Dissolved Inorganic Phosphate (DIP) respectively, reaches the open ocean although these are considered as the upper limits as estuarine processes were ignored in the study. However, there is a significant and systematic spatial variability in supply materials to the open ocean as well as the amount and kinds of nutrients supplied. Sharples et al. (2017) reported that the proportion of nutrients reaching the open ocean, from tropical and subtropical rivers tend to be the most important for nutrient delivery because the weak Coriolis force allows direct across-shelf movement of river plumes unlike in temperate and polar regions, where the Coriolis force moves freshwater flows along the shelf (Jickells et al., 2017). Hence low latitude rivers such as the Amazon, and the rivers in Southeast Asia including the Changjiang River are major sources of nutrients for the oceans or seas into which they discharge.

As nutrient loads change, so does the stoichiometry of the coastal and open ocean waters resulting mostly in increasing N:P supply ratios and consequent variations in algal communities (Glibert et al., 2014). There has been a large body of work (Anderson et al., 2002; Heisler et al., 2008; Glibert et al., 2010) on eutrophication which report that inland and coastal waters are witnessing increased algal growth and development of high biomass blooms as well as changes in species diversity from increased riverine nutrient loads. However, only a few studies document changes in regions of the open ocean where riverine nutrients are exported and which can influence phytoplankton biodiversity and productivity.

Here we compare two widely disparate river-ocean continuums, the tropical Amazon River Plume (ARP) which outflows into the Western Tropical North Atlantic and the Changjiang Diluted Water (CDW), the plume of low salinity water from the Changjiang River which extends across East China Sea (ECS).

Comparison of the Amazon River and the Changjiang River Continuums

The magnitude of discharge (120,000 m^3 s^{-1}) from the Amazon River is unique in the global oceans; the Amazon River discharges as much freshwater as the next 8 largest rivers in the world combined (Coles et al., 2013). This tremendous volume of freshwater forms a very dynamic and extensive surface plume that protrudes well offshore into the WNTA (**Figure 1a**). Because the Amazon discharges at the equator and on the western boundary of the ocean, its waters are entrained in energetic boundary currents associated with the North Brazil Current, the North Equatorial Counter Current, and the coastal Guyana Current (**Figure 1a**; Coles et al., 2013). These currents have strong seasonal variations in response to the atmospheric Intertropical Convergence Zone (ITCZ) which is located in the southern position in winter, and northern in summer. Thus, during the winter and spring months, the plume follows the North Brazil Current along the northeastern coast of South America, carrying low salinity water to the Caribbean and in summer and fall, it retroflects to the east, entrained in the North Equatorial Counter Current (Muller-Karger et al., 1988; Coles et al., 2013; Weber et al., 2017). The discharge, introduces tremendous quantities of nutrient-rich water to the Western Tropical North Atlantic, with nutrients being mostly plant derived as it traverses for over 6000 km from the Andes in Peru to the Atlantic Ocean, and covers a watershed that includes the largest tropical rainforest in the world as well as areas of dry grassland, or savannah (Del Vecchio and Subramaniam, 2004).

The Changjiang River, the third largest in the world and the largest outflowing river in China (Yan et al., 2010) discharges into the ECS, one of the world's largest marginal seas (**Figure 1b**) with 70% of its area characterized by a continental shelf slope shallower than 200 m. The freshwater discharge and total

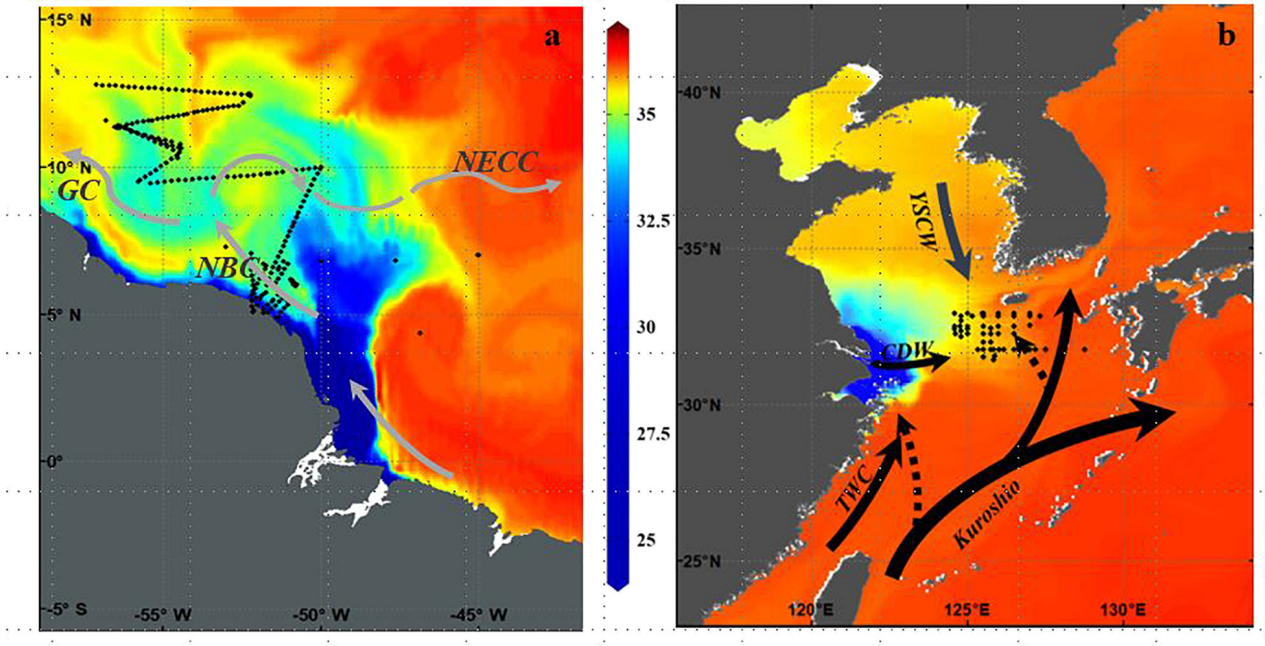

FIGURE 1 | (a) Cruise track of R/V *Knorr* cruise KN197-8 in May-June 2010 showing CTD stations occupied and underway sampling track overlaid on a map of model (1/6° HYCOM) derived salinity distribution. Currents according to Coles et al. (2013) are North Brazil Current (NBC), Guyana Current (GC), and North Equatorial Counter Current (NECC) **(b)** Sampling locations during four cruises in July (2009 to 2011 and 2013) in the mid-shelf East China Sea overlaid on a map of model (Japan Coastal Ocean Prediction Experiment) derived surface salinity distribution. Solid lines indicate the Kuroshio Current, the Changjiang Diluted Water (CDW), the Taiwan Warm Current (TWC), and Yellow Sea Coastal Water (YSCW). Dashed lines indicate two Kuroshio intrusions one into the northeast of Taiwan and the other into the southwest of Kyushu.

suspended matter from the Changjiang River spreads over the entire shelf (Sukigara et al., 2017), accounting for 90–95% of the total riverine input into the ECS (Zhang et al., 2007). Heaviest discharge is in summer in association with the monsoons with its buoyant plume, known as CDW, spreading eastward over the ECS over an area ca. 85×10^3 km^2 (Zhang et al., 2007). In winter when discharge is lower, the northerly monsoonal winds prevail over the ECS and the Changjiang discharge is restricted to the western side of the ECS with waters moving southward and forming a narrow belt along the coast of China and toward the Taiwan Strait (**Figure 1**; Zhang et al., 2007). Anthropogenic activities appear to be the principal driver of the high DIN and DIP in the coastal environment of the Changjiang River (Zhang et al., 2007) with DIN inputs having increased almost 4-fold from 1970 to 2003 (Yan et al., 2010). In contrast, the Yellow Sea Coastal water flowing from the north, provides only marginal amounts of DIP and DIN (Zhang et al., 2007). High levels of nutrients from land sources brought in by the Changjiang are usually constrained to coastal and inner-shelf regions with nutrient species in surface waters gradually decreasing from eutrophic coastal to oligotrophic open shelf waters depending on the hydrographic stages of the river (Chen, 2008). Highest nitrate concentrations are found near the Changjiang estuary with DIN concentrations often exceeding 50 μM and DIP concentrations >1 μM (Zhang et al., 2007) and in some cases N:P ratios exceeding 100 (Chen and Wang, 1999). However, large phytoplankton blooms primarily of diatoms and dinoflagellates rapidly consume the DIP which is reduced to below 0. 2 μM while DIN is still higher than 1 μM (Chen, 2008) making DIP a limiting nutrient in the shelf waters of the ECS as well as in the mid-shelf and offshore region (Wang and Wang, 2007). Off the shelf break, the northward intrusion of the nutrient-rich, sub-surface Kuroshio waters into the ECS at 50-100m depth also affects the nutrient regime of the ECS (**Figure 1b**). These waters can upwell in summer when winds are favorable (Zhang et al., 2007) alleviating the severe P limitation at least in the ECS shelf region (Yang et al., 2012; Yang et al., 2013; Tseng et al., 2014) Relative to shelf waters, the Kuroshio intrusion waters are high in DIN and DIP (Zhang et al., 2007) providing a much required DIP source to phytoplankton in the euphotic layer.

Compared to the Changjiang River which flows through highly industrialized regions (Beusen et al., 2016) where riverine N and P have increased tremendously, the Amazon river delivers relatively low anthropogenic inorganic nitrogen because of both less intensive catchment agriculture and dilution of nitrogen inputs by the high river flow (Jickells et al., 2017). The nitrate in this source water exists at sub-Redfield ratios, and hence is quickly drawn down by blooms of coastal diatoms that benefit from the DIP and Si-rich water (Stukel et al., 2014). This leaves a plume that extends more than 3000 km from the river mouth (Hu et al., 2004) which is nitrogen-poor but both Si and DIP rich. DIP and Si exhibit patterns that suggest near conservative mixing between high nutrient river water and oligotrophic oceanic water. Additional inputs of DIP from particle leaching both in the

estuary and offshore contribute to the low N:P ratios (DeMaster, 1996) establishing nitrogen limitation early in the life of the plume and propagated offshore (Weber et al., 2017). As the plume extends from the river mouth, it spreads as a thin cap well beyond the river mouth, leading to surface stratification that can impede nutrient inputs and strongly influence the structure of the phytoplankton communities.

While a considerable effort has been made to study the relative impacts of nutrients, physical forcing, and grazing on the phytoplankton niche communities along the Amazon river continuum (Subramaniam et al., 2008; Goes et al., 2014; Stukel et al., 2014; Conroy et al., 2016; Conroy et al., 2017; Weber et al., 2017)., there is sparse information on how the CDW influences the phytoplankton community structure of the ECS. Extensive studies have focused on the nutrient contribution of the Changjiang outflow to the river-ocean continuum as well as the role of sub-surface nutrient rich Kuroshio waters (Zhang et al., 2007; Chen, 2008 and references within) in modulating the nutrient regime of the ECS while others have focused either on the phytoplankton communities of the nearshore Changjiang estuary (Li et al., 2009; Guo et al., 2014) or of the Kuroshio influenced region (Jiao et al., 2005). Our recent study (Xu et al., 2018) improves the situation by examining the phytoplankton community structure in the ECS during the summers of 3 consecutive years from 2009 to 2011 as well in 2013 clearly demonstrating the interannual variability of phytoplankton communities of the ECS associated with variations in the Changjiang River discharge and its spread eastward.

In this study we compare these two highly disparate river-ocean continuums to show that variability in the stoichiometry of their waters supports two distinct gradients of phytoplankton communities as the plumes move offshore from nutrient-rich coastal waters to offshore oligotrophic regions.

MATERIALS AND METHODS

Sampling and Hydrographic Properties

ARP

In order to investigate the system of phytoplankton communities as they adapt to nutrient limitation and changing N:P ratios we undertook 3 cruises in the ARP (Coles et al., 2013; Goes et al., 2014; Stukel et al., 2014; Weber et al., 2017). This paper describes the findings of the first cruise on board the R/V *Knorr* from 22nd May to 25th June, 2010 when the discharge was at its maximum.

For a detailed description of the sampling strategies and methods, the reader is directed to Goes et al. (2014) and Weber et al. (2017). Briefly, a total of 25 stations were occupied along a cruise track (**Figure 1a**) which traversed the plume four times and extended well offshore to provide contrast with waters within the plume (Weber et al., 2017). Samples were collected with Niskin® bottles attached to a Conductivity-Temperature-Depth (CTD) Sea-Bird Electronics® Rosette from 4 depths within the euphotic zone determined from in-water profiles of photosynthetically available radiation (PAR) using a Biospherical Instruments® in-water quantum scalar radiometer (Goes et al., 2014). Additionally, surface samples were collected at hourly intervals along the cruise track from the ship's uncontaminated seawater flow-through system, filtered and stored in the same manner as the hydrocast samples. While, samples were also collected from the deep chlorophyll maximum (DCM) and from below the euphotic depth, in this paper we only discuss data from surface samples and information on depth profiles is available in Goes et al. (2014). A highly refined phytoplankton structure of surface waters was obtained using microscopically determined phytoplankton species (Goes et al., 2014) while in this paper some pigment derived phytoplankton classes have also been added.

ECS

All studies were conducted on board the T/V *Nagasaki Maru* in late July of each year (**Figure 1b**). Sampling locations were confined to the ECS, in an area extending from 124.6 to 128.8°E and from 31.4 to 33.0°N. This allowed a better understanding of how phytoplankton composition in the mid-shelf ECS can be impacted by variations in the mixing of different water masses, in particular the flow and the extent of mixing of the CDW and the Kuroshio with their different nutrient contents. A more thorough and detailed description on the methods is available in Xu et al. (2018). Briefly, a CTD was used to obtain profiles of seawater Temperature (T) and Salinity (S) of the upper 80 m. Seawater samples from the surface were collected using an acid washed bucket and analyzed for pigments, and nutrients (DIN and DIP). Nutrient samples were immediately frozen in polyethylene tubes after sampling and transferred under frozen conditions to the shore laboratory for analysis using an Auto-analyzer (AACS-IV, BLTEC).

High Pressure Liquid Chromatography (HPLC) Pigment Analysis and CHEMTAX

ARP

Total phytoplankton biomass was collected by gently filtering 1–2.5L surface seawater onto 47-mm GF/F filters, which were frozen in liquid nitrogen at sea and transported to shore for analysis by HPLC. Acetone extracted phytoplankton pigments were separated and characterized by methods described in Van Heukelem and Thomas (2001) and Hooker et al. (2005). Currently this method is recognized as one of the most efficient and reliable methods to analyze algal pigments (Serive et al., 2017). HPLC provided separation of almost 15 pigments including the primary pigment, Chlorophyll *a* (Chl *a*) and a suite of accessory pigments (carotenoids and chlorophylls) many of which are specific to individual phytoplankton taxa or groups (Mackey et al., 1996; Vidussi et al., 2001; Wright, 2005; Wright and Jeffrey, 2006) and can be used to categorize phytoplankton classes such as diatoms, dinoflagellates, prochlorophytes etc. This was undertaken using CHEMTAX, a free statistical software program that estimates algal class abundances from pigment markers by applying an iterative process to find the optimal ratio of biomarker pigment: Chl *a* (Mackey et al., 1996; Higgins et al., 2011) and then generates the fraction of the total Chl *a*

pool belonging to each pigment-determined group (Mackey et al., 1996). Accurate estimates necessitate that the initial or seed ratios be close to those of the phytoplankton populations that are being assessed (Latasa, 2007; Swan et al., 2016). As this constitutes the first report on pigment based phytoplankton distribution of the Amazon plume continuum we do not have pigment ratios exclusively for this region and have relied on the extensive and recently published synthesis of culture and field pigment ratios for major algal groups (**Table 1**; Higgins et al., 2011). These ratios have been used by Swan et al. (2016) for their global analysis and by others for select regions (Armbrecht et al., 2015; Barlow et al., 2016). However, we were also guided in our choice of ratios by microscopy data detailed in our earlier paper (Goes et al., 2014) and the extensive taxonomic report of Wood (1966) for the ARP. Another *a priori* assumption required for effective CHEMTAX analysis is that the accessory pigment-to-chl*a* ratios should be constant across the data subset under consideration i.e., the phytoplankton community must be relatively homogeneous (Swan et al., 2016). We have minimized this problem by clustering the data into subsets of pigment ratios with similarities (Dandonneau and Niang, 2007; Torrecilla et al., 2011; Wolf et al., 2014) using the statistical package PRIMER (ver. 6.1.13) on log(X + 1) transformed pigment to Chl *a* ratios from the upper 5m. Considering only linkage distances greater than 50%, our pigment ratios separated into 3 clusters (Bray Curtis similarity index) which comprised of samples from similar salinity ranges as well as coincided with the water types proposed by Goes et al. (2014) based on fluorescence data. Cluster 1 (salinity > 35) comprised mostly open ocean samples, Cluster 2 was made up of mesohaline samples in the extension of the plume (salinity 30–35), and cluster 3 were samples in the plume (salinity < 30). Each data cluster was assumed to be made up of samples of similar phytoplankton populations and CHEMTAX was run separately on each cluster.

The initial ratios or 'true' pigment ratios (**Table 1**; Higgins et al., 2011) were used to generate about 30 'artificial' ratios within a certain range (S. Wright, *personal comm.*). CHEMTAX was applied to each cluster using these initial 30 matrices. CHEMTAX quantitatively estimates the contribution of algal taxa by iteratively modifying the user-specified Pigment:Chl*a* ratios using a "steepest descent" algorithm to successively reduce the amount of unexplained pigment measured as the RMS of the residuals. The output of the matrix with the smallest RMS error was used to create 30 more matrices. However, prior to selecting this matrix, the ratios were plotted to see that they had stabilized as RMS decreased. When the RMS and the Pigment:Chl*a* ratios had stabilized, the matrices associated with the 6 best RMS were averaged. This 'best' matrix was then compared to the initial matrix to see if the ratios had deviated in which case the matrix was discarded. This procedure was repeated until we were confident that the RMSE was low but more importantly, that the pigment ratios had converged to within known ranges. The output (phytoplankton classes) from the 6 best RMS were averaged to provide the final phytoplankton classes for that cluster (Final Ratios in **Table 1**). *Prochlorococcus* sp. was quantified exclusively by its unambiguous divinyl Chlorophyll a (DVChla) signature (Chisholm et al., 1992; Swan et al., 2016) and was not included in the CHEMTAX analysis.

ECS

Pigment analysis of samples collected in the ECS was undertaken as described in Section 2.1.2 and (Xu et al., 2018). Initial pigment ratios were from (Furuya et al., 2003) and are based on earlier pigment studies in the ECS. CHEMTAX was run as described in Section ARP. Initial and Final Ratios are shown in Xu et al. (2018). For accuracy, (see Section ARP) CHEMTAX was run on surface datasets of 2009, 2010, 2011, and 2013 separately.

Phytoplankton Taxonomy

ARP

Details of sample collection and processing for phytoplankton taxonomy are in Goes et al. (2014). Briefly, phytoplankton cells were filtered onto 8 μm pore size, 47 mm diameter Nuclepore® filters and examined under an epifluorescence microscope (Carpenter et al., 1999), and enumerated within 24 h.

TABLE 1 | Initial pigment: Chl a ratios entered into the CHEMTAX program are from Higgins et al. (2011), Swan et al. (2016) and Wright, S. (personal comm.), and Final ratios are the output after completion of CHEMTAX runs.

Phytoplankton Class	Chl c3	Chl c1	Peridinin	ButFuc	Fucox	Prasinox	Violax	Hex-fuco	Zea	Allox	Chl b	Chl a
INTIAL RATIOS												
Prasinophytes-2	0	0	0	0	0	0	0.049	0	0.032	0	0.32	1
Cyyptophytes	0	0	0	0	0	0	0	0	0	0.38	0	1
Haptophytes	0.18404	0	0	0.00632	0.35	0	0	0.5	0	0	0	1
FINAL RATIOS												
Phytoplankton Class	Chl c3	Chl c1	Peridinin	ButFuc	Fucox	Prasinox	Violax	Hex-fuco	Zea	Allox	Chl b	Chl a
Prasinophytes-2	0	0	0	0	0	0.174	0.01747	0	0.01988	0	0.15524	1
Cyyptophytes	0	0	0	0	0	0	0	0	0	0.26514	0	1
Haptophytes	0.28286	0	0	0.23239	0.22161	0	0	0.82225	0	0	0	1

These ratios are for analysis of pigments from the ARP while similar ratios for the ECS can be found in Xu et al. (2018). Pigment abbreviations are Chlorophyll c3 and c1 (Chl c3, c1), Chlorophyll b (Chl b), Chlorophyll a (Chl a), 19'butanoyloxyfucoxanthin (ButFuc), Fucoxanthin (Fucox), Prasinoxanthin (Prasinox), Violaxanthin (Violax), 19'hexanoyloxyfucoxanthin (Hex-fuco), Zeaxanthin (Zea), and Alloxanthin (Allox).

ECS

Taxonomy was solely based on pigments and no microscopy was undertaken.

RESULTS

ARP

The trajectory of the ARP is clearly defined by its salinity gradient (**Figures 1a**, **2a**) as it traveled northward in narrow coastal band, broadening and dispersing off the continental shelf at around 8°N. Salinities < 35 were evident as far north as 18°N and west of 47°W (**Figure 2a**). Based on high frequency fluorescence data we previously delineated three water types along the plume continuum (Goes et al., 2014), which are coincident with the salinity based demarcations of Subramaniam et al. (2008). These water types include an oceanic type of high salinity (salinity > 35), a mesohaline type with salinities from 30-35, and plume waters with salinity < 30.

The ARP clearly influenced the nutrient (DIN, DIP, and SiO_3) concentrations of the otherwise oligotrophic Western Tropical North Atlantic. DIN was almost depleted from the waters by large coastal blooms (Goes et al., 2014; **Figure 2b**) and concentrations ranging from 0.1–1.5 μM were found at only 9 locations, 6 of them in the plume. The highest value of 1.5 μM was at 6°N (**Figure 2b**) where depth profiles indicated an upward flux of the nutrient from deeper depths (see vertical profile in Figure 4e of Goes et al., 2014). In contrast, higher concentrations of DIP (**Figure 2c**) and SiO_3 (**Figure 2d**) were measured in the plume than in the surrounding waters indicating riverine influence. Although DIP distribution followed the conservative mixing line at least below 9°N, north of this, there were strong positive deviations along the axis of the plume (Goes et al., 2014; Weber et al., 2017) which have been ascribed to the release of DIP from suspended particles and dissolved organic matter (Goes et al., 2014; Weber et al., 2017). N:P ratios of surface waters were mostly negative indicating severe nitrogen limitation. This is best illustrated using the diagnostic parameter Excess Nitrate (ExN), which measures departure from classic Redfield ratios and is calculated as ExN = DIN–(R*DIP) (R = Redfield N:P ratio of 16). ExN values of < 0 indicate DIP enrichment, while ExN > 0 μM (N:P > 16) indicates the converse (Wong et al., 1998). ExN was consistently between −17.5 and −7.5 as the plume moved northwestward indicating severe DIN limitation. Low ExN arises from a combination of rapid uptake of DIN in the plume and the addition of DIP from leaching (Fox et al., 1986). Surface SiO_3 concentrations (**Figure 2d**) ranged widely from 0.37 to 50 μM and mostly followed a conservative behavior as a function of salinity but with lower values in the plume and the northwestern edge of the plume because of high uptake rates by diatoms (**Figure 2d**).

Pigment derived phytoplankton classes and microscopically determined phytoplankton communities show the formation of niches governed by the stoichiometry of the region. A very dense and mixed bloom of diatoms comprising primarily of *Skeletonema marinoi* (*sensu lato, costatum*), *Pseudo-nitzchia* spp., *Thalasiossira alienii*, and *Chaetoceros* spp. occupied the low salinity core of the plume (**Figure 3a**). These blooms were fueled by riverine derived SiO_3 (**Figure 2d**) and cross-shore and upward flux of DIN into the surface layers. Maximum cell counts for some of the diatom species included *Pseudo-nitzschia* spp (1.5×10^6 cells L^{-1}), *Thalassiosira* spp. (3.5×10^6 cells L^{-1}), *Guinardia flaccida* (9.0×10^4 cells L^{-1}), *Chaetoceros* spp (3.6×10^5 cells L^{-1}), *Coscinodiscus* ($3.3.8 \times 10^6$ cells L^{-1}), and *Odontella sinensis* (4.5×10^7 cells L^{-1}). These blooms depleted DIN from surface waters in the mesohaline and open ocean regions (**Figure 2b**).

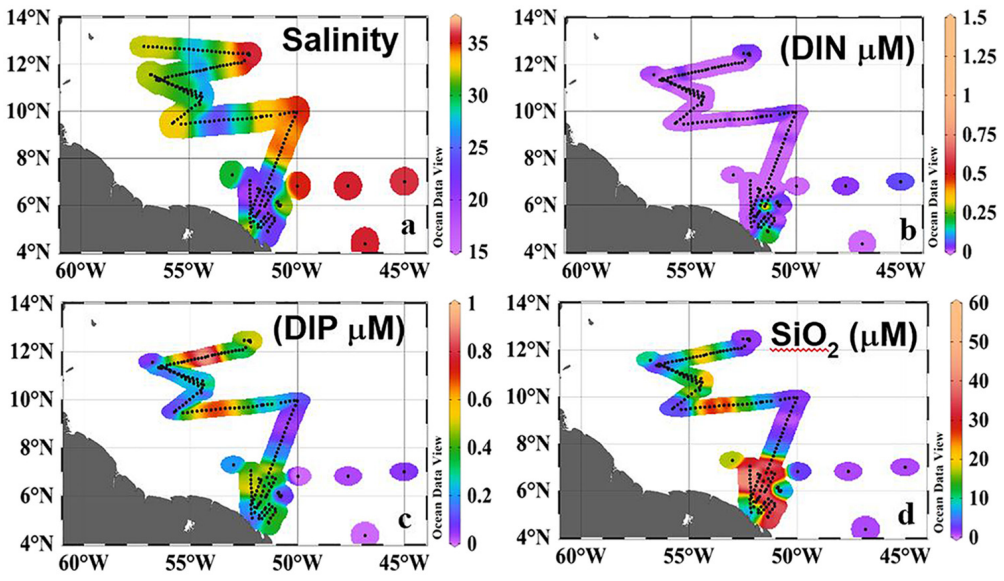

FIGURE 2 | Surface Distribution of **(a)** Salinity **(b)** Dissolved Inorganic Nitrogen (DIN, μM), **(c)** Dissolved Inorganic Phosphorous (DIP, μM), **(d)** Silicate (μM). Black dots along the track indicate sampling locations. Redrawn from Goes et al. (2014).

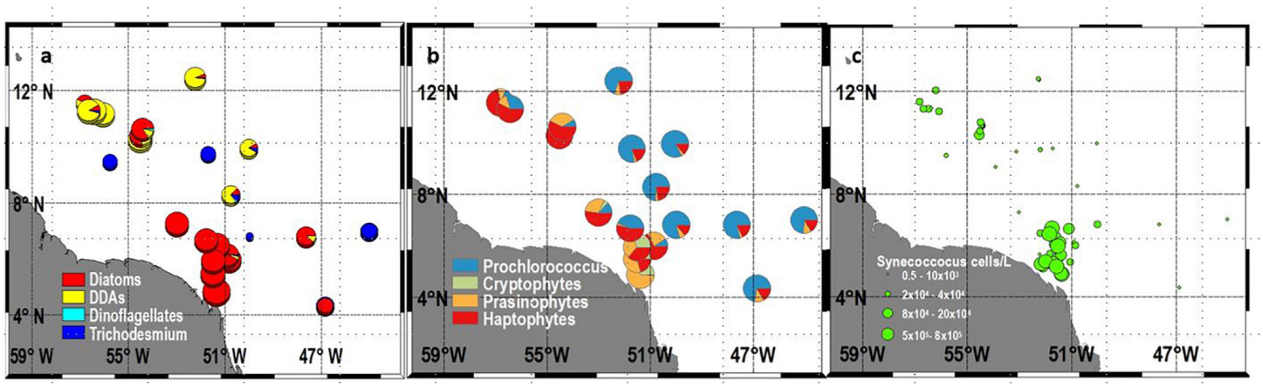

FIGURE 3 | Surface **(a)** Percent proportion of Microplankton (Diatoms, DDAs, Dinoflagellates, *Trichodesmium* **(b)** Percent proportion of Nano and Picoplankton (*Prochlorococcus*, Cryptophytes, Prasinophytes, Haptophytes), and **(c)** Total *Synechococcus* (cells L^{-1}).

Consequently, in the mesohaline waters, the moderately high Silicate (28–33 μM) and DIP (0.5–0.9 μM) allowed a very different group of diatoms, the DDAs to emerge (**Figure 3a**). These symbiotic diatom-diazotrophic assemblages are capable of photosynthesizing and growing actively in the absence of DIN, because their nitrogen requirements are met via the N_2 fixing ability of their endosymbiont *Richelia intracellularis* (Foster et al., 2007; Foster et al., 2011). The dominant DDA was *Hemiaulus hauckii* with a maximum cell count of 9.7×10^5 cells L^{-1} and high cell counts on the western side of the plume. Another DDA, *Rhizosolenia clevei* was also observed but in much smaller numbers, with maximum concentrations of about 800 cells L^{-1}. Additionally, the free living, non-symbiotic, cyanobacteria, *Trichodesmium* was also seen but more broadly distributed than the DDAs. Higher *Trichodesmium* concentrations were seen just north of the plume and in the oligotrophic waters east of the plume (**Figure 3a**). In addition to the microplankton (diatoms, dinoflagellates, and DDAs) (**Figure 3a**), nanoplankton like Cryptophytes, Prasinophytes and Haptophytes were also observed in large numbers in the two regions where DIN was available albeit at low concentrations (**Figure 3b**). This included the plume region and the mesohaline region where DDAs replenish DIN when cells disintegrate. Cryptophytes proliferated only in the low salinity plume waters with numbers ranging from 3.2×10^3–6.3×10^5 L^{-1}. This was also the case with prasinophytes but Haptophytes were seen in both the plume and the mesohaline area coincident with the DDA blooms (**Figure 3b**). Picoplanktonic *Synechoccocus* (**Figure 3c**) were also seen in large numbers especially in the plume where their numbers ranged from 5.0×10^3–6.9×10^5 L^{-1}. Outside of the plume, *Synechoccocus* were only seen in the mesohaline, DDA dominated region. Conversely, *Prochlorococcus* identified by their unique Divinyl Chl *a* signature were absent from the nutrient rich plume waters but were ubiquitous elsewhere especially in the waters east of the plume (**Figure 3b**), where all three macro nutrients were below the level of detection.

The significance of the ARP in driving changes in the hydrography, chemistry, and phytoplankton communities of the western Tropical North Atlantic is illustrated by Principal Component Analysis (PCA) of hydrographic data and microscopic and CHEMTAX derived phytoplankton communities (**Figure 4a**). PCA enables a visualization of the similarities and differences between samples, as well as the correlations between the variables. The first principle component accounted for 32% of the variance and divided the data set into phytoplankton communities that proliferated in the plume (diatoms, dinoflagellates, cryptophytes and prasinophytes) from those in the mesohaline and oligotrophic waters (DDAs, *Trichodesmium*, *Prochlorococcus,* and Haptophytes). The former group correlated with DIN indicating its importance in the growth of these micro and nanoplankton. The latter group which comprised diazotrophs, Haptophytes, and picoplanktonic *Prochlorococcus* with low nutrient requirements were found in high salinity waters outside of the plume. The PC2 axis separated DIN, the limiting nutrient from DIP and silicate which were not limiting.

ECS

Our four-year study clearly demonstrated that the hydro-chemical environment of the ECS undergoes large interannual variations linked to the discharge of the Changjiang River and the eastward movement of its plume (CDW) which strongly influences phytoplankton distribution. As in the case of the ARP, and based on T-S plots, Xu et al. (2018) defined three water types *viz*. CDW ($T > 23^oC$, $S < 28$) primarily influenced by discharge from the Changjiang River, the Kuroshio surface waters associated with the deeper, higher salinity Kuroshio waters ($S > 32.9$) and the Shelf waters. The latter is a mixed water mass (Salinity of 30–32.9) of the CDW and Kuroshio surface waters, located in the central part (125–128°E) of our study area. The large interannual variability in temperature, salinity and nutrients of the ESC was mainly from the variable influence of CDW and Kuroshio surface waters as is evident in **Figures 5a–v**. The influence of the CDW was greatest in 2010 with colder, lower salinity waters extending up to 127.5°E (**Figures 5b,f**) followed by the consecutive year of 2011 when the CDW was confined to west of 126°E (**Figures 5c,g**). In contrast, 2009 and 2013 experienced a greater influence of warmer, more saline Kuroshio surface

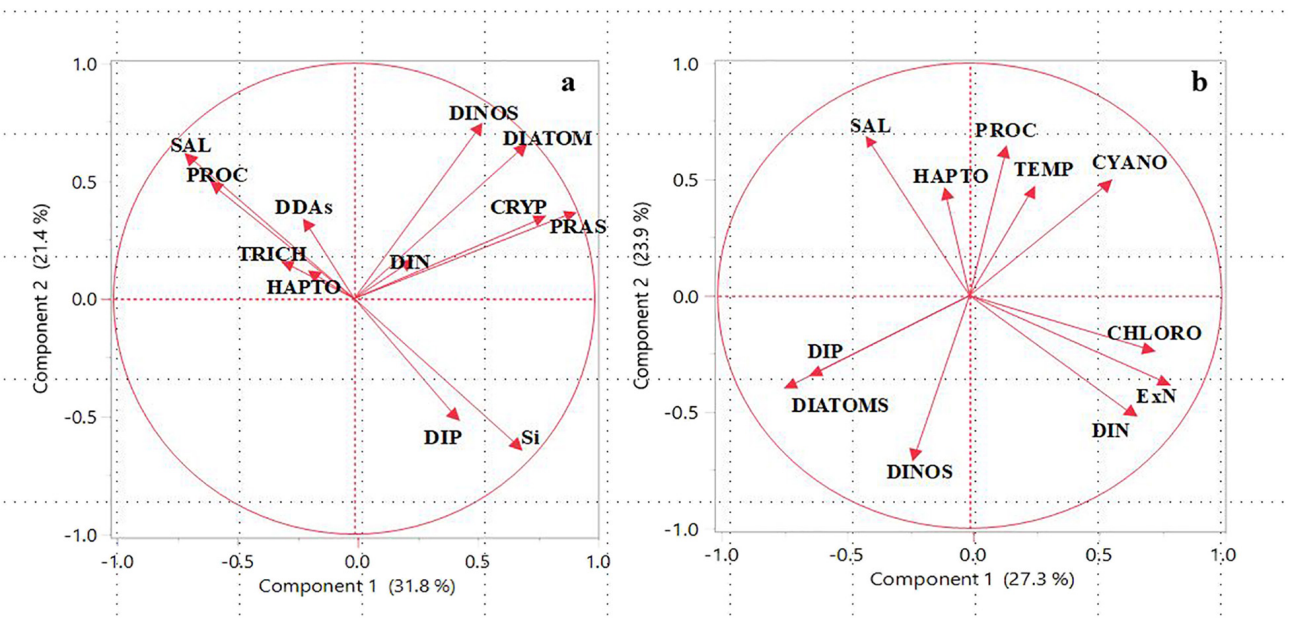

FIGURE 4 | Principal Component Analysis (PCA) of the hydrographic parameters (Temperature and Salinity), nutrients, and phytoplankton classes for **(a)** Amazon River Plume and **(b)** East China Sea. Abbreviations used: PROC (*Prochlorococcus*), DDAs (Diatom-Diazatroph Associations), TRICH (*Trichodesmium*), HAPTO (Haptophytes), DINOS (Dinoflagellates), CRYP (Cryptopytes), PRAS (Prasinophytes), SAL (Salinity), DIN (Dissolved Inorganic Nitrogen), DIP (Dissolved Inorganic Phosphorous), Si (Silicate), ExN (Excess Nitrate). Redrawn from Goes et al. (2014) and Xu et al. (2018).

waters (**Figures 5a,e,d,h**). This resulted in mixed Shelf waters covering the entire study area. During these 2 years, waters in the eastern part of the observation area were warmer (SST > 28.5°C) (**Figures 5a,d**) and more saline (>32.9) (**Figures 5e,h**).

The surface waters of the eastern region of the study area, which are less influenced by riverine discharge and in the path of the Kuroshio extension were generally depleted of nutrients during all 4 years of study. DIN in these waters ranged from 0.02 to 0.11 μM (**Figures 5i–l**), and DIP was less than 0.07 μM (**Figures 5m–p**). In these Kuroshio influenced waters, ExN measured around 0 μM (**Figures 5q–v**) indicating invariant stoichiometry. In contrast, the CDW waters showed distinct interannual differences in their nutrient regime with significantly higher (non-parametric Mann-Whitney U test, $p < 0.05$) ExN values in 2010 and 2011 (5–25 μM) (**Figures 5t,u**) indicating severe DIP limitation. This is contrast to 2009 and 2013 when ExN was <0 μM (**Figures 5q,v**). As expected, in the former years, the CDW was characterized by extremely high DIN (>10 μM, maximum of 26.1 μM) derived from the anthropogenic load of the Changjiang River (**Figures 5j,k**) but low DIP (<0.05 μM) (**Figures 5n,o**). A contrasting situation emerged in 2009 and 2013 when only one station to the west of 125°E showed high DIN (**Figures 5i,l**). DIP in 2009 and 2013 was higher (up to 0.2 mg m^{-3}) compared to concentrations in 2010 and 2011 when it was almost below the limit of detection. Statistically, the differences in DIN, DIP, and ExN between higher DIP years (2009, 2013) and high lower DIP years (2010, 2011) were highly significant ($p < 0.01$) indicating the predominant influence of the Changjiang River on the stoichiometry of the ECS. Overall, phytoplankton biomass reflected the large west-east differences in N:P ratios in the ECS. Chl *a* was higher in the CDW region (0.25–4.0 mg m^{-3}) but decreased in the shelf waters (0.14–0.9 mg m^{-3}) (**Figures 5w–z**). Lowest values were observed in Kuroshio surface waters where Chl *a* rarely exceeded 0.2 mg m^{-3}.

Similar to phytoplankton communities in the ARP continuum, those in the ECS also adapted to the changing nutrient regime influenced by the Changjiang River discharge. Phytoplankton communities of the CDW (**Figure 6**) showed clear distinctions between low DIP (2010, 2011) and high DIP (2009, 2013) years. Diatoms dominated the latter years and diatom-derived Chl *a* ranged from 3–2.1 mg m^{-3} compared to concentrations of 0.02–0.34 mg m^{-3} during low DIP years. In contrast, during 2010 and 2011, cyanobacteria dominated, contributing 6–76% of the Chl *a* as opposed to 1–20% in 2009 and 2013. A substantial population of Prymnesiophytes also contributed to the Chl *a* (25–55%) in 2013. Although we have chosen to show only the phytoplankton community structure of the CDW, it is apparent from Figure 4b of Xu et al. (2018) that there were no interannual differences in the phytoplankton structure of the mixed shelf waters. However, diatom populations did show dominance in the high DIP year of 2009 (Chl *a* contribution 28–83%). A mixture of cyanobacteria and the picoplanktonic prochlorophytes dominated (>61% of the total Chl *a*) the low Chl *a* at waters of the oligotrophic Kuroshio surface waters during all 4 years of study (Figure 4c in Xu et al., 2018). Prochlorophytes, the second highest group after cyanobacteria, comprised more than 30% of the phytoplankton community in 2009, 2010, and 2013 and 19% in 2011 (Xu et al., 2018). Diatoms were

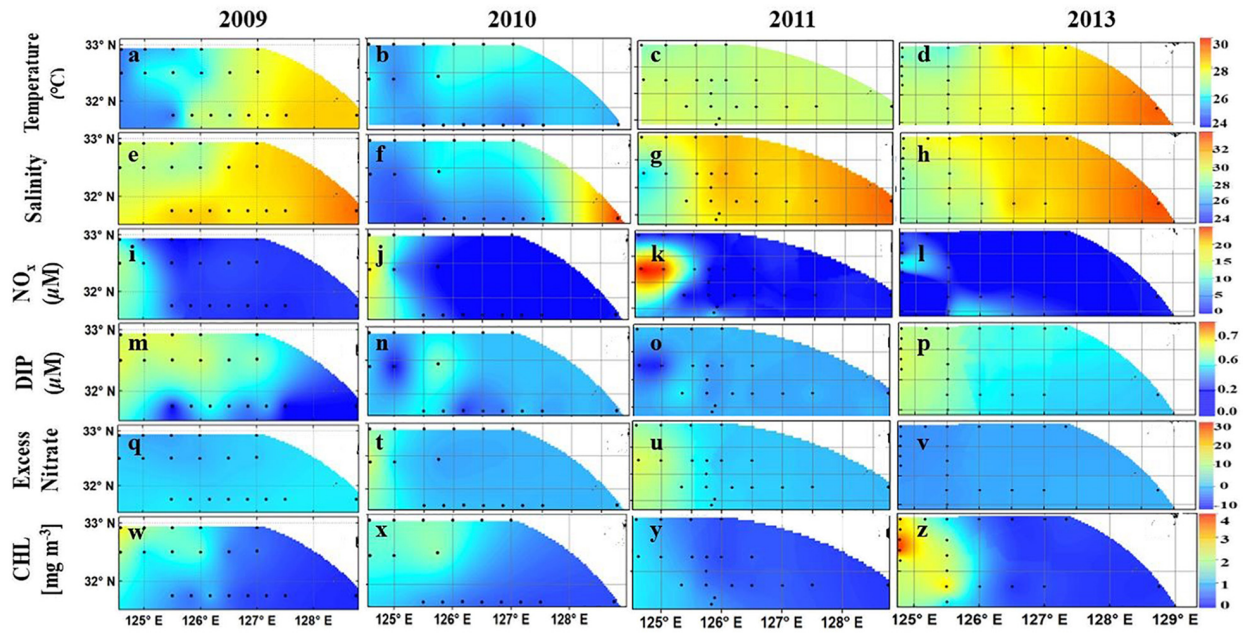

FIGURE 5 | (a–x). Surface distribution of Temperature **(a–d)**, salinity **(e–h)**, DIN **(i–l)**, DIP **(m–p)**, ExN **(q–v)**, and Chl *a* **(w–z)** in the East China Sea from 2009 to 2011 and 2013. Black dots are sampling stations. Redrawn from Xu et al. (2018).

absent or negligible except in 2011 when 18% of Chl *a* was from this group. As in the case of the ARP (Goes et al., 2014), large diatom blooms were seen in the coastal waters of the Changjiang River Continuum (Zhou et al., 2008; Guo et al., 2014) advantaged by the abundant nutrients available from the river discharge.

The possible dependence of the various algal groups on Salinity, Temperature and nutrients is also examined by means of PCA (**Figure 4b**). PC1 accounted for 27.3% of the variance in this data separating DIP and DIN. PC1 also divided the data set into large microplankton (diatoms and dinoflagellates) with high P requirements versus smaller nano and picoplankton such as Chlorophytes, Cyanobacteria and Prochlorophytes which can grow at lower DIP concentrations. DIP correlated with large microplankton (diatoms and dinoflagellates) showing it to be the limiting nutrient that determined the transition from small to large phytoplankton in the CDW. Conversely, cyanobacteria, chlorophytes, and prochlorophytes were associated with warmer waters of low DIP concentrations characteristic of Kuroshio surface waters. This is also demonstrated by the positive correlation of smaller phytoplankton with ExN on PCA1 axis and the converse with microplankton. Both PC1 and PC2 show a strong negative correlation between Salinity and DIN indicating riverine inputs of DIN. In contrast to PC1, the PC2 axis which accounted for 24% of the variance in the dataset showed a positive correlation between DIN, DIP, and diatoms but notably a negative correlation with Temperature. This typifies the intrusion of colder, upwelled waters which bring in DIP and result in the domination of diatoms. The latter is elaborated further in the Discussion section.

DISCUSSION

Revisiting and comparing the previously conducted research in two of the world's largest river-ocean systems gave us an opportunity to understand how fluctuations in nutrient availability and nutrient ratios shape phytoplankton communities along the river-ocean continuum to produce highly distinct and specialized groups that can profoundly affect the food web and carbon fluxes to deeper depths. As we discuss below, it is likely that the N:P supply ratios from the two systems determine whether or not diazotrophs are part of the community, while it is likely that supply of a single limiting nutrient (such as DIP) is responsible for the interannual variability seen in the ECS. We use resource competition theory and resource supply ratio to describe the distribution of phytoplankton communities of the ARP and CDW in relation to changing in N:P supply ratios and changing DIP supplies along the river-ocean continuums.

Simply stated, Tilman (1977)'s resource competition theory states that in an equilibrium environment, each competing phytoplankton type is capable of drawing the limiting nutrient down to distinct low subsistence concentrations, known as R*. The value of R* for any nutrient is set by the ecophysiological characteristics of the phytoplankton type and represents both the concentration of the limiting nutrient at which growth is balanced by mortality (top down) and the minimum nutrient concentration (bottom up) required for survival (Ward et al., 2014). If multiple organism types are present, the ambient resource concentration will be drawn down to the lowest R* and only that class of organisms will survive while other organisms will be excluded over time (Dutkiewicz et al., 2009). This theory then implies that the smallest cells which have higher

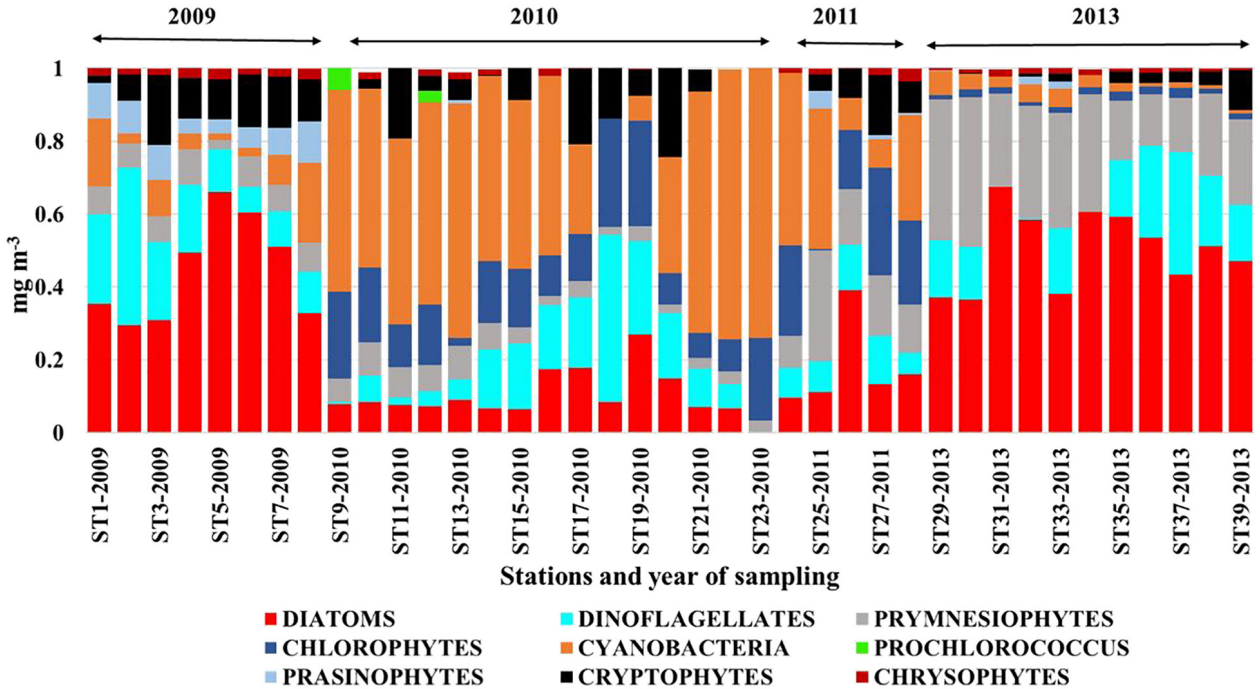

FIGURE 6 | Phytoplankton classes derived by pigment analysis and CHEMTAX in the CDW in 2009, 2010, 2011, and 2013. plot. Redrawn from Xu et al. (2018).

nutrient uptake rates should accumulate biomass by drawing down nutrients to the lowest level thus excluding any larger phytoplankton with higher nutrient requirements. However, this is not the case because the smallest and most competitive phytoplankton groups are in fact kept under control by grazing by the small zooplankton, allowing larger size classes to become established when excess nutrients become available (Ward et al., 2012; Ward et al., 2014). In this situations the R*s intersect and stable coexistence is possible. Thus, when nutrient supplies are higher, more classes of larger phytoplankton (with less efficient nutrient uptake rates) could coexist with the smallest types. This seems to the case in the ECS where the CDW waters were DIP limited. However, in years (2009, 2013) when DIP concentrations increased we saw predominance of diatoms while in years when DIP concentrations were low or beyond the level of detection, small cells like cyanobacteria and chlorophytes predominated. Dinoflagellates remained invariant during all 4 years of sampling with Chl *a* ranging from 0.1–0.4 mg m^{-3} of the total Chl *a*. Many dinoflagellates are mixotrophic, and it is possible that this mixing of trophic levels allows them to exist in all situations.

On the eastern side of our sampling grid, in the oligotrophic waters dominated by the nutrient poor Kuroshio surface waters only picoplanktonic *Prochloroccocus* proliferated (Xu et al., 2018). The increased DIP concentrations appear to be regulated by the extent of low saline CDW in the western region which as determined by the surface temperature and salinity was limited westward in 2009 and 2013. In our more extensive study (Xu et al., 2018), we have investigated the physical forces driving the higher DIP concentrations in the mid-shelf of the ECS in 2009 and 2013. All evidence points to upwelling of DIP-rich Kuroshio Intermediate Water onto the upper layers of the shelf (Tseng et al., 2014) and its advection eastward by the CDW into the mid-shelf of the ECS. In Xu et al. (2018) we explain the higher surface DIP in 2009 and 2013 and the converse situation in 2010 and 2011 as follows. In the latter, when the Changjiang River discharge was higher, DIP from coastal upwelling was not only diluted as the CDW moved eastward, vertical stratification from density differences also prevented mixing. In contrast, during low discharge years, DIP from coastal upwelling could be transported further eastward into the mid-shelf where it supported the growth of larger phytoplankton.

In case of the ARP, we can also explain the appearance of diazotrophs versus non-diazotrophs (non-nitrogen fixing marine phytoplankton) in terms of the resource supply-ratio theory. Ward et al. (2013) describes the competition between the two (diazotrophs versus non-diazotrophs) through their interaction with the three essential nutrient elements *viz*. Fe, DIN and DIP. Fe is not limiting for phytoplankton both in the ARP and the CDW largely because of intense weathering and erosion that takes place in the drainage basins of this river system (Edmond et al., 1985; Bergquist and Boyle, 2006). Whereas in the CDW, DIP appears to be the single nutrient that controls the size structure of phytoplankton communities, in the ARP, it is the N: P ratio that will determine whether diazotrophs or non-diazotrophs will establish themselves. Generally, diazotrophs exhibit slower growth rates than non-diazotrophs so they will be outcompeted if both nutrients are limited. But if there is excess DIP relative to the stoichiometric requirements of the non-diazotrophs then this DIP can fuel diazotroph growth,

since it is assumed that diazotrophs can fix N. In other words, in situations where DIP:DIN supply rates are in excess of the non-diazotroph requirements, then diazotrophs can co-exist with the non-diazotrophs (Dutkiewicz et al., 2012). In the case of the ARP, away from the inner shelf where sediment load is reduced and light levels are not limiting, large mixed blooms (Shipe et al., 2006; Goes et al., 2014) deplete the DIN and reduce DIP although the riverine Si required for diatoms was not limiting. As the plume flows offshore, DIP is replenished through desorption (Fox et al., 1986; Berner and Rao, 1994) and the system transitions to diazotrophy and the acute shortage of DIN is thus mitigated. As stated earlier, a variety of diatom diazotroph assemblages as well as non-symbiotic and non-siliceous diazotrophs like *Trichodesmium* proliferated in the mesohaline waters. Small nitrogenous inputs from symbiotic diatoms supported populations of nanoplankton such as Prasinophytes and Haptophytes which were earlier not reported but are identified in this study using pigment biomarkers. Experimental evidence from other locations (Gulf of California and the subtropical North Pacific) shows that *Richelia* fixes 81–744% more N than needed for its own growth and up to 97.3% of the fixed N is transferred to the diatom partners (Foster et al., 2011). This same study also showed that N_2 fixation rates of *Richelia* and another cyanobacterial symbiont *Calothrix* were 171–420 times higher when the cells were symbiotic compared with the rates for the cells living freely.

It is well known that diazotrophy is inhibited when DIN and/or ammonium concentrations exceed 1 μM (Knapp, 2012) and the resource supply-ratio theory suggests that high N:P supply ratios will not support diazotrophy, so it is not surprising that we did not see either DDAs or non-symbiotic diazotrophs such as *Trichodesmium* in the ECS during our 4 years of study as DIN was not a limiting nutrient in these waters. What is noteworthy about the results from the ECS is the marked interannual variability in the hydrology, stoichiometry and consequent phytoplankton community structure of ECS modulated by the extent of the Changjiang River and its DIP inputs.

Long term changes being monitored in the ECS using satellite-derived salinity algorithms (Bai et al., 2014) show that the spread and direction of CDW plume on the ECS continental shelf are affected by the Changjiang River discharge while other long term studies of summer phytoplankton community in the Changjiang estuary during the past 50 years (Jiang et al., 2014) suggest that anthropogenic loading is leading to increase in smaller phytoplankton and dinoflagellates which could exacerbate harmful algal blooms. Although similar information is not available for the Amazon River continuum, model projections of climate change effects on discharge and inundation in the Amazon basin (Sorribas et al., 2016) show a system in transition (Davidson et al., 2012). A study of all the rivers of South America (van der Struijk and Kroeze, 2010) including the Amazon river shows that exports of DIN and DIP increased between 1970 and 2000 although the increases were more prominent in rivers south of the Amazon. If DIN export were to increase and attain concentrations higher than DIP loading, then we would expect diazotrophy to disappear from the ARP. Elsewhere, nutrient reduction measures such as in the Chesapeake Bay Estuary along the east coast of the US, have resulted in a decrease in diatoms from a decrease in DIN (Harding et al., 2015) whereas the reverse was seen in Patos Lagoon Estuary, Brazil which showed increasing signs of eutrophication (Haraguchi et al., 2015). Not surprisingly and considering the extent of the rapid economic development of China during the past 30 years, the Pearl River which empties into the northern part of South China Sea showed the same situation that we observed in the ECS. While diatoms proliferated in the inner estuary, limited DIP resulted in the proliferation of picophytoplankton in the mesohaline and nearshore oceanic waters (Qiu et al., 2010).

The varied taxonomical diversity of the two river continuums should be reflected in the geochemical fluxes to deeper depth. Variations in the impact of the CDW through its nutrient supply and consequently on the phytoplankton community are also reflected in the carbon fluxes. Sukigara et al. (2017) who operated sediment traps in 2000 and 2011 in tandem with our studies, showed that sinking particles were thrice as high in 2000 when our study showed the dominance of diatoms than in 2011. Particulate carbon and nitrogen contents as well as isotope ratios, showed that the particles that sunk out the euphotic zone in 2010 were primarily from the CDW layer with a secondary contribution from the SCM layer. Concomitant with our ARP studies Chong et al. (2014), showed a distinct axis of POC and biogenic silica deposition on the deep floor aligned with the plume and a footprint of approximately 1 million km^2 of carbon and biogenic silica on the deep sea floor.

Traditionally, the elemental stoichiometry of both phytoplankton biomass and dissolved nutrient pools has been viewed as having limited variability. Expressing the relevance of the canonical Redfield ratio, Falkowski and Davis (2004) wrote that "the uniformity of elemental Redfield ratios in the oceans and the life they contain underpins our understanding of marine biogeochemistry." But just as this near-constant ratio laid the foundations for the twentieth-century advances in our understanding of marine biogeochemistry, deviations from this ratio are now providing twenty-first-century insights into the nutrient dynamics of oceans modern and ancient (Nature Geoscience, 2014). Questions remain with respect to fundamental facts such as the flexibility of phytoplankton stoichiometry and the relationship of internal ratios to resource availability and growth rates (Hillebrand et al., 2013). Relationship between available and internal N:P ratios are not necessarily linear. While Goldman et al. (1979) found that phytoplankton N:P ratios varied widely at low N:P converging to classic N:P ratio of 16 only at high growth rates, Hillebrand et al. (2013) revisited this premise to show that although N:P ratios did converge to an optimal ratio it was different for different species and phylogenetic groups. We think that river continuums with changing spatial and temporal stoichiometry are ideal environments to study the flexibility of phytoplankton stoichiometry *vis a vis* resource availability and its implications for size and functional traits.

CONCLUSION

We have compared the distribution of phytoplankton communities in the river-ocean continuums of two of the world's largest rivers, the Amazon River, the nutrient content of which is largely governed by forest derived nutrients and the Changjiang River, the waters of which are heavily impacted by human activities. We show that phytoplankton communities along the axes of their plumes are shaped largely by the initial N: P content of the rivers. In the case of the ARP, phytoplankton populations downstream of the river plume were largely controlled by the availability of inorganic nitrogenous nutrients with diatoms dominating upstream where nitrogenous were available either from the source water or from the onshore advection of nutrient rich waters from depth. In the case of the Changjiang River plume, phytoplankton communities were limited significantly by a single nutrient *viz*. inorganic phosphate and downstream of the plume, diatoms were observed during years when coastal upwelling was more intense and inorganic phosphate from deeper depths advected offshore. One of the largest differences between the ARP and the Changjiang River plume waters was the absence of DDAs and *Trichodesmium* spp. in the latter, which appears to be tied to different N:P supply ratios.

AUTHOR CONTRIBUTIONS

HG wrote the paper and conducted the Amazon plume research. QX conducted the East China Sea research. JG conducted research in the Amazon plume. EC undertook the cell counts for the Amazon plume research. JI and PY were the lead PIs on the East China Sea and Amazon Plume projects respectively.

FUNDING

This work was supported by Visiting Professorships at Nagoya University, Japan to HG and JG. Research conducted in the ECS by JI and QX was supported by JAXA GCOM-C and JSPS KAKENHI grant number JP26241009 awarded to JI. Research work in the ARP was supported by grants NSF OCE-0934095 and 1133277 to PY, JG, and HG and NASA grants NNX13AI29A and NNX16AD40G to JG and HG.

ACKNOWLEDGMENTS

We are highly indebted to Dr. Simon Wright (Australian Antarctic Division) for the CHEMTAX code and for his constant help and guidance in running CHEMTAX. We would specially like to thank Dr. Stephanie Dutkiewicz (MIT) for her time, effort and invaluable suggestions that improved this paper immensely. We thank the NASA-HPLC Center, for help with analysis of phytoplankton pigments for the ARP study. We thank Victoria Coles (Center for Environmental Science, University of Maryland) for the Salinity distribution map of the ARP and we acknowledge the Salinity map for the ECS provided by Asia-Pacific Data Research Center.

REFERENCES

Anderson, D. M., Glibert, P. M., and Burkholder, J. M. (2002). Harmful algal blooms and eutrophication: nutrient sources, composition, and consequences. *Estuaries* 25, 704–726. doi: 10.1007/BF02804901

Armbrecht, L. H., Wright, S. W., Petocz, P., and Armand, L. K. (2015). A new approach to testing the agreement of two phytoplankton quantification techniques: microscopy and CHEMTAX. *Limnol. Oceanogr.* 13, 425–437. doi: 10.1002/lom3.10037

Bai, Y., He, X., Pan, D., Chen, C.-T. A., Kang, Y., Chen, X., et al. (2014). Summertime Changjiang River plume variation during 1998–2010. *J. Geophys. Res.* 119, 6238–6257. doi: 10.1002/2014JC009866

Barlow, R., Gibberd, M. J., Lamont, T., Aiken, J., and Holligan, P. (2016). Chemotaxonomic phytoplankton patterns on the eastern boundary of the Atlantic Ocean. *Deep Sea Res. Part I* 111, 73–78. doi: 10.1016/j.dsr.2016.02.011

Bergquist, B. A., and Boyle, E. A. (2006). Iron isotopes in the Amazon River system: weathering and transport signatures. *Earth Planet. Sci. Lett.* 248, 54–68. doi: 10.1016/j.epsl.2006.05.004

Berner, R. A., and Rao, J.-L. (1994). Phosphorus in sediments of the Amazon River and estuary: implications for the global flux of phosphorus to the sea. *Geochim. Cosmochim. Acta* 58, 2333–2339. doi: 10.1016/0016-7037(94)90014-0

Beusen, A. H. W., Bouwman, A. F., Van Beek, L. P. H., Mogollón, J. M., and Middelburg, J. J. (2016). Global riverine N and P transport to ocean increased during the 20th century despite increased retention along the aquatic continuum. *Biogeosciences* 13, 2441–2451. doi: 10.5194/bg-13-2441-2016

Bouwman, A. F., Van Drecht, G., Knoop, J. M., Beusen, A. H. W., and Meinardi, C. R. (2005). Exploring changes in river nitrogen export to the world's oceans. *Global Biogeochem. Cycles* 19:GB1002. doi: 10.1029/2004GB002314

Carpenter, E. J., Montoya, J. P., Burns, J., Mulholland, M. R., Subramaniam, A., and Capone, D. G. (1999). Extensive bloom of a N2-fixing diatom/cyanobacterial association in the tropical Atlantic Ocean. *Mar. Ecol. Prog. Ser.* 185, 273–283. doi: 10.3354/meps185273

Chen, C. T. (2008). Distributions of nutrients in the East China Sea and the South China Sea connection. *J. Oceanogr.* 64, 737–751. doi: 10.1007/s10872-008-0062-9

Chen, C. T., and Wang, S. L. (1999). Carbon, alkalinity and nutrient budgets on the East China Sea continental shelf. *J. Geophys. Res.* 104, 20675–20686. doi: 10.1029/1999JC900055

Chisholm, S. W., Frankel, S. L., Goericke, R., Olson, R. J., Palenik, B., Waterbury, J. B., et al. (1992). *Prochlorococcus marinus* nov. gen. nov. sp.: an oxyphototrophic marine prokaryote containing divinyl chlorophyll a and b. *Arch. Microbiol.* 157, 297–300. doi: 10.1007/BF00245165

Chong, L. S., Berelson, W. M., Mcmanus, J., Hammond, D. E., Rollins, N. E., and Yager, P. L. (2014). Carbon and biogenic silica export influenced by the Amazon River Plume: patterns of remineralization in deep-sea sediments. *Deep Sea Res. I* 85, 124–137. doi: doi:10.1016/j.dsr.2013.12.007

Coles, V. J., Brooks, M. T., Hopkins, J., Stukel, M. R., Yager, P. L., and Hood, R. R. (2013). The pathways and properties of the Amazon River Plume in the tropical North Atlantic Ocean. *J. Geophys. Res.* 118, 6894–6913. doi: 10.1002/2013JC008981

Conroy, B. J., Steinberg, D. K., Song, B., Kalmbach, A., Carpenter, E. J., and Foster, R. A. (2017). Mesozooplankton Graze on cyanobacteria in the Amazon river plume and western tropical north Atlantic. *Front. Microbiol.* 8:1436. doi: 10.3389/fmicb.2017.01436

Conroy, B. J., Steinberg, D. K., Stukel, M. R., Goes, J. I., and Coles, V. J. (2016). Meso- and microzooplankton grazing in the Amazon River plume and western

tropical North Atlantic. *Limnol. Oceanogr.* 61, 825–840. doi: 10.3389/fmicb.2017.01436

Dandonneau, Y., and Niang, A. (2007). Assemblages of phytoplankton pigments along a shipping line through the North Atlantic and tropical Pacific. *Prog. Oceanogr.* 73, 127–144. doi: 10.1016/j.pocean.2007.02.003

Davidson, E. A., de Araújo, A. C., Artaxo, P., Balch, J. K., Brown, I. F., C, Bustamante, M. M., et al. (2012). The Amazon basin in transition. *Nature* 481, 321–328. doi: 10.1038/nature10717

Del Vecchio, R., and Subramaniam, A. (2004). Influence of the Amazon River on the surface optical properties of the western tropical North Atlantic Ocean. *J. Geophys. Res.* 109:C11001. doi: 10.1029/2004JC002503

DeMaster, D. J. (1996). Biogeochemical processes in Amazon shelf waters: chemical distributions and uptake rates of silicon, carbon and nitrogen. *Continent. Shelf Res.* 16, 617–643. doi: 10.1016/0278-4343(95)00048-8

Dutkiewicz, S., Follows, M. J., and Bragg, J. G. (2009). Modeling the coupling of ocean ecology and biogeochemistry. *Global Biogeochem. Cycles* 23:GB4017. doi: 10.1029/2008GB003405

Dutkiewicz, S., Ward, B. A., Monteiro, F., and Follows, M. J. (2012). Interconnection of nitrogen fixers and iron in the Pacific Ocean: theory and numerical simulations. *Global Biogeochem. Cycles* 26:GB1012. doi: 10.1029/2011GB004039

Edmond, J. M., Spivack, A., Grant, B. C., Ming-Hui, H., Zexiam Chen, S., and Zeng Xiushau, C. (1985). Chemical dynamics of the Changjiang estuary. *Continent. Shelf Res.* 4, 17–36. doi: 10.1016/0278-4343(85)90019-6

Falkowski, P. G., and Davis, C. S. (2004). Natural proportions. *Nature* 431:131. doi: 10.1038/431131a

Foster, R. A., Kuypers, M. M. M., Vagner, T., Paerl, R. W., Musat, N., and Zehr, J. P. (2011). Nitrogen fixation and transfer in open ocean diatom–cyanobacterial symbioses. *ISME J.* 5, 1484–1493. doi: 10.1038/ismej.2011.26

Foster, R. A., Subramaniam, A., Mahaffey, C., Carpenter, E. J., Capone, D. G., and Zehr, J. P. (2007). Influence of the Amazon River plume on distributions of free-living and symbiotic cyanobacteria in the western tropical north Atlantic Ocean. *Limnol. Oceanogr.* 52, 517–532. doi: 10.4319/lo.2007.52.2.0517

Fox, L. E., Sager, S. L., and Wofsy, S. C. (1986). The chemical control of soluble phosphorus in the Amazon estuary. *Geochim. Cosmochim. Acta* 50, 783–794. doi: 10.1016/0016-7037(86)90354-6

Furuya, K., Hayashi, M., Yabushita, Y., and Ishikawa, A. (2003). Phytoplankton dynamics in the East China Sea in spring and summer as revealed by HPLC-derived pigment signatures. *Deep Sea Res. II* 50, 367–387. doi: 10.1016/S0967-0645(02)00460-5

Glibert, P. M., Allen, J. I., Bouwman, A. F., Brown, C. W., Flynn, K. J., Lewitus, A. J., et al. (2010). Modeling of HABs and eutrophication: status, advances, challenges. *J. Mar. Syst.* 83, 262–275. doi: 10.1016/j.jmarsys.2010.05.004

Glibert, P. M., Maranger, R., Sobota, D. J., and Bouwman, L. (2014). The Haber Bosch–harmful algal bloom (HB–HAB) link. *Environ. Res. Lett.* 9:105001. doi: 10.1088/1748-9326/9/10/105001

Goes, J. I., Gomes, H. D. R., Chekalyuk, A. M., Carpenter, E. J., Montoya, J. P., Coles, V. J., et al. (2014). Influence of the Amazon River discharge on the biogeography of phytoplankton communities in the western tropical north Atlantic. *Prog. Oceanogr.* 120, 29–40. doi: 10.1016/j.pocean.2013.07.010

Goldman, J. C., Mccarthy, J. J., and Peavey, D. G. (1979). Growth rate influence on the chemical composition of phytoplankton in oceanic waters. *Nature* 279:210. doi: 10.1038/279210a0

Guo, S., Feng, Y., Wang, L., Dai, M., Liu, Z., Bai, Y., et al. (2014). Seasonal variation in the phytoplankton community of a continental-shelf sea: the East China Sea. *Mar. Ecol. Progr. Ser.* 516, 103–126. doi: 10.3354/meps10952

Haraguchi, L., Carstensen, J., Abreu, P. C., and Odebrecht, C. (2015). Long-term changes of the phytoplankton community and biomass in the subtropical shallow Patos Lagoon Estuary. Brazil. *Estuar. Coast. Shelf Sci.* 162, 76–87. doi: 10.1016/j.ecss.2015.03.007

Harding, L. W., Adolf, J. E., Mallonee, M. E., Miller, W. D., Gallegos, C. L., Perry, E. S., et al. (2015). Climate effects on phytoplankton floral composition in Chesapeake Bay. *Estuar. Coast. Shelf Sci.* 162, 53–68. doi: 10.1038/srep23773

Heisler, J., Glibert, P. M., Burkholder, J. M., Anderson, D. M., Cochlan, W., Dennison, W. C., et al. (2008). Eutrophication and harmful algal blooms: a scientific consensus. *Harmful Algae* 8, 3–13. doi: 10.1016/j.hal.2008.08.006

Higgins, H. W., Wright, S. W., and Schlüter, L. (2011). *Quantitative Interpretation of Chemotaxonomic Pigment Data: Phytoplankton Pigments: Characterization, Chemotaxonomy and Applications in Oceanography*. London: Cambridge University Press.

Hillebrand, H., Steinert, G., Boersma, M., Malzahn, A., Meunier, C. L., Plum, C., et al. (2013). Goldman revisited: faster-growing phytoplankton has lower N : P and lower stoichiometric flexibility. *Limnol. Oceanogr.* 58, 2076–2088. doi: 10.4319/lo.2013.58.6.2076

Hooker, S. B., Heukelem, L. V., Thomas, C. S., Claustre, H., Ras, J., Barlow, R., et al. (2005). *The Second SeaWiFS HPLC Analysis Round Robin Experiment (SeaHARRE-2)*. Greenbelt, MD: NASA Goddard Space Flight Center.

Hu, C., Montgomery, E. T., Schmitt, R. W., and Muller-Karger, F. E. (2004). The dispersal of the Amazon and Orinoco River water in the tropical Atlantic and Caribbean Sea: observation from space and S-PALACE floats. *Deep Sea Res. II* 51, 1151–1171. doi: 10.1016/S0967-0645(04)00105-5

Jiang, Z., Liu, J., Chen, J., Chen, Q., Yan, X., Xuan, J., et al. (2014). Responses of summer phytoplankton community to drastic environmental changes in the Changjiang (Yangtze River) estuary during the past 50 years. *Water Res.* 54, 1–11. doi: 10.1016/j.watres.2014.01.032

Jiao, N., Yang, Y., Hong, N., Ma, Y., Harada, S., Koshikawa, H., et al. (2005). Dynamics of autotrophic picoplankton and heterotrophic bacteria in the East China Sea. *Continent. Shelf Res.* 25, 1265–1279. doi: 10.1016/j.csr.2005.01.002

Jickells, T. D., Buitenhuis, E., Altieri, K., Baker, A. R., Capone, D., Duce, R. A., et al. (2017). A reevaluation of the magnitude and impacts of anthropogenic atmospheric nitrogen inputs on the ocean. *Global Biogeochem. Cycles* 31, 289–305. doi: 10.1002/2016GB005586

Knapp, A. N. (2012). The sensitivity of marine N(2) fixation to dissolved inorganic nitrogen. *Front. Microbiol.* 3:374. doi: 10.3389/fmicb.2012.00374

Latasa, M. (2007). Improving estimations of phytoplankton class abundances using CHEMTAX. *Mar. Ecol. Progr. Ser.* 329, 13–21. doi: 10.3354/meps329013

Li, J., Glibert, P. M., Zhou, M., Lu, S., and Lu, D. (2009). Relationships between nitrogen and phosphorus forms and ratios and the development of dinoflagellate blooms in the East China Sea. *Mar. Ecol. Progr. Ser.* 383, 11–26. doi: 10.3354/meps07975

Mackey, M. D., Dj, M., Hw, H., and Sw, W. (1996). CHEMTAX - a program for estimating class abundances from chemical markers: application to HPLC measurements of phytoplankton. *Mar. Ecol. Progr. Ser.* 144, 265–283. doi: 10.3354/meps144265

Muller-Karger, F. E., Mcclain, C. R., and Richardson, P. L. (1988). The dispersal of the Amazon's water. *Nature* 333, 56–59. doi: 10.1038/333056a0

Nature Geoscience (2014). Eighty years of Redfield. *Nat. Geosci.* 7:849.

Qiu, D., Huang, L., Zhang, J., and Lin, S. (2010). Phytoplankton dynamics in and near the highly eutrophic Pearl River Estuary. South China Sea. *Continent. Shelf Res.* 30, 177–186. doi: 10.1016/j.marpolbul.2011.01.018

Seitzinger, S. P., Mayorga, E., Bouwman, A. F., Kroeze, C., Beusen, A. H. W., Billen, G., et al. (2010). Global river nutrient export: a scenario analysis of past and future trends. *Global Biogeochem. Cycles* 24:GB0A08. doi: 10.1016/j.scitotenv.2009.12.015

Serive, B., Nicolau, E., Bérard, J.-B., Kaas, R., Pasquet, V., Picot, L., et al. (2017). Community analysis of pigment patterns from 37 microalgae strains reveals new carotenoids and porphyrins characteristic of distinct strains and taxonomic groups. *PLoS One* 12:e0171872. doi: 10.1371/journal.pone.0171872

Sharples, J., Middelburg, J. J., Fennel, K., and Jickells, T. D. (2017). What proportion of riverine nutrients reaches the open ocean? *Global Biogeochem. Cycles* 31, 39–58. doi: 10.1002/2016GB005483

Shipe, R. F., Curtaz, J., Subramaniam, A., Carpenter, E. J., and Capone, D. G. (2006). Diatom biomass and productivity in oceanic and plume-influenced waters of the western tropical Atlantic ocean. *Deep Sea Res. I* 53, 1320–1334. doi: 10.1016/j.dsr.2006.05.013

Sorribas, M. V., Paiva, R. C. D., Melack, J. M., Bravo, J. M., Jones, C., Carvalho, L., et al. (2016). Projections of climate change effects on discharge and inundation in the Amazon basin. *Clim. Change* 136, 555–570. doi: 10.1007/s10584-016-1640-2

Stukel, M. R., Coles, V. J., Brooks, M. T., and Hood, R. R. (2014). Top-down, bottom-up and physical controls on diatom-diazotroph assemblage growth in the Amazon River plume. *Biogeosciences* 11, 3259–3278. doi: 10.5194/bg-11-3259-2014

Subramaniam, A., Yager, P. L., Carpenter, E. J., Mahaffey, C., Björkman, K., Cooley, S., et al. (2008). Amazon River enhances diazotrophy and carbon sequestration in the tropical North Atlantic Ocean. *Proc. Natl. Acad. Sci. U.S.A.* 105, 10460–10465. doi: 10.1073/pnas.0710279105

Sukigara, C., Mino, Y., Tripathy, S. C., Ishizaka, J., and Matsuno, T. (2017). Impacts of the Changjiang diluted water on sinking processes of particulate organic matters in the East China Sea. *Continent. Shelf Res.* 151, 84–93. doi: 10.1016/j.csr.2017.10.012

Swan, C. M., Vogt, M., Gruber, N., and Laufkoetter, C. (2016). A global seasonal surface ocean climatology of phytoplankton types based on CHEMTAX analysis of HPLC pigments. *Deep Sea Res. I* 109, 137–156. doi: 10.1016/j.dsr.2015.12.002

Tilman, D. (1977). Resource competition between plankton algae: an experimental and theoretical approach. *Ecology* 58, 338–348. doi: 10.2307/1935608

Torrecilla, E., Stramski, D., Reynolds, R. A., Millán-Núñez, E., and Piera, J. (2011). Cluster analysis of hyperspectral optical data for discriminating phytoplankton pigment assemblages in the open ocean. *Remote Sens. Environ.* 115, 2578–2593. doi: 10.1016/j.rse.2011.05.014

Tseng, Y. F., Lin, J., Dai, M., and Kao, S. J. (2014). Joint effect of freshwater plume and coastal upwelling on phytoplankton growth off the Changjiang River. *Biogeosciences* 11, 409–423. doi: 10.5194/bg-11-409-2014

van der Struijk, L. F., and Kroeze, C. (2010). Future trends in nutrient export to the coastal waters of South America: implications for occurrence of eutrophication. *Global Biogeochem. Cycles* 24, doi: 10.1029/2009GB003572

Van Heukelem, L., and Thomas, C. S. (2001). Computer-assisted high-performance liquid chromatography method development with applications to the isolation and analysis of phytoplankton pigments. *J. Chromatogr. A* 910, 31–49. doi: 10.1016/S0378-4347(00)00603-4

Vidussi, F., Claustre, H., Manca, B., Luchetta, A., and Marty, J. C. (2001). Phytoplankton pigment distribution in relation to upper thermocline circulation in the eastern Mediterranean Sea during winter. *J. Geophys. Res.* 106, 939–959. doi: 10.1029/1999JC000308

Wang, B., and Wang, X. (2007). Chemical hydrography of coastal upwelling in the East China Sea. *Chin. J. Oceanol. Limnol.* 25, 16–26. doi: 10.1007/s00343-007-0016-x

Ward, B. A., Dutkiewicz, S., and Follows, M. J. (2014). Modelling spatial and temporal patterns in size-structured marine plankton communities: top–down and bottom–up controls. *J. Plank. Res.* 36, 31–47. doi: 10.1093/plankt/fbt097

Ward, B. A., Dutkiewicz, S., Jahn, O., and Follows, M. J. (2012). A size-structured food-web model for the global ocean. *Limnol. Oceanogr.* 57, 1877–1891. doi: 10.4319/lo.2012.57.6.1877

Ward, B. A., Dutkiewicz, S., Moore, C. M., and Follows, M. J. (2013). Iron, phosphorus, and nitrogen supply ratios define the biogeography of nitrogen fixation. *Limnol. Oceanogr.* 58, 2059–2075. doi: 10.4319/lo.2013.58.6.2059

Weber, S. C., Carpenter, E. J., Coles, V. J., Yager, P. L., Goes, J., and Montoya, J. P. (2017). Amazon River influence on nitrogen fixation and export production in the western tropical North Atlantic. *Limnol. Oceanogr.* 62, 618–631. doi: 10.1002/lno.10448

Wolf, C., Frickenhaus, S., Kilias, E. S., Peeken, I., and Metfies, K. (2014). Protist community composition in the Pacific sector of the Southern Ocean during austral summer 2010. *Polar Biol.* 37, 375–389. doi: 10.1007/s00300-013-1438-x

Wong, G. T. F., Gong, G. C., Liu, K. K., and Pai, S. C. (1998). 'Excess Nitrate' in the East China Sea. *Estuar. Coast. Shelf Sci.* 46, 411–418. doi: 10.1006/ecss.1997.0287

Wood, F. E. J. (1966). A Phytoplankton Study of the Amazon Region. *Bull. Mar. Sci.* 16, 102–123.

Wright, S., and Jeffrey, S. W. (2006). "Pigment markers for phytoplankton production," in *Marine Organic Matter: Biomarkers, Isotopes and DNA*, ed. J. Volkman (Berlin: Springer), 71–104. doi: 10.1007/698_2_003

Wright, S. W. (2005). *Analysis of Phytoplankton Populations using Pigment Markers. Course Notes for a Workshop Pigment Analysis of Antarctic Microorganisms*. Kuala Lumpur: University of Malaya,

Xu, Q., Sukigara, C., Goes, J. I., Do Rosario Gomes, H., Zhu, Y., Wang, S., et al. (2018). Interannual changes in summer phytoplankton community composition in relation to water mass variability in the East China Sea. *J. Oceanogr.* 322, 31–47. doi: 10.1007/s10872-018-0484-y

Yan, W., Mayorga, E., Li, X., Seitzinger, S. P., and Bouwman, A. F. (2010). Increasing anthropogenic nitrogen inputs and riverine DIN exports from the Changjiang River basin under changing human pressures0. *Global Biogeochem. Cycles* 24:GB0A06. doi: 10.1029/2009GB003575

Yang, D., Yin, B., Liu, Z., Bai, T., Qi, J., and Chen, H. (2012). Numerical study on the pattern and origins of Kuroshio branches in the bottom water of southern East China Sea in summer. *J. Geophys. Res.* 117:C05015. doi: 10.1029/2011JC007528

Yang, D., Yin, B., Sun, J., and Zhang, Y. (2013). Numerical study on the origins and the forcing mechanism of the phosphate in upwelling areas off the coast of Zhejiang province, China in summer. *J. Mar. Syst.* 12, 1–18. doi: 10.1016/j.jmarsys.2013.04.002

Zhang, J., Liu, S. M., Ren, J. L., Wu, Y., and Zhang, G. L. (2007). Nutrient gradients from the eutrophic Changjiang (Yangtze River) Estuary to the oligotrophic Kuroshio waters and re-evaluation of budgets for the East China Sea Shelf. *Progr. Oceanogr.* 74, 449–478. doi: 10.1016/j.pocean.2007.04.019

Zhou, M.-J., Shen, Z.-L., and Yu, R.-C. (2008). Responses of a coastal phytoplankton community to increased nutrient input from the Changjiang (Yangtze) River. *Continent. Shelf Res.* 28, 1483–1489. doi: 10.1016/j.csr.2007.02.009

Conflict of Interest Statement: The authors declare that the research was conducted in the absence of any commercial or financial relationships that could be construed as a potential conflict of interest.

frontiers in Environmental Science

ORIGINAL RESEARCH
published: 28 June 2018
doi: 10.3389/fenvs.2018.00062

Bioavailability of Dissolved Organic Phosphorus in Temperate Lakes

Seth K. Thompson[1]* *and James B. Cotner*[2]

[1] Water Resource Science Program, University of Minnesota, St. Paul, MN, United States, [2] Department of Ecology, Evolution and Behavior, University of Minnesota, St. Paul, MN, United States

Freshwater aquatic systems are biogeochemical hotspots, with heterotrophic bacteria rapidly cycling the compounds that pass through them. P is a key nutrient that controls primary production in many freshwater ecosystems and is important for understanding eutrophication in lakes. Previous work has often focused on the dynamics of inorganic phosphorus and its impact on primary production, however, the role of nutrients bound in more complex organic forms (such as dissolved organic phosphorus, DOP) in supporting primary production and harmful algal blooms has been neglected. Here, we quantify the bioavailability of dissolved organic carbon (DOC) and DOP in 27 aquatic systems across the Upper Midwest United States. Using exponential decay models, long-term nutrient degradation assays revealed that decay constants for DOP ranged from −0.001 per day to −0.12 per day with a median value of −0.01 per day. These rates were geographically variable and were as high or higher than DOC decay constants, which ranged from −0.003 per day to −0.024 per day with a median value of −0.01 per day. Additionally, total bioavailability of DOP ranged from 0 to 100% with a median value of 78% of the DOP pool, demonstrating that DOP bioavailability was highly variable across systems. In contrast, bioavailable DOC was more tightly constrained with values ranging from 4.37 to 53.81% of the total DOC pool with a median value of 24.95%. DOP bioavailability was negatively correlated with the DOC:DOP of the organic matter pool, suggesting that bioavailable DOP is drawn down in systems that are more likely to be P limited. Finally, we show that including estimates of DOC and DOP bioavailability reduces estimates of elemental imbalance experienced by aquatic bacteria.

Keywords: phosphorus, carbon, bioavailability, dissolved organic matter, degradation

OPEN ACCESS

Edited by:
Solange Duhamel, Lamont Doherty Earth Observatory (LDEO), United States

Reviewed by:
Monika Nausch, Leibniz Institute for Baltic Sea Research (LG), Germany
Martin Tucker Auer, Michigan Technological University, United States

***Correspondence:**
Seth K. Thompson
thom2587@umn.edu

Specialty section:
This article was submitted to Freshwater Science, a section of the journal Frontiers in Environmental Science

Received: *24 March 2018*
Accepted: *07 June 2018*
Published: *28 June 2018*

Citation:
Thompson SK and Cotner JB (2018) Bioavailability of Dissolved Organic Phosphorus in Temperate Lakes. Front. Environ. Sci. 6:62. doi: 10.3389/fenvs.2018.00062

INTRODUCTION

Freshwater systems are incredibly active biogeochemical hot spots, particularly with regards to the processing of organic matter (Cole et al., 2007; Tranvik et al., 2009). Heterotrophic bacteria are major biogeochemical players in aquatic systems (Cotner and Biddanda, 2002) and understanding how these microbes interact with organic matter is fundamental to predicting the flow of energy and nutrients through freshwaters. Dissolved organic matter (DOM) is a major resource pool for aquatic bacteria and has been the focus of numerous studies over the last 20 years. The vast majority of this work has focused on understanding how microbial modifications of DOM influence global carbon cycle processes, but it is important to remember that DOM is not solely composed of carbon. Microbial interactions with DOM are also likely important for understanding other biogeochemical

cycles in freshwater such as the phosphorus (P) cycle, but our understanding of the role DOM plays in these other nutrient cycles remains limited (Maranger et al., 2018).

Humans have had profound impacts on the global P cycle by increasing the annual flux of P through ecosystems by a factor of 4–8 (Falkowski, 2000; Schlesinger and Bernhardt, 2013). This has important biogeochemical implications and has resulted in the eutrophication of freshwater systems worldwide leading to degraded water quality on a global scale. Fundamentally, eutrophication is a biogeochemical imbalance, where excess nutrients, often P in freshwater (Schindler et al., 2008), result in excessive accumulation of carbon (C) in the form of increased algal biomass. This continued anthropogenic modification of freshwater nutrient and organic matter pools, together with observations of shifts in planktonic community composition and organic nutrient pools (Teubner et al., 2003) suggest that the bioavailability of organic nutrient pools could an important factor affecting auto-heterotrophic coupling as well as harmful algal blooms.

Previous work has often explored the role of a single inorganic nutrient controlling primary production, but our rapidly evolving understanding suggests more complex scenarios are likely involved. Specifically, there is a growing appreciation for the role of nutrients bound in complex organic forms (such as dissolved organic phosphorus, DOP) in acting as important resources for aquatic organisms (Jackson and Williams, 1985; Cotner and Wetzel, 1992; Björkman and Karl, 2003; Nausch and Nausch, 2007; Soares et al., 2017). Therefore, it is imperative to understand the bioavailability of DOP in natural systems in order to better predict its capacity to serve as a resource in the absence of (or supplementary to) inorganic phosphorus. Furthermore, understanding the composition and bioavailability of nutrients and organic matter, not just the total quantities in a system have been shown to have important impacts on the formation and toxicity of harmful algal blooms (Anderson et al., 2002; Donald et al., 2011) providing another compelling reason to further study DOP bioavailability in freshwater systems.

Organic P is the dominant form of P in most freshwater systems with DOP typically comprising 25–50% of the total P pool (Wetzel, 2001). Many studies have clearly demonstrated that at least some forms of DOP can serve as a P source for primary and secondary producers (Cotner and Wetzel, 1992; Björkman and Karl, 2003; Nausch and Nausch, 2007; Li and Brett, 2013) and DOP is therefore likely an important source of P when inorganic P is limited. While there have been some studies on DOP bioavailability specific to freshwater systems (Sonzogni et al., 1982; Boström et al., 1988; Cotner and Wetzel, 1992; Li and Brett, 2013), more studies have examined this topic in marine systems (Björkman and Karl, 1994; Ruttenberg and Sonya, 2005; Dyhrman and Ruttenberg, 2006; Nausch and Nausch, 2006, 2007). Nonetheless, in both marine and freshwaters, a portion of the DOP pool is readily available for assimilation into planktonic organisms. The relative bioavailability of specific DOP compounds can range from almost 0% to over 90% (Li and Brett, 2013). While these studies have clearly suggested that DOP may be an important source of P for aquatic microorganisms, few studies have quantified bioavailable DOP in freshwater systems or examined how organic matter stoichiometry may affect the bioavailability of DOP compounds. In this paper, we present results from DOM bioavailability assays from 27 aquatic systems in the Upper Midwest of the USA. Our goal was to quantify the bioavailability of DOC and DOP from a diverse set of aquatic ecosystems and explore the potential environmental drivers of DOM bioavailability.

MATERIALS AND METHODS

Study Sites and Sample Collection

During the summer season (June–September) water was collected from 27 freshwater systems (24 lakes and 3 streams) in Minnesota and South Dakota (Supplementary Figure 1) from the upper mixed layer (0–2 m of depth) using a Van Dorn water sampler. The 27 systems covered three different Level III ecoregions as defined by the United States Environmental Protection Agency: The Black Hills in Western South Dakota (Middle Rockies), Itasca State Park in North Minnesota (Northern Lakes and Forests), and the Twin Cities greater metropolitan area (North Central Hardwood Forests). The Black Hills and Itasca State Park systems are relatively pristine systems with watersheds primarily dominated by coniferous forest whereas the Twin Cities greater metropolitan area is highly human impacted with watersheds dominated by hardwoods with urban land use or small-scale agriculture. General characteristics of each lake system can be found in **Table 1**.

Samples were collected in acid-washed HDPE amber bottles after pre-rinsing them with ∼100 ml of sample water. Samples were stored on ice until they could be returned to the lab (always less than 4 h), where they were stored at 4°C until processed (<72 h). For processing, ∼100 ml of water was filtered through pre-combusted 0.7 μm nominal pore-size glass-fiber filters (Whatman, GF/F) and collected in pre-combusted borosilicate vials. Twenty milliliters of this sample was acidified with 10% HCL and used to measure total dissolved organic carbon (DOC) and total dissolved nitrogen (TDN) on a Shimadzu TOC-L auto-analyzer with a TNM-L module (CSH/CSN model, Shimadzu Corp). Another 20 ml of filtrate was reserved for absorbance scans (wavelengths from 200 to 800 nm) using a Cary 50 spectrophotometer, which was used to calculate the specific UV absorbance at a wavelength of 254 nm (SUVA). The remaining 60 ml of sample was used to measure total dissolved phosphorus (TDP), and soluble reactive phosphorus (SRP) using a molybdenum blue reaction with and without acid-persulfate digestion (Murphy and Riley, 1962). DOP was calculated as the difference between TDP and SRP. Additionally, the GF/F filters were collected for fluorometric quantification of chlorophyll-a after being extracted in 90% acetone (Standard Methods, 2005).

DOM Degradation Assays

DOM degradation assays were performed as long-term dark bottle incubations. Within 72 h of collecting each sample, 900 ml of lake water was filter-sterilized using a 0.22 μm pore-size filter (EMD Millipore Steritop Filters) and collected in a pre-combusted 1 L amber glass bottle. Each bottle was inoculated with 100 ml of water from the same lake that had been filtered

TABLE 1 | Table showing general characteristics of each of the 27 sampling sites.

Name	Region	DIC (μM)	DOC (μM)	TDN (μM	TDP (μM)	SRP (μM)	DOP (μM)	Chl-a (μg/L)	SUVA (L/(mg*m))	pH	Alkalinity (μeq/L)
Bismark	Black hills	1,097	790	53.5	0.49	0.06	0.43	10.29	2.40	7.5	1,157
Canyon lake	Black hills	3,051	165	13.8	0.22	0.16	0.07	0.35	1.11	8.3	3,042
Center	Black hills	779	514	21.1	0.27	0.06	0.21	4.09	2.25	7.7	830
Dark canyon	Black hills	2,912	168	6.2	0.07	<0.038	>0.32	0.25	1.38	8.6	2,939
Deerfield	Black hills	3,780	236	10.3	0.24	0.04	0.19	2.18	1.47	8.6	3,799
Pactola	Black hills	2,914	197	10.3	0.17	0.11	0.06	2.00	1.21	8.4	2,964
Roubaix	Black hills	2,623	207	10.7	0.20	0.08	0.12	5.34	2.90	8.5	2,615
Sheriden	Black hills	2,366	430	18.3	0.24	0.12	0.12	6.83	1.55	8.5	2,398
Stockade	Black hills	1,952	800	40.0	0.61	0.31	0.29	12.21	1.97	8.5	2,024
Sylvan	Black hills	803	552	22.1	0.27	0.06	0.21	8.11	1.69	8.5	857
Arco	Itasca	920	515	31.0	0.13	0.07	0.06	5.14	1.38	7.5	830
Boot	Itasca	3,086	363	19.8	0.33	0.17	0.16	1.55	1.25	8.4	2,848
Deming	Itasca	1,206	733	35.3	0.25	0.08	0.17	10.85	1.60	8.0	1,145
E. Twin	Itasca	3,083	701	28.3	0.34	0.06	0.28	3.13	2.32	7.9	2,991
Elk	Itasca	2,526	568	28.4	0.95	0.11	0.84	2.86	1.74	8.5	2,913
Itasca	Itasca	3,372	421	23.3	0.35	0.16	0.19	6.58	1.83	8.5	3,101
Josephine	Itasca	604	520	29.0	0.42	0.20	0.23	1.34	1.27	7.8	555
Long	Itasca	3,005	304	18.3	0.34	0.17	0.17	1.04	0.86	8.5	3,059
Mary	Itasca	2,847	627	26.1	0.10	0.06	0.04	1.47	1.98	8.4	2,860
Ozawindib	Itasca	1,603	690	33.0	0.35	0.05	0.30	1.92	2.25	8.2	1,631
Beckman	Twin Cities	180	993	35.0	0.14	0.05	0.09	28.27	2.30	5.4	29
Cedar Bog	Twin Cities	1,030	971	34.9	1.03	0.57	0.47	57.19	3.69	6.9	1,039
Fish	Twin Cities	374	639	40.2	0.21	0.13	0.08	–	1.78	9.2	552
Como	Twin Cities	754	738	31.8	2.31	2.16	0.15	9.61	1.83	9.1	770
Staring Creek N	Twin Cities	2,806	797	51.9	0.72	0.58	0.15	–	3.65	8.0	2,203
Staring Creek S	Twin Cities	2,303	797	48.2	0.50	0.14	0.36	–	3.05	7.9	2,292
Staring Lake	Twin Cities	2,180	805	49.9	0.50	0.11	0.39	10.29	2.82	7.8	2,718

through a 1.6 μm pore-size glass fiber filter (Whatman, GF/A). While this approach did not standardize for the absolute inoculum size (i.e., number of bacterial cells), it did provided a consistent relative inoculum source for each assay of 10% by volume, similar to previous work (Wiegner et al., 2006; Lønborg et al., 2009; Vonk et al., 2015). Furthermore, the relative size of the inoculum has been shown to have little to no effect on the overall degradation of DOC (Vonk et al., 2015). These bottles were incubated in the dark at 20°C for a minimum of 230 days. Periodically throughout the incubation period (approximately monthly for the first 6 months and less often subsequently), 100 ml samples were removed from the incubations. These samples were filtered using pre-combusted GF/F filters and DOC, TDN, DOP, SRP, and absorbance scans were measured as described above.

Data Analysis

To calculate DOM degradation rates, data were fitted to 3 unique models (linear, 2 component exponential, and 3 component exponential) and the model fit was compared using Akaike information criterion (AIC) scores. Because model fits were variable for different portions of the DOM pool, relative bioavailability of DOC and DOP was calculated by dividing the maximum nutrient loss (initial concentration minus the minimum measured concentration during the incubation period) by the starting concentration to obtain the percentage of the total pool that was degraded. This approach allowed for the direct comparison of relative lability between the DOP and DOC pools. The relationships between bioavailability and environmental parameters (such as SUVA, nutrients, etc.) were examined using simple linear regression. All analysis was performed using JMP® version 13 (SAS Institute Inc., Cary, NC, 1989–2007).

RESULTS

Bulk Nutrient Analysis

The 27 systems studied covered a trophic gradient with chlorophyll-a values ranging from 0.25 μg/L to 57.19 μg/L and total dissolved phosphorus concentrations ranging from 0.07 μM to 2.31 μM (**Table 1**). Mean chlorophyll levels were much higher the Twin Cities region compared to the two less human-impacted regions and chlorophyll values were also more variable in the Twin Cities compared to the other two regions. SUVA values were calculated for each system by dividing the specific UV absorbance at 254 nm by the DOC concentration of the system. SUVA can be used as an index of the terrestrial contribution to the

DOM pool, with higher SUVA values indicating more terrestrial influence. We sampled systems that exhibited a range of SUVA values (from 0.86 to 3.69) to cover a gradient of terrestrial influence on the DOM pool. Across the three regions sampled, chlorophyll and the relative contribution of DOC to the total dissolved carbon pool (DOC:TDC) showed strong differences, but DOP concentration and the relative contribution of DOP to TDP did not (**Figure 1**). Also, our study sites showed no regional differences in TDP or SRP concentrations, despite the fact that others have shown strong differences in P concentrations across these ecoregions (Heiskary et al., 1987). Furthermore, DOP concentration was not significantly correlated with any of the measured lake characteristics (pH, alkalinity, chlorophyll, or SUVA), but was weakly positively correlated with DOC concentration and TDN concentration (**Figure 2**). Additionally, the Twin Cities dissolved carbon pool had a much higher fractional total organic carbon signature (with a median value of approximately 40% DOC) compared to the Black Hills and Itasca where DOC contributed less (11 and 18.5% respectively) to the dissolved carbon pool (**Figure 1**).

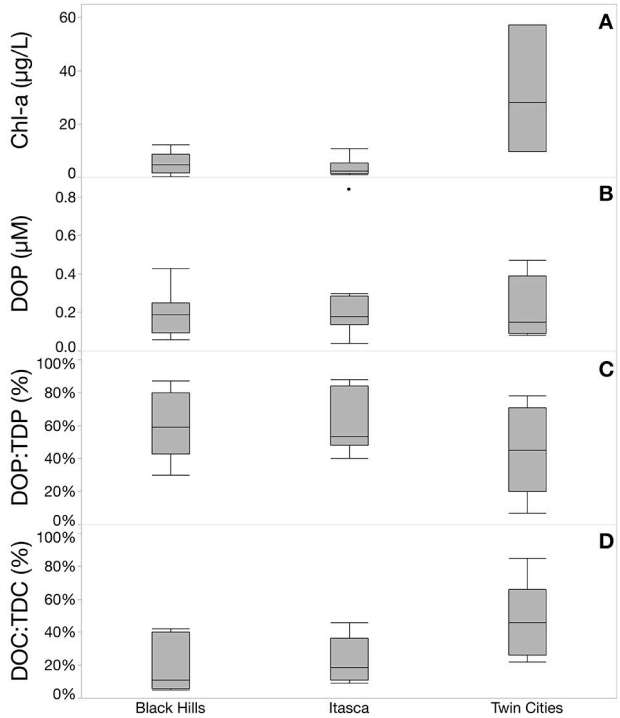

FIGURE 1 | Regional variability in measured lake characteristics. **(A)** Shows that chlorophyll concentrations were highest and most variable in the Twin Cities (urban) region. **(B)** Shows no significant differences in total DOP concentration across the three study regions and **(C)** shows no significant differences in the relative contribution of DOP to the total dissolved P pool, however the Twin Cities does show the largest range of relative DOP contribution. **(D)** Shows the contribution of DOC to the total dissolved carbon pool with the Twin Cities showing a much higher contribution of DOC compared to the other two regions, in other words, inorganic carbon dominates the dissolved carbon pool in the Black Hills and Itasca regions.

Degradation Rates of DOC and DOP

DOC degradation was best fit by an exponential decay model with a non-zero asymptote (Equation 1, model resulted in an R^2 value of 0.998 across all lakes; Supplementary Figure 2). Two lakes, Canyon Lake and Roubaix (both from the Black Hills region), resulted in model fits that had positive k values, despite both having lost DOC over the course of the incubation so they were excluded from analysis of DOC decay rates. In the remaining 25 lakes, k values ranged from −0.003 to −0.024 per day with a median value of −0.009 and quartiles of −0.006 and −0.013 or median turnover time of 111 days (**Figure 3**). DOC degradation rates were not significantly correlated to measured elemental pools (DOC, TDN, TDP, SRP) or lake characteristics (pH, chlorophyll, SUVA) and there were no significant differences in DOC decay rates across region.

$$DOC_t = BDOC^{kt} + DOC_R \quad (1)$$

Three parameter exponential decay model that was the best fit for long term DOC incubations where DOC_t is the concentration of DOC at time t, BDOC is the total pool of bioavailable DOC, k is the degradation rate, t is the time of incubation in days, and DOC_R is the size of the recalcitrant DOC pool.

TDP, SRP, and DOP incubations revealed turnover times of approximately 150 days. After this period, DOP concentrations tended to increase in the incubations suggesting internal cycling of DOP (see Supplementary Figure 3). Given that there were no external sources of P to these incubations, this increasing concentration of dissolved P likely resulted from the degradation of particulate P that had accumulated over the early portion of the incubation. To examine the degradation of DOP over the course of the incubation, we excluded all data points after 150 days of incubation and excluded points when the calculated DOP concentration was below zero (this only occurred in 6 of the 230 total measurements). A 2-parameter exponential fit model best described the DOP data [the same model as Equation (1), omitting the recalcitrant pool] resulting in a model with an overall r^2 value of 0.77.

DOP degradation rates (k) across the 27 lakes largely fell between 0 and −0.025 per day (22 of the 27 lakes). Three lakes had positive modeled k values with two of these systems in the Twin Cities metro area (Fish and Staring North) and one was in the Black Hills (Pactola, see supplementary data file). Because the model estimated k values were positive despite the fact that concentrations of DOP decreased in the incubations, these lakes were excluded from other analysis of DOP degradation rates. Additionally, two lakes form the Itasca region (Boot and Elk) had extreme negative k values of −0.096 and −0.123 respectively (**Figure 3**). The median value for all 27 systems was −0.010 corresponding to a median turnover time of 100 days. DOP degradation rates were not significantly correlated to measured elemental pools (DOC, TDN, TDP, SRP) or lake characteristics (pH, chlorophyll, SUVA).

To compare the relative rate of DOP turnover to DOC turnover, we calculated a k_{DOC}:k_{DOP} value for the 22 systems that had negative k values for both DOC and DOP. Overall, turnover

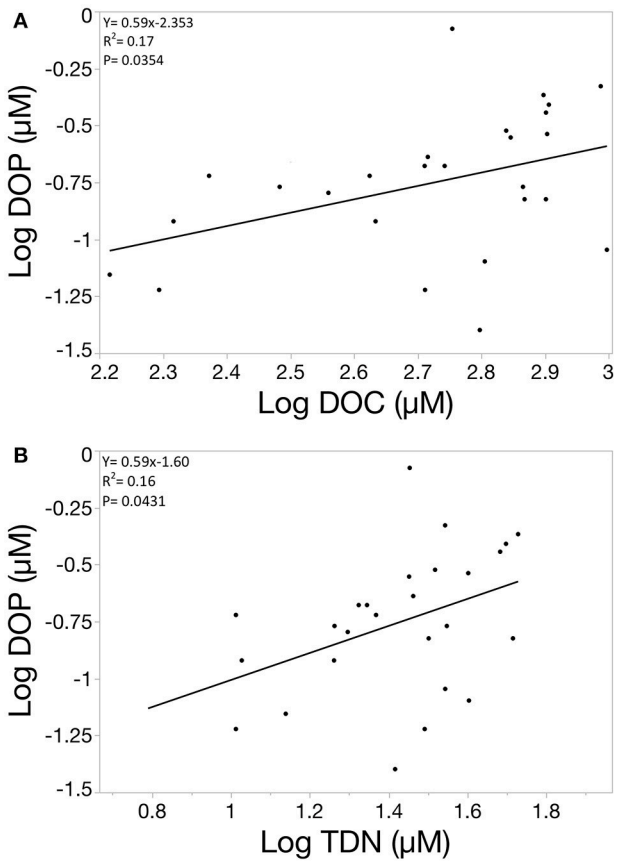

FIGURE 2 | Scatterplots showing the relationship between DOP and DOC **(A)** and between DOP and TDN **(B)**. All values are log transformed. DOP shows a significant positive correlation to both DOC and TDN, but the relationship is weak in both cases with R^2 values below 0.2 for both regressions.

rates of the two nutrients were remarkably similar with a median k_{DOC}:k_{DOP} of 0.98, upper quartile of 1.83, and lower quartile of 0.50. However, there were several lakes with more extreme values with the most extreme system having a DOP turnover rate nearly 20 times faster than DOC (Elk Lake in Itasca State Park). The Itasca region did have significantly lower k_{DOC}:k_{DOP} values than the other two regions (**Figure 4**, Chi Square Median test, $p = 0.0297$). The Itasca region also had a typical k_{DOC}:k_{DOP} value less than 1 (Wilcoxon signed-rank, $p = 0.014$), indicating that for this region DOP degradation constants were significantly higher than DOC degradation constants.

Estimates of DOC and DOP Bioavailability

It took approximately 9 months for degradation models to give reasonable predictions for the total size of the recalcitrant DOC pool (i.e., the 3 parameter fit models outperformed the 2 parameter fit models). Prior to 9 months, 2 parameter fit models outperformed the 3 parameter models so a clear asymptote was not indefinable. In contrast, for DOP, the 2-parameter fit model was always a better fit than 3 parameter fit model, so a modeled estimate of the recalcitrant DOP concentration was not possible. Therefore, in order to estimate and compare the relative sizes of the bioavailable pools of DOC and DOP, we calculated these values using the lowest measured value of DOC and DOP over the course of the incubation. By subtracting this lowest value from the starting concentration, we estimated the amount of DOC or DOP that had been degraded during the incubation period and used this as an estimator of the size of the BDOC and BDOP pools. BDOC values in these lakes ranged from ∼19 μM to ∼397 μM with a median value of 118 μM, and relative BDOC values ranged from 4.4 to 53.8% of the total DOC pool with a median value of 25.0% with no regional differences in BDOC. In contrast, a much larger portion of the DOP pool tended to be bioavailable. Eight systems had BDOP values over 95% of the total DOP pool and the median value for all the lakes was 78%. Relative BDOP was also more variable than BDOC and had an interquartile range of 40.8 to 97.5% compared to 21.0 to 30.6% for BDOC (**Figure 5**). Absolute values for BDOP concentrations ranged from 0.01 μM to 0.82 μM and three-quarters of the samples had BDOP concentrations below 0.26 μM. As with BDOC, there were no significant regional difference in BDOP.

In these systems, relative %BDOP was positively correlated to the initial concentration of DOP in the system, suggesting that systems with a larger DOP pools not only had more BDOP, but also had a larger fraction of the DOP pool that was bioavailable (**Figure 6**, $p = 0.0043$). Additionally, relative BDOP was negatively correlated to the initial DOC: DOP ratio, indicating that DOP was relatively less bioavailable when it was scarce relative to DOC (**Figure 7**, $p = 0.0002$). However, relative BDOP was not significantly correlated to other individual element pools (DOC, TDN, DIC) nor was it significantly correlated to any of the lake characteristics measured (pH, alkalinity, chlorophyll or SUVA). Temperature data were only available for the 10 lakes in the Itasca region, but within this subset of the data temperature was not a significant predictor of BDOP concentration or relative BDOP percentage. Absolute concentrations of BDOP also showed a strong negative correlation with the DOC:DOP ratio, suggesting that BDOP was being drawn down at high DOC:DOP ratios (**Figure 8**), but absolute BDOP was not significantly correlated to other elemental or lake characteristic measurements.

Relative %BDOC was not significantly correlated with any of the measured elemental parameters (initial DOC, TDN, TDP, SRP, DOP or DOC:TDN, DOC:TDP, DOC:SRP, or DOC:DOP). Interestingly, relative %BDOC was also not significantly correlated to SUVA but the absolute size of the BDOC pool did show a significant positive correlation with SUVA (**Figure 9**; $p = 0.0217$). This positive trend with SUVA is likely partially explained by the fact that high SUVA systems tend to be high in DOC (and the absolute amount of BDOC was strongly positively correlated to DOC concentration), but in combination with the fact that relative BDOC did not change with SUVA, this suggests that even systems dominated by more terrestrial-like organic matter contain large amounts of bioavailable DOC. Furthermore, absolute BDOC concentration was strongly positively correlated to TDN, TDP, and chlorophyll (**Figure 10**, $p < 0.0001$), consistent with the accumulation of labile DOC under high nutrient conditions and high productivity.

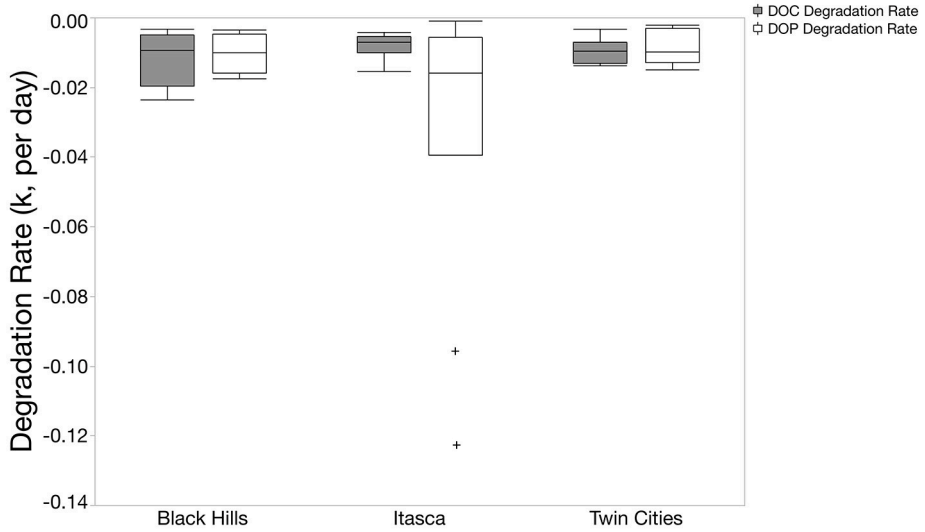

FIGURE 3 | Box and whisker plots of DOC and DOP degradation constants (k) from exponential decay models. Only lakes that had negative *k* values are included in this figure. In the Black Hills and Twin Cities regions, *k* values are very similar for DOC and DOP. However, DOP *k* values are more negative (meaning faster degradation) than DOC *k* values in the Itasca region. For figure including positive *k* values, see Supplementary Figure 1.

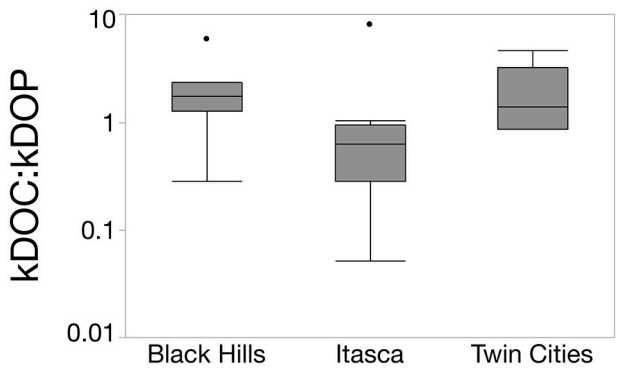

FIGURE 4 | Box and whisker plot showing the variability in kDOC:kDOP values across the three study regions. The Itasca region had a significantly lower value than the other two regions (Chi Square Median test, $p = 0.0297$) meaning DOP turnover was faster relative to DOC turnover in the Itasca region compared to the Black Hills and Twin Cities. The majority of samples form the Itasca region also had values less than 1, indicating that DOP was typically turning over faster than DOC in this region.

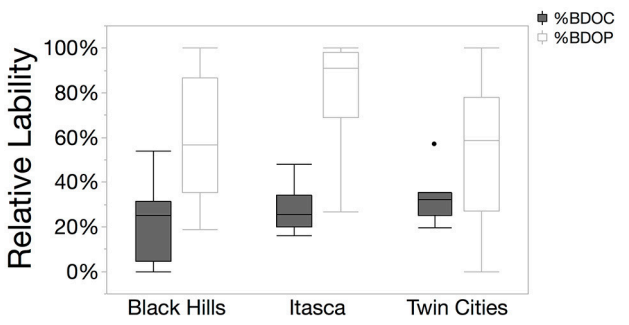

FIGURE 5 | Box and whisker plots showing the relative lability of DOC and DOP in the three regions studied. Relative %BDOP was higher than relative %BDOC in all three regions (pairwise *t*-tests, $p < 0.01$). Relative % BDOP also showed a much larger range of values compared to relative %BDOC.

Stoichiometry of Bioavailable Nutrients

Overall, ratios of bioavailable C and P were much lower than the bulk chemistry pools. DOC:TDP ratios ranged from 319 to 7122:1 with a median of 1595:1 while DOC:DOP ratios ranged from 679 to 15360:1 with a median of 2449:1 in the systems we examined. In comparison, BDOC:BTDP ranged from 133 to 8848:1 (this high point was an outlier with the next highest value being 2943) and median value of 746:1. BDOC:BDOP ranged from 144 to 9719:1 with a median value of 843:1. Previous work showed that assemblages of aquatic heterotrophic bacteria in lakes have mean biomass C:P ratios around 102:1 (Cotner et al., 2010), while individual strains can have highly variable biomass composition with values well over 1000:1 (Godwin and James, 2015). Therefore, the stoichiometry of the bioavailable nutrients measured in this study more closely match typical bacterial biomass stoichiometry than measures of bulk nutrient chemistry. Bioavailable nutrient stoichiometry was also positively correlated with bulk nutrient stoichiometry (**Figure 11**, $p < 0.0001$).

DISCUSSION

The data on degradation and bioavailability of DOC and DOP provide insights into three important areas. First, across all lakes, median BDOC and BDOP turnover times were similar equal for BDOC and BDOP (∼100 days), but in Itasca State Park lakes, BDOP turnover was significantly faster than BDOC (in

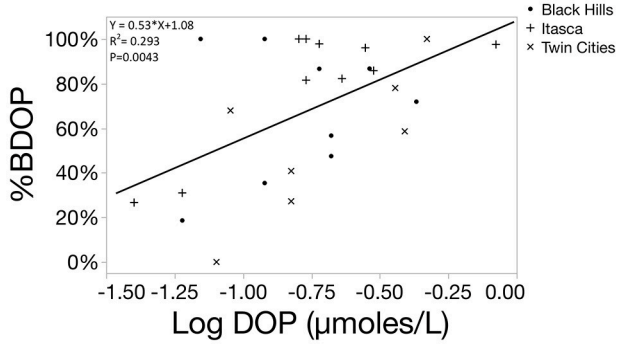

FIGURE 6 | Scatterplot showing the linear regression between the %BDOP and the original concentration of DOP in the sample (log transformed) for 26 lakes. One lake had to be excluded because the initial SRP concentration was below the method detection limit, so a DOP concentration could not be calculated. A positive relationship shows that as DOP concentration increased among systems, the relative lability of DOP increased.

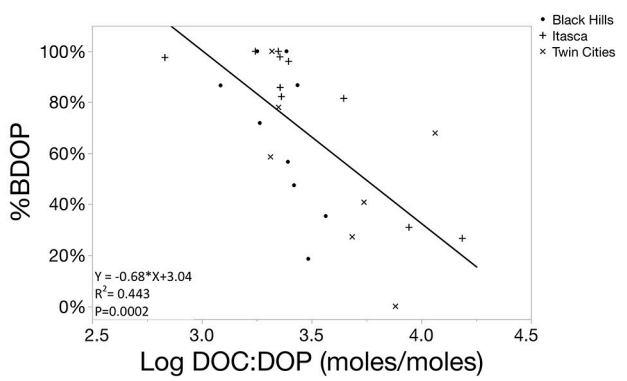

FIGURE 7 | Scatterplot showing the linear regression function comparing the percentage of BDOP to the DOC:DOP ratio of the initial sample (log transformed). The significant negative relationship demonstrates that the relative bioavailability of the DOP pool decreases as DOP becomes scarce relative to DOC.

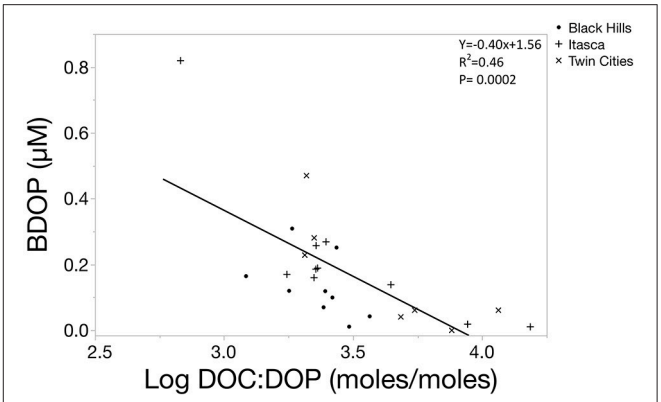

FIGURE 8 | Scatterplot showing the linear regression function comparing the concentration of BDOP to the DOC:DOP ratio of the initial sample (log transformed). The significant negative relationship demonstrates BDOP is drawn down as DOP becomes scarce relative to DOC.

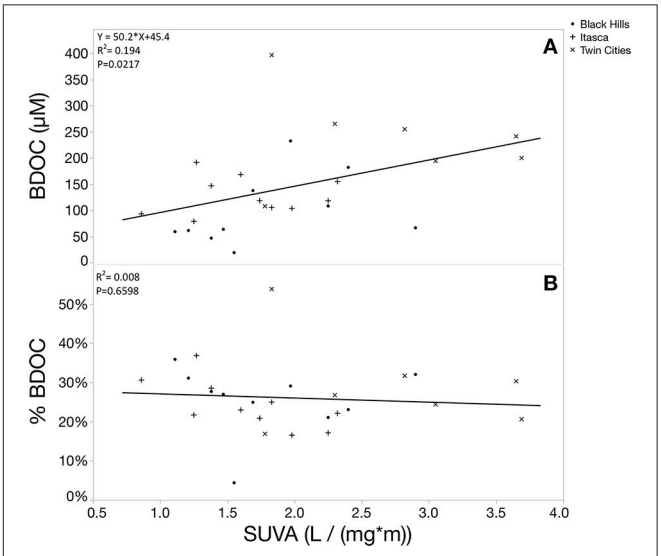

FIGURE 9 | Scatterplots showing the relationship between BDOC and SUVA. Panel **(A)** shows the absolute size of the BDOC pool and **(B)** shows the relative size of the BDOC pool. The absolute amount of BDOC showed a significant positive association with SUVA whereas the relative BDOC percentage was not significantly related to SUVA. This could be at least partially driven by the fact that high SUVA systems tend to have larger total DOC pools, but it also suggests that systems dominated by more aromatic carbon compounds (high SUVA) still have large pools of BDOC.

some cases by as much as 20 times). This spatial variability highlights the need for more empirical measurements of DOP degradation rates from a variety of systems to better understand potential spatial patterns. In our study, degradation rates of DOC and DOP could not be explained by the other elemental pool sizes or environmental characteristics, further emphasizing the need for more work in this area. Second, we show that the portion of the DOP pool that is bioavailable was extremely variable across systems, but often exceeded 50% and was strongly related to the DOC:DOP ratio of the system. BDOP was drawn down in systems with high DOC:DOP ratios (where P was more likely limiting) and therefore it is likely that in many systems, DOP represents a high-quality P resource to supplement inorganic P availability. Thirdly, the bioavailability of the DOM pool suggests that the nutrient stoichiometry of available resources in aquatic systems may be more similar to the biomass demands of aquatic microbes than previously thought. This has important implications for understanding the experienced nutrient imbalance by heterotrophic bacteria and in turn, understanding how bacteria couple multiple elemental cycles in aquatic systems.

Degradation Rates of DOC and DOP

Degradation rates of DOC in freshwater systems have been the topic a numerous papers and a recently published meta-analysis showed that DOC decay rates can vary by several orders of magnitude across different systems (Catalán et al.,

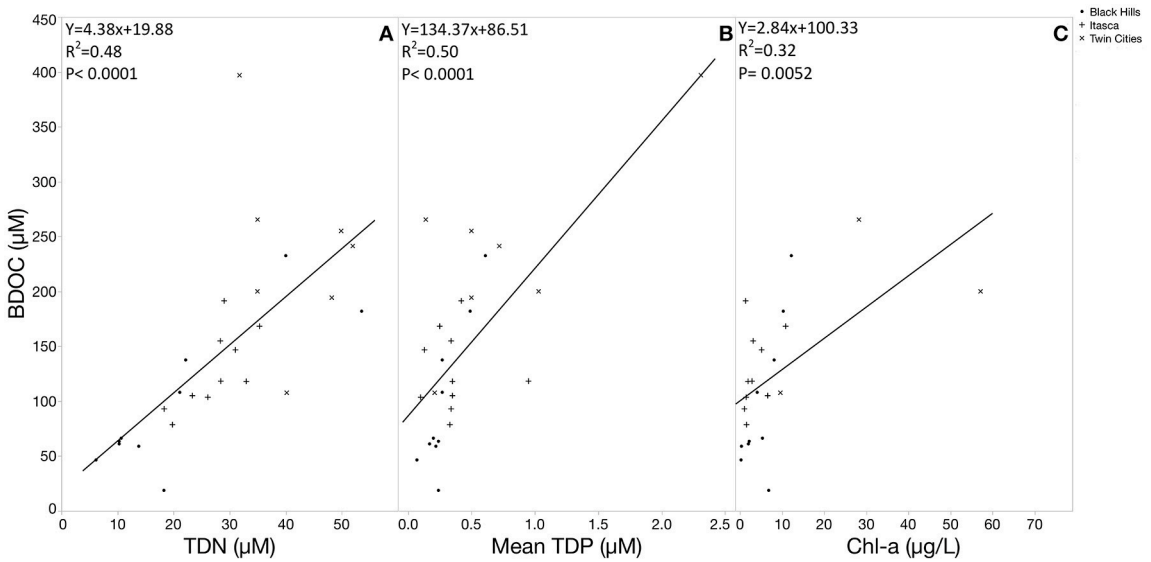

FIGURE 10 | Linear regression functions showing the relationship between BDOC concentration and trophic status indicators. Strong positive relationships between BDOC and TDN **(A)** and TDP **(B)** suggest BDOC accumulation in high nutrient conditions. BDOC is also positively correlated with productivity, measured as chlorophyll-a concentration **(C)**.

2016). Their dataset included 33 bioassay measurements from lakes in a similar climatic region to our study and these 33 lakes had a median k_{DOC} value of 0.0021, the same order of magnitude as our median value of 0.0077. Estimates of DOP degradation rates are scarcer in the literature and are dominated by estimates from marine systems. One study in the Baltic Sea estimated DOP turnover times to be between 3 to 4 days, about twice as fast as the shortest turnover time in our data set (Nausch and Nausch, 2006). In contrast, DOP turnover times from the North and South Atlantic Ocean subtropical gyres were 5.5 months and 10.5 years respectively (Mather et al., 2008). Another study from Station ALOHA, in the North Pacific Subtropical Gyre found that DOP turnover time increased with depth and ranged from 12 to 268 days at a single sampling site (Björkman and Karl, 2003). One major difference between these systems that could explain the differences in turnover times is productivity, with the Baltic being highly productive compared to Station ALOHA. However, DOP degradation rates were not significantly correlated to chlorophyll levels in our study, so within our systems, productivity was not a good predictor of DOP turnover. The variability of literature measurements, along with the variability in DOP turnover times in this study, highlight the need for more direct measurements of DOP degradation across a variety of systems to better constrain typical DOP degradation dynamics and to better understand the factors controlling them.

Here, it is also important to consider the difference in model fits between the DOC and DOP degradation curves. DOC degradation was incredible, consistent across system, allowing for the degradation models to accurately estimate the recalcitrant portion of the DOC pool and degradation rate (Supplementary Figure 2). However, in the case of DOP there was more variation in degradation pattern across systems and the proximity of many of the DOP measurements to a non-zero asymptote made it difficult to use the degradation model to accurately estimate a refractory DOP pool (Supplementary Figure 3). Nonetheless, we elected to use a two parameter decay model to estimate DOP degradation rates because the model provided a reasonable overall fit (R^2-0.77, Supplementary Figure 3) and gave rates that could be directly compared to the DOC estimates. This approach does by definition infer that a refractory DOP is not present (i.e., 100% bioavailability) and tends to homogenize the overall DOP degradation patterns. A closer view of the DOP degradation plots (Supplementary Figure 3) revealed at least three different general patterns for DOP degradation: (1) DOP was rapidly degraded to a zero intercept, (2) DOP was slowly degraded to a zero intercept, or (3) DOP degraded slowly to a non-zero intercept but a zero intercept is inferred by the fit model. This third case would suggest that there is in fact a refractory DOP pool in these systems and this observation further supports our use of measured concentrations differences rather than DOP degradation models to calculate the size of the bioavailable DOP pool in these systems.

Bioavailability of DOC and DOP

Our measurements of the relative bioavailability of DOC are well within the range measured in other aquatic systems (Sondergaard and Middelboe, 1995; Stets and Cotner, 2008; Catalán et al., 2015; Helton et al., 2015; Frey et al., 2016). All but one of the systems we measured had BDOC values less than 50% of the total DOC pool, further supporting the idea that the bulk portion of DOC in freshwater is recalcitrant. However, these relative BDOC measures are quite high compared to marine systems, suggesting

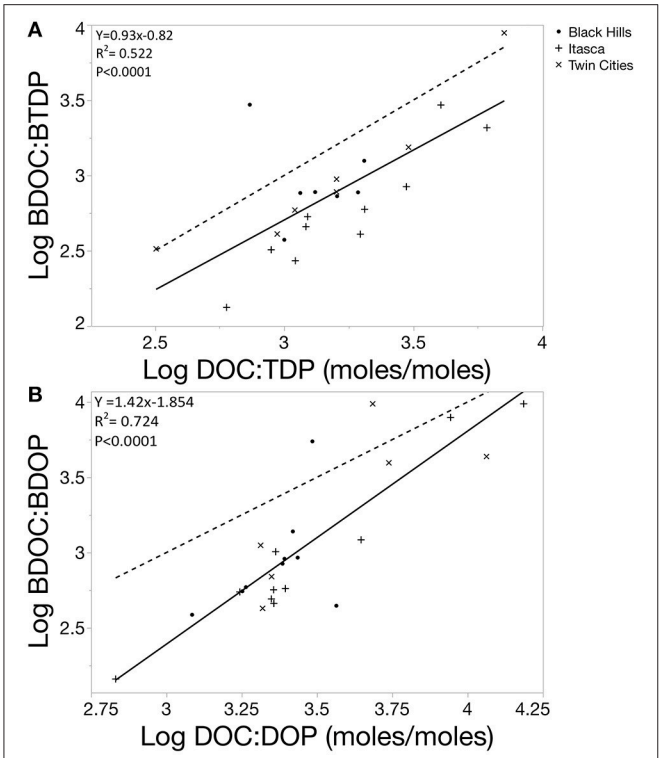

FIGURE 11 | (A) Linear regression fit (solid line) comparing the log transformed values for BDOC:BTDP ratio to the bulk DOC:TDP ratio for 24 lakes, 3 samples had to be removed from the data set because estimated BTDP was 0. Dotted line represents a 1:1 for comparison. The regression line falls below the 1:1 reference indicating that the C:P ratio of the bioavailable pool is lower than the measured C:P of the system. In other words, bulk resource ratios measured using whole water DOC:TDP would overestimate the experienced resource ratio of the microbial community (BDOC:BTDP). **(B)** Linear regression fit (solid line) comparing the log transformed values for BDOC:BDOP ratio to the bulk DOC:DOP ratio for 24 lakes, 3 samples had to be removed from the data set because estimated BTDP was 0. Dotted line represents a 1:1 for comparison. The regression line falls below the 1:1 reference indicating that the C:P ratio of the bioavailable pool is lower than the measured C:P of the system. Additionally, the slope of the regression fit is greater than 1 meaning that BDOC:BDOP ratios more closely match bulk DOC:DOP ratios when they are higher (in systems that are DOP poor relative to DOC).

that exports to freshwater represent a younger, more labile carbon source than those found in marine systems. Furthermore, absolute BDOC concentrations were strongly related to TDN, TDP, and chlorophyll concentrations suggesting that nutrient availability is an important control on the accumulation of BDOC. This finding contrasts previous work that showed no significant correlation between BDOC and nutrient conditions (Stets and Cotner, 2008); however, it should be noted that Stets and Cotner also measured positive correlations between BDOC and both TDP and chlorophyll concentrations but the relationships were not statistically significant in the 12 lakes they studied. Nonetheless, our data also suggest that stoichiometry may be an additional constraint to BDOC accumulation. The fact that the slope in **Figure 11B** was more than 1 suggested that BDOC was accumulating disproportionately when DOC:DOP ratios were highest.

It was interesting to note that while the amount of BDOC was positively correlated to SUVA, the relative lability was not (**Figure 9**). SUVA has been shown to be highly correlated with the aromaticity of the DOM pool (Weishaar et al., 2003), so this pattern suggests that increasing aromaticity of the DOM pool does not significantly decrease its bioavailability. Furthermore, SUVA is considered a useful proxy for terrigenous organic matter with higher SUVA systems receiving large terrigenous inputs. SUVA was not strongly correlated to relative or absolute concentrations of BDOP, so we suggest that terrigenous inputs in our study systems represent a labile source of organic carbon but not organic phosphorus.

As with DOP degradation kinetics, estimates of the relative pool size of BDOP are sparse. However, the values reported in the literature are in good agreement with the values we measured here. In a Baltic Sea study, the DOP pool was 75% bioavailable (Stepanauskas et al., 2002) and a similar value (33.2–60%) was reported for 3 stations in the central Baltic as part of a different study (Nausch and Nausch, 2007). A more recent analysis suggested that ∼40% of the DOP in four boreal lakes was bioavailable (Soares et al., 2017). Our study of 27 unique systems supports the idea of very labile BDOP with a median value of ∼78%, but also highlights the large amount of variability in BDOP across systems. It should be mentioned, however, that our incubations lasted much longer than these other studies (150 days compared to ∼7 days), which should have resulted in higher estimates of BDOP as our incubations would capture both rapidly degrading and slowly degrading DOP compounds. The fact that many of our incubations continued to show DOP losses up until 150 days into the incubations (Supplementary Figure 3) demonstrates the need for longer term incubations to fully describe the BDOP pool. On the other hand, our first sampling period occurred after ∼30 days of incubation, which limited our ability to describe the degradation rates of the fastest degrading DOP pool. Given the rates of degradation documented in the literature and also the fact than many of our incubations showed major losses of DOP within the first 30 days, a stratified sampling method with high frequency measurements over the first few weeks and then less frequent measurements over several months may provide the best overall picture of DOP degradation.

Our findings also suggest that organic matter stoichiometry is an important control on the bioavailability of DOP. We found that the DOC:DOP ratio was a significant predictor of both absolute and relative BDOP (**Figures 7**, **8**), with higher DOC:DOP ratios correlated to lower BDOP concentrations and percentages and a higher BDOC:BDOP ratio relative to the DOC:DOP pool (**Figure 11**). These patterns suggest that relative size of the BDOP pool decreased when the DOP was small relative to DOC. Presumably when the DOC pool size was large relative to DOP, microbes were more likely to be P-limited and consumed any bioavailable P. In lakes with lower DOC:DOP ratios, the organic matter pool would more closely resemble the biomass requirements of aquatic bacteria and/or the microbes are more likely to be limited by organic C rather than P.

Stoichiometry of Bioavailable Nutrients

Ecological stoichiometry provides a guide for predicting the cycling of multiple nutrients by examining the elemental balance between organisms and their resources. However, a fundamental problem associated with understanding these imbalances is our capacity to know what the resource availability is that organisms actually experience. Our ability to accurately describe the resource imbalance experienced by bacterial communities *in situ* is hindered by our lack of simultaneous measurements of the bioavailability of multiple elements (Berggren et al., 2014; Soares et al., 2017). Here, we observed that the experienced BDOC:BDOP resource ratios of aquatic bacterial communities were typically less than measured DOC:DOP pools (**Figure 11**). Therefore, bulk chemical measurements likely overestimate the size of the labile DOC pool or underestimate the size of the DOP pool. The fact that our measurements of BDOP indicated that large fractions of the DOP pool could be bioavailable while there clearly was a non-labile pool of DOC suggests that DOC measurements overestimate the BDOC pool, which many other studies have observed. Nonetheless, previous measurements of imbalance using bulk chemistry data likely overestimate the actual imbalance experienced by these communities particularly in more carbon-limited systems. Furthermore, our results suggest that it is at lower C:P ratios, i.e., more eutrophic systems, where chemical measurements of DOC:DOP are likely to overestimate the bioavailable pool of DOC (**Figure 11**). Although there is more BDOC being produced in these systems, the microbial biomass is more likely to be limited by the availability of organic carbon, resulting in more drawdown and an increased proportion of the DOC pool being recalcitrant. This has important implications for understanding how bacteria couple C and P cycles in freshwater because the experienced imbalance between consumer and resources governs the differential recycling of those nutrients. If heterotrophic bacteria in aquatic systems experience a more balanced resource pool in terms of the C:P ratio than previously thought, this should result in more efficient C cycling as compared to predictions based on bulk chemistry ratios.

CONCLUSIONS

The 27 aquatic systems examined in this study demonstrate that DOP bioavailability was quite variable across systems but was strongly predicted by the DOC:DOP ratio of the system. The bioavailability of DOC was more tightly constrained due to an increased proportion of recalcitrant material relative to DOP and it was not predicted by organic pool stoichiometry but rather was strongly related to nutrient conditions (both TDN and TDP concentration). Exponential decay models fit the loss of DOC tightly, but were not as strong of a fit for DOP. Given that DOP turnover times were calculated using an exponential model with no asymptote (and therefore assuming 100% bioavailable DOP in all samples) our estimates for turnover times are likely skewed high, particularly for systems with sizeable recalcitrant DOP pools. Despite these potential limitations, our data suggest that DOP turnover time was significantly faster than DOC turnover in the Itasca region (in one case, ∼20 times faster), but DOC and DOP had similar rates of turnover in the other two regions. This suggests that overall DOP in freshwater systems is turning over as quickly or more quickly than DOC. More measurements are needed in order to properly assess this spatial variability and determine if there are any broader geographic patterns in the relative turnover rates of DOC and DOP in freshwaters, particularly because variability in DOC and DOP degradation rates could not be explained by inorganic nutrient pool sizes or lake characteristics measured in this study.

Furthermore, we have shown that organic matter stoichiometry is an important control on the accumulation of bioavailable DOP in aquatic systems. Relative bioavailability of DOP was positively related to the concentration of DOP in the sample and negatively correlated to the initial DOC:DOP ratio, suggesting that DOP accumulates in systems that are less P-limited. In contrast, the initial organic matter stoichiometry was not predictive of relative or absolute BDOC. Instead, BDOC accumulation was associated with high nutrients (TDN and TDP) and high production (chlorophyll). Absolute BDOC was also strongly correlated to SUVA values, providing evidence that terrestrial subsidies represent a labile source of DOC in the systems studied. Finally, incorporating measures of nutrient bioavailability decreased the predicted nutrient imbalance experienced by heterotrophic bacteria in aquatic systems, which has important implications for understanding the coupling of C and P biogeochemical cycles.

AUTHOR CONTRIBUTIONS

ST performed the field work and data collection. JC and ST jointly contributed to the research design, data analysis, and manuscript writing.

FUNDING

This work was funded by the Itasca Graduate Student Fellowship and Moos Graduate Fellowship in the aquatic science awarded to ST by the College of Biological Sciences at the University of Minnesota and NSF award 1257571 to JC.

ACKNOWLEDGMENTS

The authors would like to thank Bri Loeks-Johnson and Dr. Lesley Knoll for their help in the field collecting samples and Andrea Little for her technical support on the project.

SUPPLEMENTARY MATERIAL

The Supplementary Material for this article can be found online at: https://www.frontiersin.org/articles/10.3389/fenvs.2018.00062/full#supplementary-material

REFERENCES

Anderson, D. M., Patricia, M. G., Joann, M. B., Donald, M. A., Patricia, M. G., Joann, M., et al. (2002). Harmful algal blooms and eutrophication: nutrient sources, composition, and consequences coastal waters : global patterns of cause and effect. *Estuaries* 25, 704–726. doi: 10.1007/BF02804901

Berggren, M., Ryan, A., Sponseller, A. R., Alves, S., and Ann, K. B. (2014). Toward an ecologically meaningful view of resource stoichiometry in DOM-dominated aquatic systems. *J. Plank. Res.* 37, 489–499. doi: 10.1093/plankt/fbv018

Björkman, K. M., and Karl, M. D. (1994). Bioavailability of inorganic and organic phosphorus compounds to natural assemblages of microorganisms in Hawaiian coastal waters. *Mar. Ecol. Process Ser.* 111, 265–273. doi: 10.3354/meps111265

Björkman, K. M., and Karl, M. D. (2003). Bioavailability of dissolved organic phosphorus in the euphotic zone at station ALOHA, north pacific subtropical gyre. *Limnol. Oceanogr.* 48, 1049–1057. doi: 10.4319/lo.2003.48.3.1049

Boström, B., Gunnar, P., and Brita, B. (1988). Bioavailability of different phosphorus forms in freshwater systems. *Hydrobiologia* 170, 133–155. doi: 10.1007/BF00024902

Catalán, N., Anne, M. K., Hannes, P., Francesc, C., and Lars, J. T. (2015). Absence of a priming effect on dissolved organic carbon degradation in lake water. *Limnol. Oceanogr.* 60, 159–168. doi: 10.1002/lno.10016

Catalán, N., Rafael, M., Dolly, N. K., and Lars, J. T. (2016). Organic carbon decomposition rates controlled by water retention time across inland waters. *Nat. Geosci.* 9, 501–504. doi: 10.1038/ngeo2720

Cole, J. J., Yves, P., Caraco, N. F., McDowell, W. H., Tranvik, L. J., Robert, G. S., et al. (2007). Plumbing the global carbon cycle: integrating inland waters into the terrestrial carbon budget. *Ecosystems* 10, 171–184. doi: 10.1007/s10021-006-9013-8

Cotner, J. B., and Biddanda, A. B. (2002). Small players, large role: microbial influence on biogeochemical processes in pelagic aquatic ecosystems. *Ecosystems* 5, 105–121. doi: 10.1007/s10021-001-0059-3

Cotner, J. B., Edward, K. H., Thad, S. J., and Mikal, H. (2010). Freshwater bacteria are stoichiometrically flexible with a nutrient composition similar to seston. *Front. Microbiol.* 1:132. doi: 10.3389/fmicb.2010.00132

Cotner, J. B., and Wetzel, R. G. (1992). Uptake of dissolved inorganic and organic phosphorus compounds by phytoplankton and bacterioplankton. *Limnol. Oceanogr.* 37, 232–243. doi: 10.4319/lo.1992.37.2.0232

Donald, D. B., Matthew, J. B., Kerri, F., and Peter, R. L. (2011). Comparative effects of urea, ammonium, and nitrate on phytoplankton abundance, community composition, and toxicity in hypereutrophic freshwaters. *Limnol. Oceanogr.* 56, 2161–2175. doi: 10.4319/lo.2011.56.6.2161

Dyhrman, S. T., and Ruttenberg, C. K. (2006). Presence and regulation of alkaline phosphatase activity in eukaryotic phytoplankton from the coastal ocean: implications for dissolved organic phosphorus remineralization. *Limnol. Oceanogr.* 51, 1381–1390. doi: 10.4319/lo.2006.51.3.1381

Falkowski, P. (2000). The global carbon cycle: a test of our knowledge of earth as a system. *Science* 290, 291–296. doi: 10.1126/science.290.5490.291

Frey, K. E., William, V. S., Paul, J. M., and Robert, M. H. (2016). Optical properties and bioavailability of dissolved organic matter along a flow-path continuum from soil pore waters to the Kolyma river mainstem, East Siberia. *Biogeosciences* 13, 2279–2290. doi: 10.5194/bg-13-2279-2016

Godwin, C. M., and James, B. C. (2015). Aquatic heterotrophic bacteria have highly flexible phosphorus content and biomass stoichiometry. *ISME J.* 9, 2324–2327. doi: 10.1038/ismej.2015.34

Heiskary, S. A., Bruce, W. C., and David, P. L. (1987). Analysis of regional patterns in lake water quality: using ecoregions for lake management in Minnesota. *Lake Reserv. Manage.* 3, 337–344. doi: 10.1080/07438148709354789

Helton, A., Meredith, W., Emily, S. B., Geoffrey, P., Rose, M. C., and Jack, S. A. (2015). Dissolved organic carbon lability increases with water residence time in the alluvial aquifer of a river floodplain ecosystem. *J. Geophys. Res.* 120, 693–706. doi: 10.1002/2014JG002832

Jackson, G. A., and Williams, M. P. (1985). Importance of dissolved organic nitrogen and phosphorus to biological nutrient cycling. *Deep Sea Res. Oceanogr. Res. Papers* 32, 223–235. doi: 10.1016/0198-0149(85)90030-5

Li, B., and Brett, M. T. (2013). The influence of dissolved phosphorus molecular form on recalcitrance and bioavailability. *Environ. Pollut.* 182, 37–44. doi: 10.1016/j.envpol.2013.06.024

Lønborg, C., Keith, D., Xosé, A., Álvarez-Salgado, and Axel, E. J. M. (2009). Bioavailability and bacterial degradation rates of dissolved organic matter in a temperate coastal area during an annual cycle. *Mar. Chem.* 113, 219–226. doi: 10.1016/j.marchem.2009.02.003

Maranger, R., Jones, S., and James, C. (2018). Stoichiometry of carbon, nitrogen, and phosphorus through the freshwater pipe. *Limnol. Oceanogr. Lett.* 3, 89–101. doi: 10.1002/lol2.10080

Mather, R. L., Reynolds, S. E., Wolff, G. A., Williams, R. G., Torres-Valdes, S., Woodward, E. M. S., et al. (2008). Phosphorus cycling in the north and south Atlantic ocean subtropical gyres. *Nat. Geosci.* 1, 439–443. doi: 10.1038/ngeo232

Murphy, J., and Riley, J. P. (1962). Determrnation single solution method for the in natural. *Anal. Chim. Acta* 27, 31–36. doi: 10.1016/S0003-2670(00)88444-5

Nausch, M., and Nausch, G. (2006). Bioavailability of dissolved organic phosphorus in the Baltic sea. *Mar. Ecol. Prog. Ser.* 321, 9–17. doi: 10.3354/meps321009

Nausch, M., and Nausch, G. (2007). Bioavailable dissolved organic phosphorus and phosphorus use by heterotrophic bacteria. *Aquat. Biol.* 1, 151–160. doi: 10.3354/ab00012

Ruttenberg, K. C., and Sonya, T. D. (2005). Temporal and spatial variability of dissolved organic and inorganic phosphorus, and metrics of phosphorus bioavailability in an upwelling-dominated coastal system. *J. Geophys. Res.* 110, 1–22. doi: 10.1029/2004JC002837

Schindler, D. W., Hecky, R. E., Findlay, D. L., Stainton, M. P., Parker, B. R., Paterson, M. J., et al. (2008). Eutrophication of lakes cannot be controlled by reducing nitrogen input: results of a 37-year whole-ecosystem experiment. *Proc. Natl. Acad. Sci. U.S.A.*105, 11254–11258. doi: 10.1073/pnas.0805108105

Schlesinger, W. H., and Bernhardt, E. S. (2013). "The global cycles of nitrogen and phosphorus," in *Biogeochemistry: An Analysis of Global Change*, 3rd Edn (Waltham MA: Academic Press), 445–467.

Soares, A. R. A., Ann, K. B., Ryan, A. S., Joanna, M. M., Reiner, G., and Emma, S. K. (2017). New insights on resource stoichiometry: assessing availability of carbon, nitrogen, and phosphorus to bacterioplankton. *Biogeosciences* 14, 1527–1539. doi: 10.5194/bg-14-1527-2017

Sondergaard, M., and Middelboe, M. (1995). A cross-system analysis of labile dissolved organic carbon. *Mar. Ecol. Prog. Ser.* 118, 283–294. doi: 10.3354/meps118283

Sonzogni, W. C., Chapra, S. C., Armstrong, D. E., and Logan, T. J. (1982). Bioavailability of phosphorus inputs to lakes1. *J. Environ. Qual.* 11, 555. doi: 10.2134/jeq1982.00472425001100040001x

Standard Methods (2005). *Standard Methods For the Examination of Water and Wastewater, 11th Edn*. Washington, DC: Standard Methods.

Stepanauskas, R., Niels, O. G., Ørgensen, J., Eigaard, O. R., and Audrius, Ž., Lars, J. T., et al. (2002). Summer inputs of riverine nutrients to the Baltic sea: bioavailability and eutrophication relevance. *Ecol. Monogr.* 72, 579–597. doi: 10.2307/3100058

Stets, E. G., and Cotner, J. B. (2008). Littoral zones as sources of biodegradable dissolved organic carbon in lakes. *Can. J. Fish. Aquat. Sci.* 65, 2454–2460. doi: 10.1139/F08-142

Teubner, K., Crosbie, N. D., Donabaum, K., Kabas, W., Kirschner, A. K., Pfister, M., et al. (2003). Enhanced phosphorus accumulation efficiency by the pelagic community at reduced phosphorus supply: a lake experiment from bacteria to metazoan zooplankton. *Limnol. Oceanogr.* 48, 1141–1149. doi: 10.4319/lo.2003.48.3.1141

Tranvik, L. J., John, A. D., James, B. C., Steven, A. L., Robert, G. S., Thomas, J. B., et al. (2009). Lakes and reservoirs as regulators of carbon cycling and climate. *Limnol. Oceanogr.* 54, 2298–2314. doi: 10.4319/lo.2009.54.6_part_2.2298

Vonk, J. E., Tank, S. E., Mann, P. J., Spencer, R. G. M., Treat, C. C., Striegl, R. G., et al. (2015). Biodegradability of dissolved organic carbon in permafrost soils and aquatic systems: a meta-analysis. *Biogeosciences* 12, 6915–6930. doi: 10.5194/bg-12-6915-2015

Weishaar, J., George, A., Brian, B., Miranda, F., Roger, F., and Kenneth, M. (2003). Evaluation of specific ultra-violet absorbance as an indicator of the chemical content of dissolved organic carbon. *Environ. Sci. Technol.* 37, 4702–4708. doi: 10.1021/es030360x

Wetzel, R. G. (2001). *Limnology: Lake and River Ecosystems*. 3rd Edn. San Diego, CA: Gulf Professional Publishing.

Wiegner, T. N., Seitzinger, S. P., Glibert, P. M., and Bronk, D. A. (2006). Bioavailability of dissolved organic nitrogen and carbon from nine rivers in the eastern United States. *Aquat. Microb. Ecol.* 43, 277–287. doi: 10.3354/ame043277

Conflict of Interest Statement: The authors declare that the research was conducted in the absence of any commercial or financial relationships that could be construed as a potential conflict of interest.

frontiers in Marine Science

ORIGINAL RESEARCH
published: 04 September 2018
doi: 10.3389/fmars.2018.00302

Phosphorus Forms in Sediments of a River-Dominated Estuary

Sheree J. Watson[1]*, *Barbara J. Cade-Menun*[2], *Joseph A. Needoba*[1,3] and *Tawnya D. Peterson*[1,3]

[1] Institute of Environmental Health, Oregon Health and Science University, Portland, OR, United States, [2] Agriculture and Agri-Food Canada, Swift Current Research and Development Centre, Swift Current, SK, Canada, [3] OHSU-PSU School of Public Health, Oregon Health and Science University, Portland, OR, United States

Estuaries are biologically productive transition zones between land and sea that play a vital role in transforming, recycling, and sequestering nutrients and organic matter, thus influencing nutrient loading to coastal systems. Yet, the processes involved in phosphorus (P) transformation and cycling among inorganic and organic P forms are poorly known in estuaries. To better understand the potential for P transformation and sequestration, we identified P forms and estimated their contributions to total P in intertidal wetland sediments of a river-dominated estuary (Columbia River, Oregon, USA) using solution ^{31}P nuclear magnetic resonance spectroscopy (P-NMR). Inorganic P forms dominated sediment P extracts throughout the estuary, with orthophosphate accounting for 71–84% of total extracted P. However, biologically-derived inorganic and organic P forms were also detected. Polyphosphates were found in sediment extracts throughout the estuary, contributing as much as 10% of extracted P. Similar to other wetlands, orthophosphate monoesters and diesters made approximately equal contributions (∼ 20%) to total extracted P. However, monoesters (e.g., phytate) were more abundant in sedimentary environments characterized by low organic matter content, while diesters (e.g., DNA) were more abundant in sedimentary environments with high organic matter, regardless of salinity. Collectively, the data show strong evidence for P transformation in sediments of a large, river-dominated estuary, which influences its transport to the coastal Pacific Ocean via the expansive Columbia River plume.

Keywords: phosphorus, ^{31}P-nuclear magnetic resonance, sediments, river, estuary

OPEN ACCESS

Edited by:
Toshi Nagata,
The University of Tokyo, Japan

Reviewed by:
Masahiro Suzumura,
National Institute of Advanced Industrial Science and Technology (AIST), Japan
Sue Newman,
South Florida Water Management District, United States

***Correspondence:**
Sheree J. Watson
shereew@hawaii.edu

Specialty section:
This article was submitted to Marine Biogeochemistry, a section of the journal Frontiers in Marine Science

Received: *28 February 2018*
Accepted: *08 August 2018*
Published: *04 September 2018*

Citation:
Watson SJ, Cade-Menun BJ, Needoba JA and Peterson TD (2018) Phosphorus Forms in Sediments of a River-Dominated Estuary. Front. Mar. Sci. 5:302. doi: 10.3389/fmars.2018.00302

INTRODUCTION

Phosphorus (P) is an essential but often limiting nutrient in freshwater aquatic and terrestrial ecosystems (Daniel et al., 1998); however, downstream systems are increasingly under threat from nutrient-stimulated eutrophication (Conley et al., 2009; Tiessen et al., 2011). Watershed losses result from inefficient recycling, or poor sequestration, and lead to P transport from soils to surface waters; ultimately, excess P ends up in estuaries and coastal systems where it often results in nutrient-driven eutrophication. Eutrophication can lead to hypoxia, acidification, and harmful algal blooms (Paerl, 2006; Bricker et al., 2008) and represents a growing worldwide threat to human health and well-being (Millenium Ecosystem Assessment, 2006).

Estuaries are biologically productive transition zones comprising a variety of habitats including wetlands, mudflats, and seagrass beds between freshwater and marine systems. They play a vital role in transforming, recycling, and sequestering nutrients and organic matter (OM) prior to entering

the coastal ocean (Barbier et al., 2011). Tidal mixing of fresh and saltwater within estuaries leads to particle flocculation (Sholkovitz, 1976) and the localized resuspension of bottom material in turbidity maxima (van Beusekom and Brockmann, 1998; Small and Prahl, 2004). Combined with downstream transport in rivers, estuaries are vulnerable to nutrient pollution because dissolved inorganic P (orthophosphate) desorption from sediment surfaces occurs when anions in seawater compete with phosphate anions for binding sites, leading to P efflux (Fox et al., 1986; Froelich, 1988; House and Warwick, 1999; Monbet et al., 2010). Moreover, the reducing conditions associated with intense OM remineralization increase P desorption, setting up a positive feedback loop whereby eutrophic conditions contribute to P mobilization and limit nutrient sequestration (Howarth et al., 2011; Li et al., 2013). This impairs the critical function of estuaries and wetlands, which is to reduce nutrient loads before they reach coastal waters (Barbier et al., 2011).

Phosphorus retention, or sequestration, in wetlands can occur via chemical, physical, or biological means. For example, orthophosphate is retained in sediment pore waters through adsorption from the water column, particularly in sediments dominated by clays and minerals (Reddy and DeLaune, 2008). Phosphorus (P) buffering is defined as the equilibrium reached between adsorption and desorption of orthophosphate at the water/sediment interface, which reduces variability in orthophosphate concentrations irrespective of input or removal processes (Froelich, 1988). High concentrations of inorganic P and minerals (i.e., Fe, Al, Ca, and Mg) in sediments result in the formation of both soluble and insoluble P compounds, predominantly Fe and Al minerals in acidic soils and Ca compounds in near-neutral to alkaline soils (Stevenson, 1986; Reddy et al., 1999; Richardson and Reddy, 2013). However, seasonality in hydrology, including flooding and drying, produces changes in soil redox conditions, which play a governing role in transformation, storage, and transport of P in wetlands.

In comparison, organic P in wetlands is associated with living systems including plants, microbes, detritus and organic matter, and commonly accounts for large fractions of total P (Vaithiyanathan and Richardson, 1997; Reddy et al., 1999). Although plant storage material is often the dominant source of organic P in wetland soils (Reddy and DeLaune, 2008), soil microbes play a key role in controlling degradation of organic matter and cycling of P in wetlands. For example, microbes secrete enzymes that readily mineralize organic P and can quickly assimilate orthophosphate released into pore water (Richardson, 1985; Kellogg and Bridgham, 2003; Noe et al., 2003). Microbes also regulate P in sediments through biomass, which can account for up to 25–50% of the total P in wetland mineral sediments (Wright et al., 2001; McDowell and Sharpley, 2003) and up to 70% of total P in hydrologically isolated sediments (Williams and Silcock, 2001).

Because the mobility and retention of P depends upon its chemical forms, the determination of chemical structures is critical for identifying possible sources and for estimating the potential for retention, sequestration, and transformation (Celi and Barberis, 2005; Condron et al., 2005; Quiquampoix and Mousain, 2005). The goal of this study was to investigate P forms and their contributions in a mesotidal, river-dominated system characterized by rapid flushing and short water residence times (1–5 d; Chawla et al., 2008; Columbia River estuary, Oregon, USA). Previous work in this estuary showed that water-column dissolved inorganic phosphate (DIP) exhibited seasonal non-conservative increases along a salinity gradient, suggesting the presence of P sources that were not accounted for when orthophosphate was measured in river and ocean end members (Gilbert et al., 2013). To address the knowledge gap, our goal was to determine what P forms are present in the peripheral bay sediments that might contribute to fluxes of DIP and to characterize variability in estuarine P forms as a function of sediment properties.

MATERIALS AND METHODS

Field Sites

The Columbia River is the second largest by discharge in the USA (Sherwood et al., 1990), culminating in a river-dominated, salt-wedge estuary with strong seasonality in salinity and biogeochemical properties (Roegner et al., 2011). The U.S. Pacific Northwest coast is strongly influenced by summer upwelling when northerly winds promote the offshore transport of surface waters, which are replaced by nutrient-rich subsurface oceanic water (Huyer, 1983; Grantham et al., 2004). The Columbia River discharge varies with season, peaking at $>10{,}000\ m^3\ s^{-1}$ during the snowmelt-driven spring freshet (April–June) and declining to $< 2{,}000\ m^3\ s^{-1}$ in the dry season (July–October). Salt intrusion into the estuary is greatest during periods of low discharge, which typically occur coincidentally with upwelling-favorable conditions between June and September (Chawla et al., 2008). The estuary exchanges the majority of water in north and south paths that run along the peripheral bays, including Baker Bay (north) and Youngs and Cathlamet Bay (south; **Figure 1**).

Compared to the estuary at large, the three peripheral bays included in this study share some similarities in terms of sediment characteristics (Sherwood et al., 1984; Sherwood and Creager, 1990); however, there are differences among them in terms of the composition (i.e., percent silt and clay vs. sand) and grain size. Although Baker and Youngs Bays receive considerable deposits of fine sand, silts, and clays, the sources of sediment deposits differ (Sherwood and Creager, 1990; Simenstad et al., 1990). Baker Bay and Cathlamet Bay receive fine sediments from suspended material, while Youngs Bay received fortnightly inputs of fine sediment from ephemeral estuarine turbidity maximum events (Sherwood and Creager, 1990). In addition, there are seasonal differences in depositional patterns, with the western side of Baker Bay receiving coarser sediment deposits than the east side in February and June. In Youngs Bay, the upstream reaches tend to accumulate a combination of long-term deposits of coarse and fine sediments, with the latter dominating on the fringes. Closer to the estuary's south channel, sediment deposits are coarser than in the other peripheral bay areas. Salinity varies throughout the year in peripheral bays as a function of river discharge; Baker Bay on the northern side of the estuary is mesohaline (i.e., brackish), with a range of 5–20 practical salinity

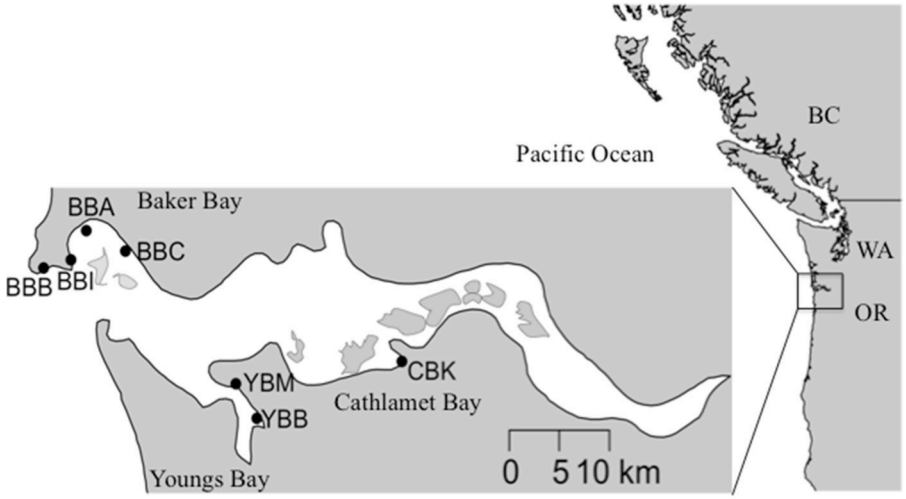

FIGURE 1 | Map of the Columbia River estuary sampling sites within tidal wetlands from three lateral bays: Baker Bay (BB), Cathlamet Bay (CB), and Youngs Bay (YB). BBB, Baker Bay, Boat Launch; BBI, Baker Bay, Ilwaco harbor; BBA, Baker Bay, airport road; BBC, Baker Bay, Chinook Harbor; YBM, Youngs Bay, Mouth; YBB, Youngs Bay, Back; CBK, Cathlamet Bay, Knappa dock.

units (PSU) during periods of relatively low flow (i.e., summer and autumn), while Youngs and Cathlamet Bays on the southern side of the estuary are oligohaline (0–5 PSU). The furthest upriver site, Cathlamet Bay, includes a diverse region of islands, tidal flats and marshes that experience seasonal exposure to salinity at depth.

Sample Collection and Chemical Analysis

Sediment texture (percent clay, silt) was determined using the hydrometer method (AgSource Laboratories, OR) on sediment samples from August 2013 prior to the collection of samples for the analysis of P forms. From September 2013–August 2014, sediment samples for the analysis of P forms were collected 1–2 h before low tide at sites within Baker Bay (four sites: BBB, BBI, BBA, BBC), Youngs Bay (two sites: YBB, YBM) and Cathlamet Bay (one site: CBK; **Figure 1**), all on exposed mudflats lacking any emergent vegetation at low tide. Cores were collected by pressing 50 mL Falcon conical centrifuge tubes with the bottom cut off into sediments. A full tube represented a sediment volume of ∼43 cm^3 (with a core diameter of 2.3 cm and a length of 10 cm). The tubes were transported back to the laboratory on ice (∼2–6 h) and kept at −20°C pending analysis. For this study, sediment cores from March–April and May–August were coarsely sieved to remove large debris, air-dried in a fume hood, ground and homogenized prior to P-NMR extraction (Cheesman et al., 2013). Total P concentrations in the unextracted sediments were determined by ignition followed by extraction with dilute H_2SO_4 (SmartChem 170, Unity Scientific, MA). Following combustion, dissolved P from the sediment extracts was determined colorimetrically (Murphy and Riley, 1962) and total OM content was estimated by loss on ignition (LOI) at 500°C (Nelson and Sommers, 1996).

Samples collected from waters overlying sediments were filtered in the field by syringe (60 mL) through combusted (4 h at 450°C) 0.7 μm, 25 mm GF/F filters (Whatman, NY) into 60 mL acid-cleaned HDPE bottles (Nalgene) and transported to the lab on dry ice in a cooler, where they were stored at −20°C pending processing. Total nitrogen (N) and total P concentrations were determined on unfiltered water samples. A rapid flow analyzer (Astoria Analyzer, Astoria Pacific, Clackamas, OR) was used for colorimetric determination of dissolved nitrate+nitrite (NO_x), ammonium, nitrite, and DIP (here measured as molybdate-reactive orthophosphate) concentrations and for measurement of total N and P after alkaline persulfate digestion (US EPA, 1983a,b; Antweiler et al., 1996; Zimmerman and Keefe, 1997; Patton and Kryskalla, 2003). Further, salinity and temperature measurements were checked during time of sampling by *in situ* sensor platforms (SATURN04, Cathlamet Bay; SATURN07, Baker Bay; SATURN09, Youngs Bay) in the Columbia River from a publicly available online database (www.stccmop.org) maintained by the Center for Coastal Margin Observation and Prediction (Baptista et al., 2015).

Extraction of Phosphorus

Using a modification of the Cade-Menun and Preston (1996) procedure, approximately 3.0 g of air-dried sediment was suspended in 30 mL of NaOH-EDTA (0.25 M NaOH, 50 mM Na_2EDTA) and sonicated (Branson Digital, Cleveland, OH) for 1 min at 20 kHz (∼55 W) in an ice bath followed by shaking at 150 rpm for 4 h. Samples were centrifuged for 10 min at 1,200 × g and the supernatant was removed, neutralized with 10% HCl and frozen at −80°C prior to lyophilization. An aliquot of each NaOH-EDTA extract was analyzed for Al, Ca, Fe, Mg, manganese (Mn), and P (mg L^{-1}) by inductively coupled plasma atomic emission spectroscopy (ICP-AES) using a Plasma 400 emission spectrophotometer (PerkinElmer, Waltham, MA).

Solution P-NMR

Lyophilized extracts were redissolved in a solution combining 0.6–0.65 mL each of D_2O, H_2O, NaOH-EDTA solution, and 10 M NaOH, vortexed, centrifuged at 1,500 × *g* for 20 min, and stored at 4°C within 12 h of analysis. If precipitate formed (observed in two samples, from BBA and BBC), it was filtered out using 0.2-μm polycarbonate syringe filters prior to analysis. Spectra were collected on a Bruker Avance 500 MHz NMR spectrometer with a 10 mm broadband probe. The NMR delay times were determined based on the ratio of concentrations of P/(Fe+Mn) within the extracts (McDowell et al., 2006). A temperature of 21°C and a 45° pulse were used, with a pulse delay of 4.5 s. Acquisition time was 0.5 s and 2,800–5,830 scans (∼4–8 h) were collected. Samples were analyzed with no spinning and no proton decoupling.

Data Analysis and Statistics

The NMR spectra were processed using NMR Utility Transform Software (NUTS; Acorn NMR, Livermore, CA, 2000 edition). Processing included standardizing the orthophosphate peak for each sample at 6.000 ppm. Phosphorus forms (P forms) were identified by their chemical shifts using published libraries for known peaks, with spiking for confirmation (Cade-Menun, 2015). Spectra were processed with 7–10 Hz line broadening for full spectra and 3 Hz line broadening to identify peaks in the orthophosphate monoester and diester regions (Cade-Menun and Liu, 2014). Corrections were made to account for orthophosphate diester degradation by summing the peak areas associated with degradation products (α- and β-glycerophosphate and mononucleotides, degraded from phospholipids and RNA respectively), subtracting this sum from the total monoester area, and adding it to the total diester area (Young et al., 2013; Schneider et al., 2016).

A constrained ordination was performed on the transformed P forms (abundance) and sediment environmental data (TotalP, LOI, Fe, Mn, Ca, and Mg). A redundancy analysis (RDA) is an extension of principal components analysis (PCA) designed to identify or reduce complexity of environmental data. The principal components were constrained to be linear combinations of the environmental variables, with the goal being to explain variation of the dependent variables (P form abundance) as much as can be explained by independent variables (sediment properties; Legendre and Legendre, 1998; Ramette, 2007). Phosphorus forms and sediment data were normalized with centered log ratio (clr) transformations (Abdi et al., 2015). Statistical analyses were performed with R using the vegan package (R Core Team, 2015).

RESULTS

Chemical Analysis

Physicochemical characteristics associated with each sample are shown in **Table 1**. It should be noted that the small number of samples analyzed in this study limits spatial and temporal comparisons made across sites and environmental characteristics. Total sediment P concentrations varied by more than two-fold, with the highest value observed at CBK (1,366 mg kg^{-1}) and the lowest at BBC (601 mg kg^{-1}). The OM (LOI%) content mirrored total sediment P (11.3% at CBK, 2.2% at BBC). Sediment texture analysis demonstrated the largest percentage of clay and silt at the western side of Baker Bay (42.4%, BBB) and at the mouth of Youngs Bay (35%, YBM), which come from different sources in the estuary including fine suspended material and estuarine turbidity maxima events, respectively (Sherwood and Creager, 1990).

TABLE 1 | Physicochemical characteristics of water and sediments collected from the estuary.

Site	Date (Time)	Water†							Sediment‡		
		DIP μM	TotP μM	NO_x μM	TotN μM	NH_4	Salinity PSU§	Temp °C§	Total P mg kg^{-1}	LOI %	Clay + Silt %
CBK	4/29/14 (1:10)	0.59	1.5	27.0	39.3	3.14	0	11.7	1,366	11.3	13.4
YBM	3/28/14 (18:55)	0.30	1.2	1.64	21.7	1.68	3	10.8	712	3.8	35.0
YBB	3/28/14 (19:19)	0.94	5.1	36.4	80.7	4.10	1	10.8	1,221	9.6	–
BBB	3/28/14 (7:04)	0.54	13.7	24.7	114.7	2.61	4	9.4	853	6.5	42.4
BBI	4/29/14 (7:30)	0.85	1.9	5.64	30.2	4.82	4	13.8	630	2.5	15.8
BBC	5/29/14 (10:15)	0.98	2.9	1.20	29.8	3.25	6	15.1	601	2.2	11.8
BBA	8/25/14 (7:50)	4.79	10.5	0.10	56.9	16.0	18	17.9	752	1.2	13.4

†Water collected above the sediments; DIP, dissolved inorganic phosphorus (P); TotP, total P; NO_x, NO_3^-+NO_2^-; TotN, total dissolved nitrate/nitrite; NH_4^+, ammonium; PSU, practical salinity units; and Temp, temperature.

‡Total P (sediment) mg kg^{-1} dry sediment weight, and organic matter was calculated as loss-on-ignition (LOI); Clay and Silt were analyzed for sediments collected in August 2013.

§Salinity and temperature collected from local autonomous sensors (SATURN04, Cathlamet Bay; SATURN07, Baker Bay; SATURN09, Youngs Bay).

Monthly measurements of DIP, NO_x, and ammonium (NH_4) at the seven sites over a nine-month period (Jan–Sep 2014) are provided in Supplemental Materials (**Figure S2**). Only the measurements that coincide with the analysis of sediment P forms are indicated in **Table 1**. Water column DIP concentrations were low from March–May; in contrast, the sample taken in August at site BBA was one of the highest observed (4.79 μM; **Table 1**). The 9-month time series confirmed that DIP levels were low in the winter and spring but increased in the late summer (**Figure S2**). Higher salinity (6–18 PSU vs. 0–4 PSU) and higher DIP concentrations were observed in the August water sample compared to the others. High concentrations of NO_x in overlying waters were observed in samples collected from March–May, with the exception of the BBC site; NO_x concentrations were lowest in late summer (**Table 1**, **Figure S2**). Ammonium concentrations mirrored DIP throughout the year (**Figure S2**), with the lowest concentrations observed in spring and the highest value in the late summer (**Table 1**).

The P recovery following sediment NaOH-EDTA extraction varied from a low of 1.5 at site BBA to a high of 24.5% at YBB (**Table 2**). The samples with the lowest OM tended to have the lowest Fe and Mn concentrations in the extracts (e.g., 0.45 and 0.34 mg kg^{-1}, respectively at BBC; **Table 2**), and therefore may have required longer delay times to be fully quantitative for extracted P. Higher concentrations of paramagnetic ions in samples (e.g., Fe, Mn) shorten ^{31}P nuclei relaxation times, reducing the delay time required between pulses (McDowell et al., 2006), but potentially increasing line-broadening of peaks. Since it is unknown whether variation in the efficiency of P extraction among the samples led to any biases due to preferential extraction of certain P forms, quantifications should be interpreted with caution. Of the cations extracted with P, Ca was most abundant, ranging from 110 to 2077 mg kg^{-1} across samples (**Table 2**), while Fe concentrations ranged from 1.5 mg kg^{-1} (BBA) to 73.7 mg kg^{-1} (YBB), however caution should be taken in interpretation as these cation concentrations do not necessarily represent their actual concentrations in sediments.

Phosphorus Forms and Their Contributions to P in Sediments

Figure 2 shows example P-NMR spectra, which demonstrate peaks associated with P forms detected in estuarine sediments of the Columbia River; the remaining spectra are included as Supplemental Data (**Figure S1**). Chemical shifts associated with the peaks are summarized in **Table S1** and the percentages of total extracted P accounted for by identified P forms are in **Table S2**.

Total extracted P was dominated by inorganic forms (P_i; **Figure 3A**), which exceeded contributions from organic P (P_o) by 2–6 times. Orthophosphate, which varied twenty-fold across sites (8.1–231.3 mg kg^{-1} at BBA and YBB, respectively), accounted for 70.7–84.4% of total P [Σ (P_i + P_o)] and 87–99% of P_i (**Table S2**). Both pyrophosphate and polyphosphate were detected at all sites except BBA in the summer (where only polyphosphate was detected). There was little variation in concentration among most sites (**Figure 3B**), with pyrophosphate and polyphosphate accounting for 1–13% of P_i and 0.8–10.6% of total P, respectively (**Table S2**). The largest total polyphosphate (pyrophosphate + polyphosphate) concentrations were observed at the west end of Baker Bay (6.2 mg kg^{-1}, BBI), while the lowest were observed in Cathlamet Bay, located in a southern bay of the estuary (CBK, 0.8 mg kg^{-1}; **Table 3**).

Concentrations of P_o ranged from 2.9 to 59.5 mg kg^{-1}, accounting for 13.5–26.6% of total extracted P in sediments (**Figure 3C**). Orthophosphate monoesters made the largest contribution to P_o, where they accounted for 66–94% of P_o and 9.4–25% of total extracted P. Identified monoesters comprised stereoisomers of inositol hexakisphosphate (IHP), including *chiro, myo, neo, scyllo*-IHP, as well as α- and β-glycerophosphate and mononucleotides. The IHP stereoisomers were broadly

TABLE 2 | Concentrations of P and selected cations in alkaline extracts from estuary lateral bay sediments.

Location	Sample	Date (Time)	NaOH-EDTA extracts						
			P	Fe	Mn	Al	Mg	Ca	P Recovery† %
			mg kg^{-1}						
Cathlamet Bay	CBK	4/29/14 (1:10)	111.0	34.1	60.3	77.0	24.5	1553.5	8.1
Youngs Bay	YBM	3/28/14 (18:55)	47.7	1.69	0.56	13.4	36.3	193.6	6.7
	YBB	3/28/14 (19:19)	298.8	73.7	34.0	205.1	16.1	1077.7	24.5
Baker Bay	BBB	3/29/14 (7:04)	204.3	12.0	6.01	58.5	73.3	1044.1	23.9
	BBI	4/29/14 (7:30)	100.1	3.29	1.39	49.6	87.6	575.5	15.9
	BBC	5/29/14 (10:15)	33.9	0.45	0.34	16.7	10.6	109.7	5.7
	BBA	8/25/14 (7:50)	11.1	1.50	0.19	16.5	12.9	79.4	1.5

† *P Recovery, Percentage of total sediment P extracted by NaOH-EDTA.*

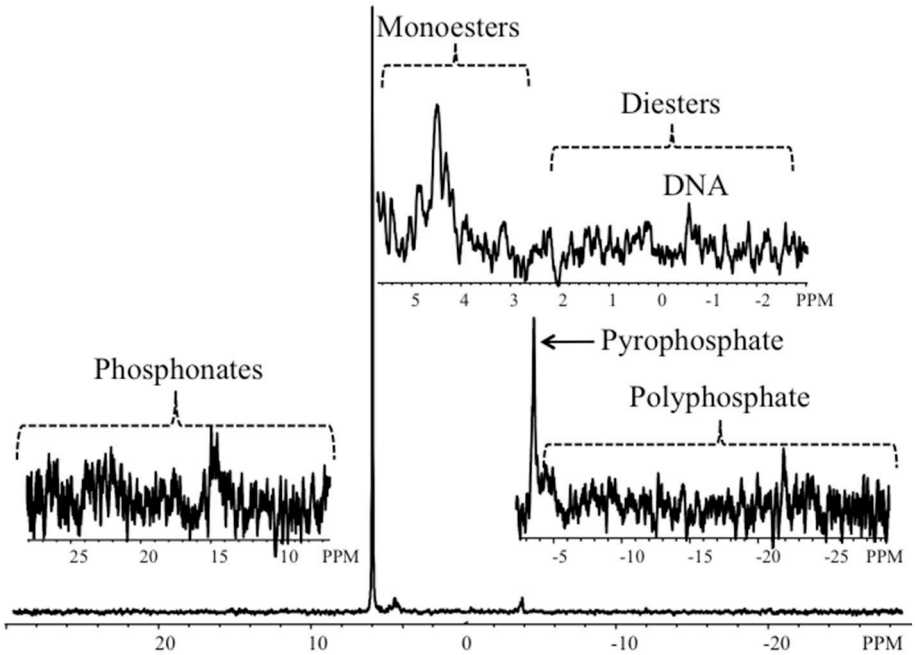

FIGURE 2 | Representative P-NMR spectrum from a sediment sample collected in Youngs Bay (YBM). The full spectrum, scaled to the orthophosphate peak at 7 Hz line-broadening, is shown at the bottom; the upper right inset shows the orthophosphate monoester and orthophosphate diester regions, including a peak corresponding to DNA, the bottom right inset shows the pyrophosphate and polyphosphate region, and the bottom left inset shows the phosphonate region.

detected in estuarine sediments at concentrations that varied considerably (1.4–54.1 mg kg^{-1}) over short distances, indicating high local heterogeneity (**Table 3**). For example, the lowest and highest IHP concentrations were observed within Baker Bay (BBB and BBI, respectively while BBA had no detectable IHP). Stereoisomers of IHP (*chiro, myo, neo, scyllo*) contributed approximately equally to IHP with the exception of BBB, where contributions from *myo*-IHP were small (**Table 3**).

Orthophosphate diesters made up 0.8–7.4% of extracted P, contributing 0.4–28.7 mg kg^{-1} of P (**Table S2**; **Figure 3C**). The highest concentration of total orthophosphate diesters was observed at YBB (28.7 mg kg^{-1}). DNA was detected throughout the estuary, contributing as little as 0.2 mg kg^{-1} of P (BBC) and as much as 4.5 mg kg^{-1} of P (YBB), which also had the highest concentration of diester degradation products (α- and β-glycerophosphate and mononucleotides; **Table 3**). Though present at low concentrations, phosphonates were detected throughout estuarine sediments (0.7–1.4% P), ranging from 0.33 to 2.1 mg kg^{-1} of total extracted sediment P (**Figure 3C**).

Redundancy Analysis

An RDA was performed to explore possible relationships among P forms and sediment characteristics within lateral bay sediments (**Figure 4**). The biplots of the RDA model display ordination between response variables (P form abundance) and explanatory variables (TotalP, LOI, Fe, Mn, Ca, and Mg; **Figure 4A**), sites (non-quantitative centroids; CBK, YBM, YBB, BBB, BBI, BBC, and BBA) and explanatory variables (**Figure 4B**). The dominant constraining variable (RDA1) was explained by variation in organic matter (LOI; 90.6%) and secondarily (RDA2) by Mg concentrations (Mg; 6.7%), which together explained 97.3% of the variation observed in P forms.

An ordination biplot was generated to look for correlative relationships among sediment characteristics and P form abundances (**Figure 4A**). For example, among the response variables (i.e., P form abundances), phytate (IHP)—and to a lesser degree, total monoesters (Mono)—were associated with low organic matter (LOI) found at BBA, BBC, BBI, and CBK (**Figures 4A,B**). In contrast, diesters (Diester), and to a weaker extent DNA were associated with high concentrations of organic matter, Ca, and Mg (LOI, Ca, Mg; **Figure 4A**), observed at YBM, YBB and BBB. Orthophosphate and phosphonates were weakly associated with high OM (LOI), and total polyphosphates (TotPoly; pyrophosphate and polyphosphates) were not associated with any explanatory variables. Differences in overlying water properties (total P, NO_x, DIP, temperature, salinity) did not explain patterns in P form abundance (data not shown).

An ordination plot of sample sites and sediment characteristics split up sites into two groups according to their associative sediment characteristics (**Figure 4B**). For example, sites BBA, BBC, CBK and to a lesser extent BBI all had low organic matter, total sediment P and concentrations of cations (Ca, Mg, Fe, and Mn; **Figure 4B**), compared to sites YBB, YBM and BBB. The BBA site separated from the other sites because of its very low organic matter (LOI) and cation concentrations (**Figure 4B**). Correlation of explanatory variables can be obtained by taking the cosine of angles between vectors;

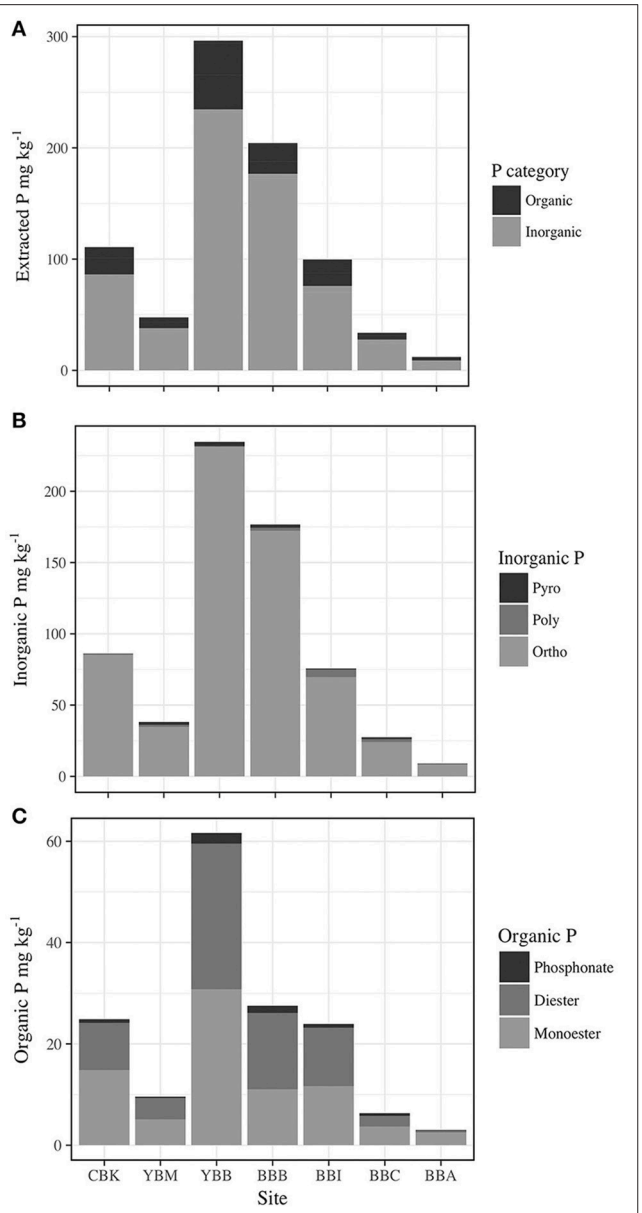

FIGURE 3 | Concentration of P by forms in sediment extracts from sampled sites in the Columbia River estuary (CBK, YBM, YBB, BBB, BBI, BBC, and BBA), including **(A)** Total organic P (P_O) and total inorganic P (P_I); **(B)** total inorganic phosphorus (P_O) as forms (Pyro, pyrophosphate; Poly, polyphosphate; Ortho, orthophosphate); and **(C)** total organic phosphorus (P_O) as forms (phosphonate; Diester, orthophosphate diester; Monoester, orthophosphate monoester).

this analysis revealed that sediment Ca and organic matter (LOI) were highly correlated, with angles $\leq 15^{\circ}$ between most vectors ($R = 0.97$; **Figures 4A,B**).

DISCUSSION

There are few studies reporting P forms in estuarine environments, and therefore the small data set presented here provides useful information about the potential for P cycling and retention in a river-dominated estuary. The time and costs associated with P-NMR often limit the number of samples that can be analyzed; in addition, samples are often homogenized and pooled, limiting potential replication. In addition, standardization of methods is being stressed in the literature so that P-NMR results can be compared across environments (Cade-Menun and Liu, 2014). For this reason, extracts were prepared from 10 cm diameter cores, which represents the homogenization of at least 1 year's worth of sediment deposition (based on rates of $\sim$6 cm year^{-1}; Sherwood and Creager, 1990). In addition, the extraction of organic P forms is notoriously difficult (Cade-Menun et al., 2006), therefore we used an alkaline extraction that optimizes the extraction of organic P forms; however, this tends to produce low extraction efficiencies, and this must be kept in mind when interpreting the data. The recovery rates reported here for NaOH-EDTA extracted P (6–24%) are comparable to other P-NMR studies in wetlands with similar sediment characteristics. For example, P recovery was 6–16% in calcareous soils and 16–30% in sediments with low OM and neutral pH (Cheesman et al., 2014). In contrast, higher recoveries (25–84%) have been reported in wetland sediments that are acidic (pH 3.6–4.8) or that have high OM (56–94%; Turner and Newman, 2005; Cheesman et al., 2014). It is likely that the residual P that was not extracted in our protocol was inorganic, alkali-stable, and associated with Ca or Mg minerals, since these forms are not readily extracted using NaOH-EDTA (Turner and Newman, 2005; Defforey et al., 2017). Nevertheless, despite low recovery of P in NaOH-EDTA extracts, we detected a range of P forms in estuarine sediments.

Polyphosphates and pyrophosphates were detected in all estuarine sediment samples, where they contributed as much as 13% of inorganic P (10% of total extracted P). In almost half the samples, polyphosphate concentrations exceeded pyrophosphate, in contrast to other studies (Turner and Newman, 2005; Zhang et al., 2009; Cheesman et al., 2010). This might be explained by the fact that, unlike the previous work cited, we included a neutralization step prior to lyophilization, which increases the stability of polyphosphate (Cade-Menun et al., 2006). Degradation of polyphosphate to pyrophosphate (either *in situ* or during sediment extraction) may also account for the fact that only a handful of studies report detection of polyphosphate in wetlands (Zhang et al., 2009; Cheesman et al., 2014).

Polyphosphate is biologically produced across the domains of life, including by bacteria, fungi, protozoa, plants, and mammals (Kornberg, 1995; Brown and Kornberg, 2004; Kulaev et al., 2004) and is thought to be indicative of microbial activity rather than linked to particular soil or sediment types (Cheesman et al., 2014). Interestingly, we detected polyphosphate in sediments with different characteristics, from brackish sediments in Baker Bay where concentrations were highest BBI (low OM, low Fe, and Mn) and BBB (high OM, high Fe, and Mn), and further supported by our RDA which found total polyphosphates not affiliated with measured sediment properties. Further, the presence of diesters (e.g., DNA) as an indicator of microbial activity was associated with high OM, Fe, and Mn concentrations and total P in sediments, suggesting that microbial biomass may be a major contributor to organic matter in river-dominated

TABLE 3 | Phosphorus form contributions at estuary lateral bay sample sites.

Location	Samples	Inorg:Org†	Mono:Di	cMono	cDi	Total IHP	cM:D	Myo:other IHP	Deg	DNA	Total Poly	Pyro:Poly
				mg kg^{-1}					mg kg^{-1}			
Cathlamet Bay	CBK	3.5	5.2	14.8	9.3	7.8	1.6	0.7	5.4	1.7	0.8	1.3
Youngs Bay	YBM	4.0	3.5	5.1	4.2	2.5	1.2	0.6	2.2	0.5	3.4	1.5
	YBB	3.8	3.2	30.8	28.7	16.4	1.0	1.0	14.3	4.5	3.3	10.0
Baker Bay	BBB	6.4	2.8	11.0	15.1	1.4	0.7	0	8.2	2.3	4.3	1.1
	BBI	3.2	2.1	11.6	11.6	54.1	1.0	0.5	4.2	4.0	6.2	0.15
	BBC	2.1	9.7	3.7	2.1	2.3	1.8	0.4	0.9	0.2	3.6	0.7
	BBA	3.0	31.3	2.5	0.4	0	7.1	0	0.3	0.02	0.9	0

†*Inorg:Org, ratio of inorganic to organic P; Mono:Di, ratio of Orthophosphate monoesters to diesters without correction for degradation; cMono, cDi, total orthophosphate monoester and diesters corrected for degradation; Total IHP, sum of myo-, scyllo-, neo- and D-chiro-inositol hexakisphosphate; Myo:other IHP, ratio of sum of myo-inositol hexakisphosphate to all sterioisomers (scyllo-, neo-, D-chiro-inositol hexakisphosphate); Deg, degradation compounds include α-glycerophosphate, β-glycerophosphate, and mononucleotides; DNA, sum of identified DNA peaks; Total Poly, sum of pyrophosphate and polyphosphate; Pyro:Poly, ratio of pyrophosphate to polyphosphate. Standard error (±) in P-NMR analysis for samples from native and tame grasslands and croplands (four replicates across land types) was 8.7% for extracted P at ≥10%, compared to 20.1% for extracted P at <10% (personal communication B. Cade-Menun, Liu et al., 2018).*

estuary sediments. Polyphosphates found throughout sediments produced by microbial activity may be a source of cycled P in dynamic, diel cycled environments such as estuaries, perhaps much more than has generally been assumed and further investigation is certainly warranted.

Although extracted P was dominated by inorganic forms, organic P accounted for ∼30% of total P and was comprised of P forms that are considered both labile (e.g., RNA, phospholipids) and stable (e.g., IHP), despite rapid flushing and a low contribution of organic P compared to other freshwater wetlands (Turner and Newman, 2005; Turner et al., 2006; Cheesman et al., 2010, 2014) or lake sediments (Carman et al., 2000). The dominant organic P form in these estuarine sediments was the orthophosphate monoester *myo*-inositol hexakisphosphate (*myo*-IHP, also called phytate), which is derived from plants, and was detected in all but one sample. Inositol phosphates (*myo*-IHP, and stereioisomers *scyllo*-, neo-, and D-*chiro*-IHP), accrue in terrestrial soils and in aquatic sediments, particularly when clay content is high and pH is low; under these conditions, phytate tends to be the dominant form (Turner et al., 2002). In the river-dominated estuary, phytate was associated with low OM in both fresh and brackish sediments, with the highest concentrations occurring in samples from Baker Bay with relatively high salinity (BBA; >15 PSU). Usually, sedimentary phytate concentrations tend to be lower in the presence of salt and under hypoxic conditions, (Suzumura and Kamatani, 1995a,b) due to the destabilization of phytate complexes (Gardolinski et al., 2004) formed through complexation with iron oxides in acidic soils or by minerals in sediments with high mineral content (Turner et al., 2002; Turner and Newman, 2005; Turner and Weckström, 2009; Cheesman et al., 2014). High variability in phytate concentrations in the higher-salinity samples may indicate a varying effect of salinity and/or sediment complexing agents as Baker Bay has the greatest variation in biogeochemical conditions.

Other Influences on P Forms and P Retention

Peripheral bay environments in this study are considered depositional environments, where fine material (mainly consisting of clays and silts) is deposited from suspended fluvial material (Sherwood and Creager, 1990). The composition of sediments and grain sizes varies seasonally in the estuary; however, the peripheral bays are consistently sites of long-term deposition of fine sediments. Differences in P forms found at the different sites within these bays could reflect differences in sediment sorting, and/or diagenetic processes. For example, sites differ in terms of the origin of deposited sediments, with Baker and Cathlamet Bay sediment originating from fluvial washload and Youngs Bay sediment originating from a combination of washload and deposits from ephemeral estuarine turbidity maxima.

In addition to sequestration of organic forms, P retention is influenced by abiotic buffering processes, which limit fluctuations in DIP through mineral precipitation with Fe, Mg, Ca, and Mn (e.g., Fe oxyhydroxides, Ca mineral precipitates; Richardson and Marshall, 1986; Froelich, 1988; Reddy et al., 1999; Bridgham et al., 2001). Retention also occurs through abiotic adsorption to sediment surfaces, particularly on fine particles (Li et al., 2013), which dominate the depositional environment of peripheral bays in the estuary. The relatively low and similar DIP concentrations in waters overlying Columbia River estuary sediments (Gilbert et al., 2013; **Figure S2**)—despite variations in total P within the sediments—may be explained by buffering of P (Froelich, 1988), which warrants further exploration as this would affect P retention in these depositional environments. In addition, the limited sample set suggests that YBB and BBB sites had high concentrations of extractable Ca^{2+}, which readily forms mineral precipitates with P if in high concentrations in sediment environments, (e.g., $CaHPO_4$ from Ca^{+2} and HPO_4^{-2}) at comparable rates with sediment P

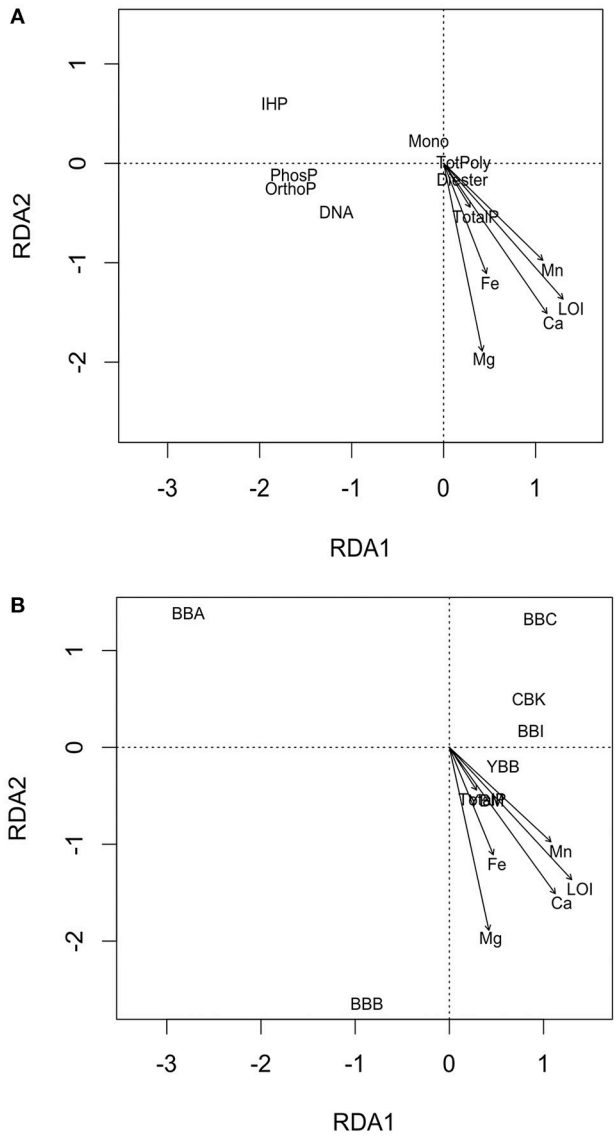

FIGURE 4 | Schematic of two RDA biplots with objects ordinated as **(A)** response variables as points (TotPoly, total of pyrophosphates and polyphosphates; IHP, inositol hexakisphosphates; Mono, monesters; Diesters, diesters; OrthoP, orthophosphate; DNA, deoxyribonucleic acid; PhosP, phosphonate), and **(B)** non-quantitative points (sites CBK, YBM, YBB, BBC, BBI, BBA, BBB), and explanatory variables as arrows (LOI, loss-on-ignition, concentrations of Fe, Mn, Ca, Mg, and TotalP, total sediment P).

sorption (Reddy et al., 1999; Li et al., 2013). Further studies should investigate relationships between P forms and total cation concentrations in different sedimentary environments within the estuary to determine how they might affect P mineralization and sequestration.

CONCLUSIONS

A variety of P forms were identified in river-dominated estuary sediment extracts, which were dominated by inorganic P. Although orthophosphate made the largest contribution to inorganic P, polyphosphate and pyrophosphate were found throughout the lateral bays, constituting up to 13% of extracted inorganic P. Organic forms accounted for ∼30% of total extracted P, and included both labile P forms (e.g., phospholipids, RNA) and resistant forms (e.g., IHP), which were detected at approximately equal concentrations throughout the estuary. Sample-to-sample variability was greatest among organic P forms, with orthophosphate monoesters such as phytate (*myo*-IHP) being most abundant when OM content was low. In contrast, orthophosphate diesters were more abundant in sediments with high OM, suggesting that microbial activity might play a larger role in P cycling in sediments with high OM. Low orthophosphate concentrations in overlying waters along with variable sediment P concentrations suggest P buffering may occur within peripheral bays. These data demonstrate that despite short water residence times and rapid flushing, sediments of a river-dominated estuary have the potential to sequester P in inorganic and inorganic forms, thus influencing P loading to the coastal ocean via the large Columbia River plume.

AUTHOR CONTRIBUTIONS

SW collected and analyzed all samples, wrote the manuscript, and managed communication among all the authors. BC-M ran the NMR experiments and analyzed spectra with SW. JN and SW analyzed water samples and JN contributed to sediment P analysis as well as design of the work. TP had substantial contributions to the conception and design of the work and along with BC-M critically revised the work for intellectual content and contributions.

FUNDING

This work was supported by the National Science Foundation (NSF OCE-0424602), a Science and Technology Center, the Center for Coastal Margin Observation and Prediction (CMOP). Further, travel grants were provided by the National Science Foundation-sponsored Consortium of Universities for the Advancement of Hydrological Science, Inc. (CUAHSI), and an N.L. Tartar Trust Research Award from Oregon Health and Science University (OHSU) for work in Canada.

ACKNOWLEDGMENTS

The NMR analysis was done at the Saskatchewan Structural Sciences Centre at the University of Saskatchewan, with support funding from Agriculture and Agri-Food Canada; we thank Drs. K. Brown and P. Zhu for their assistance. Total sediment analysis was done with J. Morse at Portland State University.

SUPPLEMENTARY MATERIAL

The Supplementary Material for this article can be found online at: https://www.frontiersin.org/articles/10.3389/fmars.2018.00302/full#supplementary-material

REFERENCES

Abdi, D., Cade-Menun, B. J., Ziadi, N., and Parent, L. E. (2015). Compositional statistical analysis of soil ^{31}P-NMR forms. *Geoderma* 257–258, 40–47. doi: 10.1016/j.geoderma.2015.03.019

Antweiler, R. C., Patton, C. J., and Taylor, H. E. (1996). *Automated Colorimetric Methods for Determination of Nitrate Plus Nitrite, Nitrite, Ammonium and Orthophosphate Ions in Natural Water Samples*. Report, USGS Report.

Baptista, A. M., Seaton, C., Wilkin, M. P., Riseman, S. F., Needoba, J. A., Maier, D., et al. (2015). Infrastructure for collaborative science and societal applications in the Columbia River estuary. *Front. Earth Sci.* 9, 659–682. doi: 10.1007/s11707-015-0540-5

Barbier, E. B., Hacker, S. D., Kennedy, C., Koch, E. W., Stier, A. C., and Silliman, B. R. (2011). The value of estuarine and coastal ecosystem services. *Ecol. Monogr.* 81, 169–193. doi: 10.1890/10-1510.1

Bricker, S. B., Longstaff, B., Dennison, W., Jones, A., Boicourt, K., Wicks, C., et al. (2008). Effects of nutrient enrichment in the nation's estuaries: a decade of change. *Harmful Algae* 8, 21–32. doi: 10.1016/j.hal.2008.08.028

Bridgham, S. D., Johnston, C. A., Schubauer-Berigan, J. P., and Weishampel, P. (2001). Phosphorus sorption dynamics in soils and coupling with surface and pore water in riverine wetlands. *Soil Sci. Soc. Am. J.* 65, 577–588. doi: 10.2136/sssaj2001.652577x

Brown, M. R., and Kornberg, A. (2004). Inorganic polyphosphate in the origin and survival of species. *Proc. Natl. Acad. Sci. U.S.A.* 101, 16085–16087. doi: 10.1073/pnas.0406909101

Cade-Menun, B. J. (2015). Improved peak identification in ^{31}P-NMR spectra of environmental samples with a standardized method and peak library. *Geoderma* 257–258, 102–114. doi: 10.1016/j.geoderma.2014.12.016

Cade-Menun, B. J., and Liu, C. W. (2014). Solution 31P-NMR spectroscopy of soils from 2005-2013: a review of sample preparation and experimental parameters. *Soil Soc. Am. J.* 78, 19–37. doi: 10.2136/sssaj2013.05.0187dgs

Cade-Menun, B. J., Navaratnam, J. A., and Walbridge, M. R. (2006). Characterizing dissolved and particulate phosphorus in water with P-31 nuclear magnetic resonance spectroscopy. *Environ. Sci. Technol.* 40, 7874–7880. doi: 10.1021/es061843e

Cade-Menun, B. J., and Preston, C. M. (1996). A comparison of soil extraction procedures for 31P NMR spectroscopy. *Soil Sci.* 161, 770–785. doi: 10.1097/00010694-199611000-00006

Carman, R., Gunnar, E., and Damberg, C. (2000). Distribution of organic and inorganic phosphorus compounds in marine and lacustrine sediments: a 31P NMR study. *Chem. Geol.* 163, 101–114. doi: 10.1016/S0009-2541(99)00098-4

Celi, L. R., and Barberis, E. (2005). "Abiotic stabilzation of organic phosphorus in the environment," in *Organic Phosphorus in the Environment*, eds B. L.Turner, E. Frossard, and D. S. Baldwin (Cambridge, MA: CABI Publishing),113–132. doi: 10.1079/9780851998220.0113

Chawla, A., Jay, D. A., Baptista, A. M., Wilkin, M., and Seaton, C. (2008). Seasonal variability and estuary-shelf interactions in circulation dynamics of a river-dominated estuary. *Estuaries Coasts.* 31, 269–288. doi: 10.1007/s12237-007-9022-7

Cheesman, A. W., Turner, B. L., Inglett, P. W., and Reddy, K. R. (2010). Phosphorus transformations during decomposition of wetland macrophytes. *Environ. Sci. Tech.* 44, 9265–9271. doi: 10.1021/es102460h

Cheesman, A. W., Turner, B. L., and Reddy, K. R. (2014). Forms of organic phosphorus in wetland soils. *Biogeosciences* 11, 6697–6710. doi: 10.5194/bg-11-6697-2014

Cheesman, A. W., Turner, B. L., and Rocca, I. (2013). "Phosphorus characterization in wetland soils by solution Phosphorus-31 nuclear magnetic resonance spectroscopy," in *Methods in Biogeochemistry of Wetlands*, eds R. D. DeLaune, C. J. Richardson, and J. P. Megonigal (Madison, WI: Soil Science Society of America), 639–665.

Condron, L. M., Turner, B. L., and Cade-Menun, B. J. (2005). "Chemistry and dynamics of soil organic phosphorus," in *Phosphorus Agriculture and the Environment*, eds J. T. Sims and A. N. Sharpley (Madison, WI: Soil Science Society of America), 87–121.

Conley, D. J., Paerl, H. W., Howarth, R. W., Boesch, D. F., Seitzinger, S. P., Havens, K. E., et al. (2009). Controlling eutrophication: nitrogen and phosphorus. *Science* 323, 1014–1015. doi: 10.1126/science.1167755

Daniel, T. C., Sharpley, A. N., and Lemuyon, J. L. (1998). Agricultural phosphorus and eutrophication: a symposium review. *J. Env. Qual.* 27, 251–257. doi: 10.2134/jeq1998.00472425002700020002x

Defforey, D., Cade-Menun, B. J., and Paytan, A. (2017). A new solution ^{31} P NMR sample preparation scheme for marine sediments. *Limnol. Oceanogr. Meth.* 15, 381–393. doi: 10.1002/lom3.10166

Fox, L. E., Sager, S. L., and Wofsy, S. C. (1986). The chemical control of soluble phosphorus in the Amazon estuary. *Geochim. Cosmochim. Acta* 50, 783–794. doi: 10.1016/0016-7037(86)90354-6

Froelich, P. N. (1988). Kinetic control of dissolved phosphate in natural rivers and estuaries: a primer on the phosphate buffer mechanism. *Limnol. Oceanogr.* 33, 649–668. doi: 10.4319/lo.1988.33.4_part_2.0649

Gardolinski, P. C., Worsfold, P. J., and McKelvie, I. D. (2004). Seawater induced release and transformation of organic and inorganic phosphorus from river sediments. *Water Res.* 38, 688–692. doi: 10.1016/j.watres.2003.10.048

Gilbert, M., Needoba, J., Koch, C., Barnard, A., and Baptista, A. (2013). Nutrient loading and transformations in the Columbia River estuary determined by high-resolution *in situ* sensors. *Estuaries Coasts.* 36, 708–727. doi: 10.1007/s12237-013-9597-0

Grantham, B. A., Chan, F., Nielsen, K. J., Fox, D. S., Barth, J. A., Huyer, A., et al. (2004). Upwelling-driven nearshore hypoxia signals ecosystem and oceanographic changes in the northeast Pacific. *Nature* 429, 749–754. doi: 10.1038/nature02605

House, W. A., and Warwick, M. S. (1999). Interactions of phosphorus with sediments in the River Swale, Yorkshire, UK. *Hydrol. Process.* 13, 1103–1115. doi: 10.1002/(SICI)1099-1085(199905)13:7<1103::AID-HYP792>3.0.CO;2-6

Howarth, R., Chan, F., Conley, D. J., Garnier, J., Doney, S. C., Marino, R., et al. (2011). Coupled biogeochemical cycles: eutrophication and hypoxia in temperate estuaries and coastal marine ecosystems. *Front. Ecol. Environ.* 9, 18–26. doi: 10.1890/100008

Huyer, A.(1983). Coastal upwelling in the California current system. *Prog. Oceanogr.* 12, 259–284. doi: 10.1016/0079-6611(83)90010-1

Kellogg, L. E., and Bridgham, S. D. (2003). Phosphorus retention and movement across an ombrotrophic-minerotrophic peatland gradient. *Biogeochemistry* 63, 299–315. doi: 10.1023/A:1023387019765

Kornberg, A. (1995). Inorganic polyphosphate: toward making a forgotten polymer unforgettable. *J. Bacteriol.* 177, 491–496. doi: 10.1128/jb.177.3.491-496.1995

Kulaev, I. S., Vagabov, V. M., and Kulakovskaya, T. V. (eds.). (2004). "The occurence of polyphosphates in living organisms," in *The Biochemistry of Inorganic Polyphosphates* (Hoboken, NJ: John Wiley and Sons), 37–44. doi: 10.1002/0470858192

Legendre, P., and Legendre, L. (1998). *Numerical Ecology, 2nd Edn*. Amsterdam: Elsevier.

Li, M., Whelan, M. J., Wang, G. Q., and White, S. M. (2013). Phosphorus sorption and buffering mechanisms in suspended sediments from the Yangtze estuary, and Hangzhou Bay, China. *Biogeosciences* 10, 3341–3348. doi: 10.5194/bg-10-3341-2013

Liu, J., Cade-Menun, B. J., Yang, J., Hu, Y., Liu, C. W., Tremblay, J., et al. (2018). Long-term land use affects phosphorus speciation and the composition of phosphorus cycling genes in agricultural soils. *Front. Microbiol.* 9:1643. doi: 10.3389/fmicb.2018.01643

McDowell, R. W., and Sharpley, A. N. (2003). Uptake and release of phosphorus from overland flow in a stream environment. *J. Environ. Qual.* 32, 937–948. doi: 10.2134/jeq2003.9370

McDowell, R. W., Stewart, I., and Cade-Menun, B. J. (2006). An examination of spin-lattice relaxation times for analysis of soil and manure extracts by liquid state phosphorus-31 nuclear magnetic resonance spectroscopy. *J. Environ. Qual.* 35, 293–302. doi: 10.2134/jeq2005.0285

Millenium Ecosystem Assessment (2006). *Ecosystems and Human Well-being Synthesis.* Washington, DC: Island Press. Available online at: https://www.millenniumassessment.org/documents/document.356.aspx.pdf

Monbet, P., McKelvie, I. D., and Worsfold, P. J. (2010). Sedimentary pools of phosphorus in the eutrophic Tamar estuary (SW England). *J. Environ. Monitor.* 12, 296–304. doi: 10.1039/B911429G

Murphy, J., and Riley, J. P. (1962). A modified single solution method for the determination of phosphate in natural waters. *Anal. Chim. Acta* 27, 31–36. doi: 10.1016/S0003-2670(00)88444-5

Nelson, D. W., and Sommers, L. E. (1996). "Total carbon, organic carbon, and organic matter," in *Methods of Soil Analysis, Part 3*, *Chemical Methods,* ed D. L. Sparks (Madison, WI: Soil Science Society of America), 961–1010.

Noe, G. B., Scinto, L. J., Taylor, J., Childers, D. L., and Jones, R. D. (2003). Phosphorus cycling and partitioning in an oligotrophic everglades wetlands ecosytem: a radioisotope tracing study. *Freshwater Biol.* 48, 1993–2008. doi: 10.1046/j.1365-2427.2003.01143.x

Paerl, H. W. (2006). Assessing and managing nutrient-enhanced eutrophication in estuarine and coastal waters: interactive effects of human and climatic perturbations. *Ecol. Eng.* 26, 40–54. doi: 10.1016/j.ecoleng.2005.09.006

Patton, C. J., and Kryskalla, J. R. (2003). *Methods of Analysis by the U.S. Geological Survey National Water Quality Laboratory - Evaluation of Alkaline Persulfate Digestion as an Alternative to Kjeldahl Digestion for Determination of Total and Dissolved Nitrogen and Phosphorus in Water*, ed USGS (Denver, CO), 1–40. Available online at: https://nwql.usgs.gov/pubs/WRIR/WRIR-03-4174.pdf

Quiquampoix, H., and Mousain, D. (2005). Enzymatic hydrolysis of organic phosphorus, in *Organic Phosphorus in the Environment* (Cambridge, MA: CABI Publishing), 89–112.

R Core Team (2015). *R: A Language and Environment for Statistical Computing.* Vienna: R Foundation for Statistical Computing.

Ramette, A. (2007). Multivariate analyses in microbial ecology. *FEMS Microbiol. Ecol.* 62, 142–160. doi: 10.1111/j.1574-6941.2007.00375.x

Reddy, K. R., and DeLaune, R. D. (eds.). (2008). "Phosphorus," in *Biogeochemistry of Wetlands: Science and Applications* (Boca Raton, FL: CRC Press, Taylor and Francis Group, LLC), 325–404. doi: 10.1201/9780203491454.ch9

Reddy, K. R., Kadlec, R. H., Flaig, E., and Gale, P. M. (1999). Phosphorus retention in streams and wetlands: a review. *Crit. Rev. Environ. Sci. Technol.* 29, 83–146. doi: 10.1080/10643389991259182

Richardson, C. J. (1985). Mechanisms controlling phosphorus retention capacity in freshwater wetlands. *Science* 228, 1424–1427. doi: 10.1126/science.228.4706.1424

Richardson, C. J., and Marshall, P. E. (1986). Processes controlling movement, storage, and export of phosphorus in a fen peatland. *Ecol. Mongr.* 56, 279–302. doi: 10.2307/1942548

Richardson, C. J., and Reddy, K. R. (2013). "Methods for soil phosphorus characterization and analysis of wetland soils," in *Methods in Biogeochemistry of Wetlands Number 10*, eds R. D. DeLaune, K. R. Reddy and C. J. Richardson (Madison, WI: Soil Science Society of America), 603–638.

Roegner, C. G., Needoba, J. A., and Baptista, A. M. (2011). Coastal upwelling supplies oxygen-depleted water to the Columbia River estuary. *PLoS ONE* 6:e18672 doi: 10.1371/journal.pone.0018672

Schneider, K. D., Cade-Menun, B. J., Lynch, D. H., and Voroney, R. P. (2016). Soil phosphorus forms from organic and forage fields. *Soil Sci.* 80, 328–340. doi: 10.2136/sssaj2015.09.0340

Sherwood, C., Jay, D. A., Harvey, R. B., Hamilton, P., and Simenstad, C. A. (1990). Historical changes in the Columbia River estuary. *Prog. Oceanogr.* 25, 299–352. doi: 10.1016/0079-6611(90)90011-P

Sherwood, C. R., and Creager, J. S. (1990). Sedimentary geology of the Columbia River estuary. *Prog. Oceanogr.* 25, 15–80. doi: 10.1016/0079-6611(90)90003-K

Sherwood, C. R., Creager, J. S., Roy, E. H., Gelfenbaum, G., and Dempsey, T. (1984). *Sedimentary Processes and Environments in the Columbia River Estuary,* Columbia River Estuary Data Development Program. Astoria, OR: Columbia River Estuary Study Taskforce.

Sholkovitz, E. R. (1976). The flocculation of dissolved organic and inorganic matter during the mixing of river and seawater. *Geochim. Cosmochim. Acta* 40, 831–845. doi: 10.1016/0016-7037(76)90035-1

Simenstad, C. A., Small, L. F., McIntire, C. D., Jay, D. A., and Sherwood, C. (1990). Columbia River estuary studies: an introduction to the estuary, a brief history, and prior studies. *Prog. Oceanogr.* 25, 1–13. doi: 10.1016/0079-6611(90)90002-J

Small, L. F., and Prahl, F. G. (2004). A particle conveyor belt process in the Columbia River estuary: evidence from chlorophyll a and particulate organic carbon. *Estuaries* 27, 999–1013. doi: 10.1007/BF02803426

Stevenson, F. J. (1986). *Cycles of Soil: Carbon, Nitrogen, Phosphorus, Sulfur, Micronutrients*. New York, NY John Wiley and Sons.

Suzumura, M., and Kamatani, A. (1995a). Mineralization of inositol hexaphosphate in aerobic and anaerobic marine sediments: implications for the phosphorous cycle. *Geochim. Cosmochim. Acta* 59, 1021–1026. doi: 10.1016/0016-7037(95)00006-2

Suzumura, M., and Kamatani, A. (1995b). Origin and distribution of inositol hexaphosphate in estuarine and coastal sediments. *Limnol. Oceanogr.* 40, 1254–1261. doi: 10.4319/lo.1995.40.7.1254

Tiessen, H., Ballester, M. V., and Salcedo, I. (2011). "Phosphorus and global change," in *Soil Biology,* eds E. K. Bünemann, A. Oberson and E. Frossard (Berlin, Heidelberg: Springer), 295–316.

Turner, B. L., and Newman, S. (2005). Phosphorus cycling in wetland soils. *J. Environ. Qual.* 34, 1921–1929. doi: 10.2134/jeq2005.0060

Turner, B. L., Newman, S., and Reddy, K. R. (2006). Overestimation of organic phosphorus in wetland soils by alkaline extraction and molybdate colorimetry. *Environ. Sci. Tech.* 40, 3349–3354. doi: 10.1021/es052442m

Turner, B. L., Paphazy, M. J., Haygarth, P. M., and Mckelvie, I. D. (2002). Inositol phosphates in the environment. *Phil. Trans. R. Soc. London Ser. B* 357, 449–469. doi: 10.1098/rstb.2001.0837

Turner, B. L., and Weckström, K. (2009). Phytate as a novel phosphorus-specific paleo-indicator in aquatic sediments. *J. Paleolimnol.* 42, 391–400. doi: 10.1007/s.10933-008-9283-6

US EPA (1983a). "Phosphorus, all forms Method 365.1 (colorimetric, automated ascorbic acid)," in *Methods for Chemical Analysis of Water and Wastes EPA-600/4-79-020* (Cincinnati, OH: Environmental Monitoring and Support Laboratory, Office of Research and Development, US EPA).

US EPA (1983b). "Sample Preservation," in *Methods for Chemical Analysis of Water and Wastes*, *EPA-600/4-79-020* (Cincinnati, OH: Environmental Monitoring and Support Laboratory, Office of Research and Development, US EPA).

Vaithiyanathan, P., and Richardson, C. J. (1997). Nutrient profiles in the everglades: examination along the eutrophication gradient. *Sci. Total Environ.* 205, 81–95. doi: 10.1016/S0048-9697(97)00191-5

van Beusekom, J. E. E., and Brockmann, U. H. (1998). Transformation of phosphorus in the elbe estuary. *Estuaries* 21, 518–526. doi: 10.2307/1353291

Williams, B. L., and Silcock, D. J. (2001). Does nitrogen addition to raised bogs influence peat phosphorus pools? *Biogeochemistry* 53, 307–321. doi: 10.1023/A:1010675601613

Wright, R. B., Lockaby, B. G., and Walbridge, M. R. (2001). Phosphorus availability in an artificially flooded southeastern floodplain forest soil. *Soil Sci. Am. J.* 65, 1293–1302. doi: 10.2136/sssaj2001.6541293x

Young, E. O., Ross, D. S., Cade-Menun, B. J., and Liu, C. W. (2013). Phosphorus speciation in riparian soils: a phosphorus-31 nuclear magnetic resonance spectroscopy and enzyme hyrdolysis study. *Soil Sci. Soc. Am. J.* 77, 1636–1647. doi: 10.2136/sssaj2012.0313

Zhang, R., Wu, F., He, Z., Zheng, J., Song, B., and Jin, L. (2009). Phosphorus composition in sediments from seven different trophic lakes, China: a phosphorus-31 NMR study. *J. Environ. Qual.* 38, 353–359. doi: 10.2134/jeq2007.0616

Zimmerman, C. F., and Keefe, C. W. (1997). *Determination of Orthophosphate in Estuary and Coastal Waters by Automated Colorimetric Analysis, EPA/600/R-15/011* (Washington, DC: US EPA).

Conflict of Interest Statement: The authors declare that the research was conducted in the absence of any commercial or financial relationships that could be construed as a potential conflict of interest.

frontiers in Marine Science

ORIGINAL RESEARCH
published: 10 July 2018
doi: 10.3389/fmars.2018.00235

Spatial and Temporal Dynamics of Inorganic Phosphate and Adenosine-5′-Triphosphate in the North Pacific Ocean

Karin M. Björkman[1], Solange Duhamel[2], Matthew J. Church[3] and David M. Karl[1]*

[1] Oceanography, University of Hawaii, Honolulu, HI, United States, [2] Lamont Doherty Earth Observatory, Palisades, NY, United States, [3] Flathead Lake Biological Station, University of Montana, Lake County, IL, United States

Temporal variability in dissolved inorganic, organic phosphate (Pi, DOP) and particulate phosphorus (PPO_4) concentrations, and microbial utilization of Pi and dissolved adenosine-5′-triphosphate (DATP) was studied at Station ALOHA (22.75°N, 158°W) in the North Pacific Subtropical Gyre (NPSG) over a multi-year period. Spatial variability of the same properties was investigated along two transects, to and from Hawaii, that traversed the NPSG boundaries to the east (2014) and north (2016). Radiotracer techniques were employed to measure the turnover time of Pi and DATP pools to calculate Pi uptake rates and the Pi hydrolysis rates of DATP. Pi concentrations were more variable, both in time and space, than DOP, ranging two orders of magnitude compared to a factor of two for DOP. The DATP pool, while constituting on average <0.15% of the total DOP-P, was as dynamic as Pi (∼1–200 pmol l^{-1}), with lowest concentrations coinciding with Pi depletion. The Pi turnover times ranged from a few hours to several weeks, and were correlated with measured Pi concentrations ($r = 0.9$; Station ALOHA, $n = 28$; 2014, $n = 14$; 2016, $n = 12$). Pi uptake rates averaged 3.6 ± 1.3 nmol-P l^{-1} d^{-1} ($n = 28$: Station ALOHA), 9.2 ± 4.7 nmol-P l^{-1} d^{-1}, ($n = 15$; 2014) and 5.1 ± 2.5 nmol-P l^{-1} d^{-1}, ($n = 12$; 2016). The turnover time of the DATP pool was typically substantially shorter (0.4–5 days) than for the Pi-pool, and uptake rates ranged from 1 to 115 pmol l^{-1} d^{-1}. However, at very low Pi and ATP concentrations, ATP turnover was longer than Pi turnover and ATP uptake rates lower. Total ATP hydrolysis was high along both transects, exceeding the ATP taken up by the microbial community, resulting in a net release of Pi into the ambient seawater. This net release was positively correlated to Pi concentration. The relative contribution by microbial size classes to total P-uptake depended on whether P was derived from ambient Pi or from DATP, with the <0.6>0.2 μm size class dominating the DATP uptake. Our results indicate that during Pi limiting conditions, regenerated P is rapidly consumed, and that Pi limitation occurs locally and transiently but does not appear to be the predominant condition in the upper water column of the NPSG.

Keywords: phosphorus cycling, North Pacific subtropical gyre, phosphate, ATP, station ALOHA

OPEN ACCESS

Edited by:
Javier Arístegui, Universidad de Las Palmas de Gran Canaria, Spain

Reviewed by:
Marta Sebastian, Instituto de Oceanografía y Cambio Global, Spain
Sarah Elizabeth Reynolds, University of Portsmouth, United Kingdom

****Correspondence:***
Karin M. Björkman
bjorkman@hawaii.edu

Specialty section:
This article was submitted to Marine Biogeochemistry, a section of the journal Frontiers in Marine Science

Received: *24 January 2018*
Accepted: *18 June 2018*
Published: *10 July 2018*

Citation:
Björkman KM, Duhamel S, Church MJ and Karl DM (2018) Spatial and Temporal Dynamics of Inorganic Phosphate and Adenosine-5′-Triphosphate in the North Pacific Ocean. Front. Mar. Sci. 5:235. doi: 10.3389/fmars.2018.00235

INTRODUCTION

Phosphorus (P) is essential for all life and is a key component of nucleic acids, cell membrane lipids and in biological energetic processes via e.g., adenosine-5′-triphosphate (ATP). Inorganic phosphate (Pi) is frequently at very low concentrations in aquatic environments and although the bioavailability of nitrogen (N) appears to be a proximately limiting resource for primary producers in marine ecosystems, P is believed to be the ultimately limiting macronutrient over geological time scales (Falkowski, 1997; Tyrell, 1999). Within the North Pacific Subtropical Gyre (NPSG) inorganic pools of P and N are generally at much lower concentrations than their respective dissolved organic pools (DOP, DON; Karl et al., 2001b), indicative of their preferential exploitation by the microbial community. The utilization of the DOP pool, at least during times of Pi-stress or limitation, should constitute a reservoir or buffer for P. Several studies have shown that microorganisms in marine environments do utilize the DOP both during P stress and under P-replete conditions in nature (Björkman and Karl, 2003; Mather et al., 2008; Lomas et al., 2010; Duhamel et al., 2011, 2017). However, the DOP pool is chemically diverse and still only partially characterized, but consists predominantly of phosphate esters and a substantial amount of phosphonates (Clark et al., 1998; Kolowith et al., 2001; Karl and Björkman, 2015; Repeta et al., 2016). Among the most commonly studied DOP compounds is ATP. ATP has several advantages as a "model" compound, among them that it is available in different radiolabeled forms. This makes it possible to discern preferential uptake of subcomponents of the molecule, and importantly, it is possible to measure its ambient particulate and dissolved concentrations (Bossard and Karl, 1986; Ammerman and Azam, 1991a; Björkman and Karl, 2001) and to follow its utilization by the microbial community (Casey et al., 2009; Björkman et al., 2012). Although ATP may only be a small portion, and not necessarily representative of the average DOP pool constituents, getting a clearer assessment of its flux through the different P-pools will aid in elucidating the behavior of the bioavailable DOP.

In this study we compare temporal and spatial variabilities in the utilization of Pi and ATP by the surface ocean microbial community, as a function of Pi, DOP and dissolved ATP (DATP) concentrations. Radiotracer techniques were used to determine the turnover times of the Pi or ATP pools respectively, as well as the Pi hydrolysis rates from the DATP pool. The temporal study was conducted at or near Station ALOHA (22.75°N, 158°W) in the North Pacific Subtropical Gyre (NPSG) over a multi-year period (2005–2015). The spatial variability in these same properties was investigated during an August-September 2014 zonal transect from California to Hawaii, and an April–May 2016 meridional transect from Hawaii to approximately 36°N along longitude 158°W. This is, to our knowledge, the first time that all the above P-pools and accompanying rates of utilization have been measured in concert within the oligotrophic oceans.

MATERIALS AND METHODS

Station Locations

Sampling for rate measurements was conducted at, or near, Station ALOHA (22.75°N, 158.00°W) on several Hawaii Ocean Time-series (HOT), or Center for Microbial Oceanography: Research and Education (C-MORE) expeditions during an 11-year time-period from 2005 to 2015. In the late summer/early fall season of 2014 (18 Aug−16 Sep, 2014), a northeast to southwest (hereafter; zonal) transect cruise was conducted onboard the R/V *New Horizon* (NH1417: Nitrogen Effects on MicroOrganisms—NEMO) originating in San Diego, CA and terminating in Honolulu, HI. This transect cruise occupied 128 stations with near daily samplings for P concentrations, P-utilization experiments and primary productivity ($n = 26$, 20, and 25 respectively; **Table 1**,**Figure 1**), providing an opportunity to assess spatial variability of the inorganic and organic P dynamics over a larger area to complement the temporal investigations at or around Station ALOHA. In the spring of 2016 (April 19–May 4), a meridional cruise onboard the R/V *Kaimikai-O-Kanaloa* (KOK 1606: SCOPE—Gradients Cruise I), originating and ending in Honolulu, HI, occupied 14 stations between 23°N and 38°N along longitude 158°W, from within the NPSG into the transition zone toward sub-polar waters. Twelve stations were sampled during the meridional transect and comprised the same suite of measurements as the NH1417 cruise but investigated a different region and season than the earlier zonal transect (**Table 1**,**Figure 1**).

Hydrography and Sample Collections

Water samples were collected using polyvinyl chloride (PVC) Niskin®-type bottles mounted on a 24-place rosette frame, equipped with conductivity, temperature and pressure (CTD) sensors. In addition to the parameters measured with the environmental sensors, discrete seawater samples were also collected. These included samples for soluble reactive phosphate (hereafter called inorganic phosphate [Pi]), total dissolved phosphorus (TDP), particulate P (PPO_4), DATP and chlorophyll *a*. With the exception of DATP samples, which were pre-filtered through a 0.2 μm polycarbonate filter, the sample collections and subsequent analyses were performed according to the HOT standard protocols for the temporal data collected at HOT (hahana.soest.hawaii.edu/hot/methods/) with slight modifications during the transect cruises. In brief, for chlorophyll *a* determinations, seawater (150 ml to 2 l) was filtered through a glass fiber filter (GF/F; Whatman) and the filter extracted in 5 ml of 100% acetone. The samples were extracted for 1–7 days at −20°C in the dark prior to fluorometric analysis (Turner Designs; model 10-AU, or TD700). Samples for nutrient concentrations were collected into acid washed, deionized water and sample rinsed, high-density polyethylene bottles, stored upright and frozen (−20°C) until analyzed (Dore et al., 1996).

Sample Analyses

The Pi concentrations were measured using the MAGnesium Induced Co-precipitation technique (MAGIC; Karl and Tien, 1992), followed by standard colorimetric assays (Murphy and Riley, 1962) using a 10 cm cuvette cell (Beckman DU 640 spectrophotometer). The Pi samples were treated to reduce arsenate to arsenite to eliminate cross reactivity with the molybdenum blue complex (Johnson, 1971). The analytical precision of this method is ± 1 nmol l^{-1} with a detection limit (DL) of ≤ 3 nmol l^{-1}, using the definition of DL = 3 x

TABLE 1 | Station number, date sampled, location co-ordinates (latitude [Lat], longitude [Long]), temperature (T; °C), salinity (PSS), chlorophyll *a* concentrations (ng l^{-1}), and ^{14}C-primary production (μg C l^{-1} d^{-1}), at 25 m during the 2014 zonal transect and 15 m during the 2016 meridional transect.

Station	Date	Lat (°N)	Long (°W)	T (°C)	Salinity	Chlorophyll *a* (ng l^{-1})	Primary production (μg C l^{-1} d^{-1})
NH1417-							
2	19 Aug 2014	33.118	120.064	19.04	33.57	420 ± 18	32.4 ± 3.4
4	20 Aug 2014	33.789	123.022	18.20	33.28	848 ± 4	33.5 ± 4.6
10	21 Aug 2014	34.604	126.226	19.89	33.12	93 ± 4	7.3 ± 0.4
20	22 Aug 2014	34.909	127.259	19.78	33.10	92 ± 8	8.1 ± 0.3
37	23 Aug 2014	33.870	128.799	21.25	33.61	99 ± 9	8.2 ± 0.3
39	24 Aug 2014	33.124	129.954	20.92	33.37	65 ± 6	5.6 ± 0.4
43	25 Aug 2014	31.640	132.509	22.19	34.03	99 ± 4	7.9 ± 0.2
46	27 Aug 2014	26.543	138.509	23.58	35.33	78 ± 1	6.8 ± 0.3
50	28 Aug 2014	25.875	138.514	24.36	35.26	77 ± 2	6.1 ± 0.1
53	29 Aug 2014	27.960	140.167	24.44	35.48	75 ± 4	6.4 ± 0.6
61	30 Aug 2014	29.584	140.783	24.25	35.30	89 ± 9	8.2 ± 0.9
69	31 Aug 2014	28.818	141.984	24.68	33.44	249 ± 3	14.3 ± 0.9
76	1 Sep 2014	28.813	143.984	24.85	35.45	222 ± 14	14.4 ± 1.3
81	2 Sep 2014	29.300	146.909	25.42	35.62	66 ± 3	6.4 ± 0.2
84	3 Sep 2014	29.610	147.704	25.57	35.62	80 ± 4	6.1 ± 0.2
88	4 Sep 2014	30.328	150.240	25.88	35.40	136 ± 7	8.0 ± 0.2
98	5 Sep 2014	30.550	150.434	26.00	35.39	104 ± 9	7.3 ± 0.2
100–5	6 Sep 2014	30.320	150.368	26.07	35.33	126 ± 15	9.0 ± 0.3
100–11	7 Sep 2014	30.322	150.370	26.08	35.39	133 ± 1	10.0 ± 0.3
100–12	7 Sep 2014	30.321	150.367	26.07	35.44	No data	No data
102	8 Sep 2014	29.400	150.222	26.03	35.52	65 ± 2	6.2 ± 0.2
106	9 Sep 2014	26.221	150.837	26.62	35.38	113 ± 1	12.7 ± 0.2
110	10 Sep 2014	23.667	151.316	26.60	35.15	148 ± 3	11.5 ± 1.1
122	11 Sep 2014	24.283	152.550	27.23	35.40	169 ± 7	12.0 ± 0.1
127–3	12 Sep 2014	24.484	152.947	27.21	35.40	112 ± 9	9.2 ± 0.7
127–9	13 Sep 2014	24.484	152.951	27.39	35.38	173 ± 10	6.5 ± 0.2
KOK1606-							
2	20 Apr 2016	23.497	158.00	24.04	35.22	80 ± 2	3.5 ± 0.9
4	22 Apr 2106	28.143	158.00	20.00	35.15	80 ± 5	3.0 ± 0.6
5	23 Apr 2016	29.452	158.00	19.80	35.21	98	2.0 ± 0.2
6	24 Apr 2016	32.583	158.00	16.17	34.60	264	9.1 ± 0.2
7	25 Apr 2016	34.058	158.00	14.82	34.42	331	7.5 ± 0.6
8	26 Apr 2016	37.302	158.00	11.40	34.18	776	9.9 ± 0.7
9	27 Apr 2016	36.570	158.00	12.01	34.13	214	5.5 ± 0.4
10	28 Apr 2016	35.463	158.00	13.33	34.05	706	11.3 ± 0.8
UW	29 Apr 2016	36.053	158.00	14.22	34.12	No data	13.7 ± 1.1
12	30 Apr 2016	33.092	158.00	16.07	34.48	604	26.6 ± 2.0
13	1 May 2016	29.700	158.00	20.91	35.15	040	5.9 ± 0.2
14	2 May 2016	26.283	158.00	23.05	35.31	047	7.2 ± 0.8
Station ALOHA		22.750	158.00	–	–	–	–
2005-2015	Apr	–	–	23.4 ± 0.5	35.1 ± 0.2	93 ± 17	6.4 ± 0.9
	Aug–Sep	–	–	26.2 ± 0.6	35.2 ± 0.2	80 ± 7	7.4 ± 1.8
2014 (HOT 265)	Sep	–	–	27.23	34.95	60 ± 0	7.8 ± 0.5
2016 (HOT 283)	Apr	–	–	24.25	34.80	69 ± 7	6.1 ± 0.1

Station ALOHA data are the mean values at the 25 m horizon for Aug–Sep and April from 2005 to 2015 (n = 20 and 10, respectively), and Sep 2014 and April 2016.

the standard deviation (s.d.) of the analytical precision. TDP was analyzed by the wet persulfate/high temperature oxidation method (Menzel and Corwin, 1965) followed by MAGIC and the standard Pi colorimetric assay. TDP measurements have an analytical precision of ± 5 nmol l^{-1}. DOP was calculated as the difference between TDP and Pi concentrations in paired samples.

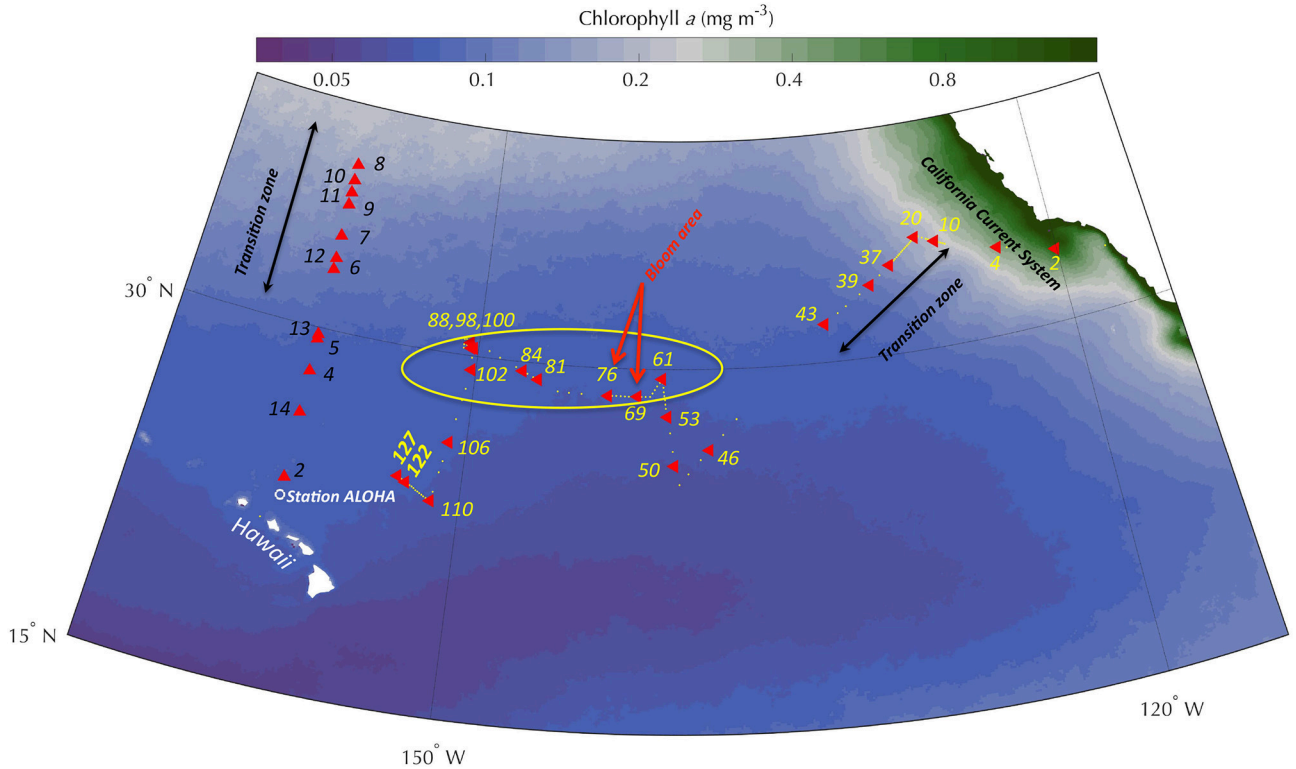

FIGURE 1 | Map over study area in the North Pacific Ocean showing a multiyear composite of chlorophyll *a* concentrations in the surface waters (OCI algorithm, MODIS; Aqua, 9 km resolution) and the station locations for the zonal transect from San Diego, CA to Honolulu, HI in August-September of 2014, and the meridional transect from Honolulu to approximately 37°N along the 158°W longitude and back in April-May 2016. Station ALOHA (white circle) located at 22.75°N, 158.00°W and is the site for the Hawaii Ocean Time-series (HOT). The zonal transect occupied 127 stations (yellow bullets) of which 20 stations where phosphorus (Pi, ATP) rate experiments were conducted, including two additional stations for ^{14}C-primary production (red triangles; yellow station numbers). Circled is the area along the 30°N meridian where Pi was depleted during the 2014 cruise. Note that Stations 88, 98, and 100 overlap in the figure, but were separated by 8–18 nmiles; the stations closest in space were separated in time by 3 days. The meridional transect (red triangles; black station numbers) occupied 14 stations of which 12 were sampled for P experiments and ^{14}C-primary production. (Zonal transect: California Current System [CCS] – Stns 1–4; Transition zone [TZ] – Stns 5–43; North Pacific Subtropical Gyre [NPSG] – Stns 46–127: Meridional transect NPSG – Stns 2–5 and 13–14; TZ – Stns 6–12).

DATP concentrations were determined as described in Björkman and Karl (2001) which is based on the co-precipitation of ATP with brucite, based on the same principal as the MAGIC method used for Pi, allowing DATP to be concentrated from seawater before analysis using firefly bioluminescence. Modifications from the original protocol were made to sample volume and concentration factors as follow; triplicate 50 ml subsamples from each field sample were amended with 250 µl 1 N NaOH, mixed and centrifuged at 1,000 × g for 60 min. The supernatant was carefully aspirated and the pellet dissolved with 50 µl 2.5 N HCl, followed by the addition of 250 µl of deionized water. Prior to analyses the sample was mixed with an equal volume of Tris buffer (pH 7.4, Sigma-Aldrich T7693). Samples for the calibration curve were made in surface seawater with the additions of known amounts of ATP and treated as samples. Blanks were made from surface seawater samples without ATP additions and treated with apyrase to hydrolyze any ATP in the sample (Sigma-Aldrich #A6132; stock 10 units ml^{-1}, 10 µl per sample:Tris mix). The DL for this assay is 9 pmol DATP l^{-1}, with the precision of ± 3 pmol l^{-1}. Data averaged from multiple observations are presented as the mean ± s.d., (n = x) where x is the number of observations. Station ALOHA core data presented here were obtained from the publicly available HOT data archive; HOT Data Organization and Graphical System (HOT-DOGS: http://hahana.soest.hawaii.edu/hot/hot-dogs/).

Incubation Experiments

Seawater was collected into acid washed, deionized water and sample rinsed, clear polycarbonate (PC) incubation bottles (Nalgene: 75–250 ml). All data presented in this study for Station ALOHA and NH1417 were collected from 25 m, and from 15 m during KOK1606. The samples were spiked with tracer amounts of either ^{32}P or ^{33}P orthophosphate (MP Biomedicals # 064014L, Perkin-Elmer #NEZ08000; carrier free) or ATP labeled at the gamma position with either ^{32}P or ^{33}P (MP Biomedicals # 01350200, Perkin-Elmer NEG302H00; specific activity 111 TBq mmol^{-1}). The final radioactivity of the samples typically ranged from 0.1 to 1 MBq l^{-1} depending on experiment. The bottles were incubated in on-deck incubators, cooled with running, surface seawater and shielded with blue plexiglass

(Arkema #2069) to achieve the approximate light level and spectral quality of the depth from which the sample water had been collected. The incubation time varied depending on location and expectancy of the rates, but all incubations were conducted during daytime. Experiments were typically performed as time-course incubations with 3–5 sampling events over a 3–6 h period. A subsample (0.1–0.5 ml) was collected from each incubation bottle to measure the total radioactivity added. Particulate activity was determined by filtering a 5–10 ml aliquot through a 0.2 μm pore size polycarbonate membrane filter (Nuclepore). Polycarbonate filters of 0.6 and 2 μm pore sizes were also included on occasion at Station ALOHA, and at all stations sampled along the two transects, to assess the relative size class contribution to community Pi or DATP pool turnover. The filters were rinsed with 3 × 2 ml of filtered seawater to remove unincorporated radioactivity, placed into a 7 ml plastic scintillation vial (Simport) and 4 ml of scintillation cocktail (Ultima Gold LLT, Perkin Elmer) added. Radioactivity was measured using a liquid scintillation counter (Perkin-Elmer, LSC 2910TR). Data were corrected for activity loss during the counting process due to decay of the short-lived isotopes. Measurements for primary productivity were performed in conjunction with the P-incubation experiments on both transect cruises. Primary productivity was determined by the ^{14}C-bicarbonate assay (^{14}C-PP) using 75 ml PC-bottles, spiked with ^{14}C-bicarbonate (MP Biomedicals 117441H) to a final radioactivity of approximately 7.4 MBq l^{-1}.

ATP Hydrolysis Rates

During the 2014 and 2016 transect cruises, and at Station ALOHA in 2013, the total hydrolysis rates of DATP were assessed from the ^{33}P-ATP incubation experiments. The protocol used was modified from Ammerman and Azam (1991b). The filtrate from the 0.2 μm filter fraction was collected during the time course incubations. Triplicate 1 ml aliquots from each sample were placed into micro-centrifuge tubes and mixed with 0.2 ml activated charcoal slurry (20 mg charcoal ml^{-1} in 0.03 N sulfuric acid: The activated charcoal selectively binds organic molecules, such as DATP, while Pi will remain in solution. This allows for the separation of hydrolyzed ^{33}P-Pi from ^{33}P-DATP). The samples were thoroughly mixed by vortex and centrifuged for 15 min at 20,800 × g. A subsample (0.75 ml) of the supernatant was placed into a scintillation vial for radioactivity counting. DATP hydrolysis was measured from the increase of radioactivity over time in the supernatant, indicating that Pi had been cleaved from ATP and released into the ambient seawater, i.e., Pi regenerated from DATP. Total DATP hydrolysis was calculated as the sum of the particulate activity retained on the 0.2 μm filters (i.e., P from DATP taken up by microbes, hereafter; PATP) and the regenerated, non-incorporated ^{33}Pi from ^{33}P-DATP in the charcoal extractions. All rates were based on time course sampling and the rates determined through linear regression over time.

Kinetic Pi Rate Experiment

During the 2014 transect at station 100 (30.32°N, 150.38°W), an additional experiment was conducted to assess the kinetic response to increasing concentrations of Pi. Very short Pi-pool turnover times were measured at this location and were presumed to be due to low ambient concentrations of Pi (this was later confirmed by chemical analysis). Seawater samples were amended with non-radioactive Pi to target additions of 0, 5, 10, 25, 50, 75, 100, and 200 nmol Pi l^{-1}. A subsample from each concentration step was placed into PC incubation bottles, spiked with ^{33}P-Pi, incubated and sampled as described above. A separate set of incubation bottles, amended with 0, 25, 50, and 100 nmol Pi l^{-1}, was spiked with ^{33}P-ATP. The remaining seawater was stored frozen (−20°C) for later analysis of Pi concentrations. Time-course sampling was conducted for the three lowest P concentrations at 5, 25, 75, and 150 min of spiking with ^{33}P-Pi. Incubations receiving 25 nmol Pi l^{-1} or above, and the ^{33}P-ATP spiked samples, were sub-sampled in triplicate after approximately 3 h of incubation.

Calculations of P Uptake Rates and Kinetic Parameters

The Pi or ATP uptake rates and turnover times in days (TOT, d) were calculated as follows: TOT(d) = t/r where t is the total radioactivity added (Bq l^{-1}) and r is the rate of radiolabel uptake into the particulate fraction (Bq l^{-1} d^{-1}). The rate was determined from linear regression of the incubation time and radioactivity of the filters from the time course experiments. This calculation assumes that the specific activity of the substrate pool is constant during the incubation period. In our experiments <10% of the radiolabel was taken up during the incubation time, with the exception of the samples from stations 88 (30.33°N, 150.24°W) and 100 (30.32°N, 150.38°W) along the 2014 transect. At station 88; >80% of the radiolabel was taken up by 80 min and at station 100; ∼40% was captured on the filters after 75 min. At such high proportions of the radiolabel taken up, the calculated uptake rate will be biased as a result of recycling, and may lead to underestimates of the actual rate of uptake. However, the finer time-course resolution and additions of Pi at station 100 allowed for the determination of rates at this station (see above *Kinetic Pi rate experiment*). In this experiment we also calculated the kinetic parameters V_{max} and K_m for the maximum uptake rate and half saturation constant, respectively, using Hanes-Woolf linear transformation of the data. This transformation uses the substrate concentration (S) and uptake velocity (V) to derive V_{max} and K_m as follows: $S/V = (1/V_{max}) \times S + V_{max}/K_m$. Here S/V is the measured TOT in our incubations, the slope of the linear regression is $1/V_{max}$, and the y-intercept is V_{max}/K_m.

The rate of Pi or PATP uptake, expressed as nmol l^{-1} d^{-1} or pmol l^{-1} d^{-1}, was calculated from the turnover time of the respective radioactive tracers and the measured concentration of Pi or DATP of the samples.

RESULTS

Transect Characterizations

The zonal transect in 2014 traversed the California Current System (CCS) for the first few stations (Stations 1–4), characterized by relatively low sea-surface temperatures (SST), high nutrient concentration, high chlorophyll *a* and ^{14}C-PP

(**Table 1**, **Figure 2B**). Stations 5–43 comprised the transition zone between the CCS and the NPSG (**Figure 1**). This region showed high eddy activity as detected by satellite estimates of sea surface height anomalies (Shilova et al., 2017), with variable chlorophyll *a* and declining Pi concentrations. Stations 44–127 were all within the NPSG with low eddy activity and unusually high SST, reaching temperatures above 27°C nearing the Hawaiian Islands. Time-series data from Station ALOHA have only rarely recorded such high temperatures, and in September 2014 was the first time in a decade to do so. The meridional transect in 2016 reached the transition zone between the NPSG and the subpolar front just south of 32°N (Station 6). This region demonstrated high spatial variability in a variety of parameters (e.g., chlorophyll *a*, salinity) likely due to entrainment and filaments of mixing water masses belonging to the oligotrophic gyre and more nutrient-enriched water in the transition zone.

Chlorophyll a and ^{14}C-Primary Productivity

Over the past decade at Station ALOHA chlorophyll *a* concentration at the 25 m horizon varied by approximately a factor of two with the lowest concentrations observed during the summer months (72 ± 16 ng l^{-1}; $n = 28$) and the highest during winter (119 ± 31 ng l^{-1}; $n = 26$) with an average concentration of 93 ± 17 ng l^{-1} (**Table 1**). Chlorophyll *a* concentrations along the 2014 zonal transect were highest within the CCS, but even within the NPSG the concentrations varied over 3-fold (Station 81; 66 ± 3 ng l^{-1}, Station 69; 249 ± 3 ng l^{-1}: **Table 1**), with the highest chlorophyll *a* found in a phytoplankton bloom (**Figure 1**,**Table 1**). During the spring 2016 meridional transect, chlorophyll *a* varied two-fold within the NPSG and at the northernmost stations reached concentrations similar to those observed in the CCS. Station ALOHA ^{14}C-PP, at the 25 m horizon, ranged from 4.5 to 11.8 μg C l^{-1} d^{-1}, with a mean for August-September of 6.4 ± 0.9 μg C l^{-1} d^{-1} ($n = 20$) and 7.4 ± 1.8 μg C l^{-1} d^{-1} ($n = 10$) for April. Along the two transects ^{14}C-PP varied by approximately a factor of 2–3 within the NPSG, but were much higher in the nutrient-enriched regions of the CCS and the northernmost stations of the 2016 transect (**Table 1**). During the zonal transect, within the NPSG, a peak in ^{14}C-PP was observed at stations 69 and 76 (∼ 14 μg C l^{-1} d^{-1}). These two stations were also associated with the highest chlorophyll *a* measured during that transect within the NPSG (**Table 1**).

P Concentrations at Station ALOHA and Along Transects

Variability in Pi concentrations at 25 m at Station ALOHA ranged approximately 25-fold over the past decade (2005–2015; 7–195 nmol P l^{-1}; **Figure 2A**), with an average concentration of 70 ± 39 nmol l^{-1} ($n = 107$), and median of 62 nmol l^{-1}. It should be noted that Pi inventories over this period displayed a rapid increase beginning in mid-2012, persisting through the end of 2013 before slowly subsiding into 2014 and 2015 (**Figure 2A**). The upper ocean inventories during this 1.5–year period were significantly higher than in the preceding 7–year period (integrated 0–100 m, [2005–2011, $n = 67$] 4.8 ± 2.4 mmol m^{-2}; [2012–2013, $n = 20$] 11.3 ± 3.5 mmol m^{-2}) and this skewed the mean Pi concentrations at the 25 m horizon upwards for the period by approximately 30% from the longer term mean for Station ALOHA. Pi concentrations during the 2014 zonal transect varied 60-fold driven by the high values found within the CCS, but were still variable by a factor of

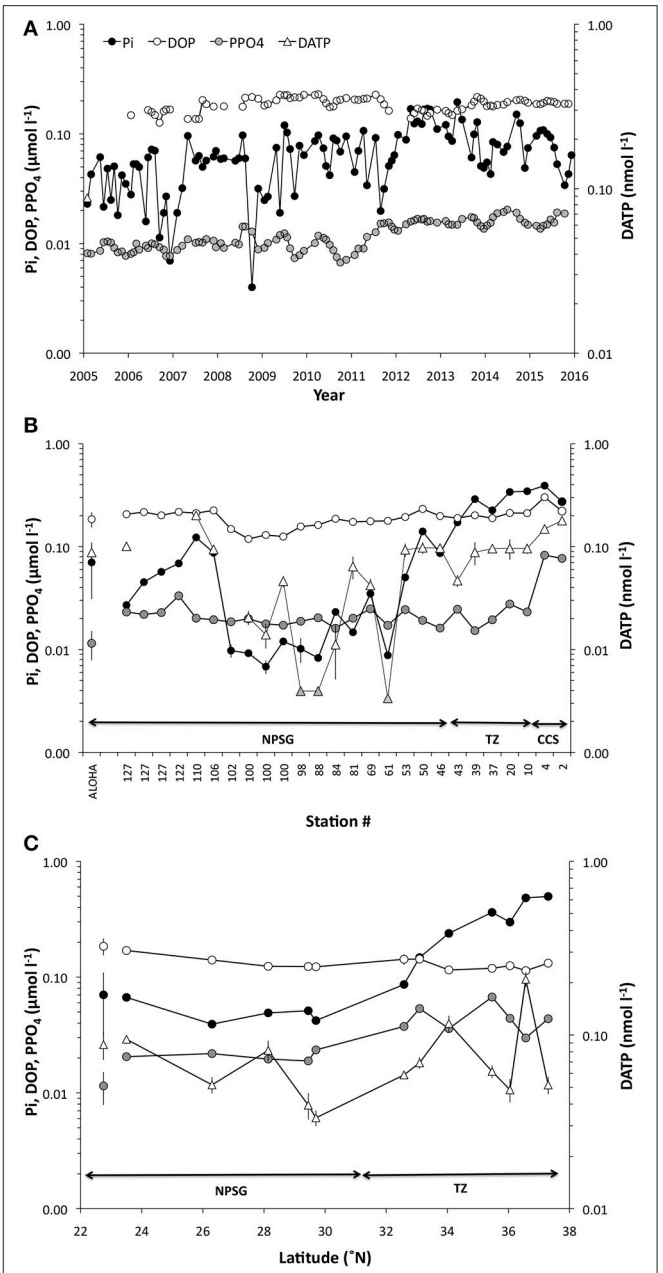

FIGURE 2 | Temporal and spatial variability in inorganic phosphate (Pi), dissolved organic phosphate (DOP) and particulate organic phosphate (PPO_4) concentrations (μmol l^{-1}) at **(A)** Station ALOHA (2005–2016), **(B)** along the zonal transect in the fall 2014 and **(C)** along the meridional transect in the spring 2016. Dissolved adenosine-5′-triphosphate (DATP) concentrations are shown in nmol l^{-1} for the two transects in **(B,C)**. The shaded triangles in **(B)** are below the stipulated detection limit, and presented only as a comparison to Pi. Arrows in **(B,C)** indicates the stations within the CCS, TZ, and NPSG as described in **Figure 1**. Note that the scale is logarithmic.

approximately 20 for stations within the NPSG (**Figure 2B**; Stations 46–127; range 7–141 nmol l^{-1}). The stations occupied within the region along 29.3–30.5°N and between 140 and 150°W (Stations 61–102), were characterized by low Pi concentrations (range 7–35 nmol l^{-1}, mean 15 ± 1 nmol l^{-1}, $n = 10$), and within the more intensely sampled region around 29.3–30.5°N, ∼150.3°W (stations 88–102) the mean Pi concentration was even lower at 9 ± 2 nmol l^{-1} ($n = 6$). During the spring 2016 meridional transect, Pi concentrations within the NPSG were 42 ± 8 nmol l^{-1}, and increased though the transition zone into the subpolar front to approximately 500 nmol l^{-1} at 37.2°N (**Figure 2C**). The concentrations of DOP were much less variable both in space and time and ranged about a factor of two with concentrations at Station ALOHA averaging 185 ± 31 nmol P l^{-1} ($n = 85$; range 109–248 nmol P l^{-1}; **Figure 2A**), and 2014 transect stations within the NPSG at 182 ± 34 nmol P l^{-1} ($n = 19$; range 119–232 nmol P l^{-1}; **Figure 2B**). The DOP concentrations were significantly lower (*t*-test, $p < 0.001$) in the region encompassing stations 61–102 compared to the other stations within the NPSG. The meridional transect in the spring of 2016 showed a more uniform distribution even into the subpolar regions, ranging from a high of 170 nmol P l^{-1} at the southernmost site to a low of 114 nmol P l^{-1} toward the subpolar front (**Figure 2C**). The relative contribution of DOP to the total dissolved P (TDP) pool at Station ALOHA varied from 45% to near 100%, with an average of 72 ± 11% ($n = 85$). Along the zonal transect DOP contributed 41–95% of the total pool, when the CCS stations were included, and 62–95% (mean 84 ± 11%, $n = 19$) for stations sampled within the NPSG. DOP concentrations were relatively low during the meridional transect, but the DOP contribution to the TDP pool within the NPSG was in the range of the long-term mean for Station ALOHA (73 ± 3%, $n = 5$). The PPO_4 concentrations varied approximately 3-fold during the 10-year period at Station ALOHA (**Figure 2A**; mean 12 ± 4 nmol l^{-1}, $n = 106$; range 6–25 nmol l^{-1}). The mean PPO_4 during 2011–2015 was 16 ± 3 nmol l^{-1} ($n = 41$). During the zonal transect in 2014, PPO_4 peaked within the CCS (**Figure 2B**), whereas concentrations within the NPSG varied approximately 2-fold (mean 21 ± 4 nmol l^{-1}, $n = 19$; range 16–33 nmol l^{-1}). Similarly, the meridional transect in 2016 showed the highest PPO_4 concentrations within the transition zone and toward the subpolar front (**Figure 2C**), while concentrations within the NPSG showed small variations averaging 20 ± 2 nmol l^{-1} ($n = 5$). DATP concentrations along the zonal transect ranged from ∼1 to 180 pmol DATP l^{-1}, with the lowest concentrations coinciding with the lowest Pi pool and shortest Pi-, and ATP-pool turnover times. The highest concentrations were found within the CCS. However, the DATP concentrations were less dynamic than the range in concentrations imply, and were typically ∼100 pmol l^{-1} for the majority of stations sampled (91 ± 15 pmol l^{-1}, $n = 11$; excluding stations where Pi < 15 nmol l^{-1}; **Figure 2B**). The meridional transect DATP concentrations ranged from 33 ± 3 to 209 ± 20 pmol l^{-1} with the highest values found within the transition zone. The average DATP concentration within the NPSG for the meridional transect 2016 was 60 ± 27 pmol l^{-1} ($n = 5$: **Figure 2C**).

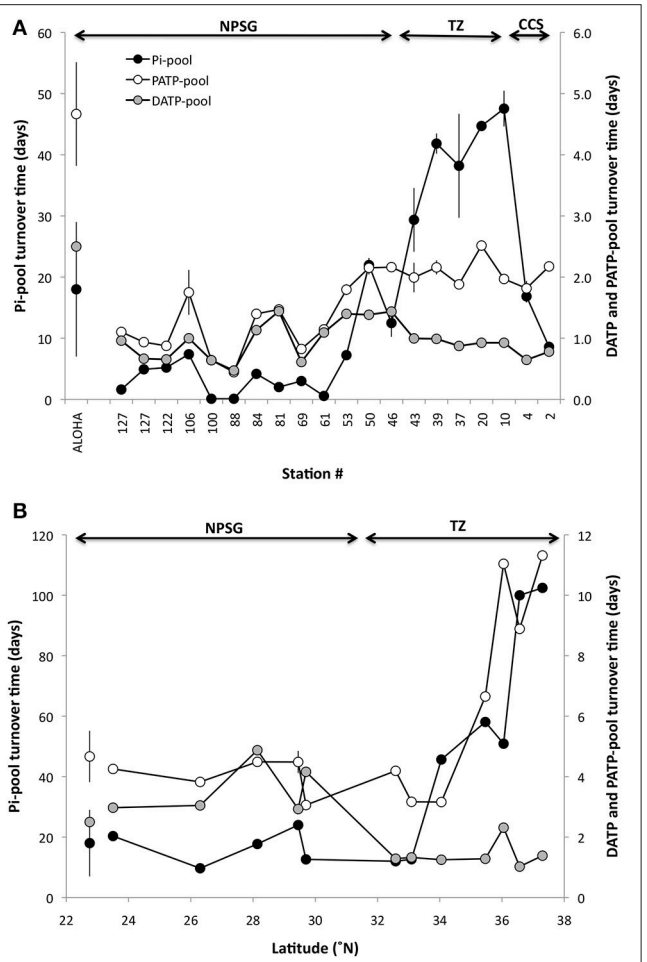

FIGURE 3 | Turnover time (days) of the Pi-pool and dissolved and particulate ATP-pools (DATP and PATP, respectively) as measured by ^{33}P radiotracer techniques. The Pi and PATP turnover times are based on the P uptake by the microbial community, whereas the DATP turnover time is the sum of the PATP and the net release of Pi originating from the hydrolysis of DATP. **(A)** zonal transect in the fall of 2014, and **(B)** meridional transect in the spring 2016. Error bars are derived from the error estimate of the regression of the time-course sampling used to calculate the turnover time. Values for Station ALOHA are mean ± 1 s.d. (Pi $n = 30$; ATP $n = 7$). Arrows indicate the stations within the CCS, TZ, and NPSG as described in **Figure 1**. Note that the scales differ among panels.

Pi Rate Measurements

Pi TOT at Station ALOHA varied from a few days to several weeks over a multi-year study with a long term mean of 18 ± 11 days ($n = 28$) and an uptake rate of 3.6 ± 1.3 nmol l^{-1} d^{-1} (range 0.6–7.1 nmol l^{-1} d^{-1}; median 3.3 nmol l^{-1} d^{-1}). The range observed for the two transects were from a few hours to 3 weeks within the NPSG, and reached 2–3 months in the CCS and subpolar transition zone respectively (**Figures 3A,B**). Very short turnover times (hours to 3 days) were found along the zonal transect around 30°N (Stations 61–100). Some of the stations (69–76) in this region were associated with a high phytoplankton biomass and enhanced primary productivity

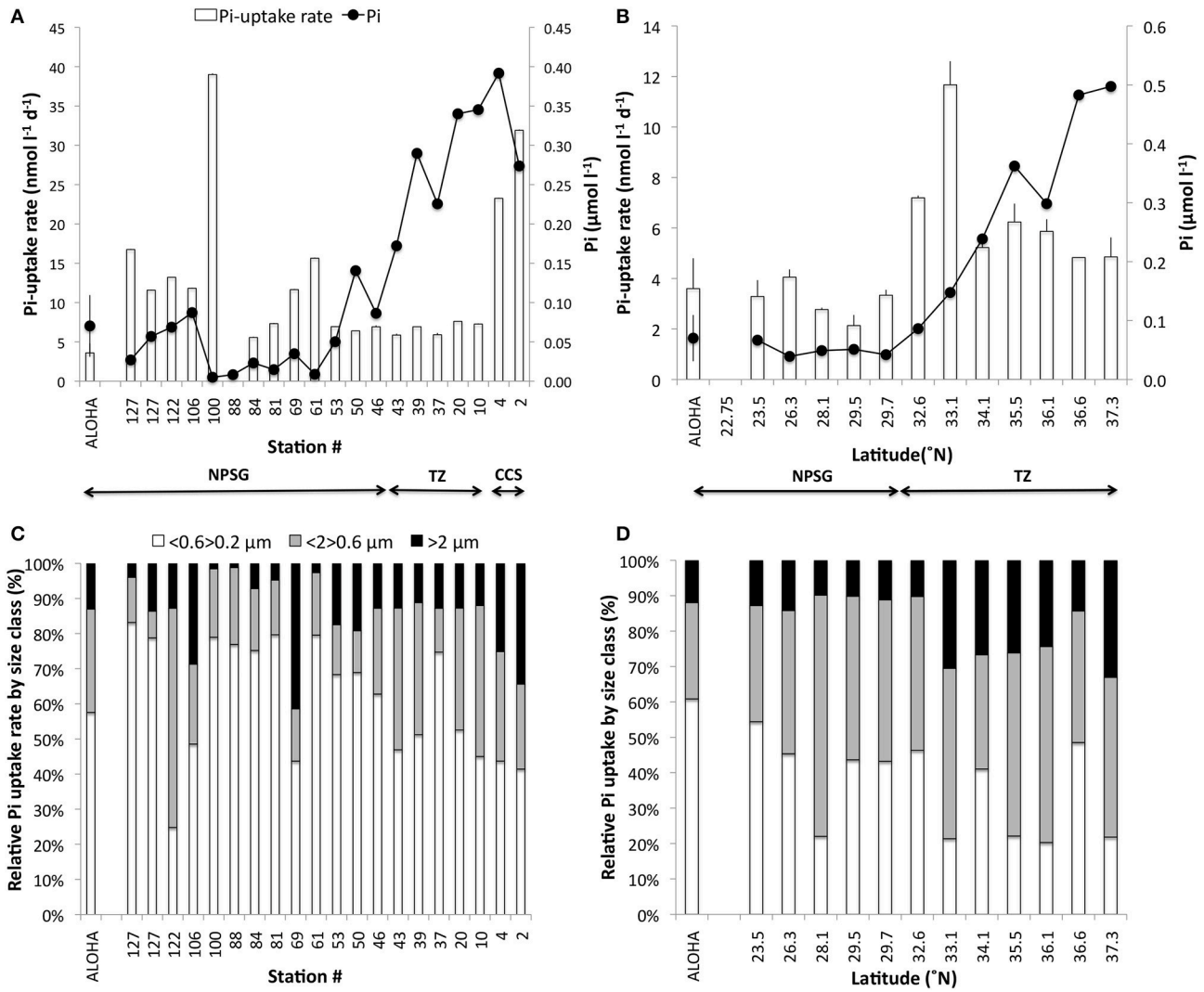

FIGURE 4 | (A,B) Pi-uptake rates (nmol l^{-1} d^{-1}; columns) and the corresponding Pi concentrations (µmol l^{-1}; bullets) and **(C,D)** the relative contribution from different microbial size classes to the Pi-uptake measured. The zonal transect is shown in **(A,C)**; the meridional transect in **(B,D)**. Station ALOHA values for Pi uptake rates and Pi concentrations are shown to the left in each panel (mean ± 1 s.d; $n = 28$). Arrows indicate the stations within the CCS, TZ and NPSG as described in **Figure 1.** Note that the scales differ among panels.

(chlorophyll a >0.2 µg l^{-1}, ^{14}C-PP ~ 14 µg C l^{-1} d^{-1}; **Table 1**). The Pi-uptake rate along the zonal transect ranged from a few nmol l^{-1} d^{-1} to approximately 15 $nmol^{-1}$ d^{-1} within the NPSG, and reached nearly 30 nmol l^{-1} d^{-1} within the CCS (**Figure 4A**). However, at the stations where we recorded the lowest Pi concentrations, and associated short turnover times, uptake rates were much enhanced (**Figure 4A**). The experiment to assess the kinetic response to increasing amounts of Pi was conducted at station 100, where there were indications of very low ambient Pi. Although the turnover time grew longer with additional Pi, as would be expected, the calculated rates for the whole water community did not show a clear kinetic response, as the calculated rates were similar for all concentrations tested (**Table 2**). A linear regression analysis gave an uptake rate estimate of 39 ± 1 nmol l^{-1} d^{-1} ($n = 8$, $r^2 = 0.991$) for the whole water community. However, the >2 µm size class did show a kinetic response with increased Pi. The Pi uptake rates in this size class tripled between 10 and 75 nmol l^{-1} Pi, and although the relative contribution of the >2 µm size class to the whole water community was small, it increased from ~2 to 8% at concentrations above 75 nmol l^{-1} Pi, indicating that cells >2 µm were P-limited at ambient concentrations at this station. The kinetic analysis indicated that the K_m for the >2 µm size class was 36 ± 7 $nmol^{-1}$ (**Table 2**), which was much above the measured ambient Pi concentration of 5 ± 1 nmol l^{-1}. Pi-uptake rates along the meridional transect were comparable to the long term mean of Station ALOHA within the NPSG (mean 2.8 ± 0.9 nmol l^{-1} d^{-1}; $n = 5$), with higher rates throughout the transition zone (range 5.5–12 nmol l^{-1} d^{-1}; **Figure 4B**).

TABLE 2 | Kinetic experiment carried out at Station 100 during the east-west transect in 2014. Seawater was amended with increasing concentrations of inorganic phosphate (Pi) to determine the turnover times (TOT) of the Pi- pool and Pi-uptake rates in different size fractions of the microbial community.

Pi (nmol l^{-1})	TOT (days)			Pi-uptake rate (nmol l^{-1} d^{-1})		
	>0.2 μm	>0.6 μm	>2μm	>0.2 μm	>0.6 μm	>2 μm
5 ± 1	0.10 ± 0.00	0.61	8.4	54 ± 11	8.8	0.6
10 ± 0	0.23 ± 0.01	0.42	10.6	42 ± 3	23.7	0.9
17 ± 1	0.33 ± 0.01	0.49	15.6	56 ± 4	35.2	1.1
31 ± 1	0.70 ± 0.03	1.39	22.2	45 ± 2	22.6	1.4
55 ± 1	1.38 ± 0.10	2.37	35.5	40 ± 3	23.4	1.6
77 ± 1	2.19 ± 0.09	3.88	28.6	35 ± 2	19.8	2.7
112 ± 1	2.55 ± 0.08	4.60	49.7	44 ± 2	24.4	2.3
189 ± 1	4.95 ± 0.11	5.50	54.1	38 ± 1	34.4	3.5
V_{max}	nmol l^{-1} d^{-1}	–	–	39 ± 1	20 ± 1	4 ± 1
K_m	nmol l^{-1}	–	–	n.d	n.d	36 ± 7

The half-saturation constant (K_m) and maximum uptake rate (V_{max}) were calculated from Hanes-Woolf linear transformation of the data. N.d, not determined, due to lack of kinetic response to added Pi.

The relative contribution by different microbial size classes to the total community Pi-uptake, although variable along the two transects, showed a clear dominance by cells <2 μm with an average of 88% of Pi taken up by this size class within the NPSG and through the transition zone, but was lower in the CCS where cells >2 μm represented ∼ 30% of the total Pi taken up (**Figures 4C,D**). Cells <0.6 μm became progressively more important to the total Pi uptake when transitioning from high Pi to low Pi environments. During the zonal transect from the CCS, transition zone to NPSG, cells <0.6 μm contributed 43 ± 2, 54 ± 12 to 67 ± 18% respectively to the total Pi uptake. The same pattern, although less pronounced, was seen during the meridional transect with 32 ± 13% at the transition zone and 42 ± 12% within the NPSG. At the stations along 30°N where Pi concentrations were <15 nmol l^{-1} (Stations 61, 81, 88, 100) the contributions from the >2 μm size class were at their lowest with <5% of the total. However, at station 69, where both chlorophyll *a* and ^{14}C-PP were enhanced, indicative of a phytoplankton bloom, the >2 μm size class represented ∼ 45% of the total Pi-uptake.

ATP Rate Measurements

The TOT of ATP, based on the rate of uptake by the microbial community, was typically much shorter than that measured for the Pi-pool (**Figures 3A,B**) at 1–2 days in most cases (zonal transect range; 0.44 ± 0.05 to 2.17 ± 0.08 days; mean 1.6 ± 0.6 days, $n = 20$: meridional range; 1.02 ± 0.06 to 11.3 ± 1.9 days; mean 5.17 ± 3.04 days, $n = 12$: **Figures 3A,B**). Only at the stations along the zonal transect where Pi concentrations were below 10 nmol l^{-1} Pi (Stations 61, 88, 100), was the ATP pool turnover longer than that for Pi (**Figure 3A**). The total DATP pool TOT (i.e., the sum of the ATP taken up by microbes and Pi regenerated from the hydrolysis of DATP and released into the ambient seawater) was less than 1 day on average along the zonal transect (0.95 ± 0.30 days: $n = 20$). The mean DATP turnover time for the meridional transect was 1.43 ± 0.47 days ($n = 12$: **Figures 3A,B**).

The total DATP hydrolysis rates ranged nearly two orders of magnitude (3–230 pmol l^{-1} d^{-1}) along the zonal transect, and approximately 10-fold along the meridional transect (**Figures 5A,B**). The very low rates were again in the region along 30°N where both Pi and DATP pools were depleted. During the zonal transect, excluding the stations where Pi and ATP were depleted, an average of 28 ± 9% ($n = 8$) of the total DATP hydrolyzed was not incorporated into cells, but regenerated as Pi within the NPSG, and an even higher proportion was regenerated within the transition zone (53 ± 4%, $n = 5$) and CCS (64 ± 0%, $n = 2$). The net Pi regenerated from DATP was even greater during the spring meridional transect with 53 ± 8% ($n = 5$) and 81 ± 8% ($n = 7$) within the NPSG and transition-sub polar regions, respectively (**Figure 5B**). The proportion (%) of Pi regenerated from DATP to total DATP hydrolysis correlated with ambient Pi concentrations, with an increasing proportion of the total not taken up with increasing Pi concentrations (**Figure 6**). Below 30 nmol Pi l^{-1} the regeneration diminished rapidly until Pi release from DATP was no longer measurable at ∼ 5 nmol Pi l^{-1} (**Figure 6**).

The relative contribution by different microbial size classes to the total community ATP-uptake, showed a different distribution than that of Pi. A great majority of P derived from ATP was incorporated into the smallest size class (<0.6>0.2 μm) with 80.1 ± 2.7% and 74.0 ± 2.0% of the total particulate uptake along the zonal and meridional transects respectively (**Figures 5C,D**). The >2 μm size class contributed <5% of the total uptake. The exceptions were at the Pi depleted stations (88, 100) and the bloom station (69) during the zonal cruise where the relative uptake by the larger size classes was considerably greater (**Figure 5C**). Furthermore, comparing the TOT of Pi and DATP for the different size classes, in paired experiments, revealed that there was no correlation between the two for the whole water community (>0.2 μm; **Figure 7A**), whereas the TOT for both Pi and DATP was similar in the >2 μm size class (**Figure 7B**,

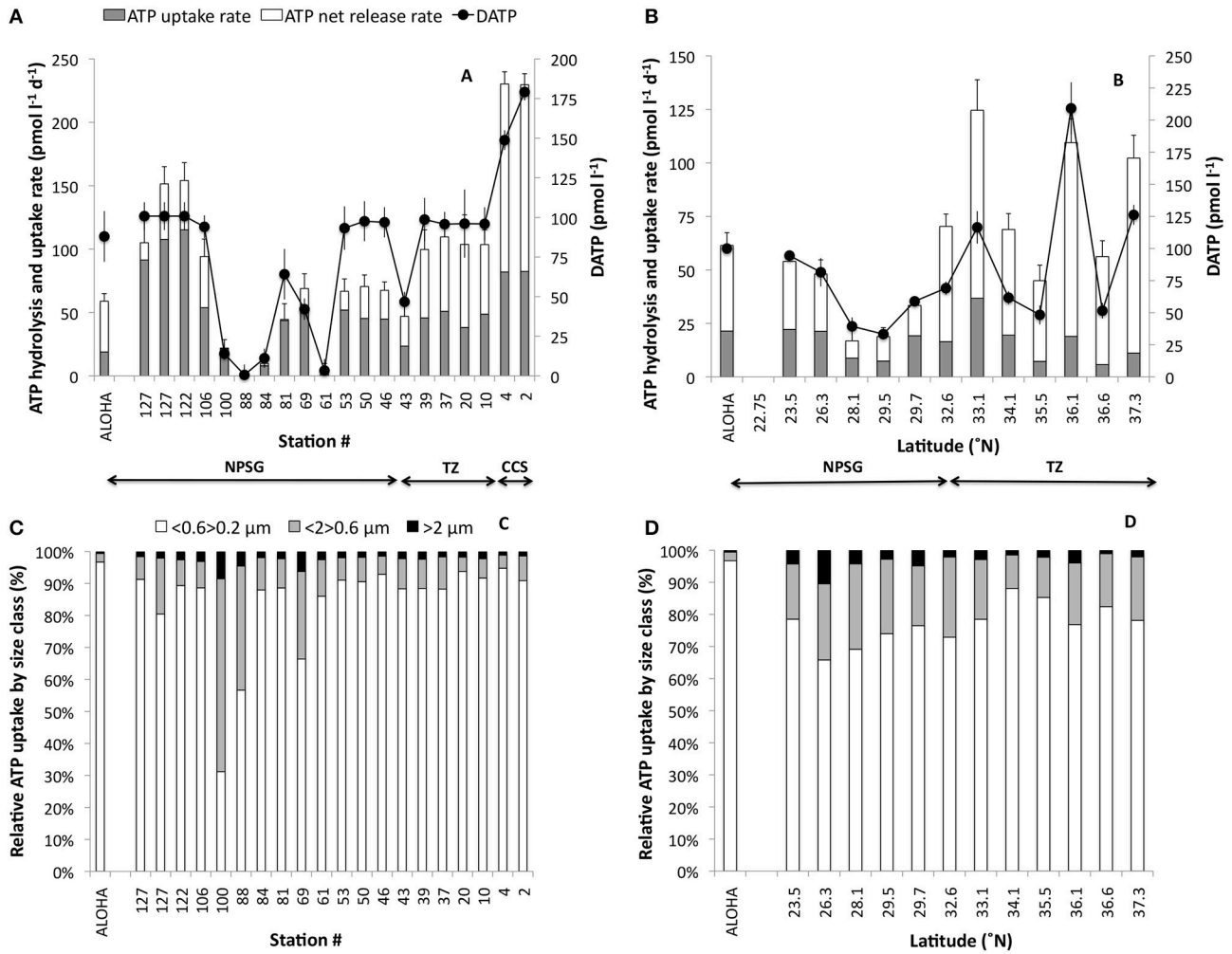

FIGURE 5 | (A,B) Total DATP hydrolysis rates (pmol l^{-1} d^{-1}) and the corresponding DATP concentrations (pmol l^{-1}; bullets). The total DATP hydrolysis rate is partitioned into rate of microbial uptake of P from ATP (gray), and the net release rate of Pi from DATP into the surrounding seawater (white). **(C,D)** Show the relative contribution from different microbial size classes to the microbial ATP-uptake measured. The zonal transect is shown in **(A,C)**; the meridional transect in **(B,D)**. Station ALOHA data for Pi uptake rates and Pi concentrations are shown to the left in each panel as the mean ± 1 s.d. ($n = 7$). Arrows indicate the stations within the CCS, TZ and NPSG as described in **Figure 1**. Note that the scales differ among panels.

$r = 0.9$). In the Pi addition experiments at Station 100, where ATP had longer TOT than Pi at ambient concentrations of Pi, the TOT did not change significantly with additional Pi in the smallest size class (<0.6>0.2 µm) at ∼ 1.3 days. However, at Pi additions of 50 and 100 nmol l^{-1}, the TOT for DATP was faster than for Pi. The TOT of DATP in the two larger size classes was more similar to Pi with additional Pi.

Correlation Between TOT, Pi, and DATP Pool Concentrations

The TOT of Pi correlated well with Pi concentrations within the NPSG (**Figure 8**). Correlation analysis of paired measurements of Pi concentrations and TOT at Station ALOHA had an $r = 0.9$ ($n = 28$); the zonal transect 2014 $r = 0.9$ ($n = 13$) and the meridional transect $r = 0.9$ ($n = 14$; **Figure 8**). However, stations within the NPSG during the meridional transect showed weaker correlation at $r = 0.7$ ($n = 5$). The relationship between TOT and Pi concentrations showed a better fit to a power function than a linear regression and it is noteworthy that below 20 nmol l^{-1} Pi, the slope of a linear regression is comparatively low, indicating that any additional Pi does not have an appreciable effect on TOT, hence additional Pi leads to an increase in uptake rate. Above ∼50 nmol l^{-1} Pi the TOT to Pi relationship stabilizes, i.e., additional Pi does not change uptake rate, so TOT instead increases. The same was not true for the TOT of DATP vs. DATP concentration, which was poorly correlated, in fact, the TOT of the DATP pool was better correlated to the Pi pool size than the DATP pool size ($r = 0.7$ vs. $r = 0.5$; data not shown).

DISCUSSION

Characterization of Study Areas

The majority of the work presented here was conducted within the NPSG, an environment characterized by its oligotrophic nature with perennially low inorganic nutrients, low standing stocks of chlorophyll and biomass, and typically low primary productivity, with Station ALOHA serving as a representative for the biome (Karl and Lukas, 1996; Karl and Church, 2014). This ecosystem is microbial based, recycling intensive, with picophytoplankton (<2 μm), specifically the cyanobacterium *Prochlorococcus,* typically the largest contributors to phytoplankton biomass and primary production (Karl, 1999; Karl et al., 2001a). The two transect cruises (zonal, 2014; meridional, 2016), presented an opportunity to compare the temporal variability in the various P-pools and microbial uptake rates of Pi and DATP observed at Station ALOHA, with spatial variability in the NPSG as well as areas within the transition zones into the CCS to the east, and toward the subpolar waters to the north of the North Pacific Ocean. The transition zones showed strong trends in both salinity and temperature with salinities and temperatures increasing from the boundaries to the east and north into the NPSG, as well as higher inorganic nutrients, chlorophyll and primary productivity compared to those of the NPSG.

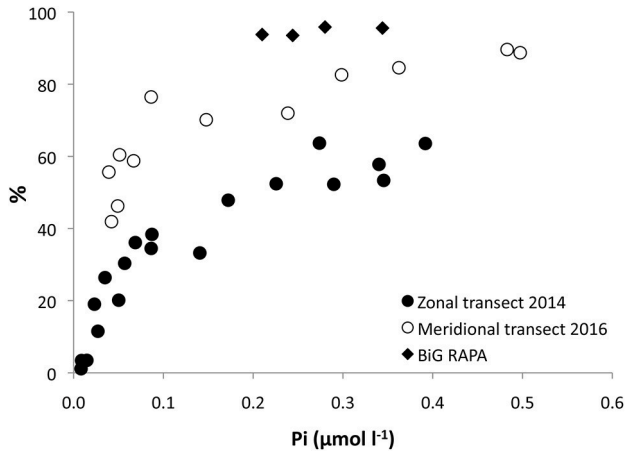

FIGURE 6 | Proportion (%) of the total DATP hydrolysis released into the surrounding seawater as dissolved Pi, versus the ambient inorganic phosphate (Pi) concentration. Zonal transect (black bullets), meridional transect (white bullets) and data from BiG RAPA transect cruise in 2010 within the South Pacific Subtropical Gyre (Duhamel et al., 2017).

P Concentrations at Station ALOHA and Along Transects

Although our understanding and knowledge of the cycling of P in the oligotrophic oceans have increased over the past decades, it is clear that these ecosystems are highly dynamic and not readily predictable. In particular the chemical composition and microbial utilization of the DOP pool, and its relative bioavailability remains an ongoing field of exploration (Karl and Björkman, 2015). Many studies have examined the bioavailability of DOP either by its susceptibility to alkaline phosphatase treatment (Moutin et al., 2008; Suzumura et al., 2012), through bioassays using known DOP compounds (Berman, 1988; Björkman and Karl, 1994; Björkman et al., 2000; Duhamel et al., 2017), or directly via specific ATP pool labeling (Karl and Bossard, 1985; Bossard and Karl, 1986; Björkman and Karl, 2005). In this study, we show the Pi-pool to be highly variable within the NPSG. Nevertheless, the range in concentrations at Station ALOHA and along the transects was similar. This suggests a mosaic upper ocean, with wide, yet limited dynamic range in terms of Pi-availability both temporally and across regions within the NPSG. In contrast, the DOP pool showed much less variability, and interestingly, the PPO_4 pool was relatively invariant within the NPSG, although always at relatively low

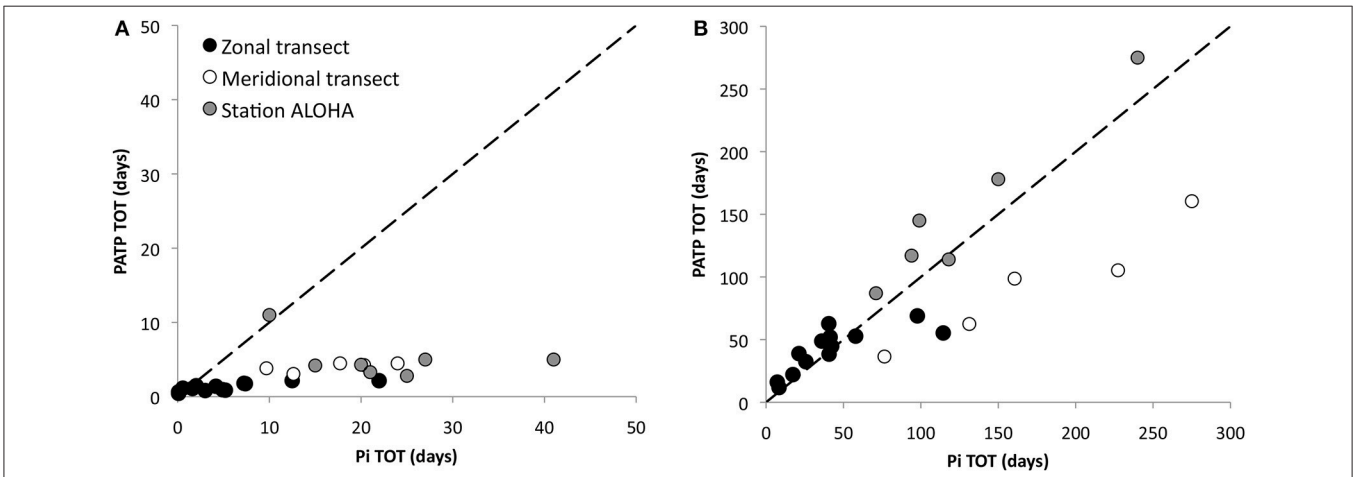

FIGURE 7 | Inorganic phosphate (Pi) turnover time (TOT; days) vs. ATP TOT (days) within the North Pacific Subtropical Gyre (NPSG) for **(A)** the whole water community (>0.2 μm), along the two transects and at Station ALOHA, and **(B)** the >2 μm size class. The dashed line indicates the 1:1 relationship.

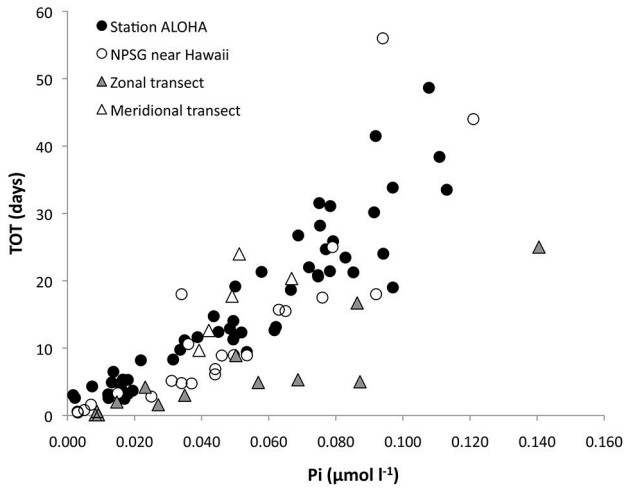

FIGURE 8 | Inorganic phosphate (Pi) concentrations vs. Pi-pool turnover times (TOT; days) within the North Pacific Subtropical Gyre (NPSG). Station ALOHA (black bullets), stations near Hawaii (white bullets), the zonal transect (gray triangles) and the meridional transect (white triangles). Correlation coefficients for these data were $r = 0.9$ for Hawaii ($n = 45$, mixed layer) and the zonal transect ($n = 13$), $r = 0.8$ for stations near Hawaii ($n = 31$), and $r = 0.7$ for the meridional transect ($n = 5$).

concentrations. This may indicate that even at very low Pi-inventories, the particulate P pool is buffered by increased utilization of the DOP pool. However, a reduction of the DOP pool in response to very low Pi is not evident at Station ALOHA, but may not be readily resolved given the analytical precision of the measurement (i.e., ability to detect a change in DOP of ±5%, or 10–15 nmol l^{-1} with sufficient certainty). Yet, during the 2014 zonal transect, in the region around 30°N where Pi was depleted, the DOP pool was significantly reduced relative to other stations along the transect, as well as compared to the long term mean at Station ALOHA. This lower DOP pool size may reflect an increased utilization of DOP due to P-limiting conditions. Nevertheless, the DOP concentrations in this region remained above 100 nM-P, indicating that a substantial fraction of the DOP pool may not be readily available to the microbial community in the surface ocean. Other studies have reached similar conclusions that only a relatively small fraction of the DOP pool appears to be bioavailable, e.g., Moutin et al. (2008) found that only 10–20% of the *in situ* DOP pool in the South Pacific Subtropical Gyre was hydrolyzable by alkaline phosphatase, similar to what Suzumura et al. (2012) reported for stations in the North Pacific near Japan (22–39%), and in the tropical and subtropical North Atlantic phosphomonoesters, substrates for alkaline phosphatase, constituted 19–37% of the DOP pool (Reynolds et al., 2014). This is also consistent with the degradation of selected DOP compounds at Station ALOHA, as well as the assessment of DOP utilization though bioassays (Björkman and Karl, 1994, 2003). An alternative explanation for high residual DOP during Pi-deplete conditions may be that other resources, such as available nitrogen or iron, are limiting or co-limiting production, and these limitations hamper further utilization of DOP. For example, in the subtropical North Atlantic, zinc has been implied as a limiting factor for the activity of alkaline phosphatase (Mahaffey et al., 2014), indicating that essential microelements may impact DOP degradation processes. The study region for the zonal transect around 30°N is known to consistently, if not predictably, harbor large, summertime phytoplankton blooms (Wilson, 2003, 2011; Villareal et al., 2012) and satellite imagery showed enhanced chlorophyll in this same area, consistent with such blooms, lasting from mid-July through September 2014. In a previous study within this same region Duhamel et al. (2010) found areas where the microbial community was under P-stress, as implied by the comparatively high alkaline phosphatase activity measured. The 2014 zonal transect coincided with late bloom stages, and areas most likely in post-bloom conditions as indicated by the vanishingly low concentrations of Pi in the surface waters.

The concentration of the DOP pool constituent DATP was quite uniform along the two transects within the NPSG, except where Pi was depleted and where the DATP pool also was drawn down to near the detection limit for our analysis. The concentrations were higher during the fall than spring transect possibly due to seasonal variability in DATP as previously observed at Station ALOHA (Björkman and Karl, 2001). Although DATP-phosphate is but a small fraction (∼0.15%) of the total DOP pool, it appears to be highly bioavailable.

P Turnover Times and Uptake Rates

The Pi pool turnover times observed in this study were within the range previously reported from the NPSG (Perry and Eppley, 1981; Björkman et al., 2000), of a few hours to several weeks, again highlighting the variability in Pi-pool dynamics within the NPSG. The Pi-pool turnover time was strongly correlated with measured Pi pool concentrations, but did show concentration dependent kinetics, i.e., increasing uptake rate with increasing Pi concentration, at low ambient Pi concentrations, as described previously for Station ALOHA (Björkman et al., 2012).

The turnover time of the DATP pool was typically substantially shorter than for the Pi-pool, reflecting both its small pool size and that the microbial hydrolysis and uptake of P from DATP proceeds separately from that of the Pi pool (Ammerman and Azam, 1985; Björkman et al., 2012; Duhamel et al., 2017). Total DATP hydrolysis was high along both transects, exceeding the uptake of Pi from DATP by the microbial community, resulting in a net release of regenerated Pi into the ambient seawater. There was a positive relationship between Pi concentrations and the proportion of the DATP hydrolyzed, i.e., net regeneration of Pi from DATP, similar to that observed by Ammerman and Azam (1991a), with a higher fraction of the total hydrolyzed P taken up at lower Pi concentrations. In the South Pacific Subtropical Gyre, where Pi concentrations are perennially higher compared to the NPSG (Moutin et al., 2008), the proportion of regenerated Pi from ATP was also higher than observed in this study (**Figure 6**) emphasizing the decoupling of DATP hydrolysis and Pi uptake at high Pi concentrations (Duhamel et al., 2017). The steepest increase in the proportion of DATP regenerated as Pi was seen at Pi concentrations <100 nmol l^{-1} Pi, indicating that the

newly regenerated Pi is of increasing importance to P-nutrition the smaller the Pi pool becomes, and the coupling between DATP hydrolysis and uptake becomes increasingly tighter, i.e., the recycling of P intensifies, as Pi concentrations drop below ∼100 nmol l^{-1}. Although the smallest components of the microbial community appear to have the highest affinity for Pi (Thingstad et al., 1993; Cañellas et al., 2000; Vadstein, 2000), and typically do not appear to be P-limited, the larger cells can capitalize at higher Pi concentrations with increased Pi-uptake rates as well as capturing a larger proportion of the total community P taken up (Björkman et al., 2012). This was observed during the two transect cruises, and demonstrated in the Pi addition experiment at station 100 where a range of Pi concentrations was used. In this experiment microorganisms in the >2 μm fraction increased both Pi uptake rate as well as the relative contribution of the total uptake with increasing Pi. The uptake of P originating from DATP was greatly dominated by the smallest size class (<0.6>0.2 μm) and likely driven by heterotrophic bacterial hydrolysis by the enzyme 5′-nucleotidase and subsequent uptake (Azam and Hodson, 1977; Bengis-Garber and Kushner, 1982; Ammerman and Azam, 1991a,b). Interestingly, at the Pi depleted stations along 30°N during the zonal transect, Pi from ATP was transferred to a greater extent into the two larger size classes, although the rates were very low. However, this partitioning was not seen in the Pi-uptake, where the largest size classes contributed the least to overall Pi uptake. Taken together, this indicates that this P depleted region was poised for rapid P assimilation, should P become available.

CONCLUSION

To gain a better appreciation for the flux of essential nutrients, such as phosphate, through biogeochemical cycles in the vast open ocean biomes, it is necessary to assess the dynamics of the P-pool and how its bioavailability may impact spatial and temporal variability in productivity and community composition. Our study showed that Pi concentrations in the surface waters within the NPSG were highly dynamic both in time and space whereas DOP and PPO_4 pools were less variable; the particulate pool potentially buffered by the much larger reservoir provided by the DOP pool. Although Pi-stress, or limitation, occurred locally or periodically, P sufficiency appears to be the prevailing condition for the dominant components of the microbial community within the NPSG. DATP was typically more rapidly turned over than the PATP pool, which turned over faster than the Pi-pool. Microbial uptake of P was dominated by the <2 μm size class; however, the turnover time for Pi or ATP in the >2 μm fraction were similar, suggesting that microbial utilization of these two phosphate pools are independent of one another within the NPSG and that DATP predominantly is processed by the smallest microbial components of this ecosystem. DATP hydrolysis commonly resulted in the net release of Pi into the ambient seawater and may increasingly contribute to P-nutrition during low Pi conditions.

AUTHOR CONTRIBUTIONS

KB and SD designed the experiments, performed the field- and laboratory work. KB wrote the manuscript. SD, DK, MC contributed significantly to the intellectual content of the manuscript. DK and MC provided funding.

ACKNOWLEDGMENTS

We thank the Captains and crew of the R/V *Kilo Moana*, R/V *Kaimikai-O-Kanaloa,* R/V *New Horizon* and R/V *Knorr*. We thank Lance Fujieki and Benedetto Barone for graphical assistance. Funding was provided by the National Science Foundation for the Hawaii Ocean Time-series program (OCE-1260164, MC, DK) and the Center for Microbial Oceanography: Research and Education (C-MORE, DBI-0424599, DK) and Dimensions in Biodiversity (OCE-124221, MC). Additional support was provided by the Gordon and Betty Moore Foundation: Marine Microbiology Initiative (3794, DK) and the Simons Foundation (SCOPE project ID 329108: DK and MC and Gradients project ID 426570SP: V. Armbrust; U. Washington, with subcontract to DK).

REFERENCES

Ammerman, J. W., and Azam, F. (1985). Bacterial 5′-nucleotidase in aquatic ecosystems: A novel mechanism of phosphorus regeneration. *Science* 227, 1338–1340. doi: 10.1126/science.227.4692.1338

Ammerman, J. W., and Azam, F. (1991a). Bacterial 5′-nucleotidase activity in estuarine and coastal marine waters: Role in phosphorus regeneration. *Limnol. Oceanogr*. 36, 1437–1447. doi: 10.4319/lo.1991.36.7.1437

Ammerman, J. W., and Azam, F. (1991b). Bacterial 5′-nucleotidase activity in estuarine and coastal waters. Characterization of enzyme activity. *Limnol. Oceanogr*. 36, 1427–1436. doi: 10.4319/lo.1991.36.7.1427

Azam, F., and Hodson, R. E. (1977). Dissolved ATP in the sea and its utilisation by marine bacteria. *Nature* 276, 696–698. doi: 10.1038/267696a0

Bengis-Garber, C., and Kushner, D. J. (1982). Role of membrane bound 5′-nucleotidase in nucleotide uptake by a moderate halophile Vibrio costicola. *J. Bacteriol*. 149, 808–815.

Berman, T. (1988). Differential uptake of orthophosphate and organic phosphorus substrates by bacteria and algae in Lake Kinneret. *J. Plankton Res*. 10, 1239–1249. doi: 10.1093/plankt/10.6.1239

Björkman, K. M., and Karl, D. M. (2001). A novel method for the measurement of dissolved adenosine and guanosine triphosphate in aquatic habitats: applications to marine microbial ecology. *J. Microb. Meth*. 47, 159–167. doi: 10.1016/S0167-7012(01)00301-3

Björkman, K. M., and Karl, D. M. (2003). Bioavailability of dissolved organic phosphorus in the euphotic zone at Station ALOHA, North Pacific Subtropical Gyre. *Limnol. Oceanogr*. 48, 1049–1057. doi: 10.4319/lo.2003.48.3.1049

Björkman, K. M., and Karl, D. M. (2005). Presence of dissolved nucleotides in the North Pacific Subtropical Gyre and their role in cycling of dissolved organic phosphorus. *Aquat. Microb. Ecol*. 39, 193–203. doi: 10.3354/ame039193

Björkman, K., and Karl, D. M. (1994). Bioavailability of inorganic and organic phosphorus compounds to natural assemblages of microorganisms in Hawaiian coastal waters. *Mar. Ecol. Prog. Ser*. 111, 265–273. doi: 10.3354/meps111265

Björkman, K., Duhamel, S., and Karl, D. M. (2012). Microbial group specific uptake kinetics of inorganic phosphate and adenosine-5′-triphosphate

(ATP) in the North Pacific Subtropical Gyre. *Front. Microbiol.* 3:189. doi: 10.3389/fmicb.2012.00189

Björkman, K., Thomson-Bulldis, A. L., and Karl, D. M. (2000). Phosphorus dynamics in the North Pacific Subtropical Gyre. *Aquat. Microb. Ecol.* 22, 185–198. doi: 10.3354/ame022185

Bossard, P., and Karl, D. M. (1986). The direct measurement of ATP and adenine nucleotide pool turnover in microorganisms: a new method for environmental assessment of metabolism, energy flux and phosphorus dynamics. *J. Plankton Res.* 8, 1–13. doi: 10.1093/plankt/8.1.1

Cañellas, M., Agusti, S., and Duarte, C. M. (2000). Latitudinal variability in phosphate uptake in the Central Atlantic. *Mar. Ecol. Prog. Ser.* 194, 283–294. doi: 10.3354/meps194283

Casey, J. R., Lomas, M. W., Michelou, V. K., Dyhrman, S. T., Orchard, E. D., Ammerman, J. W., et al. (2009). Phytoplankton taxon-specific orthophosphate (Pi) and ATP utilization in the western subtropical North Atlantic. *Aquat. Microb. Ecol.* 58, 31–44. doi: 10.3354/ame01348

Clark, L. L., Ingall, E. D., and Benner, R. (1998). Marine phosphorus is selectively remineralized. *Nature* 393:426. doi: 10.1038/30881

Dore, J. E., Houlihan, T., Hebel, D. V., Tien, G., Tupas, L., and Karl, D. M. (1996). Freezing as a method of sample preservation for the analysis of dissolved nutrients in seawater. *Mar. Chem.* 53, 173–185. doi: 10.1016/0304-4203(96)00004-7

Duhamel, S., Björkman, K. M., Repeta, D. J., and Karl, D. M. (2017). Phosphorus dynamics in biogeochemically distinct regions of the southeast subtropical Pacific Ocean. *Prog. Oceanogr.* 151, 261–274. doi: 10.1016/j.pocean.2016.12.007

Duhamel, S., Björkman, K. M., Van Wambeke, F., Moutin, T., and Karl, D. M. (2011). Characterization of alkaline phosphatase activity in the North and South Pacific Subtropical Gyres: implications for phosphorus cycling. *Limnol. Oceanogr.* 56, 1244–1254. doi: 10.4319/lo.2011.56.4.1244

Duhamel, S., Dyhrman, S. T., and Karl, D. M. (2010). Alkaline phosphatase activity and regulation in the North Pacific Subtropical Gyre. *Limnol. Oceanogr.* 55, 1414–1425. doi: 10.4319/lo.2010.55.3.1414

Falkowski, P. G. (1997). Evolution of the nitrogen cycle and its influence on the biological sequestering of CO_2 in the ocean. *Nature* 387, 272–275. doi: 10.1038/387272a0

Johnson, D. L. (1971). Simultaneous determination of arsenate and phosphate in natural waters. *Environ. Sci. Tech.* 5, 411–414. doi: 10.1021/es60052a005

Karl, D. M. (1999). A sea of change: biogeochemical variability in the North Pacific Subtropical Gyre. *Ecosystems* 2, 181–214. doi: 10.1007/s100219900068

Karl, D. M., and Björkman, K. M. (2015). "Dynamics of DOP," in *Biogeochemistry of Marine Dissolved Organic Matter*, *2nd Edn.*, eds D. Hansell and C. Carlson (Amsterdam; New York, NY: Academic Press), 233–334. doi: 10.1016/B978-0-12-405940-5.00005-4

Karl, D. M., and Bossard, P. (1985). Measurement and significance of ATP and adenine nucleotide pool turnover in microbial cells and environmental samples. *J. Microbiol. Methods* 3, 125–139. doi: 10.1016/0167-7012(85)90040-5

Karl, D. M., and Church, M. J. (2014). Microbial oceanography and the Hawaii Ocean Time-series programme. *Nat. Rev. Microbiol.* 12, 699–713. doi: 10.1038/nrmicro3333

Karl, D. M., and Lukas, R. (1996). The Hawaii Ocean Time-series (HOT) program: background, rationale and field implementation. *Deep Sea Res.* 43, 129–156. doi: 10.1016/0967-0645(96)00005-7

Karl, D. M., and Tien, G. (1992). MAGIC: A sensitive and precise method for measuring dissolved phosphorus in aquatic environments. *Limnol. Oceanogr.* 37, 105–116. doi: 10.4319/lo.1992.37.1.0105

Karl, D. M., Bidigare, R. R., and Letelier, R. M. (2001a). Long-term changes in plankton community structure and productivity in the subtropical North Pacific Ocean: the domain shift hypothesis. *Deep Sea Res.* 48, 1449–1470. doi: 10.1016/S0967-0645(00)00149-1

Karl, D. M., Björkman, K. M., Dore, J. E., Fujieki, L., Hebel, D. V., Houlihan, T., et al. (2001b). Ecological nitrogen-to-phosphorus stoichiometry at Station ALOHA. *Deep Sea Res.* 48, 1529–1566. doi: 10.1016/S0967-0645(00)00152-1

Kolowith, L. C., Ingall, E. D., and Benner, R. (2001). Composition and cycling of marine organic phosphorus. *Limnol. Oceanogr.* 46, 309–320. doi: 10.4319/lo.2001.46.2.0309

Lomas, M. W., Burke, A. L., Lomas, D. A., Bell, D. W., Shen, C., Dyhrman, S. T., et al. (2010). Sargasso Sea phosphorus biogeochemistry: an important role for dissolved organic phosphorus (DOP). *Biogeosciences* 7, 695–710. doi: 10.5194/bg-7-695-2010

Mahaffey, C., Reynolds, S., Davis, C. E., and Lohan, M. C. (2014). Alkaline phosphatase activity in the subtropical ocean: insights from nutrient, dust and trace metal addition experiments. *Front. Mar. Sci.* 1:73. doi: 10.3389/fmars.2014.00073

Mather, R. L., Reynolds, S. E., Wolff, G. A., Williams, R. G., Torres-Valdes, S., Woodward, E. M. S., et al. (2008). Phosphorus cycling in the North and South Atlantic Ocean subtropical gyres. *Nat. Geoscience* 1, 439–443. doi: 10.1038/ngeo232

Menzel, D. W., and Corwin, N. (1965). The measurement of total phosphorus in seawater based on the liberation of organically bound fractions by persulfate oxidation. *Limnol. Oceanogr.* 10, 280–282. doi: 10.4319/lo.1965.10.2.0280

Moutin, T., Karl, D. M., Duhamel, S., Rimmelin, P., Raimbault, P., Van Mooy, B., et al. and Claustre, H. (2008). Phosphate availability and the ultimate control of new nitrogen input by nitrogen fixation in the tropical Pacific Ocean. *Biogeosciences* 5, 95–109. doi: 10.5194/bg-5-95-2008

Murphy, J., and Riley, J. P. (1962). A modified single solution method for determination of phosphate in natural waters. *Anal. Chim. Acta* 27, 31–36. doi: 10.1016/S0003-2670(00)88444-5

Perry, M. J., and Eppley, R. W. (1981). Phosphate uptake by phytoplankton in the central North Pacific Ocean. *Deep Sea Res.* 28A, 39–49. doi: 10.1016/0198-0149(81)90109-6

Repeta, D. J., Ferron, S., Sosa, O. A., Johnson, C. G., Repeta, L. D., Acker, M., et al. (2016). Marine methane paradox explained by bacterial degradation of dissolved organic matter. *Nat. Geoscience* 9, 884–887. doi: 10.1038/ngeo2837

Reynolds, S., Mahaffey, C., Roussenov, V., and Williams, R. G. (2014). Evidence for production and lateral transport of dissolved organic phosphorus in the eastern subtropical North Atlantic. *Glob. Biogeochem. Cycles* 28, 805–824. doi: 10.1002/2013GB004801

Shilova, I. N., Mills, M. M., Robidart, J. C., Turk-Kubo, K. A., Björkman, K. M., Kolber, Z., et al. (2017). Differential effects of nitrate, ammonium, and urea as N sources for microbial communities in the North Pacific Ocean. *Limnol. Oceanogr.* 62, 2550–2574. doi: 10.1002/lno.10590

Suzumura, M., Hashihama, F., Yamada, N., and Kinouchi, S. (2012). Dissolved phosphorus pools and alkaline phosphatase activity in the euphotic zone of the western North Pacific Ocean. *Front. Microbiol.* 3:99. doi: 10.3389/fmicb.2012.00099

Thingstad, T. F., Skjoldal, E. F., and Bohne, R. A. (1993). Phosphorus cycling and algal-bacterial competition in Sandfjord, western Norway. *Mar. Ecol. Prog. Ser.* 99, 239–259. doi: 10.3354/meps099239

Tyrell, T. (1999). The relative influence of nitrogen to phosphorus on oceanic primary production. *Nature* 400, 525–531. doi: 10.1038/22941

Vadstein, O. (2000). Heterotrophic, planktonic bacteria and cycling of phosphorus. Phosphorus requirements, competitive ability and food web interactions. *Adv. Microb. Ecol.* 16, 115–167. doi: 10.1007/978-1-4615-4187-5_4

Villareal, T. A., Brown, C. G., Brzezinski, M. A., Krause, J. W., and Wilson, C. (2012). Summer diatom blooms in the North Pacific subtropical gyre: 2008-2009. *PLoS ONE* 7:e33109. doi: 10.1371/journal.pone.0033109

Wilson, C. (2003). Late Summer chlorophyll blooms in the oligotrophic North Pacific Subtropical Gyre. *Geophys. Res. Lett.* 30, 1–4. doi: 10.1029/2003GL017770

Wilson, C. (2011). Chlorophyll anomalies along the critical latitude at 30 degrees N in the NE Pacific. *Geophys. Res. Lett.* 38, 1–6. doi: 10.1029/2011GL048210

Conflict of Interest Statement: The authors declare that the research was conducted in the absence of any commercial or financial relationships that could be construed as a potential conflict of interest.

frontiers in Marine Science

ORIGINAL RESEARCH
published: 25 October 2018
doi: 10.3389/fmars.2018.00380

Dissolved Organic Phosphorus Utilization by Phytoplankton Reveals Preferential Degradation of Polyphosphates Over Phosphomonoesters

Julia M. Diaz[1], Alisia Holland[1], James G. Sanders[1], Karrie Bulski[1], Douglas Mollett[1,2], Chau-Wen Chou[3], Dennis Phillips[3], Yuanzhi Tang[4] and Solange Duhamel[5]*

[1] Department of Marine Sciences, Skidaway Institute of Oceanography, University of Georgia, Savannah, GA, United States, [2] Georgetown College, Georgetown, KY, United States, [3] Proteomics and Mass Spectrometry Core Facility, University of Georgia, Athens, GA, United States, [4] School of Earth and Atmospheric Sciences, Georgia Institute of Technology, Atlanta, GA, United States, [5] Division of Biology and Paleo Environment, Lamont-Doherty Earth Observatory, Palisades, NY, United States

OPEN ACCESS

Edited by:
Wolfgang Koeve, GEOMAR Helmholtz-Zentrum für Ozeanforschung Kiel, Helmholtz-Gemeinschaft Deutscher Forschungszentren (HZ), Germany

Reviewed by:
Michael William Lomas, Bigelow Laboratory for Ocean Sciences, United States
Monika Nausch, Leibniz Institute for Baltic Sea Research (LG), Germany

***Correspondence:**
Julia M. Diaz
julia.diaz@skio.uga.edu

Specialty section:
This article was submitted to Marine Biogeochemistry, a section of the journal Frontiers in Marine Science

Received: *13 May 2018*
Accepted: *28 September 2018*
Published: *25 October 2018*

Citation:
Diaz JM, Holland A, Sanders JG, Bulski K, Mollett D, Chou C-W, Phillips D, Tang Y and Duhamel S (2018) Dissolved Organic Phosphorus Utilization by Phytoplankton Reveals Preferential Degradation of Polyphosphates Over Phosphomonoesters. Front. Mar. Sci. 5:380. doi: 10.3389/fmars.2018.00380

The nutritionally available pool of dissolved organic phosphorus (DOP) supports marine primary productivity in a range of ocean ecosystems but remains poorly resolved. Here, the relative lability of model phosphorus (P) compounds representing the major P(V) bond classes of marine DOP – phosphomonoesters (P-O-C) and phosphoanhydrides (P-O-P) – was assessed in diatom cultures of the genus *Thalassiosira,* as well as coastal field sites of the western North Atlantic. In diatom samples, maximum enzymatic hydrolysis rates revealed that the P-anhydride bonds of inorganic tripolyphosphate (3poly-P), followed by the P-anhydride bonds of adenosine 5′-triphosphate (ATP), were preferentially degraded relative to the P-monoesters adenosine 5′-monophosphate (AMP) and 4-methylumbelliferone phosphate (MUF-P). Consistent with these rate measurements, targeted proteomics analysis demonstrated that the underlying phosphatase diversity present in diatom samples was dominated by P-anhydride degrading enzymes (inorganic pyrophosphatases and nucleoside triphosphatases). Furthermore, biomass-normalized rates of ATP degradation were always suppressed under P-replete conditions in diatom cultures, but the effect of overall P availability on 3poly-P degradation was inconsistent among diatom strains, suggesting that inorganic polyphosphate (poly-P) degradation may persist irrespective of prevailing P levels in the marine environment. Indeed, the majority of field sites examined in the P-replete coastal western North Atlantic exhibited significantly higher maximum rates of inorganic poly-P hydrolysis relative to P-monoester hydrolysis, which was largely driven by phytoplankton dynamics. Based on these results, the possibility that P-anhydride utilization may contribute comparably or even more substantially than P-esters to community-level P demand, phytoplankton growth, and primary productivity should be considered.

Keywords: dissolved organic phosphorus, alkaline phosphatase activity, polyphosphate, phosphoester, phosphoanhydride, phosphorus stress, *Thalassiosira,* diatom

INTRODUCTION

Marine primary productivity is fundamentally constrained by the availability of nutrients such as phosphorus (P). P is incorporated into vital biomolecules that play essential roles in cellular structure (phospholipids), the storage and transmission of genetic information (DNA and RNA), energy transduction (adenosine 5′-triphosphate; ATP), metabolic signaling (inositol trisphosphate, (de)phosphorylated proteins and metabolites), as well as stress response and homeostasis (inorganic polyphosphate; poly-P) (Kornberg et al., 1999; Gray and Jakob, 2015). Although marine primary production is principally limited by either nitrogen or iron over most of the global surface ocean (Moore et al., 2013), P can be present at low or limiting concentrations in many marine systems, from the vast oligotrophic gyres (Rivkin and Swift, 1979; Wu et al., 2000; Moore et al., 2008; Moore et al., 2013) to coastal seas (Berland et al., 1972; Fahmy, 2003; Thingstad et al., 2005; Hardison et al., 2013). Rising anthropogenic inputs of nitrogen have also led to an increasing prevalence of P limitation in many ocean environments, especially in near-shore zones (Harrison et al., 1990; Fisher et al., 1992, 1999; Huang et al., 2003; Kemp et al., 2005; Zhang et al., 2007; Xu et al., 2008; Fu et al., 2012; Laurent et al., 2012; Turner and Rabalais, 2013; Kim et al., 2014). Yet even when P is not limiting, it can be sufficiently scarce to shape microbial physiology and community composition (Moore et al., 2008).

Marine plankton communities can access a variety of P sources to satisfy nutritional P demands. Orthophosphate is considered the most biologically preferred P source, but in the open ocean where orthophosphate is scarce, i.e., <1–10% of total dissolved P (Wu et al., 2000; Lomas et al., 2010), the recycling of dissolved organic P (DOP) supports approximately 90% of gross primary productivity (Karl, 2014). Even in coastal systems that are replete with orthophosphate, a highly labile fraction of the DOP pool is rapidly recycled to support primary production (Benitez-Nelson and Buesseler, 1999). The cycling and biological utilization of DOP is therefore fundamentally tied to the productivity and function of marine ecosystems on a global scale (Letscher and Moore, 2015) across extremes in trophic status.

Natural marine DOP is an operationally defined assemblage of organic, inorganic, and polymeric P-containing molecules. Despite a high degree of heterogeneity at the molecular level, marine DOP contains consistent proportions of three major P-bond classes: P-esters, P-anhydrides, and phosphonates (Young and Ingall, 2010). P-esters contain P in its most common + V oxidation state, typically in the form of the P-O-C (monoester) or C-O-P-O-C (diester) bonds. Representative P-monoesters include nucleotides and phosphosugars, while P-diesters include phospholipids and nucleic acids. Overall, P-esters are the most abundant DOP compound class, representing ∼80% of total marine DOP (Young and Ingall, 2010). Another P(V) bond class is the P-anhydrides, which are characterized by P-O-P bonds like those present in nucleoside di- and triphosphates, inorganic pyrophosphate, and poly-P. P-anhydrides account for ∼10% of total marine DOP and are the most recently recognized DOP bond class, based on advances in techniques to recover the low molecular weight fraction of dissolved organic matter (Diaz et al., 2008; Young and Ingall, 2010). Finally, phosphonates make up ∼10% of DOP (Young and Ingall, 2010). In phosphonates, P is present in its + III oxidation state bound directly to carbon. The identities of natural marine phosphonates are not fully known but may include phosphonolipids and low molecular weight metabolites (Repeta et al., 2016).

The composition of DOP helps determine its bioavailability. For example, while phosphonate utilization may be restricted to certain prokaryotic taxa (Dyhrman et al., 2006; Ilikchyan et al., 2009; Beversdorf et al., 2010; Martinez et al., 2010), P-esters are generally recognized as the major nutritional source of DOP in the ocean (Lin et al., 2016). The widespread importance of P-esters is based on the quantitative dominance of this pool (Young and Ingall, 2010), as well as the environmental prevalence of alkaline phosphatase (AP) (Luo et al., 2009, 2011; Sebastian and Ammerman, 2009). APs are well-known P-esterases, which are active throughout the ocean (Hoppe and Ullrich, 1999; Hoppe, 2003; Mahaffey et al., 2014) and play a vital role in phytoplankton P nutritional physiology, especially in P-deplete environments (Dyhrman and Ruttenberg, 2006; Lin et al., 2016). P-anhydrides may also be a critical, yet under-characterized source of P. For instance, nucleoside triphosphates such as ATP are highly labile P sources (Moore et al., 2005; Alonso-Saez and Gasol, 2007; Michelou et al., 2011; Mazard et al., 2012; Duhamel et al., 2014) in which two-thirds of the available P is contained in P-anhydride bonds. At Station ALOHA in the oligotrophic North Pacific Subtropical Gyre (NPSG), the turnover of dissolved ATP exceeds that of the bulk DOP pool, indicating that it may be preferentially utilized over other DOP sources (Björkman and Karl, 2005). Similarly, depth profiles of inorganic poly-P in the Sargasso Sea suggest that this P-anhydride is preferentially utilized over other forms of P (Martin et al., 2014). Indeed, inorganic poly-P is bioavailable to a diversity of microorganisms, including *Prochlorococcus*, *Synechococcus* (Moore et al., 2005), eukaryotic marine phytoplankton (Diaz et al., 2016), and natural phytoplankton communities (Björkman and Karl, 1994).

Despite the widespread importance of DOP and the strong compositional control over its utilization, the relative contribution of specific DOP pools to microbial P demand and primary productivity remains unclear at the community level. Therefore, an improved understanding of compound-specific DOP dynamics is necessary to advance a mechanistic view of overall marine ecosystem productivity and functioning. In particular, a growing appreciation of inorganic poly-P cycling (Diaz et al., 2008; Martin et al., 2014; Saad et al., 2016) brings into question the importance of this P-anhydride source relative to more traditionally recognized P-esters. Therefore, in this study, the relative lability of model P-esters and P-anhydrides was assessed in representative diatom cultures of the genus *Thalassiosira*, as well as natural samples from the coastal western North Atlantic. To identify underlying mechanisms involved in the compound-specific utilization of DOP, targeted proteomic analysis of diatom culture samples was also conducted.

MATERIALS AND METHODS

Model Diatoms, Growth Conditions, and Culture Sampling

Thalassiosira oceanica CCMP1005, *Thalassiosira pseudonana* CCMP1335, and *Thalassiosira pseudonana* CCMP1014 were obtained from the National Center for Marine Algae and Microbiota (NCMA), Bigelow Laboratories, East Boothbay, Maine. Diatoms were grown in batch cultures on autoclaved (121°C, 20 min) f/2 media (Guillard and Ryther, 1962) prepared using filtered (0.2 μm) natural seawater from the South Atlantic Bight. To examine the effect of overall P availability on the degradation of model DOP sources, diatoms were grown under P-replete (+P) and P-deplete (−P) conditions. In +P media, phosphate was provided at an initial concentration of 36 μM. In −P cultures, no phosphorus source was added. Molar N:P ratios were ∼24 and >882 in +P and −P media, respectively. *T. oceanica* and *T. pseudonana* were cultivated at 23°C and 18°C, respectively, on a 14 h:10 h light:dark cycle (340 μmol photons m^{-2} s^{-1}). Phytoplankton growth was monitored daily by measuring *in vivo* chlorophyll fluorescence with an AquaFluor handheld fluorometer (Turner Designs). Cell counts were conducted using a hemocytometer counting chamber (Karlson et al., 2010).

P hydrolysis rates from a variety of model DOP substrates (see below) were investigated in diatom cultures with two types of experiments. In the first experiment type, the degradation of P sources was monitored in +P and −P cultures of each diatom strain by subsampling the cultures every 3 days across 30 days of cultivation. On a given sampling day, each subsample (6 mL) was directly filtered (0.2 μm, 33 mm) to produce the cell-free filtrate, which was then incubated with a variety of P sources for up to 24 h to determine substrate-specific P hydrolysis rates for that day, as detailed below. In the second type of P hydrolysis experiment, +P cultures of each diatom strain were sampled after 30 days of cultivation, and P hydrolysis rates for each substrate were determined, as detailed below, in whole cultures and cell-free filtrates.

To generate samples for exoproteome analysis, ∼140 mL of cell-free filtrate was sampled from +P cultures after 30 days of growth. These filtrate samples were concentrated and exchanged twice into 20 mM Tris (pH = 8.0) using a 10 kDa Centricon® Plus-70 centrifugal filter device (Millipore), to a final volume 0.5 mL.

Field Sampling

Surface seawater (5–35 m) was collected in September 2016 during two sampling campaigns in the coastal western North Atlantic (**Supplementary Table S1**). Three sites were sampled aboard the R/V *Endeavor* using a Niskin rosette sampler and incubated immediately in order to determine rates of P hydrolysis. Two sites accessible by small boat in Woods Hole Harbor and Buzzard's Bay, MA, were sampled utilizing a peristaltic pump. These samples were transported on ice packs and analyzed for P hydrolysis rates within 5–6 h of collection. Additional samples were preserved and analyzed for chlorophyll, bacteria and phytoplankton abundance, and soluble reactive P (SRP), as detailed below.

Chlorophyll

In the dark, 250 mL of seawater was filtered onto 25 mm GF/F filters. Samples were stored in the dark at −20°C until analyzed according to protocols adapted from Strickland and Parsons (1972). Briefly, samples were extracted in 90% acetone in the dark (4°C, 9 h) and measured using a 10AU fluorometer (Turner). Sample signals were calibrated using a chlorophyll-a standard (Sigma) and were corrected for pheopigments by accounting for the fluorescence of extracts before and after acidification to 0.003 M HCl.

Abundance of Bacteria and Phytoplankton

Seawater samples were preserved for flow cytometry with 0.5% glutaraldehyde (final concentration), flash frozen in liquid nitrogen and stored at −80°C until analysis. Bacteria and group-specific phytoplankton counts were conducted on a Guava EasyCyte HT flow cytometer (Millipore). Instrument-specific beads were used to calibrate the cytometer. Samples were analyzed at a low flow rate (0.24 μL s^{-1}) for 3 min. To enumerate bacteria, samples were diluted (1:100) with filtered seawater (0.01 μm). Samples and filtered seawater blanks were stained with SYBR Green I (Invitrogen) according to the manufacturer's instructions and incubated in a 96-well plate in the dark at room temperature for 1 h. Bacterial cells were counted based on diagnostic forward scatter vs. green fluorescence signals. Major phytoplankton groups were distinguished based on plots of forward scatter vs. orange fluorescence (phycoerythrin-containing *Synechococcus* sp.), and forward scatter vs. red fluorescence (eukaryotes). Size classes of eukaryotic phytoplankton were further distinguished based on forward scatter (pico-, nano- and large eukaryotes).

Soluble Reactive P

Seawater samples were collected into acid cleaned, high density polyethylene bottles. Samples used for determining *in situ* SRP concentrations were frozen and stored upright at −20°C until analysis. Field samples and diatom filtrates were both analyzed for SRP using a standard colorimetric method (Hansen and Koroleff, 1999). To determine *in situ* SRP concentrations in field samples, SRP analysis was conducted using a 4 cm glass spectrophotometry cell on triplicate subsamples, and the detection limit, defined as three times the standard deviation of replicate blank measurements, was 115 nmol L^{-1} SRP. For incubations to determine P hydrolysis rates (see below), replicate samples were analyzed in clear 96-well plates on a multimode plate reader (Molecular Devices) with a detection limit of 800 nmol L^{-1} P.

P-hydrolysis of Model DOP Substrates

Field and culture samples were incubated with a variety of model DOP substrates to determine P hydrolysis rates. Model P substrates were selected to represent the major P(V) bond classes present in natural marine DOP (**Figure 1**). The fluorogenic probe 4-methylumbeliferone phosphate (MUF-P) and the nucleotide adenosine 5′-monophosphate (AMP) were utilized as model P-esters. ATP was used as both a representative P-ester and an organic P-anhydride. Finally, two inorganic polyphosphate compounds with an average chain length of 3 or 45 P atoms (3poly-P and 45poly-P, respectively), were utilized as representative inorganic P-anhydrides. All P compounds were obtained from Millipore Sigma.

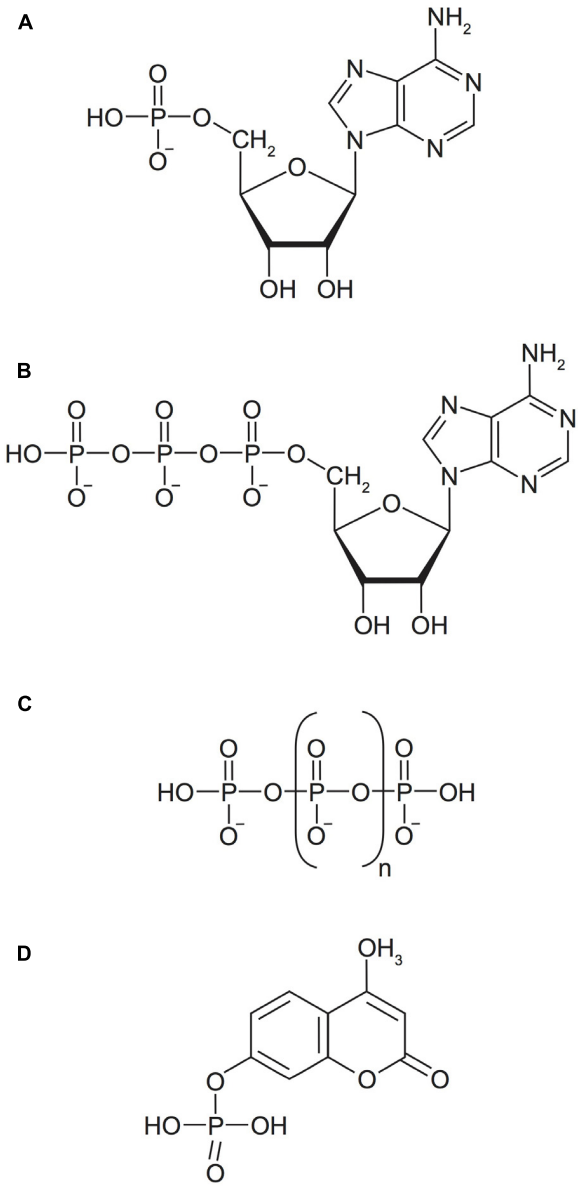

FIGURE 1 | Model P substrates utilized in this study represent the major P(V) bond classes of natural marine DOP. **(A)** Adenosine monophosphate (AMP), a P-monoester. **(B)** Adenosine triphosphate (ATP), a P-monoester and P-anhydride. **(C)** Inorganic polyphosphate (poly-P), a P-anhydride, $n \geq 1$. **(D)** 4-methylumbelliferyl phosphate (MUF-P), a fluorogenically labeled P-monoester.

P hydrolysis rates were determined in whole cultures (MUF-P only), cell-free culture filtrates (MUF-P, AMP, ATP, and 3poly-P), and whole seawater samples (MUF-P, 3poly-P, and 45poly-P). Samples were amended with each substrate at a final concentration of 20 μM P. This concentration was assumed to be rate-saturating based on preliminary experiments with natural samples. Thus, the rates of P hydrolysis reported herein represent maximum hydrolysis rates, consistent with many previous investigations of P-monoester degradation (or alkaline phosphatase activity, APA) in the marine environment [see Mahaffey et al. (2014) and references therein]. P hydrolysis rates were determined through one of the following two methods. In the first method, which was applied to all P substrates, the production of SRP was monitored over time using the colorimetric protocol outlined above. In the second method, the time-dependent hydrolysis of the fluorogenic probe MUF-P was monitored using a standard fluorescence technique (Duhamel et al., 2011). Briefly, hydrolysis of MUF-P to 4-methylumbellierone (MUF) was measured (excitation: 359 nm, emission: 449 nm) and calibrated with a multi-point standard curve of MUF (10–500 nmol L^{-1}). In both methods, samples were corrected for substrate autohydrolysis by accounting for negative controls, which were filtered (0.2 μm) and boiled (99°C, 15 min) prior to P amendment in order to eliminate enzyme activity.

In culture and field experiments, replicate samples and controls were incubated at room temperature (∼25°C) in a transparent (SRP method) or black (fluorescence method) 96-well plate. To ensure linearity of the hydrolysis rates, samples and controls were measured at multiple time points during the incubation period on a multimode plate reader (Molecular Devices). Overall incubation times were optimized depending on the sample type, P substrate, and the detection method employed. The SRP and fluorescence techniques were characterized by substantial differences in sensitivity. For example, the lower limit of detection, defined as three times the standard deviation of replicate blank measurements, was 800 nmol P L^{-1} for the SRP method and 2 nmol P L^{-1} for the fluorescence method. The upper limits of detection for the fluorescence method, defined as the P concentration above which the calibration curves begin to lose linearity, was 500 nmol L^{-1} P. Thus, samples exhibiting MUF-P hydrolysis rates within the limits of detection of the fluorescence method had to be incubated at least 1.6 times and up to 400 times longer before reaching detectable levels of SRP. The actual incubation times for the various sample types and analytical methods were as follows: whole seawater samples (fluorescence method: 12–15 h, SRP method: 24–65 h), cell-free culture filtrates (fluorescence method: 1–2 h, SRP method: 30 min to 24 h), whole culture samples (fluorescence method: 5 min to 1 h).

The SRP method was not used with whole culture samples due to interferences associated with the uptake/adsorption of enzymatically released phosphate by the cultures, which was

problematic at high cell densities. To verify the lack of such interference in whole seawater samples, SRP calibration curves (2–20 μM P) were prepared in each sample and analyzed at multiple time points throughout the incubation period.

Genome Searches

Putative APs were identified in the translated genomes of *T. pseudonana* CCMP1335 (taxid: 296543) and *T. oceanica* CCMP1005 (taxid: 159749) with NCBI's BLASTP search tool. The following protein sequences were used as queries: PhoA from *Escherichia coli* (GenBank: AAA83893), PhoD from *Bacillus subtilis* (UniProt: P42251), and PhoX from *Pseudomonas fluorescens* (Protein Data Bank: 4A9V). Only hits with an *E*-value $< 1 \times 10^{-4}$ are reported.

Proteomics

Concentrated exoproteome samples were digested using an in-solution tryptic digestion kit (ThermoScientific), according to the manufacturer's instructions. Peptide samples were analyzed at the Proteomics and Mass Spectrometry (PAMS) facility at the University of Georgia on a Thermo-Fisher LTQ Orbitrap Elite mass spectrometer coupled with a Proxeon Easy NanoLC system (Waltham, MA, United States).

The enzymatic peptides were loaded into a reversed-phase column (self-packed column/emitter with 200 Å 5 μM Bruker MagicAQ C18 resin), then directly eluted into the mass spectrometer. Briefly, the two-buffer gradient elution (0.1% formic acid as buffer A and 99.9% acetonitrile with 0.1% formic acid as buffer B) starts with 5% B, holds at 5% B for 2 min, then increases to 25% B in 60 min, to 40% B in 10 min, and to 95% B in 10 min.

The data-dependent acquisition method was used to acquire MS data. A survey MS scan was acquired first, and then the top 5 ions in the MS scan were selected following collision-induced dissociation (CID) and higher-energy collisional dissociation (HCD) MS/MS analysis. Both MS and MS/MS scans were acquired by the Orbitrap mass spectrometer at resolutions of 120,000 and 30,000, respectively. Data were acquired using Xcalibur software (version 2.2, Thermo Fisher Scientific).

Protein identification was performed using Thermo Proteome Discoverer (version 1.4) with Mascot (Matrix Science). The reference database for *T. oceanica* CCMP1005 consisted of the translated whole genome (NCBI Bioproject PRJNA36595) (Lommer et al., 2012) amended with a list of common contaminants, such as human keratin. The *T. pseudonana* CCMP1335 database was compiled from the translated nuclear (Bioproject PRJNA191), chloroplast (Bioproject PRJNA20561), and mitochondrial (Bioproject PRJNA15818) genomes (Armbrust et al., 2004; Oudot-Le Secq et al., 2007), and was also amended with common contaminant sequences. Databases included a reversed 'decoy' version for false discovery rate (FDR) analysis. The FDR of identified peptides was ∼2%. Protein matches were also filtered to exclude hits with fewer than two unique peptide identifications. Gene ontology (GO) annotations were integrated into results using the ProteinCenter Annotation node.

Statistical Analysis

P hydrolysis rates in diatom cell-free filtrates were measured throughout the growth curve of each species cultivated in replete (+P) or P-deficient (−P) media. Differences in hydrolysis rates among the three P sources under each growth condition were assessed using repeated measures analysis of variance (ANOVA) and *post hoc* testing with Tukey's honest significant difference (HSD) method. Average ratios of ATP and 3polyP hydrolysis were compared using a one-sample *T*-test. To test whether the degradation of each P source was P-regulated, cell-normalized rates of P hydrolysis were compared in +P and −P cultures using repeated measured ANOVA. Average P hydrolysis rates measured in whole cultures and in cell-free filtrates with different quantification methods were compared using Tukey's HSD test. MUF-P hydrolysis rates determined by the SRP vs. fluorescence methods were assessed using simple linear regression. Field-based rates of polyphosphate and MUF-P hydrolysis were compared at each site using an independent two-sample T-test assuming equal variance. Potential relationships between P hydrolysis rates and *in situ* chlorophyll concentrations were explored with simple linear regression. All statistical analyses were performed in Microsoft Excel® or JMP® Pro (V13.0).

RESULTS

Degradation of Model P Sources by Diatom Cultures

Relative Lability of P Sources in Cell-Free Filtrates

In order to explore the DOP nutritional preferences of *Thalassiosira* spp., the labilities of model P sources representing the major P(V) DOP bond classes (**Figure 1**) were tested in whole cultures and cell-free filtrates grown in P-replete (+P) and P-deficient (−P) media. Because P hydrolysis rates were quantified based on the production of SRP, cell-free filtrates were primarily utilized instead of whole cultures in order to avoid technical challenges associated with the analysis of SRP at high cell densities (see Discussion). All model P sources were degraded in diatom filtrates (**Figures 2–4**) and showed negligible hydrolysis (below detection) in boiled controls, consistent with enzymatic P-hydrolysis. In −P cultures, P hydrolysis rates were substantial within 1 week (*T. oceanica* and *T. pseudonana* CCMP1014) (**Figures 2B,F**) or after 2 weeks (*T. pseudonana* CCMP1335) (**Figure 2D**). In +P cultures, DOP degradation increased dramatically after about ∼2 weeks (**Figure 2**). Hydrolysis rates increased in all cultures over time, consistent with the depletion of SRP and the eventual onset of stationary phase (**Figures 2A,C,E**). Degradation rates among the three P sources were significantly different in each diatom culture and media condition throughout the growth curves (**Figure 2**). In every case, regardless of the diatom strain and the initial level of P availability, the rate of inorganic 3poly-P hydrolysis was significantly highest, followed by ATP, and finally AMP (**Figure 2**). Over the entire growth curve, ATP and AMP hydrolysis rates were statistically similar for both strains

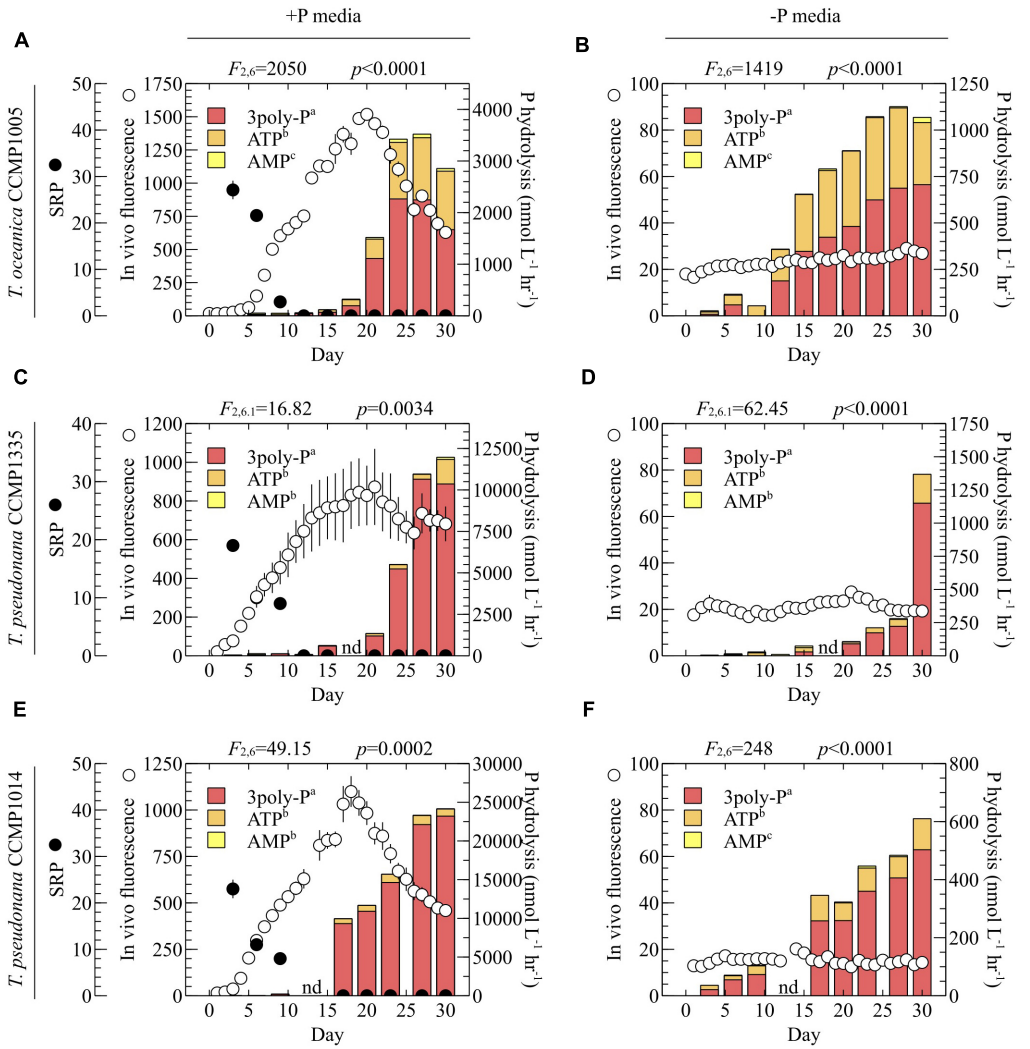

FIGURE 2 | P hydrolysis rates of model DOP compounds in diatom cell-free filtrates. **(A,B)** *T. oceanica* CCMP1005, **(C,D)** *T. pseudonana* CCMP1335, and **(E,F)** *T. pseudonana* CCMP1014. **(A,C,E)** P-replete media, and **(B,D,F)** P-deficient media. Soluble reactive phosphorus (SRP) concentrations were below detection (800 nmol L^{-1}) in –P cultures and are not depicted. Error bars indicate one standard deviation (SD) of the mean of three biological replicates. Statistical results from repeated measures ANOVA are provided above each plot and indicate the overall effect of P sources on hydrolysis rates. Results from the pairwise *post hoc* comparison of each P source via Tukey's honest significant difference test are provided next to the legend entries. P sources lacking a shared letter are significantly different ($p < 0.05$). nd, no data.

of *T. pseudonana* (**Figures 2C–E**), except for *T. pseudonana* CCMP1014 cultivated in −P media (**Figure 2F**). On the other hand, *T. oceanica* always hydrolyzed ATP significantly more than AMP, regardless of prevailing P availability (**Figures 2A,B**).

A maximum of three orthophosphate molecules can be released from ATP and 3poly-P. However, the complete degradation of phosphoanhydride bonds would produce three orthophosphate groups from 3poly-P but only two from ATP, since the final orthophosphate is bound to the adenosine moiety by a P-monoester linkage (**Figure 1**). Therefore, if the P-anhydride bonds of ATP are degraded, and the P-monoester bond remains intact, the ratio of ATP:3polyP hydrolysis should be 2/3 (or ∼66.7%). However, ratios of ATP:3poly-P hydrolysis over the last 1–2 weeks of growth were significantly less than 2/3 (**Table 1** and **Figures 2A,C–F**), except in the case of *T. oceanica* (−P) (**Table 1** and **Figure 2B**), in which ATP degradation was statistically similar to 66.7% of 3poly-P degradation.

The Effect of Overall P Availability on Substrate-Specific DOP Hydrolysis in Cell-Free Filtrates

The lability of 3poly-P, ATP, and AMP was assessed in the cell-free filtrates of diatoms cultivated in P-replete and P-deficient media. To account for differences in biomass, P hydrolysis rates were normalized to total cell counts in cultures at the respective sampling time. ATP hydrolysis was significantly upregulated under −P conditions in all diatom cultures (**Figures 3G–I**). On the other hand, P availability did not significantly affect

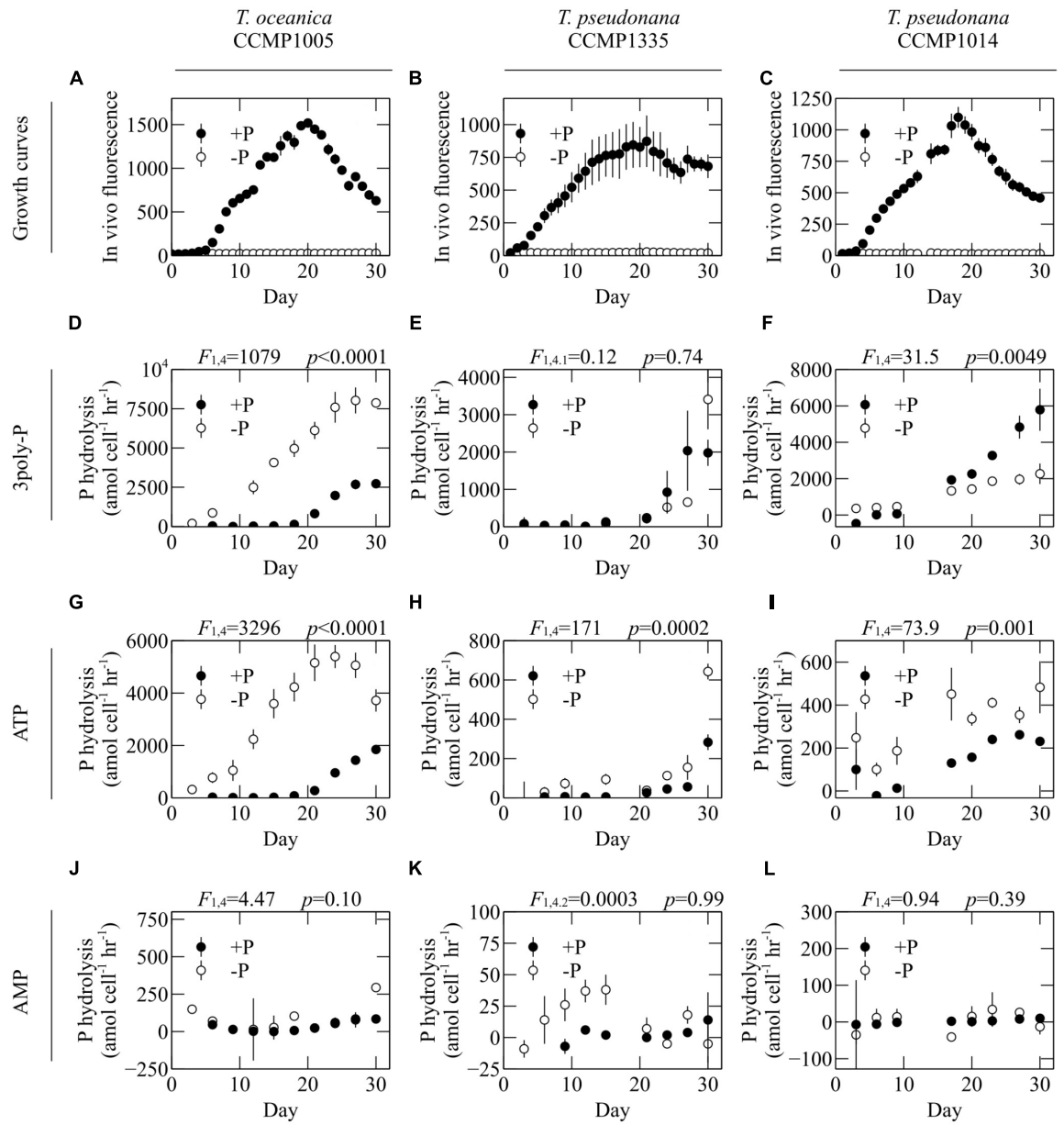

FIGURE 3 | The effect of overall P availability on DOP hydrolysis rates. **(A–C)** Growth curves and hydrolysis rates of **(D–F)** 3poly-P, **(G–I)** ATP, and **(J–L)** AMP in the cell-free filtrates of *T. oceanica* CCMP1005 **(A,D,G,J)**, *T. pseudonana* CCMP1335 **(B,E,H,K)**, and *T. pseudonana* CCMP1014 **(C,F,I,L)** cultivated under P-replete (+P) and P-deficient (–P) conditions. Error bars represent one standard deviation of the mean of three biological replicates. Statistical results from repeated measures ANOVA are provided above each plot and indicate the overall effect of P availability on hydrolysis rates.

AMP hydrolysis in any culture (**Figures 3J–L**). P-deficient conditions induced significant upregulation of 3poly-P hydrolysis by *T. oceanica* CCMP1005, significant downregulation by *T. pseudonana* CCMP1014, and no change by *T. pseudonana* CCMP1335 (**Figures 3D–F**).

Comparison to Fluorescence-Based MUF-P Hydrolysis Measurements

For all diatoms, 3poly-P hydrolysis in cell-free filtrates was significantly higher than MUF-P hydrolysis in whole cultures (**Figure 4**). ATP degradation by *T. oceanica* CCMP1005 cell-free filtrates was also significantly higher than whole culture MUF-P hydrolysis (**Figure 4A**). Rates of P-ester hydrolysis in the cell-free filtrates of all diatoms reflected strong methodological agreement. For example, AMP and MUF-P (fluorescence and SRP methods) were degraded at similar rates (**Figure 4**). In fact, SRP-based estimates of MUF-P hydrolysis systematically underestimated fluorescence-based measurements of MUF-P degradation by about ∼17% (p = 0.0008) in culture filtrates (**Figure 5**).

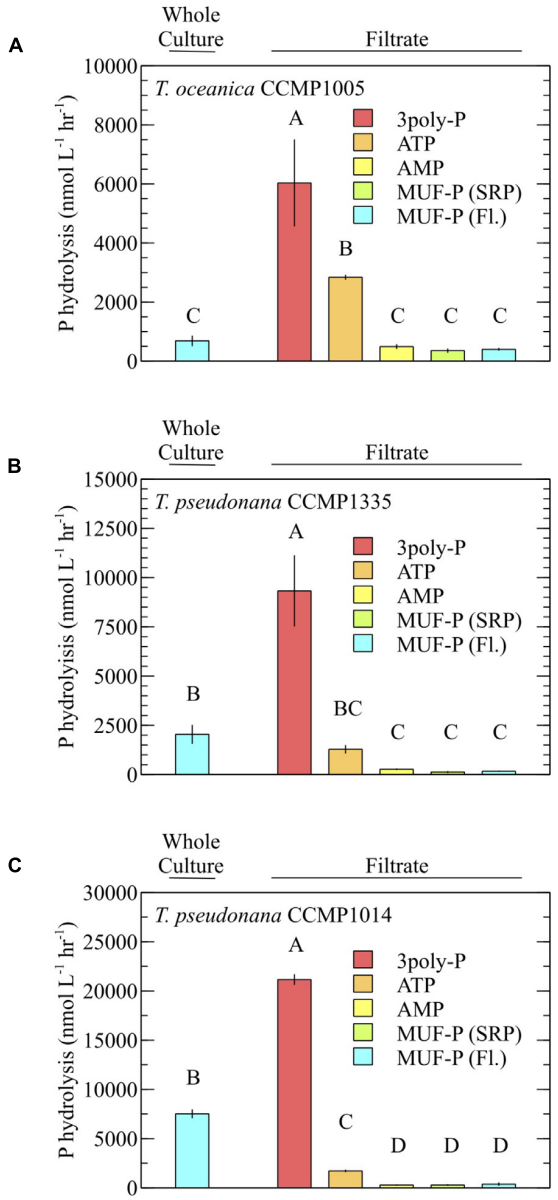

FIGURE 4 | P hydrolysis rates of model DOP compounds in the presence (whole culture) and absence (filtrate) of cells and using different detection methods. **(A)** *T. oceanica* CCMP1005, **(B)** *T. pseudonana* CCMP1335, and **(C)** *T. pseudonana* CCMP1014. All rates were quantified by measuring the accumulation of phosphate over time (SRP method), except where MUF-P degradation was quantified via the standard fluorometric method (Fl.). Cultures were analyzed after 30 days of growth. Error bars represent one standard deviation of the mean of three **(A,B)** or two **(C)** biological replicates. P hydrolysis rates lacking a shared letter are significantly different ($p < 0.05$; Tukey's honest significant difference).

Substrate-Specific P Hydrolysis Rates in the Coastal Western North Atlantic

Maximum hydrolysis rates of inorganic poly-P were measured in whole seawater samples from the coastal North Atlantic (**Figure 6A**) using the SRP method with two substrates: 3poly-P and 45poly-P. Poly-P chain length had no effect on P-hydrolysis rates, and the results from both poly-P sources were therefore combined into single average rates of inorganic poly-P hydrolysis. These rates were compared to maximum MUF-P hydrolysis rates determined via fluorescent detection. Average volume-normalized P hydrolysis rates ranged from 3.8–19.3 nmol P L^{-1} hr^{-1} and 1.4–50.6 nmol P L^{-1} hr^{-1} for inorganic poly-P and MUF-P, respectively (**Figure 6B**). Chlorophyll-normalized rates ranged from 5.6–7.7 nmol P μg chl^{-1} hr^{-1} and 2.5–20.1 nmol P μg chl^{-1} hr^{-1} for inorganic poly-P and MUF-P, respectively (**Supplementary Table S1**). SRP levels were above ∼700 nmol L^{-1}, except in a phytoplankton bloom along the New Jersey Coast, where SRP was 150 ± 15 nmol L^{-1} (avg ± SD, $n = 3$; **Supplementary Table S1**).

Inorganic poly-P hydrolysis rates were significantly higher than rates of MUF-P hydrolysis ($p < 0.05$) in four out of the five field sites sampled, by a factor of ∼1.5 to ∼2.7 (**Figure 6B** and **Table 2**). However, in one field site (Buzzard's Bay), MUF-P hydrolysis was ∼2.5-fold higher than inorganic poly-P hydrolysis ($p < 0.05$; **Figure 6B** and **Table 2**). Inorganic poly-P hydrolysis rates exhibited a significant linear correlation with chlorophyll levels ($p = 0.01$; **Figure 6C**), which was also evident for rates of MUF-P hydrolysis when the Buzzard's Bay outlier was excluded ($p = 0.04$; **Figure 6C**). However, P hydrolysis rates did not exhibit a significant relationship with bacterial abundance counts (**Figure 6D**). Bacteria cell counts (cells mL^{-1}) were ∼125 times higher than phytoplankton counts at the Buzzard's Bay site, yet only ∼17 to ∼45 times higher at all other locations (**Supplementary Table S1**).

SRP uptake/adsorption by whole seawater samples can potentially lead to the underestimation of P hydrolysis rates made by the SRP method. The degree of SRP uptake/adsorption was therefore assessed with standard additions of Na_2HPO_4 (P = 2–20 μM). Phosphate levels in these amended samples did not change over the course of the 24–65 h incubations.

Phosphatase Diversity in Diatom Cultures

The full genome data of two model diatom strains utilized in this study, *T. oceanica* CCMP1005 and *T. pseudonana* CCMP1335, are publicly available, enabling the analysis of phosphatase diversity in these two species. First, the genomes were searched for putative homologs of three bacterial alkaline phosphatase isoforms (PhoA, PhoD, and PhoX) using BLASTP analysis. In *T. oceanica* CCMP1005, results revealed the presence of two putative PhoD homologs, one putative PhoX homolog, but no homologous PhoA sequences (**Table 3**). On the other hand, *T. pseudonana* CCMP1335 possesses one putative homolog each of PhoA and PhoD, but no homologous sequences to PhoX (**Table 3**).

Since cell-free filtrates were the primary focus of substrate-specific P hydrolysis measurements, the diversity of phosphatases was investigated in cell-free filtrates of *T. oceanica* CCMP1005 and *T. pseudonana* CCMP1335 (under +P conditions for each culture only). Excluding contaminant sequences (i.e., keratin),

TABLE 1 | Comparison of ATP and 3poly-P hydrolysis rates in diatom cell-free filtrates from **Figure 2**.

Diatom	Days	Media	ATP:3poly-P (%)		*T*	df	*p*
			Avg	*SE*			
T. oceanica CCMP1005	18–30	+P	52.9	3.2	4.3	14	0.0007
		−P	70.3	4.0	0.9	14	0.38
T. pseudonana CCMP1335	21–30	+P	9.2	1.6	35.8	11	<0.0001
		−P	20.3	1.4	32.8	11	<0.0001
T. pseudonana CCMP1014	17–30	+P	6.1	0.4	167.2	14	<0.0001
		−P	23.8	1.6	26.7	14	<0.0001

T-scores (T; reported as absolute values) are calculated by subtracting from average experimental ATP:3polyP hydrolysis ratios (Avg) the proportion of ATP:3polyP hydrolysis expected from the complete degradation of phosphoanhydride bonds (66.7%), according to the following equation:

$$T = \frac{Avg - 66.7}{SE}$$

where SE is the standard error of the average ATP:3poly-P hydrolysis ratio, and df is the degrees of freedom. Two-tailed p-values are reported.

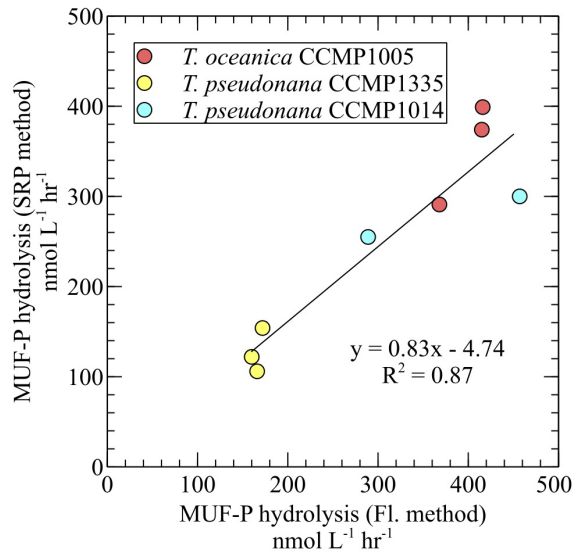

FIGURE 5 | Comparison of MUF-P hydrolysis rates obtained by the SRP quantification method and the fluorometric method in cell-free culture filtrates.

a total of 309 and 133 proteins were identified in extracellular proteomes of *T. oceanica* CCMP1005 and *T. pseudonana* CCMP1335, respectively (**Supplementary Tables S2**, **S3**). Among these hits, 24 from *T. oceanica* CCMP1005 and 9 from *T. pseudonana* CCMP1335 possess conservative domains consistent with phosphatase activity. The majority of these hits were shared among biological triplicates of each diatom (**Figure 7**). None of the putative bacterial alkaline phosphatase homologs identified through genome searches (**Table 3**) were detected in the cell-free culture filtrates, however. Rather, results indicated a diversity of other putative phosphatases, including P-anhydride- and P-ester-degrading enzymes. In fact, P-anhydride-degrading enzymes dominated the phosphatase diversity in the cell-free filtrates of both microorganisms, including inorganic pyrophosphatase and nucleoside triphosphates (**Figure 7**).

DISCUSSION

The goal of this study was to assess the relative lability of model P sources that represent the major marine DOP bond classes. The focus here was on the P(V) DOP bond classes – P-esters and P-anhydrides – because of the potential role that these compound classes have in P utilization by the bulk phytoplankton community. Maximum potential hydrolysis rates of model P-esters and P-anhydrides were assessed in the cell-free filtrates of representative diatom cultures and coastal field sites, while phosphatase diversity was also investigated in model diatom filtrates. Overall, results revealed that an innate capacity for the preferential utilization of P-anhydrides was prevalent across all of these sample types.

Degradation of Model P Sources by Diatom Cultures

In model diatoms, maximum rates of P hydrolysis were examined in cell-free filtrates that were prepared via syringe filtration of culture samples. Cell-surface and intracellular phosphatases may have been adventitiously released through the potential disruption and lysis of some cells during this process. Thus, P hydrolysis rates in these cell-free filtrates may overestimate truly dissolved rates of P hydrolysis. However, the aim here was not to quantify cell-free P hydrolysis rates *per se*, but to avoid technical barriers associated with analyzing the degradation of unlabeled P sources in the presence of cells. In particular, tracking P hydrolysis through the production of SRP becomes difficult at high cell densities because microorganisms have a strong ability to adsorb (Sanudo-Wilhelmy et al., 2004) and assimilate dissolved P.

Cell-free filtrates can only provide a glimpse into the overall DOP preferences of a culture because most DOP degradation takes place in the presence of cells. Thus, MUF-P hydrolysis in whole cultures was measured with a standard fluorometric protocol in order to help contextualize the P dynamics observed in cell-free filtrates. Surprisingly, inorganic 3poly-P degradation in the filtrates vastly exceeded MUF-P hydrolysis levels in whole cultures ($p < 0.05$), by at least ∼3-fold (*T. pseudonana*

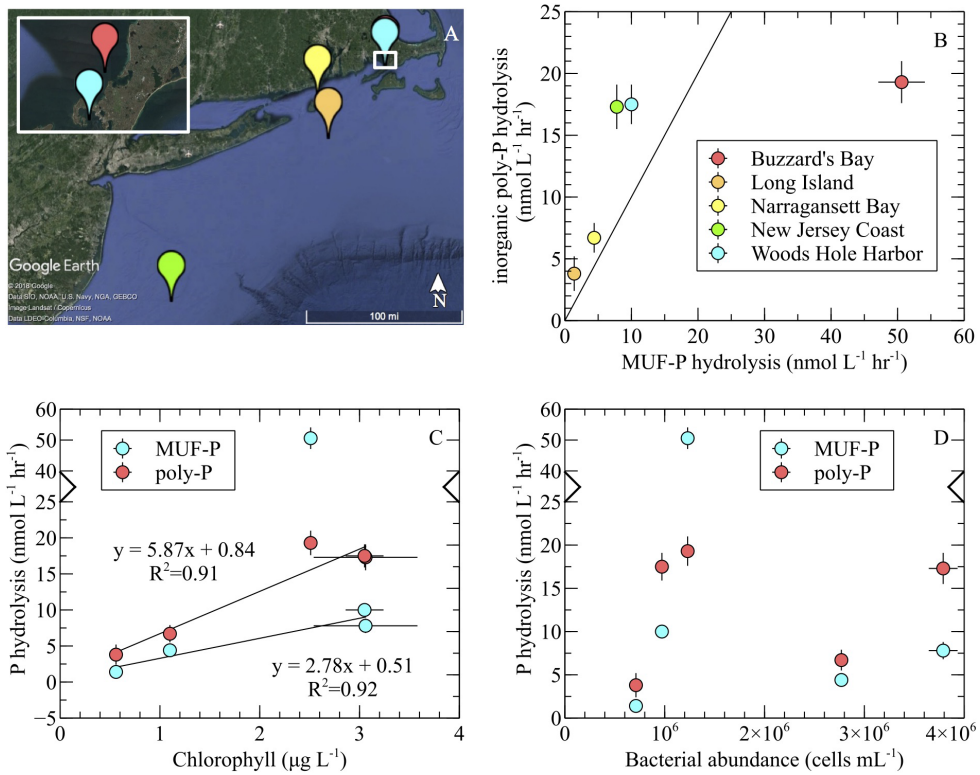

FIGURE 6 | Inorganic poly-P hydrolysis (SRP method) and MUF-P hydrolysis (fluorometric method) in the coastal western North Atlantic. **(A)** Samples were collected from the New Jersey coast (green; 39°24′43.50″N, 73°14′56.64″W), offshore Long Island (orange; 40°53′43.98″N, 71°22′49.92″W), Narragansett Bay (yellow; 41°17′12.12″N, 71°30′11.64″W), Woods Hole harbor (blue; 41°31′24.60″N, 70°40′40.80″W), and Buzzard's Bay (red; 41°32′38.28″N, 70°40′8.46″W). **(B)** Substrate-specific P hydrolysis comparison. The diagonal line depicts the 1:1 ratio of P hydrolysis rates. **(C)** Relationship of P hydrolysis rates to chlorophyll levels. For inorganic poly-P hydrolysis, the regression analysis was performed on the entire dataset (note the two overlapping data points at ~3 µg L^{-1}). For MUF-P hydrolysis, the Buzzard's Bay outlier (note broken axis) was excluded from the regression analysis. Chlorophyll correlated significantly with inorganic poly-P degradation (p = 0.01) and MUF-P hydrolysis (p = 0.04). **(D)** P hydrolysis rates and bacterial abundance. In all panels, error bars represent the standard error of the mean of replicate samples (MUF-P hydrolysis: n = 3; inorganic poly-P hydrolysis: n = 8; chlorophyll: n = 3; bacterial abundance: n = 3).

TABLE 2 | Comparison of inorganic poly-P and MUF-P hydrolysis rates in field samples from **Figure 6**.

Field site	PH_{MUF-P}	PH_{poly-P}	SE_{pooled}	T	df	p
	nmol L^{-1} hr^{-1}					
Buzzard's Bay	50.6	19.3	2.2	14.1	9	< 0.0001
Long Island	1.4	3.8	0.9	2.8	9	0.02
Narragansett Bay	4.4	6.7	0.7	3.2	9	0.01
New Jersey Coast	7.8	17.3	1.2	7.9	9	< 0.0001
Woods Hole Harbor	10.0	17.5	1.0	7.5	9	< 0.0001

T-scores (T; reported as absolute values) are calculated using an independent two-sample T-test assuming equal variance, according to the following equation:

$$T = \frac{PH_{poly-P} - PH_{MUF-P}}{SE_{pooled}}$$

where PH_{poly-P} is the average P hydrolysis rate for inorganic polyphosphate, PH_{MUF-P} is the average P hydrolysis rate for MUF-P, and SE_{pooled} is the pooled standard error of PH_{poly-P} and PH_{MUF-P}. Two-tailed p-values are reported.

CCMP1014) and up to ~9-fold (*T. oceanica* CCMP1005; **Figure 4**). This finding is probably not a result of artificially elevated 3poly-P hydrolysis due to a filtration artifact, because most extracellular DOP-degrading enzymes localize on the cell surface and thus, most of the DOP degradation capacity is removed by filtering the cells out. Indeed, MUF-P hydrolysis was significantly lower in cell-free filtrates than in whole cultures (p < 0.05; **Figure 4**). Nor are the large differences between whole-culture MUF-P hydrolysis and filtrate-based 3poly-P degradation rates a consequence of the different detection

TABLE 3 | Putative homologs of bacterial alkaline phosphatase in the genomes of *T. oceanica* CCMP1005 and *T. pseudonana* CCMP1335.

Diatom	Query	Hit	*E*-value	% Identity	% Query Coverage
T. oceanica	PhoA	No hits of any *E*-value			
CCMP1005	PhoD	EJK73971	1×10^{-15}	25	46
		EJK68987	1×10^{-37}	28	70
	PhoX	EJK47006	1×10^{-5}	25	48
T. pseudonana	PhoA	EED95980	4×10^{-15}	25	58
CCMP1335	PhoD	EED88143	2×10^{-11}	26	56
	PhoX	No hits with *E*-value below 0.011			

Hits are listed by the GenBank accession number.

methods used. In fact, the SRP method is the more conservative approach (**Figure 5**) yet still shows remarkable correspondence with the MUF-P fluorescence method (**Figure 4**), especially given the large difference in sensitivity between these two techniques.

Relatively low levels of P hydrolysis were detected in the cell-free filtrates of actively growing and late log-phase cultures (**Figure 2A**, days 6–18; **Figure 2C**, days 6–15; **Figure 2E**, days 9, 17; **Figures 3D–I**). However, P hydrolysis rates were highest during the later stages of cultivation, including stationary phase and crash (**Figures 2**, **3**). In fact, the hydrolysis of 3poly-P and ATP increased as the cultures matured, even after accounting for increases in biomass through the growth curve (**Figures 3D–I**). These results may be a consequence of differences in the release, stability, or activity of cell-free P hydrolases over the life of the culture. For example, one interpretation is that active P-hydrolyzing enzymes can be released from healthy, growing cells, but these enzymes may be more extensively released from aging and senescent cells. This release could be actively driven by the diatoms themselves and/or mediated by physical mechanisms such as turbulence (e.g., daily culture mixing) or filtering. Like natural seawater, the cell-free filtrates examined in this study likely contain a mixture of actively and passively released proteins. If cell-free P hydrolysis is indeed linked to cell aging and senescence, as our data suggest, then the dissolved P hydrolase activity of seawater may be highest under certain environmental conditions, such as the collapse of phytoplankton blooms.

All P substrates examined (MUF-P, AMP, ATP, and 3poly-P) were actively degraded in diatom filtrates, but inorganic 3-polyP, followed by ATP, were the most rapidly transformed, regardless of overall P availability (**Figures 2**, **3**). Rates of ATP hydrolysis were lower (most cases) or approximately equal (one case) to that expected from the complete degradation of P-anhydride bonds (**Table 1**). Thus, P-ester hydrolysis may not have played a role in ATP degradation, even though P-ester hydrolysis lead to a relatively small level of AMP degradation in the same samples. Assuming that only terminal phosphate groups are enzymatically labile (Huang et al., 2018), we speculate that P-anhydrides may block P-esterases from accessing the P-O-C bond of ATP. Overall, these findings suggest that *Thalassiosira* spp. may preferentially hydrolyze inorganic poly-P compared to other DOP sources under a wide range of prevailing P availability. A variety of potential mechanisms may underlie the preferential degradation of P-anhydrides in diatom cell-free filtrates, including differences

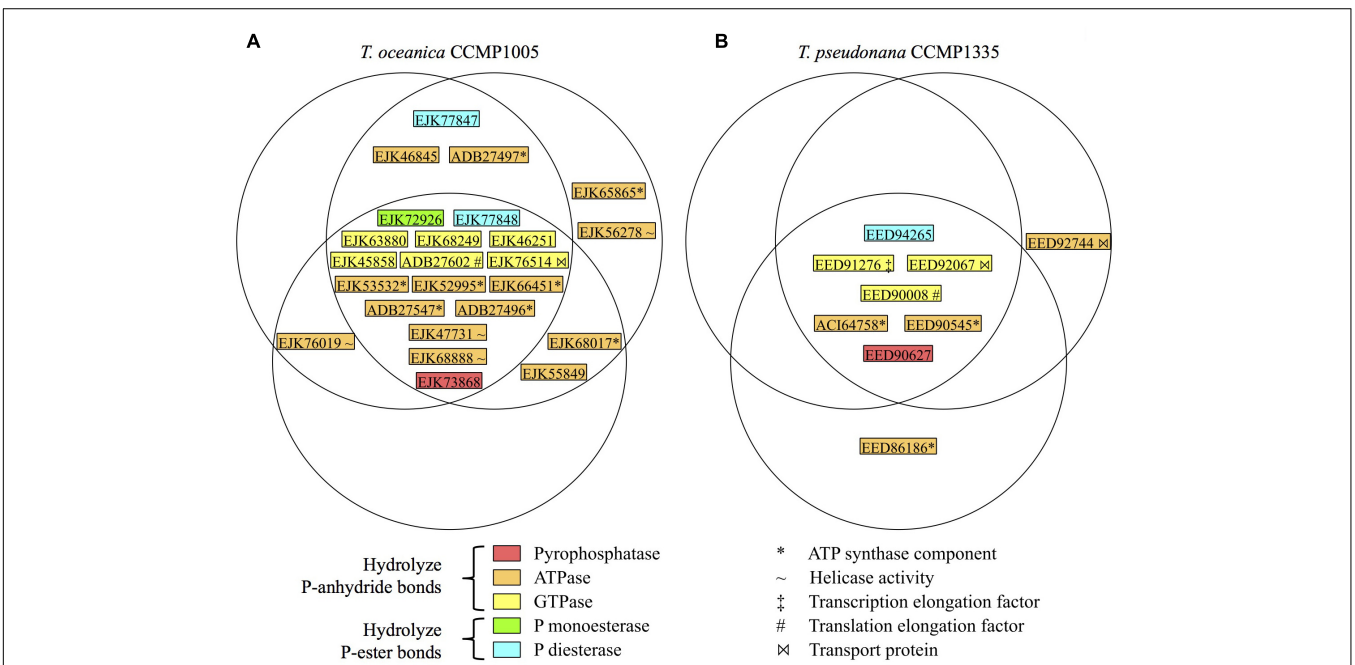

FIGURE 7 | Diversity and distribution of phosphatases in replicate cell-free filtrates of **(A)** *T. oceanica* CCMP1005 and **(B)** *T. pseudonana* CCMP1335. Each circle represents one biological replicate. GenBank accession numbers are provided. For ease of comparison to a previous study by Dyhrman et al. (2012), the JGI PID's for the *T. pseudonana* CCMP1335 phosphatases identified in this study are as follows: Genbank EED91276 (JGI PID 269148); ACI64758 (41256); EED90008 (41829); EED90627 (269348); EED90545 (269322); EED92067 (22792); EED92744 (262083); EED86186 (jgi| Thaps3_bd| 1287| e_gw1.26x41.22.1).

in the amount, substrate versatility, stability, and diversity of P-hydrolyzing enzymes.

Thalassiosira oceanica exhibited the most versatile response to P amendments, consistent with a diverse nutrient utilization profile expected in this isolate from the P-limited Sargasso Sea. For example, *T. oceanica* had the broadest potential to utilize both 3poly-P and ATP, regardless of overall P status (**Figure 2**). Furthermore, every culture upregulated the degradation of ATP under P-deplete conditions, but *T. oceanica* was the only one that also increased its capacity to degrade 3poly-P in response to P scarcity (**Figure 3**). These results suggest that while enhanced ATP utilization may be a widespread adaptation to low P availability among *Thalassiosira* spp., elevated 3poly-P utilization may not be. Rather, in *T. pseudonana*, active P-anhydride degradation may be constitutive. Overall, the P utilization potential of *T. pseudonana* CCMP1014, an oceanic isolate from the NPSG, exhibited more similarity toward *T. pseudonana* CCMP1335 than *T. oceanica*. This finding may indicate that species- rather than habitat-level factors may be a more prevalent control over DOP cycling by these diatoms, although each of these strains has been in culture for over 40 years and some genetic drift has likely occurred.

P Hydrolysis of Model DOP Sources in the Coastal Western North Atlantic

Although some SRP uptake probably occurred in our field incubations, the results suggest that it was too slow to decrease SRP concentrations by more than the detection limit of 800 nmol L^{-1}. This outcome is consistent with SRP uptake rates observed in other coastal systems with similar chlorophyll concentrations as our field sites (Harrison et al., 1977). SRP uptake therefore did not affect measured rates of inorganic poly-P hydrolysis.

Degradation rates of inorganic 3poly-P and 45poly-P were similar in field samples, which is consistent with the chain length-independent utilization of poly-P by some eukaryotic phytoplankton observed in a previous study (Diaz et al., 2016). Maximum rates of inorganic poly-P hydrolysis determined by the SRP method were significantly higher than fluorescence-based measurements of MUF-P hydrolysis in four out of five field sites examined in the coastal North Atlantic (**Figure 6B** and **Table 2**). These differences may be even more extreme, based on the finding that the SRP method for P hydrolysis is systematically conservative relative to the fluorescence-based approach (**Figure 5**).

The majority of studies on marine DOP hydrolysis have focused on P-monoester degradation in oligotrophic waters, where DOP hydrolysis is thought to function primarily as a phosphate-inhibitable phytoplankton response to P depletion (Duhamel et al., 2010; Lin et al., 2016). Above the threshold SRP level of ∼30 nmol L^{-1}, P-monoester hydrolysis is typically less than ∼1 nmol L^{-1} hr^{-1} (∼20 nmol μg chl^{-1} hr^{-1}) in these systems (Mahaffey et al., 2014). Consistent with this finding, chlorophyll-normalized rates of MUF-P and inorganic poly-P hydrolysis are less than ∼20 nmol μg chl^{-1} hr^{-1} in the relatively high-P coastal sites examined here (SRP > ∼150 nmol L^{-1}). However, because total chlorophyll levels are much higher in the waters examined in this study, the volume-normalized rates are much higher (∼4- to ∼20-fold) than in the oligotrophic ocean. Similar rates of volume-normalized P-ester hydrolysis have been previously reported from coastal systems and deep waters (Li et al., 1998; Dyhrman and Ruttenberg, 2006; Nicholson et al., 2006; Davis et al., 2014).

The strong correlation of P hydrolysis rates with chlorophyll levels (**Figure 6C**), and the lack of correlation with bacterial abundance (**Figure 6D**), suggests that the observed P dynamics were driven by phytoplankton. MUF-P hydrolysis (but not inorganic poly-P degradation) at the Buzzard's Bay site was inconsistent with the overall relationship to chlorophyll, which suggests additional, non-phytoplankton associated mechanisms of P-monoester degradation, such as contributions from heterotrophic bacteria. Heterotrophic bacteria utilize phosphatases to remineralize and acquire the carbon and nitrogen contained in DOP (Wilkins, 1972; Wanner and McSharry, 1982; Hoppe and Ullrich, 1999). Because the degradation of inorganic poly-P yields no carbon or nitrogen, heterotrophic bacteria may not contribute extensively to the degradation of inorganic poly-P sources. Thus, in a system dominated by bacterially driven DOP hydrolysis, the inorganic poly-P and P-ester dynamics may be decoupled, such that P-ester hydrolysis rates are substantially higher than inorganic poly-P degradation, consistent with results from the Buzzard's Bay site. In agreement with this hypothesis, the ratio of bacteria to phytoplankton cells was ∼3-fold higher in Buzzard's Bay than at any other location (**Supplementary Table S1**). Furthermore, White et al. (2012) found that 3poly-P was less extensively degraded than P-esters like AMP and glucose-6-phosphate in seawater incubations that had been pre-conditioned to favor bacterial growth.

Phosphatase Diversity in Diatom Cultures

Enzymes modulating the P-hydrolysis reactions observed in diatom cultures and coastal Atlantic field samples may include phosphatases such as AP, inorganic pyrophosphatase, and nucleoside triphosphatases. AP's are the best-known group of enzymes involved in DOP utilization by phytoplankton (Lin et al., 2016). These P-esterases are widely distributed in prokaryotic and eukaryotic microorganisms yet show only limited homology across these two groups (Lin et al., 2012). Furthermore, AP's are much better characterized in prokaryotes than microbial eukaryotes (Shaked et al., 2006; Xu et al., 2006, 2010; Lin et al., 2011, 2013, 2015, 2016). For example, major prokaryotic AP isoforms include PhoA, PhoX, and PhoD (Luo et al., 2009, 2011). All of these have been detected in seawater, with PhoD being the most prevalent, followed by PhoX (Luo et al., 2009; Sebastian and Ammerman, 2009; Kathuria and Martiny, 2010; Luo et al., 2011). Substrate specificities of the AP isoforms are not completely characterized, but they may exhibit a wide degree of flexibility. For example, *E. coli* PhoA is also a polyphosphatase (Lorenz and Schroder, 2001; Huang et al., 2018).

Multiple putative AP's have been recognized in the genome, transcriptome, and proteome of *T. pseudonana* CCMP1335 (Armbrust et al., 2004; Dyhrman et al., 2012), and at least one of these has been recognized for its resemblance to bacterial PhoA (Lin et al., 2016). Using BLASTP translated genome searches of *T. pseudonana* CCMP1335 and *T. oceanica* CCMP1005 with bacterial PhoA, PhoD, and PhoX queries, additional putative AP homologs were identified herein (**Table 3**). However, none of these sequences were apparent in the exoproteome data of either diatom species (**Figure 7**), suggesting that these enzymes may be exclusively cell-associated and ruling them out from participating in the P-hydrolysis dynamics observed in culture filtrates. Exoproteome samples revealed a number of other putative phosphatases, the diversity of which was biased in favor of P-anhydride degradation (**Figure 7**), consistent with the observed preferential hydrolysis of P-anhydrides in culture filtrates (**Figures 2–4**). The mechanisms leading to the appearance of these phosphatases in the exoproteome remain unclear, but may potentially include active secretion, passive dislodging of cell surface-associated enzymes during cultivation, and/or adventitious release during filtrate preparation.

Nearly all of the phosphatase hits present in the *T. pseudonana* CCMP1335 exoproteome (**Figure 7**) were also detected in its cell-associated transcriptome and proteome, which were reported in a previous study (Dyhrman et al., 2012). The only exception was the P-diesterase (GenBank EED94265). However, this sequence also could not be found in the JGI translated genome assemblies for *T. pseudonana* CCMP1335 utilized by Dyhrman et al. (2012). The absence of a protein sequence from the reference database precludes its identification in the experimental data. Thus, the absence of EED94265 in the proteome data from this previous study is at least partially a result of the different methods employed. As for the other putative phosphatases detected in the present study, none were upregulated in the *T. pseudonana* CCMP1335 transcriptome or proteome under P-deplete conditions (Dyhrman et al., 2012). In fact, three hits were upregulated under P-replete conditions: two GTPases (EED91276 in the proteome only; EED90008 in the transcriptome only) and one ATPase (transcriptome and proteome: EED92744). These results are consistent with the lack of upregulation of 3poly-P hydrolysis in the cell-free filtrate of this species under -P conditions (**Figure 3E**). On the other hand, ATP degradation was enhanced (∼2.5-fold) under low P availability in *T. pseudonana* CCMP1335 cell-free filtrates (**Figure 3H**), but this activity may not be regulated or sufficiently resolved at the transcriptional or translational levels.

Some of the exoproteome hits identified in this study may exhibit phosphatase activities by operating in the reverse direction of their annotated functions (e.g., ATP synthase components). Sequence information can identify candidate enzymes for a given biochemical function, however, these hits must be purified and assessed *in vitro* to verify their actual enzymatic reactivity. Furthermore, the presence of some protein hits in the exoproteomes may be unexpected. For example, an abundance of proteins affiliated with the ATP synthase complex were found in the exoproteomes of both diatom species. However, in some microorganisms, ATP synthase localizes in the cell membrane, utilizing the proton-motive force produced by the light activated proton-pump proteorhodopsin to generate ATP (Lin et al., 2016). In fact, proteorhodopsin expression may be an active aspect of diatom physiology (Marchetti et al., 2012; Marchetti et al., 2015). The potential localization of ATP synthase on the plasma membrane suggests that it could potentially become adventitiously dislodged without substantial cellular disruption or lysis (e.g., through daily physical mixing of cultures). Indeed, the release of cell-associated material was likely minimal during the preparation of diatom cell-free filtrates, as only 133 protein hits were detected in *T. pseudonana* CCMP1335 exoprotomes out of 1264 total protein hits reported in a prior study (Dyhrman et al., 2012).

Synthesis and Perspectives

The P-anhydride bond is essential to life. It serves as the universal basis of cellular energy transduction through the formation and hydrolysis of ATP and also plays diverse regulatory roles in the form of inorganic polyphosphates that are made by every cell in nature. As a widespread and labile constituent of marine DOP, P-anhydrides may also represent a bioavailable P source capable of supporting phytoplankton growth and productivity in the ocean. This P-anhydride pool has largely been overshadowed by the prevailing assumption that the much more abundant standing stock of marine P-esters is the most important DOP source. Based on results from this study, however, the possibility that P-anhydrides support a high degree, maybe even a majority, of DOP turnover and assimilation in diverse marine environments should be considered.

If P-esters are less preferred than P-anhydrides, then APA measurements may underestimate levels of P stress in oligotrophic systems, where phosphatase activity primarily functions in the acquisition of P by P-starved phytoplankton. In high-nutrient coastal systems, P-anhydrase activity may be constitutively expressed regardless of prevailing orthophosphate availability (Ammerman and Azam, 1991), suggesting that P-anhydrides may be a part of the highly labile DOP pool that is rapidly cycled in these environments (Benitez-Nelson and Buesseler, 1999). For example, in *T. pseudonana*, degradation of inorganic 3poly-P was just as high or higher under replete P conditions (**Figures 3E,F**). Furthermore, in *T. pseudonana* CCMP1335, this trend was consistent at the protein level, where each of the potential enzymes involved in 3poly-P degradation (**Figure 7**) were just as prevalent or more prevalent under P-rich conditions examined in a previous study (Dyhrman et al., 2012).

The degradation of dissolved P-anhydrides may be cryptic, with the relatively low abundance of this pool (Young and Ingall, 2010) masking rapid recycling rates. *In situ* P-anhydride degradation rates are dependent on the inherent degradation kinetics of the bulk P-anhydrase pool, as well as the *in situ* concentration of P-anhydride substrates. The maximum

hydrolysis rates reported herein do not necessarily reflect *in situ* degradation rates, because actual P-anhydride levels may not be rate-saturating. *In situ* DOP utilization rates have been estimated based on standing stock DOP concentrations (Duhamel et al., 2011), but cryptic cycling commonly evades detection by concentration-based approaches (Canfield et al., 2010; Hansel et al., 2015; Berg et al., 2016). Rather, cryptic transformation rates may be more readily quantified by using high-sensitivity radiotracers amended at levels similar to *in situ* substrate concentrations. Biologically mediated cryptic pathways can also be illuminated by investigating the community-level metabolic potential, as manifest in environmental genome, transcriptome, and proteome sequence data. As a step toward this goal, the present study has identified a diversity of diatom-derived phosphatases that may drive P-anhydrase reactions in the marine environment.

In addition to radiotracers and bioinformatics approaches, the study of P-anhydride degradation in marine systems would also be advanced by the availability of representative labeled substrates. For example, P-ester degradation (conventionally referred to as APA) is routinely assessed using sensitive fluorogenic and chromogenic substrates (Hoppe, 2003; Dyhrman and Ruttenberg, 2006; Mahaffey et al., 2014; Davis and Mahaffey, 2017). By quantifying the inert, signal-bearing probe that is released during P hydrolysis, these substrates can be used to track P-hydrolysis rates independently of P dynamics, which is especially important at high cell densities. Synthesis of labeled inorganic poly-P has been described (Choi et al., 2010; Hebbard et al., 2014), but these substrates were unreactive in positive controls tested in this study (data not shown).

Future work should focus on methods to assess the P hydrolysis of diverse DOP compounds by whole cells. The application of such methods should confirm whether the DOP dynamics observed here in diatom cell-free filtrates reflect broader DOP nutritional preferences. For example, the P hydrolytic potential of diatom cell-free filtrates implies that these microorganisms have a capacity, and potentially a preference in the case of 3poly-P, to utilize a diversity of P sources for growth. If cultures had been amended with 3poly-P during stationary phase, the elevated potential for 3polyP hydrolysis (**Figure 2**) may have helped the cultures avoid crashing, although this was not tested. The P-hydrolysis of DOP sources is not necessarily coupled to the biological assimilation of enzymatically released P, however (Ammerman and Azam, 1985; Duhamel et al., 2017). For instance, heterotrophic bacteria are thought to degrade organic P sources as a carbon and/or nitrogen utilization strategy, and phosphate may accumulate in seawater as a result (Hoppe and Ullrich, 1999; Hoppe, 2003). Furthermore, if phosphatases are not actively degraded, then their activity can lead to the accumulation of dissolved inorganic P when other factors besides P availability limit plankton growth. In such a case, the accumulation of enzymatically released P may have other implications for marine ecosystem functioning. For example, the primary pathway for long-term P removal is the authigenic (or *in situ*) formation of marine calcium phosphate minerals (Ruttenberg, 2014). The direct precipitation of these minerals is kinetically inhibited in most marine environments but may involve inorganic poly-P as a reactive intermediate (Schulz and Schulz, 2005; Diaz et al., 2008). In fact, the inherently high capacity for P-anhydride degradation documented in diatom cultures and natural samples in this study suggests that pulsed or spatially-heterogeneous poly-P inputs could lead to the formation of transient, submicron-scale "hotspots," which may be kinetically conducive to the formation of authigenic calcium phosphate minerals.

DATA AVAILABILITY STATEMENT

The raw data supporting the conclusions of this manuscript are deposited at the Biological and Chemical Oceanography Data Management Office (http://bco-dmo.org) under project number 747715.

AUTHOR CONTRIBUTIONS

JD, SD, and YT conceived the experiments and overall study design. JD, AH, JS, KB, DM, C-WC, and DP generated results and conducted the data analysis. All authors contributed to manuscript preparation.

FUNDING

This work was supported by the National Science Foundation under grants 1559124 (JD), 1736967 (JD), 1737083 (SD), and 1559087 (YT), as well as a Junior Faculty Seed Grant from the University of Georgia Research Foundation (JD). The Thermo-Fisher LTQ Orbitrap Elite Mass Spectrometer was purchased with funding from National Institutes of Health under grant S10RR028859.

ACKNOWLEDGMENTS

We thank Colleen Hansel, Carl Lamborg and the science party and crew of the R/V *Endeavor* during the TORCH I cruise. We thank James Morrissey for his generosity in providing fluorogenic polyphosphate for our research, and Catherine Baker for synthesizing these substrates. We also thank Lee Ann DeLeo for her help with the preparation of graphics for this paper, and we acknowledge Mohit Jain for technical assistance with proteomics data analysis.

SUPPLEMENTARY MATERIAL

The Supplementary Material for this article can be found online at: https://www.frontiersin.org/articles/10.3389/fmars.2018.00380/full#supplementary-material

REFERENCES

Alonso-Saez, L., and Gasol, J. M. (2007). Seasonal variations in the contributions of different bacterial groups to the uptake of low-molecular-weight compounds in northwestern Mediterranean coastal waters. *Appl. Environ. Microbiol.* 73, 3528–3535. doi: 10.1128/aem.02627-06

Ammerman, J. W., and Azam, F. (1985). Bacterial 5'-nucleotidase in aquatic ecosystems – A novel mechanism of phosphorus regeneration. *Science* 227, 1338–1340. doi: 10.1126/science.227.4692.1338

Ammerman, J. W., and Azam, F. (1991). Bacterial 5'-nucleotidase activity in estuarine and coastal marine waters: characterization of enzyme activity. *Limnol. Oceanogr.* 36, 1427–1436. doi: 10.4319/lo.1991.36.7.1427

Armbrust, E. V., Berges, J. A., Bowler, C., Green, B. R., Martinez, D., Putnam, N. H., et al. (2004). The genome of the diatom *Thalassiosira pseudonana*: ecology, evolution, and metabolism. *Science* 306, 79–86. doi: 10.1126/science.1101156

Benitez-Nelson, C. R., and Buesseler, K. O. (1999). Variability of inorganic and organic phosphorus turnover rates in the coastal ocean. *Nature* 398, 502–505. doi: 10.1038/19061

Berg, J. S., Michellod, D., Pjevac, P., Martinez-Perez, C., Buckner, C. R. T., Hach, P. F., et al. (2016). Intensive cryptic microbial iron cycling in the low iron water column of the meromictic Lake Cadagno. *Environ. Microbiol.* 18, 5288–5302. doi: 10.1111/1462-2920.13587

Berland, B. R., Bonin, D. J., Maestrini, S. T., and Pointer, J. R. (1972). Growth-potential bioassay of sea waters using algal cultures I. Comparison of methods of estimation. *Int. Rev. Hydrobiol.* 58, 933–944. doi: 10.1002/iroh.19720570608

Beversdorf, L. J., White, A. E., Björkman, K. M., Letelier, R. M., and Karl, D. M. (2010). Phosphonate metabolism of *Trichodesmium* IMS101 and the production of greenhouse gases. *Limnol. Oceanogr.* 55, 1768–1778. doi: 10.4319/lo.2010.55.4.1768

Björkman, K., and Karl, D. M. (1994). Bioavailability of inorganic and organic phosphorus compounds to natural assemblages of microorganisms in Hawaiian coastal waters. *Mar. Ecol. Prog. Ser.* 111, 265–273.

Björkman, K. M., and Karl, D. M. (2005). Presence of dissolved nucleotides in the North Pacific Subtropical Gyre and their role in cycling of dissolved organic phosphorus. *Aquat. Microb. Ecol.* 39, 193–203. doi: 10.3354/ame039193

Canfield, D. E., Stewart, F. J., Thamdrup, B., De Brabandere, L., Dalsgaard, T., Delong, E. F., et al. (2010). A cryptic sulfur cycle in oxygen-minimum-zone waters off the Chilean coast. *Science* 330, 1375–1378. doi: 10.1126/science.1196889

Choi, S. H., Collins, J. N. R., Smith, S. A., Davis-Harrison, R. L., Rienstra, C. M., and Morrissey, J. H. (2010). Phosphoramidate end labeling of inorganic polyphosphates: facile manipulation of polyphosphate for modulating its biological activities. *Biochemistry* 49, 9935–9941. doi: 10.1021/bi1014437

Davis, C. E., and Mahaffey, C. (2017). Elevated alkaline phosphatase activity in a phosphate-replete environment: influence of sinking particles. *Limnol. Oceanogr.* 62, 2389–2403. doi: 10.1002/lno.10572

Davis, C. E., Mahaffey, C., Wolff, G. A., and Sharples, J. (2014). A storm in a shelf sea: variation in phosphorus distribution and organic matter stoichiometry. *Geophys. Res. Lett.* 41, 8452–8459. doi: 10.1002/2014gl061949

Diaz, J., Ingall, E., Benitez-Nelson, C., Paterson, D., de Jonge, M. D., McNulty, I., et al. (2008). Marine polyphosphate: a key player in geologic phosphorus sequestration. *Science* 320, 652–655. doi: 10.1126/science.1151751

Diaz, J. M., Björkman, K. M., Haley, S. T., Ingall, E. D., Karl, D. M., Longo, A. F., et al. (2016). Polyphosphate dynamics at station ALOHA, North Pacific subtropical gyre. *Limnol. Oceanogr.* 61, 227–239. doi: 10.1002/lno.10206

Duhamel, S., Björkman, K. M., Doggett, J. K., and Karl, D. M. (2014). Microbial response to enhanced phosphorus cycling in the North Pacific Subtropical Gyre. *Mar. Ecol. Prog. Ser.* 504, 43–58. doi: 10.3354/meps10757

Duhamel, S., Björkman, K. M., Repeta, D. J., and Karl, D. M. (2017). Phosphorus dynamics in biogeochemically distinct regions of the southeast subtropical Pacific Ocean. *Prog. Oceanogr.* 151, 261–274. doi: 10.1016/j.pocean.2016.12.007

Duhamel, S., Björkman, K. M., Van Wambeke, F., Moutin, T., and Karl, D. M. (2011). Characterization of alkaline phosphatase activity in the North and South Pacific Subtropical Gyres: implications for phosphorus cycling. *Limnol. Oceanogr.* 56, 1244–1254. doi: 10.4319/lo.2011.56.4.1244

Duhamel, S., Dyhrman, S. T., and Karl, D. M. (2010). Alkaline phosphatase activity and regulation in the North Pacific Subtropical Gyre. *Limnol. Oceanogr.* 55, 1414–1425. doi: 10.4319/lo.2010.55.3.1414

Dyhrman, S. T., Chappell, P. D., Haley, S. T., Moffett, J. W., Orchard, E. D., Waterbury, J. B., et al. (2006). Phosphonate utilization by the globally important marine diazotroph *Trichodesmium*. *Nature* 439, 68–71. doi: 10.1038/nature04203

Dyhrman, S. T., Jenkins, B. D., Rynearson, T. A., Saito, M. A., Mercier, M. L., Alexander, H., et al. (2012). The transcriptome and proteome of the diatom *Thalassiosira pseudonana* reveal a diverse phosphorus stress response. *PLoS One* 7:e33768. doi: 10.1371/journal.pone.0033768

Dyhrman, S. T., and Ruttenberg, K. C. (2006). Presence and regulation of alkaline phosphatase activity in eukaryotic phytoplankton from the coastal ocean: implications for dissolved organic phosphorus remineralization. *Limnol. Oceanogr.* 51, 1381–1390. doi: 10.4319/lo.2006.51.3.1381

Fahmy, M. (2003). Water quality in the Red Sea coastal waters (Egypt): analysis of spatial and temporal variability. *Chem. Ecol.* 19, 67–77. doi: 10.1080/0275754031000087074

Fisher, T. R., Gustafson, A. B., Sellner, K., Lacouture, R., Haas, L. W., Wetzel, R. L., et al. (1999). Spatial and temporal variation of resource limitation in Chesapeake Bay. *Mar. Biol.* 133, 763–778. doi: 10.1007/s002270050518

Fisher, T. R., Peele, E. R., Ammerman, J. W., and Harding, L. W. (1992). Nutrient limitation of phytoplankton in Chesapeake Bay. *Mar. Ecol. Prog. Ser.* 82, 51–63. doi: 10.3354/meps082051

Fu, M. Z., Wang, Z. L., Pu, X. M., Xu, Z. J., and Zhu, M. Y. (2012). Changes of nutrient concentrations and N:P:Si ratios and their possible impacts on the Huanghai Sea ecosystem. *Acta Oceanol. Sin.* 31, 101–112. doi: 10.1007/s13131-012-0224-x

Gray, M. J., and Jakob, U. (2015). Oxidative stress protection by polyphosphate — New roles for an old player. *Curr. Opin. Microbiol.* 24, 1–6. doi: 10.1016/j.mib.2014.12.004

Guillard, R. R. L., and Ryther, J. H. (1962). Studies of marine planktonic diatoms. I. *Cyclotella nana* hustedt and *Detonula Confervacea* cleve. *Can. J. Microbiol.* 8, 229–239. doi: 10.1139/m62-029

Hansel, C. M., Ferdelman, T. G., and Tebo, B. M. (2015). Cryptic cross-linkages among biogeochemical cycles: novel insights from reactive intermediates. *Elements* 11, 409–414. doi: 10.2113/gselements.11.6.409

Hansen, H. P., and Koroleff, F. (1999). "Determination of dissolved inorganic phosphate," in *Methods of Seawater Analysis*, eds K. Grasshoff, K. Kremling, and M. Ehrhardt (New York, NY: Wiley), 170–174.

Hardison, D. R., Sunda, W. G., Shea, D., and Litaker, R. W. (2013). Increased toxicity of *Karenia brevis* during phosphate limited growth: ecological and evolutionary implications. *PLoS One* 8:e58545. doi: 10.1371/journal.pone.0058545

Harrison, P. J., Hu, M. H., Yang, Y. P., and Lu, X. (1990). Phosphate limitation in estuarine and coastal waters of China. *J. Exp. Mar. Biol. Ecol.* 140, 79–87. doi: 10.1016/0022-0981(90)90083-o

Harrison, W. G., Azam, F., Renger, E. H., and Eppley, R. W. (1977). Some experiments on phosphate assimilation by coastal marine plankton. *Mar. Biol.* 40, 9–18.

Hebbard, C. F. F., Wang, Y., Baker, C. J., and Morrissey, J. H. (2014). Synthesis and evaluation of chromogenic and fluorogenic substrates for high-throughput detection of enzymes that hydrolyze inorganic polyphosphate. *Biomacromolecules* 15, 3190–3196. doi: 10.1021/bm500872g

Hoppe, H. G. (2003). Phosphatase activity in the sea. *Hydrobiologia* 493, 187–200. doi: 10.1023/a:1025453918247

Hoppe, H. G., and Ullrich, S. (1999). Profiles of ectoenzymes in the Indian Ocean: phenomena of phosphatase activity in the mesopelagic zone. *Aquat. Microb. Ecol.* 19, 139–148. doi: 10.3354/ame019139

Huang, R., Wan, B., Hultz, M., Diaz, J. M., and Tang, Y. (2018). Phosphatase-mediated hydrolysis of linear polyphosphates. *Environ. Sci. Technol.* 52, 1183–1190. doi: 10.1021/acs.est.7b04553

Huang, X. P., Huang, L. M., and Yue, W. Z. (2003). The characteristics of nutrients and eutrophication in the Pearl River estuary, South China. *Mar. Pollut. Bull.* 47, 30–36. doi: 10.1016/s0025-326x(02)00474-5

Ilikchyan, I. N., McKay, R. M. L., Zehr, J. P., Dyhrman, S. T., and Bullerjahn, G. S. (2009). Detection and expression of the phosphonate transporter gene phnD in marine and freshwater picocyanobacteria. *Environ. Microbiol.* 11, 1314–1324. doi: 10.1111/j.1462-2920.2009.01869.x

Karl, D. M. (2014). Microbially mediated transformations of phosphorus in the sea: new views of an old cycle. *Annu. Rev. Mar. Sci.* 6, 279–337. doi: 10.1146/annurev-marine-010213-135046

Karlson, B., Cusak, C., and Bresnan, E. (2010). *Microscopic and Molecular Methods for Quantitative Phytoplankton Analysis*. Paris: UNESCO.

Kathuria, S., and Martiny, A. C. (2010). Prevalence of a calcium-based alkaline phosphatase associated with the marine cyanobacterium *Prochlorococcus* and other ocean bacteria. *Environ. Microbiol.* 13, 74–83. doi: 10.1111/j.1462-2920.2010.02310.x

Kemp, W. M., Boynton, W. R., Adolf, J. E., Boesch, D. F., Boicourt, W. C., Brush, G., et al. (2005). Eutrophication of Chesapeake Bay: historical trends and ecological interactions. *Mar. Ecol. Prog. Ser.* 303, 1–29. doi: 10.3354/meps303001

Kim, I.-N., Lee, K., Gruber, N., Karl, D. M., Bullister, J. L., Yang, S., et al. (2014). Increasing anthropogenic nitrogen in the North Pacific Ocean. *Science* 346, 1102–1106. doi: 10.1126/science.1258396

Kornberg, A., Rao, N. N., and Ault-Riche, D. (1999). Inorganic polyphosphate: a molecule of many functions. *Annu. Rev. Biochem.* 68, 89–125. doi: 10.1146/annurev.biochem.68.1.89

Laurent, A., Fennel, K., Hu, J., and Hetland, R. (2012). Simulating the effects of phosphorus limitation in the Mississippi and Atchafalaya River plumes. *Biogeosciences* 9, 4707–4723. doi: 10.5194/bg-9-4707-2012

Letscher, R. T., and Moore, J. K. (2015). Preferential remineralization of dissolved organic phosphorus and non-Redfield DOM dynamics in the global ocean: impacts on marine productivity, nitrogen fixation, and carbon export. *Global Biogeochem. Cycles* 29, 325–340. doi: 10.1002/2014GB004904

Li, H., Veldhuis, M. J. W., and Post, A. F. (1998). Alkaline phosphatase activities among planktonic communities in the northern Red Sea. *Mar. Ecol. Prog. Ser.* 173, 107–115. doi: 10.3354/meps173107

Lin, H. Y., Shih, C. Y., Liu, H. C., Chang, J., Chen, Y. L., Chen, Y. R., et al. (2013). Identification and characterization of an extracellular alkaline phosphatase in the marine diatom *Phaeodactylum tricornutum*. *Mar. Biotechnol.* 15, 425–436. doi: 10.1007/s10126-013-9494-3

Lin, S. J., Litaker, R. W., and Sunda, W. G. (2016). Phosphorus physiological ecology and molecular mechanisms in marine phytoplankton. *J. Phycol.* 52, 10–36. doi: 10.1111/jpy.12365

Lin, X., Wang, L., Shi, X. G., and Lin, S. J. (2015). Rapidly diverging evolution of an atypical alkaline phosphatase (PhoA(aty)) in marine phytoplankton: insights from dinoflagellate alkaline phosphatases. *Front. Microbiol.* 6:868. doi: 10.3389/fmicb.2015.00868

Lin, X., Zhang, H., Huang, B. Q., and Lin, S. J. (2011). Alkaline phosphatase gene sequence and transcriptional regulation by phosphate limitation in *Amphidinium carterae* (Dinophyceae). *J. Phycol.* 47, 1110–1120. doi: 10.1111/j.1529-8817.2011.01038.x

Lin, X., Zhang, H., Huang, B. Q., and Lin, S. J. (2012). Alkaline phosphatase gene sequence characteristics and transcriptional regulation by phosphate limitation in *Karenia brevis* (Dinophyceae). *Harmful Algae* 17, 14–24. doi: 10.1016/j.hal.2012.02.005

Lomas, M. W., Burke, A. L., Lomas, D. A., Bell, D. W., Shen, C., Dyhrman, S. T., et al. (2010). Sargasso Sea phosphorus biogeochemistry: an important role for dissolved organic phosphorus (DOP). *Biogeosciences* 7, 695–710. doi: 10.5194/bg-7-695-2010

Lommer, M., Specht, M., Roy, A. S., Kraemer, L., Andreson, R., Gutowska, M. A., et al. (2012). Genome and low-iron response of an oceanic diatom adapted to chronic iron limitation. *Genome Biol.* 13:R66. doi: 10.1186/gb-2012-13-7-r66

Lorenz, B., and Schroder, H. C. (2001). Mammalian intestinal alkaline phosphatase acts as highly active exopolyphosphatase. *Biochim. Biophys. Acta* 1547, 254–261. doi: 10.1016/S0167-4838(01)00193-5

Luo, H. W., Benner, R., Long, R. A., and Hu, J. J. (2009). Subcellular localization of marine bacterial alkaline phosphatases. *Proc. Nat. Acad. Sci. U.S.A.* 106, 21219–21223. doi: 10.1073/pnas.0907586106

Luo, H. W., Zhang, H. M., Long, R. A., and Benner, R. (2011). Depth distributions of alkaline phosphatase and phosphonate utilization genes in the North Pacific Subtropical Gyre. *Aquat. Microb. Ecol.* 62, 61–69. doi: 10.3354/ame01458

Mahaffey, C., Reynolds, S., Davis, C. E., and Lohan, M. C. (2014). Alkaline phosphatase activity in the subtropical ocean: insights from nutrient, dust and trace metal addition experiments. *Front. Mar. Sci.* 1:73. doi: 10.3389/fmars.2014.00073

Marchetti, A., Catlett, D., Hopkinson, B. M., Ellis, K., and Cassar, N. (2015). Marine diatom proteorhodopsins and their potential role in coping with low iron availability. *ISME J.* 9, 2745–2748. doi: 10.1038/ismej.2015.74

Marchetti, A., Schruth, D. M., Durkin, C. A., Parker, M. S., Kodner, R. B., Berthiaume, C. T., et al. (2012). Comparative metatranscriptomics identifies molecular bases for the physiological responses of phytoplankton to varying iron availability. *Proc. Nat. Acad. Sci. U.S.A.* 109, E317–E325. doi: 10.1073/pnas.1118408109

Martin, P., Dyhrman, S. T., Lomas, M. W., Poulton, N. J., and Van Mooy, B. A. S. (2014). Accumulation and enhanced cycling of polyphosphate by Sargasso Sea plankton in response to low phosphorus. *Proc. Nat. Acad. Sci. U.S.A.* 111, 8089–8094. doi: 10.1073/pnas.1321719111

Martinez, A., Tyson, G. W., and DeLong, E. F. (2010). Widespread known and novel phosphonate utilization pathways in marine bacteria revealed by functional screening and metagenomic analyses. *Environ. Microbiol.* 12, 222–238. doi: 10.1111/j.1462-2920.2009.02062.x

Mazard, S., Wilson, W. H., and Scanlan, D. J. (2012). Dissecting the physiological response to phosphorus stress in marine *Synechococcus* isolates. *J. Phycol.* 48, 94–105. doi: 10.1111/j.1529-8817.2011.01089.x

Michelou, V. K., Lomas, M. W., and Kirchman, D. L. (2011). Phosphate and adenosine-5′-triphosphate uptake by cyanobacteria and heterotrophic bacteria in the Sargasso Sea. *Limnol. Oceanogr.* 56, 323–332. doi: 10.4319/lo.2011.56.1.0323

Moore, C. M., Mills, M. M., Arrigo, K. R., Berman-Frank, I., Bopp, L., Boyd, P. W., et al. (2013). Processes and patterns of oceanic nutrient limitation. *Nat. Geosci.* 6, 701–710. doi: 10.1038/ngeo1765

Moore, C. M., Mills, M. M., Langlois, R., Milne, A., Achterberg, E. P., La Roche, J., et al. (2008). Relative influence of nitrogen and phosphorus availability on phytoplankton physiology and productivity in the oligotrophic sub-tropical North Atlantic Ocean. *Limnol. Oceanogr.* 53, 291–305. doi: 10.4319/lo.2008.53.1.0291

Moore, L. R., Ostrowski, M., Scanlan, D. J., Feren, K., and Sweetsir, T. (2005). Ecotypic variation in phosphorus acquisition mechanisms within marine picocyanobacteria. *Aquat. Microb. Ecol.* 39, 257–269. doi: 10.3354/ame039257

Nicholson, D., Dyhrman, S., Chavez, F., and Paytan, A. (2006). Alkaline phosphatase activity in the phytoplankton communities of Monterey Bay and San Francisco Bay. *Limnol. Oceanogr.* 51, 874–883. doi: 10.4319/lo.2006.51.2.0874

Oudot-Le Secq, M.-P., Grimwood, J., Shapiro, H., Armbrust, E. V., Bowler, C., and Green, B. R. (2007). Chloroplast genomes of the diatoms *Phaeodactylum tricornutum* and *Thalassiosira pseudonana*: comparison with other plastid genomes of the red lineage. *Mol. Genet. Genomics* 277, 427–439. doi: 10.1007/s00438-006-0199-4

Repeta, D. J., Ferrón, S., Sosa, O. A., Johnson, C. G., Repeta, L. D., Acker, M., et al. (2016). Marine methane paradox explained by bacterial degradation of dissolved organic matter. *Nat. Geosci.* 9, 884–887. doi: 10.1038/NGEO2837

Rivkin, R. B., and Swift, E. (1979). Diel and vertical patterns of alkaline phosphatase activity in the oceanic dinoflagellate *Pyrocystis noctiluca*. *Limnol. Oceanogr.* 24, 107–116. doi: 10.4319/lo.1979.24.1.0107

Ruttenberg, K. C. (2014). "The global phosphorus cycle," in *Treatise on Geochemistry: Biogeochemistry*, Vol. 10, eds D. M. Karl and W. H. Schlesinger (Amsterdam: Elsevier), 499–588.

Saad, E. M., Longo, A. F., Chambers, L. R., Huang, R., Benitez-Nelson, C., Dyhrman, S. T., et al. (2016). Understanding marine dissolved organic matter production: compositional insights from axenic cultures of *Thalassiosira pseudonana*. *Limnol. Oceanogr.* 61, 2222–2233. doi: 10.1002/lno.10367

Sanudo-Wilhelmy, S. A., Tovar-Sanchez, A., Fu, F. X., Capone, D. G., Carpenter, E. J., and Hutchins, D. A. (2004). The impact of surface-adsorbed phosphorus on phytoplankton Redfield stoichiometry. *Nature* 432, 897–901. doi: 10.1038/nature03125

Schulz, H. N., and Schulz, H. D. (2005). Large sulfur bacteria and the formation of phosphorite. *Science* 307, 416–418. doi: 10.1126/science.1103096

Sebastian, M., and Ammerman, J. W. (2009). The alkaline phosphatase PhoX is more widely distributed in marine bacteria than the classical PhoA. *ISME J.* 3, 563–572. doi: 10.1038/ismej.2009.10

Shaked, Y., Xu, Y., Leblanc, K., and Morel, F. M. M. (2006). Zinc availability and alkaline phosphatase activity in *Emiliania huxleyi*: implications for Zn-P co-limitation in the ocean. *Limnol. Oceanogr.* 51, 299–309. doi: 10.4319/lo.2006.51.1.0299

Strickland, J. D. H., and Parsons, T. R. (1972). *A Practical Handbook Of Seawater Analysis*. Ottawa, ON: Fisheries Research Board of Canada.

Thingstad, T. F., Krom, M. D., Mantoura, R. F. C., Flaten, G. A. F., Groom, S., Herut, B., et al. (2005). Nature of phosphorus limitation in the ultraoligotrophic eastern Mediterranean. *Science* 309, 1068–1071. doi: 10.1126/science.1112632

Turner, R. E., and Rabalais, N. N. (2013). Nitrogen and phosphorus phytoplankton growth limitation in the northern Gulf of Mexico. *Aquat. Microb. Ecol.* 68, 159–169. doi: 10.3354/ame01607

Wanner, B. L., and McSharry, R. (1982). Phosphate-controlled gene expression in *Escherichia coli* K12 using Mudl-directed lacZ fusions. *J. Mol. Biol.* 158, 347–363. doi: 10.1016/0022-2836(82)90202-9

White, A. E., Watkins-Brandt, K. S., Engle, M. A., Burkhardt, B., and Paytan, A. (2012). Characterization of the rate and temperature sensitivities of bacterial remineralization of dissolved organic phosphorus compounds by natural populations. *Front. Microbiol.* 3:276. doi: 10.3389/fmicb.2012.00276

Wilkins, A. S. (1972). Physiological factors in the regulation of alkaline phosphatase synthesis in *Escherichia coli*. *J. Bacteriol.* 110, 616–623.

Wu, J. F., Sunda, W., Boyle, E. A., and Karl, D. M. (2000). Phosphate depletion in the western North Atlantic Ocean. *Science* 289, 759–762. doi: 10.1126/science.289.5480.759

Xu, J., Yin, K. D., He, L., Yuan, X. C., Ho, A. Y. T., and Harrison, P. J. (2008). Phosphorus limitation in the northern South China Sea during late summer: influence of the Pearl River. *Deep Sea Res. I Oceanogr. Res. Pap.* 55, 1330–1342. doi: 10.1016/j.dsr.2008.05.007

Xu, Y., Boucher, J. M., and Morel, F. M. M. (2010). Expression and diversity of alkaline phosphatase ehap1 in *Emiliania huxleyi* (Prymnesiophyceae). *J. Phycol.* 46, 85–92. doi: 10.1111/j.1529-8817.2009.00788.x

Xu, Y., Wahlund, T. M., Feng, L., Shaked, Y., and Morel, F. M. M. (2006). A novel alkaline phosphatase in the coccolithophore *Emiliania huxleyi* (Prymnesiophyceae) and its regulation by phosphorus. *J. Phycol.* 42, 835–844. doi: 10.1111/j.1529-8817.2006.00243.x

Young, C. L., and Ingall, E. D. (2010). Marine dissolved organic phosphorus composition: insights from samples recovered using combined electrodialysis/reverse osmosis. *Aquat. Geochem.* 16, 563–574. doi: 10.1007/s10498-009-9087-y

Zhang, J., Liu, S. M., Ren, J. L., Wu, Y., and Zhang, G. L. (2007). Nutrient gradients from the eutrophic Changjiang (Yangtze River) Estuary to the oligotrophic Kuroshio waters and re-evaluation of budgets for the East China Sea Shelf. *Prog. Oceanogr.* 74, 449–478. doi: 10.1016/j.pocean.2007.04.019

Conflict of Interest Statement: The authors declare that the research was conducted in the absence of any commercial or financial relationships that could be construed as a potential conflict of interest.

frontiers in Marine Science

ORIGINAL RESEARCH
published: 10 July 2018
doi: 10.3389/fmars.2018.00234

Sensitive Determination of the Dissolved Phosphate Pool for an Improved Resolution of Its Vertical Variability in the Surface Layer: New Views in the P-Depleted Mediterranean Sea

Kahina Djaoudi[1], France Van Wambeke[1], Laurent Coppola[2], Fabrizio D'Ortenzio[2], Sandra Helias-Nunige[1], Patrick Raimbault[1], Vincent Taillandier[2], Pierre Testor[3], Thibaut Wagener[1] and Elvira Pulido-Villena[1]*

[1] Aix-Marseille Univ., Université de Toulon, Centre National de la Recherche Scientifique, IRD, MIO UM 110, Marseille, France, [2] Sorbonne Université, CNRS, Laboratoire d'Océanographie de Villefanche, LOV, Villefranche-sur-mer, France, [3] Sorbonne Université, UPMC, Université Paris 06, Centre National de la Recherche Scientifique, IRD, MNH, Laboratoire d'Océanographie et de Climatologie, IPSL, Paris, France

OPEN ACCESS

Edited by:
Christian Lønborg, Australian Institute of Marine Science (AIMS), Australia

Reviewed by:
Masahiro Suzumura, National Institute of Advanced Industrial Science and Technology (AIST), Japan
LeAnn Whitney, University of Rhode Island, United States

***Correspondence:**
Kahina Djaoudi
kahina.djaoudi@mio.osupytheas.fr

Specialty section:
This article was submitted to Marine Biogeochemistry, a section of the journal Frontiers in Marine Science

Received: *01 February 2018*
Accepted: *18 June 2018*
Published: *10 July 2018*

Citation:
Djaoudi K, Van Wambeke F, Coppola L, D'Ortenzio F, Helias-Nunige S, Raimbault P, Taillandier V, Testor P, Wagener T and Pulido-Villena E (2018) Sensitive Determination of the Dissolved Phosphate Pool for an Improved Resolution of Its Vertical Variability in the Surface Layer: New Views in the P-Depleted Mediterranean Sea. Front. Mar. Sci. 5:234. doi: 10.3389/fmars.2018.00234

An accurate understanding of the biogeochemistry of dissolved phosphate pool in the upper waters of P-depleted oceanic regions is constrained by the low sensitivity of routine phosphate measurements. In this study, by using the sensitive Liquid Waveguide Capillary Cell method, we report the first extensive cross-basin survey of nanomolar dissolved inorganic phosphate (DIP) and dissolved organic phosphate (DOP) concentration in P-depleted surface waters of the Mediterranean Sea during the stratification period. In the north western Mediterranean Sea (NWMS), DIP above the mixed layer depth (MLD) ranged between 4.9 and 26.5 nM. Along an E-W transect crossing Ionian and Tyrrhenian Seas (E-W transect), DIP above the MLD was lower, ranging between 0.9 and 11.4 nM. Contrarily to the traditional view of a depleted and invariant surface dissolved phosphate pool, a significant vertical variability of DIP and DOP was revealed in upper waters. A positive gradient of DIP was observed above the phosphacline, between the MLD and the deep chlorophyll maximum (DCM) depth, suggesting a potential diffusion of new phosphate to near-surface waters, even under stratified conditions. Interestingly, despite this apparent DIP availability, a significant negative gradient of DOP concentration was observed in the same layer. Finally, the positive gradient in DIP coincided with a significant increase in N:P ratio, suggesting a higher rate of increase of N than of P. The results obtained in this study indicate that acquiring nanomolar DIP data is a *sine qua non* condition for the comprehension and prediction of the biogeochemical functioning of P-depleted oceanic regions, such as the Mediterranean Sea.

Keywords: the Mediterranean Sea, dissolved inorganic phosphate, dissolved organic phosphate, N:P ratios, liquid waveguide capillary cell

INTRODUCTION

Nitrogen (N) and phosphorus (P) are essential macronutrients for sustaining marine organisms (Redfield, 1958). By controlling the efficiency of the biological pump, N and P determine the strength of the oceanic carbon uptake (Balino et al., 2001). Over the vast oligotrophic ocean, upper waters are often subjected to N and P exhaustion due to a strong vertical stratification and an active drawdown by biological activity (Tyrrell, 1999). N has traditionally been viewed as the limiting nutrient of primary production in marine waters (Ryther and Dunstan, 1971). However, with an increased understanding of the N cycling in the ocean, there is a growing awareness that P has also the potential to limit primary production in certain regions of the oligotrophic ocean (i.e., Wu et al., 2000; Moutin et al., 2008; Lomas et al., 2010). The Redfield N:P ratio of 16:1 has been considered as a fundamental tenet in marine biogeochemistry. Deviations from this canonical ratio have been used to provide insights, for instance, on the efficiency of carbon sequestration in the ocean (Sigman and Boyle, 2000), or on nutrient limitation of primary production (i.e., Falkowski and Raven, 1997; Moore et al., 2013). In some oligotrophic regions, such as the North Atlantic subtropical gyre, N:P ratios in near-surface waters are higher than 16:1, suggesting a depletion of P before that of N (Wu et al., 2000; Ammerman et al., 2003).

In such P-depleted oligotrophic regions, the quantification of dissolved inorganic phosphate (DIP) is a challenging task because concentrations drop to nanomolar (nM) levels, so unquantifiable using the conventional automated colorimetric procedure (CACP) which presents a limit of detection (LOD) of 20 nM, at best cases. Alternative analytical procedures have been introduced to improve the LOD and precision of DIP analysis (see review by Patey et al., 2008). The pre-concentration by magnesium-induced co-precipitation (MAGIC) method substantially improved the amount of DIP data at nM levels (Karl and Tien, 1992; Rimmelin and Moutin, 2005). During the last decade, the Liquid Waveguide Capillary Cell (LWCC) method, have gained a foothold as a reliable method for nM DIP measurements (i.e., Zhang and Chi, 2002; Patey et al., 2008). By using these high sensitive methods, studies in both the North Pacific (Karl et al., 2001 and references therein; Suzumura et al., 2012; Hashihama et al., 2013) and North Atlantic (Ammerman et al., 2003; Lomas et al., 2010) subtropical gyres have revealed DIP concentrations as low as 0.2 nM (Wu et al., 2000). Moreover, since the determination of dissolved organic phosphate (DOP) relies upon DIP measurements, some of the above cited studies have also provided accurate DOP data (i.e., Mather et al., 2008; Suzumura et al., 2012), crucially enhancing our knowledge on the biogeochemical functioning of P-depleted oceanic regions, where DOP represents a P source for sustaining community productivity (Karl and Björkman, 2015 and references therein; Sato et al., 2013).

The Mediterranean Sea is one of the world's most oligotrophic oceanic regions. It is divided into two sub-basins, western and eastern, exhibiting distinct hydrodynamics and biogeochemical features. The Mediterranean Sea exhibits low nutrient concentrations, with a west to east decreasing gradient (Krom et al., 1991; Moutin and Raimbault, 2002; De Madron et al., 2011), partly linked to its anti-estuarine thermohaline circulation (Crispi et al., 2001). Available nutrients in the Atlantic surface inflow entering the Mediterranean Sea are consumed along the way to the eastern basin and exported to deep waters (Crise et al., 1999; Lazzari et al., 2012). Consequently, the western Mediterranean basin is oligotrophic while the eastern basin is ultraoligotrophic (Moutin and Raimbault, 2002).

In the Mediterranean surface waters, DIP concentration has been shown to limit primary production, nitrogen fixation and heterotrophic bacterial activity (Van Wambeke et al., 2002; Thingstad et al., 2005). These findings are supported by low DIP concentrations measured in upper waters and a deep N:P ratio which diverges greatly from the canonical Redfield ratio, with values ranging between 21 and 23 in the Western basin (Bethoux et al., 1992) and even higher in the Eastern basin (Krom et al., 1991). Surface DIP concentration in surface waters is systematically below 20 nM (LOD of the CACP) during the stratification period, dramatically constraining data coverage in this oceanic region (i.e., Pujo-Pay et al., 2011; Céa et al., 2015). The depth at which DIP concentration becomes measurable by the CACP is usually used to define the phosphacline and it has been reported to be between 45 m and 120 m, during the stratified period, in the western and eastern Mediterranean Sea, respectively (Moutin and Raimbault, 2002). To date, lack of DIP data above this phosphacline has precluded resolving vertical variability in this key layer as has led to the traditional view of an entirely depleted and invariant dissolved phosphate surface pool. Few studies, however, by using sensitive determination of DIP, have reported low but detectable increases in nanomolar DIP concentration above the phosphacline adding evidence against this traditional view (Van Wambeke et al., 2002; Krom et al., 2005; Djaoudi et al., 2017). Nevertheless, the scarcity and the sparse nature of available nM DIP data in the Mediterranean Sea still precludes a complete assessment of DIP dynamics in the upper waters at the basin scale.

As for DIP, a critical gap in accurate DOP data (i.e., based on nanomolar DIP measurements) persists in the upper waters of the Mediterranean Sea (Moutin and Raimbault, 2002; Pujo-Pay et al., 2011). Indeed, only two studies have reported nanomolar DIP and DOP data simultaneously (Krom et al., 2005; Djaoudi et al., 2017). In the Mediterranean Sea, when DIP is exhausted, DOP becomes a possible alternative source of P as confirmed by high activities of alkaline phosphatase suggesting an active utilization of the DOP pool in upper waters (Van Wambeke et al., 2002, 2009; Thingstad and Mantoura, 2005). How and to which extent such biogeochemical dynamics induce changes in DOP concentration above the phosphacline remains unknown.

In this study, we conducted cross-basin observations of nM DIP and DOP concentration in the Mediterranean Sea with emphasis on upper waters. The main goals of this work are: (1) to extend the nM dataset of accurate paired DIP/DOP data in the upper Mediterranean Sea under stratification conditions, (2) to examine the vertical variability of both DIP and DOP above the phosphacline, under stratification conditions and, (3) to better resolve the DIN:DIP and DON:DOP ratios in the upper waters of this P-depleted oceanic region.

MATERIALS AND METHODS

Study Area and Sampling

This study was performed in the framework of two research cruises carried out in 2015 in the Mediterranean Sea, during the stratification period, MOOSE-GE (doi.org/10.18142/235) and BioArgomed (doi.org/10.17882/51678) (**Figure 1**).

The MOOSE-GE (Mediterranean Ocean Observing System for the Environment– *Grande Échelle*) cruise took place on board the R/V *Le Suroit* between 10 and 26 July in the oligotrophic North Western Mediterranean Sea (NWMS). The BioArgoMed cruise took place on board the R/V *Tethys II* between 13 May and 03 June along an east to west transect (E-W transect) crossing the ultraoligotrophic Ionian and Tyrrhenian Seas. Therefore, these cruises covered the two Mediterranean sub-basins, western and eastern, which exhibit distinct hydrological and biogeochemical features (i.e., De Madron et al., 2011).

During the two cruises, oceanographic casts were acquired using a conductivity-temperature-depth profiling system (SBE911 + CTD unit). The density profiles were calculated from temperature and salinity profiles, and linearly interpolated at 1 m depth intervals. Fluorescence profiles were provided by a Chelsea Aquatracka 3 fluorimeter interfaced with the CTD unit.

Seawater samples were collected during up casts with a carousel of Niskin bottles for analyses of dissolved phosphate (dissolved inorganic phosphate, DIP; total dissolved phosphate, TDP) and dissolved nitrogen (dissolved inorganic nitrogen, DIN; total dissolved nitrogen, TDN). In the present study, DIN includes nitrate + nitrite concentration and does not include ammonium. Pujo-Pay et al. (2011) reported NH_4^+ concentrations in the Mediterranean Sea between 0 and 10 nM, indicating that DIN data reported in this study can suffer from up to 10 nM underestimation.

Samples were collected in duplicate and filtered on board through a pre-cleaned (500 mL of ultrapure water) 0.2 μm syringe filter. Samples were then disposed into acid washed HDPE-60 mL bottles and were stored frozen (−20°C) until analysis. To check for potential N and P contamination through filtration, DIP and DIN concentration were analyzed on ultrapure water filtered the same way as samples. DIN concentration in such blanks was below the limit of detection. DIP concentrations in the blanks was 2.8 ± 0.6 nM ($n = 5$), not significantly different from the reagent blanks (2.2 ± 0.3 nM, $n = 5$).

During the MOOSE-GE cruise, seawater samples were collected at 25 stations (**Figure 1**), between the surface and 100 m at 4 different depths. Sampling depths were chosen according to the density and fluorescence depth profiles. Density profiles were used to determine the depth of the mixed layer, in which a sampling point was defined (depth 1, **Figure 2**). From the fluorescence depth profiles, which exhibited the characteristic subsurface maximum (deep chlorophyll maximum, DCM) reported for the western Mediterranean Sea during the stratification period (Lavigne et al., 2015), 3 sampling points were defined: one point at the DCM (depth 3, **Figure 2**) and two points above and below the DCM (depths 2 and 4, **Figure 2**). During the BioArgoMed cruise, seawater samples were collected from 6 stations (**Figure 1**) at 6 different depths between the surface and 120 m.

Dissolved Nutrient Analysis

DIP concentration was determined by using both the CACP (Aminot and Kérouel, 2007) and the LWCC method (Zhang and Chi, 2002). Both spectrophotometric methods are based on the molybdenum blue reaction, described by Murphy and Riley (1962). In the LWCC method, according to the Beer-Lambert law, the sensitivity of the spectrophotometric measurement is improved by increasing the optical path length of the measurement cell from 1 cm (CACP) to 2.5 m (LWCC). The LOD, estimated as three times the standard deviation of ten measurements of the blank, was 20 and 0.8 nM for the CACP and the LWCC method, respectively. For the LWCC method, the linearity of absorbance vs. DIP concentration was assessed, and the dynamic range was determined to be between 0.8 and 143 nM. Therefore, for DIP concentrations above such range, the DIP value provided by the CACP was used. Between 20 and 143 nM (range of concentrations for which both methods are comparable), the relationship between the two methods followed a linear model ($r = 0.96$; $n = 80$) with a slope of 1.14 ± 0.04, not significantly different from 1 ($p > 0.05$).

Total dissolved phosphate (TDP) concentration was analyzed by using the CACP after sample processing by the wet oxidation method (Valderrama, 1981). DOP concentrations were then estimated by subtracting nM LWCC-DIP from TDP concentrations, with an analytical precision of 7%.

Dissolved inorganic nitrogen (DIN) and total dissolved nitrogen (TDN) concentrations were measured by using the CACP with a LOD of 50 nM. As for TDP, samples for TDN were processed according to the wet oxidation method (Valderrama, 1981). Dissolved organic nitrogen (DON) concentrations were then estimated by subtracting DIN from TDN concentrations.

Data Treatment and Calculations

The mixed layer depth (MLD) was estimated from the density profiles as the depth where the difference of density from the surface reference (i.e., density at 10 m depth) was 0.03 kg m^{-3} (De Boyer Montégut, 2004).

The depth of the phosphacline was calculated as the average of 4 phosphacline depth values determined based on 4 different reported criteria following Van Wambeke et al. (2009). $Phosphacline_1$ and $phosphacline_2$ were calculated as the shallowest depths in which DIP concentrations exceeded the mixed layer value by 10 and 50 nM, respectively (Van Wambeke et al., 2009); $phosphacline_3$ and $Phosphacline_4$ were calculated as the depths in which DIP concentrations exceeded the concentration at the immediate previous depths by 20 and 100 nM, respectively (Van Wambeke et al., 2009; Pujo-Pay et al., 2011).

The Wilcoxon signed-rank test was used to assess the overall significance of the vertical differences in DIP and DOP concentration for each cruise. For each individual profile, vertical differences in DIP and DOP concentration where considered significant when they were higher than the LOD and precision of the analytical methods.

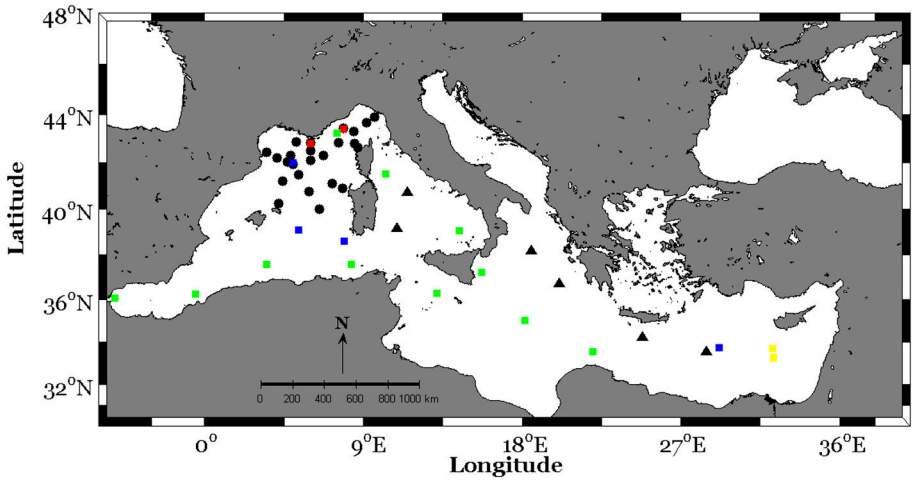

FIGURE 1 | Station locations in the North Western Mediterranean Sea (MOOSE-GE cruise, black circles) and along an E-W transect crossing Ionian and Tyrrhenian seas (BioArgomed cruise, black triangles). The squares represent sampling stations from published studies reporting nanomolar dissolved inorganic phosphate in the Mediterranean Sea (green squares: PROSOPE cruise, 1999; blue squares: BOUM cruise, 2008; red squares: MOOSE-ANTARES and MOOSE-DYFAMED fixed stations, see **Table 1** for references).

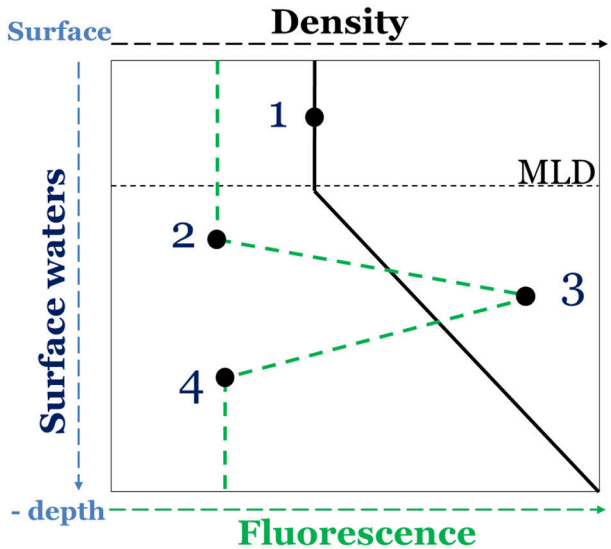

FIGURE 2 | Schematic representation of the sampling depth determination in the North Western Mediterranean Sea, based on density (black plot) and fluorescence (dashed green plot) depth profiles.

RESULTS

Over the study area and for both cruises, a stratification of the water column was observed. The MLD ranged between 6 and 30 m with an average of 13 ± 5 m ($n = 25$) during the MOOSE-GE cruise (hereafter, NWMS: for NW Mediterranean Sea) and between 14 and 20 m with an average of 17 ± 3 m ($n = 6$) during the BioArgoMed cruise (hereafter, E-W transect) (**Figure 3**). The phosphacline depth in the NWMS ranged between 30 and 89 m with an average of 56 ± 14 m for 21 stations and was higher than 100 m for the remaining 4 stations (**Figure 3**). Along the E-W transect, the phosphacline depths were higher than 120 m (maximum sampled depth) except for one value at 70 m (**Figure 3**).

Dissolved Phosphate Pools

By using the LWCC, all DIP concentrations in the upper waters of the Mediterranean Sea obtained in this study were above the LOD of 0.8 nM. Compared to the CACP, the sensitive LWCC method resulted in a 75% increase of valid DIP data and therefore of DOP data in the study area.

Surface (0–100 m) DIP concentration in the NWMS ranged over two orders of magnitude, between 3.6 and 251 nM (**Figure 3A**). Surface (0–120 m) DIP concentrations along the E-W transect were lower, ranging between 0.9 and 14.6 nM except for one single value at 127.5 nM (**Figure 3B**). DIP concentrations above the MLD ranged between 4.9 and 26.5 with an average of 12.8 ± 6.8 ($n = 28$) in the NWMS (**Figure 3A**) and between 0.9 and 11.4 nM with an average of 5.5 ± 3.6 nM ($n = 11$) along the E-W transect (**Figure 3B**).

Concerning vertical variability, DIP concentration in the NWMS exhibited a first significant increase between the MLD and the DCM depth (Wilcoxon signed-ranks test, $Z = 3.2$, $p < 0.01$, $n = 25$) (**Figure 4**). It then increased more sharply between the DCM depth and 100 m (Wilcoxon signed-ranked test, $Z = 4.0$, $p < 0.001$, $n = 25$) (**Figure 4**). In order to get a deeper insight on the observed DIP vertical variability, a gradient of DIP was calculated by dividing the difference in DIP concentration by the corresponding difference in depth. In the NWMS, the first DIP positive gradient (between the MLD and the DCM depth) was recorded in 21 out of 25 of the sampling stations (Figure S1) and ranged between 0.04 and 3.2 nM m^{-1} with an average of 0.4 ± 0.7 nM m^{-1}. The second positive gradient

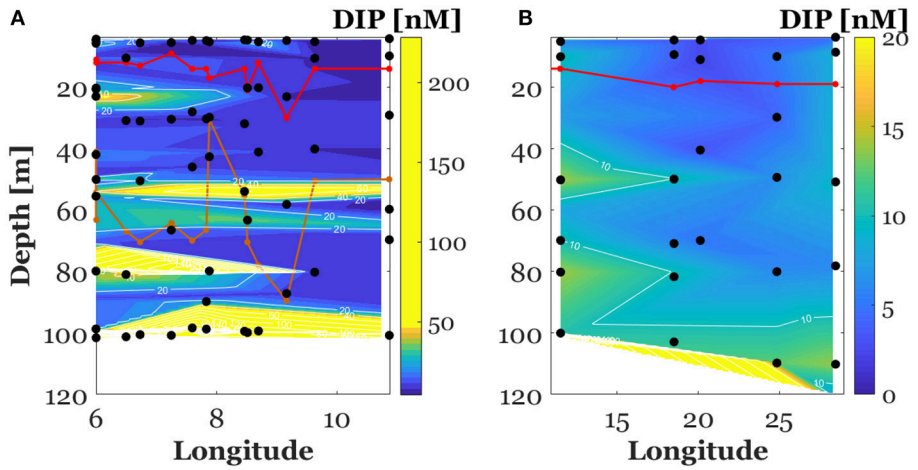

FIGURE 3 | Vertical section of dissolved inorganic phosphate concentrations (DIP) in the North Western Mediterranean Sea (between the surface and 100 m, **A**) and along the E-W transect crossing Ionian and Tyrrhenian seas (between the surface and 120 m, **B**). The red plot represents the mixed layer depth. The orange plot represents the phosphacline depth. Note that the scale of the color bar has been tightened to point out the positive gradient of DIP in the North Western Mediterranean Sea.

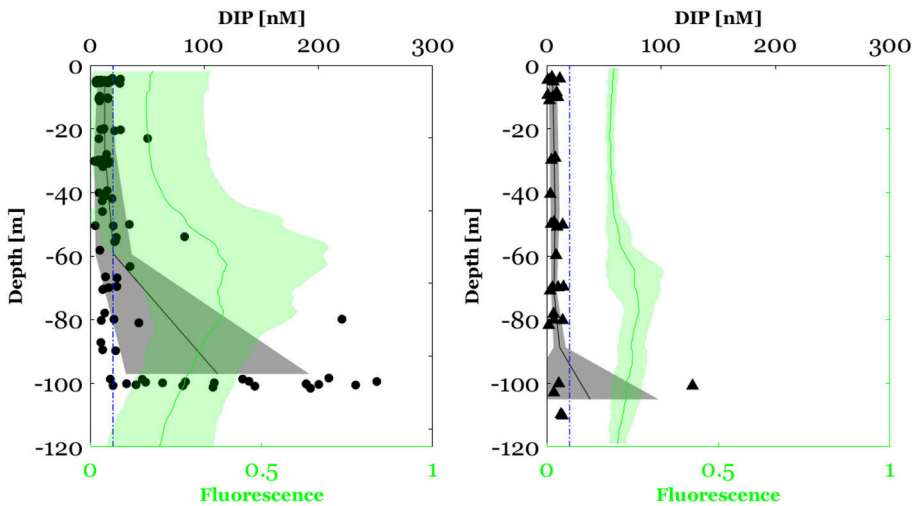

FIGURE 4 | Dissolved inorganic phosphate (DIP) concentration between the surface and 100 m in the North Western Mediterranean Sea (circles) and between the surface and 120 m along the E-W transect crossing Ionian and Tyrrhenian seas (triangles). The black plot represents the mean profile of DIP concentration and the bounded line the standard deviation from the mean. The blue dashed line corresponds to the limit of detection (LOD) of the conventional automated colorimetric procedure (20 nM). The green plot represents the fluorescence profile (mean ± standard of deviation).

(between the DCM depth and 100 m) was recorded in 21 out of 25 of the sampling stations (Figure S1) and ranged between 0.03 and 5.7 nM m^{-1} with an average of 2.6 ± 1.6 nM m^{-1}.

Likewise, along the E-W transect, a significant increase in DIP concentration was observed between the MLD and the DCM depth (Wilcoxon signed-ranks test, $Z = 2.2$, $p < 0.05$, $n = 6$) (**Figure 4**). This DIP positive gradient was recorded for all stations and ranged between 0.01 and 0.08 nM m^{-1} with an average of 0.04 ± 0.03 nM m^{-1} (Figure S1). Because in the E-W transect the maximum sampling depth was above the phosphacline, the second increase in DIP concentration below the DCM was not observed.

Surface DOP concentration in the NWMS ranged between 4 and 149 nM with an average of 44 ± 25 nM ($n = 100$) (**Figure 5A**). As for DIP, DOP concentrations were lower along the E-W transect, ranging between 15 and 64 nM with an average of 33 ± 12 nM ($n = 36$) (**Figure 5B**). DOP concentration above the MLD ranged between 17 and 139 nM with an average of 47 ± 36 ($n = 28$) in the NWMS (**Figure 5A**) and between 20 and 62 nM with an average of 35 ± 11 nM ($n = 11$) along the E-W transect (**Figure 5B**).

Concerning the vertical variability, DOP concentration in the NWMS exhibited a significant decrease between the MLD and the DCM (Wilcoxon signed-ranks test, $Z = 2.1$, $p < 0.05$,

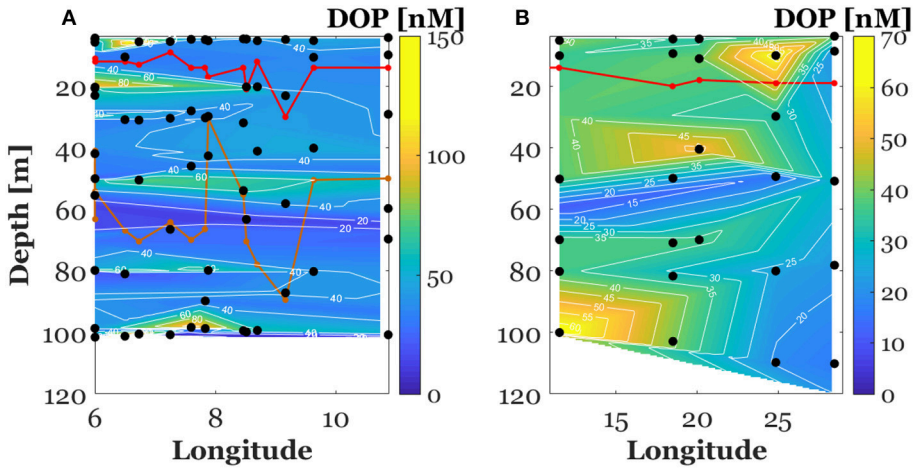

FIGURE 5 | Vertical section of dissolved organic phosphate concentrations (DOP) in the North Western Mediterranean Sea (between the surface and 100 m, **A**) and along the E-W transect crossing Ionian and Tyrrhenian seas (between the surface and 120 m, **B**). The red plot represents the mixed layer depth. The orange plot represents the phosphacline depth. Note that the scale of the color bar has been tightened to point out the negative gradient of DOP in the North Western Mediterranean Sea.

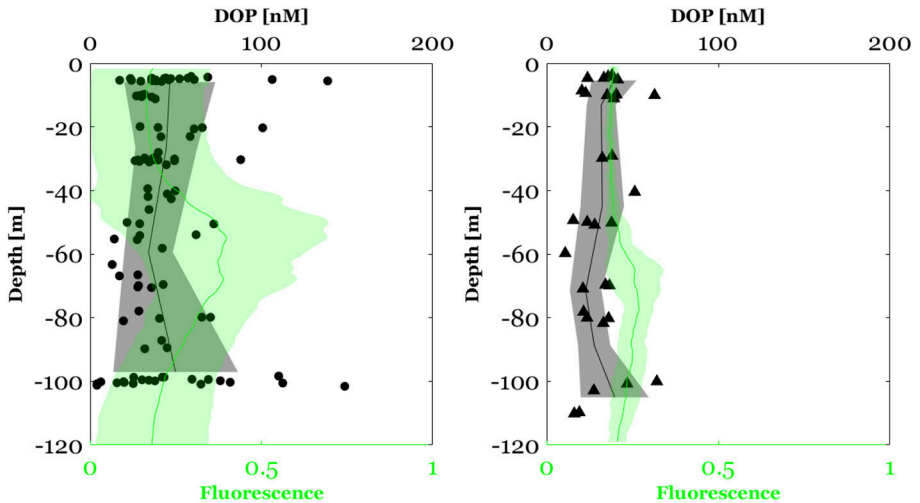

FIGURE 6 | Dissolved organic phosphate (DOP) concentration in the North Western Mediterranean Sea (circles) and Along the E-W transect crossing Ionian and Tyrrhenian seas (triangles). The black plot represents the mean depth profile of DOP concentrations and the bounded line the deviation from the mean. The green plot represents the fluorescence profile (mean ± standard of deviation).

$n = 25$) (**Figure 6**). As for DIP, a DOP gradient between the MLD and the DCM was calculated by dividing the difference in DOP concentration by the corresponding difference in depth. The negative gradient of DOP in this layer was recorded in 15 out of 25 of the sampling stations (Figure S2) and ranged between 0.05 and 2.7 nM m^{-1} with an average value of 0.6 ± 0.7 nM m^{-1}.

Along the E-W transect, no significant difference in DOP concentration was observed between the MLD and the DCM depth (Wilcoxon signed-ranks test, $Z = 0.94$, $p > 0.05$, $n = 6$).

N:P Molar Ratios in the Upper Mediterranean Sea

In the NWMS, surface (0–100 m) DIN:DIP ratios ranged between 2 and 165 (**Figure 7**) and DON:DOP ratios ranged between 55 and 525 (**Figure 8**). Above the mixed layer depth, DIN:DIP ratios ranged between 1 and 65 with an average of 20 ± 19 and DON:DOP ratios between 113 and 312 with an average of 182 ± 55. Along the E-W transect, 50% of DIN data were below the LOD of the CACP. When DIN data were available, the surface (0–120 m) DIN:DIP ratios in this area ranged between 10 and 289 (**Figure 7**) and DON:DOP ratios ranged between 67 and 252 (**Figure 8**). Along the E-W transect, DIN:DIP and DON:DOP molar ratios have not been calculated above the MLD due to insufficient valid DIN data.

Regarding vertical profiles, in the NWMS, there was a significant increase of DIN:DIP (Wilcoxon signed-ranks test, $z = 3.4$, $p < 0.001$, $n = 19$) and of DON:DOP ratios (Wilcoxon signed-ranks test, $z = 2.4$, $p < 0.05$, $n = 17$), between the MLD

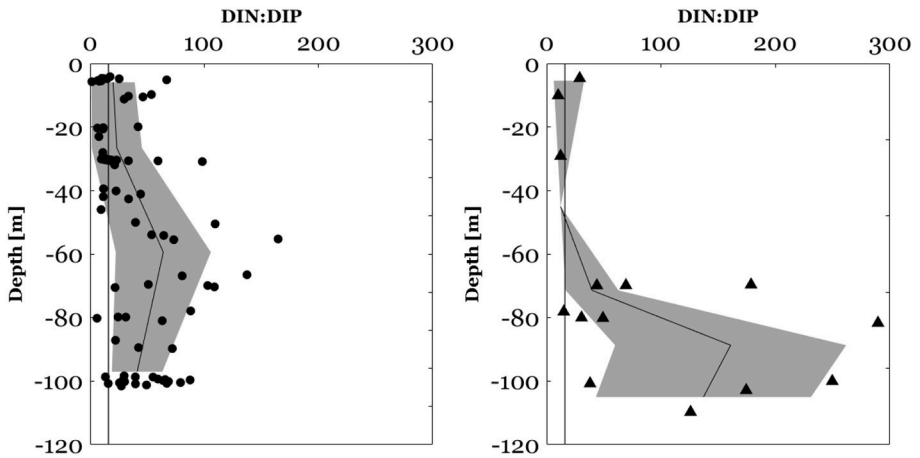

FIGURE 7 | DIN:DIP molar ratios between the surface and 100 m in the NWMS (circles) and DIN:DIP ratios between the surface and 120 m along the E-W transect (triangles). The black plot represents the mean depth profile of the DIN:DIP ratio, the bounded line the standard deviation from the mean and the dark vertical line the Redfield molar ratio of 16:1.

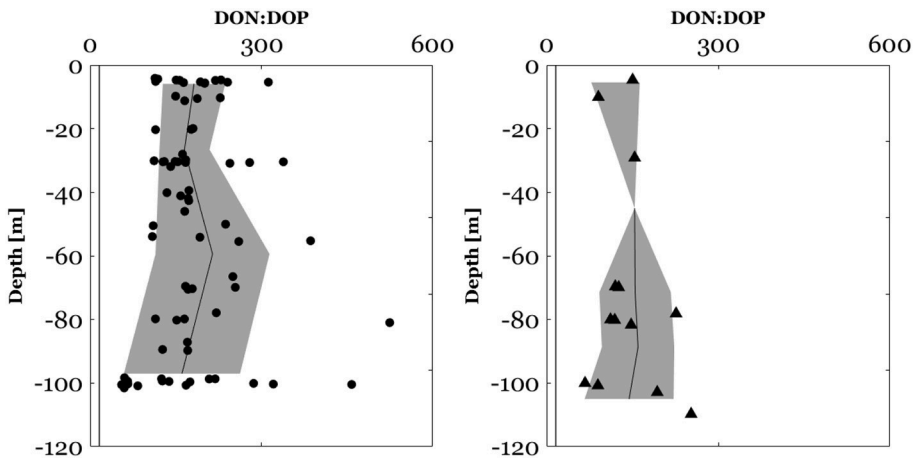

FIGURE 8 | DON:DOP ratios between the surface and 100 m in the North Western Mediterranean Sea (circles). DON:DOP molar ratios between the surface and 120 m along the E-W transect (triangles) crossing Ionian and Tyrrhenian seas. The black plot represents the mean depth profile of the DON:DOP ratio, the bounded line the standard deviation from the mean and the black vertical line the Redfield molar ratio of 16:1.

and the DCM (**Figures 7**, **8**). The increase in the DIN:DIP ratio was observed for 15 out of 19 stations (Figure S3) and ranged between 0.2 and 5.7 m^{-1}. The increase in the DON:DOP ratio within this layer was observed for 12 out of 17 stations (Figure S4) and ranged between 0.2 and 9.3 m^{-1}. Along the E-W transect, no assessment of the vertical variability of N:P ratios was made due to insufficient valid DIN data.

DISCUSSION

In the Mediterranean Sea, the existent dataset of nM measurements of DIP at both spatial and temporal scales is severely scarce. The few reported nM concentrations of DIP are limited to two cross-basin cruises (PROSOPE cruise in 1999, Moutin et al., 2002: 7 values reported; Van Wambeke et al., 2002: 2 profiles reported and BOUM cruise in 2008: Talarmin et al., 2015, 5 profiles reported) and data acquired as part of the CYCLOPS project in the eastern basin of the Mediterranean Sea (Krom et al., 2005, 3 profiles reported). Two additional studies reported 1-year time series of surface nM DIP in the NW Mediterranean Sea at fixed observation stations: DYFAMED (Pulido-Villena et al., 2010) and ANTARES (Djaoudi et al., 2017). By reporting an important amount of vertical profiles along a longitudinal gradient, the present study is the first to extensively address the distribution of nM DIP in the P-depleted Mediterranean surface waters.

The nM DIP data obtained in this study are within the range reported in the above cited few previous studies, despite

the use of different methods of analysis (**Table 1**). Regarding the longitudinal pattern of nM DIP, as previously reported by Moutin et al. (2002) for bioavailable DIP concentration in the upper layer (between 10 and 15 m), the present study shows a decreasing trend toward the East within the mixed layer with lower concentrations along the E-W transect (5.5 ± 3.6 nM) compared to the NWMS (12.8 ± 6.8 nM). This longitudinal gradient extends below the mixed layer (between the surface and 100 m), in contrast to Talarmin et al. (2015) study in which DIP concentrations (between the surface and 130 m) did not show any clear longitudinal trend crossing a W-E transect.

Regarding the vertical variability of surface DIP, the few existing data revealed a low but detectable increase of DIP concentration in the layer encompassing the DCM depth (Van Wambeke et al., 2002; Krom et al., 2005). In the present study, a significant vertical gradient of DIP but also of DOP was observed in both the NWMS and the E-W transect, allowing the generalization of this vertical pattern to the whole Mediterranean Sea. The positive gradient of DIP occurred above the phosphacline depth (Figure S1), suggesting that the phosphacline may be shallower than previously thought in both the NWMS and along the E-W transect. This result confirms that DIP in surface waters is not just a depleted invariant pool, highlighting the need to refine the criteria of the phosphacline determination.

The observed positive gradient of DIP, both in the NWMS and along the E-W transect, was higher than the bioavailable orthophosphate (<1–3 nM) reported by Moutin et al. (2002) in the upper waters (10–15 m). This means that the positive gradient of DIP observed in this study may be sufficient to sustain a biological activity in the surface waters, particularly by promoting microbial assemblages with very high-affinity transport systems and living very close to the theoretical diffusion limit for uptake. Indeed, the success of Synechococcus in the oligotrophic Mediterranean Sea has been linked to its ability to acquire phosphate even at low (<5 nM) concentrations (Moutin et al., 2002). However, the lack of biological data in this study precludes any deeper interpretation of the observed DIP gradient in a biological context.

The DIP concentration in surface waters would be the net resultant between biological and physical sources and sinks. The appearance of a positive gradient in upper waters suggests a balance in favor of DIP supply. This positive gradient of DIP could indeed arise from vertical phosphate diffusion from deep layers, suggesting the potential ability of new DIP to reach the upper waters even under stratification conditions in spite of an active biological uptake. The positive gradient of DIP above the phosphacline was, on average, higher in the NWMS than along the E-W transect, in agreement with reported differences in oligotrophy degree between the two sub-basins. Differences in DIP diffusion from deep layers, but also in rates of DOP hydrolysis could explain the observed differences in DIP gradient between the two cruises.

DOP data reported in this study are within the range of previous studies (**Table 1**), despite using different digestion methods (wet persulfate oxidation vs. UV digestion). Regarding the vertical profiles, this study revealed an important variability of DOP concentration in surface waters. Indeed, in the NWMS, a significant negative gradient of DOP was observed between the MLD and the DCM depth (av. 0.6 ± 0.7 nM m^{-1}), which could be the result of its potential bioavailability. High alkaline phosphatase activities have been reported in the NW Mediterranean basin (Van Wambeke et al., 2002; Thingstad and Mantoura, 2005), suggesting an active DOP hydrolysis of phospho-ester bonds which could explain the DOP decrease observed in our study. Interestingly, the negative DOP gradient coincided with the DIP positive gradient, suggesting a DOP utilization even under available DIP conditions. These findings could suggest a possible simultaneous biological uptake of both DIP and DOP in this layer. In a cross-basin cruise in the Mediterranean Sea, Van Wambeke et al. (2002) showed that heterotrophic prokaryotes switched from P to labile carbon limitation at depths where DIP was still undetectable by the conventional technique. Thus, another explanation for the observed DOP decreasing gradient at the DCM depth coincident with sufficiently available DIP is a possible limitation by organic carbon, based on the hypothesis that another role of alkaline phosphatase is to decompose dissolved organic matter (Nausch and Nausch, 2004; Luo et al., 2011). Therefore, if the diffusion is enough to maintain a DIP gradient in the nanomolar range and, thus, remove P limitation, then the observed DOP decrease may be a consequence of the shift from P to C limitation. Again, further studies combining nanomolar DIP and DOP measurements with biological data are needed to confirm the biological meaning of the observed gradients.

N:P Ratios

N:P ratios in the upper waters reported in this study showed a high variability in both inorganic and organic pools. This contrasts with the deep waters of the Mediterranean Sea in which N:P ratios are constrained to a narrow range of values, between 21 and 22 in the western basin, and somewhat higher in the eastern basin (Krom et al., 1991; Bethoux et al., 1992). The vertical profiles of DIN:DIP ratio exhibited the classical shape reported for the Mediterranean Sea surface waters, during the stratification period, with a marked increase of the DIN:DIP ratio in subsurface water (Diaz et al., 2001; Moutin and Raimbault, 2002; Van Wambeke et al., 2009). Based on the conventional definition of nutriclines, this increase would be due to a nitracline shallower than the phosphacline, as previously reported (Moutin and Raimbault, 2002; Van Wambeke et al., 2009; Pujo-Pay et al., 2011). In this study, the use of the sensitive LWCC technique for DIP analysis revealed that this increase of the N:P ratio occurred between the MLD and the DCM depth. As said previously, a positive gradient of nM DIP was recorded in this layer, indicating the existence of a higher gradient of DIN compared to DIP. This observation stresses the need to extend nanomolar measurements to DIN concentration for a better understanding of the controlling factors of DIN:DIP ratios variability as on other oceans, DIN also can be the first limiting nutrient (i.e., Gruber, 2008)

The DON:DOP molar ratios in the surface waters of both NWMS and along the E-W transect were higher than the corresponding DIN:DIP ratios pointing to a DOP depletion

TABLE 1 | Summary of published data on nanomolar dissolved inorganic phosphate (DIP) and dissolved organic phosphate (DOP) concentration in the Mediterranean Sea.

Location	Period of sampling	Depth [m]	DIP [nM]	Method of analysis	DOP [nM]	Method of hydrolysis	References
NW Mediterranean Sea Eastern Mediterranean Sea (PROSOPE cruise, 1999)	Stratification	10–15	3.1	Derived from turnover time of phosphate	_	_	Moutin et al., 2002
		0–150	5–100	MAGIC	_	_	Van Wambeke et al., 2002
Eastern Mediterranean Sea	Stratification	Surface waters	2–6 nM	LWCC	50 - 60	UV oxidation	Krom et al., 2005
NW Mediterranean Sea (MOOSE-DYFAMED station: 43. 41° N; 7. 87° E)	Stratification Mixing	0–40	≤6 nM 200–350	LWCC	_	_	Pulido-Villena et al., 2010
NW Mediterranean Sea Eastern Mediterranean Sea (BOUM Cruise)	Stratification	0–< 130	6 – 80	MAGIC	_	_	Talarmin et al., 2015
NW Mediterranean Sea (MOOSE-ANTARES station: 42.8 °N; 6,00°E)	Stratification	0–200	2–47 nM (above the MLD) >47–300	LWCC	24 - 130	UV oxidation	Djaoudi et al., 2017
NW Mediterranean Sea (MOOSE-GE)	Stratification	0–100	3.6–251	LWCC	4–149	Persulfate wet oxidation	This study
E-W transect (BioArgoMed)	Stratification	0–120	0.9–14.6 (one exceptional value at 127.5 nM)		15–64		

Depth of the corresponding measurements as well as the methods used for both DIP analysis and DOP hydrolysis are presented. MAGIC and LWCC relate to the magnesium induced co-precipitation and the liquid waveguide capillary cell methods, respectively.

relative to DON. This could be the result of a preferential remineralization of DOP with depth as reported by Aminot and Kérouel (2004) in the Mediterranean Sea and by Letscher and Moore (2015) at the scale of the global ocean. Similarly to the DIN:DIP molar ratios, an increase of the DON:DOP was observed at the DCM depth. This finding could be related to a biological utilization of DOP, since in this layer a negative gradient of DOP was observed. Nevertheless, accurate measurement of DON, implying nM measurements of nitrogen, would help to a better constraining of the DON:DOP variability in upper waters.

CONCLUSION

This study reports the first cross-basin distribution of nM DIP and DOP in the P-depleted Mediterranean surface waters. Surface DIP and DOP concentration showed an important variability on both longitudinal and vertical axis. Vertical profiles of DIP exhibited a significant positive gradient above the phosphacline, suggesting the potential of new phosphate to reach the near-surface waters by diffusion even under stratified conditions, and giving evidence against the traditional view of a depleted invariant DIP pool in the surface Mediterranean Sea. Despite this evidence of sufficient P availability, a significant negative gradient of DOP concentration was observed between the mixed layer depth and the DCM. Finally, the positive gradient in DIP was accompanied by a concomitant increase in N:P ratios, suggesting the existence of a higher gradient in DIN compared to DIP. The results obtained in this study indicate that acquiring nanomolar DIP data is a sine qua non condition for the comprehension and prediction of the biogeochemical functioning of the P-depleted Mediterranean Sea.

AUTHOR CONTRIBUTIONS

KD, EP-V, and FV contributed to the conception and design of the study. KD and TW did seawater sampling and sample conditioning during the MOOSE-GE and BioArgoMed cruises, respectively. KD and SH-N analyzed nutrient concentrations. VT, LC, and PT acquired hydrological data (CTD). KD organized the database and wrote the first draft of the manuscript. EP-V and FV wrote sections in the manuscript. LC and PT were chief scientists during the MOOSE-GE cruise. VT and FD were chief scientists during the BioArgoMed cruise. PR is the principal investigator of the MOOSE project. FD is the coordinator of the Mediterranean work package of the NAOS project. All authors contributed to the manuscript revision, read and approved the submitted version.

ACKNOWLEDGMENTS

The authors would like to thank the MOOSE project and the NAOS project (ANR J11R107-F, funded by the French Equipement d'Avenir) in the framework of which this study was performed. Captains and crews of the R/V *le Suroit* and the R/V *le Tethys II* are warmly acknowledged for their cooperative work at sea. The work leading to this publication has received funding from European FEDER Fund under project 1166-39417. This work is a contribution to the Labex OT-Med (n° ANR-11-LABX-0061) funded by the French Government *Investissements d'Avenir* program of the French National Research Agency (ANR) through the A*MIDEX project (n° ANR-11-IDEX-0001-02). Two reviewers are acknowledged for their relevant comments and suggestions on the manuscript.

SUPPLEMENTARY MATERIAL

The Supplementary Material for this article can be found online at: https://www.frontiersin.org/articles/10.3389/fmars.2018.00234/full#supplementary-material

REFERENCES

Aminot, A., and Kérouel, R. (2007). *Dosage Automatique des Nutriments Dans Les Eaux Marines: Méthodes en Flux Continu*. Plouzané: Ed Ifremer-Quae, 188.

Aminot, A., and Kérouel, R. (2004). Dissolved organic carbon, nitrogen and phosphorus in the N-E Atlantic and the N-W Mediterranean with particular reference to non-refractory fractions and degradation. *Deep Sea Res. Part I Oceanogr. Res. Pap.* 51, 1975–1999. doi: 10.1016/j.dsr.2004.07.016

Ammerman, J. W., Hood, R. R., Case, D. A., and Cotner, J. B. (2003). Phosphorus deficiency in the Atlantic: an emerging paradigm in oceanography. *Eos Trans. Am. Geophys. Union* 84, 165–170. doi: 10.1029/2003EO180001

Balino, B., Fasham, M., and Bowles, M. (eds.) (2001). *Ocean Biogeochemistry and Global Change: JGOFS Research Highlightings 1988–2000*, IGBP Science 2. Stockholm: IGBP, 32.

Bethoux, J. P., Morin, P., Madec, C., and Gentili, B. (1992). Phosphorus and nitrogen behavior in the Mediterranean Sea. *Deep Sea Res. Part A Oceanogr. Res. Pap.* 39, 1641–1654. doi: 10.1016/0198-0149(92)90053-V

Céa, B., Lefèvre, D., Chirurgien, L., Raimbault, P., Garcia, N., Charrière, B., et al. (2015). An annual survey of bacterial production, respiration and ectoenzyme activity in coastal NW Mediterranean waters: temperature and resource controls. *Environ. Sci. Pollut. Res. Int.* Research, 22, 13654–13668. doi: 10.1007/s11356-014-3500-9

Crise, A., Allen, J., Baretta, J., Crispi, G., Mosetti, R., and Solidoro, C. (1999). The Mediterranean pelagic ecosystem response to physical forcing. *Prog. Oceanogr.* 44, 219–243. doi: 10.1016/S0079-6611(99)00027-0

Crispi, G., Mosetti, R., Solidoro, C., and Crise, A. (2001). Nutrients cycling in Mediterranean basins: the role of the biological pump in the trophic regime. *Ecol. Model.* 138, 101–114. doi: 10.1016/S0304-3800(00)00396-3

De Boyer Montégut, C. (2004). Mixed layer depth over the global ocean: an examination of profile data and a profile-based climatology. *J. Geophys. Res.* 109, 1–20. doi: 10.1029/2004JC002378

De Madron, X. D., Guieu, C., Sempere, R., Conan, P., Cossa, D., D'Ortenzio, F., et al. (2011). Marine ecosystems' responses to climatic and anthropogenic forcings in the Mediterranean. *Prog. Oceanogr.* 91, 97–166. doi: 10.1016/j.pocean.2011.02.003

Diaz, F., Raimbault, P., Boudjellal, B., Garcia, N., and Moutin, T. (2001). Early spring phosphorus limitation of primary productivity in a NW Mediterranean coastal zone (Gulf of Lions). *Mar. Ecol. Prog. Ser.* 211, 51–62. doi: 10.3354/meps211051

Djaoudi, K., Van Wambeke, F., Barani, A., Hélias-Nunige, S., Sempéré, R., and Pulido-Villena, E. (2017). Atmospheric fluxesof soluble organic C, N and P to the Mediterranean Sea: potential biogeochemical implications in the surface layer. *Progr. Oceanogr.* 163, 59–69. doi: 10.1016/j.pocean.2017.07.008

Falkowski, P. G., and Raven, J. A. (1997). *Aquatic Photosynthesis*. Oxford: Blackwell Science.

Gruber, N. (2008). The marine nitrogen cycle: overview and challenges. *Nitrog. Mar. Environ.* 2, 1–50. doi: 10.1016/B978-0-12-372522-6.00001-3

Hashihama, F., Kinouchi, S., Suwa, S., Suzumura, M., and Kanda, J. (2013). Sensitive determination of enzymatically labile dissolved organic phosphorus and its vertical profiles in the oligotrophic western North Pacific and East China Sea. *J. Oceanogr.* 69, 357–367. doi: 10.1007/s10872-013-0178-4

Karl, D. M., and Björkman, K. M. (2015). "Dynamics of dissolved organic phosphorus," in *Biogeochemistry of Marine Dissolved Organic Matter,* eds D. A. Hansell and C. A. Carlson (Burlington: Academic Press), 579–608.

Karl, D. M., Björkman, K. M., Dore, J. E., Fujieki, L., Hebel, D. V., Houlihan, T., et al. (2001). Ecological nitrogen-to-phosphorus stoichiometry at station ALOHA. *Deep Sea Res. Part II Top. Stud. Oceanogr.* 48, 1529–1566. doi: 10.1016/S0967-0645(00)00152-1

Karl, D. M., and Tien, G. (1992). Magic - a sensitive and precise method for measuring dissolved phosphorus in aquatic environments. *Limnol. Oceanogr.* 37, 105–116. doi: 10.4319/lo.1992.37.1.0105

Krom, M. D., Kress, N., Brenner, S., and Gordon, L. I. (1991). Phosphorus limitation of primary productivity along the E-W transect. *Limnol. Oceanogr.* 36, 424–432. doi: 10.4319/lo.1991.36.3.0424

Krom, M. D., Woodward, E. M. S., Herut, B., Kress, N., Carbo, P., Mantoura, R. F. C., et al. (2005). Nutrient cycling in the south-east Levantine basin of the eastern Mediterranean: results from a phosphorus starved system. *Deep Sea Res. Part II Top. Stud. Oceanogr.* 52, 2879–2896. doi: 10.1016/j.dsr2.2005.08.009

Lavigne, H., D'Ortenzio, F., D'Alcala, M. R., Claustre, H., Sauzede, R., and Gacic, M. (2015). On the vertical distribution of the chlorophyll a concentration in the Mediterranean Sea: a basin-scale and seasonal approach. *Biogeosciences* 12, 5021–5039. doi: 10.5194/bg-12-5021-2015

Lazzari, P., Solidoro, C., Ibello, V., Salon, S., Teruzzi, A., Béranger, K., et al. (2012). Seasonal and inter-annual variability of plankton chlorophyll and primary production in the Mediterranean Sea: a modelling approach. *Biogeosciences* 9, 217–233. doi: 10.5194/bg-9-217-2012

Letscher, R. T., and Moore, J. K. (2015). Preferential remineralization of dissolved organic phosphorus and non-Redfield DOM dynamics in the global ocean: impacts on marine productivity, nitrogen fixation, and carbon export. *Global Biogeochem. Cycles* 29, 325–340. doi: 10.1002/2014GB004904

Lomas, M. W., Steinberg, D. K., Dickey, T., Carlson, C. A., Nelson, N. B., Condon, R. H., et al. (2010). Increased ocean carbon export in the Sargasso Sea linked to climate variability is countered by its enhanced mesopelagic attenuation. *Biogeosciences* 7, 57–70. doi: 10.5194/bg-7-57-2010

Luo, H., Zhang, H., Long, R. A., and Benner, R. (2011). Depth distributions of alkaline phosphatase and phosphonate utilization genes in the North Pacific Subtropical Gyre. *Aquat. Microb. Ecol.* 62, 61–69. doi: 10.3354/ame01458

Mather, R. L., Reynolds, S. E., Wolff, G. A., Williams, R. G., Torres-Valdes, S., Woodward, E. M. S., et al. (2008). Phosphorus cycling in the North and South Atlantic Ocean subtropical gyres. *Nat. Geosci.* 1, 439–443. doi: 10.1038/ngeo232

Moore, C. M., Mills, M. M., Arrigo, K. R., Berman-Frank, I., Bopp, L., Boyd, P. W., et al. (2013). Processes and patterns of oceanic nutrient limitation. *Nat. Geosci.* 6, 701–710. doi: 10.1038/ngeo1765

Moutin, T., Karl, D. M., Duhamel, S., Rimmelin, P., Raimbault, P., Van Mooy, B. A. S., et al. (2008). Phosphate availability and the ultimate control of new nitrogen input by nitrogen fixation in the tropical Pacific Ocean. *Biogeosciences* 5, 95–109. doi: 10.5194/bg-5-95-2008

Moutin, T., and Raimbault, P. (2002). Primary production, carbon export and nutrients availability in western and eastern Mediterranean Sea in early summer 1996 (MINOS cruise). *J. Mar. Syst.* 33, 273–288. doi: 10.1016/S0924-7963(02)00062-3

Moutin, T., Thingstad, T. F., Van Wambeke, F., Marie, D., Slawyk, G., Raimbault, P., et al. (2002). Does competition for nano-molarphosphate supply explain the

predominance of the cyanobacterium Synechococcus? *Limnol. Oceanogr.* 47, 1562–1567. doi: 10.4319/lo.2002.47.5.1562

Murphy, J., and Riley, J. P. (1962). A modified single solution method for the determination of phosphate in natural waters. *Anal. Chim. Acta* 27, 31–36. doi: 10.1016/S0003-2670(00)88444-5

Nausch, M., and Nausch, G. (2004). Bacterial utilization of phosphorus pools after nitrogen and carbon amendment and its relation to alkaline phosphatase activity. *Aquat. Microb. Ecol.* 37, 237–245. doi: 10.3354/ame037237

Patey, M. D., Rijkenberg, M. J. A., Statham, P. J., Stinchcombe, M. C., Achterberg, E. P., and Mowlem, M. (2008). Determination of nitrate and phosphate in seawater at nano-molarconcentrations. *TrAC Trends Analy. Chem.* 27, 169–182. doi: 10.1016/j.trac.2007.12.006

Pujo-Pay, M., Conan, P., Oriol, L., Cornet-Barthaux, V., Falco, C., Ghiglione, J. F., et al. (2011). Integrated survey of elemental stoichiometry (C, N, P) from the western to eastern Mediterranean Sea. *Biogeosciences* 8, 883–899. doi: 10.5194/bg-8-883-2011

Pulido-Villena, E., Rerolle, V., and Guieu, C. (2010). Transient fertilizing effect of dust in P-deficient LNLC surface ocean. *Geophys. Res. Lett.* 37, 1–5. doi: 10.1029/2009GL041415

Redfield, A. C. (1958). The biological control of chemical factors in the environment. *Am. Sci.* 46, 230A 205–221.

Rimmelin, P., and Moutin, T. (2005). Re-examination of the MAGIC method to determine low orthophosphate concentration in seawater. *Anal. Chim. Acta* 548, 174–182. doi: 10.1016/j.aca.2005.05.071

Ryther, J. H., and Dunstan, W. M. (1971). Nitrogen, phosphorus, and eutrophication in the coastal marine environment. *Science* 171, 1008–1013. doi: 10.1126/science.171.3975.1008

Sato, M., Sakuraba, R., and Hashihama, F. (2013). Phosphate monoesterase and diesterase activities in the North and South Pacific Ocean. *Biogeosciences* 10, 7677–7688. doi: 10.5194/bg-10-7677-2013

Sigman, D. M., and Boyle, E. A. (2000). Glacial/interglacial variations in atmospheric carbon dioxide. *Nature* 407, 859–869. doi: 10.1038/35038000

Suzumura, M., Hashihama, F., Yamada, N., and Kinouchi, S. (2012). Dissolved phosphorus pools and alkaline phosphatase activity in the euphotic zone of the western North Pacific Ocean. *Front. Microbiol.* 3:99. doi: 10.3389/fmicb.2012.00099

Talarmin, A., Van Wambeke, F., Lebaron, P., and Moutin, T. (2015). Vertical partitioning of phosphate uptake among picoplankton groups in the low Pi Mediterranean Sea. *Biogeosciences* 12, 1237–1247. doi: 10.5194/bg-12-1237-2015

Thingstad, T. F., Krom, M. D., Mantoura, R. F. C., Flaten, G. A. F., Groom, S., Herut, B., et al. (2005). Nature of phosphorus limitation in the ultraoligotrophic eastern Mediterranean. *Science* 309, 1068–1071. doi: 10.1126/science.1112632

Thingstad, T. F., and Mantoura, R. F. C. (2005). Titrating excess nitrogen content of phosphorous-deficient eastern Mediterranean surface water using alkaline phosphatase activity as a bio-indicator. *Limnol. Oceanogr. Methods* 3, 94–100. doi: 10.4319/lom.2005.3.94

Tyrrell, T. (1999). The relative influences of nitrogen and phosphorus on oceanic primary production. *Nature* 400, 525–531. doi: 10.1038/22941

Valderrama, J. C. (1981). The simultaneous analysis of total nitrogen and total phosphorus in natural water. *Mar. Chem.* 10, 102–122. doi: 10.1016/0304-4203(81)90027-X

Van Wambeke, F., Christaki, U., Giannokourou, A., Moutin, T., and Souvemerzoglou, K. (2002). Longitudinal and vertical trends of bacterial limitation by phosphorus and carbon in the Mediterranean Sea. *Microb. Ecol.* 43, 119–133. doi: 10.1007/s00248-001-0038-4

Van Wambeke, F., Ghiglione, J.-F., Nedoma, J., Mével, G., and Raimbault, P. (2009). Bottom up effects on bacterioplankton growth and composition during summer-autumn transition in the open NW Mediterranean Sea. *Biogeosciences* 6, 705–720. doi: 10.5194/bg-6-705-2009

Wu, J. F., Sunda, W., Boyle, E. A., and Karl, D. M. (2000). Phosphate depletion in the western North Atlantic Ocean. *Science* 289, 759–762. doi: 10.1126/science.289.5480.759

Zhang, J. Z., and Chi, J. (2002). Automated analysis of nano-molar concentrations of phosphate in natural waters with liquid waveguide. *Environ. Sci. Technol.* 36, 1048–1053. doi: 10.1021/es011094v

Conflict of Interest Statement: The authors declare that the research was conducted in the absence of any commercial or financial relationships that could be construed as a potential conflict of interest.

Advantages of publishing in Frontiers

OPEN ACCESS
Articles are free to read for greatest visibility and readership

FAST PUBLICATION
Around 90 days from submission to decision

HIGH QUALITY PEER-REVIEW
Rigorous, collaborative, and constructive peer-review

TRANSPARENT PEER-REVIEW
Editors and reviewers acknowledged by name on published articles

Frontiers
Avenue du Tribunal-Fédéral 34
1005 Lausanne | Switzerland

Visit us: www.frontiersin.org
Contact us: info@frontiersin.org | +41 21 510 17 00

REPRODUCIBILITY OF RESEARCH
Support open data and methods to enhance research reproducibility

DIGITAL PUBLISHING
Articles designed for optimal readership across devices

FOLLOW US
@frontiersin

IMPACT METRICS
Advanced article metrics track visibility across digital media

EXTENSIVE PROMOTION
Marketing and promotion of impactful research

LOOP RESEARCH NETWORK
Our network increases your article's readership